PLANT VIRUSES, VOLUME II: MOLECULAR PLANT VIRUS EPIDEMIOLOGY AND ITS MANAGEMENT

EDITED BY: Rajarshi kumar Gaur, Akhtar Ali, Xiaofei Cheng, Kristiina Mäkinen, Bright Agindotan and Xifeng Wang

PUBLISHED IN: Frontiers in Microbiology and Frontiers in Plant Science

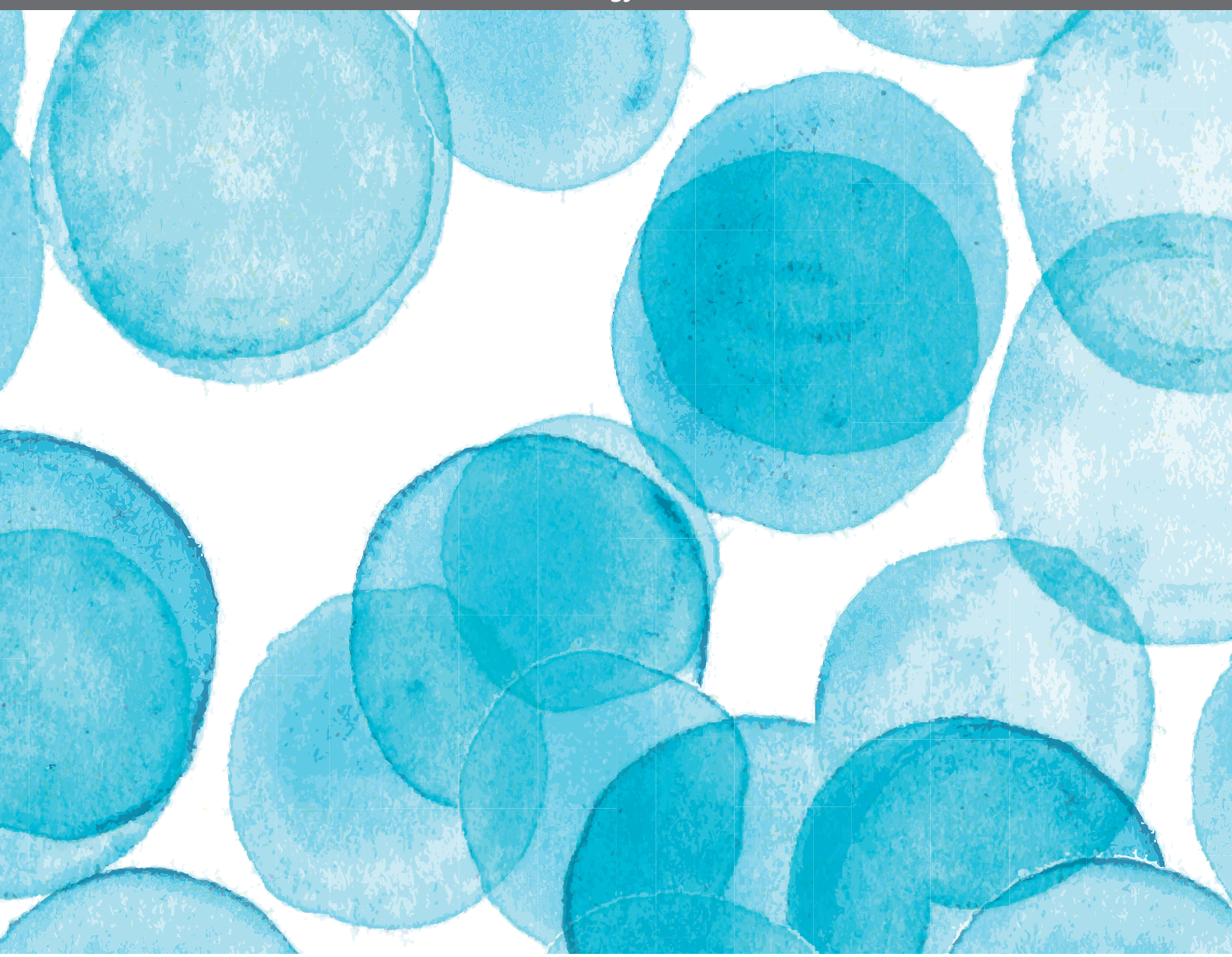

frontiers Research Topics

ISSN 1664-8714
ISBN 978-2-88971-876-4
DOI 10.3389/978-2-88971-876-4

About Frontiers

Frontiers is more than just an open-access publisher of scholarly articles: it is a pioneering approach to the world of academia, radically improving the way scholarly research is managed. The grand vision of Frontiers is a world where all people have an equal opportunity to seek, share and generate knowledge. Frontiers provides immediate and permanent online open access to all its publications, but this alone is not enough to realize our grand goals.

Frontiers Journal Series

The Frontiers Journal Series is a multi-tier and interdisciplinary set of open-access, online journals, promising a paradigm shift from the current review, selection and dissemination processes in academic publishing. All Frontiers journals are driven by researchers for researchers; therefore, they constitute a service to the scholarly community. At the same time, the Frontiers Journal Series operates on a revolutionary invention, the tiered publishing system, initially addressing specific communities of scholars, and gradually climbing up to broader public understanding, thus serving the interests of the lay society, too.

Dedication to Quality

Each Frontiers article is a landmark of the highest quality, thanks to genuinely collaborative interactions between authors and review editors, who include some of the world's best academicians. Research must be certified by peers before entering a stream of knowledge that may eventually reach the public - and shape society; therefore, Frontiers only applies the most rigorous and unbiased reviews.
Frontiers revolutionizes research publishing by freely delivering the most outstanding research, evaluated with no bias from both the academic and social point of view. By applying the most advanced information technologies, Frontiers is catapulting scholarly publishing into a new generation.

What are Frontiers Research Topics?

Frontiers Research Topics are very popular trademarks of the Frontiers Journals Series: they are collections of at least ten articles, all centered on a particular subject. With their unique mix of varied contributions from Original Research to Review Articles, Frontiers Research Topics unify the most influential researchers, the latest key findings and historical advances in a hot research area! Find out more on how to host your own Frontiers Research Topic or contribute to one as an author by contacting the Frontiers Editorial Office: frontiersin.org/about/contact

PLANT VIRUSES, VOLUME II: MOLECULAR PLANT VIRUS EPIDEMIOLOGY AND ITS MANAGEMENT

Topic Editors:
Rajarshi Kumar Gaur, Deen Dayal Upadhyay Gorakhpur University, India
Akhtar Ali, University of Tulsa, United States
Xiaofei Cheng, Northeast Agricultural University, China
Kristiina Mäkinen, University of Helsinki, Finland
Bright Agindotan, USDA APHIS Veterinary Services, United States
Xifeng Wang, Institute of Plant Protection (CAAS), China

Citation: Gaur, R. K., Ali, A., Cheng, X., Mäkinen, K., Agindotan, B., Wang, X., eds. (2021). Plant Viruses, Volume II: Molecular Plant Virus Epidemiology and its Management. Lausanne: Frontiers Media SA. doi: 10.3389/978-2-88971-876-4

Table of Contents

frontiers in Microbiology

EDITORIAL
published: 25 October 2021
doi: 10.3389/fmicb.2021.756807

Editorial: Plant Viruses, Volume II: Molecular Plant Virus Epidemiology and Its Management

Rajarshi Kumar Gaur[1]*, *Akhtar Ali*[2], *Xiaofei Cheng*[3], *Kristiina Mäkinen*[4], *Bright Agindotan*[5] *and Xifeng Wang*[6]

[1] Department of Biotechnology, Deen Dayal Upadhyaya Gorakhpur University, Gorakhpur, India, [2] Department of Biological Science, The University of Tulsa, Tulsa, OK, United States, [3] Key Laboratory of Germplasm Enhancement, Physiology and Ecology of Food Crops in Cold Region of Chinese Education Ministry, College of Agriculture, Northeast Agricultural University, Harbin, China, [4] Department of Microbiology, Viikki Plant Science Center, University of Helsinki, Helsinki, Finland, [5] Science & Technology (S&T) Beltsville Laboratory, USDA APHIS, Beltsville, MD, United States, [6] State Key Laboratory for Biology of Plant Diseases and Insect Pests, Institute of Plant Protection, Chinese Academy of Agricultural Sciences, Beijing, China

Keywords: plant virus, high throughput sequencing, transmission, mixed infections, virus-host plant interactions, resistance, CRISPR/Cas

Editorial on the Research Topic

Plant Viruses, Volume II: Molecular Plant Virus Epidemiology and Its Management

The International Committee on Taxonomy of Viruses (ICTV) lists nearly 2,000 different species of plant viruses. Plant viruses are recognized as economically important plant pathogens, because they cause significant losses in a variety of crops that we rely on. Due to the global transportation of agricultural products and planting materials and intensive agricultural farming practices, emerging new viruses and reemerging known viruses significantly threat food security. There is currently no efficient or long-term control measures for many of the plant viruses that cause serious diseases. On these lines, Zhang Z. et al. describes the occurrence and distribution of orthotospoviral diseases and their possible management strategies in China.

A big advancement in ecological plant virus research has been achieved by high throughput sequencing (HTS). HTS allows quick identification of most, if not all, viruses in plants without a need for prior information, which viruses might be present. In their expert review, Maclot et al. highlights the many opportunities that careful use of the HTS method opens up in understanding the behavior of plant virus populations in cultivated and wild plants. Velasco and Padilla consider the possibility to use HTS in certification schemes based on the results of a comparison between HTS of small RNAs and other diagnostic methods in grapevine plants. The prospects of HTS based diagnosis in controlling plant virus diseases are bright.

Plant viruses enter the plant cell by mechanical injury, when transported by insects or nematodes feeding on them or via parasitic agents such as fungi. Virus-insect vector interaction studies are essential for understanding the connections between plant viral transmission routes and virus epidemics. In their review, Zhang L. et al., discuss fijivirus outbreaks, which occur in connection to migrations of the planthopper vectors. The authors give insights into several aspects of vector transmission including the effects of viruses on the behavior and physiology of vector insects. An interesting finding presented by Du et al., is that the RNA-silencing suppressor NSs of tomato spotted wilt virus reduces the monoterpene volatiles in a way that increases the attractiveness of the plant for the transmission vector thrip *Frankliniella occidentalis*. In their paper, McGreal et al. studied the possibility to use ground cover plants as an alternative controlling strategy to reduce transmission of grapevine leafroll-associated virus 3 by mealybugs. Zhang J. et al., asked the question about the role of virus-induced expression of circular RNAs in the vector *Laodelphax striatellus* on rice black-streaked dwarf virus infection. Chen et al., found that the virus concentrations in the

Edited and reviewed by:
Elvira Fiallo-Olivé, Institute of Subtropical and Mediterranean Horticulture La Mayora, Spain

***Correspondence:**
Rajarshi Kumar Gaur
gaurrajarshi@hotmail.com

Specialty section:
This article was submitted to Virology, a section of the journal Frontiers in Microbiology

Received: *11 August 2021*
Accepted: *30 September 2021*
Published: *25 October 2021*

Citation:
Gaur RK, Ali A, Cheng X, Mäkinen K, Agindotan B and Wang X (2021) Editorial: Plant Viruses, Volume II: Molecular Plant Virus Epidemiology and Its Management. Front. Microbiol. 12:756807. doi: 10.3389/fmicb.2021.756807

salivary gland of the leafhopper vector *Nephotettix cincticeps* were higher during the intermittent period than during the transmitting period of rice dwarf virus, a plant reovirus, which led the authors to discuss a threshold-regulated release of viruses from the insect vectors.

Plant responses to mixed infections vary, but because of their many possible adverse consequences, it is important to understand how viruses interact in co-infected susceptible plants. A previously undescribed interaction of a potyvirus watermelon mosaic virus protein P1 with a crinivirus cucurbit yellow stunting disorder virus protein P25 was proposed to contribute to the complex response of the host to this virus pair (Domingo-Calap et al.). The authors demonstrate reduced RNA silencing suppression activity of the crinivirus P25 in this interaction. An interaction that reduced the activity of RNA silencing suppressor of another crinivirus cucurbit chlorotic yellows virus was discovered by Yang et al., In this case the interactor was a ribosomal protein that could negatively affect virus accumulation. These studies suggest that the silencing suppressor proteins interact with various proteins and many antiviral defense pathways during crinivirus infections. It also simply is amazing in how many ways geminiviral AC2 silencing suppressor proteins interfere with post-transcriptional gene silencing, transcriptional gene silencing and other plant defense pathways as can be learned from the review article by Veluthambi and Sunitha.

Basal immunity of non-host plant species protects plants against most plant virus diseases. Also host plants may express basal resistance at certain developmental stages. The factors underlying the mechanism of age-related resistance against a geminivirus, tomato leaf curl virus, were studied by against a geminvirus tomato yellow leaf curl virus were studied by Zhang J.-R. et al. They suggest that salicylic acid plays a major role and raise the possibility to deploy the cues obtained from these studies in managing the disease. Knowledge on the molecular mechanisms of plant virus- host interactions provides ideas and novel targets for resistance breeding. The mechanism of resistance toward rice stripe virus, achieved by expressing coat protein encoding transcripts, relates to RNA silencing in Arabidopsis as demonstrated in Sun et al. While RNA silencing-mediated resistance provides one option, it is important to explore other possibilities as well. Identification of host factors that either promote or suppress infections by interacting with viral proteins is an important study field in the search of possible novel resistance targets. Increasing body of evidence indicate that specific nuclear factors are involved in systemic spread of several viruses. The study by Alazem et al., reveals that the control of systemic spread of bamboo mosaic virus is connected to a correct homeostasis of a nuclear high mobility group protein and to processes it regulates. As reviewed in Kozieł et al., the components of cell wall affect the spread of the virus and the apoplast- and symplast-based defense mechanisms both in susceptible and resistant plants. Engineering antiviral mechanisms to host plants to prevent and control plant viruses has been and will continue to be an effective management strategy. Modern DNA/RNA editing tools based on clustered regularly interspaced short palindromic repeats (CRISPR) and CRISPR-associated Cas nucleases are reviewed by Cao et al. They discuss the challenges and opportunities provided by CRISPR/Cas systems for controlling different plant viruses by targeting either viral sequences or host susceptibility genes.

Finally, we would like to show our gratitude to all the authors who contributed to the Research Topic. The articles cover a broad spectrum of plant host-virus interactions and management strategies and open several channels for study by providing major insights into these complex relationships.

AUTHOR CONTRIBUTIONS

All authors listed have made a substantial, direct and intellectual contribution to the work, and approved it for publication.

ACKNOWLEDGMENTS

We sincerely thank all researchers who have contributed to our Research Topic.

Conflict of Interest: The authors declare that the research was conducted in the absence of any commercial or financial relationships that could be construed as a potential conflict of interest.

Publisher's Note: All claims expressed in this article are solely those of the authors and do not necessarily represent those of their affiliated organizations, or those of the publisher, the editors and the reviewers. Any product that may be evaluated in this article, or claim that may be made by its manufacturer, is not guaranteed or endorsed by the publisher.

frontiers in Microbiology

ORIGINAL RESEARCH
published: 29 September 2020
doi: 10.3389/fmicb.2020.588009

Systematic Identification and Functional Analysis of Circular RNAs During Rice Black-Streaked Dwarf Virus Infection in the *Laodelphax striatellus* (Fallén) Midgut

Jianhua Zhang[1†], Haitao Wang[1,2†], Wei Wu[1], Yan Dong[1,2], Man Wang[1,2], Dianshan Yi[3], Yijun Zhou[1,2] and Qiufang Xu[1,2]*

[1] Institute of Plant Protection, Jiangsu Academy of Agricultural Sciences, Nanjing, China, [2] Key Laboratory of Food Quality and Safety of Jiangsu Province – State Key Laboratory Breeding Base, Nanjing, China, [3] Nanjing Plant Protection and Quarantine Station, Nanjing, China

OPEN ACCESS

Edited by:
Xiaofei Cheng,
Northeast Agricultural University, China

Reviewed by:
Jing Li,
ZheJiang Academy of Agricultural Sciences, China
Tong Zhang,
South China Agricultural University, China

***Correspondence:**
Qiufang Xu
xuqiufang@jaas.ac.cn

[†] These authors have contributed equally to this work

Specialty section:
This article was submitted to Microbe and Virus Interactions with Plants, a section of the journal Frontiers in Microbiology

Received: 30 July 2020
Accepted: 14 September 2020
Published: 29 September 2020

Citation:
Zhang J, Wang H, Wu W, Dong Y, Wang M, Yi D, Zhou Y and Xu Q (2020) Systematic Identification and Functional Analysis of Circular RNAs During Rice Black-Streaked Dwarf Virus Infection in the Laodelphax striatellus (Fallén) Midgut. Front. Microbiol. 11:588009. doi: 10.3389/fmicb.2020.588009

Circular RNAs (circRNAs) are endogenous RNAs that have critical regulatory roles in numerous biological processes. However, it remains largely unknown whether circRNAs are induced in response to plant virus infection in the insect vector of the virus as well as whether the circRNAs regulate virus infection. Rice black-streaked dwarf virus (RBSDV) is transmitted by *Laodelphax striatellus* (Fallén) in a persistent propagative manner and causes severe losses in East Asian countries. To explore the expression and function of circRNAs in the regulation of virus infection, we determined the circRNA expression profile in RBSDV-free or RBSDV-infected *L. striatellus* midgut tissues by RNA-Seq. A total of 2,523 circRNAs were identified, of which thirteen circRNAs were differentially expressed after RBSDV infection. The functions of these differentially circRNAs were predicted by GO and KEGG pathway analyses. The expression changes of five differentially expressed circRNAs and eight parental genes were validated by RT-qPCR. The circRNAs-microRNAs (miRNAs) interaction networks were analyzed and two miRNAs, which were predicted to bind circRNAs, were differentially expressed after virus infection. CircRNA2030 was up-regulated after RBSDV infection in *L. striatellus* midgut. Knockdown of circRNA2030 by RNA interference inhibited the expression of its predicted parental gene phospholipid-transporting ATPase (PTA) and enhanced RBSDV infection in *L. striatellus*. However, none of the six miRNAs predicting to bind circRNA2030 was up-regulated after circRNA2030 knockdown. The results suggested that circRNA2030 might affect RBSDV infection via regulating PTA. Our results reveal the expression profile of circRNAs in *L. striatellus* midgut and provide new insight into the roles of circRNAs in virus–insect vector interaction.

Keywords: circular RNA, RNA-Seq, rice black-streaked dwarf virus, *Laodelphax striatellus*, midgut, circRNA2030

INTRODUCTION

A high-proportion of genomes can be transcribed into RNA and the majority of these RNAs are non-coding RNAs (ncRNAs). The ncRNAs, can be divided into multiple types, including microRNAs (miRNAs), PIWI-interacting RNAs (piRNAs), long non-coding RNAs (lncRNAs), and circular RNAs (circRNAs) (Huttenhofer et al., 2005; Lauressergues et al., 2015). CircRNAs have a single-strand and covalently closed structure. In general, circRNAs are generated through back-splicing the exons and introns of precursor mRNAs and joining a downstream splice donor site with an upstream splice acceptor site (Lasda and Parker, 2014). CircRNAs exist in almost all eukaryotes with abundant and tissue-specific expression patterns (Lasda and Parker, 2014; Salzman, 2016).

An increasing number of researches have shown that circRNAs play vital regulatory roles in numerous biological processes (Gan et al., 2017; Wei et al., 2017). CircRNAs can function as miRNA sponges, splicing interferences, and transcription regulators (Li et al., 2019). For example, circRNA *CDR1as* can impact the development of zebrafish midbrain through sponging miR-7 (Memczak et al., 2013). CircRNAs also play vital roles in host–virus interactions. In *Bombyx mori*, a large number of differentially expressed circRNAs were identified during cytoplasmic polyhedrosis virus (CPV) infection (Hu et al., 2018). The relative expressions of circRNAs and their parent genes were significantly alerted in the IPEC-J2 cell line after porcine endemic diarrhea virus (PEDV) infection (Chen et al., 2019). CircRNAs were involved in the response to cucumber green mottle mosaic virus (CGMMV) infection in watermelon (Sun et al., 2020). In tomato, circRNAs were identified as negative regulators following tomato yellow leaf curl virus (TYLCV) infection (Wang et al., 2018). However, the functions of circRNAs in host–virus interactions are still unclear.

Over 76% of plant viruses are transmitted via insect vectors, including planthoppers, whiteflies, thrips, and aphids (Hogenhout et al., 2008; Dader et al., 2017; Jia et al., 2018). Rice black-streaked dwarf virus (RBSDV) is a member of the genus *Fijivirus* within the family *Reoviridae* and is the causal agent of rice black-streaked dwarf and maize rough dwarf disease (Zhang et al., 2001b; Xu et al., 2014; Wu et al., 2020). RBSDV was first reported in Japan (Kuribayashi and Shinkai, 1952), with the first report in China in 1963 in Yuyao county, Zhejiang Province, and caused severe damage (Chen, 1964; Ren et al., 2016; Liu et al., 2020). RBSDV is transmitted in a persistent propagative manner by *Laodelphax striatellus* (Fallén) (Wu et al., 2020). The genome of RBSDV contains 10 double-stranded RNA (dsRNA) segments (*S1* to *S10*) and encodes 13 proteins (Milne et al., 1973; Zhang et al., 2001a; He et al., 2020). Most RBSDV genomic segments encode one protein, while S5, S7, and S9 encode two proteins. P5-1, P6, and P9-1 proteins encoded by S5, S6, and S9 are the components of the viroplasm (Li et al., 2013; Sun et al., 2013; He et al., 2020). The P10 protein, encoded by S10, is the virus outer capsid protein. P10 can promote RBSDV infection when expressed in rice and can impair the innate immunity in *L. striatellus* (Lu et al., 2019; Zhang et al., 2019).

In its insect vector, RBSDV can move from midgut lumen to hemolymph or other tissues, then to salivary gland, and finally, infect the plant during insect feeding. The midgut is an important barrier for RBSDV infection (Jia et al., 2014). In this research, we investigated the expression profiles of circRNAs in the *L. striatellus* midgut during RBSDV infection by RNA-Seq. The expression of differentially expressed circRNAs and their parental genes was verified by quantitative real-time PCR (RT-qPCR). The functions of the differentially expressed circRNAs were predicted using GO and KEGG analyses. Also, the interactive networks between differentially expressed circRNAs and miRNAs were constructed. Furthermore, the function of circRNA2030 was investigated by RNA interference (RNAi). The results provide new insight into the functions of circRNAs in regulating plant virus infection in the insect vector.

MATERIALS AND METHODS

Insect, Virus, and Sample Preparation

The non-viruliferous populations of *L. striatellus* used in this research were collected from Haian (32.57°N, 120.45°E; Jiangsu Province, China) and maintained in the incubator at 26 ± 1°C with 70%–80% humidity and 16 h light: 8 h dark photoperiod. The RBSDV-infected rice plants with typical dwarf symptom were collected for *L. striatellus* to acquire virus.

The non-viruliferous 3rd-instar nymphs of *L. striatellus* were reared on RBSDV-infected rice plants for 2 days and then transferred to healthy rice seedlings for another 2 days. Finally, the surviving nymphs of *L. striatellus* were collected as RBSDV-infected *L. striatellus*. The non-viruliferous 3rd-instar nymphs of *L. striatellus* were reared on healthy rice seedlings for 4 days, and the surviving nymphs of *L. striatellus* were collected as virus-free *L. striatellus*.

RBSDV-free (VF) and RBSDV-infected (RB) midguts were collected from 200 non-viruliferous or RBSDV-infected *L. striatellus* nymphs for RNA-Seq analysis. For midgut dissection, the nymphs were rinsed with 75% ethanol and then washed three times using sterilized-deionized water. The midgut tissue was dissected in chilled 1× phosphate-buffered saline (1× PBS, pH 7.4) with sterile forceps under a stereomicroscope. Each sample contained three independent biological repetitions.

RNA Extraction and RNA-Seq

Total RNA of *L. striatellus* midgut was extracted using TRIzol reagent (Invitrogen, United States) according to the manufacturer's instructions. The quantity and quality of total RNA was determined by spectrophotometry (NanoDrop 2000, Thermo Scientific) and agarose gel electrophoresis, respectively.

Ribosomal RNA in the total RNAs was eliminated by Epicentre Ribo-Zero Gold Kit (Illumina, United States). Thereafter, the cDNA libraries were constructed by the mRNA-Seq sample preparation kit using approximately 10 μg of RNA (Illumina, United States). Sequencing was carried out using the Illumina HiSeq 4000 platform, and the whole transcriptome was performed by Lianchuan Biotechnology (Hangzhou, China).

Bioinformatics Analysis

The sequence quality was analyzed by FastQC after removal of the reads containing low-quality bases, undetermined bases, and adaptor contamination[1]. Bowtie2, Tophat2, and tophat-fusion were used to map sequences to the genome of *L. striatellus* (GenBank No.: GCA_003335185.2) (Kim and Salzberg, 2011; Langmead and Salzberg, 2012; Kim et al., 2013). The mapped reads were de novo assembled to circRNAs using CIRCExplorer (Zhang et al., 2014, 2016; Gao et al., 2015). The unmapped reads were used to identify back splicing reads by CIRCExplorer and tophat-fusion (Kim and Salzberg, 2011; Zhang et al., 2014, 2016; Gao et al., 2015). The expression levels of circRNAs were normalized using the formula (normalized expression = (mapped reads)/(total reads) × 1,000,000). Only the comparisons with p value < 0.05 were regarded as having significant differential expression by the R package (Robinson et al., 2010). Gene Ontology (GO[2]) and Kyoto Encyclopedia of Genes and Genomes database (KEGG[3]) were performed to analyze the potential functions of circRNAs (Kanehisa et al., 2008; Young et al., 2010). The miRanda software[4] was used to detect the potential binding miRNAs of these differentially expressed circRNAs.

RT-qPCR

The cDNA was synthesized from 1 μg of total RNA with PrimeScript™ RT reagent kit with gDNA Eraser (Takara, Japan). SYBR PrimeScript™ RT-PCR Kit (Takara, Japan) and IQ™5 multicolor real-time PCR detection system (BIO-RAD, United States) were used and each experiment included three independent technical and biological replications. RT-qPCR was carried out for 40 cycles (94°C for 5 s, 60°C for 34 s) after an initial denaturation step (94°C for 30 s). RPL5 (encoding ribosome protein L5) was used as an internal reference gene (Wu et al., 2019a). U6 snRNA was used as an internal reference for miRNAs analysis (Wu et al., 2019b). The data were calculated by $2^{-\Delta\Delta Ct}$ method. The primers were designed with Beacon Designer 7.7 and listed in **Supplementary Table S1**.

RNA Interference

The T7 high yield transcription kit (Invitrogen, America) was used to synthesize double-stranded RNA (dsRNA). The RBSDV-free 3rd-instar nymphs of *L. striatellus* were immobilized on a 1% agarose plate and approximately 100 nL dsRNA (2 μg/μL) was injected into the conjunction between the prothorax and mesothorax via capillary on FemtoJet (Eppendorf, Germany) after being anesthetized with carbon dioxide. The dsRNA of enhanced green fluorescent protein (EGFP) was injected as a control. Each experiment was carried out with 30 nymphs and three independent biological repetitions.

The RNAi efficiency of circRNA2030 was determined by calculating its relative expression at 1, 3, and 5 days after injection of circRNA2030 dsRNA. Two days after microinjection, the nymphs of *L. striatellus* were reared on RBSDV-infected rice plants for 2 days. Then, the nymphs were transferred to healthy rice seedlings for another 2 days, and the RBSDV accumulation was determined by detecting the gene and protein expression of P10 using RT-qPCR and immunofluorescence, respectively.

Immunostaining

The midgut tissue was dissected in chilled 1× PBS under a stereomicroscope and fixed with 4% paraformaldehyde for 1 h. Then, the midguts were permeabilized with 2% Triton X-100 for 30 min and blocked with 3% BSA for 2 h. The primary antibody (anti-RBSDV P10 mouse mAb conjugated with FITC) was incubated with the midguts at 4°C overnight. Then, the midguts were incubated with TRITC phalloidin (Solarbio, China) for 10 min. An LSM 710 (ZEISS, Germany) was used to view the confocal imaging.

Statistical Analysis

SPSS 20.0 (IBM Corporation, United States) was used to perform the statistical analysis. One-way analysis of variance (ANOVA) with least significant difference (LSD) test was used in comparing the gene expression levels. The p-value < 0.05 and p-value < 0.01 were regarded as significant and very significant differences, respectively.

RESULTS

Profiling of CircRNAs in *L. striatellus* Midguts in Response to RBSDV Infection

Six libraries were constructed from RBSDV-free (VF) and RBSDV-infected (RB) *L. striatellus* midguts and analyzed by RNA-Seq. The sequence was deposited in the National Center for Biotechnology Information (NCBI) with accession number GSE153102. A total of 2,523 circRNAs were identified (**Supplementary Table S2**). In this study, the length of circRNAs ranged from 116 to 121,200 bp and 86.76% of circRNAs were greater than 1,000 bp (**Supplementary Figure S1A**). Source statistics showed that about 98% of the circRNAs were exonic circRNAs, and about 2% of the circRNAs were from introns (**Supplementary Figure S1B**). Due to the limitations of CIRCExplorer software analysis, none circRNAs were identified from intergenic exons and introns.

Analysis of Differentially Expressed CircRNAs

Thirteen circRNAs were differentially expressed in response to RBSDV infection in *L. striatellus* midguts, including eight up-regulated and five down-regulated circRNAs (**Supplementary Table S3**). Heat maps were generated to illustrate the expression patterns of the 13 differentially expressed circRNAs (**Figure 1**). We randomly selected three up-regulated (circRNA378, circRNA2029, and circRNA2030) and two down-regulated circRNAs (circRNA1026 and circRNA1117) to verify the

[1]http://www.bioinformatics.babraham.ac.uk/projects/fastqc/

[2]http://www.geneontology.org/

[3]http://www.kegg.jp

[4]http://www.microrna.org/microrna/home.do

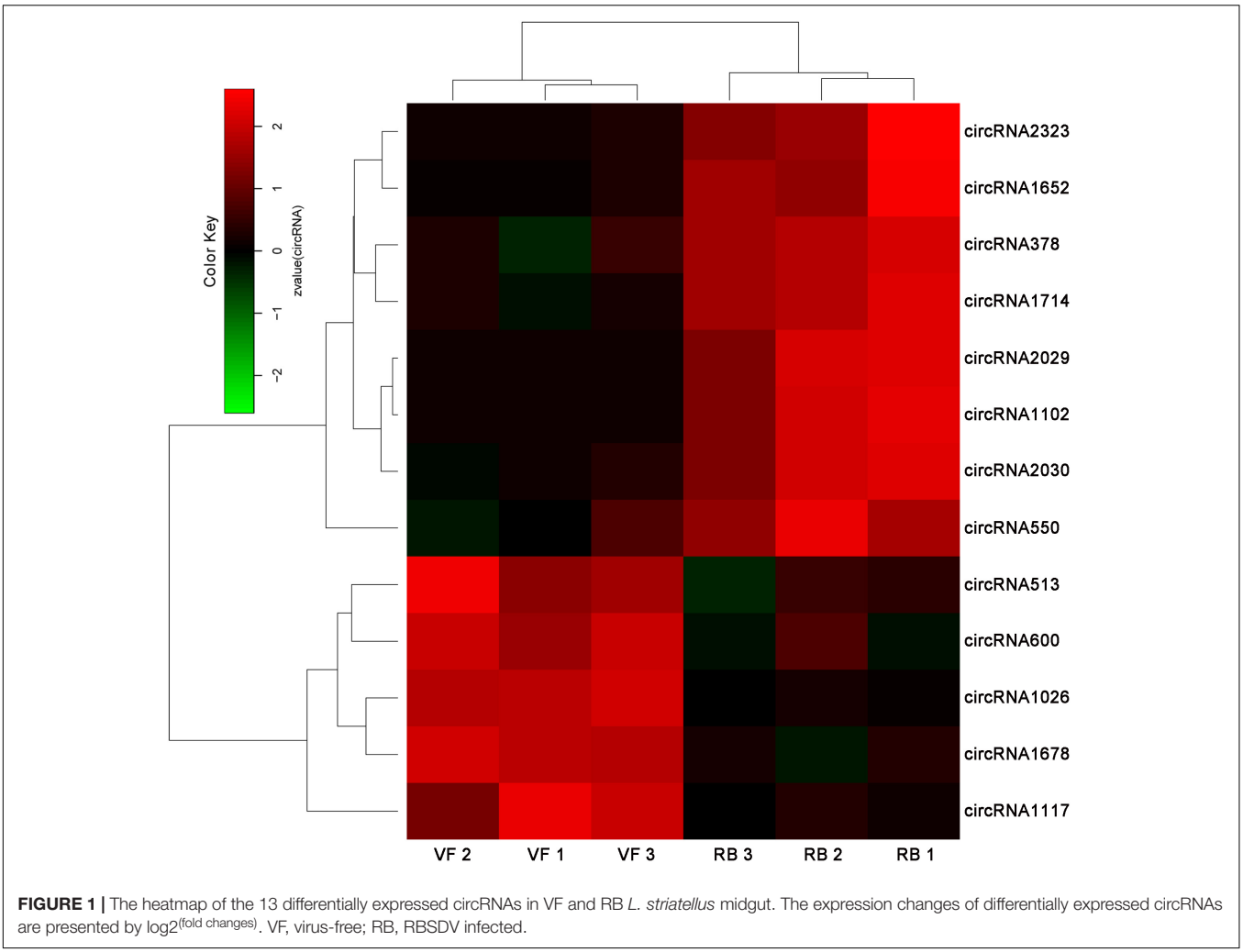

FIGURE 1 | The heatmap of the 13 differentially expressed circRNAs in VF and RB *L. striatellus* midgut. The expression changes of differentially expressed circRNAs are presented by $\log2^{(\text{fold changes})}$. VF, virus-free; RB, RBSDV infected.

circRNA expression by RT-qPCR. The expression levels of circRNA378, circRNA2029, and circRNA2030 were confirmed to be up-regulated and the expression level of circRNA1117 was down-regulated in *L. striatellus* midgut after RBSDV infection (**Figure 2**). These data were consistent with the transcriptome. However, the expression level of circRNA1026 did not have any changes after RBSDV infection (**Figure 2**).

GO and KEGG Pathway Analysis of Differentially Expressed CircRNAs

It has been reported that the function of circRNAs can be suggested through characterizing the features of parental linear mRNAs (Wei et al., 2017). In this study, 13 differentially expressed circRNAs were predicted from 11 parental genes (**Supplementary Table S4**). To predict the functions of these differentially expressed circRNAs, the GO and KEGG analyses of their parental genes were performed. GO analysis revealed that the biological process was the most significantly different subgroup (**Figure 3A**). SNARE interactions in vesicular transport and caffeine metabolism were shown as the top two most significantly enriched pathways in KEGG analysis (**Figure 3B**).

To clarify whether the parental genes of the differentially expressed circRNAs are also induced in response to RBSDV infection, the expression patterns of eight parental genes were analyzed by RT-qPCR. As shown in **Figure 4**, the expression levels of four parental genes, helicase, syntaxin, phospholipid-transporting ATPase (PTA) and multiple C2 and transmembrane domain-containing protein 1 (MCTP1) were differentially expressed. In contrast, the expression of other parental genes did not change after RBSDV infection.

CircRNAs-MiRNAs Interaction Analysis

CircRNAs can act as miRNA sponges to regulate the post-transcriptional level of miRNA's target genes (Li et al., 2019). In this study, the interactions of differentially expressed circRNAs-miRNAs were analyzed according to the miRanda software. Thirteen differentially expressed circRNAs were predicted to bind 30 miRNAs (**Table 1**). Both circRNA1102 and circRNA2030 were predicted to bind six miRNAs. Four miRNAs, miR-14-3p, miR-9a-3p, miR-92a, and miR-315-5p, were predicted to bind two or more differentially expressed circRNAs. Besides, miR-9a-3p and miR-315-5p were significantly down-regulated, and the

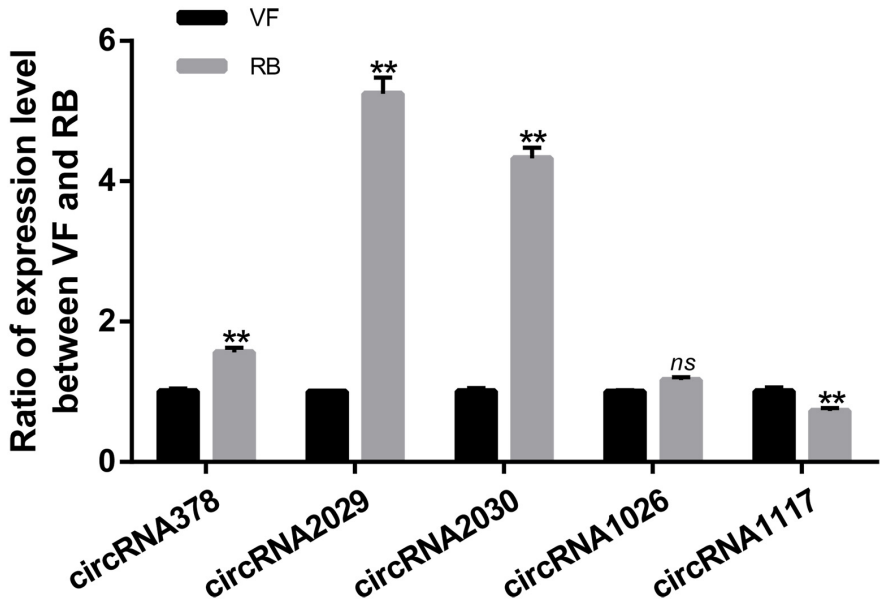

FIGURE 2 | Validation of the expression changes of five differentially expressed circRNAs by RT-qPCR in VF and RB *L. striatellus* midgut. The expressions of five differentially expressed circRNAs were analyzed through $2^{-\Delta\Delta Ct}$ method. The *ns* represents no significant difference, and the asterisks (**) indicate significant differences at $p < 0.01$ levels.

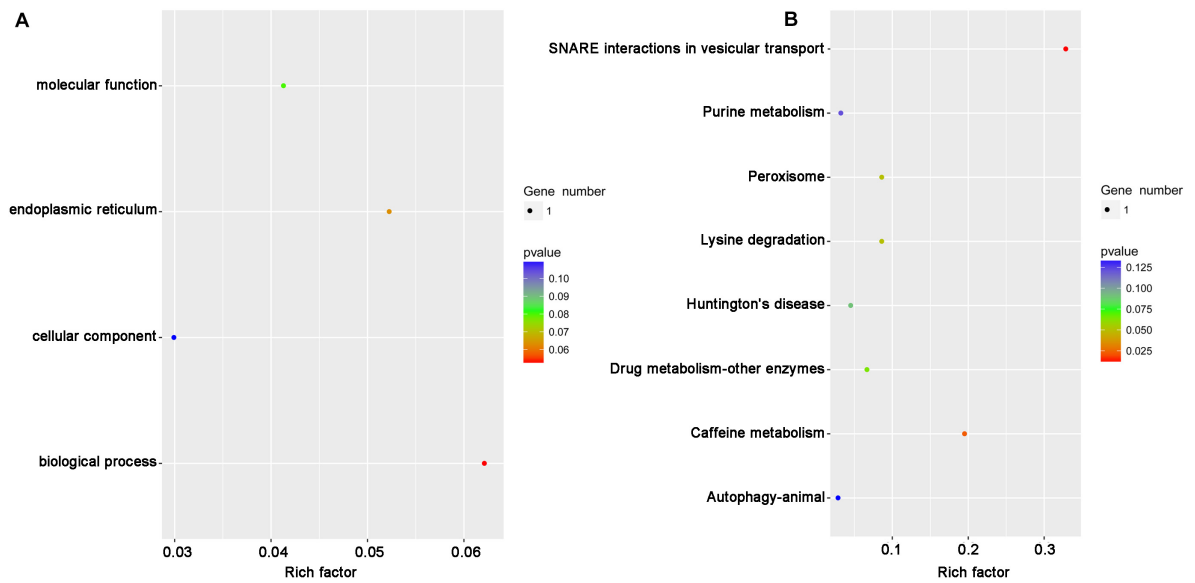

FIGURE 3 | The GO and KEGG pathway analysis of the parental genes of differentially expressed circRNAs. **(A)** The top four GO terms of parental genes were analyzed. **(B)** The top eight enriched pathways for the parental genes were analyzed. GO: gene ontology; KEGG: Kyoto Encyclopedia of Genes and Genomes.

expression levels of miR-14-3p and miR-92a did not change after RBSDV infection (**Figure 5**).

CircRNA2030 Regulated RBSDV Infection in *L. striatellus* Midgut

The expression of circRNA2030 changed more than 4.0-fold after RBSDV infection. It was predicted to bind six miRNAs. We further studied its functions in RBSDV infection of *L. striatellus* midgut. The expression patterns of circRNA2030 were examined in different developmental stages, from 1st-instar to adult and in different tissues, including fat body, midgut, ovary, and salivary gland. The expression of circRNA2030 was observed in all developmental stages and had highest level in the male adult (**Figure 6A**). The tissue expression patterns showed that circRNA2030 was highly expressed in

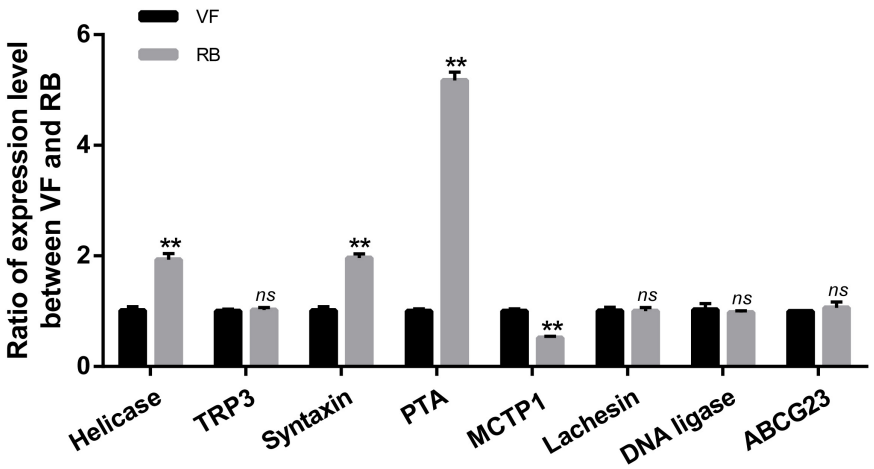

FIGURE 4 | Validation of the expression of eight parental genes by RT-qPCR. The *ns* represents no significant difference, and the asterisks (**) indicate significant differences at $p < 0.01$ levels.

the midgut (**Figure 6B**). The relative expression level of circRNA2030 was significantly decreased three and five days after dsRNA injection (**Supplementary Figure S2**). Knockdown of circRNA2030 significantly increased the expression of RBSDV *S10* in *L. striatellus* midgut, suggesting that inhibition of circRNA2030 promotes RBSDV accumulation (**Figure 7A**). Besides, immunofluorescence analysis also showed that RBSDV accumulation in *L. striatellus* midgut was also increased after knockdown of circRNA2030 (**Figure 7B**). Furthermore, the relative expression levels of RBSDV replication related genes, *S5-1*, *S6,* and *S9-1*, were significantly up-regulated after knockdown of circRNA2030 (**Figure 7C**).

In order to explore whether circRNA2030 regulates RBSDV infection via miRNA or its parental gene, the relationships between circRNA2030 and its related miRNAs (miR-8-3p, miR-184-3p, miR-277-3p, miR-315-5p, miR-277, and miR-932) or its parental gene (PTA) were investigated. In general, if circRNA2030 could act as miRNAs sponges, the expression levels of the adsorbed miRNAs should be up-regulated when circRNA2030 was knocked down. However, none of the six related miRNAs was up-regulated after knockdown of circRNA2030 (**Figure 8**). In the other hand, the expression of PTA was significantly down-regulated after knockdown of circRNA2030 (**Figure 8**). In addition, the relative expression level of PTA was significantly up-regulated after RBSDV infection (**Figure 4**). These results indicated that circRNA2030 may regulate RBSDV infection via regulating the expression of PTA at the mRNA level.

DISCUSSION

With the novel computational methodology and the advent of deep sequencing technology, numerous circRNAs have been identified in eukaryotes, including mice, *Caenorhabditis elegans*, and plants (Memczak et al., 2013; Westholm et al., 2014; Ye et al., 2015; Cortes-Lopez et al., 2018). However, functional studies of circRNAs in insects are still at preliminary stages. Recently, significant progress has been made in the identification of circRNAs in insects, especially in *Drosophila melanogaster* and *B. mori* (Westholm et al., 2014; Gan et al., 2017). It has been reported that circRNAs participate in the responses of viral infection in animal and plant, such as CPV infection in *B. mori* (Hu et al., 2018), and TYLCV infection in tomato (Wang et al., 2018). However, few studies focus on the expression profiles and functions of circRNAs in plant virus–insect vector interactions. Midgut is an important barrier for persistent circulative plant viruses to infect insect vectors (Jia et al., 2018; Qin et al., 2018). Our present research characterizes the comprehensive types and expression patterns of circRNAs in *L. striatellus* midgut during RBSDV infection for the first time. After verifying the sequence quality with FastQC, a total of 2,523 circRNAs were systematically identified in virus-free and RBSDV-infected *L. striatellus* midgut. The total number of the circRNAs identified in our research was similar to other insect species, such as *D. melanogaster* and *B. mori* (Westholm et al., 2014; Gan et al., 2017). The length of 86.76% circRNAs was over 1,000 bp in this study. Although, it is usually reported that the length of circRNA is less than 1,000 bp, there are still many circRNAs longer than 1,000 bp, even longer than 10,000 bp in circBase[5]. Also, 13 differentially expressed circRNAs were obtained after RBSDV infection. Mainly, the identification and quantification of circRNAs were dependent on the reverse splicing reads, resulting in a large intra-group difference in the identified circRNAs. Therefore, the number of differentially expressed circRNAs was quite less in this study. Altogether, these data will be helpful to identify specific circRNAs involved in virus infection in the insect vector.

Understanding the functions of parental linear mRNAs will be helpful to reveal the roles of circRNAs (Wei et al., 2017). The differentially expressed circRNAs identified in our study were predicted from 11 parental genes and were mainly predicted to be involved in SNARE interactions in vesicular transport and

[5]http://www.circbase.org/

TABLE 1 | The miRNAs predicted to bind the differentially expressed circRNAs.

Accession name	Exons	Putative miRNAs	miRanda score	miRanda energy
circRNA2323	4	miR-6497-3p	148.00	−15.32
circRNA378	2	miR-79	170.00	−13.69
		miR-305-5p	156.00	−15.86
		miR-79-3p	170.00	−13.69
		miR-9a-3p	159.00	−14.68
circRNA1714	2	miR-971	145.00	−12.45
		miR-137-5p	149.00	−14.55
		miR-1-3p	157.00	−17.34
		miR-14-3p	142.00	−11.82
		miR-1	157.00	−17.34
circRNA2029	3	miR-124-3p	154.00	−17.65
		miR-315-5p	147.00	−10.32
		miR-965-3p	141.00	−10.52
circRNA1102	4	miR-6497-5p	142.00	−15.44
		miR-92a	147.00	−12.08
		miR-92a-3p	152.00	−13.79
		miR-9a-3p	150.00	−11.67
		miR-92b-3p	152.00	−13.32
		miR-92-3p	156.00	−19.08
circRNA2030	3	miR-8-3p	146.00	−16.39
		miR-184-3p	153.00	−20.27
		miR-277-3p	163.00	−19.18
		miR-315-5p	147.00	−10.32
		miR-277	163.00	−19.18
		miR-932	148.00	−14.93
circRNA513	6	miR-252a-3p	146.00	−24.25
		miR-993a-3p	140.00	−15.24
		miR-14-3p	147.00	−10.80
		miR-34	156.00	−28.51
circRNA600	2	miR-971	158.00	−15.59
		miR-1000	148.00	−15.02
		miR-14-3p	157.00	−15.26
circRNA1026	5	miR-210	154.00	−25.91
		miR-993a-3p	151.00	−14.91
		miR-210-3p	154.00	−25.91
circRNA1678	2	miR-92a	145.00	−13.81
		miR-14-3p	170.00	−21.30
circRNA1117	2	miR-2765	149.00	−16.96

caffeine metabolism by KEGG analysis and biological process by GO analysis. The expression changes of some circRNAs were verified by RT-qPCR, and most of the results were consistent with the sequencing, indicating the accuracy results of RNA-Seq were reliable. Among the parental genes of the circRNAs, helicase, syntaxin, and PTA were significantly up-regulated, and MCTP1 was significantly down-regulated after RBSDV infection. It has been reported that syntaxin is involved in the release of hepatitis C virus (HCV) through mediating vesicles fusion (Ren et al., 2017). These differentially expressed parental genes might be involved in the infection of RBSDV in *L. striatellus* midgut. However, a relationship between circRNAs forms and their parental genes needs to be studied.

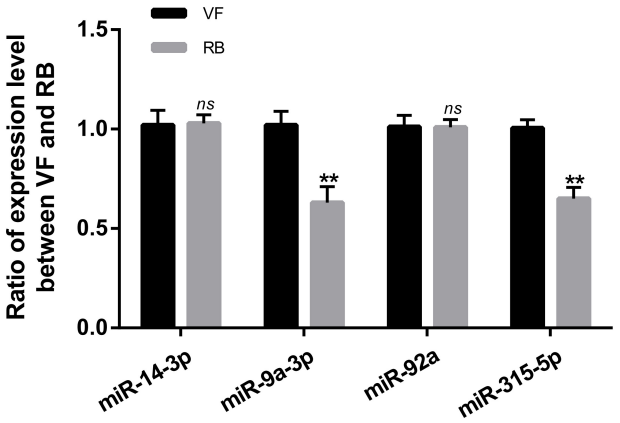

FIGURE 5 | Validation of the expression of four microRNAs by RT-qPCR. The *ns* represents no significant difference, and the asterisks (**) indicate significant differences at $p < 0.01$ levels.

A growing body of research has shown that circRNAs function as miRNA sponges to regulate the post-transcriptional level of gene expression (Li et al., 2019). To further explore the roles of the differentially expressed circRNAs during RBSDV infection, a total of 30 miRNAs were predicted to bind to the circRNAs. A single miRNA was predicted to combine with several circRNAs. For example, miR-14-3p could bind by four differentially expressed circRNAs. It has been reported that miR-14 can regulate various ecdysone-signaling pathway genes to switch off ecdysone production after ecdysis in silkworm (He et al., 2019). However, the expression level of miR-14-3p (measured by RT-qPCR) was not changed after RBSDV infection, indicating that miR-14-3p may not be directly involved in virus infection, but it might affect the development of the insect vector. In addition, we found that the expression levels of miR-9a-3p and miR-315-5p were significantly down-regulated after RBSDV infection. miR-9a is involved in the dengue virus (DENV) infection in mosquitoes (Avila-Bonilla et al., 2017). In shrimp, miR-315 could facilitate the white spot syndrome virus (WSSV) infection by targeting the expression of the gene encoding the prophenoloxidase-activating enzyme to attenuate phenoloxidase activity (Jaree et al., 2018). The results suggest that miR-9a-3p and miR-315-5p may be involved in RBSDV infection, and the mechanism is worth further study. In addition, a network of circRNA-miRNA is presented in *L. striatellus* midgut following RBSDV infection. Altogether, our results provide a new insight into the mechanism of plant virus-insect vector interactions.

CircRNA2030 was significantly expressed after RBSDV infection and bound to six miRNAs. To further study its functions in virus infection, we analyze its expression pattern. It was expressed in all developmental stages and mainly expressed in the midgut of *L. striatellus*, indicating a key biological role of circRNA2030 in the midgut. Knockdown of circRNA2030 caused a significant increase of RBSDV accumulation in *L. striatellus* midgut, indicating that circRNA2030 has antivirus functions in *L. striatellus* under RBSDV infection. To our knowledge, this is the first report that circRNA can regulate plant virus

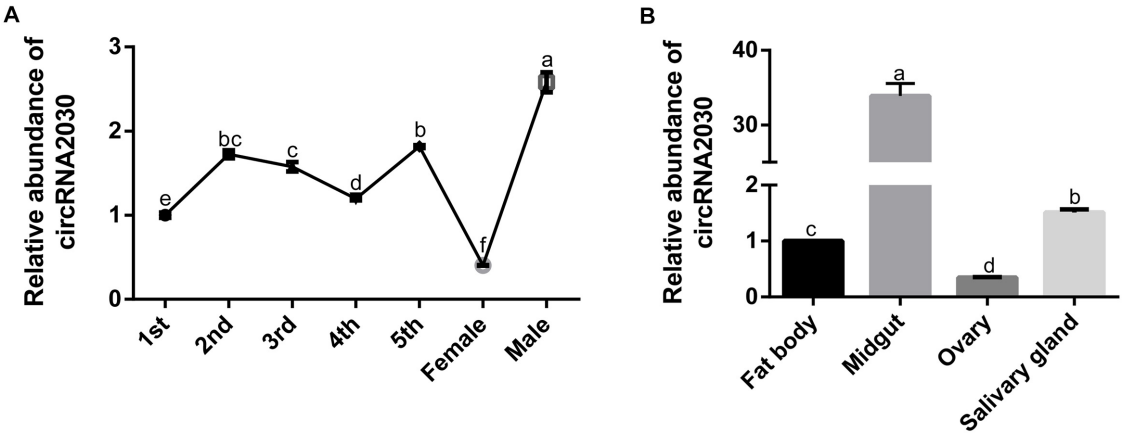

FIGURE 6 | The expressions of circRNA2030 in different developmental stages and different tissues of *L. striatellus*. **(A)** CircRNA2030 was expressed in all developmental stages and had the highest level in the male adult. **(B)** CircRNA2030 was highly expressed in the midgut. The letters a, b, c and d present significant differences ($p < 0.05$) of the expression level of circRNA2030 at different developmental stages and in different tissues.

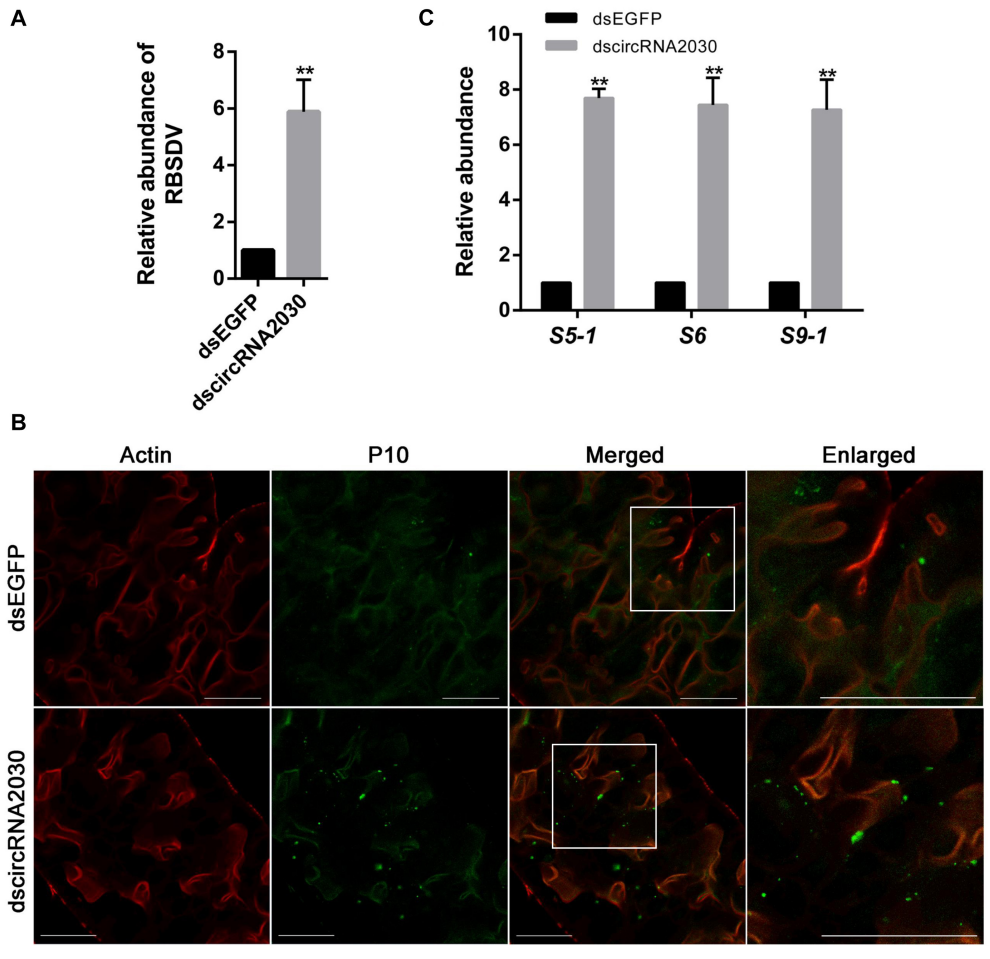

FIGURE 7 | Knockdown of circRNA2030 increased RBSDV accumulation in *L. striatellus* midgut. **(A)** RT-qPCR analyzed the expression of RBSDV *S10* after knockdown of circRNA2030 in *L. striatellus* midgut. The expression level of *S10* was used as an indicator of relative abundance of RBSDV. **(B)** Immunofluorescence analysis showed that the relative abundance of RBSDV, labeling by antibody against P10 protein and presenting as green dots, was significantly increased after knockdown of circRNA2030. **(C)** The relative expression levels of *S5-1*, *S6,* and *S9-1* genes were significantly increased after knockdown of circRNA2030. The asterisks (**) indicate significant differences at $p < 0.01$ levels. Scale bars, 50 μm.

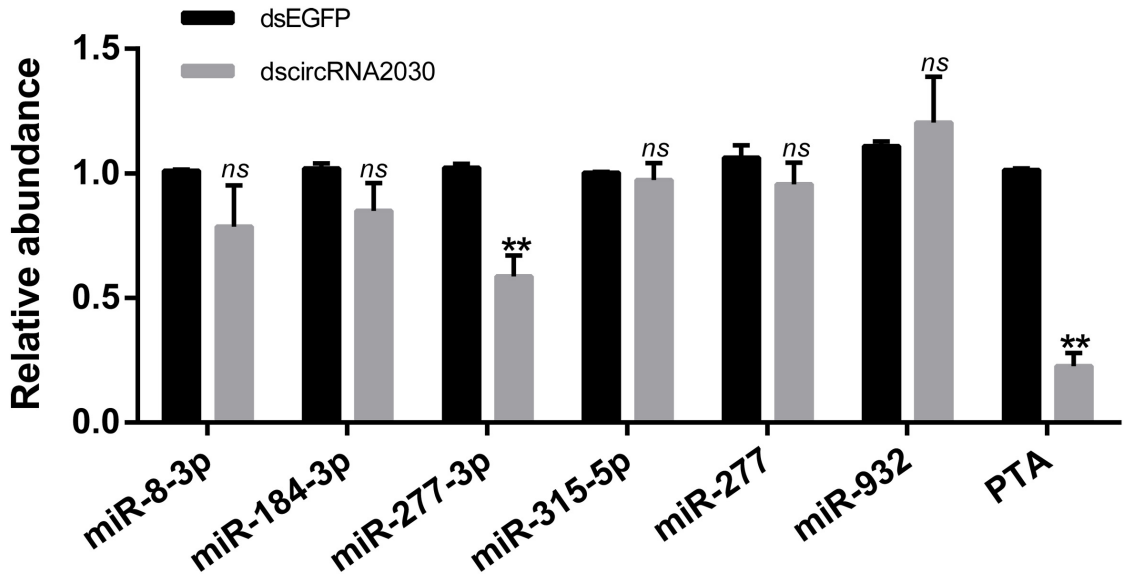

FIGURE 8 | Validation the relationships among the circRNA2030 and its related miRNAs (miR-8-3p, miR-184-3p, miR-277-3p, miR-315-5p, miR-277, and miR-932) and parental gene (PTA) by RT-qPCR. The *ns* represents no significant difference, and the asterisks (**) indicate significant differences at $p < 0.01$ levels.

infection in an insect vector. To explore the possible molecular mechanism of circRNA2030 regulating RBSDV infection, the relationships among the circRNA2030 and its related miRNAs and parental gene were investigated. The results indicated that the possible molecular mechanism of circRNA2030 regulating RBSDV infection might be via regulating the expression of PTA at the mRNA level.

CONCLUSION

The expression profile and the differentially expressed circRNAs were identified in *L. striatellus* midgut after RBSDV infection, and the function of circRNA2030 in RBSDV infection was analyzed. These results suggest that circRNAs play pivotal roles for virus infection through the insect vector.

DATA AVAILABILITY STATEMENT

The datasets presented in this study can be found in online repositories. The names of the repository/repositories and accession number(s) can be found in the article/ **Supplementary Material**.

AUTHOR CONTRIBUTIONS

JZ and QX conceived and designed the experiments. JZ, HW, WW, YD, and MW performed the experiments. JZ, HW, DY, and QX analyzed the data. JZ, HW, YZ, and QX wrote the manuscript. All authors contributed to the article and approved the submitted version.

FUNDING

This work was supported by the National Key Research and Development Program of China (2016YFD0300706/ 2016YFD0300700), the National Natural Science Foundation of China (31872639), the China Postdoctoral Science Foundation (2019M661772), the Natural Science Foundation of Jiangsu Province (BK20190268), and the Jiangsu Postdoctoral Research Foundation (2019K266).

ACKNOWLEDGMENTS

The RBSDV P10 antibody was kindly provided by Prof. Jianxiang Wu (Zhejiang University, Hangzhou, China). We would like to thank Prof. Kai Xu (College of Life Sciences, Nanjing Normal University) for revising the manuscript. We would also like to thank Dr. Paul Daly (Institute of Plant Protection, Jiangsu Academy of Agricultural Sciences) for editing and revising the English language.

SUPPLEMENTARY MATERIAL

The Supplementary Material for this article can be found online at: https://www.frontiersin.org/articles/10.3389/fmicb.2020.588009/full#supplementary-material

Supplementary Figure 1 | The length and source statistics of the 2,523 circRNAs identified from VF and RB *L. striatellus* midgut. **(A)** Length distribution of circRNAs. **(B)** Source statistics of circRNAs.

Supplementary Figure 2 | Analysis of the expression level of circRNA2030 after dsRNA injection by RT-qPCR. The *ns* represents no significant difference, and the asterisks (**) indicate significant differences at $p < 0.01$ levels.

REFERENCES

Avila-Bonilla, R. G., Yocupicio-Monroy, M., Marchat, L. A., De Nova-Ocampo, M. A., del Angel, R. M., and Salas-Benito, J. S. (2017). Analysis of the miRNA profile in C6/36 cells persistently infected with dengue virus type 2. *Virus Res.* 232, 139–151. doi: 10.1016/j.virusres.2017.03.005

Chen, J. N., Wang, H. W., Jin, L., Wang, L. Y., Huang, X., Chen, W. W., et al. (2019). Profile analysis of circRNAs induced by porcine endemic diarrhea virus infection in porcine intestinal epithelial cells. *Virology* 527, 169–179. doi: 10.1016/j.virol.2018.11.014

Chen, L. (1964). Preliminary investigation of rice black-streaked dwarf disease in Yuyao county. *Zhejiang Nongye Kexue* 3, 123–127.

Cortes-Lopez, M., Gruner, M. R., Cooper, D. A., Gruner, H. N., Voda, A. I., Van der Linden, A. M., et al. (2018). Global accumulation of circRNAs during aging in *Caenorhabditis elegans*. *BMC Genomics* 19:8. doi: 10.1186/s12864-017-4386-y

Dader, B., Then, C., Berthelot, E., Ducousso, M., Ng, J. C. K., and Drucker, M. (2017). Insect transmission of plant viruses: multilayered interactions optimize viral propagation. *Insect Sci.* 24, 929–946. doi: 10.1111/1744-7917.12470

Gan, H., Feng, T., Wu, Y., Liu, C., Xia, Q., and Cheng, T. (2017). Identification of circular RNA in the *Bombyx mori* silk gland. *Insect Biochem. Mol. Biol.* 89, 97–100. doi: 10.1016/j.ibmb.2017.09.003

Gao, Y., Wang, J., and Zhao, F. (2015). CIRI: an efficient and unbiased algorithm for de novo circular RNA identification. *Genome Biol.* 16:4. doi: 10.1186/s13059-014-0571-3

He, K., Xiao, H., Sun, Y., Situ, G., Xi, Y., and Li, F. (2019). microRNA-14 as an efficient suppressor to switch off ecdysone production after ecdysis in insects. *RNA Biol.* 16, 1313–1325. doi: 10.1080/15476286.2019.1629768

He, L., Chen, X., Yang, J., Zhang, T. Y., Li, J., Zhang, S. B., et al. (2020). Rice black-streaked dwarf virus-encoded P5-1 regulates the ubiquitination activity of SCF E3 ligases and inhibits jasmonate signaling to benefit its infection in rice. *New Phytol.* 225, 896–912. doi: 10.1111/nph.16066

Hogenhout, S. A., Ammar, E. D., Whitfield, A. E., and Redinbaugh, M. G. (2008). Insect vector interactions with persistently transmitted viruses. *Annu. Rev. Phytopathol.* 46, 327–359. doi: 10.1146/annurev.phyto.022508.092135

Hu, X., Zhu, M., Zhang, X., Liu, B., Liang, Z., Huang, L., et al. (2018). Identification and characterization of circular RNAs in the silkworm midgut following *Bombyx mori* cytoplasmic polyhedrosis virus infection. *RNA Biol.* 15, 292–301. doi: 10.1080/15476286.2017.1411461

Huttenhofer, A., Schattner, P., and Polacek, N. (2005). Non-coding RNAs: hope or hype? *Trends Genet.* 21, 289–297. doi: 10.1016/j.tig.2005.03.007

Jaree, P., Wongdontri, C., and Somboonwiwat, K. (2018). White spot syndrome virus-induced shrimp miR-315 attenuates prophenoloxidase activation via PPAE3 gene suppression. *Front. Immunol.* 9:2184. doi: 10.3389/fimmu.2018.02184

Jia, D. S., Chen, Q., Mao, Q. Z., Zhang, X. F., Wu, W., Chen, H. Y., et al. (2018). Vector mediated transmission of persistently transmitted plant viruses. *Curr. Opin. Virol.* 28, 127–132. doi: 10.1016/j.coviro.2017.12.004

Jia, D. S., Ma, Y. Y., Du, X., Chen, H. Y., Xie, L. H., and Wei, T. Y. (2014). Infection and spread of Rice black-streaked dwarf virus in the digestive system of its insect vector small brown planthopper. *Acta Phytopathol. Sin.* 44, 188–194.

Kanehisa, M., Araki, M., Goto, S., Hattori, M., Hirakawa, M., Itoh, M., et al. (2008). KEGG for linking genomes to life and the environment. *Nucleic Acids Res.* 36, 480–484. doi: 10.1093/nar/gkm882

Kim, D., Pertea, G., Trapnell, C., Pimentel, H., Kelley, R., and Salzberg, S. L. (2013). TopHat2: accurate alignment of transcriptomes in the presence of insertions, deletions and gene fusions. *Genome Biol.* 14:R36. doi: 10.1186/gb-2013-14-4-r36

Kim, D., and Salzberg, S. L. (2011). TopHat-Fusion: an algorithm for discovery of novel fusion transcripts. *Genome Biol.* 12:R72. doi: 10.1186/gb-2011-12-8-r72

Kuribayashi, K., and Shinkai, A. (1952). On the new disease of rice, black-streaked dwarf. *Ann. Phytopathol. Soc. Jpn.* 16:41.

Langmead, B., and Salzberg, S. L. (2012). Fast gapped-read alignment with Bowtie 2. *Nat. Methods* 9, 354–357. doi: 10.1038/nmeth.1923

Lasda, E., and Parker, R. (2014). Circular RNAs: diversity of form and function. *RNA* 20, 1829–1842. doi: 10.1261/rna.047126.114

Lauressergues, D., Couzigou, J. M., Clemente, H. S., Martinez, Y., Dunand, C., Becard, G., et al. (2015). Primary transcripts of microRNAs encode regulatory peptides. *Nature* 520, 190–205. doi: 10.1038/nature14346

Li, J., Xue, J., Zhang, H. M., Yang, J., Lv, M. F., Xie, L., et al. (2013). Interactions between the P6 and P5-1 proteins of southern rice black-streaked dwarf fijivirus in yeast and plant cells. *Arch. Virol.* 158, 1649–1659. doi: 10.1007/s00705-013-1660-4

Li, M. Z., Xiao, H. M., He, K., and Li, F. (2019). Progress and prospects of noncoding RNAs in insects. *J. Integrat. Agricul.* 18, 729–747.

Liu, Y., Khine, M. O., Zhang, P., Fu, Y., and Wang, X. (2020). Incidence and distribution of insect-transmitted cereal viruses in wheat in China from 2007 to 2019. *Plant Dis.* 104, 1407–1414. doi: 10.1094/PDIS-11-19-2323-RE

Lu, L. N., Wang, Q., Huang, D. Q., Xu, Q. F., Zhou, X. P., and Wu, J. X. (2019). Rice black-streaked dwarf virus p10 suppresses protein kinase c in insect vector through changing the subcellular localization of LsRACK1. *Philos. Trans. R. Soc. Lond. B Biol. Sci.* 374:20180315. doi: 10.1098/rstb.2018.0315

Memczak, S., Jens, M., Elefsinioti, A., Torti, F., Krueger, J., and Rybak, A. (2013). Circular RNAs are a large class of animal RNAs with regulatory potency. *Nature* 495, 333–338. doi: 10.1038/nature11928

Milne, R. G., Conti, M., and Lisa, V. (1973). Partial purification, structure and infectivity of complete maize rough dwarf virus particles. *Virology* 53, 130–141. doi: 10.1016/0042-6822(73)90472-8

Qin, F. L., Liu, W. W., Wu, N., Zhang, L., Zhang, Z. K., Zhou, X. P., et al. (2018). Invasion of midgut epithelial cells by a persistently transmitted virus is mediated by sugar transporter 6 in its insect vector. *PLoS Pathog.* 14:21. doi: 10.1371/journal.ppat.1007201

Ren, H., Elgner, F., Himmelsbach, K., Akhras, S., Jiang, B., Medvedev, R., et al. (2017). Identification of syntaxin 4 as an essential factor for the hepatitis c virus life cycle. *Eur. J. Cell Biol.* 96, 542–552. doi: 10.1016/j.ejcb.2017.06.002

Ren, Y. D., Lu, C. T., and Wang, X. F. (2016). Reason analysis about outbreak epidemics of rice black streaked dwarf disease: an example in Kaifeng. Henan Province. *Plant Prot.* 42, 8–16. doi: 10.3969/j.issn.0529-1542.2016.03.002

Robinson, M. D., Mccarthy, D. J., and Smyth, G. K. (2010). EDGER: a bioconductor package for differential expression analysis of digital gene expression data. *Bioinformatics* 26, 139–140. doi: 10.1093/bioinformatics/btp616

Salzman, J. (2016). Circular RNA expression: its potential regulation and function. *Trends Genet.* 32, 309–316. doi: 10.1016/j.tig.2016.03.002

Sun, L. Y., Xie, L., Andika, I. B., Tan, Z. L., and Chen, J. P. (2013). Non-structural protein P6 encoded by Rice black-streaked dwarf virus is recruited to viral inclusion bodies by binding to the viroplasm matrix protein P9-1. *J. Gen. Virol.* 94, 1908–1916. doi: 10.1099/vir.0.051698-0

Sun, Y. Y., Zhang, H. Q., Fan, M., He, Y., and Guo, P. (2020). Genome-wide identification of long non-coding RNAs and circular RNAs reveal their ceRNA networks in response to cucumber green mottle mosaic virus infection in watermelon. *Arch. Virol.* 165, 1177–1190. doi: 10.1007/s00705-020-04589-4

Wang, J. Y., Yang, Y. W., Jin, L. M., Ling, X. T., Liu, T., Chen, T. Z., et al. (2018). Re-analysis of long non-coding RNAs and prediction of circRNAs reveal their novel roles in susceptible tomato following TYLCV infection. *BMC Plant Biol.* 18:104. doi: 10.1186/s12870-018-1332-3

Wei, X., Li, H., Yang, J., Hao, D., Dong, D., Huang, Y., et al. (2017). Circular RNA profiling reveals an abundant circLMO7 that regulates myoblasts differentiation and survival by sponging miR-378a-3p. *Cell Death Dis.* 8:e3153. doi: 10.1038/cddis.2017.541

Westholm, J. O., Miura, P., Olson, S., Shenker, S., Joseph, B., Sanfilippo, P., et al. (2014). Genome-wide analysis of *Drosophila* circular RNAs reveals their structural and sequence properties and age-dependent neural accumulation. *Cell Rep.* 9, 1966–1980. doi: 10.1016/j.celrep.2014.10.062

Wu, N., Zhang, L., Ren, Y. D., and Wang, X. F. (2020). Rice black-streaked dwarf virus: from multiparty interactions among plant–virus–vector to intermittent epidemics. *Mol. Plant Pathol.* 21, 1007–1019. doi: 10.1111/mpp.12946

Wu, W., Liu, H. Q., Dong, Y., Zhang, Y., Wong, S. M., Wang, C. C., et al. (2019a). Determination of suitable RT-qPCR reference genes for studies of gene functions in Laodelphax striatellus (Fallén). *Genes* 10, 887–900. doi: 10.3390/genes10110887

Wu, W., Zhai, M., Li, C., Yu, X., Song, X., Gao, S., et al. (2019b). Multiple functions of miR-8-3p in the development and metamorphosis of the red flour beetle. *Tribolium castaneum*. *Insect Mol. Biol.* 28, 208–221. doi: 10.1111/imb.12539

Xu, H. X., He, X. C., Zheng, X. S., Yang, Y. J., and Lu, Z. X. (2014). Influence of Rice black streaked dwarf virus on the ecological fitness of non-vector planthopper *Nilaparvata lugens* (*Hemiptera*: *Delphacidae*). *Insect Sci.* 21, 507–514. doi: 10.1111/1744-7917.12045

Ye, C. Y., Chen, L., Liu, C., Qian, H. Z., and Fan, L. (2015). Widespread noncoding circular RNAs in plants. *New Phytol.* 208, 88–95. doi: 10.1111/nph.13585

Young, M. D., Wakefield, M. J., Smyth, G. K., and Oshlack, A. (2010). Gene ontology analysis for RNA-seq: accounting for selection bias. *Genome Biol.* 11:R14. doi: 10.1186/gb-2010-11-2-r14

Zhang, H. H., Tan, X. X., He, Y. Q., Xie, K. L., Li, L. L., Wang, R., et al. (2019). Rice black-streaked dwarf virus P10 acts as either a synergistic or antagonistic determinant during superinfection with related or unrelated virus. *Mol. Plant Pathol.* 20, 641–655. doi: 10.1111/mpp.12782

Zhang, H. M., Chen, J. P., and Adams, M. J. (2001a). Molecular characterisation of segments 1 to 6 of Rice black-streaked dwarf virus from China provides the complete genome. *Arch. Virol.* 146, 2331–2339. doi: 10.1007/s007050170006

Zhang, H. M., Chen, J. P., Lei, J. L., and Adams, M. J. (2001b). Sequence analysis shows that a dwarfing disease on rice, wheat and maize in China is caused by rice black-streaked dwarf virus. *Eur. J. Plant Pathol.* 107, 563–567. doi: 10.1023/A:1011204010663

Zhang, X. O., Dong, R., Zhang, Y., Zhang, J. L., Luo, Z., Zhang, J., et al. (2016). Diverse alternative back-splicing and alternative splicing landscape of circular RNAs. *Genome Res.* 26, 1277–1287. doi: 10.1101/gr.202895.115

Zhang, X. O., Wang, H. B., Zhang, Y., Lu, X. H., Chen, L. L., and Yang, L. (2014). Complementary sequence-mediated exon circularization. *Cell* 159, 134–147. doi: 10.1016/j.cell.2014.09.001

Conflict of Interest: The authors declare that the research was conducted in the absence of any commercial or financial relationships that could be construed as a potential conflict of interest.

frontiers in Microbiology

REVIEW
published: 16 October 2020
doi: 10.3389/fmicb.2020.578064

Illuminating an Ecological Blackbox: Using High Throughput Sequencing to Characterize the Plant Virome Across Scales

François Maclot[1], Thierry Candresse[2], Denis Filloux[3,4], Carolyn M. Malmstrom[5], Philippe Roumagnac[3,4], René van der Vlugt[6] and Sébastien Massart[1]**

[1] Plant Pathology Laboratory, Terra-Gembloux Agro-Bio Tech, Liège University, Gembloux, Belgium, [2] Univ. Bordeaux, INRAE, UMR BFP, Villenave d'Ornon, France, [3] CIRAD, BGPI, Montpellier, France, [4] BGPI, INRAE, CIRAD, Institut Agro, Montpellier University, Montpellier, France, [5] Department of Plant Biology and Graduate Program in Ecology, Evolution and Behavior, Michigan State University, East Lansing, MI, United States, [6] Laboratory of Virology, Wageningen University and Research Centre (WUR-PRI), Wageningen, Netherlands

OPEN ACCESS

Edited by:
Xifeng Wang,
Institute of Plant Protection (CAAS), China

Reviewed by:
Mengji Cao,
Southwest University, China
Valerian V. Dolja,
Oregon State University, United States
Ulrich Karl Melcher,
Oklahoma State University, United States

***Correspondence:**
François Maclot
francois.maclot@uliege.be
Sébastien Massart
sebastien.massart@uliege.be

Specialty section:
This article was submitted to Microbe and Virus Interactions with Plants, a section of the journal Frontiers in Microbiology

Received: *30 June 2020*
Accepted: *24 September 2020*
Published: *16 October 2020*

Citation:
Maclot F, Candresse T, Filloux D, Malmstrom CM, Roumagnac P, van der Vlugt R and Massart S (2020) Illuminating an Ecological Blackbox: Using High Throughput Sequencing to Characterize the Plant Virome Across Scales. Front. Microbiol. 11:578064. doi: 10.3389/fmicb.2020.578064

The ecology of plant viruses began to be explored at the end of the 19th century. Since then, major advances have revealed mechanisms of virus-host-vector interactions in various environments. These advances have been accelerated by new technlogies for virus detection and characterization, most recently including high throughput sequencing (HTS). HTS allows investigators, for the first time, to characterize all or nearly all viruses in a sample without *a priori* information about which viruses might be present. This powerful approach has spurred new investigation of the viral metagenome (virome). The rich virome datasets accumulated illuminate important ecological phenomena such as virus spread among host reservoirs (wild and domestic), effects of ecosystem simplification caused by human activities (and agriculture) on the biodiversity and the emergence of new viruses in crops. To be effective, however, HTS-based virome studies must successfully navigate challenges and pitfalls at each procedural step, from plant sampling to library preparation and bioinformatic analyses. This review summarizes major advances in plant virus ecology associated with technological developments, and then presents important considerations and best practices for HTS use in virome studies.

Keywords: virus ecology and evolution, plant virome, high throughput sequencing, historical advances, opportunities and challenges

INTRODUCTION

The field of plant virus ecology examines complex interactions among plant-associated viruses, their hosts and their vectors, and the environment, effectively extending the perspective of plant virus epidemiology (Jones, 2014). Traditionally, virus epidemiology investigates diseases and factors influencing their spread and population dynamics, whereas virus ecology extends the focus to include understanding patterns of virus distribution and dynamics within a given environment, their effects on community and ecosystem properties, and the reciprocal effects of the environment on virus dynamics and evolution (Gibbs, 1983; Hull, 2014; Lefeuvre et al., 2019).

As a field, plant virus ecology draws on diverse disciplines including virology, ecology, epidemiology, plant biology and entomology (Matthews and Hull, 2002). The study of viruses requires highly specialized methods and tools, which explains why at first ecologists focused their efforts on more readily observable organisms and why the history of plant virus ecology has largely been driven by technological developments (see **Figure 1**). Plant virus ecology has also been marked by the gradual divergence of virology and ecology during the 20th century, caused by the development of molecular methods from the 1970s onward, which oriented virology toward virus molecular biology and the study of viral infection in controlled conditions, away from ecological considerations (Malmstrom et al., 2011). This gap between the fields of ecology – mainly focused on wild and less managed ecosystems – and virology, centered on model or domesticated hosts, began to be bridged in the early 21st century by the use of new genomic tools and molecular approaches in ecological studies (Malmstrom et al., 2011). Most of these new tools involve High-Throughput Sequencing (HTS) technologies, also called Next Generation Sequencing (NGS). Taken together, these developments have spurred the emergence of plant virus metagenome studies. The metagenome, or "virome" when referencing viruses, corresponds to the collective genome of a microbial community within a given individual or a defined environment (Roossinck, 2012). Studying the plant virome in natural communities is currently strongly advancing knowledge of viral diversity, identifying new viral variants or species that might emerge in the future as significant pathogens, and identifying new hosts of known viruses (Roossinck et al., 2015; Massart et al., 2017). Going forward, a better understanding is needed for many aspects of virus ecology: reservoirs, exchange among hosts in various landscapes, lifestyles of plant viruses, contribution of viruses to the functioning of plant populations and communities, the impact of agricultural practices on viral populations, etc.

We describe here the evolution of the techniques used in plant virus ecology and their respective impact in this field, emphasizing new high-throughput sequencing-based approaches. Several reviews have already been published on virus ecology and HTS (Roossinck, 2012; Roossinck et al., 2015; Stobbe and Roossinck, 2014) but as of yet none has detailed the opportunities and the technical challenges of applying HTS technologies with a plant virus ecology perspective. The chronology of the major advances in plant virus ecology, as well as the technological developments supporting them, is represented in the historical timeline of **Figure 1**.

EARLY STAGES OF PLANT VIROLOGY AND OF PLANT VIRUS ECOLOGY

The first plant virus infection phenotypes were likely recorded more than 1,200 years ago in *Eupatorium* plants in Japan in AD 752, as highlighted by Saunders et al. (2003). But the early stages of plant virology were marked by the description of the first plant virus, tobacco mosaic virus (TMV), by concomitant studies of Mayer (1886), Beijerinck (1899), and Ivanovskij (1899) at the end of the 19th century, using the observation of symptoms on tobacco plants.

Since the discovery of TMV, scientists have sought to study the interactions between plants and viruses, but also to decipher how viruses are transmitted between plants. Hence, the first half of the 20th century saw the building of the foundations for plant virus ecology, thanks to the use of host symptomatology, sap transmission, indicator plants, biochemistry and microscopy (reviewed in Harrison, 2009). The first explorations of plant-virus interactions involved cultivated plants and led to important insights, such as the existence of asymptomatic infections (Nishimura, 1918) or of multiple infections (Dickson, 1925). In the 1930s plant virologists began to show interest in wild communities. Brief surveys on wild plants, carried out in Germany in 1932–33 and in England in 1948–49, revealed high rates of viral infections in weeds, and a longer-term study was implemented between 1951 and 1954 in order to determine the frequency and distribution of plant viruses in their natural environment (MacClement and Richards, 1956). Virus flow between wild and cultivated reservoirs was demonstrated (Storey and McClean, 1930), as well as asymptomatic viral infections in many wild plants (Bennett, 1944).

In parallel, virologists examined interactions between viruses and their vectors, illustrated by the discovery of the first insect vector of plant viruses in 1901 (Takami, 1901). The importance of insects in virus transmission brought the concept of the "ecological trinity" between viruses, their hosts and their vectors, as coined by Carter (1939). The relationships between insect-borne viruses and their vectors led to the notions of "persistence" or "non-persistence" according to the period over which the vector can transmit the virus following its acquisition (Carter, 1939). Other virus vectors were identified, such as fungi [*Olpidium* spp. for lettuce big vein virus, (Campbell, 1962)] and nematodes [*Xiphinema* spp. for grapevine fanleaf virus, (Hewitt et al., 1958)]. Interactions between viruses themselves were also examined, leading to the discovery of synergisms (Vanterpool, 1926; Bennett, 1944) and antagonisms between virus strains or species (Bawden and Kassanis, 1941, 1945). Finally, early stages of plant-virus-vectors interactions were illustrated in 1951 with the demonstration that a virus can manipulate its host plant and vector, through a differential effect on aphids feeding on healthy or infected plants (Kennedy, 1951).

THE DEVELOPMENT OF MOLECULAR TOOLS

The rise of serological and molecular detection tools was a golden era for the discovery of the vectors of plant viruses. Indeed, plant viruses were found to be transmitted by a wide range of agents, especially sap-sucking insects (e.g., aphids, thrips, whiteflies, leafhoppers), but also by beetles, mites, nematodes, fungi, and protists. It was also revealed that plant viruses can be vertically transmitted *via* infected pollen or seeds (reviewed by Harrison, 1981 and recently in Lefeuvre et al., 2019). Screening of plant viruses in many plants and insects by the Polymerase Chain Reaction (PCR), Enzyme-Linked ImmunoSorbent Assay

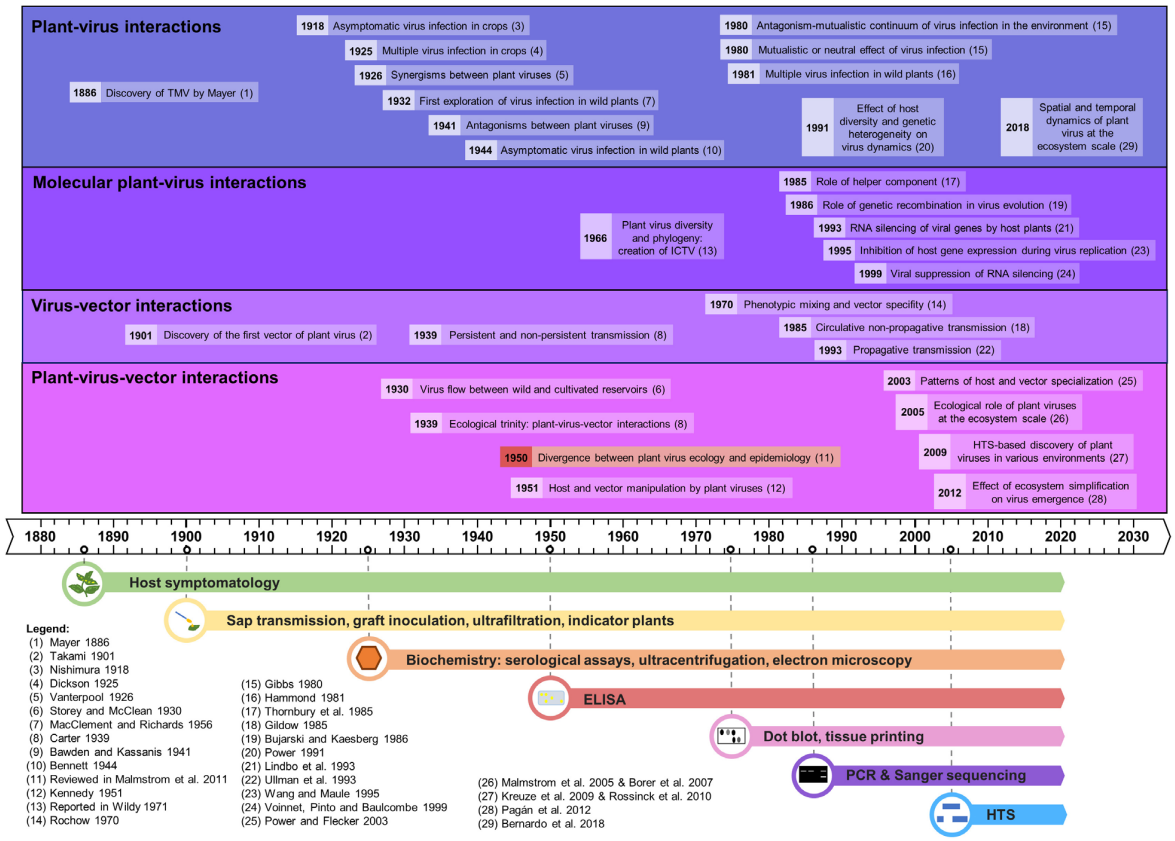

FIGURE 1 | Time line of the major advances in plant virus ecology, linked to the evolution of the detection methods.

(ELISA), and radioactivity (dot blots, tissue printings, etc.) revealed that the host and vector ranges of some plant viruses are remarkably wide (Timian, 1974; Sherwood et al., 2003; Zitter and Murphy, 2009). This variability is also reported for virus transmission, with a great diversity in host ranges for given vectors (Wijkamp, 1995; Wilson, 2014). Despite this diversity of virus biological properties, many plant viruses studied to-date are considered as host generalists and vector specialists, i.e., they have a wide host range but a narrow range of vectors (Power and Flecker, 2003). Advances in deciphering routes of virus transmission were also made, in particular concerning the description of circulative and propagative transmission modes (Gildow, 1985; Ullman et al., 1993), and the concepts of phenotypic mixing or transencapsidation (Rochow, 1970). In parallel, advances in plant-virus interactions were made at the molecular level, with for instance the discovery of the role of helper component (Thornbury et al., 1985), the concept of RNA silencing of viral genes by the host and its viral suppression (Lindbo et al., 1993; Wang and Maule, 1995; Voinnet et al., 1999), or the role of genetic recombination in virus evolution (Bujarski and Kaesberg, 1986).

Major advances in understanding plant-virus co-evolution were obtained too, with the confirmation that virus infections could commonly be found in asymptomatic wild plants (Kelley, 1994; Creamer et al., 1996; Anaya-López et al., 2003). This was extended by the suggestion that some viruses could potentially be beneficial to plants (Gibbs, 1980; Xu et al., 2008). Overall, plant-virus interactions were shown to be complex and to vary along an antagonism-mutualism continuum according to host and virus genotypes combinations and to environmental conditions (Gibbs, 1980, reviewed in Fraile and García-Arenal, 2016). In addition, co-infections with several viruses were frequently found in crops and in wild plants, further increasing the complexity of these interactions (Hammond, 1981; Jooste et al., 2015). Plant viruses were also found to be able to manipulate both their hosts and/or their vectors in order to maximize their transmission in plants (Mauck et al., 2010; Ingwell et al., 2012; Moreno-Delafuente et al., 2013), and reviewed in Mauck (2016).

THE ADVENT OF VIROMICS

Studies of plant-virus interactions at the interface between managed and natural vegetation have been conducted for nearly a century (as reviewed in Alexander et al., 2014) but became more common in the 21st century, facilitated by PCR and new sequencing techniques, most recently HTS. HTS-based metagenomic studies were initially mostly performed to explore plant virus diversity, demonstrating it to be largely underestimated (Roossinck et al., 2015; Wren et al., 2006).

Plant virus-like nucleic acids were further detected in many environments [(Culley et al., 2006; Kreuze et al., 2009) and reviewed in Roossinck, 2012; Roossinck et al., 2015], revealing an intriguing ability to circulate and persist with ecological implications that are not well understood. Viruses detected in metagenomic studies can be classified in four different types: (i) known viruses already described in the surveyed environment; (ii) known viruses not previously described in the surveyed environment; (iii) new virus species/isolates from a known family, and (iv) totally new viruses (Stobbe and Roossinck, 2014). This diversity of known/unknown plant viruses using metagenomic studies was first identified from pooled samples, further probed in analyses of individual barcoded plants [ecogenomics studies (Roossinck et al., 2010)], and then considered in an explicit spatial context [geometagenomic studies (Elena et al., 2014; Roossinck et al., 2015)].

Up to now, most HTS studies have been focused on virus identification and characterization in cultivated plants (Stobbe and Roossinck, 2014). In contrast, metagenomic studies on wild plants have been scarcer (Stobbe and Roossinck, 2014), but have confirmed that virus infections are common in nature (Muthukumar et al., 2009; Claverie et al., 2018, 2019; Susi et al., 2019) and may not cause any recognizable symptoms in wild plants in natural settings. These studies further reveal an abundance of persistent viruses (i.e., viruses that do not move between cells in plants but are transmitted in a strictly vertical manner via gametes) (Roossinck, 2010). The central value of these studies in expanding our understanding of viral diversity has been well-recognized. Indeed, a recent taxonomic position paper recommended the incorporation of viruses identified only from metagenomic data into the official classification scheme of the International Committee on Virus Taxonomy [ICTV, (Simmonds et al., 2017)], in parallel with the development of robust frameworks and safeguards for sequence-based virus taxonomy. Major discoveries in metaviromics and viral phylogenomics have caused conceptual shifts in plant virus evolution and ecology, recognition of the influence of co-divergence, host switching, and horizontal virus transfer (HVT) from invertebrates and fungi, on the origins and diversification of the plant virome (Shi et al., 2016; Zhang et al., 2019; Dolja et al., 2020). These discoveries redefined the RNA virosphere and virus evolution pathways, and enable development of the first comprehensive virus megataxonomy (Koonin et al., 2020).

Metagenomics-based inventories of plant viruses can inform significant current issues in virus ecology, including the emergence of new virus diseases, the impact of climate change or of anthropic pressures on viral populations and on plant-virus-vector interactions, the contribution of plant viruses to the functioning of wild plant populations, rules driving the assembly of viral communities etc. (as reviewed in Jones, 2014). Consequently, molecular and recent HTS-based studies have advanced our understanding of several important phenomena: (i) the reciprocal influences between the dynamics of pathogens and the structure of multispecies host communities (Power and Mitchell, 2004), illustrated with invasions of non-native plants (Malmstrom et al., 2005; Borer et al., 2007); (ii) plant virus spread among host reservoirs (wild and domestic) (Ma et al., 2020); (iii) spill-over and spill-back events (Elena et al., 2014; Roossinck and García-Arenal, 2015); (iv) effects of ecosystem simplification caused by human activities (and especially agriculture) on the biodiversity and the emergence of new viruses in crops (Pagán et al., 2012; Bernardo et al., 2018; Alonso et al., 2019, reviewed in Roossinck and García-Arenal, 2015; McLeish et al., 2019); and finally (v) effects of host diversity and genetic heterogeneity on virus dynamics (Power, 1991).

PLANT VIRUS ECOLOGY AND HTS: OPPORTUNITIES

The ability of HTS technologies to potentially detect, without *a priori* information, all or nearly all viruses within a sample offers a huge opportunity to improve virome characterization and supports the study of virus richness at multiple scales, from individual plants to entire ecosystems. In addition, these technologies also provide new insight about deciphering intra-specific viral diversity, facilitating the characterization of virus variants and better disentangling viral population genetics. In the future, HTS might also be used to quantify the relative proportions of virus species and variants within a sample or environment, thus permitting new analyses of virus prevalence and co-infection dynamics.

HTS technologies have significantly accelerated the discovery of novel viruses and of new wild hosts for known viruses. In many cases, HTS provides a strong advantage for virome characterization over the application of a large number of specific ELISA or (RT-) PCR detection protocols (Boonham et al., 2014; Massart et al., 2014), in particular when taking into account novel viruses. If the aim is to independently characterize the virome of multiple plant species within a community, the number of potentially targetable viruses becomes even greater, making targeted detection approaches more complex if not unrealistic. This fact – and the cost of large targeted efforts – explains in part why virus ecological studies have so far largely focused on a small number of virus species. Thanks to its untargeted and comprehensive approach, HTS has the potential to allow more comprehensive studies of the plant virome at community and landscape scales (Prabha et al., 2013).

Bioinformatic advances leverage the power of HTS technologies and provide further insight about viral genomes. Given sufficient sequencing depth or target availability, contigs assembled from short reads (e.g., from Illumina™ sequencing) or native long-reads (e.g., from Nanopore™) can potentially represent the full or nearly full genome of a virus.

PLANT VIRUS ECOLOGY AND HTS: CHALLENGES

HTS technologies can provide a comprehensive analysis of the viruses and variants present within a sample, and allow their detection, sequence characterization and, potentially in the future, relative quantification. Nevertheless, HTS application in plant virus ecology may be hindered by challenges that limit

the sensitivity and/or specificity of species/variant detection and their relative quantification (see **Figure 2**). Until recently, HTS technologies have been widely used on single plants to discover new viruses or strains or to study viral population genetics within individual plants. A current issue is to ensure smooth and smart transition from sequencing individual plants to large plant populations. The central challenge is that whereas low cost (RT-)PCR and ELISA tests can be carried out on large numbers of individual plants, the high per sample cost of HTS technologies often requires balancing sequencing depth/cost with the number of plants analyzed, for example by the pooling of plant samples. This pooling step has consequences for the interpretation of results. Thus, the transition to work at broader scales raises a series of issues that must be surmounted. Here we consider these issues in more detail.

Selection of Plant Sampling Strategy

Depending on the research aim – which might be the study of a single virus or of holistic virome diversity – there are several possible plant sampling strategies, including one-time and repeated measures. For one-time sampling, the crucial point is to determine the optimal sampling date in relation to the research objectives, perhaps when virus titers are highest (see below), at periods of greatest viral diversity, or after a certain period of virus spread, etc. For virome diversity studies, the lack of information makes it very complicated (perhaps impossible) to determine the optimal sampling period for novel viruses. In that case, it may be best to use repeated sampling.

Virus Concentration (Titer)

Several factors influence the multiplication rate of viruses and their accumulation within plant hosts: the time of sampling, i.e., days post-infection (DPI); environmental conditions (Cordoba et al., 1991; Nachappa et al., 2016); phenological stage of the plant (Dal Zotto et al., 1999); sampled organ(s) (Kogovšek et al., 2011; Constable et al., 2012; Lacroix et al., 2016), and plant and virus genotypes (Azizi and Shams-bakhsh, 2014). The detection sensitivity for a single virus, as well as its genome coverage, depend on its concentration in the sample, on the sample processing method, and on sample sequencing depth (Visser et al., 2016). The genome of a low-titer virus is therefore less likely to be completely sequenced with good coverage, which will impose limits on population genetics studies.

There is generally no optimal sampling, but virus titers are typically higher in actively-growing, green vegetation than in senescent plant tissues. In-depth knowledge of biology of the known viruses within the plant community is therefore a bonus and should guide the choice of sampling time(s). For instance, temperate climate pathosystems involving aphids may be preferentially sampled in spring and autumn, when plants are growing actively and vector populations are expanding and actively disseminating (Harris and Maramorosch, 1977). This would therefore warrant sampling at multiple time points to provide a dynamic vision of the virome. If the budget is limited, a smart approach can be to first conduct large-scale screening by HTS followed by assessment of the kinetics of targeted virus prevalence by ELISA or (RT-)PCR.

Co-infection by Several Viruses

The broad application of HTS technologies for plant virus detection has driven a paradigm change: co-infections are now recognized to be much more frequent than single infections (reviewed in Mascia and Gallitelli, 2016). Such co-infections may have consequences for symptom expression and/or virus concentration, and therefore the probability of detection. Indeed, interactions of multiple viruses within a single plant or tissue can lead to a variety of relationships ranging from antagonism (Wintermantel et al., 2008; Tatineni et al., 2010; Syller and Grupa, 2014) to synergism (Wang et al., 2002; Martínez et al., 2013), depending on host, viruses involved and infection history (defined as the succession of infection events).

Co-infection may also cause competition among viral targets for sequencing reads; a low-titer virus could theoretically be missed in a co-infection if the other virus(es) have high titer. The presence of several strains or several viruses sharing regions of homology can also hamper the proper reconstruction of viral genomes. Indeed, around the homologous region (for which a single contig will be generated), several 5′ and 3′ flanking reads and contigs can be assembled, which can *in fine* produce chimeric assemblies. This issue has been demonstrated for closely related species most particularly, but not only, when using a small RNA sequencing protocol (Massart et al., 2019).

Field Sampling

The protocol used for collection of samples from the field is critical but often poorly documented in virological reports. To support robust data analysis and interpretation, it is essential to consider the relationships among the question to be investigated, the overall study design, and the sampling strategy. Three common aims of field sampling for HTS studies are (i) to quantify *infection prevalence* – the proportion of individual plants that have detectable virus infection; (ii) to characterize the *species (or variant) composition* of a viral community or population; and (iii) to evaluate patterns of viral *diversity*, including viral *taxa richness* – the number of taxonomic units, such as species, genera, or families within a community. There are both general and aim-specific sampling considerations.

General Sampling Considerations

Many practical ecological and epidemiological texts offer guidance about field sampling strategies, including the classic "Measuring and Monitoring Plant Populations" (available online)[1]. Sampling insect communities raises additional considerations beyond the scope of this article. The interested reader is directed to specific literature on this question, in particular (Dayaram et al., 2015). Questions to consider include: What spatial pattern and areal extent of sampling will be the most suitable? What host species will be chosen? When and how frequently should sampling occur? How many individuals of each sampling group will be selected? What will be the specific process for plant selection – will developmental stage, size, or

[1]https://digitalcommons.unl.edu/cgi/viewcontent.cgi?article=1016&context=usblmpub

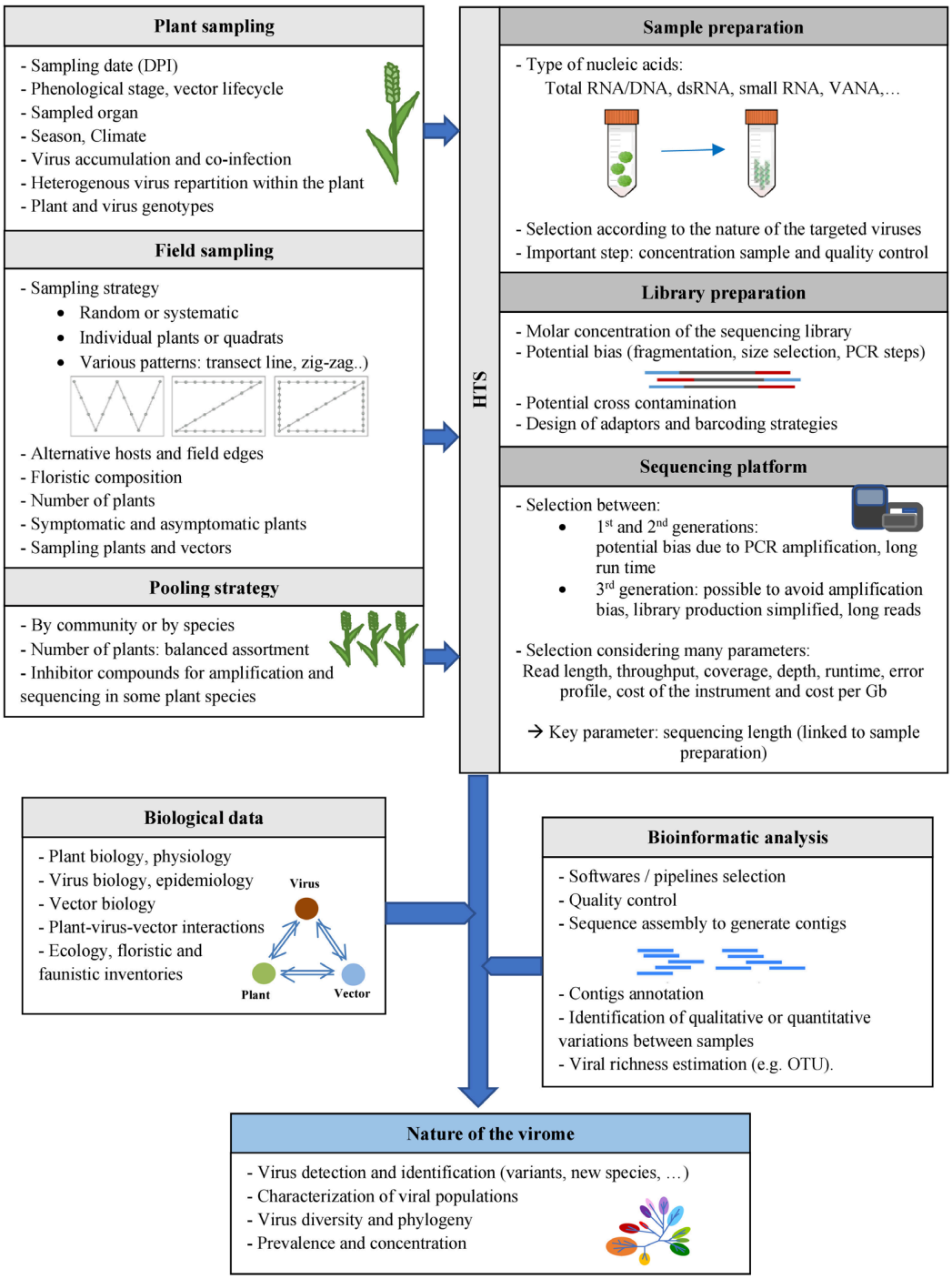

FIGURE 2 | Methods for characterizing the viromes of plant communities. Various factors may potentially impact HTS-based viral ecology studies, at the different steps of these studies: plant sampling at days post-infection (DPI), field sampling, pooling strategies, sample and library preparation methods, selection of the sequencing platforms and bioinformatic analyses. Biological data on the viruses, their host plants and vectors (if known) could also be useful for viral ecology studies.

symptom status be considered? The answers to these questions will influence the nature of the statistical analyses that can be conducted and the inferences drawn.

In heterogeneous landscapes, planning may further involve discernment of plant community types within a larger sampling unit and development of a stratified sampling scheme in which sampling effort is allocated to each community type as a function of its relative area. If a larger unit is 40% dry meadow and 60% wet meadow, for example, sampling effort might be allocated proportionately.

Once sampling compartments are identified, protocols must be developed for determining (i) at which points material will be collected, and (ii) how much of each plant(s) will be collected at each point. Decisions about sampling locations are best made prior to entering the field to remove user bias. For example, pre-determined points can be selected in the lab with a Geographic Information System (GIS) and then located with a Global Positioning System (GPS) in the field. These points might be located completely randomly or be selected in a grid for systematic sampling (Bernardo et al., 2018). If a grid is used, care must be taken that the spacing does not align with a regular interval in the vegetation pattern that would lead to oversampling of some vegetation types and undersampling of others. Alternatively, sampling may be conducted at predetermined intervals along transects, an approach that requires less technology to implement (Wilson, 2014). One method is to walk along one or several transects within a community or landscape, collecting samples every certain number of paces (Sseruwagi et al., 2004; Turechek et al., 2010). Transect start points and headings may be selected randomly or deliberately chosen to capture particular features, such as distance from edge (Ingwell et al., 2017) or border communities containing alternative host species (Byamukama et al., 2011; Muñoz et al., 2014).

Once sampling points are chosen, it is also essential to develop a protocol guiding the selection of individual samples at each point. The sampling unit might be an individual plant, several plants, or a quadrat from which all or some of the plants are collected (Byamukama et al., 2011). A sample-selection protocol is necessary to prevent introduction of bias by the sampler whose eyes may be drawn, for example, to symptomatic plants (Wilson, 2014) or to larger ones. Selection may be made through a specific randomization process or selection pattern (e.g., the individual closest to the right of the point is sampled, irrespective of condition or size).

Infection Prevalence

Studies aimed at quantifying infection prevalence – a common objective in agricultural research – focus on determining the proportion of plants carrying infection. In this context, virus infection can be considered as a plant characteristic, and plants can be sampled using standard plant ecology methods. Individual plants may be barcoded separately and sequenced. Alternatively, pooled plants may be sequenced and then viruses of interest targeted in individual plants with specific (RT-)PCR or ELISA methods. A critical consideration is to ensure that individuals are sampled without regard to symptoms and that all age/size classes of interest are evaluated.

Virus Community Composition

A more complex aim is to characterize the virus community ("virome") within a given area, plant community, or plant population. Typically, the objective is to identify all or most of the viral taxa within the study unit and perhaps also to compare virus community composition across host species, locations, or treatments. Important questions include, (i) Will the sampling protocol return a representative sample of the study unit? (ii) Can the desired comparisons across study units be fairly made?

To characterize the virome infecting a given plant community, the sampling effort may be structured to reflect the relative representation of the plant community's members, as evident in their relative abundance, relative cover, or relative biomass. A virome reflecting the relative abundance of individual plant species could be achieved, for example, by complete random sampling of individual plants, given sufficient sampling effort. Alternatively, sampling that is representative of plant species' relative abundances might also be achieved by first evaluating plant community composition and then conducting stratified sampling in which each plant species is sampled in proportion to its relative abundance. A third approach is to harvest all of the plants within numerous randomly-placed quadrats (often called the "lawn-mower" strategy) (Ramsell et al., 2008; Roossinck, 2012). This approach might be the most suited for analyses that aim to characterize an areal-based virome, but may also reflect to varying degrees the relative abundance, cover, or biomass of individual plant species. A critical issue for all methods is the extent of spatial dispersion or aggregation of samples, which will influence estimates of viral community composition and its comparability. For example, plants and viruses that are sampled in close proximity to each other are likely to be more similar than those with greater separation. Thus, samples taken from quadrats may miss species found in completely random sampling.

A related issue is the sampling effort – how many samples are to be taken overall? Typically, greater sampling effort uncovers greater species numbers, and the prevalence of individual viruses, as well as the relative representation of their plant hosts, will directly influence their probabilities of detection. If the prevalence or titer of a given virus is low, more sampling effort will be required to detect it, as it is also true for rare host species (Abarshi et al., 2010). *Taxon accumulation curves (collector's curves*) illustrate the gain in species numbers detected with increasing sampling effort, but do not predict species identity. They are sometimes used, however, to roughly assess the sampling effort at which species number begins to saturate (Gotelli and Colwell, 2001).

In addition to capturing a representative plant community virome, some studies also seek to compare the viromes of individual plant species within it. This is straightforward if the relative abundances and samples of the plant taxa to be compared are similar. However, if one plant species is common and the other is rare, the sample size of the rare species in a community-representative sample may be too small to be effectively compared. For such comparisons, additional equal-numbers sampling of each plant species might be conducted, while keeping in mind that equal numbers will not represent equal proportions of the host populations. For example, 30 individuals might represent 80% of a rare population but only 1% of a common one. Thus, the virome of the rare host population will likely be more complete than that of the common host. For discussion of an alternative approach, standardizing to equal coverage, see Chao et al. (2014). To reduce sampling costs, the host-comparative and community–representative approaches might be combined by sampling all individual plant species in

high numbers and then creating a community-representative assessment by subsampling each plant taxon in proportion to its relative abundance (this can be done multiple times to evaluate variability in outcomes). Such a combined approach is probably most tractable when barcoded plants are sequenced individually, because pooling steps in library preparation add complexity.

Virus Richness and Diversity

A third key aim of HTS studies is to evaluate patterns of *virus diversity*, as distinct from determining the taxonomic composition of the virome. Diversity is a core ecological property that can be complex to measure [for an introductory overview, see McCabe (2011)]; and further discussion in Gotelli and Colwell, 2001, 2011]. The simplest measure is *taxa richness* (*S*) or the number of different taxonomic units within a community sample. A related measure is *taxa density*, the number of taxonomic units per unit area. More complex indices, such as the Shannon-Wiener diversity index (*H'*) and Simpson's diversity index (D_1), incorporate information about both taxa richness and their relative abundance or evenness; the choice of index – of which there are many – may strongly influence the interpretation of results (Chao et al., 2014). Diversity is classically considered at several scales, as alpha, beta and gamma diversity. To simplify, alpha diversity describes diversity within a given subunit (sample, field, etc.), whereas beta diversity describes diversity among subunits or along environmental gradients. Gamma diversity represents diversity across an entire landscape, and incorporates both alpha- and beta- components (Whittaker, 1960).

In comparing diversity values, it is critical to consider equitability of sampling effort because the number of taxa discovered will increase with sampling intensity, as noted earlier. It is also important to note that sampling for diversity metrics may be either "individual-based" or "sample-based." Individual-based assessments examine randomly chosen individuals in the field, whereas sample-based assessments evaluate the number and identity of the target taxa in collective sampling units such as quadrats (Gotelli and Colwell, 2001). Because of within-patch similarities, species richness values from sample-based assessments will generally be lower than equivalent individual-based assessments. When assessing viral diversity, essentially all measures will be sample-based, because viruses are not sampled directly as individuals standing independently in the field but rather as entities embedded within particular host environments, be they individual plants or multi-plant collections.

With regard to sampling effort, richness in the simplest example quantifies the number of taxa represented by a given number of enumerated individuals. For example, if one finds 100 individual viruses (virus counts, however defined) in each of two communities and this number represents 7 taxa in community A and 25 in community B, then viral taxa richness is much greater in community B, all else being equal. (In practice, richness values may be adjusted to account for differences in detection rates among species and other issues beyond the scope of this review). In this example, comparisons between the two communities are straightforward because the same number of viruses has been enumerated in each. If the number differed, then rarefaction curves could be used to estimate how many taxa would be represented if the larger sample were subsampled to match the size of the smaller one (Gotelli and Colwell, 2001; McCabe, 2011). Alternatively, taxa accumulation curves could be used to estimate how many more species would be gained if the number of individuals enumerated in the smaller sample (Gotelli and Colwell, 2001). For in-depth consideration of such issues, see (Chao et al., 2014).

One must recall that "individual" in this context refers to an individual viral unit, however defined, not to an individual plant, and that "sample-based" assessments include assessments of individual or multiple plants. So with individual-based assessments, for example, one evaluates the number of distinct taxa represented by a given number of virus individuals and then might compare this richness value across treatments. For instance, 100 virus individuals might represent seven taxa in one treatment, and twenty-five in another, giving the latter greater virus richness. One advantage of working with richness values is that taxa accumulation curves and corresponding rarefaction curves may be more directly useful in permitting comparisons. Rarefaction determines how many taxa would likely be present in smaller subsamples of the total sampled population (McCabe, 2011). Thus, a treatment with more individuals can be rarefied to allow more equitable comparison of virus richness with another containing fewer individuals.

Pooling Strategy

Another crucial parameter is the strategy for pooling individuals or samples for sequencing (e.g., in library preparation), which can be necessary to reduce costs. Individual plants might be pooled, for instance, by species (a subsample of each species present) or by sampling location (all sampled plant species from one quadrat or location). The optimal pool size depends on striking a sometime difficult balance between the number of pools to be sequenced and the number of individual plants per pool. Increasing pool size is likely to exacerbate competition among viruses for sequencing reads; the larger the pool, the higher the probability that some low prevalence or low concentration viruses may be missed if other viruses are present in high abundance (dilution effect). An example is the current practice of inoculating a mild strain of pepino mosaic virus in tomato production to prevent the infection by severe strains. This mild strain is present in high concentration in the plants (up to 25% of total RNA reads, unpublished data). If such plants are included in a pool, the majority of viral reads might come from the PepMV mild strain, hampering the detection of other viruses at low abundance.

This issue is arguably most important in studies that seek to characterize the complete viral community, and perhaps less important for relative comparisons among sampling groups. Nested sample pooling is one approach for determining optimal pooling strategy. In this approach, a series of pools with increasing number of pooled plants from the same community or from an increasing number of communities is collected and sequenced. The results will give a preliminary overview of the geographic heterogeneity of the sampled population and thus of the sample size required for good representation. In all cases, it

is advisable to collect and store individual plants for downstream confirmation of HTS results.

Pooling strategies should also consider that some plant species may contain inhibitors (i.e., secondary metabolites) that can negatively affect the amplification and sequencing steps in some protocols (Lacroix et al., 2016). A preliminary study of the potential inhibitory effect of all host species sampled may need to be performed using targeted RT-PCR and mixing experiments (e.g., Lacroix et al., 2016). If inhibition is evident, the preferred solution would be to employ nucleic acid extraction protocols sufficiently robust for all plant hosts sampled. If no other option is available, it may be necessary to exclude the problematic plants species from the study. The dsRNA purification protocol (Tzanetakis and Martin, 2008; Okada et al., 2015; Nwokeoji et al., 2017; Ma et al., 2019) appears to be relatively robust, but in any case, the possibility of limitations for particular plant species should always be considered.

Selection of Method for Sample Preparation and Sequencing

The selection of the target nucleic acids population is critical as it defines the types of viral sequences that will be detected, including total RNA/DNA, RNA-Seq, Virion-Associated Nucleic Acids (VANA), dsRNA, small RNA, circular ssDNA or amplification of targeted PCR products using generic primers. While HTS technologies have the theoretical capacity to target any viral nucleic acid in any host plant or vector, the available protocols present distinct advantages and limitations as reviewed previously (Roossinck et al., 2015) and summarized in **Figure 3** and **Table 1**.

These limitations warrant a careful *a priori* evaluation of the viruses and viroids potentially infecting the plants in the study area. However, neither the viruses, nor their (genomic) characteristics are *a priori* all known. Hence protocol selection may be influenced most strongly by information about which viruses are common in the study area or are most interesting given the question(s) addressed. The research question and the objectives of the study will thus be crucial for protocol selection, along with a botanical inventory. For example, there are currently no viroids known to infect *Poaceae*. So, the VANA method – which concentrates DNA and RNA associated with virions but not viroids – could be a good choice when studying grassland samples, as long as it is understood that the analysis would likely miss any novel *Poaceae*-infecting viroids.

There are additional important considerations in sample and library preparation. For example, many current metagenomics-based protocols include a random PCR amplification step prior to sequencing, which can create chimeric reads and introduce bias in the relative proportion of sequences. This, among others, has so far limited the ability to evaluate the relative frequencies of viral sequences in a sample. Moreover, HTS-based approaches have already proven to be as susceptible to between-samples contamination as PCR-based assays (Massart et al., 2014; Galan et al., 2016), thus requiring specific precautions and controls. These contaminating reads can result from laboratory contaminations but also from read misassignment (also called index-hopping) when multiple libraries that include multiplexed samples are sequenced on the same Illumina lane (Vezzi et al., 2017). In ecogenomic studies where the establishment of a direct link between host plants and virus species is sought, cross-contamination among samples would result in the erroneous identification of virus-host combinations. For example, a plant species might be erroneously identified as a low-titer reservoir for a particular virus. Therefore, the same precautions and standards currently implemented in (RT)-PCR-based assays must be implemented for HTS technologies (Massart et al., 2014; Galan et al., 2016), such as the use of a series of controls (positive/negative, internal/external, spiking) at each step of the HTS pipeline [for example, as developed in the guidelines of the European VALITEST project (Lebas and Massart, 2020)]. In addition, verification of the virus found in individual samples by other independent methods is highly recommended.

In the sequencing phase, proper read length selection is a key consideration. For small RNA sequencing, the very short length of small RNAs (21–24 nt) complicates sequence assembly and annotation, and makes genome reconstruction and strain identification more difficult (Massart et al., 2017, 2019). More typically, read lengths generated by Illumina™ platforms range from 75 to 300 nt for single or paired reads, with error rates increasing with longer reads (Sameith et al., 2016). Pacific Biosciences™ or Oxford Nanopore™ technologies can generate much longer reads (and therefore a better reconstruction of genomes and isolates) but with lower sequencing accuracy (Filloux et al., 2018).

Sequencing depth is directly correlated with an improved ability to detect viruses present at low abundance/concentration, as shown for small RNA sequencing (Massart et al., 2019). On the other hand, a higher sequencing depth increases the probability of false positive detection because of potential contamination problems (i.e., contaminants are more likely to be sequenced) and increases the price per sample (Massart et al., 2014). Protocols allowing an enrichment of viral sequences, such as VANA or dsRNA will significantly improve the sensitivity of virus detection for a given sequencing depth. These protocols are therefore very popular for ecological studies (Djikeng et al., 2009; Coetzee et al., 2010; Blouin et al., 2016; Palanga et al., 2016). On the other hand, total RNA/DNA may still be used despite the requirement of higher sequencing depth (Ng et al., 2011; Bernardo et al., 2013; Gil et al., 2016; Akinyemi et al., 2016). Nevertheless, on the long term, if the cost of sequencing continues to decrease and the efficiency of ribodepletion protocols to increase, the use of total RNA could also be envisioned, provided sufficient sequencing depth is sought (in the range of 100x more than for VANA or dsRNA), as illustrated in grapevine viruses and a 35x enrichment for dsRNA (Al Rwahnih et al., 2009).

Bioinformatic Analysis

Detection, Characterization, and Taxonomic Assignment of Viral Reads and Contigs

Bioinformatic analyses may be performed to examine viral reads and assign them to virus taxonomic units, in order to estimate virus(es) genetic structure and diversity (richness and evenness),

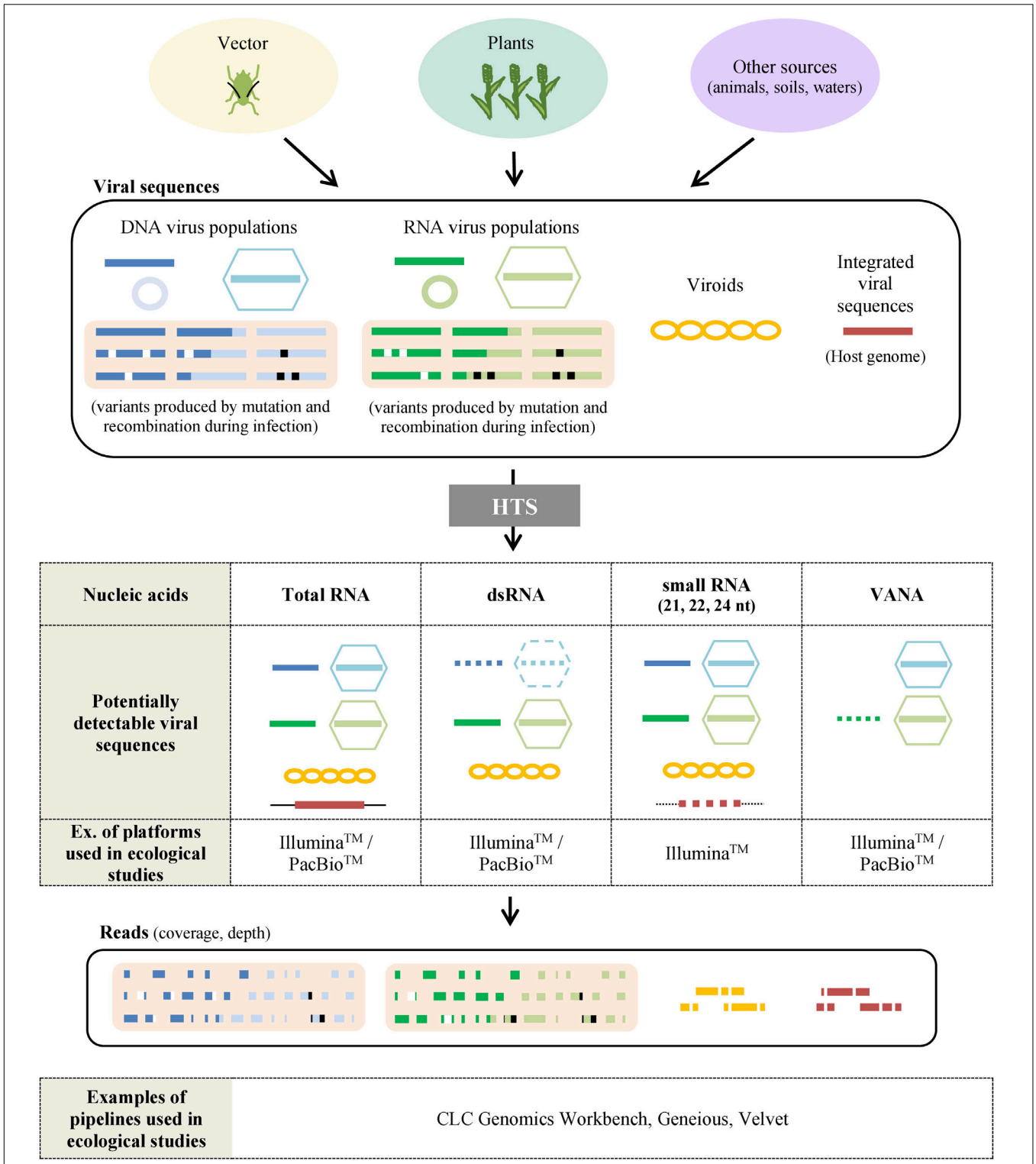

FIGURE 3 | Sample preparation for virus ecological studies using HTS. Samples taken from plants, vectors or other sources (waters, animals, etc.) may contain various viral sequences including DNA viruses (blue), RNA viruses (green), viroids (yellow) or viral sequences integrated in the host genome (red). Variants can be produced by mutations (white) and recombinations (black) during the infection. The most frequently used protocols to analyze viral sequences by HTS are based on the extraction of total RNA, dsRNA, small RNA, and Virion-Associated Nucleic Acids (VANA). By using sequencing platforms, sets of reads are obtained and have then to be processed by bioinformatic pipelines to reassemble them in order to detect, identify and quantify the virus and viroids present. Dotted figures correspond to viral sequences sometimes detected with the preparation method described.

TABLE 1 | Advantages and drawbacks of different sample preparations for HTS-based virus ecological studies.

Nucleic acids	Total RNA	dsRNA	Small RNA (21, 22, 24 nt)	VANA
Advantages	• Detection of any RNA or DNA virus and viroids. • For individual plants and pooled samples.	• All RNA viruses including viroids. • Enrichment of viral sequences in the data. • For individual plants and pooled samples.	• Screen any kind of virus and viroid targeted by silencing mechanism. • For individual plant samples.	• All viral particles, detection of DNA and RNA viruses. • Enrichment of viral sequences in the data. • For individual plants and pooled samples.
Drawbacks	• High sequencing depth is needed as there is a high background of rDNA (even with depletion of ribosomal RNAs). • No enrichment of viral sequences. • Limited sensitivity to detect viruses in low concentration	• Labor intensive. • Limited or no detection of DNA viruses. • Introduction of technical bias (enrichment) for quantification of variants and species.	• Cumbersome extraction methods (Trizol and CTAB-based). • Difficult annotation of sequences and genome reconstruction due to the small size of the sequences. • Only detects actively replicating agents targeted by plant silencing. • Many viruses can have very low sRNA titer in woody crops. • Not yet applied on sample pools for ecological studies. • Complicated assembly requires high sequencing depth in order to be able to assemble and identify viruses. • No enrichment of viral sequences. • Limited sensitivity to detect viruses in low concentration.	• In theory, no detection of viroids or virus nucleic acid not encapsided or with unstable particles. But endornaviruses were demonstrated to be detected with this technique. • Introduction of technical bias (enrichment) for quantification of variants and species. • Highly variable in recovery of viruses.

The four most frequently used protocols are considered: total RNA, dsRNA, smallRNA, and Virion-Associated Nucleic Acids (VANA) (Cf. ***Figure 3****). Their advantages and drawbacks are presented, in terms of detection, sensitivity, enrichment, convenience, and eventual bias.*

or even to characterize novel virus species. However, different population-based or taxonomy-based terms are often used in these analyses, such as virus species, isolates, strains, operational taxonomic unit (OTU) or quasispecies, while their definition has been discussed by virologists (Van Regenmortel, 2007; Adams et al., 2013; Peterson, 2014) and these terms have sometimes been inconsistently used in the literature. The crucial point is thus to define clearly the fundamental unit used for diversity estimation (Claverie et al., 2018). In recent geometagenomics work (Bernardo et al., 2018), virus family was for example defined as the base "individual" unit enumerated to evaluate virus richness per sample, i.e., the number of virus families represented (if any) as determined by BLAST matches of viral contigs. Consequently, this approach was deliberately conservative (to avoid double-counting contigs representing the same viral genome), but could not distinguish and enumerate co-infections of multiple isolates from the same species or of multiples species in the same or in related genera belonging to a family, that can be frequent in nature. Other strategies for estimating the viral diversity from metagenomics-based approaches have been recently used, relying on the use of a clustering of viral conserved protein motifs such as RNA-dependent RNA polymerases (RdRp) to define OTUs representing an acceptable proxy to viral species (Lefebvre et al., 2019; Ma et al., 2019) (see also next section).

Even for a single plant sample, identifying all viral agents present may be a non-trivial bioinformatic challenge and many elements have to be taken into consideration when trying to select a pipeline/strategy and optimize parameters (Massart et al., 2019). The presence of a novel viral species in a sample is not always easily detected and, to some extent, its detection still depends on the expertise of the researcher (Massart et al., 2019). In addition, homology-based annotation approaches, like BLASTn or BLASTx, have limitations because a significant proportion of sequence reads may have no detectable homologs in the sequence databases (Lefebvre et al., 2019) or because some sequences are wrongly annotated databases, which may lead to mis-identifications. Due to these limitations, current virome studies probably still miss part of the viral community but the proportion of viral sequences that are thus unidentified remains a matter of debate. Other approaches like Markov profile (Mistry et al., 2013) or k-mer analyses (Wood et al., 2019) can be used to try to identify novel virus species but without totally solving this issue since their performances are either incomplete or not properly known. Moreover, read assignment can be refined using statistical phylogenetic placement methodology, as recently illustrated by a study focusing on the appropriate phylogenetic position of viral metagenomic reads on a reference phylogenetic *Mastrevirus* tree (Claverie et al., 2019). Beside these homology-based annotation methods, sequence-independent strategies have been developed to identify novel viral sequences without using sequence databases, e.g., through the examination of characteristics of virus-derived small RNAs (Aguiar et al., 2015).

Another crucial issue for taxonomic assignment is the fact that viruses detected in plant samples by HTS technologies may

include not only viruses infecting the plant host itself but also those infecting any other organisms caught up in the sample, including microscopic arthropods, bacteria, or fungi living on or in the plant (Shi et al., 2016; Zhang et al., 2019). Some viral taxa may be readily assigned to hosts, on the basis of relationships to existing known viruses. However, the process can be complex if the taxa appear highly novel, are not well accommodated by existing phylogenies, or fall in an intermediate zone of host transition (Dolja et al., 2020; Koonin et al., 2020). Special attention should be paid to the contribution of these "contaminating viruses" to the plant virome, and to the potential influence of sample preparation techniques (e.g., dsRNA isolation might result in overrepresentation of fungal viruses with dsRNA genome as compared to ssRNA plant viruses) (Ma et al., 2019).

The characterization of the biology (host range, transmission mode, symptomatology, geographical distribution, etc.) of any newly identified virus can be challenging too. Indeed, the identification of a putative new virus alone will be of limited usefulness in a range of ecological studies. A characterization framework has recently been published, proposing a scaled approach to progressively and efficiently characterize the biology of a newly identified virus and the associated risks for the wild and domesticated plants (Massart et al., 2017).

Viral Richness and Diversity

As discussed, *taxa richness* (the number of taxa present within a sample or environment) and *taxa diversity* (which takes into account both taxa richness and *evenness*, the relative proportions of each taxa) are two key ecological metrics (Whittaker, 1965; Colwell, 1997; Witzany, 2012). To measure richness and diversity from HTS data for viruses is not a trivial task, due to: (i) incomplete virus genome assemblies potentially resulting in different viruses being represented by non-overlapping genome regions (e.g., viral species 1 being represented by its capsid protein gene while viral species 2 is represented by it polymerase gene); (ii) chimeric assembly due to homologous regions as explained in "Co-infection by Several Viruses"; and (iii) the challenge of defining enurable viral units (see above). Non-homogeneous taxonomic criteria between viral families and the absence of universally conserved genomic region shared by all viruses further complicate viral richness estimation. This difficulty will also impact alpha, beta or gamma diversity analyses, with the added complexity of simultaneously necessitating quantitative abundance or prevalence data for each individual agent (see section on "Infection Prevalence").

A proposed strategy is to measure a proxy of virus species richness by enumerating OTUs. This can be achieved by aligning a conserved region, often part of the polymerase region, setting an arbitrary distance separating OTUs (more than a fixed percentage of divergence) and then performing a sequence clustering. Other proxys have been used to estimate viral richness, for example the number of viral families or genera, or OTUs defined using other approaches but these other proxys tend to have even more limitations than the use of OTUs based on a clustering approach. A very good description of this approach for virus classification was presented by Simmonds (2015). It has recently been implemented in at least one annotation pipeline (Lefebvre et al., 2019), and already used at the family level in ecological analyses combined to plant spatial distribution (Bernardo et al., 2018) and near species level for the benchmarking of sequencing strategies (Ma et al., 2019). The study of taxa richness based on similarities/divergence between sequences offers the possibility to taxonomically "assign" the large number of virus sequences generated by HTS, but also presents some pitfalls. Indeed, while numerous virus genomes have experienced recombination and reassortment event(s), only complete genomes or at least complete coding regions of virus genomes are suitable for reliable taxonomic assignments (Simmonds, 2015). However, despite these limitations to precise taxonomic assignment, distance-based methods can be used as the only source of information for virus richness estimation from HTS data.

Single-Nucleotide Polymorphisms (SNPs) and Virus Populations

Viral populations can evolve quickly by mutation and/or recombination at each replication cycle. The resulting variants may bear large genome rearrangements as well as single-nucleotide polymorphism (SNP) mutations. Accessing viral intra-specific diversity through HTS has value for specific scientific aims (Beerenwinkel and Zagordi, 2011), such as to better measure and map evolutionary footprints of virus emergence at the plant community scale. For example, the detailed characterization of viral isolates will be needed in order to compare the virus population in a primary host and in potential reservoir(s).

To genotype and haplotype SNPs remains a challenging bioinformatic task for a single virus in a single sample. It becomes obviously more complex with samples containing multiple viruses from multiple hosts. In the case of mixtures of isolates, reconstruction of genomic sequences may be particularly complex, if not altogether impossible, especially when multiple closely related isolates are involved or for quasi-species with high variability. Moreover, the differentiation between SNP and sequencing errors is intrinsically difficult for low frequency variants. It can be impacted by the quality of the HTS sequences produced, by read length, but also by the algorithms used for quality control, contig assembly, and SNP identification. The statistical approach selected for the haplotyping analysis is another key factor to consider; its performance is determined by mutation rate and was demonstrated to decrease with genetic diversity of the sample (see McCrone and Lauring, 2016; Posada-Cespedes and Seifert, 2017; Eliseev et al., 2020).

The confirmation of SNPs represents another challenge: targeted real-time PCR could be used but the need to design and produce two probes per SNP remains costly. Another potential way to reinforce the significance of the analysis is to sequence duplicates of each sample or to combine the use of different HTS approaches that have different distribution of sequencing errors. While costly, these approaches have the potential to distinguish true SNPs from sequencing errors. Running duplicates is a strategy that is often performed for HTS-based barcoding (Razzauti et al., 2015) and could be applied to virus ecology.

CONCLUSION

The study of plant virus ecology, which began at the end of the 19th century, has been accelerated by the evolution of new methods used to detect plant viruses in various environments and in many plants simultaneously: the HTS technologies offer huge opportunities to improve virome characterization and address novel questions such as the examination of virus spread among host reservoirs (wild and domestic), the effects of ecosystem simplification caused by human activities (and agriculture) on the biodiversity, and the emergence of new viruses in crops. Recently, conceptual shifts in the understanding of the origins and diversification of the plant virome were achieved, leading to the design of the first comprehensive virus megataxonomy. Nevertheless, the use of HTS in ecological studies is associated with a series of challenges and pitfalls described in detail in this review for each procedural step in the field, in the laboratory and for bioinformatic analyses. The rapid evolution of the sequencing platforms and bioinformatic pipelines promises numerous findings in viral metagenomic studies over the coming years. These novel approaches developed in plant virology will directly be transferable to other models for a better understanding of host-virus interactions and ecological virology in general.

AUTHOR CONTRIBUTIONS

FM and SM conceived and wrote the manuscript. FM created the figures and prepared the final version of the manuscript and all authors approved it. In particular, PR and CM edited the viromics advances and field sampling sections, respectively. TC, CM, PR, RV, and DF edited the bioinformatics sections. All authors collectively revised and improved the manuscript and made useful suggestions on all sections of the review article.

FUNDING

This work was supported by the Fonds de la Recherche Scientifique – FNRS under Grant No. 1.1.309.19F06.

REFERENCES

Abarshi, M. M., Mohammed, I. U., Wasswa, P., Hillocks, R. J., Holt, J., Legg, J. P., et al. (2010). Optimization of diagnostic RT-PCR protocols and sampling procedures for the reliable and cost-effective detection of Cassava brown streak virus. *J. Virol. Methods* 163, 353–359. doi: 10.1016/j.jviromet.2009.10.023

Adams, M. J., Lefkowitz, E. J., King, A. M. Q., and Carstens, E. B. (2013). Recently agreed changes to the International Code of Virus Classification and Nomenclature. *Arch. Virol.* 158, 2633–2639. doi: 10.1007/s00705-013-1749-9

Aguiar, E. R. G. R., Olmo, R. P., Paro, S., Ferreira, F. V., De Faria, I. J. D. S., Todjro, Y. M. H., et al. (2015). Sequence-independent characterization of viruses based on the pattern of viral small RNAs produced by the host. *Nucleic Acids Res.* 43, 6191–6206. doi: 10.1093/nar/gkv587

Akinyemi, I. A., Wang, F., Zhou, B., Qi, S., and Wu, Q. (2016). Ecogenomic survey of plant viruses infecting Tobacco by Next generation sequencing. *Virol. J.* 13:181. doi: 10.1186/s12985-016-0639-7

Al Rwahnih, M., Daubert, S., Golino, D., and Rowhani, A. (2009). Deep sequencing analysis of RNAs from a grapevine showing Syrah decline symptoms reveals a multiple virus infection that includes a novel virus. *Virology* 387, 395–401. doi: 10.1016/j.virol.2009.02.028

Alexander, H. M., Mauck, K. E., Whitfield, A. E., Garrett, K. A., and Malmstrom, C. M. (2014). Plant-virus interactions and the agro-ecological interface. *Eur. J. Plant Pathol.* 138, 529–547. doi: 10.1007/s10658-013-0317-1

Alonso, P., Gladieux, P., Moubset, O., Shih, P. J., Mournet, P., Frouin, J., et al. (2019). Emergence of southern rice black-streaked dwarf virus in the centuries-old Chinese Yuanyang Agrosystem of Rice Landraces. *Viruses* 11:985. doi: 10.3390/v11110985

Anaya-López, J. L., Torres-Pacheco, I., González-Chavira, M., Garzon-Tiznado, J. A., Pons-Hernandez, J. L., Guevara-González, R. G., et al. (2003). Resistance to geminivirus mixed infections in Mexican wild peppers. *HortScience* 38, 251–255. doi: 10.21273/HORTSCI.38.2.251

Azizi, A., and Shams-bakhsh, M. (2014). Impact of cucumber mosaic virus infection on the varietal traits of common bean cultivars in Iran. *VirusDisease* 25, 447–454. doi: 10.1007/s13337-014-0233-9

Bawden, F. C., and Kassanis, B. (1941). Some properties of tobacco etch virus. *Ann. Appl. Biol.* 28, 107–118. doi: 10.1111/j.1744-7348.1941.tb07544.x

Bawden, F. C., and Kassanis, B. (1945). The suppression of one plant virus by another. *Ann. Appl. Biol.* 32, 52–57. doi: 10.1111/j.1744-7348.1945.tb06759.x

Beerenwinkel, N., and Zagordi, O. (2011). Ultra-deep sequencing for the analysis of viral populations. *Curr. Opin. Virol.* 1, 413–418. doi: 10.1016/j.coviro.2011.07.008

Beijerinck, M. (1899). Ueber ein Contagium vivum fluidum als Ursache der Fleckenkrankheit der Tabaksbl"atter. *Cent. Bakteriol. Parasitenkd. Infekt. II Abt* 5, 27–33.

Bennett, C. W. (1944). Latent virus of dodder and its effect on sugar beet and other plants. *Phytopathology* 34, 77–91.

Bernardo, P., Charles-Dominique, T., Barakat, M., Ortet, P., Fernandez, E., Filloux, D., et al. (2018). Geometagenomics illuminates the impact of agriculture on the distribution and prevalence of plant viruses at the ecosystem scale. *ISME J.* 12, 173–184. doi: 10.1038/ismej.2017.155

Bernardo, P., Golden, M., Akram, M., Naimuddin, Nadarajan, N., Fernandez, E., et al. (2013). Identification and characterisation of a highly divergent geminivirus: evolutionary and taxonomic implications. *Virus Res.* 177, 35–45. doi: 10.1016/j.virusres.2013.07.006

Blouin, A. G., Ross, H. A., Hobson-Peters, J., O'Brien, C. A., Warren, B., and MacDiarmid, R. (2016). A new virus discovered by immunocapture of double-stranded RNA, a rapid method for virus enrichment in metagenomic studies. *Mol. Ecol. Resour.* 16, 1255–1263. doi: 10.1111/1755-0998.12525

Boonham, N., Kreuze, J., Winter, S., van der Vlugt, R., Bergervoet, J., Tomlinson, J., et al. (2014). Methods in virus diagnostics: from ELISA to next generation sequencing. *Virus Res.* 186, 20–31. doi: 10.1016/j.virusres.2013.12.007

Borer, E. T., Hosseini, P. R., Seabloom, E. W., and Dobson, A. P. (2007). Pathogen-induced reversal of native dominance in a grassland community. *Proc. Natl. Acad. Sci. U.S.A.* 104, 5473–5478. doi: 10.1073/pnas.0608573104

Bujarski, J. J., and Kaesberg, P. (1986). Genetic recombination between RNA components of a multipartite plant virus. *Nature* 321, 528–531. doi: 10.1038/321528a0

Byamukama, E., Robertson, A. E., and Nutter, F. W. (2011). Quantifying the within-field temporal and spatial dynamics of Bean pod mottle virus in Soybean. *Plant Dis.* 95, 126–136. doi: 10.1094/PDIS-07-09-0469

Campbell, R. N. (1962). Relationship between the lettuce big-vein virus and its vector, olpidium brassicae. *Nature* 195, 675–677. doi: 10.1038/195675a0

Carter, W. (1939). Populations of Thrips tabaci, with special reference to virus transmission. *J. Anim. Ecol.* 8, 261–276. doi: 10.2307/1234

Chao, A., Gotelli, N. J., Hsieh, T. C., Sander, E. L., Ma, K. H., Colwell, R. K., et al. (2014). Rarefaction and extrapolation with Hill numbers: a framework for sampling and estimation in species diversity studies. *Ecol. Monogr.* 84, 45–67. doi: 10.1890/13-0133.1

Claverie, S., Bernardo, P., Kraberger, S., Hartnady, P., Lefeuvre, P., Lett, J. M., et al. (2018). From spatial metagenomics to molecular characterization of plant viruses: a geminivirus case study. *Adv. Virus Res.* 101, 55–83. doi: 10.1016/bs.aivir.2018.02.003

Claverie, S., Ouattara, A., Hoareau, M., Filloux, D., Varsani, A., Roumagnac, P., et al. (2019). Exploring the diversity of Poaceae-infecting mastreviruses on Reunion Island using a viral metagenomics-based approach. *Sci. Rep.* 9:12716. doi: 10.1038/s41598-019-49134-9

Coetzee, B., Freeborough, M.-J., Maree, H. J., Celton, J.-M., Rees, D. J. G., and Burger, J. T. (2010). Deep sequencing analysis of viruses infecting grapevines: virome of a vineyard. *Virology* 400, 157–163. doi: 10.1016/j.virol.2010.01.023

Colwell, R. R. (1997). Microbial diversity: the importance of exploration and conservation. *J. Ind. Microbiol. Biotechnol.* 18, 302–307. doi: 10.1038/sj.jim.2900390

Constable, F. E., Connellan, J., Nicholas, P., and Rodoni, B. C. (2012). Comparison of enzyme-linked immunosorbent assays and reverse transcription-polymerase chain reaction for the reliable detection of Australian grapevine viruses in two climates during three growing seasons. *Aust. J. Grape Wine Res.* 18, 239–244. doi: 10.1111/j.1755-0238.2012.00188.x

Cordoba, A. R., Taleisnik, E., Brunotto, M., and Racca, R. (1991). Mitigation of tomato spotted Wilt Vims infection and symptom expression by water stress. *J. Phytopathol.* 133, 255–264. doi: 10.1111/j.1439-0434.1991.tb00160.x

Creamer, R., Luque-Williams, M., and Howo, M. (1996). Epidemiology and incidence of beet curly top geminivirus in naturally infected weed hosts. *Plant Dis.* 80, 533–535. doi: 10.1094/pd-80-0533

Culley, A. I., Lang, A. S., and Suttle, C. A. (2006). Metagenomic analysis of coastal RNA virus communities. *Science* 312, 1795–1798. doi: 10.1126/science.1127404

Dal Zotto, A., Nome, S. F., Di Rienzo, J. A., and Docampo, D. M. (1999). Fluctuations of Prunus Necrotic Ringspot Virus (PNRSV) at Various Phenological Stages in Peach Cultivars. *Plant Dis.* 83, 1055–1057. doi: 10.1094/PDIS.1999.83.11.1055

Dayaram, A., Potter, K. A., Pailes, R., Marinov, M., Rosenstein, D. D., and Varsani, A. (2015). Identification of diverse circular single-stranded DNA viruses in adult dragonflies and damselflies (Insecta: Odonata) of Arizona and Oklahoma, USA. *Infect. Genet. Evol.* 30, 278–287. doi: 10.1016/j.meegid.2014.12.037

Dickson, B. T. (1925). TOBACCO AND TOMATO MOSAIC. *Science* 62, 398–399. doi: 10.1126/science.62.1609.398

Djikeng, A., Kuzmickas, R., Anderson, N. G., and Spiro, D. J. (2009). Metagenomic analysis of RNA viruses in a fresh water lake. *PLoS One* 4:e7264. doi: 10.1371/journal.pone.0007264

Dolja, V. V., Krupovic, M., and Koonin, E. V. (2020). Deep roots and splendid boughs of the global plant virome. *Annu. Rev. Phytopathol.* 58, 23–53. doi: 10.1146/annurev-phyto-030320-041346

Elena, S. F., Fraile, A., and García-Arenal, F. (2014). Evolution and emergence of plant viruses. *Adv. Virus Res.* 88, 161–191. doi: 10.1016/B978-0-12-800098-4.00003-9

Eliseev, A., Gibson, K. M., Avdeyev, P., Novik, D., Bendall, M. L., Pérez-Losada, M., et al. (2020). Evaluation of haplotype callers for next-generation sequencing of viruses. *Infect. Genet. Evol.* 82:104277. doi: 10.1016/j.meegid.2020.104277

Filloux, D., Fernandez, E., Loire, E., Claude, L., Galzi, S., Candresse, T., et al. (2018). Nanopore-based detection and characterization of yam viruses. *Sci. Rep.* 8:17879. doi: 10.1038/s41598-018-36042-7

Fraile, A., and García-Arenal, F. (2016). Environment and evolution modulate plant virus pathogenesis. *Curr. Opin. Virol.* 17, 50–56. doi: 10.1016/j.coviro.2016.01.008

Galan, M., Razzauti, M., Bard, E., Bernard, M., Brouat, C., Charbonnel, N., et al. (2016). 16S rRNA amplicon sequencing for epidemiological surveys of bacteria in wildlife. *mSystems* 1:e00032-16. doi: 10.1101/03982-16

Gibbs, A. (1980). A plant virus that partially protects its wild legume host against herbivores. *Intervirology* 13, 42–47. doi: 10.1159/000149105

Gibbs, A. J. (1983). "Virus Ecology — "Struggle" of the Genes," in *Physiological Plant Ecology III*, eds O. L. Lange, P. S. Nobel, C. B. Osmond, and H. Ziegler (Berlin: Springer), 537–558. doi: 10.1007/978-3-642-68153-0_15

Gil, J. F., Adams, I., Boonham, N., Nielsen, S. L., and Nicolaisen, M. (2016). Molecular and biological characterisation of two novel pomo-like viruses associated with potato (*Solanum tuberosum*) fields in Colombia. *Arch. Virol.* 161, 1601–1610. doi: 10.1007/s00705-016-2839-2

Gildow, F. E. (1985). Transcellular Transport of Barley Yellow Dwarf Virus Into the Hemocoel of the Aphid Vector, Rhopalosiphum padi. *Phytopathology* 75, 292–297. doi: 10.1094/phyto-75-292

Gotelli, N. J., and Colwell, R. K. (2001). Quantifying biodiversity: procedures and pitfalls in the measurement and comparison of species richness. *Ecol. Lett.* 4, 379–391. doi: 10.1046/j.1461-0248.2001.00230.x

Gotelli, N. J., and Colwell, R. K. (2011). "Estimating species richness," in *Biological Diversity: Frontiers in Measurement and Assessment*, eds A. E. Magurran and B. J. McGill (Oxford: Oxford University Press, 39–54.

Hammond, J. (1981). Viruses occurring in Plantago species in England. *Plant Pathol.* 30, 237–243. doi: 10.1111/j.1365-3059.1981.tb01263.x

Harris, K. F., and Maramorosch, K. (eds) (1977). *Aphids as Virus Vectors, Aphids As Virus Vectors*. New York, NY: Academic Press. doi: 10.1016/c2013-0-10831-8

Harrison, B. D. (1981). Plant virus ecology: ingredients, interactions and environmental influences. *Ann. Appl. Biol.* 99, 195–209. doi: 10.1111/j.1744-7348.1981.tb04787.x

Harrison, B. D. (2009). A brief outline of the development of plant virology in the 20th century. *J. Plant Pathol.* 91, 509–520.

Hewitt, W. B., Raski, D. J., and Goheen, A. C. (1958). Nematode vector of soil-borne fanleaf virus of grapevines. *Phytopathology* 48, 586–595.

Hull, R. (2014). *Plant Virology, Plant Virology*. New York, NY: Academic Press. doi: 10.1016/B978-0-12-384871-0.00014-5

Ingwell, L. L., Eigenbrode, S. D., and Bosque-Pérez, N. A. (2012). Plant viruses alter insect behavior to enhance their spread. *Sci. Rep.* 2:578.

Ingwell, L. L., Lacroix, C., Rhoades, P. R., Karasev, A. V., and Bosque-Pérez, N. A. (2017). Agroecological and environmental factors influence Barley yellow dwarf viruses in grasslands in the US Pacific Northwest. *Virus Res.* 241, 185–195. doi: 10.1016/j.virusres.2017.04.010

Ivanovskij, D. (1899). Ueber die Mosaikkrankheit der Tabakspflanze. *Cent. Bakteriol. Parasitenkd. Infekt. II Abt* 5, 250–254.

Jones, R. A. C. (2014). Plant virus ecology and epidemiology: historical perspectives, recent progress and future prospects. *Ann. Appl. Biol.* 164, 320–347. doi: 10.1111/aab.12123

Jooste, A. E. C., Molenaar, N., Maree, H. J., Bester, R., Morey, L., de Koker, W. C., et al. (2015). Identification and distribution of multiple virus infections in Grapevine leafroll diseased vineyards. *Eur. J. Plant Pathol.* 142, 363–375. doi: 10.1007/s10658-015-0620-0

Kelley, S. E. (1994). "Viral pathogens and the advantage of sex in the perennial grass *Anthoxanthum odoratum*," in *Infection, Polymorphism and Evolution*, eds W. D. Hamilton and J. C. Howard (Dordrecht: Springer), 25–32. doi: 10.1007/978-94-009-0077-6_3

Kennedy, J. S. (1951). Benefits to aphids from feeding on galled and virus-infected leaves. *Nature* 168, 825–826. doi: 10.1038/168825a0

Kogovšek, P., Kladnik, A., Mlakar, J., Žnidariè, M. T., Dermastia, M., Ravnikar, M., et al. (2011). Distribution of potato virus Y in Potato Plant Organs, Tissues, and Cells. *Phytopathology* 101, 1292–1300. doi: 10.1094/PHYTO-01-11-0020

Koonin, E. V., Dolja, V. V., Krupovic, M., Varsani, A., Wolf, Y. I., Yutin, N., et al. (2020). Global organization and proposed megataxonomy of the virus world. *Microbiol. Mol. Biol. Rev.* 84:e00061-19. doi: 10.1128/mmbr.00061-19

Kreuze, J. F., Perez, A., Untiveros, M., Quispe, D., Fuentes, S., Barker, I., et al. (2009). Complete viral genome sequence and discovery of novel viruses by deep sequencing of small RNAs: a generic method for diagnosis, discovery and sequencing of viruses. *Virology* 388, 1–7. doi: 10.1016/j.virol.2009.03.024

Lacroix, C., Renner, K., Cole, E., Seabloom, E. W., Borer, E. T., and Malmstrom, C. M. (2016). Methodological guidelines for accurate detection of viruses in wild plant species. *Appl. Environ. Microbiol.* 82, 1966–1975. doi: 10.1128/AEM.03538-15

Lebas B., and Massart S. (2020). Guidelines for the selection, development, validation and routine use of high-throughput sequencing analysis in plant diagnostic laboratories. *Valitest* Available onlie at: https://www.valitest.eu/

Lefebvre, M., Theil, S., Ma, Y., and Candresse, T. (2019). The VirAnnot Pipeline: a Resource for Automated Viral Diversity Estimation and Operational Taxonomy Units Assignation for Virome Sequencing Data. *Phytobiomes J.* 3, 256–259. doi: 10.1094/PBIOMES-07-19-0037-A

Lefeuvre, P., Martin, D. P., Elena, S. F., Shepherd, D. N., Roumagnac, P., and Varsani, A. (2019). Evolution and ecology of plant viruses. *Nat. Rev. Microbiol.* 17, 632–644. doi: 10.1038/s41579-019-0232-3

Lindbo, J. A., Silva-rosales, L., Proebsting, W. M., and Dougherty, W. G. (1993). lnduction of a highly specific antiviral state in transgenic plants: lmplications for regulation of gene expression and virus resistance. *Plant Cell* 5, 1749–1759. doi: 10.1105/tpc.5.12.1749

Ma, Y., Marais, A., Lefebvre, M., Faure, C., and Candresse, T. (2020). Metagenomic analysis of virome cross-talk between cultivated Solanum lycopersicum and wild *Solanum nigrum*. *Virology* 540, 38–44. doi: 10.1016/j.virol.2019.11.009

Ma, Y., Marais, A., Lefebvre, M., Theil, S., Svanella-Dumas, L., Faure, C., et al. (2019). Phytovirome analysis of wild plant populations: comparison of double-stranded RNA and virion-associated nucleic acid metagenomic approaches. *J. Virol.* 94:e01462-19. doi: 10.1128/jvi.01462-19

MacClement, W. D., and Richards, M. G. (1956). Virus in wild plants. *Can. J. Bot.* 34, 793–799. doi: 10.1139/b56-060

Malmstrom, C. M., McCullough, A. J., Johnson, H. A., Newton, L. A., and Borer, E. T. (2005). Invasive annual grasses indirectly increase virus incidence in California native perennial bunchgrasses. *Oecologia* 145, 153–164. doi: 10.1007/s00442-005-0099-z

Malmstrom, C. M., Melcher, U., and Bosque-Pérez, N. A. (2011). The expanding field of plant virus ecology: historical foundations, knowledge gaps, and research directions. *Virus Res.* 159, 84–94. doi: 10.1016/j.virusres.2011.05.010

Martínez, F., Elena, S. F., and Daròs, J.-A. (2013). Fate of artificial MicroRNA-mediated resistance to plant viruses in mixed infections. *Phytopathology* 103, 870–876. doi: 10.1094/PHYTO-09-12-0233-R

Mascia, T., and Gallitelli, D. (2016). Synergies and antagonisms in virus interactions. *Plant Sci.* 252, 176–192. doi: 10.1016/j.plantsci.2016.07.015

Massart, S., Candresse, T., Gil, J., Lacomme, C., Predajna, L., Ravnikar, M., et al. (2017). A framework for the evaluation of biosecurity, commercial, regulatory, and scientific impacts of plant viruses and viroids identified by NGS technologies. *Front. Microbiol.* 8:45. doi: 10.3389/fmicb.2017.00045

Massart, S., Chiumenti, M., De Jonghe, K., Glover, R., Haegeman, A., Koloniuk, I., et al. (2019). Virus detection by high-throughput sequencing of small RNAs: large-scale performance testing of sequence analysis strategies. *Phytopathology* 109, 488–497. doi: 10.1094/PHYTO-02-18-0067-R

Massart, S., Olmos, A., Jijakli, H., and Candresse, T. (2014). Current impact and future directions of high throughput sequencing in plant virus diagnostics. *Virus Res.* 188, 90–96. doi: 10.1016/j.virusres.2014.03.029

Matthews, R. E. F., and Hull, R. (2002). *Matthews' Plant Virology*. Houston, TX: Gulf Professional Publishing.

Mauck, K. E. (2016). Variation in virus effects on host plant phenotypes and insect vector behavior: what can it teach us about virus evolution? *Curr. Opin. Virol.* 21, 114–123. doi: 10.1016/j.coviro.2016.09.002

Mauck, K. E., De Moraes, C. M., and Mescher, M. C. (2010). Deceptive chemical signals induced by a plant virus attract insect vectors to inferior hosts. *Proc. Natl. Acad. Sci. U.S.A.* 107, 3600–3605. doi: 10.1073/pnas.0907191107

Mayer, A. (1886). Über die Mosaikkrankheit des Tabaks. *Die Landwirtsch. Versuch. Stat.* 32, 451–467.

McCabe, D. J. (2011). Sampling biological communities. *Nat. Educ. Knowl.* 3:63.

McCrone, J. T., and Lauring, A. S. (2016). Measurements of intrahost viral diversity are extremely sensitive to systematic errors in variant calling. *J. Virol.* 90, 6884–6895. doi: 10.1128/JVI.00667-16

McLeish, M. J., Fraile, A., and García-Arenal, F. (2019). Evolution of plant–virus interactions: host range and virus emergence. *Curr. Opin. Virol.* 34, 50–55. doi: 10.1016/j.coviro.2018.12.003

Mistry, J., Finn, R. D., Eddy, S. R., Bateman, A., and Punta, M. (2013). Challenges in homology search: HMMER3 and convergent evolution of coiled-coil regions. *Nucleic Acids Res.* 41:e121. doi: 10.1093/nar/gkt263

Moreno-Delafuente, A., Garzo, E., Moreno, A., and Fereres, A. (2013). A plant virus manipulates the behavior of its whitefly vector to enhance its transmission efficiency and spread. *PLoS One* 8:e61543. doi: 10.1371/journal.pone.0061543

Muñoz, R. M., Lerma, M. L., Lunello, P., and Schwartz, H. F. (2014). Iris yellow spot virus in Spain: incidence, epidemiology and yield effect on onion crops. *J. Plant Pathol.* 96, 97–103. doi: 10.4454/JPP.V96I1.029

Muthukumar, V., Melcher, U., Pierce, M., Wiley, G. B., Roe, B. A., Palmer, M. W., et al. (2009). Non-cultivated plants of the Tallgrass Prairie Preserve of northeastern Oklahoma frequently contain virus-like sequences in particulate fractions. *Virus Res.* 141, 169–173. doi: 10.1016/j.virusres.2008.06.016

Nachappa, P., Culkin, C. T., Saya, P. M., Han, J., and Nalam, V. J. (2016). Water stress modulates soybean aphid performance, feeding behavior, and virus transmission in soybean. *Front. Plant Sci.* 7:552. doi: 10.3389/fpls.2016.00552

Ng, T. F. F., Duffy, S., Polston, J. E., Bixby, E., Vallad, G. E., and Breitbart, M. (2011). Exploring the diversity of plant DNA viruses and their satellites using vector-enabled metagenomics on whiteflies. *PLoS One* 6:19050. doi: 10.1371/journal.pone.0019050

Nishimura, M. (1918). A carrier of the mosaic disease. *Bull. Torrey Bot. Club* 45, 219–233. doi: 10.2307/2479806

Nwokeoji, A. O., Kung, A. W., Kilby, P. M., Portwood, D. E., and Dickman, M. J. (2017). Purification and characterisation of dsRNA using ion pair reverse phase chromatography and mass spectrometry. *J. Chromatogr. A* 1484, 14–25. doi: 10.1016/j.chroma.2016.12.062

Okada, R., Kiyota, E., Moriyama, H., Fukuhara, T., and Natsuaki, T. (2015). A simple and rapid method to purify viral dsRNA from plant and fungal tissue. *J. Gen. Plant Pathol.* 81, 103–107. doi: 10.1007/s10327-014-0575-6

Pagán, I., González-Jara, P., Moreno-Letelier, A., Rodelo-Urrego, M., Fraile, A., Piñero, D., et al. (2012). Effect of biodiversity changes in disease risk: exploring disease emergence in a plant-virus system. *PLoS Pathog.* 8:e1002796. doi: 10.1371/journal.ppat.1002796

Palanga, E., Filloux, D., Martin, D. P., Fernandez, E., Gargani, D., Ferdinand, R., et al. (2016). Metagenomic-based screening and molecular characterization of cowpea-infecting viruses in Burkina Faso. *PLoS One* 11:e0165188. doi: 10.1371/journal.pone.0165188

Peterson, A. T. (2014). Defining viral species: making taxonomy useful. *Virol. J.* 11:131. doi: 10.1186/1743-422X-11-131

Posada-Cespedes, S., and Seifert, D. (2017). Recent advances in inferring viral diversity from high-throughput sequencing data. *Virus Res.* 239, 17–32. doi: 10.1016/J.VIRUSRES.2016.09.016

Power, A. G. (1991). Virus spread and vector dynamics in genetically diverse plant populations. *Ecology* 72, 232–241. doi: 10.2307/1938917

Power, A. G., and Flecker, A. S. (2003). "Virus specificity in disease systems: are species redundant?" in *The Importance of Species*, eds P. Kaveira and S. A. Levin (Princeton, NJ: Princeton University Press), 330–347. doi: 10.1515/9781400866779-023

Power, A. G., and Mitchell, C. E. (2004). Pathogen spillover in disease epidemics. *Am. Nat.* 164, S79–S89. doi: 10.1086/424610

Prabha, K., Baranwal, V. K., and Jain, R. K. (2013). Applications of next generation high throughput sequencing technologies in characterization, discovery and molecular interaction of plant viruses. *Indian J. Virol.* 24, 157–165. doi: 10.1007/s13337-013-0133-4

Ramsell, J. N. E., Lemmetty, A., Jonasson, J., Andersson, A., Sigvald, R., and Kvarnheden, A. (2008). Sequence analyses of Wheat dwarf virus isolates from different hosts reveal low genetic diversity within the wheat strain. *Plant Pathol.* 57, 834–841. doi: 10.1111/j.1365-3059.2008.01862.x

Razzauti, M., Galan, M., Bernard, M., Maman, S., Klopp, C., Charbonnel, N., et al. (2015). A comparison between transcriptome sequencing and 16S metagenomics for detection of bacterial pathogens in wildlife. *PLoS Negl. Trop. Dis.* 9:e0003929. doi: 10.1371/journal.pntd.0003929

Rochow, W. F. (1970). Barley Yellow Dwarf Virus: phenotypic mixing and vector specificity. *Science* 167, 875–878. doi: 10.1126/science.167.3919.875

Roossinck, M. J. (2010). Lifestyles of plant viruses. *Philos. Trans. R. Soc. Lond. B. Biol. Sci.* 365, 1899–1905. doi: 10.1098/rstb.2010.0057

Roossinck, M. J. (2012). Plant virus metagenomics: biodiversity and ecology. *Annu. Rev. Genet* 46, 359–369. doi: 10.1146/annurev-genet-110711-155600

Roossinck, M. J., and García-Arenal, F. (2015). Ecosystem simplification, biodiversity loss and plant virus emergence. *Curr. Opin. Virol.* 10, 56–62. doi: 10.1016/j.coviro.2015.01.005

Roossinck, M. J., Martin, D. P., and Roumagnac, P. (2015). Plant virus metagenomics: advances in virus discovery. *Phytopathology* 105, 716–727. doi: 10.1094/PHYTO-12-14-0356-RVW

Roossinck, M. J., Saha, P., Wiley, G. B., Quan, J., White, J. D., Lai, H., et al. (2010). Ecogenomics: using massively parallel pyrosequencing to understand virus ecology. *Mol. Ecol.* 19(Suppl. 1), 81–88. doi: 10.1111/j.1365-294x.2009.04470.x

Sameith, K., Roscito, J. G., and Hiller, M. (2016). Iterative error correction of long sequencing reads maximizes accuracy and improves contig assembly. *Brief. Bioinform.* 18:bbw003. doi: 10.1093/bib/bbw003

Saunders, K., Bedford, I. D., Yahara, T., and Stanley, J. (2003). Aetiology: the earliest recorded plant virus disease. *Nature* 422:831. doi: 10.1038/422831a

Sherwood, J. L., German, T. L., Moyer, J. W., and Ullman, D. (2003). Tomato spotted wilt. *Plant Heal. Instr.* 20. doi: 10.1094/PHI-I-2003-0613-02 [Epub ahead of print].

Shi, M., Lin, X. D., Tian, J. H., Chen, L. J., Chen, X., Li, C. X., et al. (2016). Redefining the invertebrate RNA virosphere. *Nature* 540, 539–543. doi: 10.1038/nature20167

Simmonds, P. (2015). Methods for virus classification and the challenge of incorporating metagenomic sequence data. *J. Gen. Virol.* 96, 1193–1206. doi: 10.1099/jgv.0.000016

Simmonds, P., Adams, M. J., Benkō, M., Breitbart, M., Brister, J. R., Carstens, E. B., et al. (2017). Consensus statement: virus taxonomy in the age of metagenomics. *Nat. Rev. Microbiol.* 15, 161–168. doi: 10.1038/nrmicro.2016.177

Sseruwagi, P., Sserubombwe, W. S., Legg, J. P., Ndunguru, J., and Thresh, J. M. (2004). Methods of surveying the incidence and severity of cassava mosaic disease and whitefly vector populations on cassava in Africa: a review. *Virus Res.* 100, 129–142. doi: 10.1016/j.virusres.2003.12.021

Stobbe, A. H., and Roossinck, M. J. (2014). Plant virus metagenomics: What we know and why we need to know more. *Front. Plant Sci.* 5:150. doi: 10.3389/fpls.2014.00150

Storey, H., and McClean, A. P. D. (1930). The transmission of streak disease between maize, sugar cane and wild grasses. *Ann. Appl. Biol.* XVII, 691–719. doi: 10.1111/j.1744-7348.1930.tb07240.x

Susi, H., Filloux, D., Frilander, M. J., Roumagnac, P., and Laine, A. L. (2019). Diverse and variable virus communities in wild plant populations revealed by metagenomic tools. *PeerJ* 7:e7216. doi: 10.7717/peerj.6140

Syller, J., and Grupa, A. (2014). The effects of co-infection by different Potato virus Y (PVY) isolates on virus concentration in solanaceous hosts and efficiency of transmission. *Plant Pathol.* 63, 466–475. doi: 10.1111/PPA.12095

Takami, N. (1901). On dwarf disease of rice plant and "tsumaguro-yokabai". *J. Jpn. Agric. Soc.* 241, 22–30.

Tatineni, S., Graybosch, R. A., Hein, G. L., Wegulo, S. N., and French, R. (2010). Wheat Cultivar-Specific Disease Synergism and Alteration of Virus Accumulation During Co-Infection with Wheat streak mosaic virus and Triticum mosaic virus. *Phytopathology* 100, 230–238. doi: 10.1094/PHYTO-100-3-0230

Thornbury, D. W., Hellmann, G. M., Rhoads, R. E., and Pirone, T. P. (1985). Purification and characterization of potyvirus helper component. *Virology* 144, 260–267. doi: 10.1016/0042-6822(85)90322-8

Timian, R. G. (1974). The range of symbiosis of barley and barley strip mosaic virus. *Phytopathology* 64, 342–345. doi: 10.1094/phyto-64-342

Turechek, W. W., Kousik, C. S., and Adkins, S. (2010). Distribution of four viruses in single and mixed infections within infected watermelon plants in Florida. *Phytopathology* 100, 1194–1203. doi: 10.1094/PHYTO-01-10-0018

Tzanetakis, I. E., and Martin, R. R. (2008). A new method for extraction of double-stranded RNA from plants. *J. Virol. Methods* 149, 167–170. doi: 10.1016/j.jviromet.2008.01.014

Ullman, D. E., German, T. L., Sherwood, J. L., Westcot, D. M., and Cantone, F. A. (1993). Tospovirus replication in insect vector cells: immunocytochemical evidence that the nonstructural protein encoded by the S RNA of tomato spotted wilt tospovirus is present in thrips vector cells. *Phytopathology* 83, 456–463. doi: 10.1094/phyto-83-456

Van Regenmortel, M. H. V. (2007). Virus species and virus identification: past and current controversies. *Infect. Genet. Evol.* 7, 133–144. doi: 10.1016/j.meegid.2006.04.002

Vanterpool, T. C. (1926). Streak or winter blight of tomato in Quebec. *Phytopathology* 16, 311–331.

Vezzi, F., Ormestad, M., Dalen, L., and Guschanski, K. (2017). Estimating the rate of index hopping on the Illumina HiSeq X platform. *bioRxiv* [Preprint]. doi: 10.1101/179028

Visser, M., Bester, R., Burger, J. T., and Maree, H. J. (2016). Next-generation sequencing for virus detection: covering all the bases. *Virol. J.* 13:85. doi: 10.1186/s12985-016-0539-x

Voinnet, O., Pinto, Y. M., and Baulcombe, D. C. (1999). Suppression of gene silencing: a general strategy used by diverse DNA and RNA viruses of plants. *Proc. Natl. Acad. Sci. U.S.A.* 112, 14147–14152. doi: 10.1073/pnas.1513950112

Wang, D., and Maule, A. J. (1995). Inhibition of host gene expression associated with plant virus replication. *Science* 267, 229–231. doi: 10.1126/science.267.5195.229

Wang, Y., Gaba, V., Yang, J., Palukaitis, P., and Gal-On, A. (2002). Characterization of synergy between cucumber mosaic virus and potyviruses in cucurbit hosts. *Phytopathology* 92, 51–58. doi: 10.1094/PHYTO.2002.92.1.51

Whittaker, R. H. (1960). Vegetation of the Siskiyou Mountains, Oregon and California. *Ecol. Monogr.* 30, 279–338. doi: 10.2307/1943563

Whittaker, R. H. (1965). Dominance and Diversity in Land Plant Communities: numerical relations of species express the importance of competition in community function and evolution. *Science* 147, 250–260. doi: 10.1126/science.147.3655.250

Wijkamp, I. (1995). Distinct levels of specificity in thrips transmission of Tospoviruses. *Phytopathology* 85, 1069–1074. doi: 10.1094/Phyto-85-1069

Wildy, P. (1971). "1st Report of the International Committee on Nomenclature of Viruses," in *Monographs in Virology. Vol* 5. Classification and Nomenclature of Viruses, ed. P. Wildy (Basel: Karger Publishers), 7–23. doi: 10.1159/000392076

Wilson, C. R. (2014). *Applied Plant Virology*. Wallingford: CABI Press.

Wintermantel, W. M., Cortez, A. A., Anchieta, A. G., Gulati-Sakhuja, A., and Hladky, L. L. (2008). Co-infection by two criniviruses alters accumulation of each virus in a host-specific manner and influences efficiency of virus transmission. *Phytopathology* 98, 1340–1345. doi: 10.1094/phyto-98-12-1340

Witzany, G. (2012). *Viruses: Essential Agents of Life*. Bürmoos: Springer.

Wood, D. E., Lu, J., and Langmead, B. (2019). Improved metagenomic analysis with Kraken 2. *Genome Biol.* 20:257. doi: 10.1186/s13059-019-1891-0

Wren, J. D., Roossinck, M. J., Nelson, R. S., Scheets, K., Palmer, M. W., and Melcher, U. (2006). Plant virus biodiversity and ecology. *PLoS Biol.* 4:e80. doi: 10.1371/journal.pbio.0040080

Xu, P., Chen, F., Mannas, J. P., Feldman, T., Sumner, L. W., and Roossinck, M. J. (2008). Virus infection improves drought tolerance. *New Phytol.* 180, 911–921. doi: 10.1111/j.1469-8137.2008.02627.x

Zhang, Y. Z., Chen, Y. M., Wang, W., Qin, X. C., and Holmes, E. C. (2019). Expanding the RNA virosphere by Unbiased Metagenomics. *Annu. Rev. Virol.* 6, 119–139. doi: 10.1146/annurev-virology-092818-015851

Zitter, T. A., and Murphy, J. F. (2009). The plant health instructor: cucumber mosaic virus [WWW Document]. *Am. Phytopathol. Soc.* doi: 10.1094/PHI-I-2009-0518-01

Conflict of Interest: The authors declare that the research was conducted in the absence of any commercial or financial relationships that could be construed as a potential conflict of interest.

frontiers in Microbiology

MINI REVIEW
published: 26 October 2020
doi: 10.3389/fmicb.2020.593700

Control of Plant Viruses by CRISPR/Cas System-Mediated Adaptive Immunity

Yongsen Cao[1], Huanbin Zhou[1], Xueping Zhou[1,2] and Fangfang Li[1]**

[1] State Key Laboratory for Biology of Plant Diseases and Insect Pests, Institute of Plant Protection, Chinese Academy of Agricultural Sciences, Beijing, China, [2] State Key Laboratory of Rice Biology, Institute of Biotechnology, Zhejiang University, Hangzhou, Zhejiang, China

Plant diseases caused by invading plant viruses pose serious threats to agricultural production in the world, and the antiviral engineering initiated by molecular biotechnology has been an effective strategy to prevent and control plant viruses. Recent advances in clustered regularly interspaced short palindromic repeats (CRISPR)/CRISPR-associated (Cas) system-mediated DNA or RNA editing/interference in plants make them very attractive tools applicable to the plant protection field. Here, we review the development of CRISPR/Cas systems and summarize their applications in controlling different plant viruses by targeting viral sequences or host susceptibility genes. We list some potential recessive resistance genes that can be utilized in antiviral breeding and emphasize the importance and promise of recessive resistance gene-based antiviral breeding to generate transgene-free plants without developmental defects. Finally, we discuss the challenges and opportunities for the application of CRISPR/Cas techniques in the prevention and control of plant viruses in the field.

Keywords: CRISPR, Cas proteins, plant virus, recessive resistance genes, antiviral engineering

OPEN ACCESS

Edited by:
Kristiina Mäkinen, University of Helsinki, Finland

Reviewed by:
Donato Gallitelli, University of Bari Aldo Moro, Italy
Vicente Pallas, Polytechnic University of Valencia, Spain

****Correspondence:***
Xueping Zhou
zzhou@zju.edu.cn
Fangfang Li
lifangfang@caas.cn;
Elva1988@163.com

Specialty section:
This article was submitted to Microbe and Virus Interactions with Plants, a section of the journal Frontiers in Microbiology

Received: *11 August 2020*
Accepted: *28 September 2020*
Published: *26 October 2020*

Citation:
Cao Y, Zhou H, Zhou X and Li F (2020) Control of Plant Viruses by CRISPR/Cas System-Mediated Adaptive Immunity. Front. Microbiol. 11:593700. doi: 10.3389/fmicb.2020.593700

INTRODUCTION

Plant diseases caused by plant pathogens, including bacteria, fungi, nematodes, and viruses in different crops, lead to enormous economic losses worldwide. Plant viruses cause almost half of plant diseases, and the annual global cost of viral infection of cultivated crops is estimated to be more than US$ 30 billion (Nicaise, 2014; Sastry and Zitter, 2014). About 1,500 plant virus species, grouped into 26 families, have been identified and characterized based on viral genome sequences so far[1]. Plant viruses are a class of obligate intracellular parasites, with minimal coding capacity, which heavily rely on their host to complete their infection/life cycle. Unlike in the case of other pathogens, there are barely any efficient antibiotics or other chemicals that can eliminate an infecting plant virus without perturbing host cells. Therefore, molecular plant breeding plays a pivotal role in generating virus immunity, virus resistance, or virus-tolerant plants in agricultural production to prevent and control plant viruses.

CRISPR (clustered regularly interspaced short palindromic repeats)/CRISPR-associated (Cas) systems, derived from bacterial and archaeal sources, serve as an important adaptive immunity against invading nucleic acids. With the fast development of our understanding of CRISPR/Cas systems, they have been converted into convenient tools to edit endogenous and exogenous DNA or RNA sequences in different organisms. To date,

[1]https://talk.ictvonline.org/taxonomy/

a simplified CRISPR system only contains an easily engineered guide RNA (gRNA) and a Cas effector protein. Based on the different characteristics of Cas proteins in sequence, structure, and function, CRISPR/Cas systems are separated into two distinct classes (Makarova et al., 2015, 2017a,b). Class 1 of CRISPR/Cas systems contains types I, III, and IV, which utilize a multi-protein effector complex (Makarova et al., 2017a). In contrast, class 2 of CRISPR/Cas systems includes types II, V, and VI, which achieve target editing only with a single effector protein (Makarova et al., 2017b; Shmakov et al., 2017). Therefore, class 2 CRISPR/Cas systems have been widely adopted and utilized for nucleic acid manipulation and detection (Hsu et al., 2013; Garcia-Doval and Jinek, 2017; Ji et al., 2019; **Table 1**). Among them, the type II and V Cas proteins are utilized to edit DNA, and the type VI Cas proteins are applied for editing RNA. In the past few years, CRISPR/Cas system-mediated gene editing technology has been introduced rapidly into plant genetic engineering to generate resistance against viruses and other pathogens (Hadidi et al., 2016; Ma et al., 2016; Langner et al., 2018; Mahas and Mahfouz, 2018; Chen et al., 2019; Li and Wang, 2019; Li et al., 2019; Zhang et al., 2019b). Generally, there are two main strategies to utilize CRISPR/Cas technology to control plant viruses (**Figure 1**). One approach is to target, destroy, and interfere with the viral genome to inhibit the replication and infection of invading viruses. The other one is to manipulate host susceptibility factors required for the viral infection/life cycle in order to enhance plant immunity and block virus invasion.

CRISPR/Cas SYSTEM-MEDIATED RESISTANCE TO PLANT VIRUSES BY TARGETING THE VIRAL GENOME

CRISPR/Cas System-Mediated Resistance to Plant DNA Viruses

Geminiviridae and Caulimoviridae are two major destructive plant DNA virus families that contain 485 species with single-stranded DNA (ssDNA) genome and 85 species with double-stranded DNA (dsDNA) genome, respectively, see text foot note 1. Multiple independent works have aimed to directly target and destroy the genomic DNA of geminiviruses or caulimoviruses by plant gene editing technologies. Before the emergence of the CRISPR/Cas systems, the zinc finger nucleases (ZFNs) and transcription activator-like effector nucleases (TALENs) have been applied to manipulate the host and viral DNAs in plants. ZFN- and TALEN-mediated resistance to several geminiviruses, including tomato yellow leaf curl China virus (TYLCCNV) and tobacco curly shoot virus (TbCSV), by targeting the viral genomic replication-associated region has been reported (Chen et al., 2014; Cheng et al., 2015). Compared to ZFN- and TALEN-mediated DNA editing technologies, CRISPR/Cas systems have more advantages in manipulation, so they have rapidly become more popular and promising in antiviral engineering in plants.

CRISPR/Cas9 constructs with single guide RNAs (sgRNAs) targeting the viral replication-associated region, or intergenic region (IR), have exhibited effective DNA interference and conferred viral resistance against beet severe curly top virus (BSCTV), cotton leaf curl Multan virus (CLCuMuV), and bean yellow dwarf virus (BeYDV) in transgenic *Nicotiana benthamiana* or *Arabidopsis thaliana* plants, respectively (Baltes et al., 2015; Ji et al., 2015; Yin et al., 2019). Targeting the tomato yellow leaf curl virus (TYLCV) genome with Cas9–single guide RNA at the sequences encoding the coat protein (CP) or replicase (Rep) resulted in efficient virus interference, as evidenced by the low accumulation of the TYLCV DNA genome in the transgenic tomato and *N. benthamiana* plants (Tashkandi et al., 2018). The sgRNAs targeting the stem-loop sequence compared to the sgRNAs targeting the viral CP region and the replication-associated region within the IR displayed a more effective interference of several geminiviruses including the monopartite geminivirus, cotton leaf curl Kokhran virus (CLCuKoV), the bipartite geminivirus, Merremia mosaic virus (MeMV), and different severe and mild strains of TYLCV geminiviruses (Ali et al., 2016). These findings suggest that CRISPR/Cas9-induced variants in open reading frames (ORFs) but not the IR of geminiviruses are capable of replication and systemic movement, thereby evading the CRISPR/Cas9 machinery. The use of this system by a single sgRNA targeting the conserved stem-loop sequence of the origin of replication in the TYLCV intergenic region was also able to render plants broad-spectrum resistance to other geminiviruses, including a monopartite geminivirus, beet curly top virus (BCTV), and a bipartite geminivirus, MeMV (Ali et al., 2015).

With the fast development of CRISPR/Cas9 system-based technologies, more and more successful examples show the promising resistance to plant DNA viruses. For example, a CRISPR/Cas9 system duplexed with sgRNAs targeting the movement protein (MP) or CP region established resistance to wheat dwarf virus (WDV) or banana streak virus (BSV), respectively (Kis et al., 2019; Tripathi et al., 2019). This approach shall also provide new avenues for engineering cotton against cotton leaf curl disease (CLCuD), mediated by cotton leaf curl virus (CLCuV), a key limiting factor for cotton productivity worldwide (Uniyal et al., 2019). The initial success of transgenic plants engineered by CRISPR/Cas9 systems resistant to geminiviruses points out the potential of a similar strategy against other severe ssDNA viruses, like banana bunchy top virus (BBTV), which causes devastating damage to the whole banana industry in Southern China (Rao et al., 2017).

In addition, CRISPR/Cas9-mediated immunity has been recently utilized to defend against plant dsDNA viruses. *A. thaliana* transgenic plants consistently expressing both Cas9 protein and sgRNAs targeting the CP region of cauliflower mosaic virus (CaMV) in the Caulimoviridae family conferred effective resistance to this species (Liu et al., 2018).

CRISPR/Cas System-Mediated Resistance to Plant RNA Viruses

Recently, some RNA targeting and editing CRISPR-associated proteins were found, such as Cas9 derived from *Francisella novicida* (FnCas9) and Cas13a (formerly called C2c2) from *Leptotrichia shahii* (LshCas13a) (Price et al., 2015; Shmakov et al.,

TABLE 1 | CRISPR/Cas system-mediated resistance to plant viruses by targeting the viral genome, host factors, and some potential recessive targets using genome editing systems.

Targets	Viruses	Applied systems	Potential recessive resistance targets (Without development defects)	Viruses
Viral replication region	TYLCCNV, TbCSV	ZFN	AOCl,AT4CLI,BAMI,CML38,CML39,	Geminiviruses
Viral IR region/replication region	TYLCCNV, TbCSV	TALEN	CPHSC70-1, CSNs, deltaCOP, GRAB2, HSC70, NSI, NsAK, PLP2, rgs-CaM, SCE1, SK4-I/SKK, SYTA1	
Vil-HI IR region /replication region	BeYDV. CLCuMuV	CRlSPR/SpCas9		
Viral IR region/replication region/ CP	BCTV, CLC'uKoV, McMV, TYLCV	CRJSPR/SpCas9	u-EXPA, bZIP60, CK2, cPGK, DBP1, DDXs, DnaJ-like proteins, eEFl A, eEFIB, eEF4E, eEF4G, eEF4G2, eEF(iso)4E, GRF6, IREl A, IRE1B, NBR1, PABPs, PCaPl, PVIPs, RAV2, RHs (RH8, RH9), Sec24a, SYTA1, SYP71	Potyviruses
Viral genome region	BSCTV	C'RISPR/SpCas9	l > ZIP60, CAT1, cPGK, eEFIB, EXA1	Potexviruses
Viral long IR region/MP/CP/ replication region	WDV, BSV	CRlSPR/SpCas9	ARL8a/8b, eEFIA, SYTA1, TOM1, TOM2A, TOM3	Tobamoviruses
Viral CP	CaMV	CRISPR/SpCas9	Chl-PCK, eEFlA	BaMV
Viral coding ORF/non-coding region/3′ UTR	TMV, CMV	CRISPR/FnCas9	PDIL5-1	BaYMV, BaMMV
Viral HC-Pro/CP/GFP region	TuMV (TuMV-GFP)	CRISPR/LshCasl3a, Rfi(Casl3d	FDH, CRT3, HAT1, HAT2, HAT3, VPS41	CMV
Viral coding ORF	TMV, SRBSDV	(RlSPR LshCa.sl3a	PDLP1/PDLP2/PDLP3	GFLV.CaMV
Viral NIh/P3/Cl/CP region	PVY	C'RISPR/LshCasl3a	EXAI	LoLV
Host gene elF4E	CVYV, ZYMV, PRSV-W, TuMV	CRISPR'SpCas9	eEFIA, ESCRT, GAPDH, RAB5, SYPK1	TBSV
Host gene elF4E	C1YVV	CRISPR/nCaaS-cytidine deaminase	SYTA1	TVCV
Host gene el F4G	RTSV	CRISPR/SpCas9	CPR5	RYMV
Host gene elF(iso)4E	TuMV	CRISPR/SpCas9	RIM1.SAMS1	RDV
Host gene nCBP-l/nCBP-2	CBSV	CRISPR/SpCas9	RHD3	TSWV

The known targets in light blue background are used in antiviral engineering by genome editing technologies, which can be viral replication regions, viral open reading frames (ORFs), viral non-coding regions, or the host factors required for viral infection. The potential recessive targets in light yellow background which are suppressors of plant defenses, the susceptibility factors required for viral translation/replication/movement or other life cycles, the factors in the cellular metabolism, or the modified factors for the benefit of the viral infection or viral protein functions, etc., can be utilized in antiviral engineering by genome editing technologies. The abbreviations of the virus names in this table are as follows: BaMMV, barley mild mosaic virus; BaYMV, barley yellow mosaic virus. Caulimoviruses: BSV, banana streak virus; CaMV, cauliflower mosaic virus; CMV, cucumber mosaic virus; CMV-GFP, cucumber mosaic virus carrying GFP. Geminiviruses: BCTV, beet curly top virus; BeYDV, bean yellow dwarf virus; BSCTV, beet severe curly top virus; CLCuKoV, cotton leaf curl Kokhran virus; CLCuMuV, cotton leaf curl Multan virus; MeMV, Merremia mosaic virus; TbCSV, tobacco curly shoot virus; TYLCCNV, tomato yellow leaf curl China virus; TYLCV, tomato yellow leaf curl virus; TYLCSV, tomato yellow leaf curl Sardinia virus; WDV, wheat dwarf virus; GFLV, grapevine fan leaf virus; LoLV, Lolium latent virus. Potyviruses: CBSV, cassava brown streak virus; ClYVV, clover yellow vein virus; CVYV, cucumber vein yellowing virus; PRSV-W, papaya ringspot virus-W; PVY, potato virus Y; TuMV, turnip mosaic virus; TuMV-GFP, turnip mosaic virus carrying GFP; ZYMV, zucchini yellow mosaic virus; TBSV, tomato bushy stunt virus; RDV, rice dwarf virus; RTSV, rice tungro spherical virus; RYMV, rice yellow mottle virus; SRBSDV, southern rice black-streaked dwarf virus; TMV, tobacco mosaic virus; TMV-GFP, tobacco mosaic virus carrying GFP; TSWV, tomato spotted wilt virus. The abbreviations of the gene names in this table are listed as follows. Potential recessive resistance targets that function in the infection of geminiviruses: AOC1, allene oxide cyclase 1; AT4CL1, 4-coumarate: CoA ligase; BAM1, barely any meristem 1; CML38/39, calmodulin-like protein 38/39; CPHSC70-1, chloroplastic HSC70-1; CSNs, COP9 signalosome subunits; delta COP, coatomer delta subunit; GRAB2, geminivirus Rep A-binding; HSC70, heat shock protein cognate; NSI, nuclear acetyltransferase I; NsAK, a proline-rich extensin-like receptor protein kinase (PERK); PLP2, patatin-like protein 2; rgs-CaM, regulator of RNA silencing, calmodulin-like protein; SCE1, SUMO, conjugating enzyme E1; SK4-1/SKK, shaggy-related kinase proteins. Potential recessive resistance targets that function in the infection of potyviruses: α-EXPA1, expansin; bZIP60, basic-leucine zipper transcription factor 60; cPGK, nuclear-encoded chloroplast phosphoglycerate kinase; DDXs or RHs, DEAD-box RNA helicase; eEF1, eukaryotic translation elongation factor 1A/1B; eIF4s/eIF(iso)4s, eukaryotic translation initiation factors 4/isoform factors 4 [eIF4E, eIF4G, eIF4G2, eIF(iso)4E, etc.]; GRF6, 4-3-3 family protein; IRE1, inositol requiring protein-1; NBR1, neighbor of BRCA1 gene 1; PABPs, polyA-binding proteins; PCaP1, plasma membrane-associated cation-binding protein-1; PVIPs, potyvirus VPg-interacting proteins; RAV2, ethylene-inducible host transcription factor; Sec24a, a COPII coatomer; SYTA1, synaptotagmin 1; Syp71, snare protein 71. Potential recessive resistance targets that function in the infection of CMV: FDH, formate dehydrogenase; CRT3, calreticulin-3; HATs, homeodomain-leucine zipper proteins 1/2/3; VPS41, vacuolar protein sorting 41. Potential recessive resistance targets that function in the infection of potexviruses: bZIP60; CAT1, catalase 1; cPGK; EXA1, essential for poteXvirus accumulation 1, including a putative eIF4E-binding motif and a GYF domain protein. Potential recessive resistance targets that function in the infection of tobamoviruses: ARL8a/8b, a small GTP-binding ARF family protein 8a/8b; TOM, tobamovirus multiplication (TOM1, TOM2A, and TOM3). Potential recessive resistance targets that function in the infection of some other viruses: chl-PGK, chloroplast phosphoglycerate kinase; CPR5, also referred to as the RYMV2 gene; ESCRT, endosomal sorting complexes required for transport; GAPDH, glyceraldehyde 3-phosphate dehydrogenase; PDIL5-1, protein disulfide isomerase-like 5-1; PDLP1/2/3, plasmodesmata-located proteins 1/2/3; RHD3, root hair defective 3; RIM1, rice dwarf virus multiplication 1, related to an Arabidopsis NAC domain protein (ANAC028); SAMS, S-adenosyl-L-methionine synthetase.

2015). Among them, LshCas13a is the first Cas13 ortholog to be harnessed for programmable RNA-targeting activities, which expanded the application of CRISPR/Cas systems from DNA to RNA (Abudayyeh et al., 2016). The LshCas13a protein combined with the protospacers can be bioengineered to knock down specific mRNAs in bacteria (Abudayyeh et al., 2017), which offered virologists an alternative CRISPR/Cas system to fight against pathogenic RNA viruses. Therefore, RNA viruses can

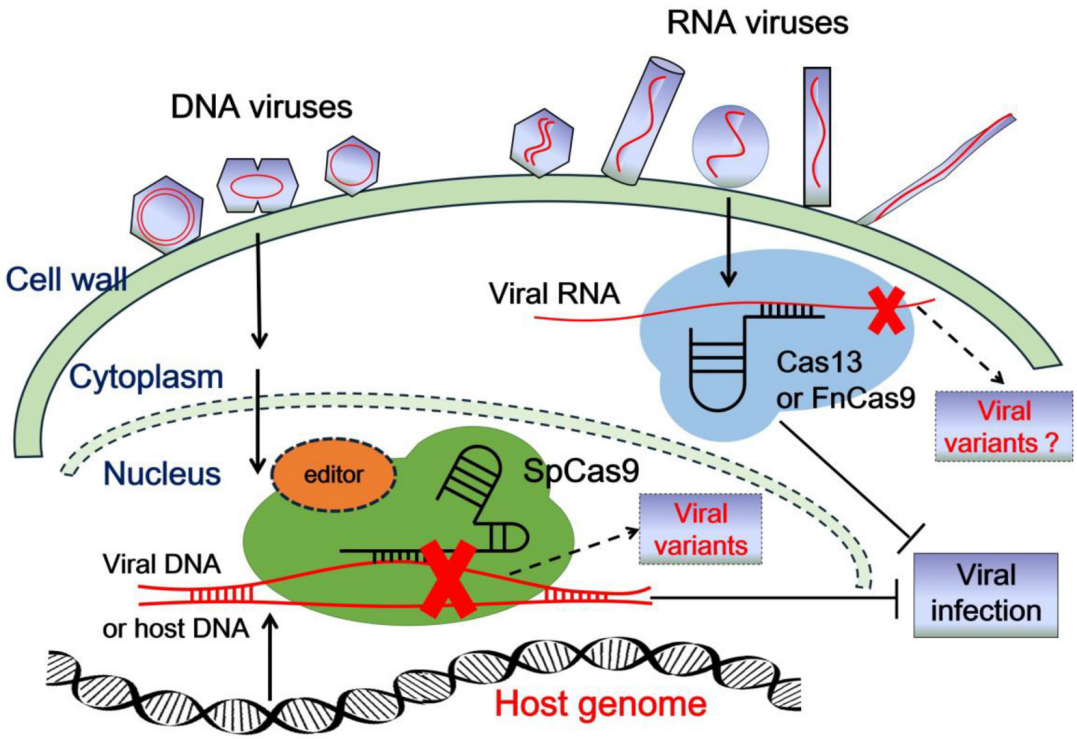

FIGURE 1 | Schematic representation of class 2 CRISPR/Cas systems to confer resistance to plant viruses. After plant viruses enter into plant cells, the viral genome is uncoated and transcribed, or translated with the help of host factors. Plant viruses then multiply their genome in the nucleus or in the cytoplasm. The viral genome DNA or RNA can be targeted, destroyed, or interfered with by CRISPR/Cas9 or CRISPR/Cas13 (or FnCas9) systems in the nucleus or in the cytoplasm, respectively, which inhibits viral infection. In addition, the mutation or deficiency in host susceptibility factors edited by the CRISPR/Cas9 system also perturbs viral infection. However, some new viral variants might be generated as by-products when CRISPR/Cas systems edit the viral genome, which might drive the risk of viral evolution.

be directly interfered with by targeting their genome through a CRISPR/Cas system with these new types of Cas effector proteins. Programmable FnCas9 protein and an RNA-targeting gRNA (rgRNA) could target a single-stranded RNA (ssRNA) virus, hepatitis C virus (HCV) in mammalian cells, resulting in the inhibition of viral protein production (Price et al., 2015). A plant codon-optimized version of FnCas9 paired with rgRNA targeting plant ssRNA viruses was also employed to gain viral resistance to cucumber mosaic virus (CMV) and tobacco mosaic virus (TMV) in transgenic *N. benthamiana* and *A. thaliana* plants, respectively (Zhang T. et al., 2018).

Another RNA-targeting CRISPR/Cas system using the class 2 type VI-A CRISPR/Cas effector, LshCas13a, has been characterized and programmed to cleave ssRNA viruses in plants. As expected, LshCas13a with a sgRNA targeting viral RNA sequences exhibited rapid and effective RNA interference to turnip mosaic virus (TuMV), wherein sgRNA was driven by a pea early browning virus (PEBV) promoter in a tobacco rattle virus (TRV)-based vector in LshCas13a transgenic *N. benthamiana* or *A. thaliana* plants, respectively (Aman et al., 2018a,b). Similarly, resistance to TMV, rice stripe mosaic virus (RSMV), and Southern rice black-streaked dwarf virus (SRBSDV) in transgenic tobacco and rice harboring LshCas13a specifically targeting viral RNA was also confirmed using this system (Zhang et al., 2019a). By targeting the P3-, NIb-, or CP-coding sequences in the potato virus Y (PVY) genomic region, this CRISPR/Cas13a system also showed its effectiveness in interfering with and inhibiting PVY infection (Zhan et al., 2019).

Furthermore, a new protein of Cas13 from *Ruminococcus flavefaciens* was characterized and classified into the type VI-D effector, named Cas13d (CasRx). This Cas13d effector with two higher eukaryotic and prokaryotic nucleotide-binding domains (HEPN) that dictate CRISPR RNA maturation and target cleavage also possesses RNase activity to target ssRNA (Konermann et al., 2018). Researchers found that Cas13d showed great advantages over Cas13a, Cas13b, or other Cas13 variants when it was used to interfere with TuMV infection by targeting the GFP, CP, or HC-Pro region in the TuMV-GFP genome (Mahas et al., 2019). Similarly, the Cas13d-mediated RNA interference system was also applied in mammalian cells to combat the novel coronavirus SARS-CoV-2 as well as influenza (Abbott et al., 2020).

CRISPR/Cas SYSTEM-MEDIATED RESISTANCE TO PLANT VIRUSES BY TARGETING HOST FACTORS

Plant viruses recruit their host cellular translation factors not only to translate their viral RNAs but also to facilitate

their other infection processes, so the translation-related host factors were initially identified as pro-viral factors. Later, more and more pro-viral host factors, including translation/replication/movement/metabolism-related genes, have been identified and characterized and exploited to control viral diseases in plants. Recessive resistance is conferred by a recessive gene mutation that encodes a host factor critical for viral infection/life cycle or encodes a negative regulator of plant defense responses (Hashimoto et al., 2016). Therefore, it is ideal for obtaining a targeted recessive gene mutant by CRISPR/Cas systems. Eukaryotic translation initiation factors eIF4E, eIF4G, and their isoforms, eIF(iso)4E and eIF(iso)4G, are the most widely exploited recessive resistance genes required for plant RNA virus–protein translation processes in several crop species, and they are effective in defending against a subset of viral species (Lellis et al., 2002; Robaglia and Caranta, 2006; Wang and Krishnaswamy, 2012; Sanfaçon, 2015; Wang, 2015; Hashimoto et al., 2016). It has been reported that CRISPR/Cas9-edited *eIF4E*-knockout cucumber showed complete resistance to zucchini yellow mosaic virus (ZYMV), papaya ringspot mosaic virus-W (PRSV-W), and cucumber vein yellowing virus (CVYV) (Chandrasekaran et al., 2016). Also, a novel allele of rice, *eIF4G*, generated by CRISPR/Cas9-targeted mutagenesis showed resistance to rice tungro spherical virus (RTSV) (Macovei et al., 2018). The induced mutation in CRISPR/Cas9-mediated *eIF(iso)4E* in cassava and *A. thaliana* conferred full resistance to cassava brown streak virus (CBSV) or TuMV-GFP, respectively (Pyott et al., 2016; Gomez et al., 2019). Cassava encodes some alternative eIF4E-like proteins: novel cap-binding protein-1 (nCBP-1) and nCBP-2. When CRISPR/SpCas9 was used to target nCBP-1 or nCBP-2 in cassava plants, the mutant plants displayed successful resistance to CBSV (Gomez et al., 2019). The newly emerged CRISPR–Cas9n–cytidine base editor was also applied in antivirus engineering, which could convert the *Arabidopsis eIF4E1* susceptibility allele into a resistance allele by introducing the N176K mutation to generate clover yellow vein virus (ClYVV)-resistant plants (Bastet et al., 2019). Recently, a soybean PBS1 decoy protein modified to contain a cleavage site for the soybean mosaic virus (SMV) NIa protease triggers cell death in soybean protoplasts, indicating that this CRISPR/Cas system can also be utilized to generate soybean resources resistant to SMV (Helm et al., 2019).

However, the current establishment of efficient, recessive resistance-type antiviral strategies was mainly dependent on eIF4s and their homologs against potyviruses and some related plant viruses. Therefore, more host susceptibility genes need to be identified and applied to obtain effective genetic resources against many other economically important plant viruses.

THE PROMISING HOST SUSCEPTIBILITY GENES FOR ANTIVIRAL ENGINEERING IN PLANTS

Although many dominant resistance genes against plant viruses have been identified, they are often genetically linked to undesired traits, including low yield, poor flavor, small size, and even developmental abnormities. Therefore, these resistance genes would not be valuable in antivirus engineering. Similarly, many host susceptibility genes involved in viral infection also affect plant viability. For example, the *Arabidopsis ssi2* mutant, which accumulates high levels of the plant defense hormone salicylic acid (SA), confers resistance to CMV, but shows an abnormal growth phenotype (Sekine et al., 2004).

Here, we list some promising potential host factors to explore for antiviral breeding whose mutation or deficiency would not perturb plant growth or development, but can still confer resistance to many plant viruses mainly based on these reports (Lozano-Durán et al., 2011; Wang, 2015; Hashimoto et al., 2016; Garcia-Ruiz, 2018; Li and Wang, 2019; Li et al., 2019; Mäkinen, 2020; **Table 1**). Most of these host factors are related to viruses of the Geminiviridae family (nine genera, 485 species) and the Potyviridae family (12 genera, 228 species), which constitute almost half of the plant viruses described to date see text foot note 1 and cause devastating diseases in economically important crops. Based on the functions of these host factors, we classified them into four groups as follows:

(1) The negative regulators of plant defenses, such as rgs-CaM that inhibited RNA silencing through repressing the transcription level of RDR6 and degrading the SGS3 protein *via* autophagy (Li et al., 2018), and homeodomain leucine zipper protein 1 (HAT1) and its related genes HAT2 and HAT3, whose mutation conferred loss-of-susceptibility to CMV infection by accumulating high levels of SA and jasmonic acid (JA) (Zou et al., 2016).

(2) The susceptible factors involved in viral replication/translation/movement or other life cycles, such as tobamovirus multiplication 1 (TOM1) and its homologs involved in the replication of tobamoviruses (Yamanaka et al., 2000), eEF1A and eEF4s involved in the translation of potyviruses, and PCaP1 (plasma membrane-associated cation-binding protein-1) and Sec24a(a COPII coatomer) involved in the movement of potyviruses (Wang, 2015).

(3) The host factors participating in the modification of viral proteins to achieve their effective function in the infection, such as shaggy-related protein kinases (SK4-1, NsAK, etc.) which could interact with and phosphorylate geminiviral C4 proteins, and are required to trigger disease symptoms (Lozano-Durán et al., 2011). The CP protein of potato virus A (PVA) is phosphorylated by cellular CK2, and the phosphorylated CP interacts with ubiquitin ligase CP-interacting protein (CPIP) and HSP90, which is required for PVA replication and CP accumulation (Lõhmus et al., 2017).

(4) The factors involved in the cellular processes beneficial for virus behaviors, such as phenylpropanoid metabolism factor (4-coumarate:CoA ligase1, 4CL1) or secondary cell wall synthesis factor (Bearskin2B, BRN2), whose silencing in phloem tissue delays geminivirus infection (Lozano-Durán et al., 2011).

The above recessive genetic resources can be obtained by a regular CRISPR/Cas9 system, and the corresponding transgene-free resources can also be further generated by genetic crossing to remove the Cas9 protein out. Different strategies to deliver the constructs expressing Cas proteins or sgRNAs to the plant have been reported and improved. The use of viral vectors to deliver sgRNAs and/or Cas proteins vastly enhanced the efficiency of

this system due to the rapid and robust amplification/expression of sgRNAs and/or Cas proteins during virus infection. In addition, the virus vector-based CRISPR/Cas9 system was able to produce plants with the desired traits without the involvement of laborious and time-intensive tissue culture practices. For example, the CRISPR/Cas9 system based on DNA viruses (BeYDV, WDV, and cabbage leaf curl virus) and RNA viruses (TRV, PEBV, TMV, beet necrotic yellow vein virus, and barley stripe mosaic virus) have demonstrated efficient gene targeting frequencies in model plants (*N. benthamiana* and *A. thaliana*) and crops (potato, tomato, rice, wheat, and maize) (Cody et al., 2017; Zaidi and Mansoor, 2017; Hameed et al., 2018; Hu et al., 2019; Jiang et al., 2019). In order to decrease the off-target effects of antiviral strategies mediated by the CRISPR/Cas9 system in plants, (Ji et al., 2018) developed two virus-induced gene editing vectors, in which the pV86 and pC86 promoters of BSCTV were *trans*-activated by co-infecting BSCTV. These BSCTV-inducible vectors were spatially and temporally responsive and inhibited BSCTV accumulation in both transient (*N. benthamiana*) and transgenic (*A. thaliana*) assays without off-target defect. A recent report showed that the sonchus yellow net virus (SYNV)-delivered transgene-free CRISPR/Cas9 system could generate the genetic resources only by one step (Ma et al., 2020), which would save time and labor in breeding procedures. In addition, SYNV is a negative-stranded RNA virus that cannot be integrated into the plant genome or inherited into the next seedlings. Therefore, it is promising to deliver some other CRISPR/Cas editing agents by this system, such as base editors and primer editors, in order to achieve more specific and accurate gene editing results in the future (Anzalone et al., 2020). However, the SYNV-delivered transgene-free CRISPR/Cas9 system only works in *N. benthamiana* plants, which would limit its application in crops. Therefore, more convenient and optimized virus-mediated CRISPR/Cas9 systems need to be explored and applied in antiviral engineering.

THE POTENTIAL RISK OF CRISPR/CAS SYSTEMS IN ANTIVIRAL ENGINEERING

The CRISPR/Cas systems provide many valuable tools and new thoughts in creating gene loss-of-function and gain-of-function mutants of plants, especially for economic crops. In the plant virus-combating arsenal, the interaction and battle between host plants and viruses never end. When plant virologists are determined to control the dissemination of plant DNA virus by using CRISPR/Cas9 technology to interfere with and destroy viral genome DNA, some accompanying challenges also come out.

The mutation or recombination of endogenous genes would lead to inactivate their function, while the sequence variations of plant viruses generated by genome editing technologies would probably facilitate viral evolution. It has been shown that mutation, recombination, and reassortment are the main driving forces of plant RNA viruses, and the first two are that of plant DNA viruses. Mehta et al. found transgenic cassava plants with the expressions of both Cas9 and a sgRNA targeting the overlapping regions of AC2 and AC3 of African cassava mosaic virus (ACMV) failing to confer any resistance to ACMV infection. The depth analysis of the full-length viral genomes in transgenic plants revealed about 33–48% of inserted geminiviruses. Although these new variants of ACMV generated by CRISPR/Cas9 could not proliferate themselves alone, they are able to rely on wild-type ACMV to accumulate in *N. benthamiana* (Mehta et al., 2019). Ali et al. and Liu et al. also showed the CRISPR/Cas9-mediated targeting of viral ORFs that generated more viral variants, which may result in different levels of viral escape events, raising the possibility that this system has the potential to create and allow the dissemination of mutant viruses from plants even with multiple gRNAs (Ali et al., 2016; Liu et al., 2018). However, the combinations of two single gRNAs, especially those far from each other, would substantially delay resistance breakdown compared to a single sgRNA (Liu et al., 2018). Also, there exist off-target effects when the CRISPR/Cas9 system was applied in *A. thaliana* plants, indicating that this system would possibly entail unpredictable risks (Zhang Q. et al., 2018). In addition, the presence of folded dsRNA domains in sgRNAs could generate small interfering RNAs (siRNAs), which could reduce the abundance of sgRNAs, a possibility that should be considered in the future application of the CRISPR/Cas9 system.

Therefore, the cases and risks that viruses escaped from the CRISPR/Cas system-mediated antiviral immunity in plants warn that the CRISPR/Cas system may be considered as a double-edged sword in antiviral engineering. Although it can target, destroy, or interfere with the viral genome to inhibit viral infection, it raises an important issue that the new viral variants or species may be generated as genome editing by-products, indicating that it would speed up the virus evolution or that the obtained transgenic crops may lose their specific resistance to these viruses.

CONCLUSION AND FUTURE PERSPECTIVES

Molecular breeding has played a pivotal role in the prevention and control of plant viruses causing diseases, and the emergence and development of CRISPR/Cas technologies would speed up the generation and obtainment of new resistance resources. With the development and understanding of CRISPR/Cas systems and the exploration and function identification of recessive resistance genes, the resistance materials with the mutation or deficiency in host susceptibility factors generated by CRISPR/Cas systems would better benefit viral prevention and control in the field. Compared to targeting, destroying, or interfering with viral genomes, which might increase the risks of viral evolution, the editing of recessive resistance genes would have a promising perspective in engineering-resistant plants against plant viruses. Additionally, host susceptibility genes for insect vectors can be important targets by CRISPR/Cas systems to prevent the viral spread and dissemination. Of note is that it is also useful for antiviral engineering by utilizing newly developed CRISPR/Cas systems. For instance, the transcriptional

activation of many plant-dominant resistance genes by CRISPR-Act2.0 would enhance the plant immunity to confer a broad range of resistance to different kinds of pathogens (Lowder et al., 2018), and the primer editor is also an interesting alternative applied into the antiviral engineering (Anzalone et al., 2019). The multiplexed CRISPR technologies, in which numerous gRNAs or Cas proteins are expressed at once, have vastly enhanced the scope and efficiency of genetic editing and transcriptional regulation (McCarty et al., 2020). However, the application of these multiplexed CRISPR technologies into the field to control plant viruses is still on the way, mainly because of the complexity of experimental manipulation, the limitations of the genetic transformation of several simultaneous Cas proteins into one plant, and the lack of validated and effective endogenous targets against different viruses, among other things (McCarty et al., 2020).

AUTHOR CONTRIBUTIONS

FL, HZ, and XZ conceived the project. YC, FL, and XZ wrote the manuscript with contributions from all authors.

FUNDING

This work was funded by the National Natural Science Foundation of China (31972244 and 31930089).

ACKNOWLEDGMENTS

Apologies to colleagues whose work could not be discussed due to space limitations.

REFERENCES

Abbott, T., Dhamdhere, G., Liu, Y., Lin, X., Goudy, L., Zeng, L., et al. (2020). Development of CRISPR as an antiviral strategy to combat SARS-CoV-2 and influenza. *Cell* 181, 865–876. doi: 10.1016/j.cell.2020.04.020

Abudayyeh, O., Gootenberg, J., Essletzbichler, P., Han, S., Joung, J., Belanto, J., et al. (2017). RNA targeting with CRISPR-Cas13. *Nature* 550, 280–284.

Abudayyeh, O., Gootenberg, J., Konermann, S., Joung, J., Slaymaker, I., Cox, D., et al. (2016). C2c2 is a single-component programmable RNA-guided RNA-targeting CRISPR effector. *Science* 353:aaf5573. doi: 10.1126/science.aaf5573

Ali, Z., Abulfaraj, A., Idris, A., Ali, S., Tashkandi, M., and Mahfouz, M. (2015). CRISPR/Cas9-mediated viral interference in plants. *Genome Biol.* 16:238.

Ali, Z., Ali, S., Tashkandi, M., Zaidi, S. S., and Mahfouz, M. (2016). CRISPR/Cas9-mediated immunity to geminiviruses: differential interference and evasion. *Sci. Rep.* 6:26912.

Aman, R., Ali, Z., Butt, H., Mahas, A., Aljedaani, F., Khan, M. Z., et al. (2018a). RNA virus interference via CRISPR/Cas13a system in plants. *Genome Biol.* 19:1.

Aman, R., Mahas, A., Butt, H., Aljedaani, F., and Mahfouz, M. (2018b). Engineering RNA virus interference via the CRISPR/Cas13 machinery in *Arabidopsis*. *Viruses* 10:732. doi: 10.3390/v10120732

Anzalone, A., Koblan, L., and Liu, D. (2020). Genome editing with CRISPR-Cas nucleases, base editors, transposases and prime editors. *Nat. Biotechnol.* 38, 824–844. doi: 10.1038/s41587-020-0561-9

Anzalone, A., Randolph, P., Davis, J., Sousa, A., Koblan, L., Levy, J., et al. (2019). Search-and-replace genome editing without double-strand breaks or donor DNA. *Nature* 576, 149–157. doi: 10.1038/s41586-019-1711-4

Baltes, N., Hummel, A., Konecna, E., Cegan, R., Bruns, A., Bisaro, D., et al. (2015). Conferring resistance to geminiviruses with the CRISPR-Cas prokaryotic immune system. *Nat. Plants.* 1:15145.

Bastet, A., Zafirov, D., Giovinazzo, N., Guyon-Debast, A., Nogué, F., Robaglia, C., et al. (2019). Mimicking natural polymorphism in eIF4E by CRISPR-Cas9 base editing is associated with resistance to potyviruses. *Plant Biotechnol. J.* 17, 1736–1750. doi: 10.1111/pbi.13096

Chandrasekaran, J., Brumin, M., Wolf, D., Leibman, D., Klap, C., Pearlsman, M., et al. (2016). Development of broad virus resistance in non-transgenic cucumber using CRISPR/Cas9 technology. *Mol. Plant Pathol.* 17, 1140–1153. doi: 10.1111/mpp.12375

Chen, K., Wang, Y., Zhang, R., Zhang, H., and Gao, C. (2019). CRISPR/Cas genome editing and precision plant breeding in agriculture. *Annu. Rev. Plant Biol.* 70, 667–697. doi: 10.1146/annurev-arplant-050718-100049

Chen, W., Qian, Y., Wu, X., Sun, Y., Wu, X., and Cheng, X. (2014). Inhibiting replication of begomoviruses using artificial zinc finger nucleases that target viral-conserved nucleotide motif. *Virus Genes.* 48, 494–501. doi: 10.1007/s11262-014-1041-4

Cheng, X., Li, F., Cai, J., Chen, W., Zhao, N., Sun, Y., et al. (2015). Artificial TALE as a convenient protein platform for engineering broad-spectrum resistance to begomoviruses. *Viruses* 7, 4772–4782. doi: 10.3390/v7082843

Cody, W. B., Scholthof, H. B., and Mirkov, T. E. (2017). Multiplexed gene editing and protein overexpression using a tobacco mosaic virus viral vector. *Plant Physiol.* 175, 23–35. doi: 10.1104/pp.17.00411

Garcia-Doval, C., and Jinek, M. (2017). Molecular architectures and mechanisms of Class 2 CRISPR-associated nucleases. *Curr. Opin. Struct. Biol.* 47, 157–166. doi: 10.1016/j.sbi.2017.10.015

Garcia-Ruiz, H. (2018). Susceptibility genes to plant viruses. *Viruses* 10:484. doi: 10.3390/v10090484

Gomez, M., Lin, Z., Moll, T., Chauhan, R., Hayden, L., Renninger, K., et al. (2019). Simultaneous CRISPR/Cas9-mediated editing of cassava eIF4E isoforms nCBP-1 and nCBP-2 reduces cassava brown streak disease symptom severity and incidence. *Plant Biotechnol. J.* 17, 421–434. doi: 10.1111/pbi.12987

Hadidi, A., Flores, R., Candresse, T., and Barba, M. (2016). Next-generation sequencing and genome editing in plant virology. *Front. Microbiol.* 7:1325. doi: 10.3389/fmicb.2016.01325

Hameed, A., Zaidi, S. S., Shakir, S., and Mansoor, S. (2018). Applications of new breeding technologies for potato improvement. *Front. Plant Sci.* 9:925. doi: 10.3389/fpls.2018.00925

Hashimoto, M., Neriya, Y., Yamaji, Y., and Namba, S. (2016). Recessive resistance to plant viruses: potential resistance genes beyond translation initiation factors. *Front. Microbiol.* 7:1695. doi: 10.3389/fmicb.2016.01695

Helm, M., Qi, M., Sarkar, S., Yu, H., Whitham, S., and Innes, R. (2019). Engineering a decoy substrate in soybean to enable recognition of the soybean mosaic virus NIa protease. *Mol. Plant Microbe Interact.* 32, 760–769. doi: 10.1094/mpmi-12-18-0324-r

Hsu, P., Scott, D., Weinstein, J., Ran, F., Konermann, S., Agarwala, V., et al. (2013). DNA targeting specificity of RNA-guided Cas9 nucleases. *Nat. Biotechnol.* 31, 827–832. doi: 10.1038/nbt.2647

Hu, J., Li, S., Li, Z., Li, H., Song, W., Zhao, H., et al. (2019). A barley stripe mosaic virus-based guide RNA delivery system for targeted mutagenesis in wheat and maize. *Mol. Plant Pathol.* 20, 1463–1474. doi: 10.1111/mpp.12849

Ji, X., Si, X., Zhang, Y., Zhang, H., Zhang, F., and Gao, C. (2018). Conferring DNA virus resistance with high specificity in plants using virus-inducible genome-editing system. *Genome Biol.* 19:197.

Ji, X., Wang, D., and Gao, C. (2019). CRISPR editing-mediated antiviral immunity: a versatile source of resistance to combat plant virus infections. *Sci. China Life Sci.* 62, 1246–1249. doi: 10.1007/s11427-019-9722-2

Ji, X., Zhang, H., Zhang, Y., Wang, Y., and Gao, C. (2015). Establishing a CRISPR-Cas-like immune system conferring DNA virus resistance in plants. *Nat. Plants.* 1:15144.

Jiang, N., Zhang, C., Liu, J. Y., Guo, Z. H., Zhang, Z. Y., Han, C. G., et al. (2019). Development of beet necrotic yellow vein virus-based vectors for multiple-gene expression and guide RNA delivery in plant genome editing. *Plant Biotechnol. J.* 17, 1302–1315. doi: 10.1111/pbi.13055

Kis, A., Hamar, É, Tholt, G., Bán, R., and Havelda, Z. (2019). Creating highly efficient resistance against wheat dwarf virus in barley by employing CRISPR/Cas9 system. *Plant Biotechnol. J.* 17, 1004–1006. doi: 10.1111/pbi.13077

Konermann, S., Lotfy, P., Brideau, N., Oki, J., Shokhirev, M., and Hsu, P. (2018). Transcriptome engineering with RNA-targeting type VI-D CRISPR effectors. *Cell* 173, 665–676.e14.

Langner, T., Kamoun, S., and Belhaj, K. (2018). CRISPR crops: plant genome editing toward disease resistance. *Annu. Rev. Phytopathol.* 56, 479–512. doi: 10.1146/annurev-phyto-080417-050158

Lellis, A., Kasschau, K., Whitham, S., and Carrington, J. (2002). Loss-of-susceptibility mutants of Arabidopsis thaliana reveal an essential role for eIF(iso)4E during potyvirus infection. *Curr. Biol.* 12, 1046–1051. doi: 10.1016/s0960-9822(02)00898-9

Li, F., Liu, W., and Zhou, X. (2019). Pivoting plant immunity from theory to the field. *Sci. China Life Sci.* 62, 1539–1542. doi: 10.1007/s11427-019-1565-1

Li, F., and Wang, A. (2019). RNA-targeted antiviral immunity: more than just RNA silencing. *Trends Microbiol.* 27, 792–805. doi: 10.1016/j.tim.2019.05.007

Li, F., Yang, X., Bisaro, D., and Zhou, X. (2018). The βC1 protein of geminivirus-betasatellite complexes: a target and repressor of host defenses. *Mol. Plant.* 11, 1424–1426. doi: 10.1016/j.molp.2018.10.007

Liu, H., Soyars, C., Li, J., Fei, Q., He, G., Peterson, B., et al. (2018). CRISPR/Cas9-mediated resistance to cauliflower mosaic virus. *Plant Direct.* 2:e00047. doi: 10.1002/pld3.47

Lõhmus, A., Hafrén, A., and Mäkinen, K. (2017). Coat protein regulation by CK2, CPIP, HSP70, and CHIP is required for potato virus a replication and coat protein accumulation. *J. Virol.* 91:e01316.

Lowder, L., Zhou, J., Zhang, Y., Malzahn, A., Zhong, Z., Hsieh, T., et al. (2018). Robust transcriptional activation in plants using multiplexed CRISPR-Act2.0 and mTALE-Act systems. *Mol. Plant.* 11, 245–256. doi: 10.1016/j.molp.2017.11.010

Lozano-Durán, R., Rosas-Díaz, T., Luna, A. P., and Bejarano, E. R. (2011). Identification of host genes involved in geminivirus infection using a reverse genetics approach. *PLoS One* 6:e22383. doi: 10.1371/journal.pone.0022383

Ma, X., Zhang, X., Liu, H., and Li, Z. (2020). Highly efficient DNA-free plant genome editing using virally delivered CRISPR-Cas9. *Nat. Plants* 6, 773–779. doi: 10.1038/s41477-020-0704-5

Ma, X., Zhu, Q., Chen, Y., and Liu, Y. (2016). CRISPR/Cas9 platforms for genome editing in plants: developments and applications. *Mol. Plant* 9, 961–974. doi: 10.1016/j.molp.2016.04.009

Macovei, A., Sevilla, N., Cantos, C., Jonson, G., Slamet-Loedin, I., Èermák, T., et al. (2018). Novel alleles of rice eIF4G generated by CRISPR/Cas9-targeted mutagenesis confer resistance to Rice tungro spherical virus. *Plant Biotechnol. J.* 16, 1918–1927. doi: 10.1111/pbi.12927

Mahas, A., Aman, R., and Mahfouz, M. (2019). CRISPR-Cas13d mediates robust RNA virus interference in plants. *Genome Biol.* 20:263.

Mahas, A., and Mahfouz, M. (2018). Engineering virus resistance via CRISPR-Cas systems. *Curr. Opin. Virol.* 32, 1–8. doi: 10.1016/j.coviro.2018.06.002

Makarova, K., Wolf, Y., Alkhnbashi, O., Costa, F., Shah, S., Saunders, S., et al. (2015). An updated evolutionary classification of CRISPR-Cas systems. *Nat. Rev. Microbiol.* 13, 722–736.

Makarova, K. S., Zhang, F., and Koonin, E. V. (2017a). SnapShot: class 1 CRISPR-Cas systems. *Cell* 168:946-946.e1.

Makarova, K. S., Zhang, F., and Koonin, E. V. (2017b). SnapShot: class 2 CRISPR-Cas systems. *Cell* 168:328-328.e1.

Mäkinen, K. (2020). Plant susceptibility genes as a source for potyvirus resistance. *Ann. Appl. Biol.* 176, 122–129. doi: 10.1111/aab.12562

McCarty, N. S., Graham, A. E., Studená, L., and Ledesma-Amaro, R. (2020). Multiplexed CRISPR technologies for gene editing and transcriptional regulation. *Nat. Commun.* 11:1281.

Mehta, D., Stürchler, A., Anjanappa, R., Zaidi, S., Hirsch-Hoffmann, M., Gruissem, W., et al. (2019). Linking CRISPR-Cas9 interference in cassava to the evolution of editing-resistant geminiviruses. *Genome Biol.* 20:80.

Nicaise, V. (2014). Crop immunity against viruses: outcomes and future challenges. *Front. Plant Sci.* 5:660. doi: 10.3389/fpls.2014.00660

Price, A., Sampson, T., Ratner, H., Grakoui, A., and Weiss, D. (2015). Cas9-mediated targeting of viral RNA in eukaryotic cells. *Proc. Natl. Acad. Sci. U. S. A.* 112, 6164–6169. doi: 10.1073/pnas.1422340112

Pyott, D., Sheehan, E., and Molnar, A. (2016). Engineering of CRISPR/Cas9-mediated potyvirus resistance in transgene-free *Arabidopsis* plants. *Mol. Plant Pathol.* 17, 1276–1288. doi: 10.1111/mpp.12417

Rao, X., Wu, Z., Zhou, L., Sun, J., and Li, H. (2017). Genetic diversity of banana bunchy top virus isolates from China. *Acta. Virol.* 61, 217–222. doi: 10.4149/av_2017_02_13

Robaglia, C., and Caranta, C. (2006). Translation initiation factors: a weak link in plant RNA virus infection. *Trends. Plant Sci.* 11, 40–45. doi: 10.1016/j.tplants.2005.11.004

Sanfaçon, H. (2015). Plant translation factors and virus resistance. *Viruses* 7, 3392–3419. doi: 10.3390/v7072778

Sastry, S. K., and Zitter, T. A. (2014). "Management of virus and viroid diseases of crops in the tropics," in *Plant Virus and Viroid Diseases in the Tropics, Vol. 2. Epidemiology and Management*, (Dordrecht: Springer), 149–480. doi: 10.1007/978-94-007-7820-7_2

Sekine, K., Nandi, A., Ishihara, T., Hase, S., Ikegami, M., Shah, J., et al. (2004). Enhanced resistance to cucumber mosaic virus in the *Arabidopsis thaliana* ssi2 mutant is mediated via an SA-independent mechanism. *Mol. Plant Microbe Interact.* 17, 623–632. doi: 10.1094/mpmi.2004.17.6.623

Shmakov, S., Abudayyeh, O., Makarova, K., Wolf, Y., Gootenberg, J., Semenova, E., et al. (2015). Discovery and functional characterization of diverse Class 2 CRISPR-Cas systems. *Mol. Cell* 60, 385–397. doi: 10.1016/j.molcel.2015.10.008

Shmakov, S., Smargon, A., Scott, D., Cox, D., Pyzocha, N., Yan, W., et al. (2017). Diversity and evolution of class 2 CRISPR-Cas systems. *Nat. Rev. Microbiol.* 15, 169–182.

Tashkandi, M., Ali, Z., Aljedaani, F., Shami, A., and Mahfouz, M. M. (2018). Engineering resistance against tomato yellow leaf curl virus via the CRISPR/Cas9 system in tomato. *Plant Signal. Behav.* 13:e1525996. doi: 10.1080/15592324.2018.1525996

Tripathi, J., Ntui, V., Ron, M., Muiruri, S., Britt, A., and Tripathi, L. (2019). CRISPR/Cas9 editing of endogenous banana streak virus in the B genome of *Musa spp*. overcomes a major challenge in banana breeding. *Commun. Biol.* 2:46.

Uniyal, A. P., Yadav, S. K., and Kumar, V. (2019). The CRISPR-Cas9, genome editing approach: a promising tool for drafting defense strategy against begomoviruses including cotton leaf curl viruses. *J. Plant Biochem. B.* 28, 121–132. doi: 10.1007/s13562-019-00491-6

Wang, A. (2015). Dissecting the molecular network of virus-plant interactions: the complex roles of host factors. *Annu. Rev. Phytopathol.* 53, 45–66. doi: 10.1146/annurev-phyto-080614-120001

Wang, A., and Krishnaswamy, S. (2012). Eukaryotic translation initiation factor 4E-mediated recessive resistance to plant viruses and its utility in crop improvement. *Mol. Plant Pathol.* 13, 795–803. doi: 10.1111/j.1364-3703.2012.00791.x

Yamanaka, T., Ohta, T., Takahashi, M., Meshi, T., Schmidt, R., Dean, C., et al. (2000). TOM1, an Arabidopsis gene required for efficient multiplication of a tobamovirus, encodes a putative transmembrane protein. *Proc. Natl. Acad. Sci. U.S.A.* 97, 10107–10112. doi: 10.1073/pnas.170295097

Yin, K., Han, T., Xie, K., Zhao, J., Song, J., and Liu, Y. (2019). Engineer complete resistance to cotton leaf curl Multan virus by the CRISPR/Cas9 system in *Nicotiana benthamiana*. *Phytopathol. Res.* 1:9.

Zaidi, S. S., and Mansoor, S. (2017). Viral vectors for plant genome engineering. *Front. Plant Sci.* 8:539. doi: 10.3389/fpls.2017.00539

Zhan, X., Zhang, F., Zhong, Z., Chen, R., Wang, Y., Chang, L., et al. (2019). Generation of virus-resistant potato plants by RNA genome targeting. *Plant Biotechnol. J.* 17, 1814–1822. doi: 10.1111/pbi.13102

Zhang, Q., Xing, H.-L., Wang, Z.-P., Zhang, H.-Y., Yang, F., Wang, X.-C., et al. (2018). Potential high-frequency off-target mutagenesis induced by CRISPR/Cas9 in *Arabidopsis* and its prevention. *Plant Mol. Biol.* 96, 44–456.

Zhang, T., Zheng, Q., Yi, X., An, H., Zhao, Y., Ma, S., et al. (2018). Establishing RNA virus resistance in plants by harnessing CRISPR immune system. *Plant Biotechnol. J.* 16, 1415–1423. doi: 10.1111/pbi.12881

Zhang, T., Zhao, Y., Ye, J., Cao, X., Xu, C., Chen, B., et al. (2019a). Establishing CRISPR/Cas13a immune system conferring RNA virus resistance in both dicot and monocot plants. *Plant Biotechnol. J.* 17, 1185–1187. doi: 10.1111/pbi.13095

Zhang, Y., Malzahn, A., Sretenovic, S., and Qi, Y. (2019b). The emerging and uncultivated potential of CRISPR technology in plant science. *Nat. Plants.* 5, 778–794. doi: 10.1038/s41477-019-0461-5

Zou, L., Deng, X., Han, X., Tan, W., Zhu, L., Xi, D., et al. (2016). Role of transcription factor HAT1 in modulating Arabidopsis thaliana response to cucumber mosaic virus. *Plant Cell Physiol.* 57, 1879–1889.

Conflict of Interest: The authors declare that the research was conducted in the absence of any commercial or financial relationships that could be construed as a potential conflict of interest.

frontiers in Microbiology

ORIGINAL RESEARCH
published: 13 November 2020
doi: 10.3389/fmicb.2020.591619

Rice Stripe Virus Coat Protein-Mediated Virus Resistance Is Associated With RNA Silencing in *Arabidopsis*

Feng Sun[1], Peng Hu[1,2], Wei Wang[1,3], Ying Lan[1], Linlin Du[1], Yijun Zhou[1] and Tong Zhou[1,3]**

[1] Jiangsu Key Laboratory for Food Quality and Safety-State Key Laboratory Cultivation Base of Ministry of Science and Technology, Institute of Plant Protection, Jiangsu Academy of Agricultural Sciences, Nanjing, China, [2] The State Key Laboratory of Crop Genetics and Germplasm Enhancement, Nanjing Agricultural University, Nanjing, China, [3] College of Plant Protection, Nanjing Agricultural University, Nanjing, China

OPEN ACCESS

Edited by:
Xifeng Wang,
State Key Laboratory for Biology of Plant Diseases and Insect Pests, Institute of Plant Protection (CAAS), China

Reviewed by:
Won Kyong Cho,
Seoul National University, South Korea
Yongliang Zhang,
China Agricultural University, China
Hongying Zheng,
Ningbo University, China
Fei Yan,
Ningbo University, China

***Correspondence:**
Feng Sun
sunfeng1201@126.com
Tong Zhou
zhoutong@jaas.ac.cn

Specialty section:
This article was submitted to Microbe and Virus Interactions with Plants, a section of the journal Frontiers in Microbiology

Received: 05 August 2020
Accepted: 26 October 2020
Published: 13 November 2020

Citation:
Sun F, Hu P, Wang W, Lan Y, Du L, Zhou Y and Zhou T (2020) Rice Stripe Virus Coat Protein-Mediated Virus Resistance Is Associated With RNA Silencing in Arabidopsis. Front. Microbiol. 11:591619. doi: 10.3389/fmicb.2020.591619

Rice stripe virus (RSV) causes rice stripe disease, which is one of the most serious rice diseases in eastern Asian countries. It has been shown that overexpression of RSV coat protein (CP) in rice plants enhances resistance against virus infection. However, the detailed mechanism underlying RSV CP-mediated virus resistance remains to be determined. In this study, we show that both translatable and non-translatable RSV CP transgenic *Arabidopsis* plants exhibited immunity to virus infection. By using deep sequencing analysis, transgene-derived small interfering RNAs (t-siRNAs) from non-translatable CP transgenic plants and virus-derived small interfering RNAs (vsiRNAs) mapping in the CP region from RSV-infected wild-type plants showed similar sequence distribution patterns, except for a significant increase in the abundance of t-siRNA reads compared with that of CP-derived vsiRNAs. To further test the correlation of t-siRNAs with RSV immunity, we developed RSV CP transgenic *Arabidopsis* plants in an siRNA-deficient *dcl2/3/4* mutant background, and these CP transgenic plants showed the same sensitivity to RSV infection as non-transgenic plants. Together, our data indicate that the expression of RSV CP protein from a transgene is not a prerequisite for virus resistance and RSV CP-mediated resistance is mostly associated with the RNA silencing mechanism in *Arabidopsis* plants.

Keywords: Rice stripe virus, CP-mediated resistance, RNA silencing, deep sequence, *dcl2/3/4*

INTRODUCTION

RNA silencing is a conserved antiviral defense mechanism that has been used to increase resistance to plant virus infections (Pumplin and Voinnet, 2013; Guo et al., 2019). In antiviral RNA silencing, host Dicer-like ribonucleases (DCLs) cleave viral double-stranded RNAs (dsRNAs) that are formed during virus replication and transcription into 21-24-nucleotide (nt) viral small interfering RNAs (vsiRNAs) (Pumplin and Voinnet, 2013; Guo et al., 2019). Secondary vsiRNAs can be produced by dicing secondary viral dsRNA synthesized by host-encoded RNA-dependent RNA polymerases (RdRps) (Wassenegger and Krczal, 2006; Zhang et al., 2015). These vsiRNAs

are mainly loaded into the Argonaute (Ago) protein-containing RNA-induced silencing complex (RISC) to posttranscriptionally repress target viral and host RNAs by sequence complementarity (Carbonell and Carrington, 2015; Fang and Qi, 2016). The *Arabidopsis thaliana* genome encodes four DCLs, among which DCL1 produces microRNA, whereas DCL2, DCL3, and DCL4 produces 22-, 24-, and 21-nt vsiRNAs, respectively (Guo et al., 2019). DCL4 and DCL2 are the primary components of antiviral defense in plants and exhibit redundant or cooperative functions (Diaz-Pendon et al., 2007; Guo et al., 2019). The 21-nt vsiRNA produced by DCL4 is the most dominant species of vsiRNA in RNA virus-infected plants (Deleris et al., 2006; Wang et al., 2010). DCL2-dependent 22-nt vsiRNAs also accumulate abundantly when DCL4 is absent or suppressed by viruses, and these 22-nt vsiRNAs seem to be less effective at mediating antiviral RNA silencing (Wang et al., 2011). DCL3 produces 24-nt siRNAs that are associated with transcriptional repression of transposons and repeat sequences in plants (Blevins et al., 2015; Singh et al., 2019) and may enhance antiviral defense against DNA viruses (Raja et al., 2008; Jackel et al., 2016). In *Arabidopsis* plants, AGO1 and AGO2 are the two major plant antiviral argonautes against RNA viruses by associating with vsiRNAs based on the identity of the 5′ terminal nucleotide (Mi et al., 2008; Carbonell and Carrington, 2015).

Rice stripe virus (RSV) is the type species in the genus *Tenuivirus* and causes rice stripe disease, which is one of the most serious rice diseases in eastern Asia (Falk and Tsai, 1998; Xiong et al., 2008). It is transmitted by the small brown planthopper (SBPH) (*Laodelphax striatellus* Fallén) in a circulative and propagative manner (Falk and Tsai, 1998; Li et al., 2015). Under experimental control, RSV also infects *Nicotiana benthamiana* by mechanical sap inoculation and *Arabidopsis* plants by viruliferous SBPH inoculation (Xiong et al., 2008; Sun et al., 2011, 2016). The genome of RSV contains four single-stranded RNA segments, RNA1, RNA2, RNA3, and RNA4, in order of their decreasing molecular weights (Toriyama and Watanabe, 1989). RNA1 is negative sense and encodes a putative viral RdRp (Barbier et al., 1992). The other small three RNA segments encode two proteins using an ambisense coding strategy. RNA2 encodes NS2, a viral RNA silencing suppressor (Du et al., 2011), and NSvc2, a putative membrane glycoprotein (Yao et al., 2014). RNA3 encodes NS3, another RNA silencing suppressor (Xiong et al., 2009) and a coat protein (CP). SP (a disease-specific protein) (Kong et al., 2014) and NSvc4 (a movement protein) (Xiong et al., 2008) are encoded by RNA4.

To manage rice stripe disease caused by RSV, the use of insecticides against SBPH vectors and the exploitation of genetically resistant cultivars are the most effective approaches; however, they all have concerning features, such as high costs, environmental pollution, insecticide resistance and limited resistance resources (Otuka, 2013). Recently, RNA silencing-based resistance has been shown to be an effective and powerful method to enhance plant resistance against viruses in transgenic plants (Galvez et al., 2014; Lindbo and Falk, 2017). Plants transformed with a hairpin construct consisting of an inverted repeat virus-specific sequence are able to induce RNA silencing and exhibit immunity to virus infection (Lindbo and Falk, 2017). For RSV, transgenic rice plants with the RSV CP or NSvc4 hairpin constructs exhibit near immunity against RSV infection (Shimizu et al., 2011; Sasaya et al., 2014). Chimeric CP/SP RNA silencing construct transgenic rice plants show strong resistance against two different RSV isolates (Ma et al., 2011). In addition to hairpin constructs, plant expression of the viral CP gene also confers plant viral resistance, which is mostly but not completely due to an RNA silencing-mediated resistance mechanism (Lindbo and Falk, 2017). It has been shown that overexpression of the RSV CP gene in transgenic rice plants enhances resistance against the virus (Hayakawa et al., 1992). Recent research has also shown that RSV CP mediates virus resistance through jasmonate-AGO18 signaling in rice plants (Han et al., 2020; Yang et al., 2020). However, considering that AGO18 is the key component of RNA silencing in rice plants, whether RSV CP-mediated virus resistance involves the RNA silencing pathway remains to be addressed.

In this study, using the RSV-*Arabidopsis* pathosystem, we showed that both translatable and non-translatable RSV CP transgenic *Arabidopsis* plants exhibit immunity to RSV infection. By using deep sequencing analysis and comparing transgenic-derived siRNAs (t-siRNAs) from non-translatable versions of CP transgenic plants and CP-derived virus-derived siRNAs (vsiRNAs) from RSV-infected wild-type plants, we found that siRNA mapped to the CP sequence segment showed a similar pattern in both transgenic plants and virus-infected wild-type plants, except that greater accumulation of siRNAs was seen in transgenic immune plants. In the siRNA-deficient *dcl2/3/4* mutant background, CP transgenic plants showed the same RSV susceptibility as non-transgenic plants. Together, our collective results indicated that RSV CP-mediated virus resistance depends on the function of DCLs and mostly involved in RNA silencing in *Arabidopsis* plants.

MATERIALS AND METHODS

Sources of Virus, Vectors, and Plant Materials

Rice stripe virus-infected rice plants were collected from Jiangsu Province in China, and the virus was confirmed by using a western blot assay (Sun et al., 2016). Non-viruliferous instar nymphs of SBPHs reared on rice seedlings (*Oryza sativa* L. cv. Wuyujing No. 3) were collected and fed on RSV-infected rice plants for 3 days to acquire the virus. The virus was maintained by successive transovarial infections in SBPHs on rice seedlings in an insect-rearing room at 25°C.

Arabidopsis thaliana (Col-0) and *dcl2/3/4* mutant seeds were obtained from Dr. Xiuren Zhang (Texas A&M University, College Station, United States) and grown in potting soil in a growth chamber at 23°C under 200 μmol m^{-2} s^{-1} illumination and 16-h light/8-h dark cycle conditions.

RSV Inoculation Assay

Transgenic and wild-type *Arabidopsis* plants at 2 weeks were inoculated with 10 viruliferous SBPHs per plant and were kept in a glass incubator containing ten plants. SBPHs were sprayed

with insecticide after a 4-day inoculation access period. Plants were kept in a growth chamber for symptom development, and non-viruliferous insects were used for mock inoculation. To evaluate of resistance to RSV, thirty *Arabidopsis* plants of each line were inoculated with RSV. The seedlings were harvested at different time points for RNA and protein extractions. Each RSV inoculation assay was repeated three times.

DNA Constructs and Transgenic Plants

The RSV *CP* gene was amplified from RSV-infected rice plant leaf tissue using RT-PCR performed with CP-specific primers (**Supplementary Table S1**). The CP PCR products were cloned into the pDONR-zero vector (Invitrogen, Carlsbad, CA, United States) and subsequently transferred into the binary vector pBA-Flag-Myc4-DC (Zhang et al., 2005) using the Gateway cloning system following the manufacturer's instructions (Invitrogen Corporation). The constructed binary vector pBA-Flag-Myc4-CP was transformed into *Arabidopsis* plants using *Agrobacterium tumefaciens* strain ABI by the floral dip method (Clough and Bent, 1998; Zhang et al., 2006). The CP overexpression transgenic *Arabidopsis* plants were selected on standard MS medium containing 10 mg/L glufosinate ammonium (Sigma-Aldrich, St. Louis, MO, United States).

Western Blot Assay

Western blot was performed following the protocol described by Sun et al. (2016). In brief, *Arabidopsis* total proteins were separated by 10% SDS-PAGE and transferred to PVDF membranes. The membranes were blocked and inoculated with an anti-RSV SP (our laboratory), anti-Myc (Sigma-Aldrich, St. Louis, MO, United States), anti-YFP (Genscript, Nanjing, China) or anti-actin antibody (Enogene, Nanjing, China) overnight at 4°C. Signals were developed in ECL buffer (Transgen Biotech, Beijing, China) and recorded with a Tanon 5200 Luminescent Imaging Workstation (Tanon, Shanghai, China).

RT-PCR

Total RNA was isolated from the plant samples using RNAiso Plus reagent (Takara, Dalian, China), and first-strand cDNA was synthesized from 1 μg of total RNA using an iScript™ cDNA Synthesis Kit (Bio-Rad, Hercules, CA, United States). PCR amplification was performed using 2 × Taq Master Mix (Vazyme Biotech, Nanjing, China) with RSV CP-specific primers (**Supplementary Table S1**). *EF1a* was used as a loading control.

Quantitative Reverse-Transcription PCR

Total RNA was isolated from the plant samples using RNAiso Plus reagent (Takara, Dalian, China), and cDNA synthesis and PCR were performed as described previously (Sun et al., 2016). Briefly, first-strand cDNA was synthesized from 1 μg of total RNA using an iScript™ cDNA Synthesis Kit (Bio-Rad, Hercules, CA, United States). qRT-PCR was performed using SsoFast EvaGreen Supermix (Bio-Rad, Hercules, CA, United States) with a Bio-Rad iQ5 Real-Time PCR system with gene-specific primers (**Supplementary Table S1**). *EF1a* was used as an internal standard, and all qRT-PCR experiments were performed at least three times.

Deep Sequencing and Analysis of Small RNA Sequences

Total RNA was extracted from RSV-infected and mock-treated NOP-CP transgenic or non-transgenic plants each with triplicate biological replicates, using RNAiso Plus reagent (Takara, Dalian, China), and used for small RNA library construction. A total of 12 small RNA libraries were sequenced using an Illumina HiSeq 4000 sequencer to generate single-end 50-bp sequences at the Beijing Genome Institute (BGI, Shenzhen, China). Raw data were obtained after removing the adapter sequences using cutadapt (v1.16) (Martin, 2011). The clean data were then mapped to the RSV genome (NCBI accession numbers: NC_003755.1, NC_003754.1, NC_003776.1, NC_003753.1), allowing up to one mismatch. Reads showing matches with the RSV reference sequences were retained and further analyzed using the CLC Genomics Workbench program (QIAGEN, Hilden, Germany), Perl scripts and Excel tools. Small RNA-seq data was deposited in the NCBI BioProject database with accession code PRJNA649376.

RESULTS

RSV CP Transgenic *Arabidopsis* Plants Show Immunity to RSV Infection

Previous studies demonstrated that transgenic rice plants expressing RSV CP exhibited a significant level of resistance to virus infection (Hayakawa et al., 1992; Yang et al., 2020). Our previous studies also showed that RSV infected *Arabidopsis* plants and caused significant symptoms, including stunted growth and vein chlorosis on leaves (Sun et al., 2011, 2016). To test whether RSV CP-mediated resistance can be extended to *Arabidopsis* plants, we first generated CP transgenic *Arabidopsis* plants. Full-length RSV CP was cloned from virus-infected rice plants and transferred into the binary vector pBA-Flag-Myc4-DC (Zhang et al., 2005) using the Gateway cloning system (**Figure 1B**). This recombinant vector was transformed into *Arabidopsis* plants (Col-0 ecotype) by the floral dip method (Clough and Bent, 1998; Zhang et al., 2006). These T2 generation transgenic plants overexpressing RSV CP with Flag-Myc4 epitopes were examined by western blot assay. The expression of Flag-Myc4-CP was detected only in transgenic plants with an anti-Myc antibody (**Figure 1B**).

To test RSV resistance, both CP transgenic (CP#4, CP#18) and wild-type (Col-0 ecotype) *Arabidopsis* plants were challenged with RSV by viruliferous SBPHs at 2-week-old stages. In three independent experiments, all wild-type plants showed typical RSV symptoms, including severe stunting at 4 weeks post-inoculation. In contrast, all the CP transgenic *Arabidopsis* plants did not show any symptoms and displayed resistance to RSV infection (**Figure 1A**). Moreover, RSV-encoded SP protein was detected in wild-type *Arabidopsis* plants by western blot assay at 14 to 28 days post-inoculation (dpi) but not in CP transgenic plants (**Figure 1C**). qRT-PCR assays showed that RSV SP mRNA

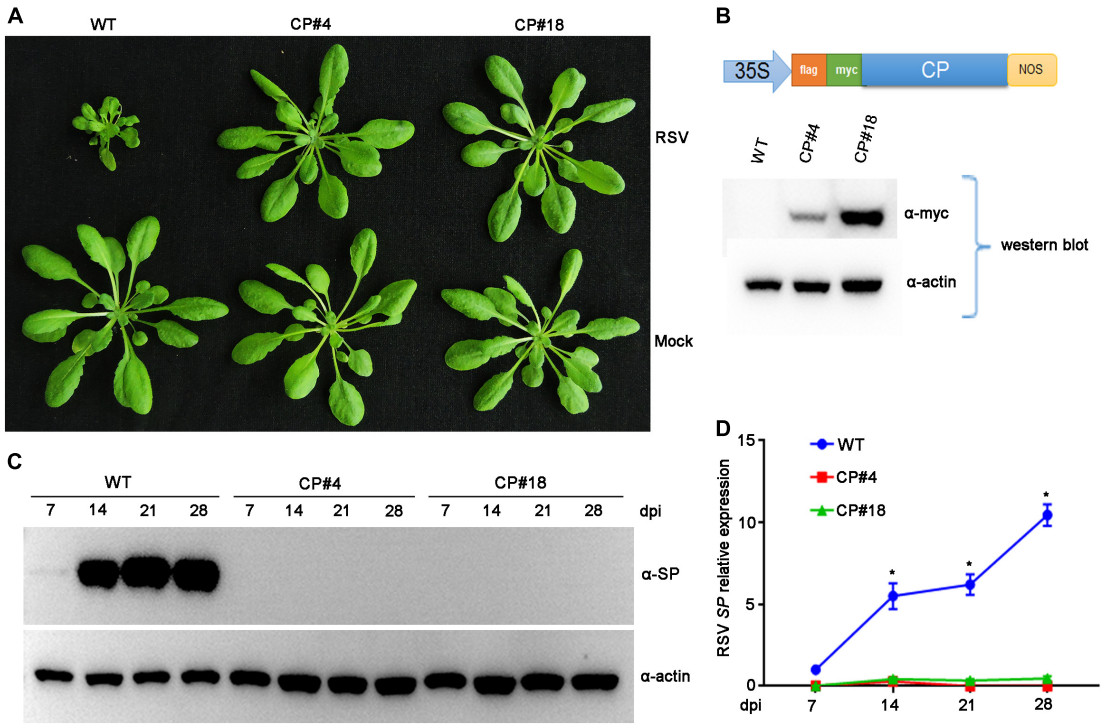

FIGURE 1 | Examination of the Rice stripe virus (RSV) resistance of CP transgenic *Arabidopsis* plants. **(A)** Symptoms of mock-inoculated and RSV-infected CP transgenic (CP#4, CP#18) and wild-type (WT) *Arabidopsis* plants. Photographs were taken at 4 weeks post-inoculation. **(B)** The upper panel shows the schematic representation of the constructed binary vector pBA-Flag-Myc4-CP, and the lower panel shows western blot analysis of CP transgenic lines with an anti-Myc antibody. The actin protein level served as a loading control. **(C)** Western blot analysis of the time course of RSV-encoded SP protein accumulation in RSV-infected CP transgenic (CP#4, CP#18) and WT *Arabidopsis* plants using an SP-specific antibody. The actin protein level served as a loading control. **(D)** qRT-PCR analysis of the time course of RSV SP mRNA transcription levels in RSV-infected CP transgenic and WT *Arabidopsis* plants. Signal intensities for each transcript were normalized with those for *EF1*-α. Values are means ± SD ($n = 3$). *$p \leq 0.05$ (Student's *t*-test).

accumulated to significantly higher levels in wild-type plants than in CP transgenic plants (**Figure 1D**). These results therefore show that RSV CP induces virus resistance in *Arabidopsis* plants.

Expression of CP Protein From a Transgene Is Not a Prerequisite for Resistance in *Arabidopsis* Plants

Previous studies demonstrated that the mechanism of CP-mediated resistance depended on the particular virus system and transgenic plants being analyzed (Lindbo and Falk, 2017). To demonstrate whether expression of RSV CP protein is necessary for resistance, we generated *Arabidopsis* plants overexpressing a non-translatable protein mutant of RSV CP (NOP-CP) in which the first codon ATG of the CP gene was replaced with TAG (**Figure 2B**), and the NOP-CP sequence was inserted into the pBA-Flag-Myc4-DC vector and tagged with Flag-Myc4 epitopes. These T2 generation transgenic plants were confirmed by RT-PCR and western blot assays. As expected, transcripts of NOP-CP mRNA were detected with primers specific to the CP sequence only in transgenic *Arabidopsis* plants (**Figure 2B**). However, signals of NOP-CP protein were not visible in either transgenic or wild-type plants with an anti-Myc antibody. These results indicate that NOP-CP transgenic *Arabidopsis* plants expressed only CP mRNA but not protein. To further analyze whether there was still a truncated RSV CP protein encoding C-terminal truncation in the corresponding region of CP nucleotides in NOP-CP gene. YFP-tagged CP or NOP-CP in C-terminal were transiently expressed in *Nicotiana benthamiana*. The transcripts of NOP-CP-YFP mRNA were detected in *Nicotiana benthamiana* (**Supplementary Figure S1B**). However, signals of NOP-CP-YFP protein were not visible in tobacco plants using confocal imaging and western blot assays (**Supplementary Figures S1A,C**). These data indicated that NOP-CP-YFP gene expressed only CP mRNA but not protein in *Nicotiana benthamiana*.

To test RSV resistance, NOP-CP transgenic (NOP-CP#7, NOP-CP#9) and wild-type *Arabidopsis* plants were inoculated with RSV viruliferous SBPHs. In three independent trials, no RSV symptoms were observed in the NOP-CP transgenic *Arabidopsis* plants (**Figure 2A**), in contrast with the severe stunting symptoms in wild-type plants. Consistently, the accumulation of viral SP protein was not detected in the NOP-CP transgenic plants by western blot (**Figure 2C**), and fewer SP mRNA transcripts were detected in NOP-CP transgenic plants than in wild-type plants (**Figure 2D**). These results show that *Arabidopsis* transgenic plants with a non-translatable RSV CP sequence are immune to virus infection and that RSV CP-mediated resistance is independent of CP protein expression.

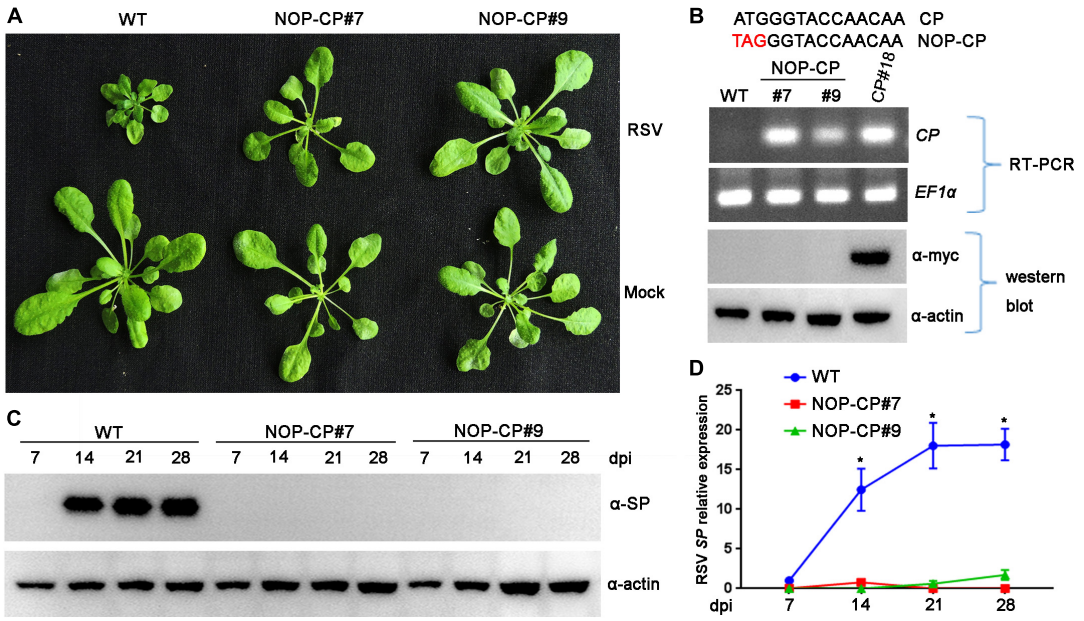

FIGURE 2 | Evaluation of NOP-CP transgenic *Arabidopsis* plants for resistance to Rice stripe virus (RSV). **(A)** Symptoms of mock-inoculated and RSV-infected NOP-CP transgenic (NOP-CP#7, NOP-CP#9) and wild-type (WT) *Arabidopsis* plants. Photographs were taken at 3 weeks post-inoculation. **(B)** The upper panel shows the schematic representation of the NOP-CP nucleotide sequence. The middle panel shows RT-PCR analysis of NOP-CP mRNA transcription levels of NOP-CP transgenic lines, and the EF1-α mRNA level served as a loading control. The lower panel shows western blot analysis of NOP-CP transgenic lines with an anti-Myc antibody, and the actin protein level served as a loading control. **(C)** Western blot analysis of the time course of RSV-encoded SP protein accumulation in RSV-infected NOP-CP transgenic (NOP-CP#7, NOP-CP#9) and WT *Arabidopsis* plants using an SP-specific antibody. The actin protein level served as a loading control. **(D)** qRT-PCR analysis of the time course of RSV SP mRNA transcription levels in RSV-infected NOP-CP transgenic and Col-0 *Arabidopsis* plants. Signal intensities for each transcript were normalized with those for *EF1-α*. Values are means ± SD ($n = 3$). $^*p \leq 0.05$ (Student's *t*-test).

Deep Sequencing of Small RNA From NOP-CP Transgenic and Wild-Type *Arabidopsis* Plants

To better resolve whether the small RNA population is associated with RSV CP-mediated resistance and minimize the impact of CP protein on the immune response, 12 libraries were constructed with small RNA isolated from mock- and RSV-infected NOP-CP transgenic and wild-type *Arabidopsis* plants. Each library generated 7–15 million clean reads ranging from 18 to 30 nt (**Table 1**). Three biological replicates of each group were analyzed and showed very similar patterns. The results described below were derived from the average generated from three biological replicates. The size distributions of total small RNAs within these different treatments were similar; the dominant size was 22 nt, followed by 21 nt and 23 nt (**Figure 3A**). We mapped clean small RNA (18–30 nt) reads to the RSV genome and CP transgenic sequence and obtained RSV-derived, CP-derived siRNAs. In RSV-infected wild-type *Arabidopsis* plants, we identified 160,436 vsiRNAs, accounting for 1.55% of the total, whereas only 1,481 reads matched to the RSV genome in mock control plants. In NOP-CP transgenic *Arabidopsis* plants, almost all reads matched to the RSV genome were generated from the NOP-CP segment sequence, accounting for 0.09% of the total reads in RSV-infected plants and 0.27% in mock plants (**Table 1**). Unexpectedly, in NOP-CP transgenic *Arabidopsis* plants, RSV infection resulted in less accumulation of NOP-CP-derived small RNA than in mock plants despite generating more small RNA reads mapped to other RSV genomic regions (**Table 1**). The sequencing results confirmed that the accumulation of NOP-CP-derived siRNAs from transgenic sequences was associated with the immunity of these plants to RSV infection.

Characterization of vsiRNA in RSV-Infected Wild-Type *Arabidopsis* Plants

To further decipher the regulatory functions of vsiRNAs, we studied the profiles of vsiRNA in RSV-infected *Arabidopsis* plants. Size distribution analysis showed that RSV-derived vsiRNAs were predominantly 20 and 21 nt, accounting for 45% and 25% of the total, respectively (**Figure 3B**). For CP-derived t-siRNAs, the dominant sizes were 21 nt and 22 nt (**Figure 3C**), whereas the most dominant sizes of CP-derived vsiRNAs were 20 nt and 21 nt (**Figure 3D**), suggesting that DCL4 is the major producer of CP-derived t-siRNA and that RSV vsiRNA production involves multiple DCL functions.

The canonical 21–24-nt small RNAs from the viral sequences were further analyzed. The 21–24-nt vsiRNA reads were mapped to the RSV genomic sequence to explore their origin. As shown in **Figure 4A** and **Supplementary Figures S2, S3**, the proportions of vsiRNAs from both polarities were almost continuous, but some genomic regions showed higher mapping frequencies. In

TABLE 1 | Twelve libraries constructed with small RNAs from wild-type (WT) and NOP-CP transgenic (NOP-CP) *Arabidopsis* plants after mock control (Mock) or RSV inoculation (RSV), including three biological replicates each.

Library	Total 18–30 nt reads	Number of reads on RSV	Percentage of RSV reads (%)	Number of reads on CP	Percentage of CP reads (%)
NOP-CP-Mock1	8,955,649	20,391	0.23	20,326	0.23
NOP-CP-Mock2	7,625,242	13,531	0.18	13,455	0.18
NOP-CP-Mock3	9,991,991	40,589	0.41	40,473	0.41
NOP-CP-Mock (average)	8,857,627	24837	0.27	24751	0.27
NOP-CP-RSV1	11,577,160	9,423	0.08	8,058	0.07
NOP-CP-RSV2	8,858,390	9,017	0.10	7,610	0.09
NOP-CP-RSV3	9,430,632	7,036	0.07	6,826	0.07
NOP-CP-RSV (average)	9,955,394	8492	0.09	7498	0.08
WT-Mock1	14,727,568	64	0.00	1	0.00
WT-Mock2	15,054,977	71	0.00	0	0.00
WT-Mock3	15,943,020	4,307	0.03	333	0.00
WT-Mock (average)	15,241,855	1,481	0.01	111	0.00
WT-RSV1	8,726,871	69,622	0.80	4,878	0.06
WT-RSV2	9,272,442	111,136	1.20	10,252	0.11
WT-RSV3	11,340,961	300,550	2.65	23,138	0.20
WT-RSV (average)	9,780,091	160436	1.55	12756	0.12

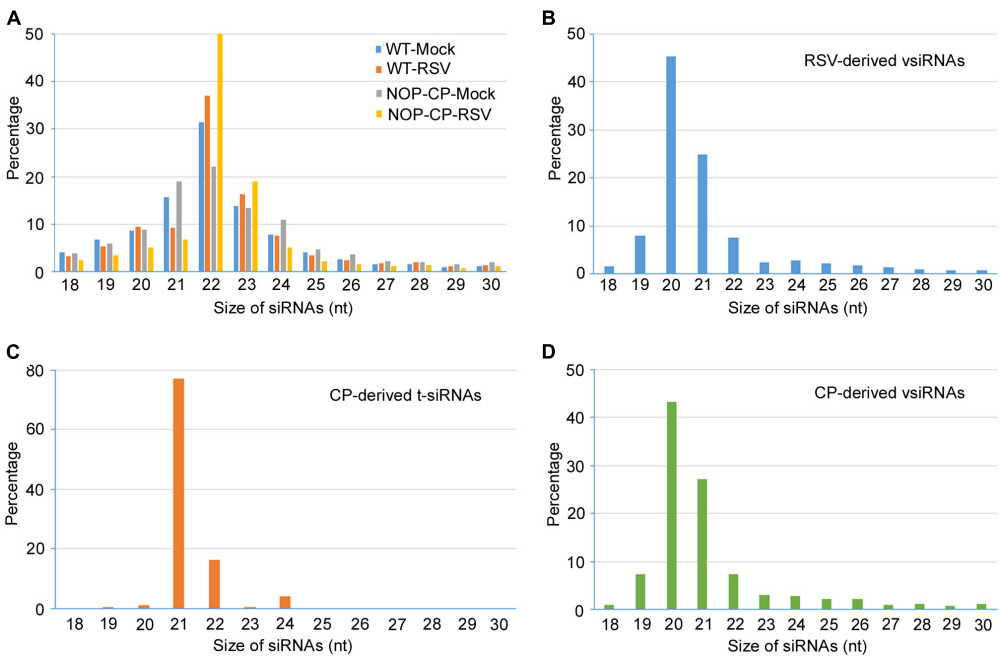

FIGURE 3 | Size distribution of 18–30 nucleotide small RNAs. **(A)** Size distribution of total small RNA from mock-inoculated and RSV-infected NOP-CP transgenic and Col-0 *Arabidopsis* plants. **(B)** Size distribution of small RNA from vsiRNAs from RSV-infected Col-0 *Arabidopsis* plants. **(C)** Size distribution of CP-derived t-siRNAs from NOP-CP transgenic plants. **(D)** Size distribution of CP-derived vsiRNAs from RSV-infected Col-0 plants.

the RSV RNA1 genome, the complementary strand of the 3′ terminus produced significantly more vsiRNAs, and other RNA segments also exhibited some hotspots for vsiRNA generation (**Figure 4A** and **Supplementary Figures S2, S3**). The sense and antisense RSV RNA strands generated almost equivalent amounts of sense (49.5%) and antisense (50.5%) vsiRNA (**Figure 4B**). In addition, preferential occurrence of A/U at the 5′ terminus was identified in vsiRNAs (**Figure 4C**). These results suggest that RSV vsiRNAs are potentially loaded into AGO1/AGO2-containing RISCs.

Characterization of t-siRNA in NOP-CP Transgenic *Arabidopsis* Plants

To understand the significance of t-siRNA in CP-mediated RSV resistance, we characterized and compared t-siRNAs generated

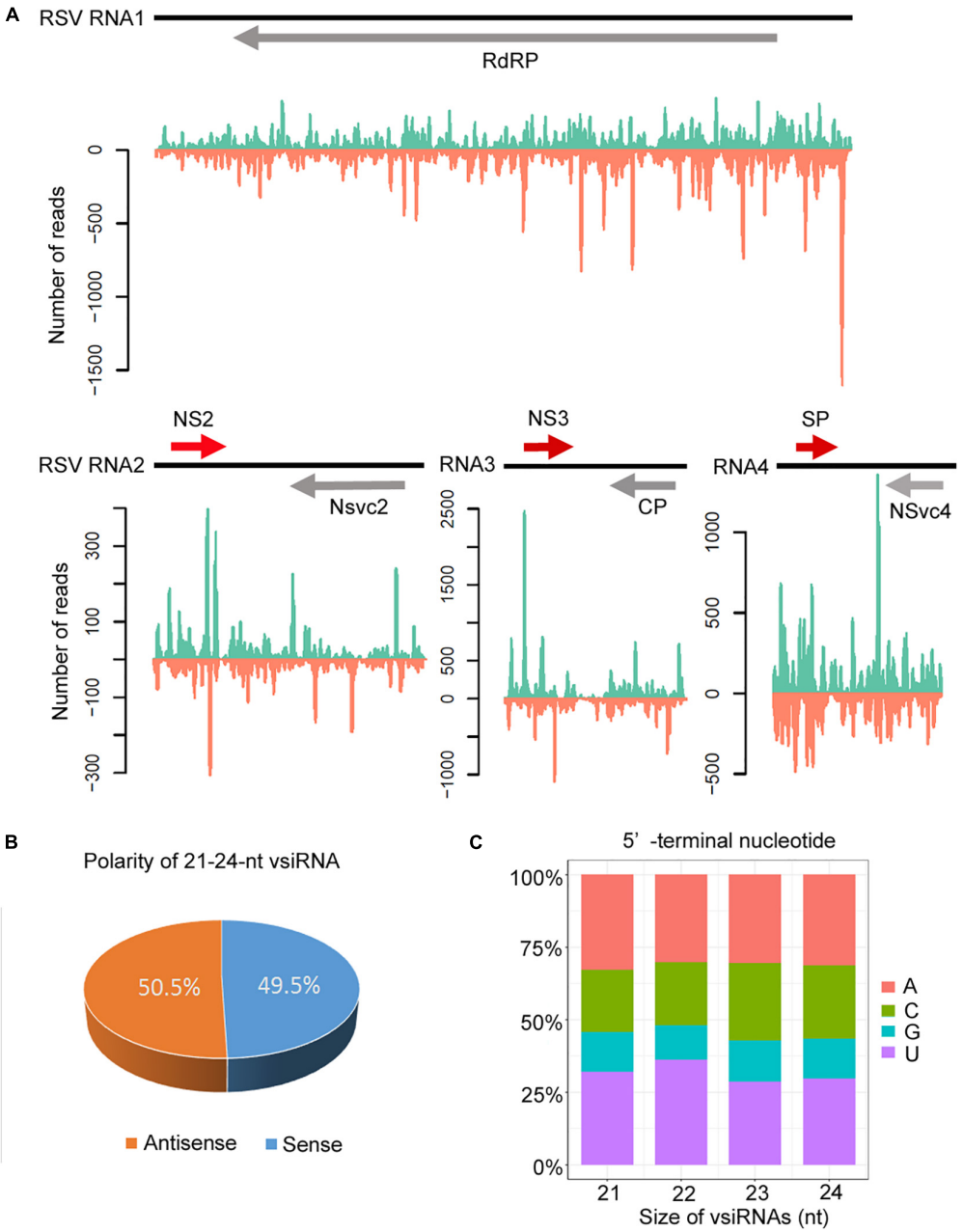

FIGURE 4 | Profile of 21–24 nucleotide (nt) virus-derived small interfering (vsiRNA) derived from RSV-infected Col-0 plants. **(A)** Distribution of vsiRNAs along the RSV genome in both positive (blue) and negative (red) polarity. Genome organization of RSV positioned proportionally above. CP, coat protein; RdRp, RNA-dependent RNA polymerase; SP, disease-specific protein. **(B)** Accumulation of sense and antisense vsiRNAs. **(C)** 5′-terminal nucleotide frequency of 21–24 nt vsiRNAs.

from the NOP-CP transgene of transgenic *Arabidopsis* plants and vsiRNAs mapping to the same region (CP-derived vsiRNA) in RSV-infected wild-type plants. The sequence distribution profile of 21–24-nt t-siRNA from the NOP-CP transgene region showed that t-siRNA accumulated in several hotspot regions throughout the transgenic sequence. Interestingly, CP vsiRNAs mapping to the CP region also showed a very similar profile, with peaks in the same position, although the t-siRNA peak read number was much higher than that for vsiRNAs (**Figure 5A** and **Supplementary Figure S4**). The similar t-siRNA and vsiRNA distribution profiles indicated that a sequence bias in the t-siRNA population depends on a nucleotide sequence preference and that there is a similar mechanism for t-siRNA and vsiRNA generation.

The size distributions of t-siRNAs showed that 21 nt was the most dominant size, representing 80% of the total t-siRNAs (**Figure 5B**). Similarly, the 21-nt classes accounted for the majority of the CP vsiRNAs, representing 70% of the total

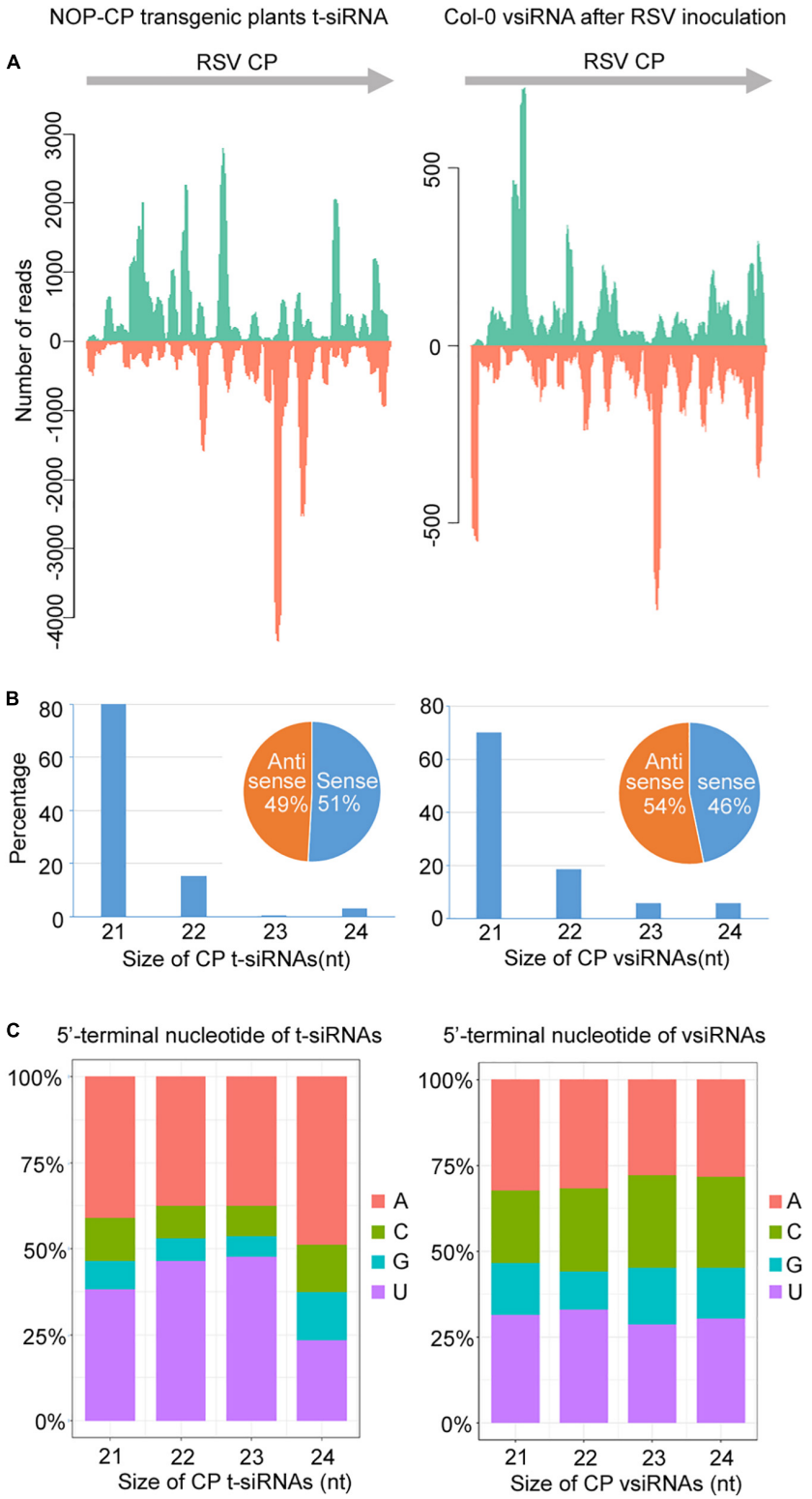

FIGURE 5 | Characterization and comparison of 21–24 nt transgenic-derived small interfering RNA (t-siRNA) mapped to the CP sequence in NOP-CP transgenic plants (left) and virus-derived small interfering RNA (vsiRNA) mapped to the RSV CP sequence in RSV-infected Col-0 plants (right). **(A)** Distribution of t-siRNAs and vsiRNAs along the CP sequence in both positive (blue) and negative (red) polarity. Note that the scale used for the NOP-CP transgenic plants is different from that used for the RSV-infected Col-0 plants. **(B)** Size distribution of t-siRNAs and vsiRNAs. Pie graph showing the percentage of the sense and antisense t-siRNAs and vsiRNAs. **(C)** 5′-terminal nucleotide frequency of 21–24 nt t-siRNAs and vsiRNAs.

CP vsiRNAs (**Figure 5B**), indicating similar sRNA processing properties in transgene- and virus-derived sRNA. To explore the origin of t-siRNAs, the strand specificity and locations of t-siRNAs were analyzed. As shown in **Figures 5A,B**, almost equivalent proportions of sense and antisense sRNAs were generated in both t-siRNAs and CP vsiRNAs, although the sense (51%) t-siRNA amounts were slightly greater than the antisense orientation amounts (49%), whereas for CP vsiRNAs, more reads were counted in the antisense (54%) orientation. The 5′ terminal nucleotides were characterized for 21–24 nt t-siRNAs and CP-vsiRNAs. The U/A were the most abundant 5′ nucleotides in all four sizes of both t-siRNAs and CP-vsiRNAs (**Figure 5C**).

Furthermore, we also characterized and compared the t-siRNA populations of NOP-CP transgenic *Arabidopsis* plants with mock treatment and RSV inoculation. The results showed that the t-siRNAs of NOP-CP transgenic plants after mock and RSV inoculation shared highly similar distribution profiles, although the read number of total t-siRNAs in RSV inoculation plants was significantly less than that in the mock treatment plants (**Supplementary Figure S5** and **Table 1**). Characterization of t-siRNAs in NOP-CP transgenic *Arabidopsis* plants indicates that NOP-CP-derived t-siRNAs may be associated with CP-mediated RSV resistance in *Arabidopsis*.

Plant DCLs 2, 3, and 4 Are Indispensable for CP-Mediated RSV Resistance in *Arabidopsis*

Previous studies have demonstrated that plant DCLs are responsible for generating transgene-derived t-siRNAs and virus-derived vsiRNAs (Guo et al., 2019). To test our hypothesis that the accumulation of t-siRNAs is associated with RSV resistance in CP transgenic *Arabidopsis* plants, we generated CP transgene plants in the *Arabidopsis dcl2/3/4* mutant background. These T2 generation transgenic plants were confirmed by western blot using an anti-Myc antibody (**Figure 6B**). An RSV infection assay showed that CP transgenic *Arabidopsis* plants in the *dcl2/3/4* background (*dcl2/3/4*;CP) developed severe stunting symptoms similar to those of non-transgenic *dcl2/3/4* and Col-0 plants (**Figure 6A**). Western blot and qRT-PCR results both showed that both RSV SP mRNA and proteins accumulated to similar levels in *dcl2/3/4*;CP plants and non-transgenic *dcl2/3/4* and Col-0 plants (**Figures 6C,D** and **Supplementary Figure S6**). These results indicate that CP-mediated RSV resistance depends on the function of DCLs in *Arabidopsis*.

DISCUSSION

Since the concept of pathogen-derived resistance (PDR) was proposed (Sanford and Johnston, 1985) and confirmed by expressing tobacco mosaic virus (TMV) CP in transgenic tobacco plants, resulting in TMV resistance (Abel et al., 1986), CP-mediated resistance has been widely used to protect various plant species against virus infection (Galvez et al., 2014). In the case of RSV, the overexpression of CP in rice plants resulted in partial resistance to virus infection, but no related mechanism was determined (Hayakawa et al., 1992). Recent studies have also demonstrated that the RSV CP triggers jasmonate accumulation and subsequently induces the plant antiviral immune response

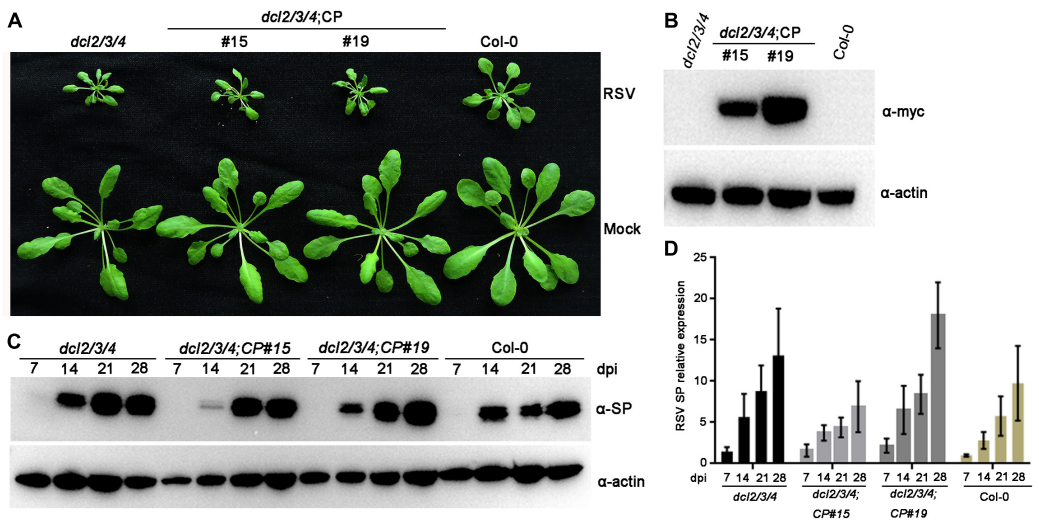

FIGURE 6 | Rice stripe virus resistance examination of CP transgenic plants in the *dcl2/3/4* background. **(A)** Symptoms of mock-inoculated and RSV-infected CP transgenic plants in the *dcl2/3/4* background (*dcl2/3/4*;CP#15, *dcl2/3/4*;CP#19) and *dcl2/3/4* and Col-0 *Arabidopsis* plants. Photographs were taken at 4 weeks post-inoculation. **(B)** Western blot analysis of CP transgenic lines in the *dcl2/3/4* background with an anti-Myc antibody. The actin protein level served as a loading control. **(C)** Western blot analysis of the time course of RSV-encoded SP protein accumulation in RSV-infected CP transgenic plants in the *dcl2/3/4* background and *dcl2/3/4* (*dcl2/3/4*;CP#15, *dcl2/3/4*;CP#19) and Col-0 *Arabidopsis* plants using an SP-specific antibody. The actin protein level served as a loading control. **(D)** qRT-PCR analysis for the time course of RSV SP mRNA transcription levels in RSV-infected CP transgenic plants in the *dcl2/3/4* background (*dcl2/3/4*;CP#15, *dcl2/3/4*;CP#19) and *dcl2/3/4* and Col-0 *Arabidopsis* plants. Signal intensities for each transcript were normalized with those for *EF1-α*. Values are means ± SD ($n = 3$).

(Han et al., 2020; Yang et al., 2020) and that RSV CP-mediated resistance requires AGO18 protein expression in rice plants (Yang et al., 2020). Thus, RSV CP-mediated resistance appears to be a protein-mediated phenomenon in rice plants, similar to TMV CP-mediated resistance in tobacco plants (Lindbo and Falk, 2017). However, the effectiveness of transgene-induced silencing could not be ruled out in these previous studies, as some resistant lines containing translatable transgenes also generated RNA-mediated resistance correlating with t-siRNAs. In this study, we provide evidence that the expression of RSV CP in transgenic *Arabidopsis* plants is not a prerequisite for CP-mediated resistance. First, both translatable and non-translatable versions of CP transgenic *Arabidopsis* plants all showed immunity to RSV infection. Second, by using deep sequencing analysis, CP-mediated resistance in transgenic *Arabidopsis* plants was associated with high accumulation of 21–24-nt t-siRNAs. Third, CP overexpression in the *dcl2/3/4* mutant background resulted in similar sensitivity to RSV infection in non-transgenic *dcl2/3/4* plants. Our results strongly indicate that RSV CP-mediated resistance is due to an RNA silencing-mediated resistance mechanism in *Arabidopsis*, similar to that indicated in tobacco etch virus (TEV) CP-mediated resistance (Lindbo et al., 1993) and tomato spotted wilt virus (TSWV) N (nucleocapsid)-mediated resistance (Catoni et al., 2013).

RNA silencing-directed resistance is mediated by 21–24 nt siRNAs (Hamilton et al., 2002; Ruiz-Ferrer and Voinnet, 2009) generated through the cleavage of a double-stranded or an imperfect stem-loop RNA molecule by plant DCLs (Moazed, 2009). In this paper, Illumina deep sequencing was performed to characterize the small RNA population and gain insights into the RNA-based virus resistance mechanism during RSV-*Arabidopsis* interactions. Bioinformatic analysis of the deep sequencing data indicated that RSV infection triggered the generation of relatively large amounts of vsiRNA, accounting for 1.55% of the total 18–30-nt reads in *Arabidopsis* plants (**Table 1**), in contrast with an average of 0.29% of the total small RNA reads mapped to the RSV genome in RSV-infected natural host rice plants (Yang et al., 2018). This difference is probably a result of the different virus titers in different RSV-host pathosystems. In general, DCL4-generated 21-nt vsiRNAs are the most abundant class, following DCL-dependent 22-nt vsiRNAs (Guo et al., 2019). In RSV-infected *Arabidopsis*, 20-nt vsiRNAs was the most abundant species (**Figure 3B**). This result is similar to the rice ragged stunt virus (RRSV) vsiRNAs in rice plants (Li et al., 2018). In RSV-infected rice and tobacco plants, 20 nt vsiRNAs also account for the high proportion (Yan et al., 2010; Jiang et al., 2012; Xu et al., 2012). These results indicate that 20 nt vsiRNAs may play a role in RSV-plants interaction. The mechanism of biogenesis and function of 20 nt visRNA remains elusive, though the biogenesis of 20 nt miRNAs is dependent on DCL1 (Lee et al., 2015). Further studies are needed to elucidate the role of *Arabidopsis* DCL1 in the production RSV vsiRNAs.

In *Arabidopsis*, AGO1 and AGO2 play crucial roles in antivirus defense (Carbonell and Carrington, 2015) and associate with small RNAs that exhibit uridine and adenosine at their 5′ ends, respectively (Mi et al., 2008). Our study also revealed preferential occurrence of uridine or adenosine residues at the 5′ terminus in RSV vsiRNA, showing the conserved AGO complexes binding vsiRNA for antivirus defense. Compared with previous studies, the 5′-terminal nucleotides of RSV visRNAs from *Arabidopsis*, rice and tobacco plants were similar (Yan et al., 2010; Jiang et al., 2012; Xu et al., 2012; Yang et al., 2018), suggesting that AGO1 and AGO2 play an important role in virus defense against RSV in plants.

Regarding the genomic regions from which RSV vsiRNAs were generated, fewer vsiRNAs were produced from RNA2 than from the other three RNA segments in *Arabidopsis* (**Figure 4**); however, in RSV-infected rice plants, RNA1 generated fewer vsiRNAs than the other three RNA segments (Xu et al., 2012; Yang et al., 2018). These distinct RSV vsiRNA origins in plant hosts might be explained by the evolutionary adaptation of RSV, which escapes RNA silencing antivirus machinery, thus facilitating successful virus infection in rice plants. In this study, RSV-derived vsiRNAs equally originate from the sense and antisense strands (**Figure 4B**), consistent with previous reports in RSV-rice interaction (Yan et al., 2010; Yang et al., 2018). These results indicate that the RSV vsiRNAs may originated from double-stranded replication intermediates.

To characterize CP t-siRNAs that confer resistance to RSV infection, the origin, composition and abundance of CP sequence-derived t-siRNAs were analyzed and compared with those of CP-derived vsiRNAs. The sequence distribution, 5′ terminal nucleotides and strand specificity exhibited very similar patterns between CP-derived t-siRNAs and CP-derived vsiRNAs, except that the amount of t-siRNAs was nearly twice that of vsiRNAs, indicating that the activation of t-siRNAs mediates antiviral defense derived from the transgene. A prerequisite step for t-siRNA biogenesis is a sufficient quantity of transgene RNA that has a dsRNA nature. Multiple studies have demonstrated that transgenes can often integrate into the host genome in complex structures, such as multiple copies inverted to each other, and transcription of transgenic DNA from these complex integrations could lead to dsRNA structures (Lindbo and Falk, 2017). Another possibility is that the single-stranded RNA transcript from transgene DNA is converted to dsRNAs by SUPPRESSOR OF GENE SILENCING 3 (SGS3) and RNA-DEPENDENT RNA POLYMERASE 6 (RDR6) (Guo et al., 2019). Further genetic and biochemical studies will be necessary to address which pathway is responsible for t-siRNA biogenesis in CP transgenic *Arabidopsis* plants.

In *Arabidopsis* plants, DCL4, DCL2 and DCL3 process transgene-derived dsRNAs to 21–24 nt siRNAs in a redundant and hierarchical manner (Deleris et al., 2006), which are incorporated into AGO1 or AGO2 effectors to guide cleavage of target RNAs (Pumplin and Voinnet, 2013). To further confirm our hypothesis that the accumulation of t-siRNAs was associated with RSV immunity in CP transgenic *Arabidopsis* plants, CP transgenic plants in the *dcl2/3/4* triple mutant background were developed. As expected, these transgenic plants exhibited susceptibility to RSV infection similar to that of non-transgenic plants, thus supporting our hypothesis. Our results also showed that *dcl2/3/4* triple mutant plants exhibited increased severity of disease symptoms and virus titers compared with those of Col-0

plants in RSV challenge assays, and similar results were obtained with other RNA viruses (Guo et al., 2019). Further investigation is needed to elucidate the special role of DCLs in producing t-siRNAs in CP transgenic *Arabidopsis* plants. The mechanism of RSV CP-mediated virus resistance revealed by this study provides an in-depth understanding of RNA-based antiviral immunity in RSV-*Arabidopsis* interactions.

DATA AVAILABILITY STATEMENT

The datasets presented in this study can be found in online repositories. The names of the repository/repositories and accession number(s) can be found in the article/ **Supplementary Material**.

AUTHOR CONTRIBUTIONS

FS and TZ conceived and designed the experiments. FS, PH, and WW conducted the experiments. YL, LD, FS, and TZ analyzed the data. FS and TZ wrote the manuscript. All authors read and approved the manuscript.

FUNDING

This research was supported by the National Key R&D Program of China (grant no. 2017YFD0100400), the Natural Science Foundation of Jiangsu Province (grant no. BK20171322), the National Natural Science Foundation of China (grant no. 31761143012), and TA CR-JSTD Bilateral Co-funding R&D Project (grant no. BZ2020024).

ACKNOWLEDGMENTS

We are grateful Dr. Xiuren Zhang at Texas A&M University for providing pBA-Flag-Myc4-DC vector and *Arabidopsis* Col-0 and *dcl2/3/4* mutant seeds.

SUPPLEMENTARY MATERIAL

The Supplementary Material for this article can be found online at: https://www.frontiersin.org/articles/10.3389/fmicb.2020.591619/full#supplementary-material

Supplementary Figure S1 | Characterization and expression of CP-YFP and NOP-CP-YFP in *Nicotiana benthamiana*. **(A)** Confocal imaging assays show the expression of CP-YFP but not NOP-CP-YFP in *Nicotiana benthamiana*. **(B)** RT-PCR analysis of CP mRNA transcription levels of CP-YFP and NOP-CP-YFP in *Nicotiana benthamiana.* The *ubc* mRNA level served as a loading control. **(C)** Western blot analysis of the expression of CP-YFP and NOP-CP-YFP in *Nicotiana benthamiana* using an YFP-specific antibody. The actin protein level served as a loading control.

Supplementary Figure S2 | Profile of 21–24 nucleotide (nt) virus-derived small interfering RNA (vsiRNA) derived from RSV-infected Col-0 plants, biological replicate 2.

Supplementary Figure S3 | Profile of 21–24 nucleotide (nt) virus-derived small interfering (vsiRNA) derived from RSV-infected Col-0 plants biological replicate 3.

Supplementary Figure S4 | Characterization and comparison of 21–24 nt transgenic-derived small interfering RNA (t-siRNA) mapped to the CP sequence in NOP-CP transgenic plants **(left)** and virus-derived small interfering RNA (vsiRNA) mapped to the RSV CP sequence in RSV-infected Col-0 plants **(right)** from two other biological replicates.

Supplementary Figure S5 | Characterization and comparison of 21–24 nt transgenic-derived small interfering RNA (t-siRNA) mapped to the CP sequence in NOP-CP transgenic plants after mock control (left) and RSV inoculation (right). **(A)** Distribution of t-siRNAs along the CP sequence in both positive (blue) and negative (red) polarity. Note that the scale used for the mock control is different from that used for the RSV inoculation. **(B)** Size distribution of t-siRNAs. Pie graph showing the percentage of the sense and antisense t-siRNAs. **(C)** 5′-terminal nucleotide frequency of 21–24 nt t-siRNAs.

Supplementary Figure S6 | Comparison of RSV resistance in CP transgenic plants in *dcl2/3/4* and Col-0 background. **(A)** Western blot analysis of RSV-encoded SP protein accumulation in RSV-infected CP transgenic *Arabidopsis* plants in *dcl2/3/4* and Col-0 background at 28 dpi. The actin protein level served as a loading control. **(B)** qRT-PCR analysis of RSV SP mRNA transcription levels in RSV-infected CP transgenic plants in *dcl2/3/4* and Col-0 background at 28 dpi. Signal intensities for each transcript were normalized with those for *EF1-α*. Values are means ± SD ($n = 3$). *$p \leq 0.05$ (Student's *t*-test).

Supplementary Table S1 | Primer sequence used for the cloning of transgenes and testing the viral infection.

REFERENCES

Abel, P. P., Nelson, R. S., De, B., Hoffmann, N., Rogers, S. G., Fraley, R. T., et al. (1986). Delay of disease development in transgenic plants that express the tobacco mosaic virus coat protein gene. *Science* 232, 738–743. doi: 10.1126/science.3457472

Barbier, P., Takahashi, M., Nakamura, I., Toriyama, S., and Ishihama, A. (1992). Solubilization and promoter analysis of RNA polymerase from rice stripe virus. *J. Virol.* 66, 6171–6174. doi: 10.1016/0166-0934(92)90013-4

Blevins, T., Podicheti, R., Mishra, V., Marasco, M., Wang, J., Rusch, D., et al. (2015). Identification of Pol IV and RDR2-dependent precursors of 24 nt siRNAs guiding de novo DNA methylation in *Arabidopsis*. *eLife* 4:e09591. doi: 10.7554/eLife.09591

Carbonell, A., and Carrington, J. C. (2015). Antiviral roles of plant ARGONAUTES. *Curr. Opin. Plant Biol.* 27, 111–117. doi: 10.1016/j.pbi.2015.06.013

Catoni, M., Lucioli, A., Doblas-Ibáñez, P., Accotto, G. P., and Vaira, A. M. (2013). From immunity to susceptibility: virus resistance induced in tomato by a silenced transgene is lost as TGS overcomes PTGS. *Plant J.* 75, 941–953. doi: 10.1111/tpj.12253

Clough, S. J., and Bent, A. F. (1998). Floral dip: a simplified method for *Agrobacterium*-mediated transformation of *Arabidopsis thaliana*. *Plant J.* 16, 735–743. doi: 10.1046/j.1365-313x.1998.00343.x

Deleris, A., Gallego-Bartolome, J., Bao, J. S., Kasschau, K. D., Carrington, J. C., and Voinnet, O. (2006). Hierarchical action and inhibition of plant dicer-like proteins in antiviral defense. *Science* 313, 68–71. doi: 10.1126/science.1128214

Diaz-Pendon, J. A., Li, F., Li, W. X., and Ding, S. W. (2007). Suppression of antiviral silencing by Cucumber Mosaic Virus 2b protein in *Arabidopsis* is associated with drastically reduced accumulation of three classes of viral small interfering RNAs. *Plant Cell* 19, 2053–2063. doi: 10.1105/tpc.106.047449

Du, Z., Xiao, D., Wu, J., Jia, D., Yuan, Z., Liu, Y., et al. (2011). p2 of rice stripe virus (RSV) interacts with OsSGS3 and is a silencing suppressor. *Mol. Plant Pathol.* 12, 808–814. doi: 10.1111/j.1364-3703.2011.00716.x

Falk, B. W., and Tsai, J. H. (1998). Biology and molecular biology of viruses in the genus Tenuivirus. *Annu. Rev. Phytopathol.* 36, 139–163. doi: 10.1146/annurev.phyto.36.1.139

Fang, X., and Qi, Y. (2016). RNAi in plants: an argonaute-centered view. *Plant Cell* 28, 272–285. doi: 10.1105/tpc.15.00920

Galvez, L. C., Banerjee, J., Pinar, H., and Mitra, A. (2014). Engineered plant virus resistance. *Plant Sci.* 228, 11–25. doi: 10.1016/j.plantsci.2014.07.006

Guo, Z., Li, Y., and Ding, S. W. (2019). Small RNA-based antimicrobial immunity. *Nat. Rev. Immunol.* 19, 31–44. doi: 10.1038/s41577-018-0071-x

Hamilton, A., Voinnet, O., Chappell, L., and Baulcombe, D. (2002). Two classes of short interfering RNA in RNA silencing. *EMBO J.* 21, 4671–4679. doi: 10.1093/emboj/cdf464

Han, K., Huang, H., Zheng, H., Ji, M., Yuan, Q., Cui, W., et al. (2020). Rice stripe virus coat protein induces the accumulation of jasmonic acid, activating plant defence against the virus while also attracting its vector to feed. *Mol. Plant Pathol*. doi: 10.1111/mpp.12995 [Epub ahead of print].

Hayakawa, T., Zhu, Y., Itoh, K., Kimura, Y., Izawa, T., Shimamoto, K., et al. (1992). Genetically engineered rice resistant to rice stripe virus, an insect-transmitted virus. *Proc. Natl. Acad. Sci. U.S.A.* 89, 9865–9869. doi: 10.1073/pnas.89.20.9865

Jackel, J. N., Storer, J. M., Coursey, T., and Bisaro, D. M. (2016). *Arabidopsis* RNA polymerases IV and V are required to establish H3K9 methylation, but not cytosine methylation, on geminivirus chromatin. *J. Virol.* 90, 7529–7540. doi: 10.1128/JVI.00656-16

Jiang, L., Qian, D., Zheng, H., Meng, L. Y., Chen, J., Le, W. J., et al. (2012). RNA-dependent RNA polymerase 6 of rice (oryza sativa) plays role in host defense against negative-strand RNA virus, rice stripe virus. *Virus Res.* 163, 512–519. doi: 10.1016/j.virusres.2011.11.016

Kong, L., Wu, J., Lu, L., Xu, Y., and Zhou, X. (2014). Interaction between rice stripe virus disease-specific protein and host PsbP enhances virus symptoms. *Mol. Plant* 7, 691–708. doi: 10.1093/mp/sst158

Lee, W. C., Lu, S. H., Lu, M. H., Yang, C. J., Wu, S. H., and Chen, H. M. (2015). Asymmetric bulges and mismatches determine 20-nt microRNA formation in plants. *RNA Biol.* 12, 1054–1066. doi: 10.1080/15476286.2015.1079682

Li, S., Wang, S., Wang, X., Li, X., Zi, J., Ge, S., et al. (2015). Rice stripe virus affects the viability of its vector offspring by changing developmental gene expression in embryos. *Sci. Rep.* 5:7883. doi: 10.1038/srep07883

Li, Z., Zhang, T., Huang, X., and Zhou, G. (2018). Impact of two reoviruses and their coinfection on the rice RNAi system and vsiRNA production. *Viruses* 10:594. doi: 10.3390/v10110594

Lindbo, J. A., and Falk, B. W. (2017). The impact of "Coat Protein-Mediated Virus Resistance" in applied plant pathology and basic research. *Phytopathology* 107, 624–634. doi: 10.1094/PHYTO-12-16-0442-RVW

Lindbo, J. A., Silva-Rosales, L., Proebsting, W. M., and Dougherty, W. G. (1993). lnduction of a highly specific antiviral state in transgenic plants: implications for regulation of gene expression and virus resistance. *Plant Cell* 5, 1749–1759. doi: 10.1105/tpc.5.12.1749

Ma, J., Song, Y., Wu, B., Jiang, M., Li, K., Zhu, C., et al. (2011). Production of transgenic rice new germplasm with strong resistance against two isolations of rice stripe virus by RNA interference. *Transgenic Res.* 20, 1367–1377. doi: 10.1007/s11248-011-9502-1

Martin, M. (2011). Cutadapt removes adapter sequences from high-throughput sequencing reads. *EMBnet J.* 17, 10–12. doi: 10.14806/ej.17.1.200

Mi, S., Cai, T., Hu, Y., Chen, Y., Hodges, E., Ni, F., et al. (2008). Sorting of small RNAs into *Arabidopsis argonaute* complexes is directed by the 5′ terminal nucleotide. *Cell* 133, 116–127. doi: 10.1016/j.cell.2008.02.034

Moazed, D. (2009). Small RNAs in transcriptional gene silencing and genome defence. *Nature* 457, 413–420. doi: 10.1038/nature07756

Otuka, A. (2013). Migration of rice planthoppers and their vectored re-emerging and novel rice viruses in East Asia. *Fron.t Microbiol.* 4:309. doi: 10.3389/fmicb.2013.00309

Pumplin, N., and Voinnet, O. (2013). RNA silencing suppression by plant pathogens: defence, counter-defence and counter-counter-defence. *Nat. Rev. Microbiol.* 11, 745–760. doi: 10.1038/nrmicro3120

Raja, P., Sanville, B. C., Buchmann, R. C., and Bisaro, D. M. (2008). Viral genome methylation as an epigenetic defense against geminiviruses. *J. Virol.* 82, 8997–9007. doi: 10.1128/JVI.00719-08

Ruiz-Ferrer, V., and Voinnet, O. (2009). Roles of plant small RNAs in biotic stress responses. *Annu. Rev. Plant Biol.* 60, 485–510. doi: 10.1146/annurev.arplant.043008.092111

Sanford, J. C., and Johnston, S. A. (1985). The concept of parasite-derived resistance-deriving resistance genes from the parasite's own genome. *J. Theor. Biol.* 113, 395–405. doi: 10.1016/s0022-5193(85)80234-4

Sasaya, T., Nakazono-Nagaoka, E., Saika, H., Aoki, H., Hiraguri, A., Netsu, O., et al. (2014). Transgenic strategies to confer resistance against viruses in rice plants. *Front. Microbiol.* 4:409. doi: 10.3389/fmicb.2013.00409

Shimizu, T., Nakazono-Nagaoka, E., Uehara-Ichiki, T., Sasaya, T., and Omura, T. (2011). Targeting specific genes for RNA interference is crucial to the development of strong resistance to rice stripe virus. *Plant Biotechnol. J.* 9, 503–512. doi: 10.1111/j.1467-7652.2010.00571.x

Singh, J., Mishra, V., Wang, F., Huang, H. Y., and Pikaard, C. S. (2019). Reaction mechanisms of Pol IV, RDR2, and DCL3 drive RNA channeling in the siRNA-directed DNA methylation pathway. *Mol. Cell* 75, 576.e5–589.e5. doi: 10.1016/j.molcel.2019.07.008

Sun, F., Fang, P., Li, J., Du, L., Lan, Y., Zhou, T., et al. (2016). RNA-seq-based digital gene expression analysis reveals modification of host defense responses by rice stripe virus during disease symptom development in *Arabidopsis*. *Virol. J.* 13:202. doi: 10.1186/s12985-016-0663-7

Sun, F., Yuan, X., Zhou, T., Fan, Y., and Zhou, Y. (2011). *Arabidopsis* is susceptible to rice stripe virus infections. *J. Phytopathol.* 159, 767–772. doi: 10.1111/j.1439-0434.2011.01840.x

Toriyama, S., and Watanabe, Y. (1989). Characterization of single- and double-stranded RNAs in particles of rice stripe virus. *J. Gen. Virol.* 70, 505–511. doi: 10.1099/0022-1317-70-3-505

Wang, X. B., Jovel, J., Udomporn, P., Wang, Y., Wu, Q., Li, W. X., et al. (2011). The 21-nucleotide, but not 22-nucleotide, viral secondary small interfering RNAs direct potent antiviral defense by two cooperative argonautes in *Arabidopsis thaliana*. *Plant Cell* 23, 1625–1638. doi: 10.1105/tpc.110.082305

Wang, X. B., Wu, Q., Ito, T., Cillo, F., Li, W. X., Chen, X., et al. (2010). RNAi-mediated viral immunity requires amplification of virus-derived siRNAs in *Arabidopsis thaliana*. *Proc. Natl Acad. Sci. U.S.A.* 107, 484–489. doi: 10.1073/pnas.0904086107

Wassenegger, M., and Krczal, G. (2006). Nomenclature and functions of RNA directed RNA polymerases. *Trends Plant Sci.* 11, 142–151. doi: 10.1016/j.tplants.2006.01.003

Xiong, R., Wu, J., Zhou, Y., and Zhou, X. (2008). Identification of a movement protein of the tenuivirus rice stripe virus. *J. Virol.* 82, 12304–12311. doi: 10.1128/JVI.01696-08

Xiong, R., Wu, J., Zhou, Y., and Zhou, X. (2009). Characterization and subcellular localization of an RNA silencing suppressor encoded by rice stripe tenuivirus. *Virology* 387, 29–40. doi: 10.1016/j.virol.2009.01.045

Xu, Y., Huang, L., Fu, S., Wu, J., and Zhou, X. (2012). Population diversity of rice stripe virus-derived siRNAs in three different hosts and RNAi-based antiviral immunity in *Laodelphgax striatellus*. *PLoS One* 7:e46238. doi: 10.1371/journal.pone.0046238

Yan, F., Zhang, H., Adams, M. J., Yang, J., Peng, J., Antoniw, J. F., et al. (2010). Characterization of siRNAs derived from rice stripe virus in infected rice plants by deep sequencing. *Arch. Virol.* 155, 935–940. doi: 10.1007/s00705-010-0670-8

Yang, M., Xu, Z., Zhao, W., Liu, Q., Li, Q., Lu, L., et al. (2018). Rice stripe virus-derived siRNAs play different regulatory roles in rice and in the insect vector *Laodelphax striatellus*. *BMC Plant Biol.* 18:219. doi: 10.1186/s12870-018-1438-7

Yang, Z., Huang, Y., Yang, J., Yao, S., Zhao, K., Wang, D., et al. (2020). Jasmonate signaling enhances RNA silencing and antiviral defense in rice. *Cell Host Microbe* 28, 89–103. doi: 10.1016/j.chom.2020.05.001

Yao, M., Liu, X., Li, S., Xu, Y., Zhou, Y., Zhou, X., et al. (2014). Rice stripe tenuivirus NSvc2 glycoproteins targeted to the golgi body by the N-terminal transmembrane domain and adjacent cytosolic 24 amino acids via the COP I- and COP II-dependent secretion pathway. *J. Virol.* 88, 3223–3234. doi: 10.1128/JVI.03006-13

Zhang, C., Wu, Z., Li, Y., and Wu, J. (2015). Biogenesis, function, and applications of virus-derived small RNAs in plants. *Front. Microbiol.* 6:1237. doi: 10.3389/fmicb.2015.01237

Zhang, X., Garreton, V., and Chua, N. H. (2005). The AIP2 E3 ligase acts as a novel negative regulator of ABA signaling by promoting ABI3 degradation. *Genes Dev.* 19, 1532–1543. doi: 10.1101/gad.1318705

Zhang, X., Henriques, R., Lin, S. S., Niu, Q. W., and Chua, N. H. (2006). *Agrobacterium*-mediated transformation of *Arabidopsis thaliana* using the floral dip method. *Nat. Protoc.* 1, 641–646. doi: 10.1038/nprot.2006.97

Conflict of Interest: The authors declare that the research was conducted in the absence of any commercial or financial relationships that could be construed as a potential conflict of interest.

frontiers in Microbiology

ORIGINAL RESEARCH
published: 10 December 2020
doi: 10.3389/fmicb.2020.590451

NSs, the Silencing Suppressor of Tomato Spotted Wilt Orthotospovirus, Interferes With JA-Regulated Host Terpenoids Expression to Attract *Frankliniella occidentalis*

Jiao Du[1,2†], Xiao-yu Song[2,3†], Xiao-bin Shi[2†], Xin Tang[2], Jian-bin Chen[2], Zhan-hong Zhang[4], Gong Chen[1], Zhuo Zhang[2], Xu-guo Zhou[5], Yong Liu[1,2] and De-yong Zhang[1,2*]*

[1] College of Plant Protection, Hunan Agricultural University, Changsha, China, [2] Hunan Academy of Agricultural Sciences, Institute of Plant Protection, Changsha, China, [3] High & New Technology Research Center of Henan Academy of Sciences, Zhengzhou, China, [4] Hunan Academy of Agricultural Sciences, Institute of Vegetable, Changsha, China, [5] Department of Entomology, University of Kentucky, Lexington, KY, United States

Tomato spotted wilt orthotospovirus (TSWV) causes serious crop losses worldwide and is transmitted by *Frankliniella occidentalis* (Pergande) (Thysanoptera: Thripidae). NSs protein is the silencing suppressor of TSWV and plays an important role in virus infection, cycling, and transmission process. In this research, we investigated the influences of NSs protein on the interaction of TSWV, plants, and *F. occidentalis* with the transgenic *Arabidopsis thaliana*. Compared with the wild-type Col-0 plant, *F. occidentalis* showed an increased number and induced feeding behavior on transgenic *Arabidopsis thaliana* expressing exogenous NSs. Further analysis showed that NSs reduced the expression of terpenoids synthesis-related genes and the content of monoterpene volatiles in *Arabidopsis*. These monoterpene volatiles played a repellent role in respect to *F. occidentalis*. In addition, the expression level of plant immune-related genes and the content of the plant resistance hormone jasmonic acid (JA) in transgenic *Arabidopsis* were reduced. The silencing suppressor of TSWV NSs alters the emission of plant volatiles and reduces the JA-regulated plant defenses, resulting in enhanced attractiveness of plants to *F. occidentalis* and may increase the transmission probability of TSWV.

Keywords: tomato spotted wilt orthotospovirus, NSs, *Frankliniella occidentalis*, monoterpene, insect behavior

OPEN ACCESS

Edited by:
Xiaofei Cheng, Northeast Agricultural University, China

Reviewed by:
Yongliang Zhang, China Agricultural University, China
Kira C. M. Neller, York University, Canada

***Correspondence:**
Yong Liu
haoasliu@163.com
De-yong Zhang
dyzhang78@163.com

[†] These authors have contributed equally to this work

Specialty section:
This article was submitted to Microbe and Virus Interactions with Plants, a section of the journal Frontiers in Microbiology

Received: *04 August 2020*
Accepted: *13 November 2020*
Published: *10 December 2020*

Citation:
Du J, Song X, Shi X, Tang X, Chen J, Zhang Z, Chen G, Zhang Z, Zhou X, Liu Y and Zhang D (2020) NSs, the Silencing Suppressor of Tomato Spotted Wilt Orthotospovirus, Interferes With JA-Regulated Host Terpenoids Expression to Attract Frankliniella occidentalis. Front. Microbiol. 11:590451. doi: 10.3389/fmicb.2020.590451

INTRODUCTION

In plant-virus-insect interactions, plants have evolved a complicated defense system against herbivores and viruses, such as the defense of secondary metabolites. For instance, plants emit repellent terpenoids as soon as herbivores damage plants (Dahlin et al., 2015; Magalhaes et al., 2018). In addition, when plants are attacked by herbivores and viruses, the plant hormone jasmonic

acid (JA) is rapidly synthesized, to activate the expression of defense compounds such as alkaloids and terpenoids, which directly and indirectly increase plant resistance (De Geyter et al., 2012; Okada et al., 2015; Rondoni et al., 2018). Correspondingly, insect-vector transmitted viruses overcome this system by increasing the capability of their insect vectors to promote virus spread (Luan et al., 2014; Shi et al., 2014, 2018; Yan and Xie, 2015). Some plant viruses can induce the synthesis of terpenoids to change the preference of insect vectors (Eigenbrode et al., 2002; Mann et al., 2012; Chen et al., 2017; Shi et al., 2017). Plant viruses have also evolved effective mechanisms to interfere with the JA-mediated defense response by targeting key proteins to inhibit the JA signaling pathway (De Geyter et al., 2012; Attaran et al., 2014; Cole et al., 2014; Gimenez-Ibanez et al., 2014).

Tomato spotted wilt orthotospovirus (TSWV) is a notorious virus in agriculture worldwide, which has a wide range of host plants, such as pepper, tomato, eggplant, broad bean, and lettuce (Turina et al., 2016). *Arabidopsis* is also the host plant for TSWV (Abe et al., 2011). TSWV is transmitted by thrips in a persistent propagative manner (Wan et al., 2020), of which the *Frankliniella occidentalis* (Pergande) (Thysanoptera: Thripidae) is the main species (Rotenberg et al., 2015; Cao et al., 2018). To resist virus infection, plants often exploit RNA silencing in their defense system, while plant viruses encode many RNA silencing suppressors as a corresponding countermeasure. The NSs protein of TSWV is an RNA silencing suppressor which plays many roles in the TSWV infection, replication, and transmission process (Rotenberg et al., 2015). For example, NSs protein suppressed post-transcriptional gene silencing in plants and interfered with RNA silencing in arthropod cell lines (Takeda et al., 2002; Garcia et al., 2006). In addition, NSs protein has been proven to be necessary in virus accumulation in viruliferous thrips (Margaria et al., 2014).

Recent evidence has shown that the silencing suppressor of plant viruses is involved in JA expression and plant volatile manipulation to promote insect vector survival and viral transmission (Yan and Xie, 2015). For example, 2b protein, the silencing suppressor of cucumber mosaic virus (CMV), was identified to prevent JA-induced degradation of JAZ1, and therefore enhanced odor-dependent attraction of the aphid vector (Wu et al., 2017). Similarly, βC1 protein, the RNA silencing suppressor of tomato yellow leaf curl China virus (TYLCCNV), which interacts with the JA-related transcription factor MYC2 and suppresses the JA-regulated synthesis of terpenoids, results in the promotion of virus transmission by the insect vector whitefly, *Bemisia tabaci* (Salvaudon et al., 2013). Up to now, whether there is a role in TSWV silencing suppressors in reducing plant defenses and promoting the preference and feeding behavior of *F. occidentalis* remains unknown.

To investigate the interaction between NSs protein, the silencing suppressor of TSWV, plants, and *F. occidentalis*, we (1) produced transgenic *Arabidopsis* expressing exogenous NSs genes; (2) compared the host preference and feeding behavior of *F. occidentalis* with wild-type *Arabidopsis* and transgenic *Arabidopsis* expressing NSs; (3) profiled plant volatiles using GC-MS and functionally characterized specific volatile compounds using a Y-tube olfactometer; (4) investigated endogenous hormones of plants; and (5) analyzed differentially expressed genes involved in terpenoid biosynthesis and plant-pathogen interaction using RNA-seq.

RESULTS

Preference and Feeding Behavior of *F. occidentalis*

A two-choice test was conducted with a Y-tube to investigate the preference of *F. occidentalis* on NSs transgenic plants and wild-type plants. The results showed that approximately 64% of *F. occidentalis* preferred the NSs transgenic plants, whereas 36% of *F. occidentalis* preferred wild-type *Arabidopsis* (Student's *t*-test, $T = -2.45$, df = 16, $P < 0.01$) (**Figure 1**). *F. occidentalis* preferred the transgenic plants expressing NSs over wild-type *Arabidopsis*.

An electrical penetration graph (EPG) was used to explore the feeding behavior of *F. occidentalis*. As the results showed, the number of total ingestion probes (TI), non-ingestion probes (NI), short-ingestion probes (SI), and long-ingestion probes (LI) was 2.76, 2.74, 2.90, and 1.93 times greater, respectively, for *F. occidentalis* on NSs plants than on WT plants (TI: Student's *t*-test, $T = -2.86$, df = 78, $P < 0.01$; NI: Student's *t*-test, $T = -2.68$, df = 78, $P = 0.01$; SI: Student's *t*-test, $T = -2.73$, df = 78, $P = 0.01$; LI: Student's *t*-test, $T = -2.14$, df = 78, $P = 0.04$; **Figure 2A**). The duration of the total ingestion probes (TI), non-ingestion probes (NI), short-ingestion probes (SI), and long-ingestion probes (LI) was 1.80, 2.94, 1.95, and 1.09 times greater, respectively, for *F. occidentalis* on NSs plants than on WT plants (TI: Student's *t*-test, $T = -3.53$, df = 78, $P < 0.01$; NI: Student's *t*-test, $T = -4.72$, df = 78, $P < 0.01$; SI: Student's *t*-test, $T = -2.28$, df = 78, $P = 0.03$; LI: Student's *t*-test, $T = -0.38$, df = 78, $P = 0.71$; **Figure 2B**). *F. occidentalis* preferred to feed on NSs plants than on wild-type plants, which means that the silencing suppressor NSs attracts *F. occidentals* to the plants.

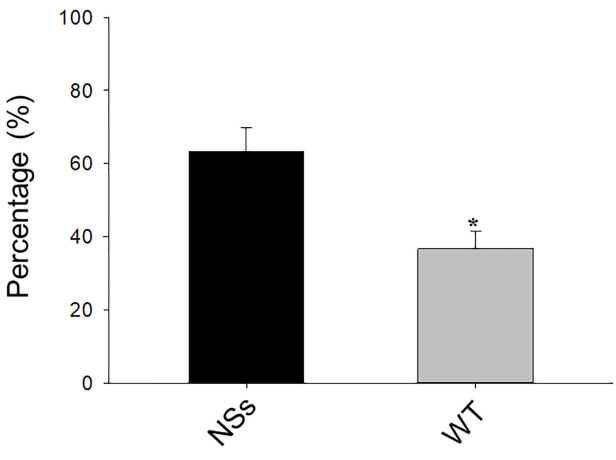

FIGURE 1 | Preference of *F. occidentalis* in Y-tube olfactometer bioassay. WT, wild-type control plants; NSs, Transgenic plants expressing NSs gene. Data are shown as percentages, and * indicate a significant difference between two bars ($n = 9$, Student's *t*-test, $P < 0.05$).

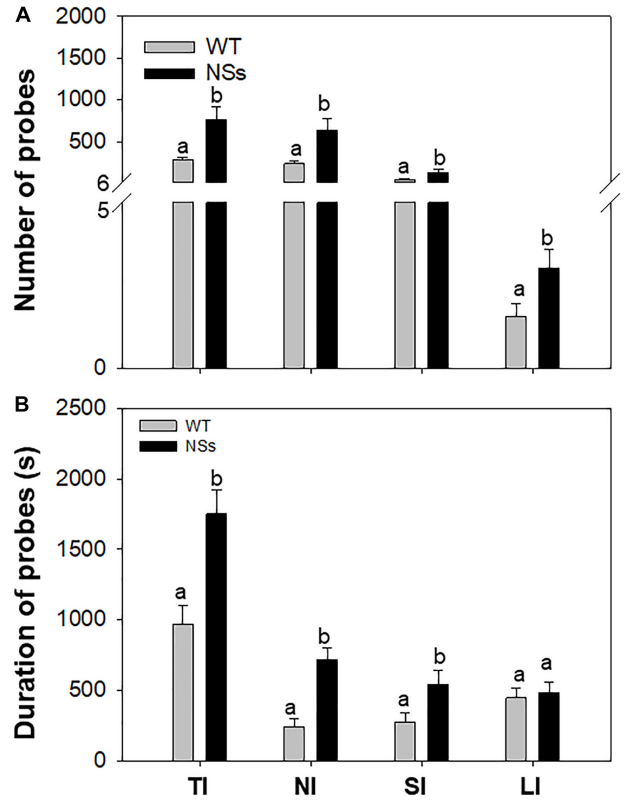

FIGURE 2 | Feeding behavior of *F. occidentalis*. Number and duration were recorded from each of two 1 h period for each individual thrip. **(A)** Number of *F. occidentalis* probes on NSs plants and WT plants; **(B)** Duration of *F. occidentalis* probes on NSs plants and WT plants. WT, wild-type control plants; NSs, transgenic plants expressing NSs gene. TI, total ingestion probes; NI, non-ingestion probes; SI, short-ingestion probes; LI, long-ingestion probes. Different lowercase letters (a, b) indicate significant differences between two bars (n = 40, Student's t-test, $P < 0.05$).

Extraction and Functional Analysis of Plant Volatiles

The volatiles were measured in the headspace of NSs transgenic plants and wild-type plants. Three terpene volatiles including (E)-β-ocimene, γ-terpinene, and β-phellandrene were detected, and they were all found to be monoterpene. Compared with wild-type *Arabidopsis*, the levels of the three monoterpene volatiles in the transgenic plants expressing NSs were significantly reduced (Student's t-test, $T = 3.56$, df = 4, $P < 0.05$ for (E)-β-ocimene; $T = 3.37$, df = 4, $P < 0.05$ for γ-terpinene; $T = 4.56$, df = 4, $P < 0.05$ for β-phellandrene) (**Figure 3**). The results indicate that the silencing suppressor NSs attracts *F. occidentalis* by suppressing host terpenoids.

F. occidentalis Preference Tests With Volatiles From Arabidopsis

To confirm whether (E)-β-ocimene, γ-terpinene, and β-phellandrene had a repellent effect on *F. occidentalis*, Y-tube olfactory-choice tests of *F. occidentalis* between volatiles and purified air were performed. The number of *F. occidentalis* was significantly higher on the arm of purified air compared with the arm with (E)-β-ocimene, γ-terpinene, and β-phellandrene. Among them, γ-terpinene showed the most obvious repelling effect (Student's t-test, $T = -3.76$, df = 16, $P < 0.01$ for (E)-β-ocimene; $T = -4.75$, df = 16, $P < 0.01$ for γ-terpinene; T = −3.01, df = 16, $P < 0.05$ for β-phellandrene) (**Figure 4A**).

In each pair of the volatile mixture and control, the number of *F. occidentalis* was higher in the Y-tube arm of purified air control than in the arm of the volatile mixture (Student's t-test, $T = -6.30$, df = 16, $P < 0.01$ for (E)-β-ocimene + γ-terpinene; $T = -5.06$, df = 16, $P < 0.01$ for (E)-β-ocimene + β-phellandrene; T = −8.74, df = 16, $P < 0.01$ for γ-terpinene + β-phellandrene; $T = -3.50$, df = 16, $P < 0.05$ for (E)-β-ocimene + γ-terpinene + β-phellandrene) (**Figure 4B**).

Quantification of Plant Endogenous Hormone

The endogenous hormones were measured in NSs transgenic plants and wild-type plants. Transgenic plants expressing NSs had one third JA compared with wild-type *Arabidopsis* (Student's t-test, $T = -3.05$, df = 4, $P < 0.05$). However, there was no significant difference in the level of MeJA and SA between the wild-type Arabidopsis and transgenic plants expressing NSs (MeJA: Student's t-test, $T = 0.61$, df = 4, $P > 0.05$; SA: Student's t-test, $T = 1.05$, df = 4, $P > 0.05$) (**Figure 5**). It suggests that NSs interferes with JA-regulated host terpenoid expression to attract *F. occidentals*.

RNA-Seq of Wild-Type and Transgenic Plants

The RNA-seq was performed to confirm the effect of NSs, which suppressed host terpenoids to attract *F. occidentals*. For RNA-seq, an average of 52 million clean reads were produced that mapped onto the *Arabidopsis* genome at an average rate of 92%, representing an average of 16,289 genes that were expressed for each sample (**Supplementary Table S2**). Compared with wild-type *Arabidopsis*, 204 differentially expressed genes (DEGs) were upregulated and 1054 DEGs were downregulated in transgenic plants expressing NSs (**Figures 6A,B** and **Supplementary Table S3**). KEGG analysis indicated that a total of 89 KEGG pathways were enriched for the DEGs (**Supplementary Table S4**). Most pathways were involved in the plant-pathogen interaction (ath04626), plant hormone signal transduction (ath04075), terpenoid backbone biosynthesis (ath00900), and sesquiterpenoid and triterpenoid biosynthesis (ath00909).

A total of five genes involved in terpenoid biosynthesis were lower in transgenic plants expressing NSs than in wild-type *Arabidopsis* among 1258 DEGs. The five DEGs were identified as terpenoid biosynthesis encoded squalene synthase 2 (SQS2), FAD/NAD (P)-binding oxidoreductase family protein (XF1), squalene epoxidase 3 (SQE3), 3-hydroxy-3-methylglutaryl-CoA reductase 2 (HMG2), and GHMP kinase family protein (AT3G54250) (**Figure 6C**). In addition, 10

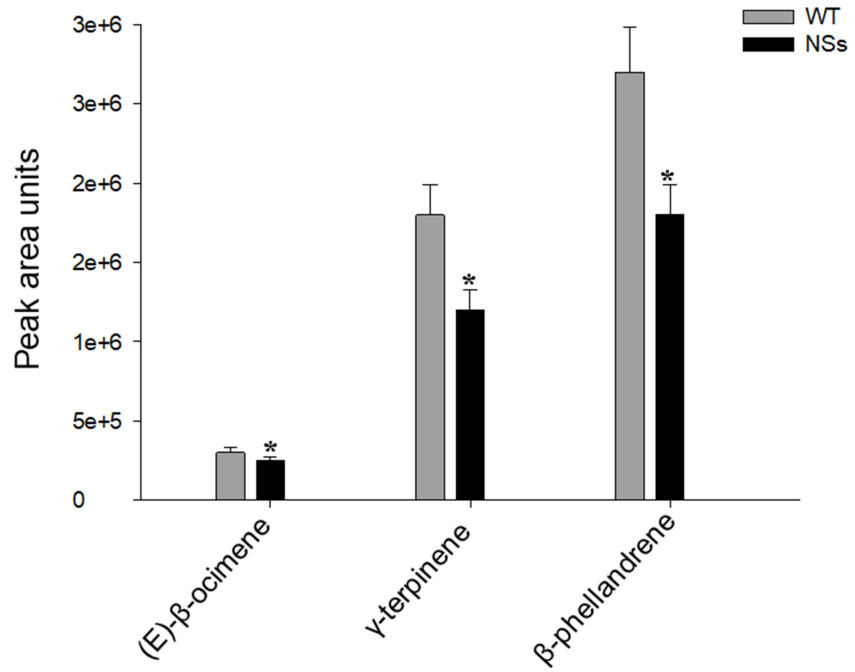

FIGURE 3 | Plant volatiles from wild-type *Arabidopsis* and transgenic plants expressing NSs at the flowering stages. WT, wild-type control plants; NSs, transgenic plants expressing NSs gene. * indicates a significant difference between two bars ($n = 3$, Student's t-test, $P < 0.05$).

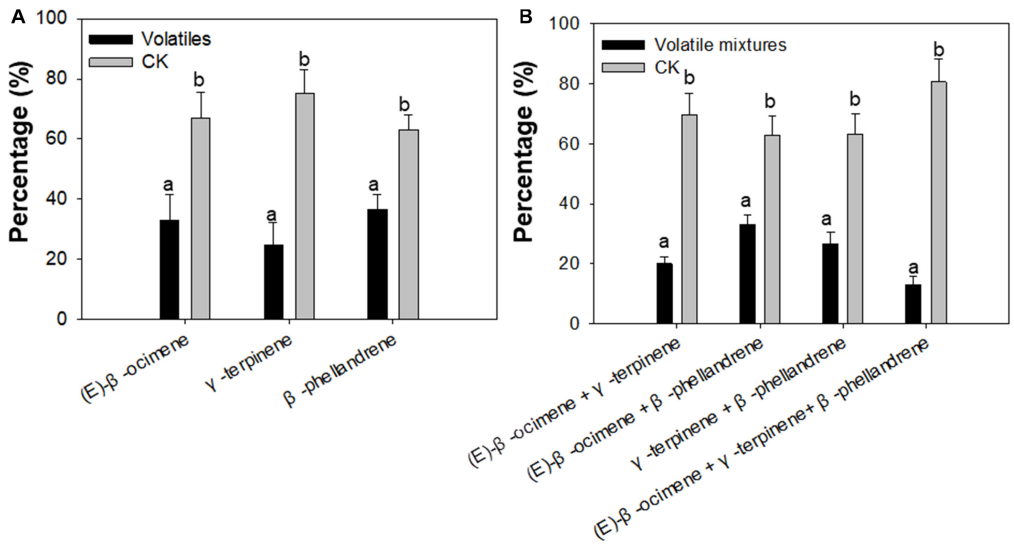

FIGURE 4 | Preference of *F. occidentalis* for selected plant volatiles, including (E)-β-ocimene, β-phellandrene, γ-terpinene, and a mixture of the three volatiles using a Y-tube olfactometer. **(A)** Preference of *F. occidentalis* for respective plant volatiles; **(B)** Preference of *F. occidentalis* for plant volatile mixtures. Standards of volatiles were used in the assay. Volatiles, (E)-β-ocimene or β-phellandrene or γ-terpinene; CK, purified air control; Volatile mixtures, mixture of (E)-β-ocimene, β-phellandrene, γ-terpinene. Different lowercase letters (a, b) indicate a significant difference between two bars ($n = 9$, Student's t-test, $P < 0.05$).

DEGs involved in the plant-pathogen interaction were also identified, including cyclic nucleotide gated channel 9 (CNGC9), calcium-binding EF hand family protein (TCH3), calmodulin 9 (CAM9), calmodulin 2 (CAM2), calmodulin 8 (CAM8), MAP kinase/ERK kinase 1 (MEK1), pathogenesis-related protein 1 (PR1), phosphatase-like protein (SGT1A), heat shock protein 81-2 (HSP81-2), and heat shock protein 81-3 (HSP81-3) (**Figure 6C**).

Validation of RNA-Seq Data by qRT-PCR

The qRT-PCR was conducted to validate RNA-seq data. As expected, compared with wild-type *Arabidopsis*, all nine

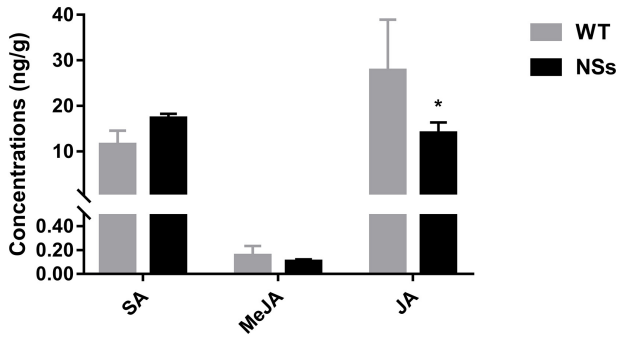

FIGURE 5 | The JA, MeJA, and SA content in wild-type *Arabidopsis* and transgenic *Arabidopsis* expressing NSs at the flowering stages. * indicates a significant difference between two bars ($n = 3$, Student's t-test, $P < 0.05$).

genes were downregulated in transgenic plants expressing NSs (**Figure 7A**). To further validate the correlation of RNA-seq data and qRT-PCR data, the r-squared value of Pearson's correlation test was used. Compared with RNA-seq results, all nine genes (genes in NSs transgenic plants compared to wild-type plants) showed downregulated expressions in the qRT-PCR results ($0 < r < 1$), which confirmed the reliability of RNA-seq data (**Figure 7B**). The results of RNA-seq and qRT-PCR confirmed that NSs interferes with JA-regulated host terpenoid expression to attract *F. occidentals*.

DISCUSSION

During the co-evolution of plant viruses with insect vectors, plant viruses influenced the performance of their vectors by manipulating plant volatile release. Although the specific molecular mechanism by which viruses interfere with the expression of host volatiles is not clear, some effectors have been found to be associated with them (Ziebell et al., 2011; Salvaudon et al., 2013; Casteel et al., 2014). Most effectors belong to silencing suppressors but the function of manipulation is independent of its silencing inhibition activity (Wu et al., 2017). In this study, we reported that NSs, the silencing suppressor of TSWV, reduced the expression of JA and led to a decrease in monoterpene volatile formation, thereby indirectly attracting *F. occidentalis* to plants. In addition, we found that feeding male thrips on NSs plants resulted in an almost threefold increase in the number of total ingestion, non-ingestion, and short-ingestion than on WT plants. Previous research showed that infected males made three times more total probes than uninfected males (Stafford et al., 2011). We found that even without a TSWV infection in the body of the thrip, only an infection of the NSs transgenic plants could induce the feeding behavior of thrips, and NSs may be the key factor of TSWV to induce thrip feeding. The NSs protein of TSWV is an RNA silencing suppressor which plays a key role in TSWV infection (Wu et al., 2019), and here we found a new role for NSs protein in helping the TSWV manipulate the feeding behavior of thrips.

Terpenoids emitted from plants, which are airborne signals for plant defense can repel herbivores (Kendra et al., 2016). Terpenoids are induced when plants are attacked by herbivores in response to herbivore damage and work to repel herbivores (Keeling and Bohlmann, 2006; Heiling et al., 2010). The content of (E)-β-ocimene increased in the volatiles of *Arabidopsis* infested with *Pieris rapae* (Faldt et al., 2003). Headspace volatiles from lima beans infested with spider mites often contain many terpenoids, such as (E)-β-ocimene, 4,8-dimethyl-1,3(E), and 7-non-atriene (Bouwmeester et al., 1999). In addition, γ-terpinene has the acaricidal activity against adult *Hyalomma marginatum* (Cetin et al., 2010). In our research, three monoterpene volatiles were detected: (E)-β-ocimene, β-phellandene, and γ-terpinene, and emissions of these three monoterpene volatiles in the transgenic plants expressing NSs were lower than those of wild-type *Arabidopsis* (**Figure 3**). Moreover, the Y-tube olfactometer assay showed that *F. occidentalis* was repelled by these three volatiles individually, and the volatile mixtures indicated that plant volatiles act as a repellent to reduce *F. occidentalis* numbers on plants and then reduce damage to *Arabidopsis* (**Figure 4**). These results indicated that the preference of *F. occidentalis* for transgenic plants expressing NSs was due to the inhibition of monoterpene volatile emissions by NSs. In this research, the terpenoid volatiles detected were different from Wu et al. (2019), as different host plants (Arabidopsis and pepper) were used in the two studies. The volatiles detected were all monoterpenes. It is possible that in different host plants, NSs may reduce the monoterpene synthesis through different volatile pathways to induce the feeding behavior and preference of *F. occidentalis*. Our results indicated that a viral silencing suppressor, such as NSs, plays an important role in inhibiting the synthesis of many kinds of monoterpenes in different host plants.

In addition, RNA-seq and qRT-PCR showed that the reduction of terpenoids was due to the inhibition of the gene expression of terpenoid synthesis pathways by NSs (**Figures 6C**, **7**). The expression of five genes (HMG2, AT3G54250, SQS2, SQE3, and XF1) in the terpenoid synthesis pathway was inhibited. Among them, the enzyme 3-hydroxy-3-methylglutaryl coenzyme A reductase (HMGR), which contains two functionally active HMGR isoforms (HMG1, HMG2), was reported to catalyze the main rate-limiting step in terpenoid biosynthetic pathways (Caelles et al., 1989; Enjuto et al., 1994). For example, the levels of triterpenes were reduced by 65 and 25% in HMG1 and HMG2 mutants, compared to those in wild-type plants, respectively (Ohyama et al., 2007). Moreover, the expression level of sterol in transgenic *Arabidopsis* overexpressing HMGR was increased (Manzano et al., 2004).

Jasmonic acid is the master switch in plant defense systems against herbivores and viruses, activating gene expression associated with terpenoid volatiles synthesis (Okada et al., 2015). For example, caterpillars (*Spodoptera littoralis)* feeding on lima beans increases the expression of JA and induces the synthesis and emission of terpenoids such as (E)-β-ocimene (Arimura et al., 2008). Conversely, after tomato mutant plants (def-1), which are deficient in JA biosynthesis, were attacked by phytophagous mites, the production of terpenoids did not increase as in wild tomatoes

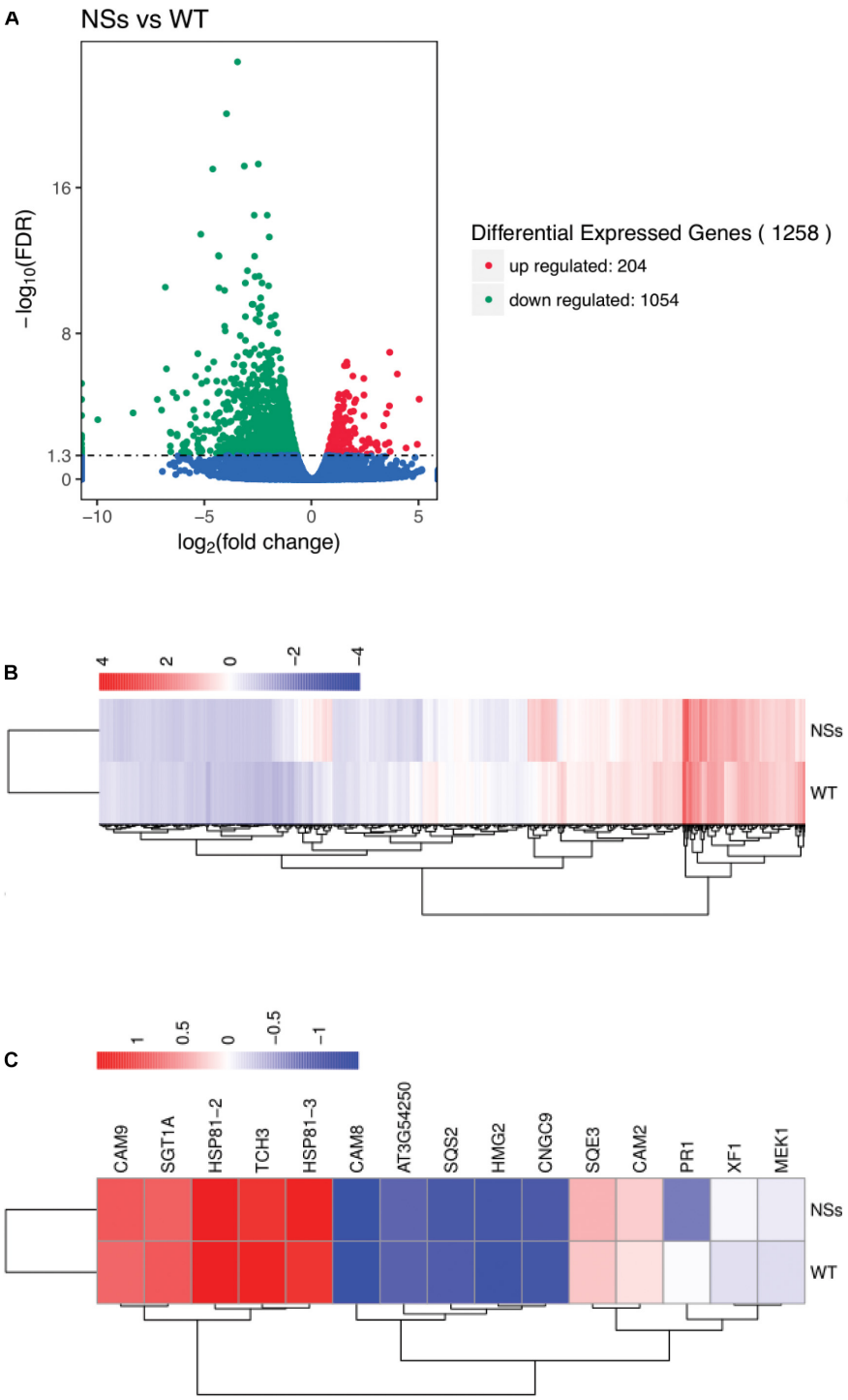

FIGURE 6 | Gene expression profiling by RNA-seq. **(A)** Volcano plot for differentially expressed genes between NSs and WT; **(B)** Cluster analysis of differentially expressed genes; **(C)** Cluster analysis of terpenoid biosynthesis-related genes and plant-pathogen interaction-related genes using RNA-seq data. Total RNA was extracted from transgenic *Arabidopsis* expressing NSs and wild-type *Arabidopsis* and sequenced using the Illumina HiSeq platform. DEGs were defined according to FDR < 0.05. NSs, transgenic plants expressing NSs gene; WT, wild-type plants.

(Ament et al., 2004). Moreover, JA and SA have an obvious antagonistic relationship in terpenoid biosynthesis, when *Arabidopsis* is infested with aphids (Girling et al., 2008). SA interferes with JA's positive regulation of terpenoids synthesis. However, in our study, NSs reduced the expression of JA in plants but had no effect on SA (**Figure 5**). These results

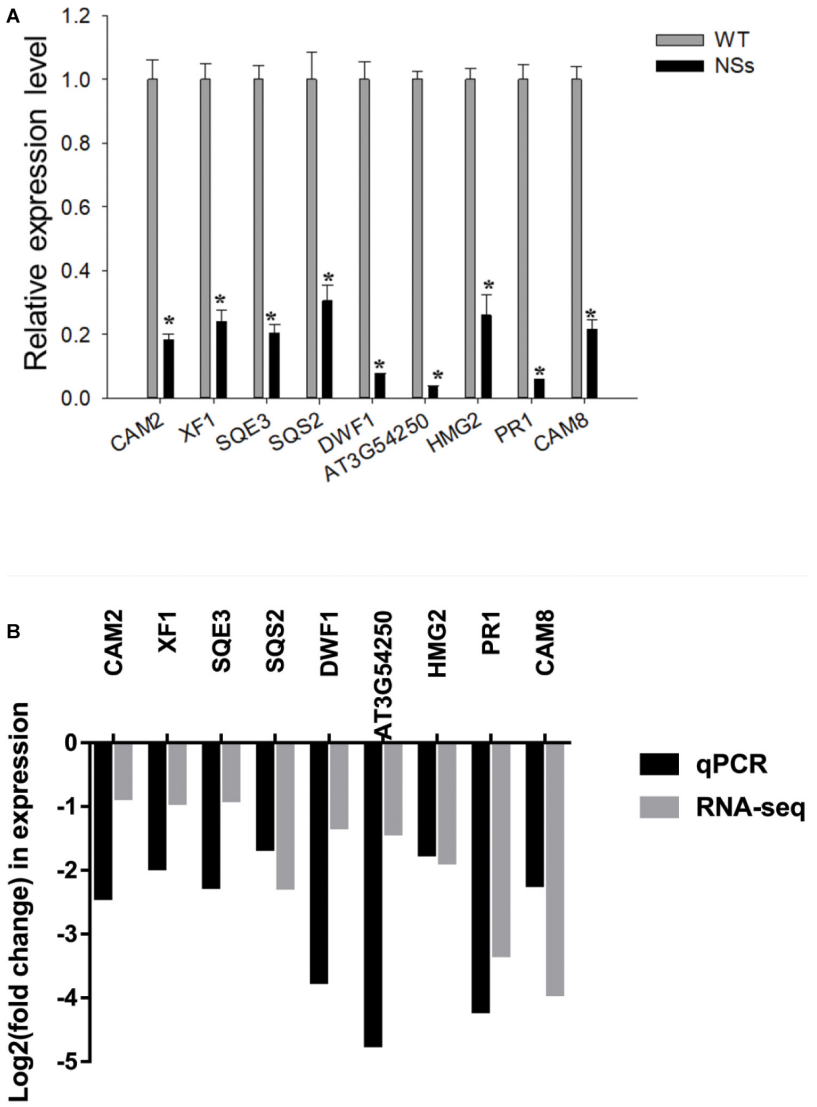

FIGURE 7 | Validation analysis of RNA-seq data by qRT-PCR. **(A)** Quantitative RT-PCR analysis of five selected terpenoid biosynthesis-related and four selected plant-pathogen interaction-related genes. * indicates a significant difference between two bars ($n = 3$, Student's t-test, $^*P < 0.05$); **(B)** The correlation analysis of five selected terpenoid biosynthesis-related and four selected plant-pathogen interaction-related genes between RNA-seq data and qRT-PCR data (Pearson's correlation test, $0 < r < 1$).

suggest that the synthesis of terpenoids may be regulated by JA signaling pathways.

In conclusion, our study shows that the silencing suppressor NSs of TSWV reduces the emission of plant monoterpene volatiles, to increase the attraction of plants to *F. occidentalis*, by interfering with JA-regulated plant defense systems and reducing the resistant volatiles. Insect vectors are extremely important for the epidemic of their transmitted viruses, since the spread of viruses between plants requires the transport of insect vectors. These viruses commonly change the physiology of plants to increase the attractiveness and adaptability of plants to insect vectors (Beanland et al., 2000; Lacroix et al., 2005; Jiu et al., 2007; Wang et al., 2012; Luan et al., 2014). The phenomenon that viruses alter plant volatiles to increase the attraction of plants to insect vectors is also found in other plant-virus-insect interactions (Eigenbrode et al., 2002; Mann et al., 2012; Chen et al., 2017). Combining these results, we speculate that "odor manipulation" is a common strategy for plant viruses to indirectly promote their own transmission.

MATERIALS AND METHODS

Thrip Strain and TSWV Inoculation

TSWV was obtained in Kunming, Yunnan Province of China from tomato plants in 2018. Then TSWV was purified, identified, designated as TSWV-YN, and mechanically inoculated on *Nicotiana tabacum* cv. Samsun NN. The mechanical inoculation

of TSWV involved an inoculum consisting of infected leaf sap in 0.1 M phosphate buffer, 0.2% sodium sulfite and 0.01 M mercaptoethanol, and 1% each of celite 545 and carborundum 320 grit. Cotton swabs were used to draw inoculum and gently rub the fresh leaves of the plant (Mandal et al., 2008; Shalileh et al., 2016). The symptoms were observed after 7–14 days, and the reverse transcription polymerase chain reaction (RT-PCR) method was used to detect whether the plant was successfully infected with the TSWV. The specific primers were NSs-F: ATGTCTTCAAGTGTTTATGAGT and NSs-R: TTATTTTGATCCTGAAGCATATG. To maintain the TSWV strain, some of the TSWV isolates were flash frozen with liquid nitrogen and then placed in a refrigerator at −80°C. The other TSWV isolates were maintained on *N. tabacum* plants by thrip transmission to avoid the viral mutants and the reduced transmissibility.

An isolate of *F. occidentalis* was obtained from Dr. Qing-jun Wu of the Chinese Academy of Agricultural Sciences (Beijing, China). Virus-free stock colonies of *F. occidentalis* were reared on bean pods (*Phaseolus vulgarisin*) in glass jars, closed on top with a 64 μm thrip-proof nylon net in a greenhouse at 25 ± 1°C, 60 ± 10% RH, and a 14 L: 10 D photoperiod. The bean pods were replaced daily, and the harvested pods with eggs were transferred to new glass jars to synchronize larvae growth. *F. occidentalis* used in all the experiments were from synchronized rearing (Mandal et al., 2008).

Wild-type Col-0 *Arabidopsis* was also obtained from the Chinese Academy of Agricultural Sciences (Beijing, China). Wild-type and transgenic *Arabidopsis* were grown in a greenhouse at a temperature of 22 ± 1°C, relative humidity of 55 ± 10%, and a photoperiod of 14 h.

Construction of Plasmids and Generation of Transgenic Plants

To obtain the NSs ORF, total RNA was extracted from 100 mg of TSWV-infected *N. benthamiana* leaves using Trizol (Invitrogen, United States). The NSs cDNA was obtained by RT-PCR with specific primers using a HiScript II 1st Strand cDNA Synthesis Kit (Vazyme, China). The full length coding sequence of NSs was amplified using pCB-NSs-F (*Xba*I) and pCB-NSs-R (*Pst*I) and inserted between the *Xba*I and *Pst*I sites of the pCambia1301 vector under the control of the cauliflower mosaic virus (CaMV) 35S promoter to generate pCambia1301-NSs. The obtained expression vector was verified by PCR and sequencing. pCambia1301-NSs was transferred into *Agrobacterium tumefaciens* GV3101 by electroporation, and then transferred into Col-0 plants by the floral dip method (Clough and Bent, 2010). Successfully transformed T1 plants were obtained on MS medium containing 50 μg/mL hygromycin B and confirmed by RT-PCR (**Supplementary Figure S1A**). Therefore, the T3 transgene-homozygote lineages generated from T1 plants through continuous self-pollination (selfing), and RT-PCR identification were used for the experiments. Western blot analysis was used to check for protein expression in the transgenic plants. Total protein of *Arabidopsis thaliana* was extracted using a Plant Protein Extraction Kit (Solarbio, China). Then, the protein was resolved by SDS-PAGE and transferred to a PVDF Membrane (BIO-RAD, United States). The membrane was blocked with TBS-T containing 5% skimmed milk, and incubated with the polyclonal antibody of TSWV NSs protein. Detection was performed incubating with the horseradish peroxidase-conjugated goat anti-rabbit IgG antibody (Thermo Fisher Scientific, United States) and the Pierce™ ECL Plus Western Blotting Substrate (Thermo Fisher Scientific, United States) (**Supplementary Figure S1B**). Wild-type *Arabidopsis* was used as a negative control. Tubulin was used as a loading control.

Preference and Feeding Behavior of *F. occidentalis*

According to previous references, the volatile components are mainly released from flowers (Aharoni et al., 2003). To investigate the preference of *F. occidentalis* on wild-type *Arabidopsis* and transgenic plants expressing NSs, plants at the flowering stages were used for pair-wise comparison using the Y-tube. In each preference test, five wild-type plants and five transgenic plants expressing NSs were placed into two odor source bottles, which were connected to the two arms of the Y-tube (stem 10 cm; arms 20 cm, 60° angle; inner diameter 2 cm). Under the action of the gas generator pump, two streams of purified airflow were metered into the arms of the Y-tube at 100 mL/min^{-1}.

F. occidentalis adults were used in the preference test for approximately 5 days. Thrips were starved for 8 h and were individually introduced at the end of the Y-tube stem. In each test there were 50 thrips, and each thrip was observed for a maximum of 5 min. A "choice" was recorded when a thrip entered one arm for more than 3 cm and a "no choice" was recorded when they remained inactive for 5 min. In each test, the preference of 50 thrips was counted and the number at each arm was recorded. In total, there were nine replicate tests, and there was a total of 450 thrips used in this research. The position of two odor-source bottles was changed to eliminate the effect of potential asymmetry (Cao et al., 2019). The Y-tube was replaced every 10 thrip tests, and in each preference test, the Y-tube was replaced 5 times. The used Y-tube was then washed with 75% ethanol and placed in a 65°C oven to dry.

The feeding behavior of *F. occidentalis* on wild-type *Arabidopsis* and transgenic plants expressing NSs was compared by electrical penetration graphs using a DC-system (a Giga-8 DC-amplifier with a 10^9 –Ω input resistance, Wageningen University, Netherlands) (Liu et al., 2013). There were two treatments, with each of 20 replicate plants in five to six-leaf stages. The 5 d-old male thrips were cooled on a glass dish on an ice-pack before recording. After that, a 15 μm diameter, 2 cm long gold wire was attached to the thorax of a thrip with a drop of water-soluble silver glue. Each wired thrip was connected to the Giga-8 probe input and then placed on the surface of the back of upper leaf of a plant. The thrip feeding behavior was analyzed with a DI710-UL analog-to-digital converter (Dataq Instruments, Akron, OH) and the output was acquired and stored with the PROBE3.4 software (Wageningen University, Netherlands). EPGs were observed and recorded continuously for 8 h with each thrip. Waveforms of EPG were identified according to a previous publication

(Stafford et al., 2011). Each 8 h observation period was divided into two 4 h halves, and a 1 h period from each half was randomly selected for analysis. For each selected 1 h period, the single and total number and duration of non-ingestion, short-ingestion, and long-ingestion probes were measured.

Extraction and Analysis of Plant Volatiles

Volatiles emitted by *Arabidopsis* at the flowering stages were collected using a dynamic headspace collection system. The soil with the roots of each plant was carefully wrapped in aluminum foil, and five plants were placed in 4 L glass jars with gas inlets and outlets. One stream of purified airflow was metered into a glass jar at 300 mL/min^{-1} from the inlet, and a glass tube filled with 300 mg of PoraPak Q 80/100 mesh (Waters, United States) was used to trap plant volatiles at the outlet. Volatiles were eluted with 800 μL n-hexane (Sigma Aldrich, United States) that contained 160 ng of n-dodecane as an internal standard after 8 h collection under continuous light. Then a 1 μL sample of the solution was subjected to GC/MS analysis. The whole experiment was repeated three times.

GC analysis was performed using a DB-1 (Agilent Technologies, United States) column (30 m × 0.25 mm × 0.25 μm). The temperature profile was as follows: 60°C for 2 min; then increased to 130°C at a programmed rate of 5°C/min^{-1} and kept for 2 min, followed by a rate of 5°C/min^{-1} to 180°C, then followed by rate of 20°C/min^{-1} to 250°C and kept for 5 min. MS conditions were as follows: the temperature of the ion source was 200°C; the scan mass range was 40–500 U. Then the compounds were identified by comparison of GC retention times with those of authentic standards and by comparison of mass spectra with spectra of the National Institute of Standards and Technology (NIST) database. The peak area of the volatile expressed as a proportion of the peak area of the internal standard was used for quantification.

F. occidentalis Preference Tests With Volatiles From Arabidopsis

Based on the GC/MS analysis results, the preference of male *F. occidentalis* to plant volatiles was tested in a Y-tube olfactometer using the standard chemical of detected volatiles (Sigma Aldrich, United States). In the Y-tube olfactometer bioassay, two glass containers, one of the standard chemical and one of purified air as control, were connected into the olfactometer arms (Shi et al., 2018). The preference of *F. occidentalis* was observed as described in "Preference and feeding behavior of *F. occidentalis*."

Quantification of Plant Endogenous Hormone

Transgenic plants and wild plants of *Arabidopsis* at the flowering stages were used for quantification of the plant endogenous hormone with 1 g/plant. Leaves of *Arabidopsis* were ground with 10 mL isopropanol/hydrochloric acid and shaken at 4°C for 30 min (You et al., 2016). There were 9 transgenic plants and 9 wild plants. Subsequently, 20 mL dichloromethane was added. The mixture was shaken at 4°C for 30 min and centrifuged at 13,000 rpm at 4°C for 5 min. The organic fraction was separated and then dried under nitrogen in darkness. The solid residue was re-suspended in 400 μL methanol/0.1% methanoic acid. The sample was filtered with a 0.22 μm filter membrane before HPLC-MS/MS analysis.

HPLC analysis was performed using a poroshell 120 SB-C18 (Agilent, United States) column (150 × 2.1 mm × 2.7 μm). The mobile phase A solvents consisted of methanol + 0.1% methanoic acid and the mobile phase B solvents consisted of ultrapure water + 0.1% methanoic acid. The injection volume was 2 μL. MS conditions were as follows: the spray voltage was 4,500 V; the pressure of the air curtain, nebulizer, and aux gas were 15, 65, and 70 psi, respectively, and the atomizing temperature was 400°C.

RNA-Seq of Wild-Type and Transgenic Plants

Total RNA was extracted from wild-type *Arabidopsis* and transgenic plants (above-ground parts) expressing NSs using Trizol (Invitrogen, United States), respectively. There were three biological replicates of NSs plants and three biological replicates of control wild-type plants. Sequencing libraries were constructed using the NEBNext® UltraTM RNA Library Prep Kit for Illumina® (NEB, United States) and sequenced using the Illumina HiSeq platform. To obtain clean reads, sequencing data of the raw reads were firstly processed through in-house perl scripts. Clean reads were obtained by removing reads containing adapter, reads containing ploy-N, and low quality reads from raw data. At the same time, Q20, Q30, and GC content clean data were calculated. All the downstream analyses were based on the clean data with high quality.

The paired-end clean reads were mapped to the reference genome downloaded from the *Arabidopsis* information resource[1]. To quantify the gene expression level, the mapped clean reads were calculated and then normalized into transcripts per million (TPM) (Patro et al., 2017). Genes with a false discovery rate (FDR < 0.05) were assigned as differentially expressed using the DESeq R package (1.18.0). Gene ontology (GO) enrichment analysis of differentially expressed genes was implemented by the GOseq R package, GO terms with an FDR less than 0.05 were considered significantly enriched by differential expressed genes. With a cut-off of 0 < FDR < 1, the statistical enrichment of differential expression genes was tested by the KOBAS software in Kyoto Encyclopedia of Genes and Genomics (KEGG) pathways[2].

Validation of RNA-Seq Data by qRT-PCR

To validate the results from RNA-seq data, we selected nine genes from the terpenoid biosynthesis-related genes and plant-pathogen interaction genes for qRT-PCR analysis. First-strand cDNA was synthesized from RNA using the HiScript® II 1st Strand cDNA Synthesis Kit (Vazyme, China). The specific primers for qRT-PCR were designed using qPrimerDB (Lu et al., 2018)[3] and two reference genes, β-TUBULIN-2 and ACTIN1 were

[1]https://www.arabidopsis.org

[2]http://www.genome.jp/kegg/

[3]https://biodb.swu.edu.cn/qprimerdb

used as controls for constant transcript level expression (Wang et al., 2009; Ramadoss et al., 2018). The stable expression of β-TUBULIN-2 and ACTIN1 were determined under our experimental conditions. A total of 0.5 μl 10 μM primers were used in the 20 μl qRT-PCR reaction system, the primer sequences are listed in **Supplementary Table S1**. In addition, qRT-PCR was performed using the AceQ qRT-PCR SYBR-Green Master Mix (Vazyme, China) and was analyzed using the $2^{-\Delta\Delta Ct}$ analysis method (Livak and Schmittgen, 2001). In total, there were three biological replicates and three technical replicates per treatment in this test.

The r-squared value of Pearson's correlation test was used to validate the correlation of RNA-seq data and qRT-PCR data. When the r-squared value is $0 < R < 1$, it means there is a positive correlation between RNA-seq data and qRT-PCR data.

Data Analysis

All proportional data were arcsine-square root transformed before analyses. Student's *t*-test for independent samples was used to compare the preference of *F. occidentalis*, the feeding behavior of *F. occidentalis*, the volatile, plant hormone, and qRT-PCR performed on wild-type *Arabidopsis* and transgenic plants expressing NSs. Student's *t*-test for independent samples was also used to compare *F. occidentalis* preference to volatiles and volatile mixtures from *Arabidopsis*. Pearson's correlation test was used to validate the correlation of RNA-seq data and qRT-PCR data. SPSS 22.0 (SPSS Software, United States) was used for all statistical analyses.

DATA AVAILABILITY STATEMENT

The original contributions presented in the study are publicly available. This data can be found here: https://www.ncbi.nlm.nih.gov/bioproject?term=PRJNA674939. BioSample accessions: SAMN16680812, SAMN16680813, SAMN16680814, SAMN16680815, SAMN16680816, and SAMN16680817.

AUTHOR CONTRIBUTIONS

XBS and DYZ designed the experiment. JD and XYS performed the experiment. XT, JBC, ZHZ, GC, ZZ, XGZ, and YL contributed reagents and materials. XBS, JD, and XYS wrote the manuscript. All authors contributed to the article and approved the submitted version.

FUNDING

This work was supported by the National Natural Science Foundation of China (Grant Nos. 31872932, 31871935, 31571981, and 31672003), the National Key R&D Program of China (2018YFE0112600), the Agriculture Research System of China (CARS-23-D-02); and the National Agricultural Outstanding Talent Program [(2015)62].

ACKNOWLEDGMENTS

We thank Prof. You-zhi Li (Hunan Agricultural University) and Prof. Feng-ming Yan (Henan Agricultural University) for kindly providing the instrument and materials for the EPG experiment.

SUPPLEMENTARY MATERIAL

The Supplementary Material for this article can be found online at: https://www.frontiersin.org/articles/10.3389/fmicb.2020.590451/full#supplementary-material

REFERENCES

Abe, H., Tomitaka, Y., Shimoda, T., Seo, S., Sakurai, T., Kugimiya, S., et al. (2011). Antagonistic plant defense system regulated by phytohormones assists interactions among vector insect, thrips and a *Tospovirus*. *Plant Cell Physiol.* 53, 204–212. doi: 10.1093/pcp/pcr173

Aharoni, A., Giri, A. P., Deuerlein, S., Griepink, F., De Kogel, W.-J., Verstappen, F. W., et al. (2003). Terpenoid metabolism in wild-type and transgenic *Arabidopsis* plants. *Plant Cell* 15, 2866–2884. doi: 10.1105/tpc.016253

Ament, K., Kant, M. R., Sabelis, M. W., Haring, M. A., and Schuurink, R. C. (2004). Jasmonic acid is a key regulator of spider mite-induced volatile terpenoid and methyl salicylate emission in tomato. *Plant Physiol.* 135, 2025–2037. doi: 10.1104/pp.104.048694

Arimura, G., Kopke, S., Kunert, M., Volpe, V., David, A., Brand, P., et al. (2008). Effects of feeding *Spodoptera littoralis* on lima bean leaves: IV. diurnal and nocturnal damage differentially initiate plant volatile emission. *Plant Physiol.* 146, 965–973. doi: 10.1104/pp.107.111088

Attaran, E., Major, I. T., Cruz, J. A., Rosa, B. A., Koo, A. J., Chen, J., et al. (2014). Temporal dynamics of growth and photosynthesis suppression in response to jasmonate signaling. *Plant Physiol.* 165, 1302–1314. doi: 10.1104/pp.114.239004

Beanland, L., Hoy, C. W., Miller, S. A., and Nault, L. R. (2000). Influence of aster yellows phytoplasma on the fitness of aster leafhopper (*Homoptera*: *Cicadellidae*). *Ann. Entomol. Soc. Am.* 93, 271–276. doi: 10.1603/0013-8746(2000)093[0271:ioaypo]2.0.co;2

Bouwmeester, H. J., Verstappen, F. W., Posthumus, M. A., and Dicke, M. (1999). Spider mite-induced (3S)-(E)-nerolidol synthase activity in cucumber and lima bean. The first dedicated step in acyclic C11-homoterpene biosynthesis. *Plant Physiol.* 121, 173–180. doi: 10.1104/pp.121.1.173

Caelles, C., Ferrer, A., Balcells, L., Hegardt, F. G., and Boronat, A. (1989). Isolation and structural characterization of a cDNA encoding *Arabidopsis thaliana* 3-hydroxy-3-methylglutaryl coenzyme a reductase. *Plant Mol. Biol.* 13, 627–638. doi: 10.1007/bf00016018

Cao, Y., Li, C., Yang, H., Li, J., Li, S., Wang, Y., et al. (2019). Laboratory and field investigation on the orientation of *Frankliniella occidentalis* (*Thysanoptera*: *Thripidae*) to more suitable host plants driven by volatiles and component analysis of volatiles. *Pest Manag. Sci.* 75, 598–606. doi: 10.1002/ps.5223

Cao, Y., Zhi, J. R., Zhang, R. Z., Li, C., Liu, Y., Lv, Z. Y., et al. (2018). Different population performances of *Frankliniella occidentalis* and thrips hawaiiensis on flowers of two horticultural plants. *J. Pest Sci.* 91, 79–91. doi: 10.1007/s10340-017-0887-3

Casteel, C. L., Yang, C., Nanduri, A. C., De Jong, H. N., Whitham, S. A., and Jander, G. (2014). The NIa-Pro protein of Turnip mosaic virus improves growth and reproduction of the aphid vector, *Myzus persicae* (green peach aphid). *Plant J.* 77, 653–663. doi: 10.1111/tpj.12417

Cetin, H., Cilek, J. E., Oz, E., Aydin, L., Deveci, O., and Yanikoglu, A. (2010). Acaricidal activity of Satureja thymbra L. essential oil and its major components, carvacrol and gamma-terpinene against adult *Hyalomma marginatum* (*Acari*: *Ixodidae*). *Vet. Parasitol.* 170, 287–290. doi: 10.1016/j.vetpar.2010.02.031

Chen, G., Su, Q., Shi, X., Liu, X., Peng, Z., Zheng, H., et al. (2017). Odor, not performance, dictates *Bemisia tabaci*'s selection between healthy and virus infected plants. *Front Physiol.* 8:146. doi: 10.3389/fphys.2017.00146

Clough, S. J., and Bent, A. F. (2010). Floral dip: a simplified method for Agrobacterium-mediated transformation of *Arabidopsis thaliana*. *Plant J.* 16, 735–743. doi: 10.1046/j.1365-313x.1998.00343.x

Cole, S. J., Yoon, A. J., Faull, K. F., and Diener, A. C. (2014). Host perception of jasmonates promotes infection by Fusarium oxysporum formae speciales that produce isoleucine- and leucine-conjugated jasmonates. *Mol. Plant Pathol.* 15, 589–600. doi: 10.1111/mpp.12117

Dahlin, I., Vucetic, A., and Ninkovic, V. (2015). Changed host plant volatile emissions induced by chemical interaction between unattacked plants reduce aphid plant acceptance with intermorph variation. *J. Pest Sci.* 88, 249–257. doi: 10.1007/s10340-014-0625-z

De Geyter, N., Gholami, A., Goormachtig, S., and Goossens, A. (2012). Transcriptional machineries in jasmonate-elicited plant secondary metabolism. *Trends Plant Sci.* 17, 349–359. doi: 10.1016/j.tplants.2012.03.001

Eigenbrode, S. D., Ding, H., Shiel, P., and Berger, P. H. (2002). Volatiles from potato plants infected with Potato leafroll virus attract and arrest the virus vector, *Myzus persicae* (*Homoptera*: *Aphididae*). *Proc. Biol. Sci.* 269, 455–460. doi: 10.1098/rspb.2001.1909

Enjuto, M., Balcells, L., Campos, N., Caelles, C., Arro, M., and Boronat, A. (1994). *Arabidopsis thaliana* contains two differentially expressed 3-hydroxy-3-methylglutaryl-CoA reductase genes, which encode microsomal forms of the enzyme. *Proc. Natl. Acad. Sci. U.S.A.* 91, 927–931. doi: 10.1073/pnas.91.3.927

Faldt, J., Arimura, G., Gershenzon, J., Takabayashi, J., and Bohlmann, J. (2003). Functional identification of AtTPS03 as (E)-beta-ocimene synthase: a monoterpene synthase catalyzing jasmonate- and wound-induced volatile formation in *Arabidopsis thaliana*. *Planta* 216, 745–751. doi: 10.1007/s00425-002-0924-0

Garcia, S., Billecocq, A., Crance, J. M., Prins, M., Garin, D., and Bouloy, M. (2006). Viral suppressors of RNA interference impair RNA silencing induced by a Semliki forest virus replicon in tick cells. *J. Gen. Virol.* 87, 1985–1989. doi: 10.1099/vir.0.81827-0

Gimenez-Ibanez, S., Boter, M., Fernandez-Barbero, G., Chini, A., Rathjen, J. P., and Solano, R. (2014). The bacterial effector HopX1 targets JAZ transcriptional repressors to activate jasmonate signaling and promote infection in *Arabidopsis*. *PLoS Biol.* 12:e1001792. doi: 10.1371/journal.pbio.1001792

Girling, R. D., Madison, R., Hassall, M., Poppy, G. M., and Turner, J. G. (2008). Investigations into plant biochemical wound-response pathways involved in the production of aphid-induced plant volatiles. *J. Exp. Bot.* 59, 3077–3085. doi: 10.1093/jxb/ern163

Heiling, S., Schuman, M. C., Schoettner, M., Mukerjee, P., Berger, B., Schneider, B., et al. (2010). Jasmonate and ppHsystemin regulate key malonylation steps in the biosynthesis of 17-Hydroxygeranyllinalool diterpene glycosides, an abundant and effective direct defense against herbivores in *Nicotiana attenuata*. *Plant Cell* 22, 273–292. doi: 10.1105/tpc.109.071449

Jiu, M., Zhou, X. P., Tong, L., Xu, J., Yang, X., Wan, F. H., et al. (2007). Vector-virus mutualism accelerates population increase of an invasive whitefly. *PLoS One* 2:e182. doi: 10.1371/journal.pone.0000182

Keeling, C. I., and Bohlmann, J. (2006). Diterpene resin acids in conifers. *Phytochemistry* 67, 2415–2423. doi: 10.1016/j.phytochem.2006.08.019

Kendra, P. E., Montgomery, W. S., Deyrup, M. A., and Wakarchuk, D. (2016). Improved lure for redbay ambrosia beetle developed by enrichment of alpha-copaene content. *J. Pest Sci.* 89, 427–438. doi: 10.1007/s10340-015-0708-5

Lacroix, R., Mukabana, W. R., Gouagna, L. C., and Koella, J. C. (2005). Malaria infection increases attractiveness of humans to mosquitoes. *PLoS Biol.* 3:e298. doi: 10.1371/journal.pbio.0030298

Liu, B., Preisser, E. L., Chu, D., Pan, H., Xie, W., Wang, S., et al. (2013). Multiple forms of vector manipulation by a plant-infecting virus: *Bemisia tabaci* and Tomato yellow leaf curl virus. *J. Virol.* 87, 4929–4937. doi: 10.1128/jvi.03571-12

Livak, K. J., and Schmittgen, T. D. (2001). Analysis of relative gene expression data using real-time quantitative PCR and the $2-\Delta\Delta CT$ method. *Methods.* 25, 402–408. doi: 10.1006/meth.2001.1262

Lu, K., Li, T., He, J., Chang, W., Zhang, R., Liu, M., et al. (2018). qPrimerDB: a thermodynamics-based gene-specific qPCR primer database for 147 organisms. *Nucleic Acids Res.* 46, 1229–1236.

Luan, J. B., Wang, X. W., Colvin, J., and Liu, S. S. (2014). Plant-mediated whitefly-begomovirus interactions: research progress and future prospects. *Bull. Entomol. Res.* 104, 267–276. doi: 10.1017/s000748531400011x

Magalhaes, D. M., Borges, M., Laumann, R. A., and Moraes, M. C. B. (2018). Influence of multiple- and single-species infestations on herbivore-induced cotton volatiles and *Anthonomus grandis* behaviour. *J. Pest Sci.* 91, 1019–1032. doi: 10.1007/s10340-018-0971-3

Mandal, B., Csinos, A. S., Martinez-Ochoa, N., and Pappu, H. R. (2008). A rapid and efficient inoculation method for *Tomato spotted* wilt *Tospovirus*. *J. Virol. Methods* 149, 195–198. doi: 10.1016/j.jviromet.2007.12.007

Mann, R. S., Ali, J. G., Hermann, S. L., Tiwari, S., Pelz-Stelinski, K. S., Alborn, H. T., et al. (2012). Induced release of a plant-defense volatile 'deceptively' attracts insect vectors to plants infected with a bacterial pathogen. *PLoS Pathog.* 8:e1002610. doi: 10.1371/journal.ppat.1002610

Manzano, D., Fernandez-Busquets, X., Schaller, H., Gonzalez, V., Boronat, A., Arro, M., et al. (2004). The metabolic imbalance underlying lesion formation in *Arabidopsis thaliana* overexpressing farnesyl diphosphate synthase (isoform 1S) leads to oxidative stress and is triggered by the developmental decline of endogenous HMGR activity. *Planta* 219, 982–992. doi: 10.1007/s00425-004-1301-y

Margaria, P., Bosco, L., Vallino, M., Ciuffo, M., Mautino, G. C., Tavella, L., et al. (2014). The NSs protein of *Tomato spotted wilt virus* is required for persistent infection and transmission by *Frankliniella occidentalis*. *J. Virol.* 88, 5788–5802. doi: 10.1128/jvi.00079-14

Ohyama, K., Suzuki, M., Masuda, K., Yoshida, S., and Muranaka, T. (2007). Chemical phenotypes of the hmg1 and hmg2 mutants of *Arabidopsis* demonstrate the in-planta role of HMG-CoA reductase in triterpene biosynthesis. *Chem. Pharm. Bull.* 55, 1518–1521. doi: 10.1248/cpb.55.1518

Okada, K., Abe, H., and Arimura, G. (2015). Jasmonates induce both defense responses and communication in monocotyledonous and dicotyledonous plants. *Plant Cell Physiol.* 56, 16–27. doi: 10.1093/pcp/pcu158

Patro, R., Duggal, G., Love, M. I., Irizarry, R. A., and Kingsford, C. (2017). Salmon provides fast and bias-aware quantification of transcript expression. *Nat. Methods* 14, 417–419. doi: 10.1038/nmeth.4197

Ramadoss, N., Gupta, D., Vaidya, B. N., Joshee, N., and Basu, C. (2018). Functional characterization of 1-aminocyclopropane-1-carboxylic acid oxidase gene in *Arabidopsis thaliana* and its potential in providing flood tolerance. *Biochem. Bioph. Res. Commun.* 503, 365–370. doi: 10.1016/j.bbrc.2018.06.036

Rondoni, G., Bertoldi, V., Malek, R., Djelouah, K., Moretti, C., Buonaurio, R., et al. (2018). Vicia faba plants respond to oviposition by invasive Halyomorpha halys activating direct defences against offspring. *J. Pest Sci.* 91, 671–679. doi: 10.1007/s10340-018-0955-3

Rotenberg, D., Jacobson, A. L., Schneweis, D. J., and Whitfield, A. E. (2015). Thrips transmission of tospoviruses. *Curr. Opin. Virol.* 15, 80–89. doi: 10.1016/j.coviro.2015.08.003

Salvaudon, L., De Moraes, C. M., Yang, J. Y., Chua, N. H., and Mescher, M. C. (2013). Effects of the virus satellite gene βC1 on host plant defense signaling and volatile emission. *Plant Signal. Behav.* 8:e23317. doi: 10.4161/psb.23317

Shalileh, S., Ogada, P. A., Moualeu, D. P., and Poehling, H. M. (2016). Manipulation of *Frankliniella occidentalis* (*Thysanoptera*: *Thripidae*) by *Tomato spotted wilt virus* (*Tospovirus*) via the host plant nutrients to enhance its transmission and spread. *Environ. Entomol.* 45, 1235–1242. doi: 10.1093/ee/nvw102

Shi, X., Chen, G., Pan, H., Xie, W., Wu, Q., Wang, S., et al. (2018). Plants pre-infested with viruliferous MED/Q cryptic species promotes subsequent *Bemisia tabaci* infestation. *Front. Microbiol.* 9:1404. doi: 10.3389/fmicb.2018.01404

Shi, X., Tang, X., Zhang, X., Zhang, D., Li, F., Yan, F., et al. (2017). Transmission efficiency, preference and behavior of *Bemisia tabaci* MEAM1 and MED under the influence of Tomato chlorosis virus. *Front. Plant Sci.* 8:2271. doi: 10.3389/fpls.2017.02271

Shi, X. B., Pan, H. P., Xie, W., Jiao, X. G., Fang, Y., Chen, G., et al. (2014). Three-way interactions between the tomato plant, Tomato yellow leaf curl virus, and *Bemisia tabaci* (*Hemiptera*: *Aleyrodidae*) facilitate virus spread. *J. Econ. Entomol.* 107, 920–926. doi: 10.1603/ec13476

Stafford, C. A., Walker, G. P., and Ullman, D. E. (2011). Infection with a plant virus modifies vector feeding behavior. *P. Natl. Acad. Sci. U.S.A.* 108, 9350–9355. doi: 10.1073/pnas.1100773108

Takeda, A., Sugiyama, K., Nagano, H., Mori, M., Kaido, M., Mise, K., et al. (2002). Identification of a novel RNA silencing suppressor, NSs protein of *Tomato spotted wilt virus*. *FEBS Lett.* 532, 75–79. doi: 10.1016/s0014-5793(02)03632-3

Turina, M., Kormelink, R., and Resende, R. O. (2016). Resistance to tospoviruses in vegetable crops: epidemiological and molecular aspects. *Annu. Rev. Phytopathol.* 54, 347–371. doi: 10.1146/annurev-phyto-080615-095843

Wan, Y., Hussain, S., Merchant, A., Xu, B., Xie, W., Wang, S., et al. (2020). *Tomato spotted wilt orthotospovirus* influences the reproduction of its insect vector, western flower thrips, *Frankliniella occidentalis*, to facilitate transmission. *Pest Manag. Sci.* 76, 2406–2414. doi: 10.1002/ps.5779

Wang, J., Bing, X. L., Li, M., Ye, G. Y., and Liu, S. S. (2012). Infection of tobacco plants by a begomovirus improves nutritional assimilation by a whitefly. *Entomol. Exp. Appl.* 144, 191–201. doi: 10.1111/j.1570-7458.2012.01278.x

Wang, J. W., Czech, B., and Weigel, D. (2009). miR156-regulated SPL transcription factors define an endogenous flowering pathway in *Arabidopsis thaliana*. *Cell* 138, 738–749. doi: 10.1016/j.cell.2009.06.014

Wu, D., Qi, T., Li, W., Tian, H., Gao, H., Wang, J., et al. (2017). Viral effector protein manipulates host hormone signaling to attract insect vectors. *Cell Res.* 27, 402–415. doi: 10.1038/cr.2017.2

Wu, X. J., Xu, S., Zhao, P. Z., Zhang, X., Yao, X. M., Sun, Y. W., et al. (2019). The Orthotospovirus nonstructural protein NSs suppresses plant MYC-regulated jasmonate signaling leading to enhanced vector attraction and performance. *PLoS Pathog.* 15:e1007897. doi: 10.1371/journal.ppat.1007897

Yan, C., and Xie, D. (2015). Jasmonate in plant defence: sentinel or double agent? *Plant Biotechnol. J.* 13, 1233–1240. doi: 10.1111/pbi.12417

You, C., Zhu, H., Xu, B., Huang, W., Wang, S., Ding, Y., et al. (2016). Effect of removing superior spikelets on grain filling of inferior spikelets in rice. *Front. Plant Sci.* 7:1161. doi: 10.3389/fpls.2016.01161

Ziebell, H., Murphy, A. M., Groen, S. C., Tungadi, T., Westwood, J. H., Lewsey, M. G., et al. (2011). Cucumber mosaic virus and its 2b RNA silencing suppressor modify plant-aphid interactions in tobacco. *Sci. Rep.* 1:187.

Conflict of Interest: The authors declare that the research was conducted in the absence of any commercial or financial relationships that could be construed as a potential conflict of interest.

frontiers in Plant Science

ORIGINAL RESEARCH
published: 16 December 2020
doi: 10.3389/fpls.2020.597665

Disrupting the Homeostasis of High Mobility Group Protein Promotes the Systemic Movement of *Bamboo mosaic virus*

*Mazen Alazem†, Meng-Hsun He, Chih-Hao Chang, Ning Cheng and Na-Sheng Lin**

Institute of Plant and Microbial Biology, Academia Sinica, Taipei, Taiwan

OPEN ACCESS

Edited by:
Kristiina Mäkinen, University of Helsinki, Finland

Reviewed by:
Eugene I. Savenkov, Swedish University of Agricultural Sciences, Sweden
Michael Taliansky, The James Hutton Institute, United Kingdom

***Correspondence:**
Na-Sheng Lin
nslin@sinica.edu.tw

†Present address:
Mazen Alazem, Plant Genomics and Breeding Institute, College of Agriculture and Life Sciences, Seoul National University, Seoul, South Korea

Specialty section:
This article was submitted to Plant Pathogen Interactions, a section of the journal Frontiers in Plant Science

Received: *21 August 2020*
Accepted: *11 November 2020*
Published: *16 December 2020*

Citation:
Alazem M, He M-H, Chang C-H, Cheng N and Lin N-S (2020) Disrupting the Homeostasis of High Mobility Group Protein Promotes the Systemic Movement of Bamboo mosaic virus. Front. Plant Sci. 11:597665. doi: 10.3389/fpls.2020.597665

Viruses hijack various organelles and machineries for their replication and movement. Ever more lines of evidence indicate that specific nuclear factors are involved in systemic trafficking of several viruses. However, how such factors regulate viral systemic movement remains unclear. Here, we identify a novel role for *Nicotiana benthamiana* high mobility group nucleoprotein (NbHMG1/2a) in virus movement. Although infection of *N. benthamiana* with Bamboo mosaic virus (BaMV) decreased *NbHMG1/2a* expression levels, nuclear-localized NbHMG1/2a protein was shuttled out of the nucleus into cytoplasm upon BaMV infection. *NbHMG1/2a* knockdown or even overexpression did not affect BaMV accumulation in inoculated leaves, but it did enhance systemic movement of the virus. Interestingly, the positive regulator Rap-GTPase activation protein 1 was highly upregulated upon infection with BaMV, whereas the negative regulator thioredoxin h protein was greatly reduced, no matter if *NbHMG1a/2a* was silenced or overexpressed. Our findings indicate that NbHMG1/2a may have a role in plant defense responses. Once its homeostasis is disrupted, expression of relevant host factors may be perturbed that, in turn, facilitates BaMV systemic movement.

Keywords: high mobility group proteins, virus movement, *Bamboo mosaic virus*, plant-virus interaction, nucleoprotein

INTRODUCTION

Viruses hijack various cellular machineries to utilize the molecules, subcellular structures, and trafficking systems required for their replication and movement (Huang et al., 2017a; Pitzalis and Heinlein, 2017). For local movement, viruses move from one cell into neighboring cells through plasmodesmata (PD), whereas viruses enter veins and traffic through the vascular system for systemic movement (Lough and Lucas, 2006; Hipper et al., 2013). Depending on the virus group, mobilized viral forms can be either viral nucleoprotein complexes or virions, with both forms usually being assisted by specific virus-encoded non-structural proteins (Hipper et al., 2013; Solovyev and Savenkov, 2014; Pitzalis and Heinlein, 2017). In the Potexvirus group, such proteins are encoded by triple gene block (TGB), which are translated into three movement proteins (MPs) TGBp1, 2, and 3 (Solovyev et al., 2012).

Ever more lines of evidence indicate that the translocation of viral MPs to nuclei, where they interact with specific nucleoproteins, is an essential step in promoting systemic viral infection (Lukhovitskaya et al., 2013; Solovyev and Savenkov, 2014; Lukhovitskaya et al., 2015). These interactions lead to transcriptional programming that reregulate the cell to confer optimal conditions for virus replication and spread (Solovyev and Savenkov, 2014). In addition, a few studies have reported that entry of specific viral proteins into the nucleus results in the export of specific host nuclear proteins to the cytoplasm (Krichevsky et al., 2006; Chang et al., 2016; Li et al., 2018). However, depending on the type of exported protein, this relocalization might be virus-regulated to assist trafficking or be a plant defense reaction that triggers an immune response. We previously identified the nucleolar protein fibrillarin as being a critical factor required for autonomous movement of the satellite RNA of *Bamboo mosaic virus* (satBaMV). The satBaMV-encoded P20 protein forms a complex with fibrillarin in the nucleolus and punctate structures associated with PDs (Chang et al., 2016). However, export of other nuclear proteins beyond the nucleus might represent a plant response to invading pathogens. For example, Arabidopsis high mobility group (HMG) protein B3 is exported to the apoplast where it functions as a damage-associated molecular pattern (DAMP), recognizes avirulent factors of the nectrophic fungus *Botrytis cinerea*, and triggers defenses mediated by salicylic acid (SA) (Choi et al., 2016).

To date, a few nuclear factors have been identified as being involved in the systemic movement of certain viruses (Hipper et al., 2013; Li et al., 2018). A previous study demonstrated that translocation of TGBp1 from *Potato mop-top virus* (PTMV) into the nucleus, mediated by the shuttle protein importin-α, is important for systemic trafficking of the virus, with importin-α knockdown reducing viral accumulation in upper leaves (Lukhovitskaya et al., 2015). However, it is not known how TGBp1 functions in the nucleus to enable PTMV to move systemically. In another example, TGBp1 of *Barley stripe mosaic virus* (BSMV) interacts with and exports fibrillarin-2 (Fib2) to PD. Fib2 also associates with the ribonucleoprotein (RNP) movement complex of BSMV, providing direct evidence of the ability of viral TGBp1 to hijack and employ Fib2 for BSMV cell-to-cell movement (Li et al., 2018). Previous works have indicated that such nuclear factors may regulate transcriptome profiles, inducing other factors required for systemic movement (Solovyev and Savenkov, 2014). Interestingly, several such nuclear factors are nucleolus-related proteins (Hiscox, 2007). For example, interaction of *Groundnut rosette virus* (GRV) open reading frame 3 (ORF3) with fibrillarin in the nucleolus is essential for re-localization of fibrillarin to the cytoplasm, as well as for the assembly of cytoplasmic RNP particles (ORF3-RNA-Fibrillarin) required for long-distance movement (Kim et al., 2007).

HMG proteins represent a heterogeneous class of ubiquitous and relatively abundant non-histone proteins associated with chromatin. They modulate chromatin structure and act as architectural factors in the assembly of nucleoprotein (Wu et al., 2003; Bianchi and Agresti, 2005; Reeves, 2010). HMGAs (previously known as HMG1s) bind specifically to AT-rich DNA through a small DNA binding motif, termed the AT-hook, and they are involved in diverse nuclear and cellular processes, including gene transcription (Lewis et al., 2001; Reeves and Beckerbauer, 2001; Bianchi and Agresti, 2005; Reeves, 2010). A role for HMGs in host-pathogen interactions has been reported previously (Choi et al., 2016; Sprague et al., 2018), playing a positive role in host defense against fungal or viral pathogens. For example, *Arabidopsis thaliana* HMGB3 (AtHMGB3) was identified as a DAMP molecule that mediates innate immune responses upon infection with *B. cinerea* (Choi et al., 2016). AtHMGB3 translocalizes to the apoplast upon infection with *B. cinerea*, activates MAPK, induces callose accumulation, and triggers the expression of defense-related genes, which collectively reduces levels of *B. cinerea*. Silencing AtHMGB3 increased *A. thaliana* susceptibility to *B. cinerea* (Choi et al., 2016). Similarly, the mouse cell lines NIH-3T3 and 3T6-Swiss secreted HMGB1 upon infection with *Herpes simplex virus* strain HSV1716, an oncolytic herpes virus. An HMGB1 knockdown cell line revealed its role in restricting HSV1716, indicating that it acts as a DAMP to regulate pro-inflammatory cytokine release and inflammation (Sprague et al., 2018; Hong et al., 2019).

Focusing on host nuclear factors is an emerging field of study in host-pathogen interactions, yet their involvement in viral movement remains largely unexplored (Solovyev and Savenkov, 2014). Here, we used BaMV to investigate the role of *Nicotiana benthamiana* HMGs (NbHMGs) in systemic movement of BaMV. BaMV is a flexuous Potexvirus with a single-stranded positive-sense RNA genome of 6.4 kb that encodes five ORFs (Lin et al., 1992; DiMaio et al., 2015; Hsu et al., 2018). The first ORF encodes a 155 kDa protein that functions as a replicase with methyltransferase (Li et al., 2001a; Huang et al., 2004), helicase (Li et al., 2001b) and RNA-dependent RNA polymerase (RdRp) domains (Li et al., 1998). The second to fourth ORFs encode three TGBp proteins; TGBp1 of 28 kDa, TGBp2 of 13 kDa, and TGPp3 of 6 kDa, respectively (Lin et al., 1994; Yang et al., 1997). These TGBp proteins assist in cell-to-cell movement of BaMV (Lin et al., 2006; Hsu et al., 2008; Chou et al., 2013). The fifth ORF encodes a 25 kDa capsid protein (CP) that is involved in virus encapsidation, symptom formation (Lan et al., 2010), and viral movement (Lee et al., 2011). When BaMV replicates, three major RNAs are generated; a genomic RNA (gRNA) of 6.4 kb and two sub-genomic RNAs (sgRNA) denoted sgRNA1 and sgRNA2 of 2 and 1 kb, respectively (Lin et al., 1994; Yang et al., 1997).

In this study, we identified two *HMG1* genes in *N. benthamiana* in which only *NbHMG1/2a* was detectable and downregulated upon infection with BaMV. NbHMG1/2a localized exclusively in the nucleus but, upon BaMV infection, it was also detected in the cytoplasm. Knockdown or overexpression of *NbHMG1/2a* did not affect BaMV accumulation in inoculated leaves. Interestingly, under both scenarios (*NbHMG1/2a*-silenced or -overexpressed), we observed significantly enhanced systemic BaMV. Moreover, previously identified host factors required for BaMV cell-to-cell and systemic movement were not affected by the status of HMG in BaMV-infected plants, except for two important host factors–Rap-GTPase activation protein 1 (Rap-GAP1) (Huang et al., 2013) and thioredoxin h protein (TRXh2) (Chen et al., 2018)–that played a positive and negative role, respectively, in

local and systemic movement of BaMV. These results provide evidence for the role of HMG protein in systemic movement of an RNA virus.

RESULTS

Orthologs of *Arabidopsis* HMGB3 in *N. benthamiana*

In order to identify the orthologs of *AtHMGB3* in *N. benthamiana*, we blasted the coding sequence of *AtHMGB3* against *N. benthamiana* genome database v1.0.1 in the Sol Genome network (solgenomics.net). The blast analysis identified two accessions; Niben101Scf09442g05005.1 and Niben101Scf02041g04034.1 with 86.55 and 82.35% identities covering 103 and 98 amino acids (aa), respectively, of the 119-aa *AtHMGB3* sequence (**Figure 1A**). Both sequences show high identity to each other in the coding region (CDS) (95%) (**Figure 1A**) and in the 5′ untranslated region (UTR) (93%), but share low similarity in the 3′ UTR (43.5%) (**Supplementary Figure S1**). The region of high similarity corresponds to the high mobility group box domain (**Figure 1A**). However, our phylogenetic analysis of HMG orthologs from different species clustered these two accessions in close proximity to *HMG1/2* from different *Nicotiana* and *Solanum* species, prompting us to denote the two accessions Niben101Scf02041g04034.1 and Niben101Scf09442g05005.1 as *NbHMG1/2a* and *b*, respectively (**Figure 1B**). We then measured the expression levels of *NbHMG1/2a* and *b* in *N. benthamiana* plants in response to BaMV infection. Although expression of *NbHMG1/2a* was significantly decreased upon BaMV infection in both inoculated and systemic leaves at 6 days post infection (dpi) (**Figure 1C**), we did not detect any expression of *NbHMG1/2b* using different pairs of primers targeting the CDS and 3′ UTR under various conditions [healthy plants or plants infected with BaMV infectious clone pKBG or infiltrated with empty vector (EV) of the *Tobacco rattle virus* (TRV) (TRV-EV)]. These data suggest that *NbHMG1/2a* might be involved in the interaction between BaMV and *N. benthamiana*, but *NbHMG1/2b* may not be expressed in *N. benthamiana* leaves under normal growth conditions or when it is under viral attack.

NbHMG1/2a Localizes in the Nucleus and Nucleolus

Next, we identified the functional domains of NbHMG1/2a. The conserved domain database of NCBI (Marchler-Bauer et al., 2015) predicted a DNA binding domain in a motif corresponding to aa 36-101 of NbHMG1/2a protein, with an *E*-value of 8.37e-15 (**Figure 2A**). A nucleus localization signal (NLS) and a nucleolus localization signal (NoLS) were also predicted in motifs at 4–56 and 15–42 aa, respectively, using cNLS and NoD mappers (Kosugi et al., 2009b; Scott et al., 2011; **Figure 2A**). No nucleus export signal was identified in the coded protein using the LocNES server (Xu et al., 2015), but the NetNES 1.1 server (la Cour et al., 2004) predicted a weak signal (below threshold) in a motif at 44–50 aa. To confirm these findings, we cloned the full *NbHMG1/2a* coding sequence with a 3HA-mCherry tag into the pBin61 expression vector (Chang et al., 2016). Transient expression of NbHMG1/2a in *N. benthamiana* leaves showed that this protein clearly localizes in the nucleus (**Figure 2B**), the nucleolus, and the nucleoplasm (**Figure 2C**), but no cytoplasmic localization was detected across 3 days of observation (1.5, 2, and 3 dpi) (**Supplementary Figures S2–S4**). Thus, under normal plant growth conditions, NbHMG1/2a localizes in the nucleus and nucleolus.

Both Silencing and Overexpression of *NbHMG1/2a* Increase Systemic Movement of BaMV

We examined the effects of silencing *NbHMG1/2a* to determine if it has any effect on BaMV accumulation or spread. To avoid silencing any off-target genes, we employed the virus-induced gene silencing (VIGS) tool in the Sol genomics database to assess the full CDS of *NbHMG1/2a* (Fernandez-Pozo et al., 2015). The VIGS tool recommended using any fragment within the first 300 base pairs (bp) of the *NbHMG1/2a* CDS to avoid silencing off-target genes (**Supplementary Table S2**). A 21-mer siRNA generated from this silencing construct would have large numbers of matches with both *NbHMG1/2a* (404 matches) and *NbHMG1/2b* (101 matches), but no other potential genes were identified as being off-target (except for two accessions each with one match) (**Supplementary Table S2**). To silence *NbHMG1/2a*, TRV silencing vector carrying *NbHMG1/2a* partial fragments was agroinfiltrated into 18-day-old *N. benthamiana* plants to silence *NbHMG1/2a.* The *Phytoene desaturase* (*PDS*) gene acted as an indicator of silencing efficiency and mCherry functioned as an EV negative control. After a strong bleaching phenotype appeared on *PDS*-silenced plants, the upper leaves (leaves 7 and 8) were agroinfiltrated with pKBG (**Figure 3A**). Silencing of *NbHMG1/2a* resulted in a stunted phenotype compared to EV- or *PDS*-silenced plants (**Figure 3B**). Nonetheless, leaf size was similar among control and silenced plants (**Figure 3B**). Levels of BaMV RNA or CP were comparable in inoculated leaves at 4, 5, and 6 dpi among EV- and *NbHMG1/2a*-silenced plants (**Figure 3C**). However, BaMV spread more rapidly to the upper systemic leaves (leaves 11 and 12) and exhibited greater accumulation (∼3.1-fold relative to EV-silenced plants) in *NbHMG1/2a*-silenced plants at 6 dpi (**Figure 3D**). To confirm these results, we carried out RTqPCR for samples collected at 6 dpi (**Supplementary Figure S5A**). Using primers targeting BaMV genomic RNA (RNA-dependent RNA polymerase "RDR"), the RTqPCR showed that *RDR* accumulated equally in the BaMV-inoculated leaves of EV and the *NbHMG1/2a*-silenced plants, but showed ∼ 6.7-fold upregulation of *RDR* in the systemically infected leaves (**Supplementary Figure S5A**). We next tested whether the TRV silencing vector is affected by BaMV or the reduced level of *NbHMG1/2a*. While TRV-RDR accumulated equally in the control and BaMV inoculated leaves, TRV-RDR exhibited 50% increase in the systemically infected leaves (**Supplementary Figure S5B**). Of note, VIGS resulted in significant decrease of NbHMG1/2a in both BaMV-inoculated leaves as well as in the systemically infected leaves (**Supplementary Figure S5C**). This

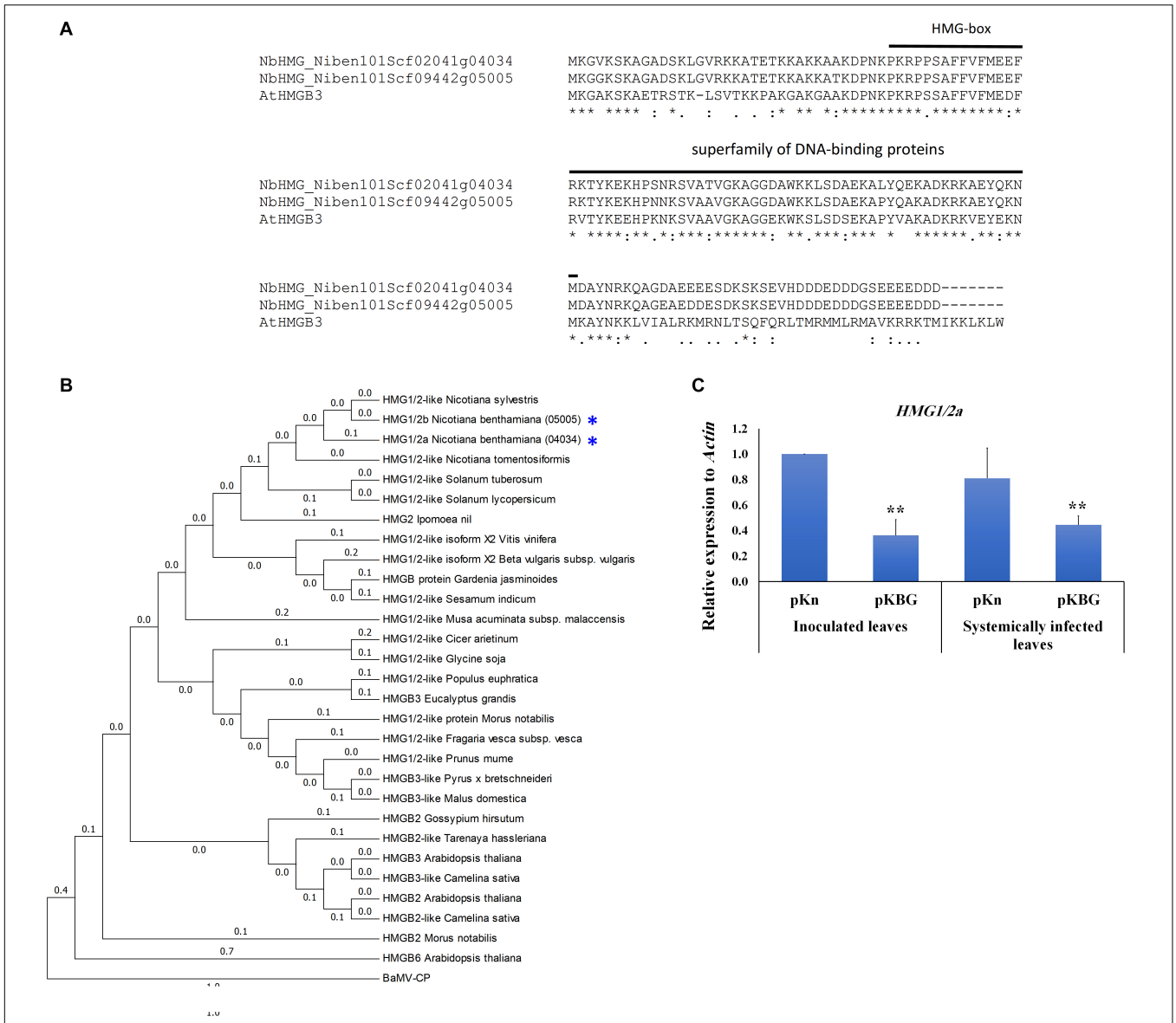

FIGURE 1 | Phylogenetic and expression analyses of *Nicotiana benthamiana HMG1/2* genes. **(A)** Similarities of *NbHMG* accessions to *Arabidopsis thaliana HMGB3*. Two *NbHMG* accessions with high similarity to *AtHMGB3* were obtained by blasting the AtHMGB3 coding sequence against the *N. benthamiana* database (Sol Genomics Networks), i.e., NbHMG_101Scf02041g04034 (*NbHMG1/2a*) and NbHMG_101Scf09442g05005 (*NbHMG1/2b*). **(B)** Phylogenetic analysis of *NbHMG1/2* with orthologs from other species. The HMG phylogeny was generated using the Neighbor Joining method in MEGA 6.0 software. Numbers represent relative phylogenetic distance. BaMV capsid protein (CP) was used as an outgroup to root the tree. **(C)** Relative expression levels of *NbHMG1/2a* by RTqPCR in *N. benthamiana* plants infected with BaMV infectious clone (pKBG) compared with plants infiltrated with empty vector (pKn). Inoculated leaves were tested at 3 days post infiltration (dpi), and the systemic leaves were tested at 6 dpi. Actin was used as an internal control. Data represent the mean ± standard deviation from three biological replicates. One-sided student *t*-tests were performed to determine significant differences. Asterisks indicate significant differences relative to control lines (infiltrated with pKn), with ** representing $P < 0.01$.

indicates that BaMV infection may allow faster spread of the silencing vector TRV.

Since *NbHMG1/2a*-silenced plants displayed enhanced systemic movement and accumulation of BaMV, we assessed the impact of transient overexpression of *NbHMG1/2a* (fused with HA-mCherry tag) on both local and systemic BaMV accumulation. Although levels of BaMV RNA and CP protein were similar in the inoculated leaves of control and overexpressing plants, accumulation of BaMV was enhanced (∼3.6-fold relative to control) in the systemically infected leaves at 6 dpi (**Figure 4A**). To confirm these results, BaMV-*RDR* expression level was measured at 6 dpi using RTqPCR (**Supplementary Figure S6**). BaMV-RDR showed no difference in the inoculated leaves of the control and NbHMG1/2a-overexpressing plants. However, the accumulation level was threefold upregulated in the systemically infected leaves

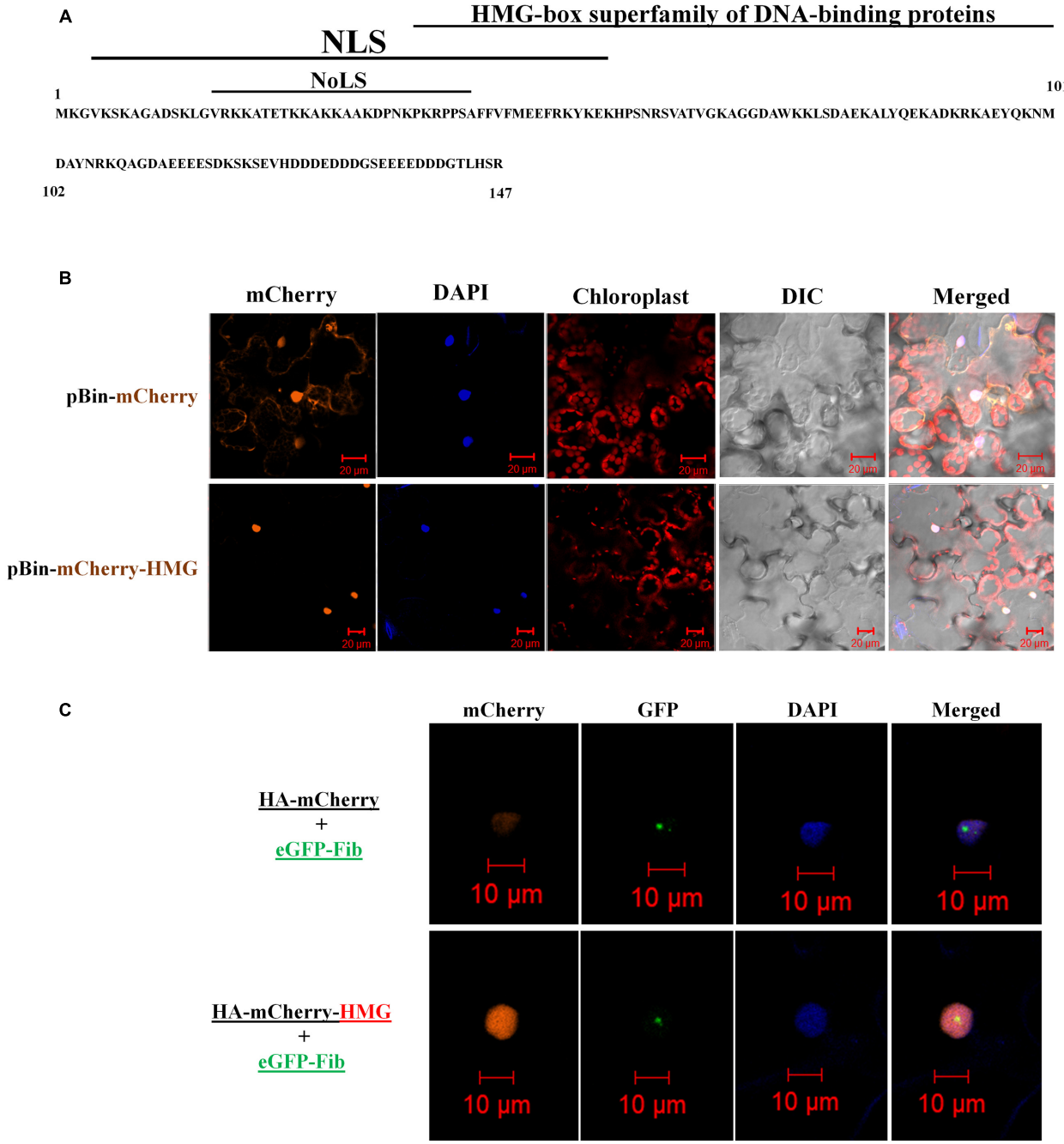

FIGURE 2 | Domain analysis and localization of NbHMG1/2a. **(A)** Predicted domains encoded in NbHMG1/2a: a nuclear localization signal (NLS) between 4 and 56 amino acids (aa), a nucleolar localization signal (NoLS) between 15 and 42 aa, and a DNA-binding domain between 36 and 101 aa. No nuclear export signal was found. **(B)** NbHMG1/2a localizes in the nucleus. *N. benthamina* leaves were infiltrated with *Agrobacterium* carrying pBin61-HA-HMG-mCherry or with control vector pBin61-HA-mCherry. **(C)** NbHMG1/2a localizes in the nucleolus. *N. benthamina* leaves were infiltrated with *Agrobacterium* carrying HA-mCherry and nucleolus-localized fibrillarin fused with eGFP (eGFP-Fib), or with HA-mCherry-HMG and eGFP-Fib. DAPI was used for nuclear staining. Images were taken 3 days after infiltration, and bars represent a measurement scale of 20 and 10 μm for the nucleus and nucleolus, respectively. The experiment was repeated three times with similar results and representative images are shown.

overexpressing NbHMG1/2a compared with the infected control (**Supplementary Figure S6**). Notably, the overexpressed *NbHMG1/2a* was detectable in inoculated leaves (**Figure 4A**), and it did not result in systemic silencing of *NbHMG1/2a* as RT-qPCR revealed that transcript levels of the endogenous *NbHMG1/2a* were comparable between control and overexpressing plants, and the overexpressed gene accumulated 2.5-fold more than the endogenous gene in the inoculated leaves (**Figure 4B**).

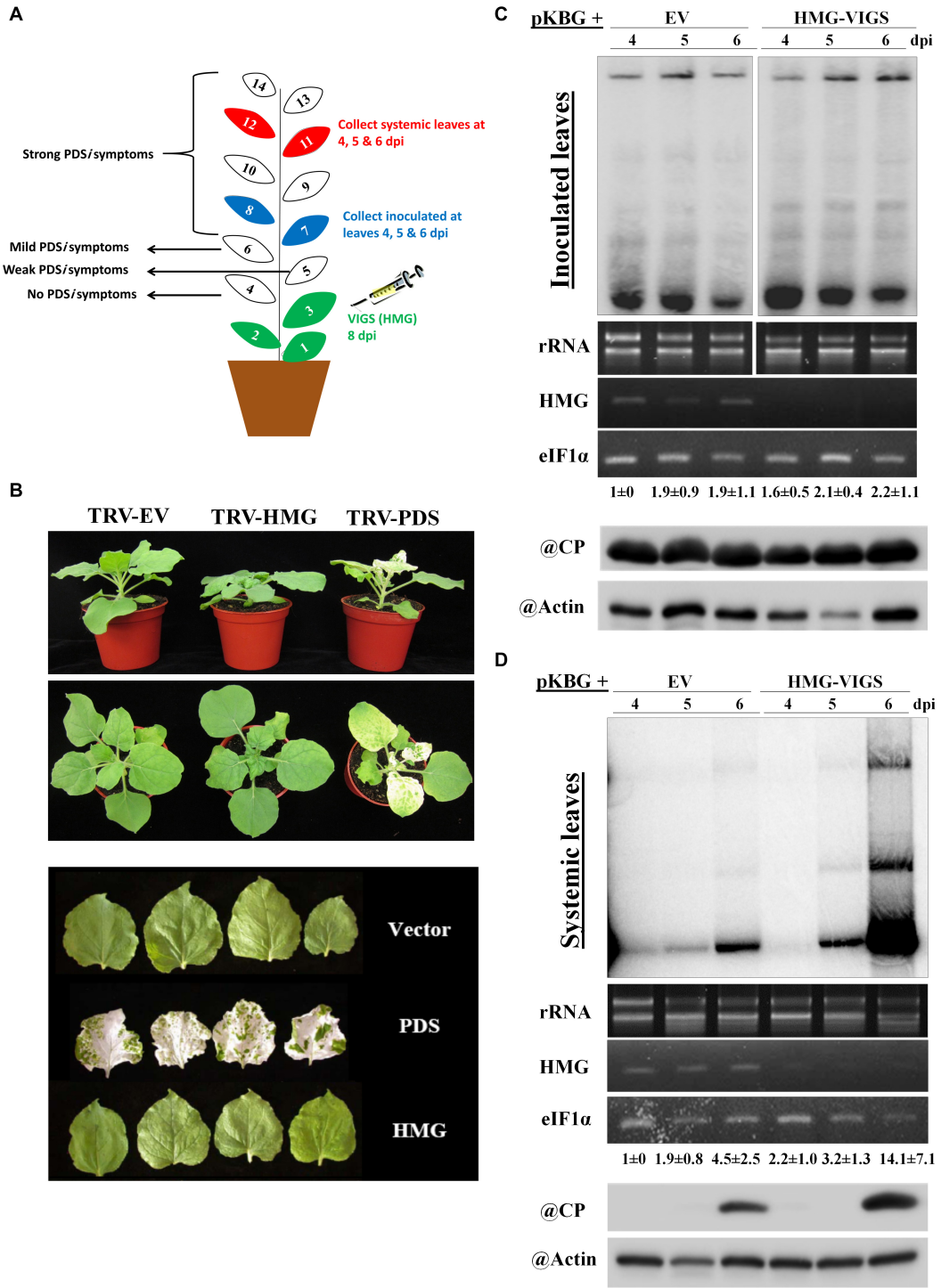

FIGURE 3 | Effects of silencing *NbHMG1/2a* on plant growth and resistance to BaMV. **(A)** Schematic illustration of our VIGS experimental design. The first three leaves of *N. benthamiana* plants were infiltrated with the silencing vector TRV carrying the *NbHMG1/2a* fragment or control mCherry fragment. Eight days later, leaves 7 and 8 were infiltrated with pBin61 carrying BaMV (pKBG). Inoculated leaves (leaves 7 and 8) and systemic leaves (leaves 11 and 12) were collected at 3, 4, and 6 days after BaMV infection (dpi). **(B)** Phenotype of *NbHMG1/2a*-silenced plants. Plants infiltrated with TRV-mCherry, TRV-HMG, and TRV-PDS. Photos were taken 8 days after agroninfiltration with TRVs. Upper and middle panel show plant height and spread, and lower panel shows leaf size. **(C,D)** RNA blot of BaMV in the inoculated leaves **(C)** and systemic leaves **(D)** of control plants (infiltrated with TRV-mCherry) and *NbHMG1/2a*-silenced plants (HMG-VIGS). The second panel represents rRNA levels as internal control. The third panel shows *NbHMG1/2a* levels in the control and silenced plants. eIF1α was used as an internal control. Values represent average accumulation of BaMV genomic RNA from three biological replicates ± standard deviation. Lower panels represent protein blots of BaMV capsid protein (CP) (25 kDa) and actin in the control and silenced plants.

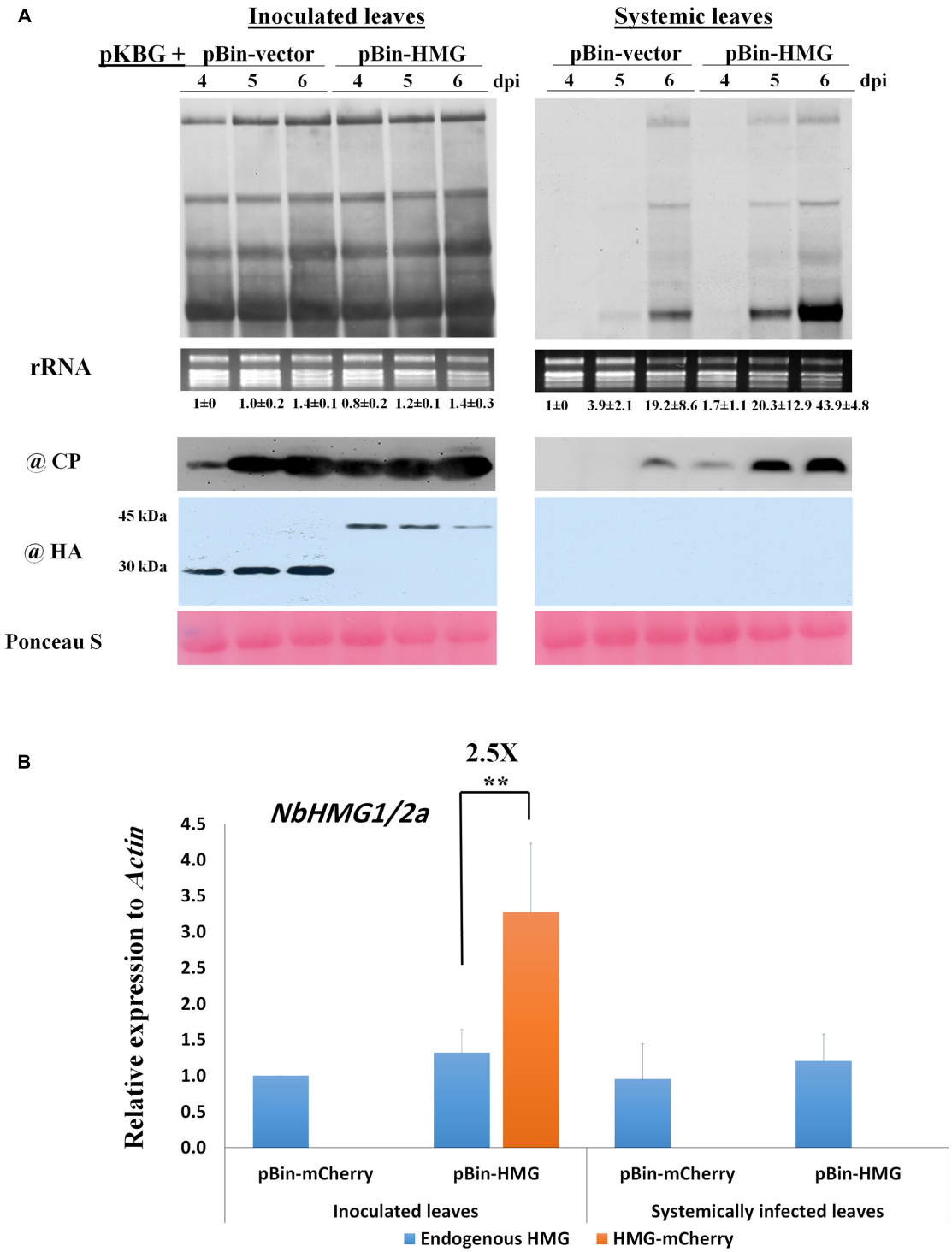

FIGURE 4 | Overexpression of *NbHMG1/2a* enhances systemic movement of BaMV. **(A)** Twenty-four-day-old *N. benthamiana* plants were co-agroinfiltrated with pKBG and pBin-HA-mCherry or pBin-HA-mCherry-HMG. Samples were collected from inoculated and systemic leaves at 4, 5, and 6 dpi. Upper panels are Northern blots for BaMV, with rRNA used as a loading control. Lower panels are protein blots of BaMV CP and HA-tag to detect HA-mCherry (30 kDa) and HA-mCherry-HMG (45 kDa). Ponceau S was used as a loading control. The experiment was conducted with three biological replicates, which generated similar results. Values below Northern blots represent average accumulation of BaMV genomic RNA from three biological replicates ± SD. **(B)** Relative expression of endogenous *NbHMG1/2a* and the overexpressed gene *NbHMG1/2a-mCherry* in inoculated and systemic leaves of *NbHMG1/2a*-overexpressing plants based on RTqPCR. According to one-sided student *t*-test, asterisk indicates significant difference for the expression of *NbHMG1/2a-mCherry* relative to the endogenous *NbHMG1/2a*, with ** representing $P < 0.01$. Actin was used as an internal control. Error bars represent the standard deviation from three biological replicates.

These results confirmed that transcript level of *NbHMG1/2a* was boosted by transient expression in the inoculated leaves.

Host Factors Required for BaMV Systemic Movement Are Regulated in *NbHMG1/2a*-Silenced and -Overexpressing Plants

Several host factors required for BaMV cell-to-cell and systemic movement have been identified previously (Cheng, 2017; Huang et al., 2017a). These factors include the activating protein Rab GTPase (*Rab-GAP1*) (Huang et al., 2013), casein kinase 2α (*CK2*α) (Hung et al., 2014), serine/threonine kinase-like protein (*STKL*) (Cheng et al., 2013), and thioredoxin h protein (*TRXh2*) (Chen et al., 2018). *TRXh2* plays a negative role in BaMV accumulation, whereas the other genes enhance local BaMV accumulation, with *RAB-GAP1* increasing BaMV accumulation in both inoculated and systemic leaves (Huang et al., 2013). In BaMV-inoculated leaves, we found that expression of *Rab-GAP1, CK2*α, and *STKL* all increased following BaMV infection of TRV-EV control plants (**Figures 5A–C**), whereas expression of *TRXh2* remained unchanged (**Figure 5D**). In *NbHMG1/2a*-silenced plants (*TRV-HMG*), only *CK2*α presented a slight increase in expression compared to TRV-EV control (**Figure 5B**). However, upon BaMV infection of *NbHMG1/2a*-silenced plants, *Rab-GAP1* was the only gene exhibiting a significant increase in expression relative to TRV-EV control plants (**Figure 5A**). Of note, expression of *TRXh2* decreased in TRV-HMG-agroinfiltrated plants compared to TRV-EV control plants (**Figure 5D**).

Expression of *Rab-GAP1*, *STKL,* and *TRXh2* was significantly increased in plants transiently overexpressing *NbHMG1/2a* (pHMG) compared to plants infiltrated with the mCherry-expressing vector (mCh) (**Figures 5E,G,H**), whereas that of *CK2*α was not affected (**Figure 5F**). After BaMV infection, *Rab-GAP1* and *STKL* were upregulated (**Figures 5E,G**), and *TRXh2* was downregulated (**Figure 5F**). Only *Rab-GAP1* was significantly increased in BaMV-infected pHMG-overexpressing plants compared to mCh-infected ones (**Figure 5E**). These findings indicate that only *Rab-GAP1* was significantly increased in both silenced and overexpressing plants following BaMV infection. Moreover, *TRXh2* was downregulated (∼ 2.5-fold) in the infected pHMG-overexpressing plants when compared to mCh-infected plants (**Figure 5H**). Together, these findings imply that enhanced systemic accumulation of BaMV may be attributable to coordinated upregulation of *Rab-GAP1* expression and downregulation of *TRXh2*. Previously, it was proposed that Rab-GAP1 triggers one of the RabGTPases to release vesicles containing the BaMV-movement complex for trafficking to the PD (Huang et al., 2013, 2017a). The speed at which viral movement complex is delivered to the PD affects the onset and swiftness of systemic trafficking (Rodrigo et al., 2014).

BaMV Infection Triggers Relocalization of NbHMG1/2a to the Cytoplasm

We have shown that NbHMG1/2a localizes exclusively in the nucleus (**Figure 2**). This observation was confirmed at 1.5, 2, and 3 dpi (**Supplementary Figures S4–S6**), and BaMV did not appear to affect this localization within these timeframes. We tried to extend our observations to the late stage of infection, but levels of transiently-expressed proteins had greatly declined, resulting in undetectable signal at 6 dpi (**Supplementary Figure S7**). To overcome this problem, we agroinfiltrated very limited amounts of pKBG (BaMV infectious clone carrying GFP) (OD_{600} = 0.005) into a defined region of leaves (**Figure 6A**, green circle). mCherry-HMG (OD_{600} = 0.5) was then expressed in the whole leaves. Two days later, GFP fluorescent signals were only detected in close proximity to the pKBG-infiltrated regions (upper white circle), but no fluorescent signals were observed in the distal cells (lower white circle) (**Figure 6A**). Surprisingly, in cells showing BaMV-GFP infection, mCherry-HMG signals were not only detected in the nucleus but also in cytosol (**Figure 6A**, upper panel). However, mCherry-HMG signals remained localized in the nucleus where no BaMV-GFP signals were observed (**Figure 6A**). To confirm the mCherry-HMG is localized in both the cytosol and the nucleus following BaMV-GFP infection, cell fractionation was carried out to separate the nuclei from the cytoplasm. First, *N. benthamiana* leaves were infiltrated with HA-mCherry or HA-mCherry-HMG, and the HA signal in the infiltrated tissues was detected by protein blot at 48 h after infiltration (**Figure 6B**). We next purified nuclei from control and the BaMV-infected leaves at 7 dpi, and the presence of HMG, CP, Histone H2 (a nuclear marker protein), and Tubulin (a cytoplasmic marker protein) was determined by protein blots from nuclear extracts. HMG and CP were found in the nuclear and the supernatant fractions, whereas Histone H2 was detectable only in the nuclear fraction, and Tubulin was found only in the supernatant fraction (**Figure 6C**). We conclude that NbHMG1/2a is translocalized to the cytoplasm upon BaMV infection. Using a similar approach, we observed that a substantial amount of mCherry-HMG moved from the nucleus to cytoplasm upon infection with pKBG (**Supplementary Figure S8**), whereas mCherry-HMG remained in the nucleus upon pKn infiltration (**Supplementary Figure S8**), indicating that the relocalization of mCherry-HMG is triggered by BaMV infection.

No Evidence of Interaction Between Plant NbHMG1/2a and Viral CP or TGBp1 Proteins

Previously, TGBp1 and CP proteins were reported to localize in the nucleus and cytosol and that they play crucial roles in BaMV cell-to-cell and systemic movement (Lin and Chen, 1991; Chang et al., 1997; Palani et al., 2009). Our observations of the localization of NbHMG1/2a in the nucleus and its trans-localization to the cytoplasm prompted us to test if CP or TGBp1 interacts with NbHMG1/2a. However, yeast two-hybrid analysis revealed that neither of these BaMV proteins directly interacts with NbHMG1/2a (**Supplementary Figure S9**), suggesting that the effect of BaMV on NbHMG1/2a localization is indirect. These observations imply that NbHMG1/2a may not be involved in regulating cell-to-cell movement of BaMV, but it might have other functions related to anti-BaMV defenses.

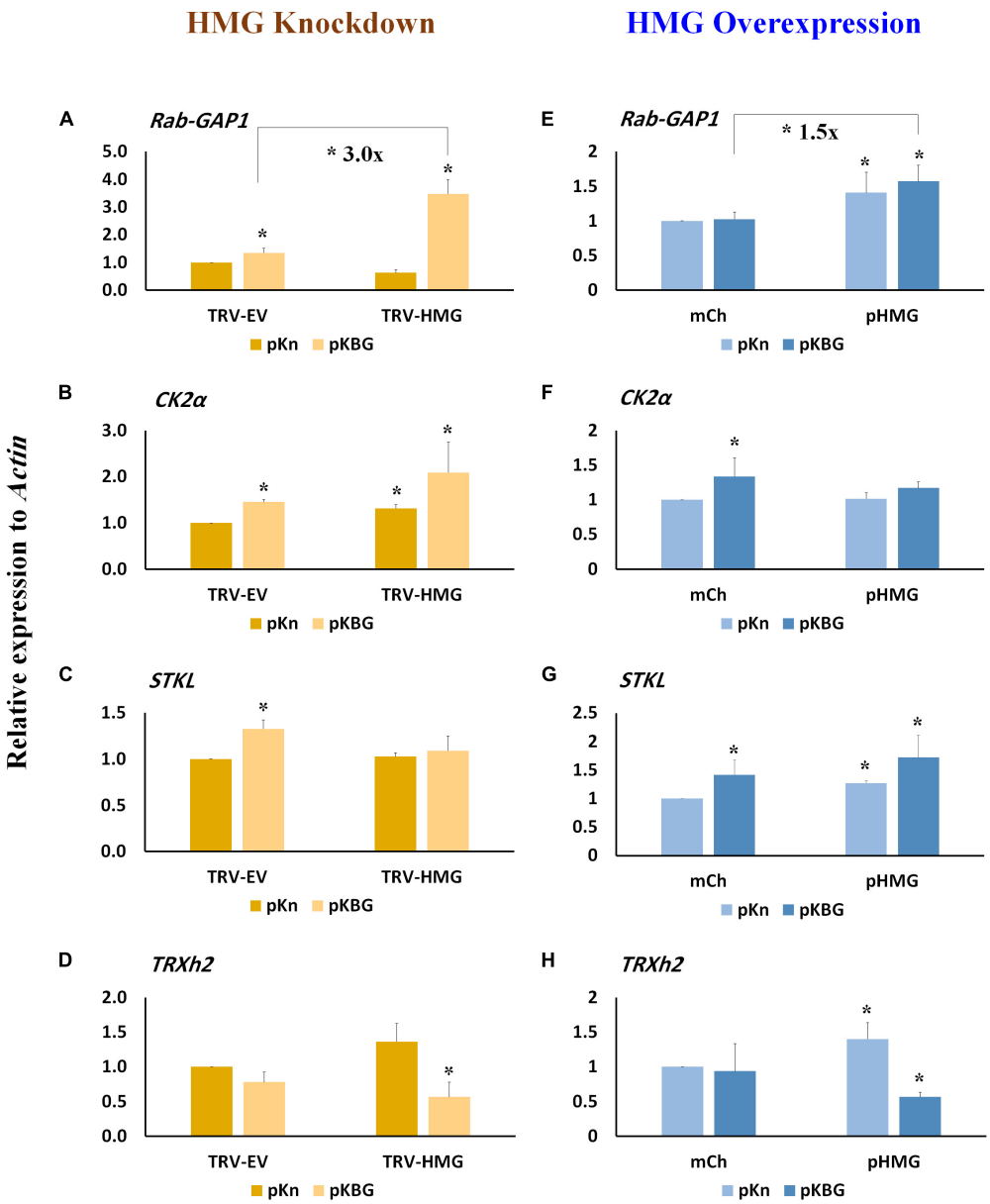

FIGURE 5 | Relative expression of host genes involved in BaMV movement in *NbHMG1/2a*- knockdown and -overexpressing plants. Transcript levels of *RAB-GAP1* **(A,E)**, *CK2α* **(B,F)**, *STKL* **(C,G)**, and *TRXh2* **(D,H)** in *N. benthamiana* plants infected with pKBG or pKn and upon *HMG* being knocked-down or overexpressed, respectively. Expression level was measured in the BaMV-inoculated leaves at 6 dpi in both HMG-silenced and HMG-overexpressed plants. Actin was used as an internal control. Data represent the mean ± SD from three biological replicates. One-sided Student's *t*-tests were performed to determine significant differences. Asterisks indicate significant differences relative to mock lines (infiltrated with pKn and pBin-mCherry), with * representing $P < 0.05$.

DISCUSSION

Entry of specific viral proteins into the nucleus and their interaction with certain nuclear or nucleolar proteins are critical processes for the systemic movement of several viruses (Solovyev and Savenkov, 2014). Yet, how these interactions locally or systemically alter plant mechanisms has not been fully uncovered, despite a few studies suggesting transcriptional reprogramming conditions the cell for enhanced viral replication and movement (Chen et al., 2013; Levy et al., 2013; Solovyev and Savenkov, 2014).

Cell-regulated export of certain nuclear proteins in response to viral infection is intriguing and implies specific functions after viral attack. Taking HMG proteins as an example, several works have reported roles for these proteins in chromatin modification and transcriptional regulation, requiring nuclear localization (Ju et al., 2006; Launholt et al., 2006; Antosch et al., 2012). However, upon infection with *B. cinerea*, export of AtHMGB3

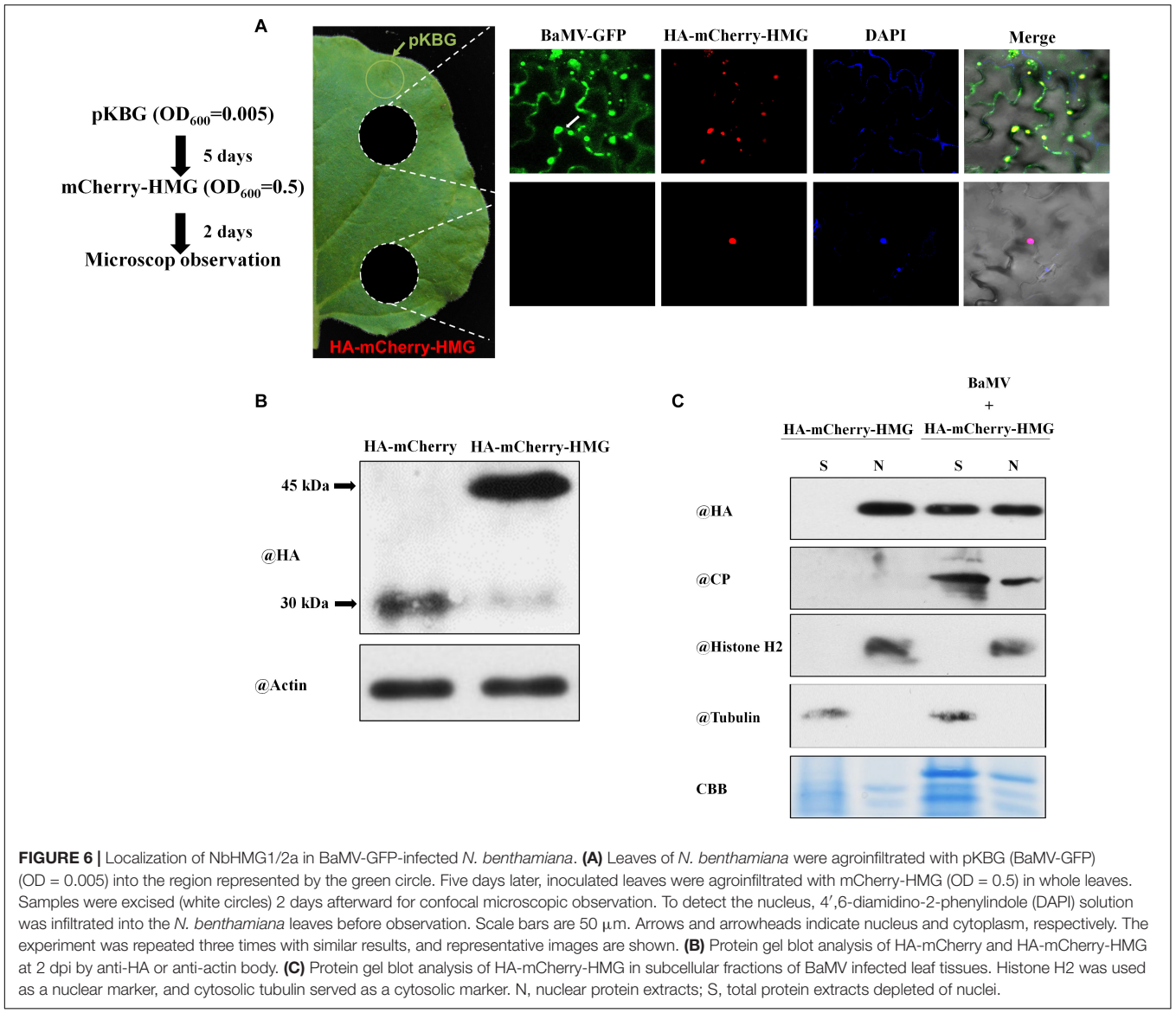

FIGURE 6 | Localization of NbHMG1/2a in BaMV-GFP-infected *N. benthamiana*. **(A)** Leaves of *N. benthamiana* were agroinfiltrated with pKBG (BaMV-GFP) (OD = 0.005) into the region represented by the green circle. Five days later, inoculated leaves were agroinfiltrated with mCherry-HMG (OD = 0.5) in whole leaves. Samples were excised (white circles) 2 days afterward for confocal microscopic observation. To detect the nucleus, 4′,6-diamidino-2-phenylindole (DAPI) solution was infiltrated into the *N. benthamiana* leaves before observation. Scale bars are 50 μm. Arrows and arrowheads indicate nucleus and cytoplasm, respectively. The experiment was repeated three times with similar results, and representative images are shown. **(B)** Protein gel blot analysis of HA-mCherry and HA-mCherry-HMG at 2 dpi by anti-HA or anti-actin body. **(C)** Protein gel blot analysis of HA-mCherry-HMG in subcellular fractions of BaMV infected leaf tissues. Histone H2 was used as a nuclear marker, and cytosolic tubulin served as a cytosolic marker. N, nuclear protein extracts; S, total protein extracts depleted of nuclei.

to the apoplast has been deemed critical for initiation of innate immunity. AtHMGB3 acts as a DAMP molecule that recognizes avirulent factors of *B. cinerea* to trigger SA-mediated defenses (Choi et al., 2016). Here, our data also shows that NbHMG1/2a is normally localized in the nucleus (**Figure 2**), but substantial amounts of NbHMG1/2a can be detected in the cytoplasm but not at PDs in response to BaMV late infection (**Figure 6**), potentially excluding a direct role of NbHMG1/2a in BaMV cell-to-cell movement. Our observation that *NbHMG1/2a* expression is reduced upon BaMV infection indicates that the virus may exert this effect to modulate the host for optimal infection conditions (**Figure 1C**). Indeed, this possibility is supported by our finding that systemic spread of BaMV was faster in *NbHMG1/2a*-silenced plants relative to control plants (**Figure 3**). In addition, neither CP nor TGBp1, both of which localize in the nucleus and cytoplasm, were found to interact directly with NbHMG1/2a (**Supplementary Figure S9**). These findings do not exclude the notion that NbHMG1/2a relocalization to the cytosol is defense-related. In fact, other HMGs, such as mouse HMGB1, contribute to cell defense against the HSV1716 oncolytic herpes virus (Sprague et al., 2018). Overall, studies of HMGs from different species suggest several members of this protein group function in defense against pathogens.

Expression levels of host factors required for local and systemic movement of BaMV indicate that Rab-GAP1 might be regulated by NbHMG1/2a because levels of this protein increased when NbHMG1/2a was transiently overexpressed (**Figure 5E**), but remained unaffected in *NbHMG1/2a*-silenced plants (**Figure 5A**). However, in response to BaMV infection, expression levels of *Rab-GAP1* were upregulated 3-fold in *NbHMG1/2a*-silenced plants (**Figure 5A**). It was reported previously that silencing of *Rab-GAP1* drastically reduced systemic and local BaMV accumulation by ∼98 and 50%, respectively, but had no effect on protoplast levels (Huang

et al., 2013). Thus, Rab-GAP1 serves as a positive regulator of BaMV movement. In contrast, BaMV infection reduced the expression of *TRXh2* only in *NbHMG1/2a*-silenced plants but not in EV-control plants. NbTRXh2 may target TGBp2, disrupting its structural integrity and its association with TGBp1 and TGBp3 (Chen et al., 2018). Regulation of these factors may explain the enhanced systemic accumulation of BaMV in *NbHMG1/2a*-silenced plants and it suggests a role for NbHMG1/2a in transcriptional regulation of Rab-GAP1 and TRXh2, and probably for other factors necessary for the BaMV infection cycle. Previous works have reported roles for HMGs in transcription (Reeves and Beckerbauer, 2001; Ju et al., 2006; Launholt et al., 2006; Reeves, 2010; Antosch et al., 2012), strengthening the notion that other host factors involved in BaMV systemic movement might also be transcriptionally regulated by HMG.

Interestingly, transient overexpression of *NbHMG1/2a* also enhanced systemic movement of BaMV, but it did not affect its local accumulation (**Figure 4**). Levels of the positive regulator of BaMV movement, Rap-GAP1, were significantly increased upon BaMV infection (**Figure 5E**), whereas *TRXh2* that impedes systemic BaMV movement was downregulated in infected plants overexpressing *NbHMG1/2a* (**Figure 5H**). Thus, coordinated upregulation of *Rab-GAP1* expression and downregulation of *TRXh2* may explain the enhanced systemic accumulation of BaMV. It could be speculated that BaMV affects the transcription-related function of NbHMG1/2a because BaMV enhanced the expression of *Rab-Gap1* in the overexpression and silenced plants (**Figures 5A,E**). While BaMV reduces the expression level of *NbHMG1/2a* (enhanced by the VIGS-mediated transient silencing), BaMV forces the remaining *NbHMG1/2a* to translocalize from the nucleus to the cytosol (**Figure 6**). Both cases resulted in increased expression of Rab-GAP1, which may suggest that NbHMG1/2a may act as a negative regular for *Rap-GAP1* in the presence of BaMV. The VIGS results support this notion, however, further experimental validations are required to explain how NbHMG1/2a affect the expression of several host factors with/without BaMV infection.

While it could be interpreted that a homeostatic imbalance of HMG affects the expression of factors involved in BaMV movement, these findings may also rule out the potential involvement of antiviral defenses (e.g., callose deposition, antiviral RNA silencing pathway, accumulation of reactive oxygen species, and salicylic and abscisic acids) on systemic BaMV movement. The impacts of these antiviral defenses would be apparent for both inoculated and systemic leaves, as well as at cellular levels (Alazem et al., 2017, 2019; Huang et al., 2019). However, since the effect of NbHMG1/2a was only significant for systemic leaves, those antiviral defenses might not be affected by HMG homeostasis. In a similar example where silencing and overexpression of specific genes induced plant susceptibility to viral infection, a previous study showed that the chloroplast gene *Increased Size Exclusion Limit 2* (*ISE2*) enhanced systemic accumulation of *Tobacco mosaic virus* (TMV) and *Turnip mosaic virus* (TuMV) under conditions of both silencing and overexpression, albeit most likely through different mechanisms (Ganusova et al., 2017). Whereas silencing of *ISE2* enhanced symplastic flux, thereby increasing systemic movement of both TMV and TuMV, levels of the Dicer-like protein of the antiviral RNA pathway was reduced in *ISE2*-overexpressing plants, perhaps explaining the enhanced susceptibility to TMV and TuMV via abrogation of antiviral defense mechanisms (Ganusova et al., 2017). *ISE2* is involved in the chloroplast-to-nucleus retrograde signaling that regulates formation of PD, consequently affecting intercellular viral movement (Ganusova et al., 2020). In our study, the nuclear-localized protein NbHMG1/2a regulates expression of host factors involved in systemic movement of BaMV with no effect observed in the inoculated leaves. The cytoplasmic role of NbHMG1/2a under conditions of BaMV infection warrants further investigation.

CONCLUDING REMARKS

Local and systemic viral trafficking requires specific cellular host factors. These factors vary depending on each stage of movement, such as passage through PDs, movement into companion cells, phloem entry, and exit from the vascular system into the upper leaves. Our study presents evidence of the involvement of a nuclear protein, HMG1/2a, in the systemic movement of plant viruses. HMG1/2a homeostasis affects levels of Rap-GAP1 and TRXh2 to regulate systemic BaMV movement and we speculate that HMG1/2a may affect other factors involved in the infection cycle of BaMV, potentially linked to its reported nuclear function in transcriptional regulation or to its unknown function in the cytoplasm. Viral interactions with host nuclear proteins and subsequent export of these latter into the cytoplasm seem to be diverse phenomena, which are probably infection stage-related. Further studies on how host nuclear factors mediate virus-host interactions will shed light on how viruses control their movement and replication by hijacking host nuclear factors and their downstream pathways.

MATERIALS AND METHODS

HMG Domain Prediction

Nucleus localization signal was predicted using cNLS Mapper with a cut-off score of 5.6[1] (Kosugi et al., 2009a). Nucleolus localization signal was predicted using NoD with a cut-off score of 0.81/1.00[2] (Scott et al., 2011). The conserved domains of HMG were defined by querying against conserved domains in NCBI[3] (Jones et al., 2014; Marchler-Bauer et al., 2015; Marchler-Bauer et al., 2017). The NetNES 1.1 server was used to predict a nuclear export signal, which indicated that a motif at 44–50 aa is responsible for nuclear export, albeit with a weak signal (below threshold) (la Cour et al., 2004).

[1]http://nls-mapper.iab.keio.ac.jp

[2]http://www.compbio.dundee.ac.uk/www-nod/

[3]https://www.ncbi.nlm.nih.gov/Structure/cdd/wrpsb.cgi

Phylogenetic Analysis

Protein sequences of NbHMG1/2 were blasted against the NCBI database. Similar sequences (with at least 70% similarity) were used to generate phylogenetic trees in MEGA 6.0 software and by applying the Neighbor Joining method.

Plant Growth and Virus Induced Gene Silencing (VIGS)

N. benthamiana plants were grown at 28°C in a walk-in plant growth chamber under a 16-h-light/8-h-dark cycle with a white light (Philips TLD 36W/840 ns) intensity of 185–222 μmol m^{-2} s^{-1} at the leaf surface, and a relative humidity of approximately 70%. VIGS was carried out as described previously (Senthil-Kumar and Mysore, 2014). In brief, 18-day-old *N. benthamiana* plants where infiltrated with *Agrobacterium* strain C58C1 carrying either TRV1 or TRV2 vector, with the latter carrying ∼300 bp fragments of NbHMG1 or PDS as a phenotype control. In addition, the TRV2 vector (with mCherry insert) was agroinfiltrated alongside TRV1 as a vector control (TRV-EV). Seven-to-eight days post-infiltration (dpi), the control plants silenced with PDS presented a bleached phenotype, indicating that silencing was effective. Leaves 7 and 8 of *NbHMG1/2a*-silenced plants were later infiltrated with pKBG to assess the effect of *NbHMG1/2a*-silencing on BaMV movement (Liou et al., 2014). pKBG-infiltrated leaves (leaves 7 and 8) and systemically infected leaves (leaves 11 and 12) were collected at 4, 5, and 6 dpi for further analyses. The VIGS experiment was tested in three biological replicates, each of which consisted of three plants.

Overexpression of *NbHMG1/2a*

Full-length *NbHMG1/2a* was cloned into the expression vector pBin61, with 3xHA-mCherry tagged on the N-terminus of NbHMG1/2a (pBin-HMG). The vector pBin61-3HA-mCherry (pBin-mCherry) was used as a control (Huang et al., 2017b). The BaMV infectious clone pKBG (BaMV construct expressing GFP) (Liou et al., 2014) was used to infect plants, and the empty vector pKn was used as a control. All clones were transferred into *A. tumefaciens* C58C1 strain for agroinfiltration. Fully expanded *N. benthamiana* leaves (leaves 7 and 8) were co-infiltrated with four different construct combinations: pBin-HMG with pKBG, pBin-HMG with pKn, pKBG with pBin-mCherry, or pKn with pBin-mCherry. Infiltrated leaves (leaves 7 and 8) and systemic leaves (leaves 11 and 12) were collected at 4, 5, and 6 dpi for further analysis. The results were tested in three biological replicates, each of which consisted of three plants.

RNA Analyses

Total RNA Extraction

Total RNA was extracted from leaves using TRIzol (Invitrogen, Carlsbad, CA, United States), purified according to the phenol-chloroform method, and then precipitated in 0.1 volume of 3 M NaOAc and 2.5 volume of 100% ethanol.

Northern Blot Analysis

BaMV RNA was detected as described previously (Alazem et al., 2014, 2017). In brief, total RNA (2 μg) was glyoxylated and then separated by electrophoresis on a 1% agarose gel. The RNA was then transferred onto a Hybond-N^+ membrane (GE Healthcare, Little Chalfont, Buckinghamshire, United Kingdom), cross-linked under UV light, and hybridized against P^{32}-labeled (–)CP to detect (+)BaMV (Lin et al., 1993).

Real-Time Quantitative PCR (RTqPCR)

Each RNA sample (2 μg) was treated with RQ1-DNase (Promega, Madison, WI, United States) for 30 min at 37°C. RNA samples were then subjected to first-strand cDNA synthesis with Superscript III (Invitrogen). cDNA was then diluted to a final concentration of 20 ng/μl. Primers used for RTqPCR are listed in **Supplementary Table S1**. All RTqPCR reactions were performed with SYBR Green Supermix (Applied Biosystems, Foster City, CA, United States), following the manufacturer's instructions. RTqPCR was carried out on three biological replicates, with three technical replicates for each biological replicate.

Protein Blot

Total protein from *N. benthamiana* leaves was extracted as described previously (Alazem et al., 2014). Briefly, leaves (approximately 0.1 g) were ground to fine powder in liquid nitrogen and homogenized by adding a similar volume of extraction buffer [0.1 M glycine NaOH (pH 9.0), 0.1 M NaCl, 0.5 mM EDTA, 2% sodium dodecyl sulfate (SDS), and 1% sodium laurosarcosine] (Varallyay et al., 2017). Samples were boiled for 5 min and subsequently centrifuged at 13,000 rpm for 5 min. Supernatants were then transferred to new tubes. For BaMV CP detection, crude protein extract (25 μl) was loaded with 2 × dye (1 M Tris, 10% SDS, 100% glycerol, and 900 ml of β-mercaptoethanol in 50 ml of H_2O) onto 10% SDS-polyacrylamide gels for Western blot analysis, and membranes were hybridized with BaMV anti-CP sera (Lin et al., 1992), anti-HA, anti-Histone H2, anti-Tubulin, or anti-actin (Sigma).

Nuclear fractionation was performed based on the protocol described by Kinkema et al. (2000). Briefly, *N. benthamiana* leaves were homogenized in Honda buffer (2.5% Ficoll 400, 5% dextran T40, 0.4 M sucrose, 25 mM Tris-HCl, pH 7.4, 10 mM $MgCl_2$, 10 mM β-mercaptoethanol, and a proteinase inhibitor cocktail) by using a mortar and pestle and then filtered through 62-μm (pore-size) nylon mesh. Triton X-100 was added to a final concentration of 0.5%, and the mixture was incubated on ice for 15 min. The solution was centrifuged at 1,500 g for 5 min, and the pellet was washed with Honda buffer containing 0.1% Triton X-100. The pellet was resuspended gently in 1 ml of Honda buffer and transferred to a microcentrifuge tube. This nucleus-enriched preparation was centrifuged at 100 g for 1 min to pellet starch and cell debris. The supernatant was centrifuged subsequently at 1,800 g for 5 min to pellet the nuclei (Kinkema et al., 2000).

Yeast Two-Hybrid Assay

Yeast two-hybrid assays were performed according to protocols of the manufacturers of the GAL4 Two-Hybrid Phagemid Vector kits (Agilent Technologies, Inc., 2011). The full-length coding sequences of NbHMG1/2a, BaMV-CP and BaMV-TGBp1 were cloned downstream of the GAL4 activation domain (AD) or GAL4 DNA-binding domain (BD). Rich medium yeast extract, peptone, dextrose (YPD) was used to grow yeast under non-selective conditions. To test the interaction between NbHMG1/2a and CP or TGBp1, we coexpressed the constructs in YRG-2 yeast cells, and selected by incubation in leucine-tryptophan-histidine medium at 28°C for 2–3 days until colonies appeared. Each experiment was repeated three times.

Confocal Microscopy

To view the subcellular localization of NbHMG1/2a, *N. benthamiana* leaves were infiltrated with Agrobacterium strain C58C1 carrying pBin-mCherry or pBin-mCherry-HMG, and images were taken by confocal microscopy at various timeframes after infiltration. In some agroinfiltrated leaves, pBin-eGFP-Fib was co-expressed as a nucleolar marker. For BaMV infection, leaves were first agroinfiltrated with pKBG (OD, 0.005), agroinfiltrated with pBin-mCherry or pBin-mCherry-HMG (OD, 0.5) 5 days later, and leaves were then observed after a further 2 days. To visualize nuclei in leaf epidermal cells, DAPI (4′,6-diamidino-2-phenylindole) was infiltrated into *N. benthamiana* leaves and then leaves were visualized immediately using a Zeiss LSM510 laser scanning microscope with a 403/1.2 W Korr UV-VIS-IR objective lens. Images were captured using LSM510 software with filters for DAPI (excitation/emission: 405 nm/480–510 nm), GFP (excitation/emission: 488 nm/505–575 nm), and mCherry (excitation/emission: 543 nm/560–615 nm). All images were processed and cropped using Zeiss LSM Image Browser and Photoshop CS5 (Adobe).

DATA AVAILABILITY STATEMENT

The original contributions presented in the study are included in the article/**Supplementary Material**, further inquiries can be directed to the corresponding author/s.

AUTHOR CONTRIBUTIONS

MA and N-SL designed the research. MA, M-HH, C-HC, and NC performed the research. MA and N-SL analyzed the data and wrote the manuscript which was approved by all authors.

SUPPLEMENTARY MATERIAL

The Supplementary Material for this article can be found online at: https://www.frontiersin.org/articles/10.3389/fpls.2020.597665/full#supplementary-material

Supplementary Figure 1 | Sequence similarity between NbHMG1/2 a and b for the coding region (CDS), 5′ UTR, and 3′ UTR.

Supplementary Figure 2 | NbHMG1/2a localization in BaMV-infected *N. benthamiana* at 1.5 dpi. *N. benthamiana* leaves were co-agroinfiltrated with pKBG or empty vector (pKn) combined with either pBin-HA-mCherry or pBin-HA-mCherry-HMG, as described in the legend of **Figure 6**. Confocal microscopic observation was carried out at 1.5 dpi. Scale bars represent 50 μm. The experiment was repeated three times with similar results, and representative images are shown.

Supplementary Figure 3 | NbHMG1/2a localization in BaMV-infected *N. benthamiana* at 2 dpi. The experiment was carried out as described in **Supplementary Figure S2**, except confocal analyses were conducted at 2 dpi.

Supplementary Figure 4 | NbHMG1/2a localization in BaMV-infected *N. benthamiana* at 3 dpi. The experiment was carried out as described in **Supplementary Figure S2**, except confocal analyses were conducted at 3 dpi.

Supplementary Figure 5 | Expression levels of *BaMV-RDR*, *TRV-RDR*, and *NbHMG1/2a in N. benthamiana* plants silenced with *NbHMG1/2a*. Transcript levels of *BaMV-RDR* **(A)**, *TRV-RDR* **(B)**, and *NbHMG1/2a* **(C)** in BaMV-inoculated *N. benthamiana* leaves at 6 dpi. Plants were already infiltrated with the empty TRV-silencing vector (EV), or with TRV-HMG (HMGi) 7–8 days before BaMV infection. Statistical analysis was carried out as described in **Figure 3**, with * and ** representing $P < 0.05$ and < 0.01, respectively.

Supplementary Figure 6 | Expression of BaMV-RDR in *N. benthamiana* plants transiently expressing NbHMG1/2a-mCherry. Transcript levels of *BaMV-RDR* in BaMV-inoculated *N. benthamiana* leaves at 6 dpi in control plants (pBin-mCherry) and NbHMG1/2a-mCherry expressing plants (pBin-HMG). Statistical analysis was carried out as described in **Figure 3**, with ** representing $P < 0.01$.

Supplementary Figure 7 | Protein blot for HA-mCherry (30 kDa) or HA-HMG-mCherry (45 kDa) in leaves infiltrated with the control vector (pKn). Leaves from *N. benthamiana* plants were collected at 4, 5, and 6 dpi for analysis. The experiment was carried out as indicated in the legend of **Figure 5**, and was repeated three times with similar results. Ponceau S was used as a loading control.

Supplementary Figure 8 | NbHMG1/2a localization in BaMV-infected *N. benthamiana*. Leaves of *N. benthamiana* were first agroinfiltrated with pKBG (BaMV) or pKn (vector), and then agroinfiltrated with mCherry or mCherry-HMG 5 days later. Samples were collected 2 days after mCherry or mCherry-HMG expression for confocal microscopic observation. DAPI was infiltrated into *N. benthamiana* leaves before observation to detect nuclei. Scale bars represent 20 μm. The experiment was repeated three times with similar results, and representative images are shown.

Supplementary Figure 9 | Yeast two-hybrid assay of HMG against BaMV proteins. Binding assays were performed for HMG against BaMV CP and TGBp1 proteins. Yeast cells were grown in liquid media to an OD_{600} of 0.1 and then subjected to a 10^{-1}, 10^{-2}, and 10^{-3} dilution series. Ten microliters of liquid medium were grown on SD medium lacking Trp and Leu, or lacking Trp, Leu, and His. Images were taken 3 days after incubation.

Supplementary Table 1 | Primers used in the study.

Supplementary Table 2 | Probable targets of silencing if the first 300 bp of HMG1/2a is targeted for silencing.

REFERENCES

Alazem, M., He, M. H., Moffett, P., and Lin, N. S. (2017). Abscisic acid induces resistance against Bamboo mosaic virus through Argonaute2 and 3. *Plant Physiol.* 174, 339–355. doi: 10.1104/pp.16.00015

Alazem, M., Lin, K. Y., and Lin, N. S. (2014). The abscisic acid pathway has multifaceted effects on the accumulation of Bamboo mosaic virus. *Mol. Plant Microbe Interact.* 27, 177–189. doi: 10.1094/mpmi-08-13-0216-r

Alazem, M., Widyasari, K., and Kim, K. H. (2019). An avirulent strain of soybean mosaic virus reverses the defensive effect of abscisic acid in a susceptible soybean cultivar. *Viruses* 11:879. doi: 10.3390/v11090879

Antosch, M., Mortensen, S. A., and Grasser, K. D. (2012). Plant proteins containing high mobility group box DNA-binding domains modulate different nuclear processes. *Plant Physiol.* 159, 875–883. doi: 10.1104/pp.112.198283

Bianchi, M. E., and Agresti, A. (2005). HMG proteins: dynamic players in gene regulation and differentiation. *Curr. Opin. Genet. Dev.* 15, 496–506. doi: 10.1016/j.gde.2005.08.007

Chang, B. Y., Lin, N. S., Liou, D. Y., Chen, J. P., Liou, G. G., and Hsu, Y. H. (1997). Subcellular localization of the 28 kDa protein of the triple-gene-block of bamboo mosaic potexvirus. *J. Gen. Virol.* 78(Pt 5), 1175–1179. doi: 10.1099/0022-1317-78-5-1175

Chang, C. H., Hsu, F. C., Lee, S. C., Lo, Y. S., Wang, J. D., Shaw, J., et al. (2016). The nucleolar fibrillarin protein is required for helper virus-independent long-distance trafficking of a subviral satellite RNA in plants. *Plant Cell* 28, 2586–2602. doi: 10.1105/tpc.16.00071

Chen, I. H., Chen, H. T., Huang, Y. P., Huang, H. C., Shenkwen, L. L., Hsu, Y. H., et al. (2018). A thioredoxin NbTRXh2 from *Nicotiana benthamiana* negatively regulates the movement of Bamboo mosaic virus. *Mol. Plant Pathol.* 19, 405–417. doi: 10.1111/mpp.12532

Chen, L., Zhang, L., Li, D., Wang, F., and Yu, D. (2013). WRKY8 transcription factor functions in the TMV-cg defense response by mediating both abscisic acid and ethylene signaling in *Arabidopsis*. *Proc. Natl. Acad. Sci. U.S.A.* 110, E1963–E1971.

Cheng, C. P. (2017). Host factors involved in the intracellular movement of Bamboo mosaic virus. *Front. Microbiol.* 8:759.

Cheng, S. F., Huang, Y. P., Chen, L. H., Hsu, Y. H., and Tsai, C. H. (2013). Chloroplast phosphoglycerate kinase is involved in the targeting of Bamboo mosaic virus to chloroplasts in *Nicotiana benthamiana* plants. *Plant Physiol.* 163, 1598–1608. doi: 10.1104/pp.113.229666

Choi, H. W., Manohar, M., Manosalva, P., Tian, M., Moreau, M., and Klessig, D. F. (2016). Activation of plant innate immunity by extracellular high mobility group box 3 and its inhibition by salicylic acid. *PLoS Pathog.* 12:e1005518. doi: 10.1371/journal.ppat.1005518

Chou, Y. L., Hung, Y. J., Tseng, Y. H., Hsu, H. T., Yang, J. Y., Wung, C. H., et al. (2013). The stable association of virion with the triple-geneblock protein 3-based complex of Bamboo mosaic virus. *PLoS Pathog.* 9:e1003405. doi: 10.1371/journal.ppat.1003405

DiMaio, F., Chen, C. C., Yu, X., Frenz, B., Hsu, Y. H., Lin, N. S., et al. (2015). The molecular basis for flexibility in the flexible filamentous plant viruses. *Nat. Struct. Mol. Biol.* 22, 642–644. doi: 10.1038/nsmb.3054

Fernandez-Pozo, N., Rosli, H. G., Martin, G. B., and Mueller, L. A. (2015). The SGN VIGS tool: user-friendly software to design virus-induced gene silencing (VIGS) constructs for functional genomics. *Mol. Plant* 8, 486–488. doi: 10.1016/j.molp.2014.11.024

Ganusova, E. E., Reagan, B. C., Fernandez, J. C., Azim, M. F., Sankoh, A. F., Freeman, K. M., et al. (2020). Chloroplast-to-nucleus retrograde signalling controls intercellular trafficking via plasmodesmata formation. *Philos. Trans. R. Soc. B Biol. Sci.* 375:20190408. doi: 10.1098/rstb.2019.0408

Ganusova, E. E., Rice, J. H., Carlew, T. S., Patel, A., Perrodin-Njoku, E., Hewezi, T., et al. (2017). Altered expression of a chloroplast protein affects the outcome of virus and nematode infection. *Mol. Plant Microbe Interact.* 30, 478–488. doi: 10.1094/mpmi-02-17-0031-r

Hipper, C., Brault, V., Ziegler-Graff, V., and Revers, F. (2013). Viral and cellular factors involved in Phloem transport of plant viruses. *Front. Plant Sci.* 4:154.

Hiscox, J. A. (2007). RNA viruses: hijacking the dynamic nucleolus. *Nat. Rev. Microbiol.* 5, 119–127. doi: 10.1038/nrmicro1597

Hong, B., Muili, K., Bolyard, C., Russell, L., Lee, T. J., Banasavadi-Siddegowda, Y., et al. (2019). Suppression of HMGB1 released in the glioblastoma tumor microenvironment reduces tumoral edema. *Mol. Ther. Oncolytics* 12, 93–102. doi: 10.1016/j.omto.2018.11.005

Hsu, H. T., Chou, Y. L., Tseng, Y. H., Lin, Y. H., Lin, T. M., Lin, N. S., et al. (2008). Topological properties of the triple gene block protein 2 of Bamboo mosaic virus. *Virology* 379, 1–9. doi: 10.1016/j.virol.2008.06.019

Hsu, Y. H., Tsai, C. H., and Lin, N. S. (2018). Editorial: molecular biology of Bamboo mosaic Virus-A type member of the *Potexvirus* genus. *Front. Microbiol.* 9:6.

Huang, Y. L., Han, Y. T., Chang, Y. T., Hsu, Y. H., and Meng, M. (2004). Critical residues for GTP methylation and formation of the covalent m7GMP-enzyme intermediate in the capping enzyme domain of bamboo mosaic virus. *J. Virol.* 78, 1271–1280. doi: 10.1128/jvi.78.3.1271-1280.2004

Huang, Y. P., Chen, I. H., and Tsai, C. H. (2017a). Host factors in the infection cycle of Bamboo mosaic virus. *Front. Microbiol.* 8:437.

Huang, Y. P., Chen, J. S., Hsu, Y. H., and Tsai, C. H. (2013). A putative Rab-GTPase activation protein from *Nicotiana benthamiana* is important for Bamboo mosaic virus intercellular movement. *Virology* 447, 292–299. doi: 10.1016/j.virol.2013.09.021

Huang, Y. P., Huang, Y. W., Chen, I. H., Shenkwen, L. L., Hsu, Y. H., and Tsai, C. H. (2017b). Plasma membrane-associated cation-binding protein 1-like protein negatively regulates intercellular movement of BaMV. *J. Exp. Bot.* 68, 4765–4774. doi: 10.1093/jxb/erx307

Huang, Y. W., Hu, C. C., Tsai, C. H., Lin, N. S., and Hsu, Y. H. (2019). *Nicotiana benthamiana* Argonaute10 plays a pro-viral role in Bamboo mosaic virus infection. *New Phytol.* 224, 804–817. doi: 10.1111/nph.16048

Hung, C. J., Huang, Y. W., Liou, M. R., Lee, Y. C., Lin, N. S., Meng, M. H., et al. (2014). Phosphorylation of coat protein by protein kinase CK2 regulates cell-to-cell movement of Bamboo mosaic virus through modulating RNA binding. *Mol. Plant Microbe Interact.* 27, 1211–1225. doi: 10.1094/mpmi-04-14-0112-r

Jones, P., Binns, D., Chang, H. Y., Fraser, M., Li, W., Mcanulla, C., et al. (2014). InterProScan 5: genome-scale protein function classification. *Bioinformatics* 30, 1236–1240. doi: 10.1093/bioinformatics/btu031

Ju, B. G., Lunyak, V. V., Perissi, V., Garcia-Bassets, I., Rose, D. W., Glass, C. K., et al. (2006). A topoisomerase IIbeta-mediated dsDNA break required for regulated transcription. *Science* 312, 1798–1802. doi: 10.1126/science.1127196

Kim, S. H., Macfarlane, S., Kalinina, N. O., Rakitina, D. V., Ryabov, E. V., Gillespie, T., et al. (2007). Interaction of a plant virus-encoded protein with the major nucleolar protein fibrillarin is required for systemic virus infection. *Proc. Natl. Acad. Sci. U.S.A.* 104, 11115–11120. doi: 10.1073/pnas.0704632104

Kinkema, M., Fan, W. H., and Dong, X. N. (2000). Nuclear localization of NPR1 is required for activation of PR gene expression. *Plant Cell* 12, 2339–2350. doi: 10.2307/3871233

Kosugi, S., Hasebe, M., Matsumura, N., Takashima, H., Miyamoto-Sato, E., Tomita, M., et al. (2009a). Six classes of nuclear localization signals specific to different binding grooves of importin alpha. *J. Biol. Chem.* 284, 478–485. doi: 10.1074/jbc.m807017200

Kosugi, S., Hasebe, M., Tomita, M., and Yanagawa, H. (2009b). Systematic identification of cell cycle-dependent yeast nucleocytoplasmic shuttling proteins by prediction of composite motifs. *Proc. Natl. Acad. Sci. U.S.A.* 106, 10171–10176. doi: 10.1073/pnas.0900604106

Krichevsky, A., Kozlovsky, S. V., Gafni, Y., and Citovsky, V. (2006). Nuclear import and export of plant virus proteins and genomes. *Mol. Plant Pathol.* 7, 131–146. doi: 10.1111/j.1364-3703.2006.00321.x

la Cour, T., Kiemer, L., Molgaard, A., Gupta, R., Skriver, K., and Brunak, S. (2004). Analysis and prediction of leucine-rich nuclear export signals. *Protein Eng. Des. Sel.* 17, 527–536. doi: 10.1093/protein/gzh062

Lan, P., Yeh, W. -B., Tsai, C. -W., and Lin, N. -S. (2010). A unique glycine-rich motif at the N-terminal region of *Bamboo mosaic virus* coat protein is required for symptom expression. *Mol. Plant Microbe Interact.* 23, 903–914. doi: 10.1094/MPMI-23-7-0903

Launholt, D., Merkle, T., Houben, A., Schulz, A., and Grasser, K. D. (2006). *Arabidopsis* chromatin-associated HMGA and HMGB use different nuclear targeting signals and display highly dynamic localization within the nucleus. *Plant Cell* 18, 2904–2918. doi: 10.1105/tpc.106.047274

Lee, C. C., Ho, Y. N., Hu, R. H., Yen, Y. T., Wang, Z. C., Lee, Y. C., et al. (2011). The interaction between Bamboo mosaic virus replication protein and coat protein is critical for virus movement in plant hosts. *J. Virol.* 85, 12022–12031. doi: 10.1128/jvi.05595-11

Levy, A., Zheng, J. Y., and Lazarowitz, S. G. (2013). The tobamovirus turnip vein clearing virus 30-kilodalton movement protein localizes to novel nuclear filaments to enhance virus infection. *J. Virol.* 87, 6428–6440. doi: 10.1128/jvi.03390-12

Lewis, R. T., Andreucci, A., and Nikolajczyk, B. S. (2001). PU.1-mediated transcription is enhanced by HMG-I(Y)-dependent structural mechanisms. *J. Biol. Chem.* 276, 9550–9557. doi: 10.1074/jbc.m008726200

Li, Y. I., Chen, Y. J., Hsu, Y. H., and Meng, M. (2001a). Characterization of the AdoMet-dependent guanylyltransferase activity that is associated with the N terminus of bamboo mosaic virus replicase. *J. Virol.* 75, 782–788. doi: 10.1128/jvi.75.2.782-788.2001

Li, Y. I., Cheng, Y. M., Huang, Y. L., Tsai, C. H., Hsu, Y. H., and Meng, M. (1998). Identification and characterization of the *Escherichia coli*-expressed RNA-dependent RNA polymerase of bamboo mosaic virus. *J. Virol.* 72, 10093–10099. doi: 10.1128/jvi.72.12.10093-10099.1998

Li, Y. I., Shih, T. W., Hsu, Y. H., Han, Y. T., Huang, Y. L., and Meng, M. (2001b). The helicase-like domain of plant potexvirus replicase participates in formation of RNA 5' cap structure by exhibiting RNA 5'-triphosphatase activity. *J. Virol.* 75, 12114–12120. doi: 10.1128/jvi.75.24.12114-12120.2001

Li, Z. G., Zhang, Y. L., Jiang, Z. H., Jin, X. J., Zhang, K., Wang, X. B., et al. (2018). Hijacking of the nucleolar protein fibrillarin by TGB1 is required for cell-to-cell movement of Barley stripe mosaic virus. *Mol. Plant Pathol.* 19, 1222–1237. doi: 10.1111/mpp.12612

Lin, M. K., Hu, C. C., Lin, N. S., Chang, B. Y., and Hsu, Y. H. (2006). Movement of potexviruses requires species-specific interactions among the cognate triple gene block proteins, as revealed by a trans-complementation assay based on the bamboo mosaic virus satellite RNA-mediated expression system. *J. Gen. Virol.* 87, 1357–1367. doi: 10.1099/vir.0.81625-0

Lin, N. S., Chai, Y. J., Huang, T. Y., Chang, T. Y., and Hsu, Y. H. (1993). Incidence of Bamboo mosaic potexvirus in Taiwan. *Plant Dis.* 77, 448–450. doi: 10.1094/pd-77-0448

Lin, N. S., and Chen, C. C. (1991). Association of Bamboo mosaic-virus (Bomv) and Bomv-specific electron-dense crystalline bodies with chloroplasts. *Phytopathology* 81, 1551–1555. doi: 10.1094/phyto-81-1551

Lin, N. S., Lin, B. Y., Lo, N. W., Hu, C. C., Chow, T. Y., and Hsu, Y. H. (1994). Nucleotide sequence of the genomic RNA of bamboo mosaic potexvirus. *J. Gen. Virol.* 75(Pt 9), 2513–2518. doi: 10.1099/0022-1317-75-9-2513

Lin, N. S., Lin, F. Z., Huang, T. Y., and Hsu, Y. H. (1992). Genome properties of Bamboo mosaic-virus. *Phytopathology* 82, 731–734. doi: 10.1094/phyto-82-731

Liou, M. R., Huang, Y. W., Hu, C. C., Lin, N. S., and Hsu, Y. H. (2014). A dual gene-silencing vector system for monocot and dicot plants. *Plant Biotechnol. J.* 12, 330–343. doi: 10.1111/pbi.12140

Lough, T. J., and Lucas, W. J. (2006). Integrative plant biology: role of phloem long-distance macromolecular trafficking. *Annu. Rev. Plant Biol.* 57, 203–232. doi: 10.1146/annurev.arplant.56.032604.144145

Lukhovitskaya, N. I., Cowan, G. H., Vetukuri, R. R., Tilsner, J., Torrance, L., and Savenkov, E. I. (2015). Importin-alpha-mediated nucleolar localization of potato mop-top virus TRIPLE GENE BLOCK1 (TGB1) protein facilitates virus systemic movement, whereas TGB1 self-interaction is required for cell-to-cell movement in *Nicotiana benthamiana*. *Plant Physiol.* 167, 738–752. doi: 10.1104/pp.114.254938

Lukhovitskaya, N. I., Gushchin, V. A., Solovyev, A. G., and Savenkov, E. I. (2013). Making sense of nuclear localization: a zinc-finger protein encoded by a cytoplasmically replicating plant RNA virus acts a transcription factor: a novel function for a member of large family of viral proteins. *Plant Signal. Behav.* 8:e25263. doi: 10.4161/psb.25263

Marchler-Bauer, A., Bo, Y., Han, L., He, J., Lanczycki, C. J., Lu, S., et al. (2017). CDD/SPARCLE: functional classification of proteins via subfamily domain architectures. *Nucleic Acids Res.* 45, D200–D203.

Marchler-Bauer, A., Derbyshire, M. K., Gonzales, N. R., Lu, S., Chitsaz, F., Geer, L. Y., et al. (2015). CDD: NCBI's conserved domain database. *Nucleic Acids Res.* 43, D222–D226.

Palani, P. V., Chiu, M., Chen, W., Wang, C. C., Lin, C. C., Hsu, C. C., et al. (2009). Subcellular localization and expression of bamboo mosaic virus satellite RNA-encoded protein. *J. Gen. Virol.* 90, 507–518. doi: 10.1099/vir.0.004994-0

Pitzalis, N., and Heinlein, M. (2017). The roles of membranes and associated cytoskeleton in plant virus replication and cell-to-cell movement. *J. Exp. Bot.* 69, 117–132. doi: 10.1093/jxb/erx334

Reeves, R. (2010). Nuclear functions of the HMG proteins. *Biochim. Biophys. Acta* 1799, 3–14. doi: 10.1016/j.bbagrm.2009.09.001

Reeves, R., and Beckerbauer, L. (2001). HMGI/Y proteins: flexible regulators of transcription and chromatin structure. *Biochim. Biophys. Acta* 1519, 13–29. doi: 10.1016/s0167-4781(01)00215-9

Rodrigo, G., Zwart, M. P., and Elena, S. F. (2014). Onset of virus systemic infection in plants is determined by speed of cell-to-cell movement and number of primary infection foci. *J. R. Soc. Interface* 11:20140555. doi: 10.1098/rsif.2014.0555

Scott, M. S., Troshin, P. V., and Barton, G. J. (2011). NoD: a nucleolar localization sequence detector for eukaryotic and viral proteins. *BMC Bioinformatics* 12:317.

Senthil-Kumar, M., and Mysore, K. S. (2014). Tobacco rattle virus-based virus-induced gene silencing in *Nicotiana benthamiana*. *Nat. Protoc.* 9, 1549–1562. doi: 10.1038/nprot.2014.092

Solovyev, A. G., Kalinina, N. O., and Morozov, S. Y. (2012). Recent advances in research of plant virus movement mediated by triple gene block. *Front. Plant Sci.* 3:276.

Solovyev, A. G., and Savenkov, E. I. (2014). Factors involved in the systemic transport of plant RNA viruses: the emerging role of the nucleus. *J. Exp. Bot.* 65, 1689–1697. doi: 10.1093/jxb/ert449

Sprague, L., Lee, J. M., Hutzen, B. J., Wang, P. Y., Chen, C. Y., Conner, J., et al. (2018). High mobility group box 1 influences HSV1716 spread and acts as an adjuvant to chemotherapy. *Viruses* 10:132. doi: 10.3390/v10030132

Varallyay, E., Valoczi, A., Agyi, A., Burgyan, J., and Havelda, Z. (2017). Plant virus-mediated induction of miR168 is associated with repression of ARGONAUTE1 accumulation (vol 29, pg 3507, 2010). *EMBO J.* 36:1641. doi: 10.15252/embj.201797083

Wu, Q., Zhang, W., Pwee, K. H., and Kumar, P. P. (2003). Rice HMGB1 protein recognizes DNA structures and bends DNA efficiently. *Arch. Biochem. Biophys.* 411, 105–111. doi: 10.1016/s0003-9861(02)00721-x

Xu, D., Marquis, K., Pei, J., Fu, S. C., Cagatay, T., Grishin, N. V., et al. (2015). LocNES: a computational tool for locating classical NESs in CRM1 cargo proteins. *Bioinformatics* 31, 1357–1365. doi: 10.1093/bioinformatics/btu826

Yang, C. C., Liu, J. S., Lin, C. P., and Lin, N. S. (1997). Nucleotide sequence and phylogenetic analysis of a bamboo mosaic potexvirus isolate from common bamboo (*Bambusa vulgaris* McClure). *Bot. Bull. Acad. Sin.* 38, 77–84.

Conflict of Interest: The authors declare that the research was conducted in the absence of any commercial or financial relationships that could be construed as a potential conflict of interest.

frontiers in Microbiology

ORIGINAL RESEARCH
published: 04 February 2021
doi: 10.3389/fmicb.2021.639445

Viral Release Threshold in the Salivary Gland of Leafhopper Vector Mediates the Intermittent Transmission of Rice Dwarf Virus

*Qian Chen, Yuyan Liu, Zhirun Long, Hengsong Yang and Taiyun Wei**

Fujian Province Key Laboratory of Plant Virology, Institute of Plant Virology, Vector-borne Virus Research Center, Fujian Agriculture and Forestry University, Fuzhou, China

Numerous piercing-sucking insects can persistently transmit viral pathogens in combination with saliva to plant phloem in an intermittent pattern. Insect vectors maintain viruliferous for life. However, the reason why insect vectors discontinuously transmit the virus remains unclear. Rice dwarf virus (RDV), a plant reovirus, was found to replicate and assemble the progeny virions in salivary gland cells of the leafhopper vector. We observed that the RDV virions moved into saliva-stored cavities in the salivary glands of leafhopper vectors via an exocytosis-like mechanism, facilitating the viral horizontal transmission to plant hosts during the feeding of leafhoppers. Interestingly, the levels of viral accumulation in the salivary glands of leafhoppers during the transmitting period were significantly lower than those of viruliferous individuals during the intermittent period. A putative viral release threshold, which was close to 1.79×10^4 copies/μg RNA was proposed from the viral titers in the salivary glands of 52 leafhoppers during the intermittent period. Thus, the viral release threshold was hypothesized to mediate the intermittent release of RDV from the salivary gland cells of leafhoppers. We anticipate that viral release threshold-mediated intermittent transmission by insect vectors is the conserved strategy for the epidemic and persistence of vector-borne viruses in nature.

Keywords: intermittent transmission, rice dwarf virus, insect vectors, salivary glands, viral release threshold

OPEN ACCESS

Edited by:
Xiaofei Cheng,
Northeast Agricultural University, China

Reviewed by:
Il-Ryong Choi,
International Rice Research Institute (IRRI), Philippines
Wenwen Liu,
Chinese Academy of Agricultural Sciences, China

***Correspondence:**
Taiyun Wei
weitaiyun@fafu.edu.cn

Specialty section:
This article was submitted to Virology, a section of the journal Frontiers in Microbiology

Received: *09 December 2020*
Accepted: *18 January 2021*
Published: *04 February 2021*

Citation:
Chen Q, Liu Y, Long Z, Yang H and Wei T (2021) Viral Release Threshold in the Salivary Gland of Leafhopper Vector Mediates the Intermittent Transmission of Rice Dwarf Virus. Front. Microbiol. 12:639445. doi: 10.3389/fmicb.2021.639445

INTRODUCTION

Several persistent plant viruses of agricultural importance are transmitted to plants by piercing–sucking insect vectors, such as leafhoppers, planthoppers, and whiteflies (Jia et al., 2018). These vectors are usually infected with viruses throughout their lifetime, yet they transmit the virus intermittently (Gamez, 1973; Reynaud and Peterschmitt, 1992; Muniyappa et al., 2000; Ammar and Nault, 2002; Pu et al., 2012). Intermittent transmission refers to the phenotype that after the latent period of persistent virus, insect vectors discontinuously transmit the virus for life, rather than transmitting it daily. The intermittent period ranges from 2 to 14 days, in which the insect vectors still remain viruliferous (Muniyappa et al., 2000; Pu et al., 2012). However, the reason why insect vectors intermittently transmit viruses and the association of intermittent transmission with viral infection in the plant hosts remain unknown. To address the mechanism that underlies the

intermittent transmission of viruses by insect vectors, it is essential to understand how the viruses are released from the salivary glands of insect vectors.

In the salivary glands of insects, most salivary gland cells are filled with abundant apical plasmalemma-lined cavities in which saliva is stored (Mao et al., 2017). Virions are generally secreted together with saliva to the salivary cavities (Hogenhout et al., 2008; Wei and Li, 2016). The virions then successively move with saliva into a canal that leads to the salivary canal and a duct that allows virus-laden saliva to exit the stylets. The virions are ultimately ejected into the phloem of the plant, while insect vectors feed on susceptible hosts (Hogenhout et al., 2008; Wei and Li, 2016). Therefore, the salivary glands of insects serve as the last barrier for the circulation of the viral pathogen and determines whether an insect can transmit the virus. A better understanding of the mechanism that underlies how the virus overcomes the salivary glands barriers is essential to provide a basis for the control of viral diseases. Previous studies showed that the salivary gland release barrier referred to the apical plasmalemma that separates the salivary cavities for saliva storage (Gray and Gildow, 2003; Mao et al., 2017). Virus in the cytoplasm of salivary glands must pass through the apical plasmalemma and disseminate into the salivary cavities for transmission by insect vectors. Therefore, the transmission efficiency by insect vectors is correlated with the viral ability to overcome the salivary gland release barrier.

Rice dwarf virus (RDV), belonging to the *Phytoreovirus* genus of *Reoviridae* family, was the first plant virus discovered to be transmitted by insect vectors (Ishikawa, 1928; Attoui et al., 2012). RDV causes rice dwarf disease, which results in yield losses in southern China, Japan, and southeast Asia (Boccardo and Milne, 1984). This virus is primarily transmitted by the leafhopper vector *Nephotettix cincticeps* in a persistent-propagative manner, and the transmission process includes infective and non-infective periods (Ishikawa, 1928; Fukushi, 1940; Zhong et al., 2003). The virion is icosahedral and approximately 70 nm in diameter (Attoui et al., 2012). The viral genome possesses 12 double-stranded RNA (dsRNA) segments (S1-S12) that encode seven structural proteins (P1, P2, P3, P5, P7, P8, and P9) and five non-structural proteins (Pns4, Pns6, Pns10, Pns11, and Pns12) (Omura and Yan, 1999; Nakagawa et al., 2003; Miyazaki et al., 2010; Chen et al., 2015a). Once the virus gains access to the alimentary canal of leafhopper via the stylet and esophagus, the RDV virions specifically recognize and bind to the undefined receptors of the filter chamber and enter the epithelium (Chen et al., 2011). The viral life cycle begins when the viroplasm, which is composed of the matrix aggregated by non-structural proteins Pns6, Pns11, and Pns12, is generated for viral propagation (Wei et al., 2006b; Chen et al., 2015b). At approximately 12 days post first access to diseased plants (padp), the RDV reaches the salivary glands of the most viruliferous leafhoppers (Chen et al., 2011). The leafhopper then becomes RDV transmittable at approximately 14 days padp (Honda et al., 2007; Chen et al., 2011). However, how the leafhopper transmits RDV and how RDV releases from the salivary glands and infects plants via the stylets of the leafhopper vector remain unknown.

To understand how a virus releases from the salivary gland and infects plant hosts, the system of RDV–leafhopper system was investigated. In this study, by applying immunofluorescence and electron microscopy analyses, RDV infection, replication in, and release from the salivary gland cells of leafhopper vectors were characterized. The properties of viral intermittent transmission by leafhoppers were also shown. Finally, we proposed a putative threshold for viral release to interpret the phenotype of viral intermittent transmission by the leafhopper vectors. We hypothesized that this viral intermittent release threshold mediates the viral release from leafhopper vectors for the effective infection of the virus into the plant host.

MATERIALS AND METHODS

Insects, Viruses, and Antibodies

Uninfected *N. cincticeps* leafhopper individuals were collected from Yunnan Province, southwest China and propagated for several generations at 25 ± 3°C in the laboratory. Rice samples infected with RDV were also initially collected from Yunnan Province. These diseased plants served as an original viral source for transmission by *N. cincticeps* to rice plants (*Oryza sativa* L. ssp. *Japonica*, variety *Nipponbare*) under greenhouse conditions. The infected rice plants were tested using RT-PCR and PCR assays to make sure that the rice plants were singly infected with RDV in the absence of rice orange leaf phytoplasma.

Rabbit polyclonal antisera specific for RDV and Pns6 were provided by Dr. Toshihiro Omura (National Agricultural Research Center, Japan). IgGs of RDV and Pns6 were directly conjugated to fluorescein isothiocyanate (FITC) and rhodamine, respectively, according to manufacturer's instructions (Thermo Fisher Scientific, United States). The virus-FITC and Pns6-rhodamine were used for immunofluorescence detection. Actin dye rhodamine-phalloidin was obtained from Thermo Fisher Scientific (Waltham, MA, United States). The antibodies against the glyceraldehyde-3-phosphate dehydrogenase (GADPH) were obtained from Sangon Biotech (Shanghai, China).

Virus Acquisition and Transmission

Uninfected second-instar nymphs were first allowed to feed on rice plants with RDV for 2 days and then transferred to healthy plants for 12 days. At 14 days padp, the salivary glands were dissected for immunofluorescence assays or electron microscopy.

To characterize the profile of RDV transmission by a group of leafhoppers, the leafhoppers that fed on diseased rice plants were then sequentially kept on healthy rice seedlings for 10 days and individually fed on a healthy rice seedling in one glass tube for 24 h (**Supplementary Figure 1**). The leafhoppers were then transferred daily to new healthy rice seedlings for 13 days (**Supplementary Figure 1**). All of the rice seedlings tested were planted in an insect-proof greenhouse for 60 days (**Supplementary Figure 1**). To determine whether RDV was transmitted by leafhoppers to plants, RT-PCR was performed to test the presence/absence of the RDV P8 gene, which encodes a major outer capsid protein, in the tested plants.

To determine the viral genome copies in the salivary glands of viruliferous leafhoppers in the transmitting and intermittent periods at 19 days padp, leafhoppers that had previously fed

on diseased plants for 2 days were individually fed on a healthy rice seedling in a glass tube for 24 h. The bodies of tested leafhoppers were then collected for RT-PCR to determine whether or not the insects were infected. The tested rice seedlings were grown for 60 days and then examined using RT-PCR for the presence of the RDV P8 gene to determine whether or not RDV was transmitted by leafhoppers, ultimately enabling the transmitting or non-transmitting leafhoppers to be distinguished from the population tested. RT-qPCR was then conducted on the corresponding salivary glands of transmitting or non-transmitting leafhoppers to determine the viral gene copies of the major outer capsid protein P8.

To visualize the viral accumulation in salivary glands of leafhoppers during the transmitting or intermittent periods, the salivary glands of the leafhoppers tested post 24 h inoculation feeding were dissected for immunofluorescence assays. The methods of viral acquisition, transmission, and distinguishment for transmitting or non-transmitting viruliferous leafhoppers from the population tested were the same as those described above.

RNA Extraction and RT-qPCR Detection

To extract the total RNA of individual insect bodies, the individual insects were collected in one 1.5 mL Eppendorf tube. The tubes were then placed in liquid nitrogen. The insect bodies were ground with pestles and then lysed with 200 μL TRIzol reagent (Thermo Fisher Scientific). To extract the total RNA of salivary glands of each individual insect, a pair of salivary glands was dissected and collected in one 0.5 mL tube. The salivary glands were then lysed with 100 μL TRIzol reagent. The subsequent procedures were conducted following the manufacturer's instructions. The final concentration of RNAs was determined using a NanoDrop 1000 (Thermo Fisher Scientific).

To absolutely quantify the viral titers in the salivary glands of infected leafhoppers, a standard curve of RDV P8 was first established. In brief, the concentration of the plasmid DNA, including the RDV P8 gene, was determined using the NanoDrop 1000. A 10-fold dilution series of plasmid was then prepared in RNase-free water, and the copy number of the RDV P8 gene was calculated using the following formula: (DNA amount $\times$ 6.022 $\times$ 10^{23})/(plasmid length $\times$ 1 $\times$ 10^9 $\times$ 650). The diluted plasmids were analyzed for their Ct value using qPCR assays with specific primers of RDV P8 (forward primer 5′-tacagccatcagctaagccaaa-3′) and reverse primer 5′-ccgcaacagaccgaaaca-3′). The qPCR assays were performed in a Mastercycler Realplex4 real-time PCR system (Eppendorf, Hamburg, Germany) using GoTaq qPCR Master Mix kit (Promega, Madison, WI). Based on the correlation of the logarithm of plasmid copy number to base 10 with the corresponding Ct value, the equation y = –3.506x + 42.981 (x is the logarithm of plasmid copy number to base 10, y is the Ct value, and R^2 = 0.9987) was established.

The viral titers in the salivary glands of infected leafhoppers were then determined. The first-strands cDNA of RDV P8 derived from the RNAs of salivary glands were synthesized using the specific primer (forward primer 5′-tacagccatcagctaagccaaa-3′) and then analyzed for their Ct values using qPCR assays. The system and program of the qPCR assay for cDNA were the same as those of the qPCR assay for plasmid DNA. Based on the Ct value of each cDNA and the equation y = –3.506x + 42.981, the copy number of RDV P8, which was used to judge for viral genome copy, was determined as the log of the copy number per microgram of insect RNA.

Immunofluorescence Assay

To characterize the viral infection in and release from salivary glands, uninfected second-instar nymphs were allowed to feed on rice plants infected with RDV for 2 days and were then kept on healthy rice seedlings. At 12 days padp, the salivary glands of these tested leafhoppers were dissected, fixed in 4% paraformaldehyde in PBS for 10 h, and then permeabilized in 0.2% Triton X-100 for 24 h. Following previously described methods (Chen et al., 2017), the salivary glands were ultimately immunolabeled with antibodies against virus-FITC for RDV particles, Pns6-rhodamine for viroplasm, or rhodamine-phalloidin for actin. The resulting samples were observed using a Leica TCS SP5 inverted confocal microscope (Wetzlar, Germany).

Electron Microscopy

The salivary glands dissected from infected *N. cincticeps* were fixed, dehydrated, and embedded. Ultrathin sections were then cut as previously described (Mao et al., 2017).

Statistical Analyses

All data for viral titers in the salivary glands of leafhoppers were analyzed using a two-tailed *t*-test in GraphPad Prism 6 (San Diego, CA, United States).

RESULTS

RDV Infection and Replication in Salivary Gland Cells

To address how RDV was released from the cells of salivary gland to overcome the salivary gland release barrier, the accumulation of RDV in the salivary glands was first studied. The salivary glands of *N. cincticeps* consist of a pair of principal and accessory salivary glands. The principal gland contains six types of cells (I–VI) (**Figures 1A,B**). The type III-cell was the largest and separated from each other, while the type VI-cells situated at the center of the type V-cells were the smallest. Immunofluorescence assays showed that at 12 days padp, RDV antigens were localized to the type III-cells (**Figure 1C**); type II- and III-cells (**Figure 1D**); type III-cells, type IV-cells, and accessory salivary glands (**Figure 1E**), or they were found throughout the principal salivary glands (**Figure 1F**). These results indicated the high frequency of RDV infection in the type III-cells.

The antibodies against the viral non-structural protein Pns6, which is a component of the viroplasm matrix (Wei et al., 2006b; Chen et al., 2015b), were used to examine viral replication. Immunofluorescence assays showed that various amounts of viroplasm were distributed in each type of cell, such as type

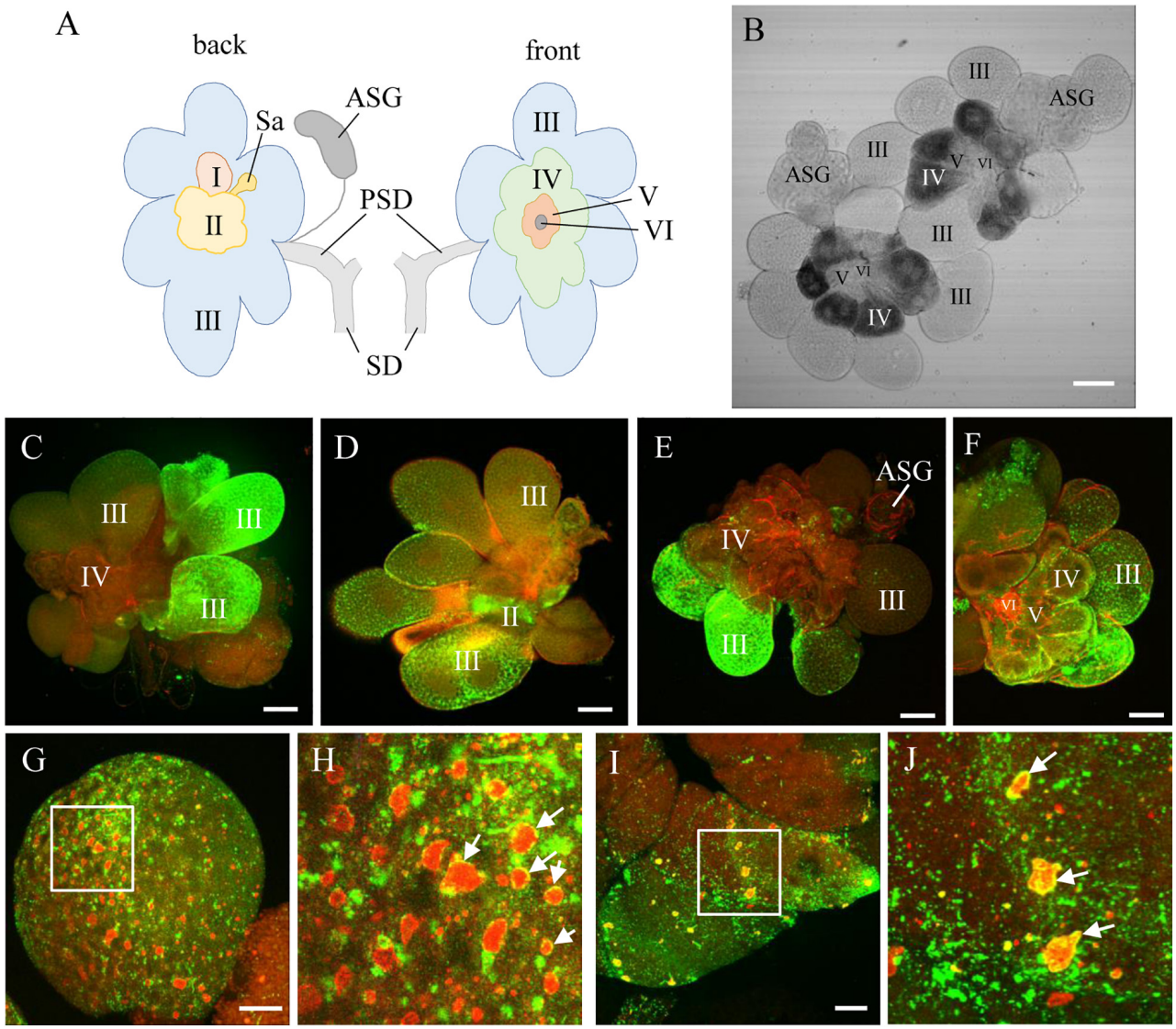

FIGURE 1 | RDV infection and replication in the salivary gland cells of viruliferous leafhoppers. **(A)** Schematic illustration of a salivary gland from an *N. cincticeps* leafhopper, modified from Sogawa (1965). **(B)** Transmission light micrograph of one pair of salivary glands from an *N. cincticeps* leafhopper. The principal salivary gland of *N. cincticeps* consists of six types of cells (I to IV). **(C–F)** Immunofluorescence microscopy showing RDV infection in different types of salivary gland cells. **(G,H)** RDV replication in type III- **(G,H)** and IV- **(I,J)** cells. Salivary glands of leafhoppers at 12 days padp were stained with virus-FITC (green), actin dye phalloidin-rhodamine (red) **(C–F)**, or Pns6-rhodamine (red) **(G,H)**, and then examined by confocal microscopy. The arrows indicate viroplasm. Panels **(H,J)** are enlarged images of the boxed areas in panels **(G,I)**, respectively. PSD, principal salivary duct; SD, salivary duct; Sa, spherical appendage; ASG, accessory salivary gland. Bars, 100 μm **(B–F)**, 20 μm **(G,I)**.

III- and IV-cells (**Figures 1G–J**). As indicated by the yellow in **Figures 1G–J**, RDV was clearly localized at the periphery of viroplasm. These results indicated that RDV could replicate more progeny virions in most cells of the salivary gland.

RDV Release From Salivary Gland Cells

Using immunofluorescence assays, we then investigated the process of RDV release from salivary gland cells into salivary cavities. The type III-cells were filled with apical plasmalemma-lined saliva-storing cavities, which formed the loose network establishing the intracellular space of secretory cells (**Figure 2A**). At 12 days padp, the RDV virions appeared as discrete, punctate inclusions inside or at the periphery of salivary cavities in type III- and VI-cells (**Figures 2A–C**). In type IV-cells, intracellular canaliculi, which discharged the main protein components for the sheath saliva (Sogawa, 1967), were immunostained with the actin dye phalloidin-rhodamine and penetrated the cytoplasm in a coarse reticular manner (**Figure 2D**). A large number of virions were scattered throughout the cytoplasm of type IV-cells or located within the canaliculi (**Figure 2D**). Together, these results provide evidence for the viral release from salivary gland cells via entry into the cavities or intracellular canaliculi.

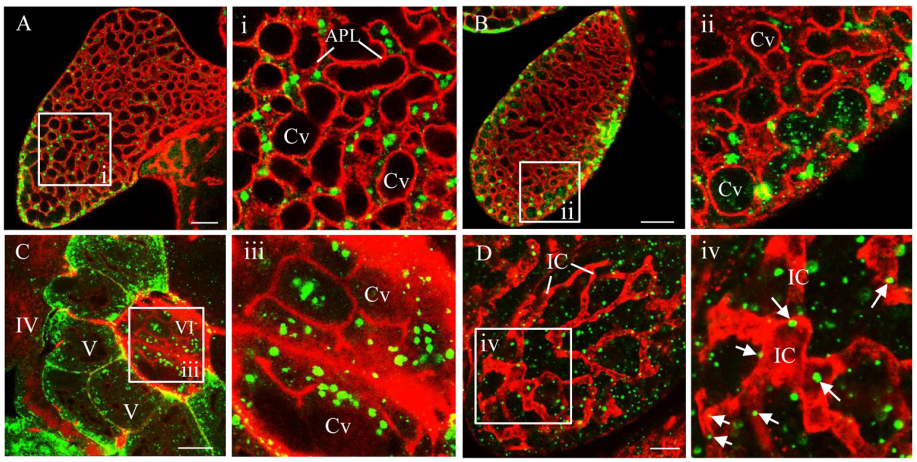

FIGURE 2 | Immunofluorescence microscopy showing the release of RDV from salivary gland cells. **(A)** Abundant RDV virions that have accumulated inside the cytoplasm at the periphery of apical plasmalemma of type III-cells of salivary gland. **(B–D)** A number of RDV virions entering the cavities of type III **(B)** or VI **(C)** cells or into the canaliculi of type IV-cells of salivary gland **(D)**. The salivary glands of leafhoppers at 12 days padp were stained with virus-FITC (green) or actin dye phalloidin-rhodamine (red), and then examined by confocal microscopy. Arrows indicate virus in the canaliculi. Panels i to iv are enlarged images of the boxed areas in panels **(A–D)**, respectively. APL, apical plasmalemma; Cv, cavity; IC, intracellular canaliculi. Bars, 20 μm **(A–C)**, 10 μm **(D)**.

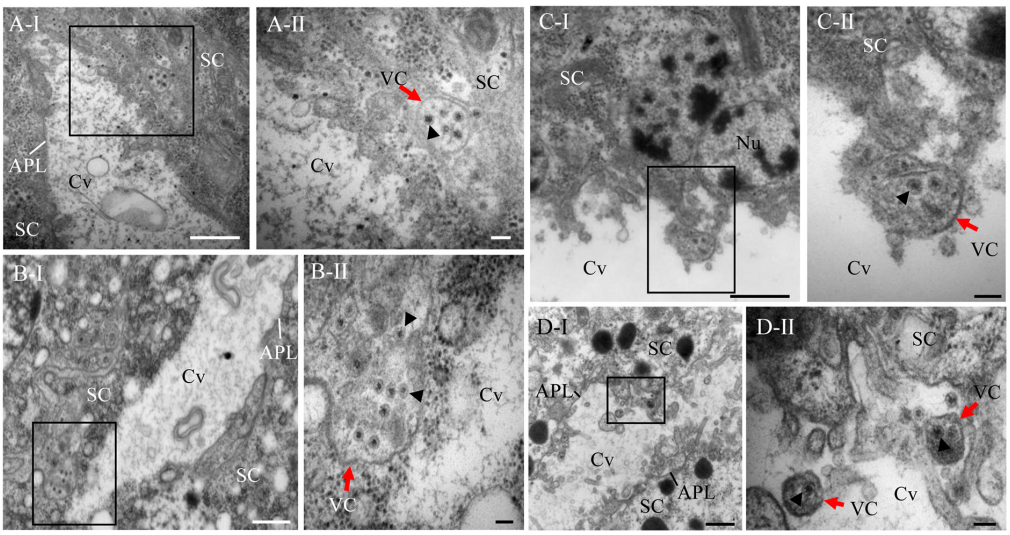

FIGURE 3 | Electron micrographs demonstrating the entry of RDV into cavities by utilizing vesicular compartments via an exocytosis-like process. **(A)** Virus-laden vesicular compartments within the cytoplasm of salivary gland cells. **(B)** Virus-laden vesicular compartments in the cytoplasm moving close to the salivary cavities. **(C)** Virus-laden vesicular compartments enter into the salivary cavities by fusing with the apical plasmalemma. **(D)** Virus-laden vesicular compartments interspersing within the salivary cavities. Red arrows indicate virus-laden vesicular compartments. Black arrow heads indicate the virions in vesicular compartments. Panels II are enlarged images of the boxed areas in panels I of **(A–D)**, respectively. SC, salivary cytoplasm; APL, apical plasmalemma; Cv, cavity; VC, vesicular compartment. Bars, 500 nm **(A-I,B-I,C-I,D-I)**, and 100 nm **(A-II,B-II,C-II,D-II)**.

In addition, electron microscopy showed that double-layered RDV particles of approximately 70 nm in diameter were sequestered within vesicular compartments in various sizes in the cytoplasm of salivary gland cells or at the periphery of salivary cavities (**Figures 3A,B**). The migration of virus-laden vesicular compartments that were close to the salivary cavities led to the fusion of the apical plasmalemma with the vesicular compartments (**Figure 3C**). Finally, virus-laden vesicular compartments were released to the salivary cavities (**Figure 3D**). These observations indicate that the release of RDV virions into the saliva-stored cavities takes advantage of vesicular compartments via an exocytosis-like manner.

Intermittent Transmission of RDV by *N. cincticeps*

To understand the effect of RDV release via virus-laden vesicular compartments on viral transmission, the profiles of

RDV transmission by *N. cincticeps* from 13 to 26 days padp was characterized. The curve for the daily transmission rates of RDV by individual *N. cincticeps* showed a wave pattern rather than a stable trend (**Figure 4A**), revealing a viral intermittent transmission pattern (**Table 1**). Approximately 61.8% of individual *N. cincticeps* showed the following pattern: they transmitted RDV for 1 day, then ceased transmission, and then some days later transmitted the virus for 1 day. The period of intermittent transmission ranged from 1 to 13 days (**Table 2**). Approximately 38.2% of *N. cincticeps* displayed the ability to continuously transmit RDV, and the period of transmission ranged from 2 to 5 days. The intermittence of viral transmission by individual *N. cincticeps* clarified the wave pattern observed in the graph of the daily transmission rate (**Figure 4A**).

A Release Threshold Mediating Viral Intermittent Release

To address the reason for viral intermittent transmission by *N. cincticeps* leafhoppers, the viral titers in salivary glands of *N. cincticeps* during the intermittent or transmitting periods were analyzed. The gene copy number of RDV P8 in the salivary glands of *N. cincticeps* served as viral titers. The results showed that the total RNA amount of a pair of salivary glands of one adult leafhopper ranged from 822 to 1,524 ng. The total RNA amount of one adult leafhopper ranged from 2,145 to 9,769 ng. At 19 days padp, the mean copy number of the viral genome in the salivary glands of 50 transmitting adult leafhoppers was 2.76×10^1 copies/μg RNA, which was significantly lower than the mean copy number of 3.8×10^3 copies/μg RNA in the salivary glands of 52 leafhoppers during the intermittent period (**Figure 4B**). The immunofluorescence assays showed that the RDV antigens in the salivary glands of leafhoppers during the transmitting period were less than those of the leafhoppers during the intermittent period (**Figure 4C**). Western blots also indicated a lower accumulation of RDV P8 in the salivary glands of *N. cincticeps* vectors during the transmitting period compared with those of viruliferous leafhoppers during the intermittent period (**Figure 4D**). These findings indicated that the viral load in the salivary glands decreased significantly owing to viral release into the rice plants, which was also the process of viral transmission by leafhoppers. Moreover, the transmitting and non-transmitting behaviors of viruliferous leafhoppers could result from a release threshold for viral release.

We then analyzed the number of viral genome copies in the salivary glands of 52 leafhoppers in the intermittent period (copy number ranging from 1.03×10^0 to 1.79×10^4 copies/μg RNA; **Table 2**) and deduced that the highest 1.79×10^4 copies/μg RNA were very close to the viral release threshold. Below this putative RDV release threshold, the RDV tended to accumulate, and few of the virions could release from the salivary gland cells in most leafhoppers (**Table 2**). Once the viral accumulation in the salivary glands of leafhoppers increased above the viral release threshold, the virus was released from the salivary gland cells and entered the salivary cavities for transmission by most leafhoppers. Therefore, this release threshold possibly mediated the intermittent transmission of RDV by *N. cincticeps*.

DISCUSSION

To date, few reports have clarified the mechanism by which viruses overcome the salivary glands release barrier. Non-propagative persistent luteoviruses and propagative rhabdoviruses can overcome this barrier via transcytosis or membrane budding (Gildow, 1982; Brault et al., 2006; Mao et al., 2017). The propagative rice gall dwarf virus (RGDV) utilizes virus-induced inclusion as a vehicle and causes an exocytosis-like process for viral release into the salivary cavities (Mao et al., 2017). In this study, we found that the progeny RDV could release from salivary gland cells and enter the salivary cavities utilizing virus-laden vesicular compartments via the exocytosis-like process (**Figures 1–3**). These viral releases caused intermittent transmission of RDV by most leafhopper vectors (**Table 1**). Most importantly, the viral titers in the salivary glands of leafhoppers, which were in the transmitting period, were significantly lower than the viral titers in the salivary glands of leafhoppers, which were in the intermittent period (**Figure 4**). We proposed that the putative RDV release threshold (close to 1.79×10^4 copies/μg RNA) (**Table 2**) mediated the viral intermittent transmission by leafhoppers, thus, facilitating RDV effective infection in the plant host.

Salivary Gland Release Barrier

The salivary gland of leafhoppers secretes two different types of saliva, namely, coagulable and watery saliva (Sogawa, 1968). At the beginning of feeding, leafhoppers eject coagulable saliva to form salivary sheaths that surround the stylets for protection (Hattori et al., 2005). The watery saliva, which lubricates the stylet and introduces enzymes, ejects when the stylet penetrates the host plant tissues (Hattori et al., 2005). Simultaneously, virus is introduced with the watery saliva into the plant. Type III-cells secrete watery saliva; type IV-cells secrete the components of coagulable saliva, and type V-cells primarily secrete phenolase (Sogawa, 1967, 1968). We found that the virus passed through the apical plasmalemma of type III- and VI-cells, which then accessed the salivary cavities and mixed with watery saliva for release. In type IV-cells, the RDV entered the intracellular canaliculi and mixed with coagulable saliva for release. However, the biological significance of virus introduction with coagulable saliva that would solidify into the salivary sheath was unknown. However, we hypothesized that the main pathway of viral entry into plants hosts is the viral release from type III-cells and introduction into watery salivary, which is owing to the highest number of type III-cells and well liquidity and the high volume of watery saliva. Therefore, most viral release is associated with the apical plasmalemma of type III-cells, and the intermittent release from salivary gland cells may be primarily controlled in type III-cells.

Because the viral replication, accumulation, and spread in insect vectors are persistent, it was thought that salivary glands acted as the key barriers that affected viral intermittent release from salivary gland cells, leading to viral intermittent transmission. Salivary glands acted as a viral reservoir. If the viral release was simultaneous with viral replication, the viral titers would be stable, and the viral titers would be non-distinctive among the salivary glands of leafhoppers. However, we found that

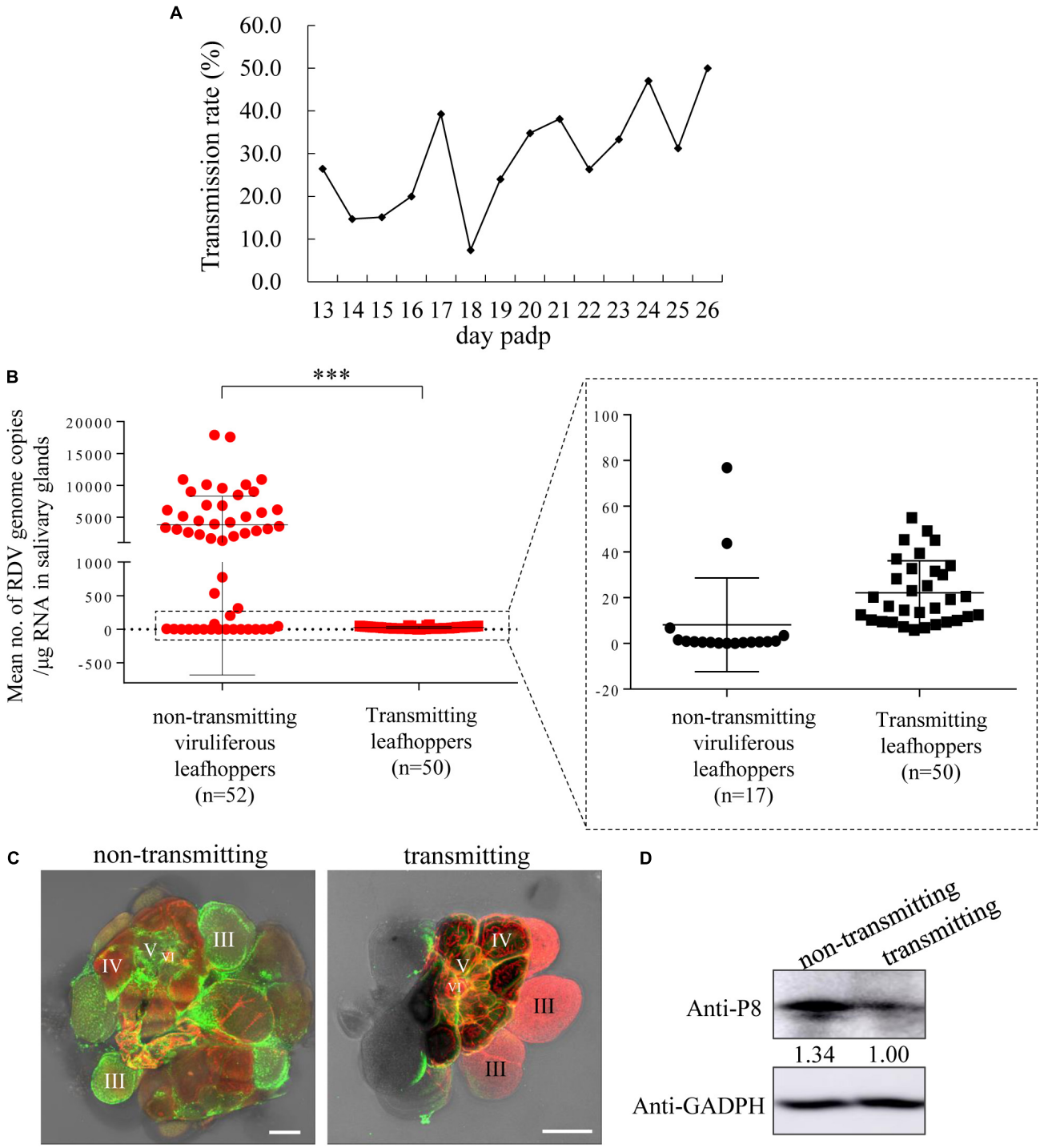

FIGURE 4 | RDV titers in the salivary glands of leafhoppers during the transmitting period were significantly lower than those in the salivary glands of viruliferous leafhoppers during the intermittent period. **(A)** The profile of transmission rate of RDV by a group of leafhoppers per day. The transmission rate was determined using RT-PCR to detect the presence of RDV P8 gene in plants. **(B)** Viral titers in the salivary glands of transmitting and viruliferous leafhoppers during the intermittent period. An RT-qPCR assay of viral titers in the salivary glands of transmitting leafhoppers was highly significantly lower than that of the non-transmitting viruliferous leafhoppers at 19 days padp. $***P < 0.0001$. **(C)** Immunofluorescence microscopy exhibiting low viral infection in the salivary glands of the transmitting leafhoppers compared with viruliferous leafhoppers during the intermittent period. **(D)** Western blot of RDV P8 and GADPH in the salivary glands of transmitting leafhoppers and viruliferous leafhoppers during the intermittent period. The samples were separated by SDS-PAGE and the presence of P8 was examined with P8-specific antibodies. The relative intensities of bands in the analyses of P8 are shown below the bands. GADPH detected with GADPH-specific IgG is shown to demonstrate the loading of equal amounts of protein.

TABLE 1 | Pattern of daily transmission of RDV by individual leafhoppers.

Insect no.	Day padp													
	13	14	15	16	17	18	19	20	21	22	23	24	25	26
1	○	●	○	○	○	○	○	○	D					
2	○	○	○	○	○	○	○	○	○	○	○	●	●	●
3	●	○	○	●	●	○	●	●	●	●	●	D		
4	●	○	D											
5	○	○	○	○	○	○	○	○	●	○	●	●	●	●
6	○	○	○	●	●	●	○	○	●	○	D			
7	●	○	●	○	○	○	○	●	○	○	●	●	●	●
8	●	○	●	○	○	○	D							
9	○	○	○	○	○	○	○	●	○	○	○	○	○	○
10	○	○	○	○	○	○	○	○	○	○	●	●	D	
11	●	○	○	○	○	○	○	○	○	○	○	○	○	○
12	○	○	●	●	○	D								
13	○	●	○	○	○	○	○	●	●	○	○	○	○	●
14	○	○	○	○	○	○	●	●	●	D				
15	●	○	○	○	D									
16	○	○	○	○	○	○	○	○	○	○	○	○	○	●
17	●	○	D											
18	○	○	●	○	●	○	●	○	○	○	○	○	○	○
19	○	○	○	○	○	●	●	●	○	●	○	●	●	●
20	○	●	○	D										
21	●	○	○	●	○	○	○	○	○	○	○	○	○	○
22	○	○	○	○	●	○	●	○	●	D				
23	○	○	●	○	D									
24	○	○	○	○	●	○	○	○	●	○	○	○	○	○
25	○	○	○	○	●	○	○	●	D					
26	○	○	○	○	●	○	○	○	●	●	●	●	○	●
27	○	○	○	○	○	○	○	○	○	●	○	●	○	○
28	●	○	○	D										
29	○	●	○	●	●	○	●	D						
30	○	○	○	○	●	○	○	○	○	○	○	○	○	○
31	○	●	○	D										
32	○	○	○	●	○	○	○	●	○	●	●	●	●	●
33	○	○	○	○	●	○	D							
34	○	○	○	○	●	○	○	D						

○, tested plant was not infected; ●, tested plant was infected; D, the insect died.

the viral titers within the salivary glands of leafhoppers during the transmitting period was significantly lower than the viral titers within the salivary glands of leafhoppers during the intermittent period. Moreover, in the group of viruliferous leafhoppers during the intermittent period, the viral titers in salivary glands were not consistent, and different individuals had large variations in viral titers (**Table 2**). Therefore, it was presumed that a certain threshold of viral release likely existed during a period of viral accumulation.

Viral Release Threshold

Among the viral titers in salivary glands of viruliferous leafhoppers during the intermittent period, the highest viral titer was likely to be close to the viral release threshold. A model for viral intermittent transmission controlled by viral

TABLE 2 | Viral genome copies in the salivary glands of viruliferous leafhoppers during the intermittent period.

Insect no.	Copies/μg RNA
1	1.09E + 04
2	2.84E + 03
3	6.88E + 03
4	1.62E + 03
5	1.96E + 03
6	2.46E + 03
7	5.06E + 03
8	1.20E + 01
9	4.02E + 01
10	5.35E + 02
11	2.26E + 03
12	1.01E + 04
13	8.98E + 03
14	6.10E + 03
15	7.75E + 02
16	1.03E + 00
17	8.49E + 03
18	3.13E + 03
19	1.76E + 04
20	4.42E + 03
21	5.12E + 03
22	4.15E + 03
23	6.79E + 03
24	1.01E + 04
25	2.59E + 03
26	6.36E + 00
27	1.09E + 04
28	1.56E + 00
29	4.38E + 01
30	5.71E + 03
31	8.52E + 00
32	8.98E + 03
33	3.88E + 03
34	3.35E + 03
35	9.55E + 03
36	6.15E + 03
37	3.11E + 02
38	3.55E + 03
39	1.28E + 03
40	7.34E + 00
41	3.46E + 00
42	1.79E + 04
43	5.55E + 00
44	2.04E + 02
45	5.11E + 00
46	7.68E + 01
47	3.84E + 00
48	6.76E + 00
49	6.56E + 00
50	7.27E + 00
51	9.77E + 00
52	3.07E + 03

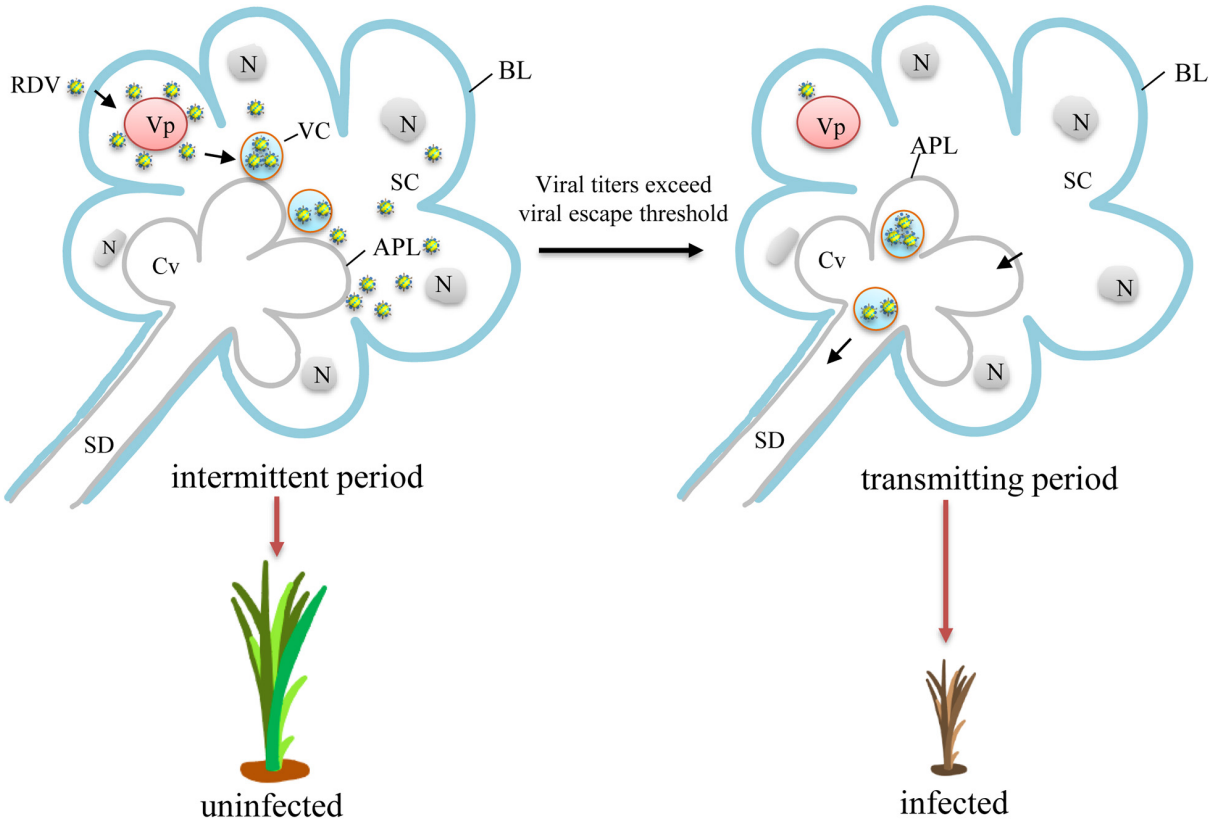

FIGURE 5 | A proposed model for viral intermittent transmission controlled by the viral release threshold. Viruses first access the cytoplasm of salivary glands and begin replication for the production of progeny virions. Abundant new virions are then formed and sequestered in vesicular compartments before their final release to salivary cavities in an exocytosis-like manner. During this process, the level of viral accumulation is still below the virus release threshold, and the leafhopper does not transmit the virus. Therefore, intermittent periods of viral transmission are observed. With the continued replication, the level of viral accumulation gradually exceeds the virus release threshold. Thus, the newly formed virions traverse the apical plasmalemma and enter the salivary cavities in a free form or using virus-laden vesicular compartments. The virions then enter the salivary duct. Once the insects feed or probe, virions are ejected with saliva into the phloem of plant hosts, causing viral infection and transmission. Vp, viroplasm; APL, apical plasmalemma; BL, basal lamina; Cv, cavity; N, nucleus; SC, salivary cytoplasm; SD, salivary duct; VC, vesicular compartment.

release threshold was then proposed (**Figure 5**). Viruses in the salivary glands of viruliferous leafhoppers during the intermittent period are still accumulating (**Figure 5**). Once the level of viral accumulation exceeds the threshold, virions are released from the salivary gland cells and infect the plant hosts. We consider this to be the threshold-controlled viral release strategy. When the level of viral accumulation decreases below the virus release threshold, leafhoppers enter the intermittent period (**Figure 5**). Once the level of viral accumulation reaches or exceeds the virus release threshold, the leafhopper once again transmits the virus (**Figure 5**).

An example of a viral release threshold that controls the release of plant viruses has previously described to have taken place during the infection of Southern rice black-streaked dwarf virus (SRBSDV) in planthoppers (Lan et al., 2016). The reason why the SRBSDV could infect but not be transmitted by the incompetent vectors is that the viral titers in the midgut epithelium are unable to reach the threshold needed for viral dissemination into the midgut muscles and then into the salivary glands (Lan et al., 2016). This suggests that the viral release threshold plays an important and universal role in mediating the viral ability to overcome barriers in insect vectors.

Viral Intermittent Transmission

The intermittent transmission of insect-borne plant viruses has been shown to occur in leafhoppers, planthoppers, and whiteflies (Gamez, 1973; Reynaud and Peterschmitt, 1992; Muniyappa et al., 2000; Ammar and Nault, 2002; Pu et al., 2012). However, the mechanism that underlies the intermittent transmission remains unknown. Among rice-infecting viruses, the SRBSDV, which over the past decade has caused the severe loss of rice production throughout southern China and northern Vietnam, has been recorded to be continuously transmitted by planthopper vectors (Pu et al., 2012). The longest period of continuous transmission of SRBSDV could be up to 22 days (Pu et al., 2012), while we found that the period of continuous transmission for RDV was only 5 days. Therefore, the longer period of continuous transmission of SRBSDV compared with that of RDV may be one of the reasons why SRBSDV has caused greater damage to rice production than RDV.

What is the biological significance of viral intermittent transmission by insect vector? We hypothesize that there are two points at least. (1) It was presumed that the intermittent transmission correlated with the viral replication cycle, because in the salivary gland cells, the period from the RDV replication to the assembly of progeny virions, together with the induction of various inclusion bodies formation, such as vesicles, requires at least one cycle of viral replication (24 h) (Wei et al., 2006a,b; Chen et al., 2012). (2) It is known that to establish an infection in a plant host, a certain viral titer (dilution limit point) is required. The virus, which accumulated to some degree, guaranteed the successful and effective infection of the virus into the plant host after release. From these perspectives, viral intermittent transmission and the existence of virus release threshold are reasonable. We anticipate that the viral release threshold-mediated intermittent transmission by insect vectors is the conserved strategy for the epidemic and persistence of vector-borne viruses in nature.

DATA AVAILABILITY STATEMENT

All datasets generated for this study are included in the article/supplementary material, further inquiries can be directed to the corresponding author/s.

AUTHOR CONTRIBUTIONS

QC and TW designed the experiments, wrote and revised the manuscript. YL conducted the transmission electron microscopy experiments. QC, ZL, and HY collected the samples and conducted the biological experiments. QC conducted the immunofluorescence assay. All authors contributed to the article and approved the submitted version.

FUNDING

This work was supported by grants from the National Key R&D Program of China (Grants 2017YFD0200900), the National Natural Science Foundation of China (31772124 and 31972239), and the Program for New Century Excellent Talents in Fujian Province University (Grants Kla18057A).

ACKNOWLEDGMENTS

We are grateful to Toshihiro Omura (National Agricultural Research Center, Japan) for providing the antibodies against intact viral particles.

SUPPLEMENTARY MATERIAL

The Supplementary Material for this article can be found online at: https://www.frontiersin.org/articles/10.3389/fmicb.2021.639445/full#supplementary-material

REFERENCES

Ammar, E., and Nault, L. R. (2002). Virus transmission by leafhoppers, planthoppers and treehoppers (auchenorrhyncha, homoptera). *Adv. Bot. Res.* 36, 141–167. doi: 10.1016/S0065-2296(02)36062-2

Attoui, H., Mertens, P. P. C., Becnel, J., Belaganahalli, S., Bergoin, M., Brussaard, C. P., et al. (2012). "Family reoviridae," in *Virus Taxonomy: Ninth Report of theInternational Committee for the Taxonomy of Viruses*, eds A. M. Q. King, M. J. Adams, E. B. Carstens, and E. J. Lefkowits (New York, NY: Elsevier), 541–637. doi: 10.1007/BF01309873

Boccardo, G., and Milne, R. G. (1984). "Plant reovirus group," in *CMI/AAB Descriptions of Plant Viruses, no. 294*, eds A. F. Morant and B. D. Harrison (Kew: Commonwealth Microbiology Institute/Association of Applied Biology), 294.

Brault, V., Herrbach, E., and Reinbold, C. (2006). Electron microscopy studies on luteovirid transmission by aphids. *Micron* 38, 302–312. doi: 10.1016/j.micron.2006.04.005

Chen, H., Chen, Q., Omura, T., Uehara-Ichiki, T., and Wei, T. (2011). Sequential infection of rice dwarf virus in the internal organs of its insect vector after ingestion of virus. *Virus Res.* 160, 389–394. doi: 10.1016/j.virusres.2011.04.028

Chen, Q., Chen, H., Jia, D., Mao, Q., Xie, L., and Wei, T. (2015b). Nonstructural protein Pns12 of Rice dwarf virus is a principal regulator for viral replication and infection in its insect vector. *Virus Res.* 210, 54–61. doi: 10.1016/j.virusres.2015.07.012

Chen, Q., Chen, H., Mao, Q., Liu, Q., Shimizu, T., Uehara-Ichiki, T., et al. (2012). Tubular structure induced by a plant virus facilitates viral spread in its vector insect. *PLoS Pathog.* 8:e1003032. doi: 10.1371/journal.ppat.1003032

Chen, Q., Zhang, L., Chen, H., Xie, L., and Wei, T. (2015a). Nonstructural protein Pns4 of rice dwarf virus is essential for viral infection in its insect vector. *Virol. J.* 12:211. doi: 10.1186/s12985-015-0438-6

Chen, Q., Zhang, L., Zhang, Y., Mao, Q., and Wei, T. (2017). Tubules of plant reoviruses exploit tropomodulin to regulate actin-based tubule motility in insect vector. *Sci. Rep.* 7:38563. doi: 10.1038/srep38563

Fukushi, T. (1940). Further studies on the dwarf disease of rice plant. *J. Fac. Agr. Hokkaido Imperial Univ.* 45, 83–154.

Gamez, R. (1973). Transmission of rayado fino virus of maize (Zea mays) by *Dalbulus maidis*. *Ann. Appl. Biol.* 73, 285–292. doi: 10.1111/j.1744-7348.1973.tb00935.x

Gildow, F. E. (1982). Coated vesicle transport of luteoviruses through salivary glands of *Myzus persicae*. *Phytopathology* 72, 1289–1296. doi: 10.1099/vir.0.19415-0

Gray, S., and Gildow, F. E. (2003). Luteovirus-aphid interactions. *Annu. Rev. Phytopathol.* 41, 539–566. doi: 10.1146/annurev.phyto.41.012203.105815

Hattori, M., Konishi, H., Tamura, Y., Konno, K., and Sogawa, K. (2005). Laccase-type phenoloxidase in salivary glands and watery saliva of the green rice leafhopper, *Nephotettix cincticeps*. *J. Insect. Physiol.* 51, 1359–1365. doi: 10.1016/j.jinsphys.2005.08.010

Hogenhout, S. A., Ammar el, D., Whitfield, A. E., and Redinbaugh, M. G. (2008). Insect vector interactions with persistently transmitted viruses. *Annu. Rev. Phytopathol.* 46, 327–359. doi: 10.1146/annurev.phyto.022508.092135

Honda, K., Wei, T., Hagiwara, K., Higashi, T., Kimura, I., Akutsu, K., et al. (2007). Retention of Rice dwarf virus by descendants of pairs of viruliferous vector insects after rearing for 6 years. *Phytopathology* 97, 712–716. doi: 10.1094/PHYTO-97-6-0712

Ishikawa, T. (1928). The merit of Hatsuzo Hashimoto, the earliest investigator of stunt disease of rice plant. *Nippon Plant Protect. Soc.* 15, 218–222.

Jia, D., Chen, Q., Mao, Q., Zhang, X., Wu, W., Chen, H., et al. (2018). Vector mediated transmission of persistently transmitted plant viruses. *Curr. Opin. Virol.* 28, 127–132. doi: 10.1016/j.coviro.2017.12.004

Lan, H., Chen, H., Liu, Y., Jiang, C., Mao, Q., Jia, D., et al. (2016). Small interfering RNA pathway modulates initial viral infection in midgut epithelium of insect after ingestion of virus. *J. Virol.* 90, 917–929. doi: 10.1128/JVI.01835-15

Mao, Q., Liao, Z., Li, J., Liu, Y., Wu, W., Chen, H., et al. (2017). Filamentous structures induced by a phytoreovirus mediate viral release from salivary glands in its insect vector. *J. Virol.* 91:e00265-17. doi: 10.1128/JVI.00265-17

Miyazaki, N., Wu, B., Hagiwara, K., Wang, C. Y., Xing, L., Hammar, L., et al. (2010). The functional organization of the internal components of rice dwarf virus. *J. Biochem.* 147, 843–850. doi: 10.1093/jb/mvq017

Muniyappa, V., Venkatesh, H. M., Ramappa, H. K., Kulkarni, R. S., Zeidan, M., Tarba, C. Y., et al. (2000). Tomato leaf curl virus from Bangalore (ToLCV-Ban4): sequence comparison with Indian ToLCV isolates, detection in plants and insects, and vector relationships. *Arch. Virol.* 145, 1583–1598. doi: 10.1007/s007050070078

Nakagawa, A., Miyazaki, N., Taka, J., Naitow, H., and Ogawa, A. (2003). The atomic structure of rice dwarf virus reveals the self-assembly mechanism of component proteins. *Structure* 11, 1227–1238. doi: 10.1016/j.str.2003.08.012

Omura, T., and Yan, J. (1999). Role of outer capsid proteins in transmission of phytoreovirus by insect vectors. *Adv. Virus Res.* 54, 15–43. doi: 10.1016/s0065-3527(08)60364-4

Pu, L., Xie, G., Ji, C., Ling, B., Zhang, M., Xu, D., et al. (2012). Transmission characteristics of southern rice black-streaked dwarf virus by rice planthoppers. *Crop Prot.* 41, 71–76. doi: 10.1016/j.virusres.2017.11.012

Reynaud, B., and Peterschmitt, M. (1992). A study of the mode of transmission of maize streak virus by cicadulina mbila using an enzyme-linked immunosorbent assay. *Ann. Appl. Biol.* 121, 85–94. doi: 10.1111/j.1744-7348.1992.tb03989.x

Sogawa, K. (1965). Studies on the salivary glands of rice plant leafhoppers. I. Morphology and histology. *Jpn. J. Appl. Entomol. Zool.* 9, 275–290. doi: 10.1303/jjaez.9.275

Sogawa, K. (1967). Studies on the salivary glands of rice plant leafhoppers. II. Origins of the structural precursors of the sheathmaterial. *Appl. Entomol. Zool.* 2, 195–202. doi: 10.1303/aez.2.195

Sogawa, K. (1968). Studies on the salivary glands of rice plant leafhoppers. III. Saliva phenolase. *Appl. Entomol. Zool.* 3, 13–25. doi: 10.1303/aez.3.13

Wei, T., Kikuchi, A., Moriyasu, Y., Suzuki, N., Shimizu, T., Hagiwara, K., et al. (2006a). The spread of Rice dwarf virus among cells of its insect vector exploits virus-induced tubular structures. *J. Virol.* 80, 8593–8602. doi: 10.1128/JVI.00537-06

Wei, T., and Li, Y. (2016). Rice Reoviruses in insect vectors. *Ann. Rev. Phytopathol.* 54, 99–120. doi: 10.1146/annurev-phyto-080615-095900

Wei, T., Shimizu, T., Hagiwara, K., Kikuchi, A., Moriyasu, Y., Suzuki, N., et al. (2006b). Pns12 protein of rice dwarf virus is essential for formation of viroplasms and nucleation of viral-assembly complexes. *J. Gen. Virol.* 87, 429–438. doi: 10.1099/vir.0.81425-0

Zhong, B., Kikuchi, A., Moriyasu, Y., Higashi, T., Hagiwara, K., and Omura, T. (2003). A minor outer capsid protein, P9, of rice dwarf virus. *Arch. Virol.* 148, 2275–2280. doi: 10.1007/s00705-003-0160-3

Conflict of Interest: The authors declare that the research was conducted in the absence of any commercial or financial relationships that could be construed as a potential conflict of interest.

frontiers in Microbiology

REVIEW
published: 24 February 2021
doi: 10.3389/fmicb.2021.628262

Insights Into Insect Vector Transmission and Epidemiology of Plant-Infecting Fijiviruses

Lu Zhang[1], *Nan Wu*[1], *Yingdang Ren*[2]* *and Xifeng Wang*[1]*

[1] State Key Laboratory for Biology of Plant Diseases and Insect Pests, Institute of Plant Protection, Chinese Academy of Agricultural Sciences, Beijing, China, [2] Institute of Plant Protection, Henan Academy of Agricultural Sciences, Zhengzhou, China

Viruses in genus *Fijivirus* (family *Reoviridae*) have caused serious damage to rice, maize and sugarcane in American, Asian, European and Oceanian countries, where seven plant-infecting and two insect-specific viruses have been reported. Because the planthopper vectors are the only means of virus spread in nature, their migration and efficient transmission of these viruses among different crops or gramineous weeds in a persistent propagative manner are obligatory for virus epidemics. Understanding the mechanisms of virus transmission by these insect vectors is thus key for managing the spread of virus. This review describes current understandings of main fijiviruses and their insect vectors, transmission characteristics, effects of viruses on the behavior and physiology of vector insects, molecular transmission mechanisms. The relationships among transmission, virus epidemics and management are also discussed. To better understand fijivirus-plant disease system, research needs to focus on the complex interactions among the virus, insect vector, insect microbes, and plants.

Keywords: plant-infecting fijiviruses, planthopper vectors, transmission, molecular determinants, virus epidemics

OPEN ACCESS

Edited by:
Jesús Navas-Castillo, Institute for Mediterranean and Subtropical Horticulture "La Mayora", Spain

Reviewed by:
Rajagopalbabu Srinivasan, University of Georgia, United States
Mariana del Vas, National Agricultural Technology Institute (Argentina), Argentina

***Correspondence:**
Xifeng Wang
xfwang@ippcaas.cn
Yingdang Ren
renyd@126.com

Specialty section:
This article was submitted to Virology, a section of the journal Frontiers in Microbiology

Received: *11 November 2020*
Accepted: *08 February 2021*
Published: *24 February 2021*

Citation:
Zhang L, Wu N, Ren Y and Wang X (2021) Insights Into Insect Vector Transmission and Epidemiology of Plant-Infecting Fijiviruses. Front. Microbiol. 12:628262. doi: 10.3389/fmicb.2021.628262

INTRODUCTION

Plant-infecting fijiviruses have double-shelled, icosahedral particles approximately 70 nm in diameter, with spherical, short surface spikes (A spikes) on each of the 12 vertices of the icosahedron (Harding et al., 2006; Attoui et al., 2012). The outer shell is very fragile, leaving the inner shell with 12 B spikes (Teakle and Steindl, 1969; Hatta and Francki, 1977). The viral genome, which contains 10 segmented double-stranded RNAs (dsRNA) varying from approximately 1.8–4.5 kb, is approximately 29 kb within the core capsid of the virus particle (Milne et al., 1973). Segments 1–4, 6, 8, and 10 are monocistronic (only one open reading frame, ORF), while segments 5 (some fijiviruses), each of 7 and 9 of plant-infecting fijiviruses contains two ORFs (Azuhata et al., 1992; Isogai et al., 1998; Firth and Atkins, 2009; Shimizu et al., 2011; Huang and Li, 2020).

Fijiviruses are transmitted by delphacid planthoppers in a persistent-propagative manner (Pu et al., 2012). In general, after eggs hatched, the nymphs will develop to adults through five instars and both nymphs and adults can transmit viruses (Holder and Wilson, 1992). Planthoppers acquire fijiviruses when feeding in infected plants using their piercing-sucking mouthparts. Then, the virions enter and replicate into the midgut epithelia. After replication, the newly assembled virions disseminate into the hemolymph or other tissues followed by moving into the salivary glands.

Finally, the virions are released from saliva to plant phloem cells when feeding (Hogenhout et al., 2008; Danthi et al., 2010). The viruses replicate and induce small tumors or enations in phloem cells of susceptible plants in families Cyperaceae, Gramineae, and Liliaceae (Huang and Li, 2020).

In nature, plant infecting fijiviruses are only spread by planthoppers vectors except garlic dwarf virus (GDV) through vegetative propagation materials (Nault, 1994). In most cases, fijivirus epidemics around the world can largely be attributed to the population density and transmission efficiency of their planthopper vectors among the different crops or gramineous weeds. Understanding the transmission mechanisms is crucial for accurate forecast and management. This review summarizes current insights of vectors for different fijiviruses, effect of viruses on the behavior and physiology of vectors, molecular determinants involved in the interaction between vector insects and the viruses, and ecological impacts of transmission biology on disease epidemiology.

FIJIVIRUSES, PLANT HOSTS, DISEASE DESCRIPTION AND DISTRIBUTION

Eight plant-infecting fijiviruses (**Table 1**) and one insect-specific fijivirus, Nilaparvata lugens reovirus, have been acknowledged by The International Committee on Taxonomy of Viruses, ICTV) (Attoui et al., 2012). Recently, another insect specific fijivirus, Psammotettix alienus reovirus, was also reported (Fu et al., 2020). Common plant hosts include flatsedge (*Juncellus serotinus* [Rottb.] C. B. Clarke) and variable flatsedge (*Cyperus difformis* L.) in family *Cyperaceae*, oat (*Avena sativa* L.), rice (*Oryza sativa* L.), sugarcane (*Saccharum officinarum* L.), maize (*Zea mays* L.), barley (*Hordeum vulgare* L.), rye (*Secale cereale* L.), wheat (*Triticum aestivum* L.), and pangola grass (a sterile triploid of *Digitaria decumbens* Stent) in family Gramineae, and garlic (*Allium sativum* L.) in family Liliaceae (Boito and Ornaghi, 2008; Li et al., 2012; Lefkowitz et al., 2018; Wu et al., 2020).

Fiji disease virus (FDV), the first of eight known plant infecting fijiviruses, was reported in 1886 in Fiji (Egan et al., 1989). By 1906, the virus had destroyed thousands of acres of sugarcane (Hughes and Robinson, 1961). Now, FDV is known to cause this serious disease of sugarcane in Southeast Asian and Pacific countries, including New Guinea, Fiji, Australia, Madagascar, Vanuatu, the Philippines, and Samoa (Harding et al., 2006; Magarey et al., 2019). Its only known naturally infected host is sugarcane (*S. officinarum* L.), but other *Saccharum* species, *Sorghum* species, and maize can be experimentally inoculated with viruliferous planthoppers (Hughes and Robinson, 1961; Dhileepan et al., 2003). GDV, the only fijivirus that infects *Allium* species, has only been reported from southeastern France where it has caused occasional epidemics since 1988 (Lot et al., 1994). Although it is considered to be of low economic importance because of its limited distribution, the epidemics have caused high yield losses (Lot et al., 1994). Maize rough dwarf virus (MRDV) was initially found in northern Italy and then several European countries, where it had severe outbreaks because of the planting of maize hybrids that have higher yields but are more susceptible to the virus (Milne and Lovisolo, 1977; Marzachi et al., 1996). The hosts on which MRDV has so far been found naturally occurring are maize and some gramineous weeds, including *Digitaria sanguinalis* (L.) Scopoli, *Echinochloa crus-galli* (L.) P. Beauv, and *Cynodon dactylon* (L.) Persoon (Lovisolo, 1971). Mal de Río Cuarto virus (MRCV), initially reported as a strain of MRDV, was first reported at the end of the 1960s in maize fields in Río Cuarto County in Argentina and is now a major constraint to maize production in Argentina (Nome, 1981; Distefano et al., 2002). In addition to maize, it can also infect winter small grains (barley, oat, rye, and wheat), spring–summer grains (millet and sorghum) as well as several annual and perennial weeds (Nome, 1981; Pardina et al., 1998; Ornaghi et al., 2000). Oat sterile dwarf virus (OSDV), originally studied simultaneously in the former Czechoslovakia and in Sweden (Catherall, 1970), causes dwarfing, a dark blue-green leaf color, and profuse tillering in infected oat plants, which remain green and grass-like at harvest but lack heads. The same virus may also have been found in Netherlands, Finland, Poland, and Britain (Milne and Lovisolo, 1977). Pangola stunt virus (PaSV), first described as a devastating disease of pangola grass in Surinam (Dirven and van Hoof, 1960), is a serious threat to the cultivation of pangola grass, a sterile triploid of *Digitaria decumbens* Stent grown as a pasture grass on millions of hectares throughout the world, particularly in Florida, the Caribbean islands, and Central and South America. The virus has now been reported in other countries (regions), including Guyana, Brazil, Peru, Fiji, and Taiwan Province of China (Karan et al., 1994). Rice black streaked dwarf virus (RBSDV) was first found in Japan, where it has been present for decades but was only recognized as distinct from rice dwarf virus by Kuribayashi and Shinkai (1952). Now, it is considered to be the causal agent of rice black streaked dwarf and maize rough dwarf diseases, responsible for intermittent epidemics in East Asia and substantial yield losses over the last decades. Rice, maize, wheat, oats, and barley are its natural hosts with the similar symptoms as those of MRDV (Azuhata et al., 1993; Wu et al., 2020). In 2008, a RBSDV-like new virus, southern rice black streaked dwarf virus (SRBSDV), was reported in the south of China (Zhou et al., 2008) and caused serious yield losses in China, Vietnam and Japan during 2010s (Zhou et al., 2013). The global distribution of plant-infecting fijiviruses is shown in **Figure 1**.

VECTOR INSECTS

Plant-infecting fijiviruses are primarily transmitted by delphacid planthoppers, which belong to a large, diverse superfamily Fulgoroidea, even though the insect vector of GDV has not been found yet. The species (*Fiji disease virus*, *Mal de Río Cuarto virus*, *Maize rough dwarf virus*, *Pangola stunt virus*, *Rice black streaked dwarf virus*, *Southern rice black streaked dwarf virus*, *Oat sterile dwarf virus* and *Garlic dwarf virus*) in genus *Fijivirus* and any known vectors are described in **Table 1**. FDV is transmitted by *Perkinsiella saccharicida* Kirkaldy, *Perkinsiella vituensis*, and *Perkinsiella vastatrix* (Toohey and Nielsen, 1972; Mungomery and Bell, 1933; Hughes et al., 2008). Both MRDV

TABLE 1 | Species of plant-infecting fijiviruses, their insect vectors and transmission characteristics.

Species	Vector	Acquisition	Latency period	Inoculation	Transovarial transmission	Citations
Subgroup 1						
Fiji disease virus	*Perkinsiella saccharicida* Kirkaldy, *P. vituensis*, *Perkinsiella vastatrix* Breddin	2 h	12–14 days	1 day	Yes (no exact data for efficiency)	Mungomery and Bell, 1933; Toohey and Nielsen, 1972; Chang, 1977; Egan and Ryan, 1986; Hughes et al., 2008
Subgroup 2						
Mal de Río Cuarto virus	*Delphacodes kuscheli* Fennah, *Chionomus haywardi* Muir, *Peregrinus maidis* Ashmead, *Toya propinqua* Fieber, *Caenodelphax teapae* Fowler, *Pyrophagus tigrinus* Remes Lenicov, *Tagosodes orizicolus* Muir	5 h	10 days	30 min	Not assessed	Remes Lenicov et al., 1985; Velázquez et al., 2003, 2006, 2017; Mattio et al., 2008
Maize rough dwarf virus	*Laodelphax striatellus* Fallén	10–15 min	10–15 days	15–30 min	Yes, max. 4%	Harpaz and Klein, 1969; Conti, 1974; Achon et al., 2013
Pangola stunt virus	*Sogatella furcifera* Horváth, *Sogatella kolophon* Kirkaldy	2 days	15–21 days	2–4 days	No	Greber et al., 1988; Teakle et al., 1988
Rice black streaked dwarf virus	*Laodelphax striatellus* Fallén, *Unkanodes sapporona* Matsumura, *U. albifascia* Matsumura	30 min	7 days	5 min	No	Shinkai, 1962; Shikata and Kitagawa, 1977; Nault, 1994; Wu et al., 2020
Southern rice black streaked dwarf virus	*Sogatella furcifera* Horváth	5 min	2–6 days	30 min	No	Jia et al., 2012; Pu et al., 2012; Zhou et al., 2013
Subgroup 3						
Oat sterile dwarf virus	*Javesella pellucida* Fabricius, *Calligypona pellucida* Fabr.	30–60 min	3–4 weeks	30 min	Yes, 0.2%	Vacke, 1966; Milne and Lovisolo, 1977
Subgroup 4						
Garlic dwarf virus	Unknown					

and RBSDV are naturally transmitted by the small brown planthopper *Laodelphax striatellus* Fallén (Achon et al., 2013; Nault, 1994). Two other planthoppers *Unkanodes sapporona* Matsumura and *Unkanodes albifascia* are not of great importance for RBSDV epidemic because of their low density in the field, though they also transmit RBSDV (Wu et al., 2020). Different planthopper species in Argentina can transmit MRCV, but *Delphacodes kuscheli* Fennah is the most plentiful and recurring species in areas where the virus is endemic (Remes Lenicov et al., 1985). Many other planthopper species, including *Chionomus haywardi* Muir, *Peregrinus maidis* Ashmead, *Toya propinqua* Fieber, *Caenodelphax teapae* Fowler, *Pyrophagus tigrinus* Remes Lenicov and *Tagosodes orizicolus* Muir are also known to transmit MRCV (Velázquez et al., 2003, 2006, 2017; Mattio et al., 2008). MRCV epidemics are largely related to the abundance, frequency and transmission efficiency of the vectors in early stages of the maize crop (Ornaghi et al., 1999; Laguna et al., 2002; Velázquez et al., 2003). The planthopper *Javesella pellucida* Fabricius is the natural vector of OSDV, but the leafhopper *Calligypona pellucida* Fabr also transmits OSDV (Milne and Lovisolo, 1977). *Sogatella kolophon* Kirkaldy and *Sogatella furcifera* were shown to vector PaSV (Greber et al., 1988; Teakle et al., 1988). SRBSDV has been identified as being transmitted by *S. furcifera*, but *L. striatellus* can also acquire it but not transmit to plants (Jia et al., 2012; Pu et al., 2012; Zhou et al., 2013).

TRANSMISSION CHARACTERISTICS

Like other persistent and propagative viruses, plant-infecting fijiviruses must initially infect and replicate in the epithelial cells of the insect's midgut, and then disseminate in different tissues, eventually spread to salivary glands, where are excreted to plants through saliva during insect feeding (Hogenhout et al., 2008; Mainou and Dermody, 2012). To complete the whole cycle of virus transmission, vector insects must undergo specific periods for acquisition, latency and inoculation. Some fijiviruses can be transovarially transmitted with low efficiency.

Acquisition

The acquisition periods range from several minutes to a few days for most plant-infecting fijiviruses, which have been mainly found in the phloem (Francki and Boccardo, 1983; Conti, 1984). Generally, the virus is more efficiently acquired by nymphs than by adults. In two similar examples, FDV is transmitted by *P. saccharicida* only if the virus is acquired by first-instar

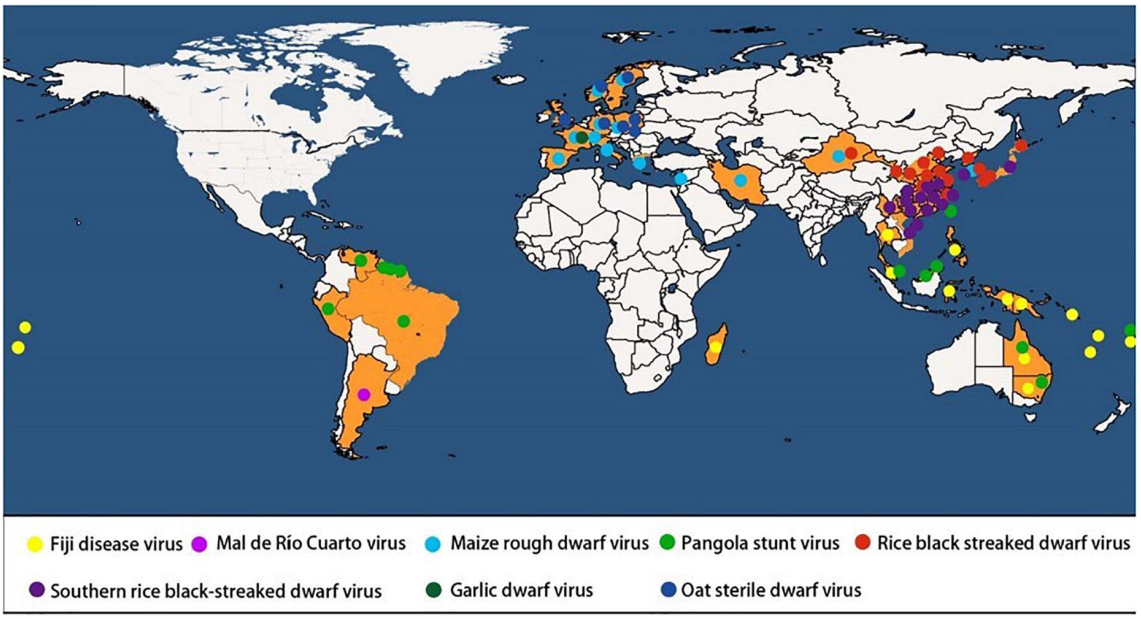

FIGURE 1 | Distribution of plant-infecting Fijiviruses in the world.

nymphs, but not older instars or adults, and first-instar nymphs of *D. kuscheli* transmit MRCV with higher efficiency compared with older instar nymphs (Hutchinson and Francki, 1973; Arneodo et al., 2005).

Latency and Inoculation

Once inside the planthoppers, the virus multiplies during a 1–4 weeks latency period when it is also disseminating into other tissues, including the salivary glands (Greber et al., 1988). When the latency period is complete, that is, the viral titre has reached a certain level, the insects can frequently transmit virus in their lifetime (Conti, 1984; Hughes et al., 2008; Argüello Caro et al., 2013; Hajano et al., 2015). For RBSDV, the minimum inoculation threshold has been shown to be as short as 5 min (Shikata and Kitagawa, 1977), but the minimum so far observed for MRDV is 15–30 min (Conti, 1974).

Transovarial Transmission

Only a few studies have shown that fijiviruses are transovarially transmitted in their planthopper vectors (Chang, 1977; Conti, 1985). For FDV, transovarial transmission in *P. saccharicida* was reported but no data were included (Chang, 1977). Transovarial transmission of MRDV in *L. striatellus* was reported to be about 4% (Harpaz and Klein, 1969), but none of 300 progenies from *L. striatellus* eggs deposited on sorghum were viruliferous (Harpaz, 1972). For OSDV, only 0.2% transovarial transmission was found in one case (Vacke, 1966) and no evidence found in another case for *J. pellucida* (Lindsten, 1974). Also, RBSDV and SRBSDV are not transmitted through the eggs of the vector *L. striatellus* and *S. furcifera* (Shinkai, 1962; Pu et al., 2012). Times for acquisition, latency and inoculation vary among the different combinations of viruses and vectors and are shown in **Table 1**.

VIRUS EFFECTS ON BEHAVIOR AND PHYSIOLOGY OF VECTOR INSECTS

Because fijiviruses must infect, multiply, and spread in their vector insect cells, virus infections have multiple effects on the behavior and physiology of their vector insects. Reports on these effects, however, are contradictory. Adverse effects include extending the nymphal stages, shortening the lifespan of adults, decreasing survival rate or fecundity (Harpaz and Klein, 1969; Nakasuji and Kiritani, 1970; Wei and Li, 2016). For example, Harpaz and Klein (1969) reported that MRDV viruliferous females of *L. striatellus* laid 30–50% fewer eggs than non-viruliferous females did and that the viability of these eggs was poor (14% vs. 99% for hatch from non-viruliferous). In those cases where hatching did occur, the incubation period was longer by up to 3 days (about 25%) than that of eggs from non-viruliferous females, and the mortality of the resulting larvae was high. Similarly, compared with non-viruliferous *S. furcifera*, SRBSDV-viruliferous females deposited fewer eggs and the viruliferous nymphs spent longer time developing into adults (Xu et al., 2014). In contrast, Zhang et al. (2014) reported that SRBSDV infection in rice led to an increase in the fecundity of *S. furcifera* and population size of macropterous adults (Zhang et al., 2014).

Feeding behavior of SRBSDV-viruliferous *S. furcifera* also differs from that of non-viruliferous insects; the frequency of phloem sap ingestion of viruliferous *S. furcifera* is significantly higher, but total feeding duration does not increase markedly (Xu et al., 2014). When SRBSDV-viruliferous *S. furcifera* feed on uninfected plants, they spend longer time in salivation and have more frequent phloem sap ingestion than did non-viruliferous insects (Xu et al., 2014). These behavioral alterations might

be adapted to the benefit of virus acquisition and inoculation (Lei et al., 2016). The infection of certain plants by MRDV can also modify the capacity of those plants to support MRDV vectors (Klein and Harpaz, 1969; Harpaz, 1972). For example, *L. striatellus* is unable to survive on non-infected *Cynodon dactylon* (L.) Pers. (Bermuda grass) for longer than 4–7 days and does not molt or lay eggs on this plant, but it can survive and breed successfully when the plants are infected with MRDV or the planthopper is already MRDV-viruliferous when placed on the plant (Klein and Harpaz, 1969).

These adverse or beneficial changes might be due to the changes of physiological and metabolic components caused by virus-plant/insect interactions. The physiology is altered in MRCV-infected wheat plants; the contents of total soluble sugar, starch, protein and malondialdehyde levels increase noticeably, but chlorophyll content decreases considerably. These variations are indicative of oxidative damage associated with biotic stress in these plants (Di Feo et al., 2010). MRCV-infected wheat plants had more than 3,000 differentially accumulated transcripts (DATs) at 21 days post inoculation, and exhibited higher levels of soluble sugars, starch, trehalose 6-phosphate (Tre6P), and organic and amino acids, but decreased transcripts levels for TaSWEET13, which are involved in sucrose phloem loading (de Haro et al., 2019). Similarly, the physiology and metabolism of viruliferous insect vectors change greatly. In SRBSDV-viruliferous *S. furcifera* with viral titer-specific monotonic transcriptome changes: 1,906 genes increase and 1,467 genes decrease in expression (Wang et al., 2016). In gas chromatography-time of flight-mass spectra, the major categories of metabolites differentially regulated after SRBSDV infection are nucleic acids and fatty acids, whereas the compounds relative to tricarboxylic acid cycle, sugars, and polyols are differentially regulated after temperature stress (Zhang et al., 2018).

COMPETITION OR SYNERGISM OF CO-INFECTING VIRUSES IN RELATION TO TRANSMISSION

Mal de Río Cuarto virus has been detected in co-infection with an isolate of maize yellow striate virus (MYSV, genus *Cytorhabdovirus*, family *Rhabdoviridae*) in maize (Dumón et al., 2015, 2017). Both viruses can naturally infect maize and several grasses through transmission by *D. kuscheli*. Although most of planthoppers could be viruliferous after feeding on mixed-infected plants, planthoppers with notably higher MRCV titers are able to transmit the virus, meaning that efficient MRCV transmission is positively correlated with virus accumulation in the insect (Argüello Caro et al., 2013). Plants doubly-infected by MRCV and the rhabdovirus showed typical symptoms of MRCV earlier than that single infected with MRCV, but the planthoppers fed on doubly-infected plants only acquired lower MRCV titers and transmitted inefficiency, indicating that these two viruses have antagonism in host plants and vector insects (Dumón et al., 2017).

Conversely, the epidemics of rice ragged stunt virus (RRSV, genus *Oryzavirus*, family *Reoviridae*), transmitted by *Nilaparvata lugens* Stal, has become more frequent in southern China since its co-infection with SRBSDV during 2010s (Wang et al., 2013). Rice plants doubly-infected by both viruses showed earlier and enhanced symptoms. *S. furcifera* and *N. lugens,* respectively, acquired SRBSDV and RRSV from doubly-infected plants with higher efficiency (Li et al., 2014). Furthermore, the non-viruliferous *N. lugens* significantly preferred feeding on virus-free plants, whereas viruliferous *N. lugens* preferred SRBSDV-infected rice plants (Wang et al., 2013). The attractiveness of the SRBSDV- or RRSV-infected rice plants to planthoppers is mainly caused by the changes of rice volatiles (Lu et al., 2016). Fecundity of *N. lugens* feeding on SRBSDV-infected rice plants is higher than those that fed on uninfected plants, but nymphal duration of males is significantly prolonged (Xu et al., 2016). Thus, these two viruses may alter the vectors' host preference to the benefit of their spread.

INSECT MICROBES

Various microbes in vector insects have also been known to directly affect virus infection or transmission (Mousson et al., 2012; Kliot and Ghanim, 2013; Jupatanakul et al., 2014). The symbiont *Chromobacterium* could reduce the susceptibility *of Aedes aegypti* to dengue virus infection and another symbiont *Wolbachia* in *Aedes albopictus* decreased virus transmission efficiency through decreasing the titer of viruses in host cells (Moreira et al., 2009; Jupatanakul et al., 2014; Kliot et al., 2014). On the contrary, acquisition and transmission of tomato yellow leaf curl virus by *Bemisia tabaci* were significantly enhanced by *Rickettsia* (Kliot et al., 2014). Moreover, the microbiota might contribute to the higher fecundity of *L. striatellus*, which in turn may be associated with the outbreaks of the virus (Liu et al., 2020). Besides microbes in vector insects, some insect-specific viruses have also been found in *L. striatellus* or *S. furcifera* (Wu et al., 2018, 2019). These new insect-specific viruses might affect fijivirus replication and transmission.

MOLECULAR MECHANISMS INVOLVED IN TRANSMISSION

Replication and spread of plant-infecting fijiviruses in different organs of their vector insects require specific interactions between virus and vector components. Some of these viral determinants and insect components which might be related to transmission of plant-infecting fijiviruses by their respective insect vectors have recently been identified.

Viral Determinants Involved in Viral Transmission

Complete genomic sequences are available for FDV, MRCV, MRDV, RBSDV, and SRBSDV, but only partial sequence genome information is available for OSDV. For RBSDV and SRBSDV, the whole genome encodes 13 viral proteins, including six putative structural proteins: P1 (the RNA-dependent RNA polymerase), P2 (major core structural protein), P3 (capping enzyme), P4

(outer shell B-spike protein), P8 (minor core protein), and P10 (major outer capsid protein), seven putative non-structural proteins P5-1, P5-2, P6, P7-1, P7-2, P9-1, and P9-2 (Attoui et al., 2012). These viral proteins can directly or indirectly affect viral transmission. The major outer capsid protein P10 plays key roles for virus invasion and transmission in vector insects (Than et al., 2016). P7-1 forms the tubule structures that serve as vehicles to transport the virions across the basal lamina and enable intercellular movement of the virus within insect cells (Jia et al., 2014, 2016).Non-structural proteins P9-1, P6 and P5-1 indirectly contribute to virus transmission since they constitute cytoplasmic inclusion bodies called viroplasms where virus replication takes place and in turn high replication and consequent high virus titers result in successful transmission (Zhang et al., 2008; Maroniche et al., 2010; Jia et al., 2012).

In plants and insects, small interfering RNA (siRNA) pathway plays a key role in antiviral defense (Ding, 2010; Zvereva and Pooggin, 2012; Gammon and Mello, 2015). In vector insects, this pathway may affect virus titers, persistence and transmission efficiency. Virus-derived siRNAs (vsiRNAs) mainly given rise by Dicer-2 in *Drosophila melanogaster* and mosquitoes to limit viral infection have been extensively studied (Fragkoudis et al., 2009; Blair, 2011; Donald et al., 2012). VsiRNAs accumulate in RBSDV-viruliferous *L. striatellus*, indicating that fijivirus replication might induce an RNAi-mediated antiviral response in its insect vector (Li et al., 2013). Similarly, SRBSDV infection induced the siRNA pathway in the midguts of an incompetent vector *L. striatellus*. Interfering with Dicer-2 significantly increased virus replication in midgut epithelial cells of *L. striatellus*, so that viral titers reached a threshold and disseminated to the *L. striatellus* midgut muscle layer (Lan et al., 2016). de Haro et al. (2017) also provided evidence that the silencing mechanism of plants and insect vectors for MRCV could distinguish viral genomes, and thus produced different vsiRNAs, which suggested fijiviruses might encounter different and distinctive defense strategies both in host plants and vector insects.

Insect Components Involved in Transmission

For successful transmission, fijiviruses have to break through various transmission barriers in midgut, salivary gland, and defense immune response of their vector insects. Multiple interactions among virus and vector components are necessary for finishing above processes (Liu et al., 2018). Based on a yeast two-hybrid system (Y2H), proteins in vector *S. furcifera* were identified to interact with P6, P7-1 or P10 of SRBSDV. Five proteins (bromodomain-containing protein [BRD], succinyl-CoA ligase [ADP-forming] subunit beta [SUCLSB], 40S ribosomal protein SA [RPSA], toll-interacting protein [TOLIP] and signal transducing adapter molecule 1 [STAM1]) interacted with SRBSDV P6, and they are mainly involved in gene transcription, protein translation, protein post-translational modification and protein synthesis (Zhao et al., 2019). In *S. furcifera*, 18 proteins were confirmed interacting with SRBSDV P7-1 and six of them (neuroglian, myosin light chain 2 [MLC2], polyubiquitin, E3 ubiquitin ligase, ribophorin II, and profilin) exhibited different levels in five organs: neuroglian, MLC2, polyubiquitin and profilin highest in the gut, but ribophorin II and E3 ubiquitin ligase highest in the salivary glands and hemolymph, respectively, which indicated that they might play specific roles in viral progresses in different organs (Mar et al., 2014). Besides, 28 proteins interacted with the P10 of SRBSDV were identified. The mRNA level of vesicle-associated membrane protein 7 (VAMP7) was highest in the gut, but vesicle transport V-SNARE protein (Vti1A) and Growth hormone-inducible transmembrane protein (Ghitm) was highest in malpighian tubule compared with other tissues (Than et al., 2016). Based on the known data, we proposed a model for SRBSDV trafficking in midgut epitheliums of its insect vector, *S. furcifera* (**Figure 2**). SRBSDV virions invade into midgut epithelial cells by endocytosis through the interactions between the major outer capsid protein P10 and receptors in insects. Then the virus replicates in the viroplasm where P5-1, P6, P9-1 play vital roles in viroplasm formation. Insect proteins interacting with P6 might also assist recruit P5-1 and P9-1. After replication, the virions disseminate into hemolymph freely or in tubular vehicles through the interaction between P7-1 and cytoskeleton.

VIRUS EPIDEMICS AND MANAGEMENT

As discussed earlier, transmission by insect vectors is essential for the spread and epidemics of plant-infecting fijiviruses because they are not transmitted by seeds or mechanical means. Here, we discuss the impacts of transmission on virus epidemics in different crops.

Relationship Between Transmission and Epidemics

Fiji disease virus can cause Fiji leaf gall (FLG), a major problem for Australian sugarcane industry. The virus epidemics led to serious yield losses during 1970–1990 because FLG-susceptible cultivar NCo310 was planted in a large area and the vector *P. saccharicida* was present at a high density (Ryan, 1988). Besides, the vector planthopper of FDV occurs in all sugarcane-growing areas of Queensland and New South Wales. If only a species of *Perkinsiella* in the sugarcane on the east coast of Australia, the movement of insects from areas without FDV to areas with FDV is not important (Egan and Ryan, 1986; Egan et al., 1989; Dhileepan and Croft, 2003). On the other hand, if a species exists in northern Queensland but not in southern Queensland, and transmits FDV more efficiently than the current population of *P. saccharicida* in southern Queensland, then the migration of these northern insects will pose a risk to the southern region (Magarey et al., 2019).

Mal de Río Cuarto disease is the most important maize viral disease in Argentina (March et al., 1993, 2002; Lenardón et al., 1998). Although the vector *D. kuscheli* does not reproduce on maize, it breeds on MRCV susceptible winter cereals such as oat, wheat and rye, which serve as virus reservoirs (Trumper et al., 1996). Generally, viruliferous *D. kuscheli* migrate from senescent winter cereals to maize and then transmit MRCV when it feeds on maize (Ornaghi et al., 1993, 1999; March et al., 1995). If the major

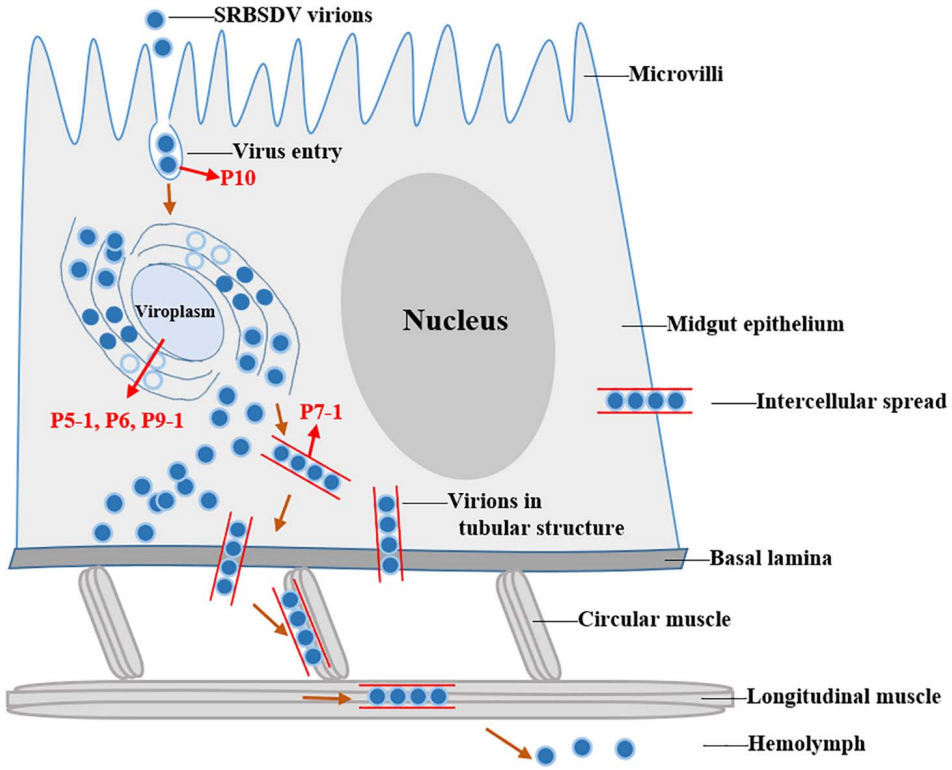

FIGURE 2 | Model of SRBSDV replication and transmission in midgut epithelium of *Sogatella furcifera*. SRBSDV enters into midgut epithelium by endocytosis through the interactions between the major outer capsid protein P10 and receptors in cell membrane and replicates in viroplasms, which are composed of non-structural proteins P9-1, P6, and P5-1. After replication, virions-containing P7-1 tubular structures directly pass across the basal lamina, traffic along the internal muscle tissues and then disseminate virions into hemolymph.

immigration period of high density of insect vectors is consistent with maize early growth stages (the first 3 weeks after maize emergence) of susceptible maize genotypes, severe outbreaks will occur (Ornaghi et al., 1993). Similarly, the epidemics of maize rough dwarf disease caused by MRDV in Spain has close relationship with the population density and distribution of its vector *L. striatellus*, especially at early stages of crop development, and to the susceptibility of the maize varieties (Conti, 1976; Trumper et al., 1996). In northern China, a double-cropping system for interplanted and intercropped maize and wheat was widely implemented in the 1980s. Such cropping system provide enough food sources for vector *L. striatellus*, resulting in its high population density and the opportunity for overwintering. In addition, the virus can be transmitted easily among different hosts, leading to outbreaks of maize rough dwarf diseases in these regions (Ren et al., 2016). As already mentioned, two fijiviruses, RBSDV and SRBSDV, are known to infect rice and cause serious yield losses in East Asian countries. For RBSDV or SRBSDV epidemics, migration and virus transmission of *L. striatellus* or *S. furcifera* among the different crops or gramineous weeds are essential. Field investigations have shown that outbreaks of SRBSDV-induced rice black streaked dwarf disease usually coincide with mass long distance migration of *S. furcifera* between or within Vietnam, Myanmar, Japan, South Korea, and China (**Figure 3**). Typhoons may carry migrating insects from southern China to northern Vietnam in the late fall or early winter, and then overwinter in tropic regions (Zhao et al., 2011; Matsukura, 2013), revealing that vector *S. furcifera* plays a crucial role in the SRBSDV epidemics. Under normal circumstances, the viruliferous macropterous adults are driven by winds to the Pearl River Basin (Guangdong) and Honghe Prefecture (Yunnan) in March. In central and eastern China, initial infection usually occurs in late spring and early summer from the viruliferous *S. furcifera* population that migrates with air flows from southern provinces of China and northern Vietnam or Myanmar (Zhou et al., 2013). In most regions with RBSDV epidemics in China, the disease incidence is closely related to the population density and viruliferous rate of the vector *L. striatellus*, which can finish its life cycle and seasonally migrate in wheat, barley, and some gramineous weeds in most regions (Wu et al., 2020).

Management

Integrated management strategies are urgently needed to reduce heavy losses caused by fijiviruses. At present, an economical and effective method for managing diseases is controlling vector insects on account of lacking disease-resistant varieties. Covering plant seedling nurseries with insect-proof nets is broadly used to control black streaked dwarf diseases caused by RBSDV or SRBSDV in China. Postponing sowing time of maize is available to prevent the peak period of *L. striatellus* planthopper

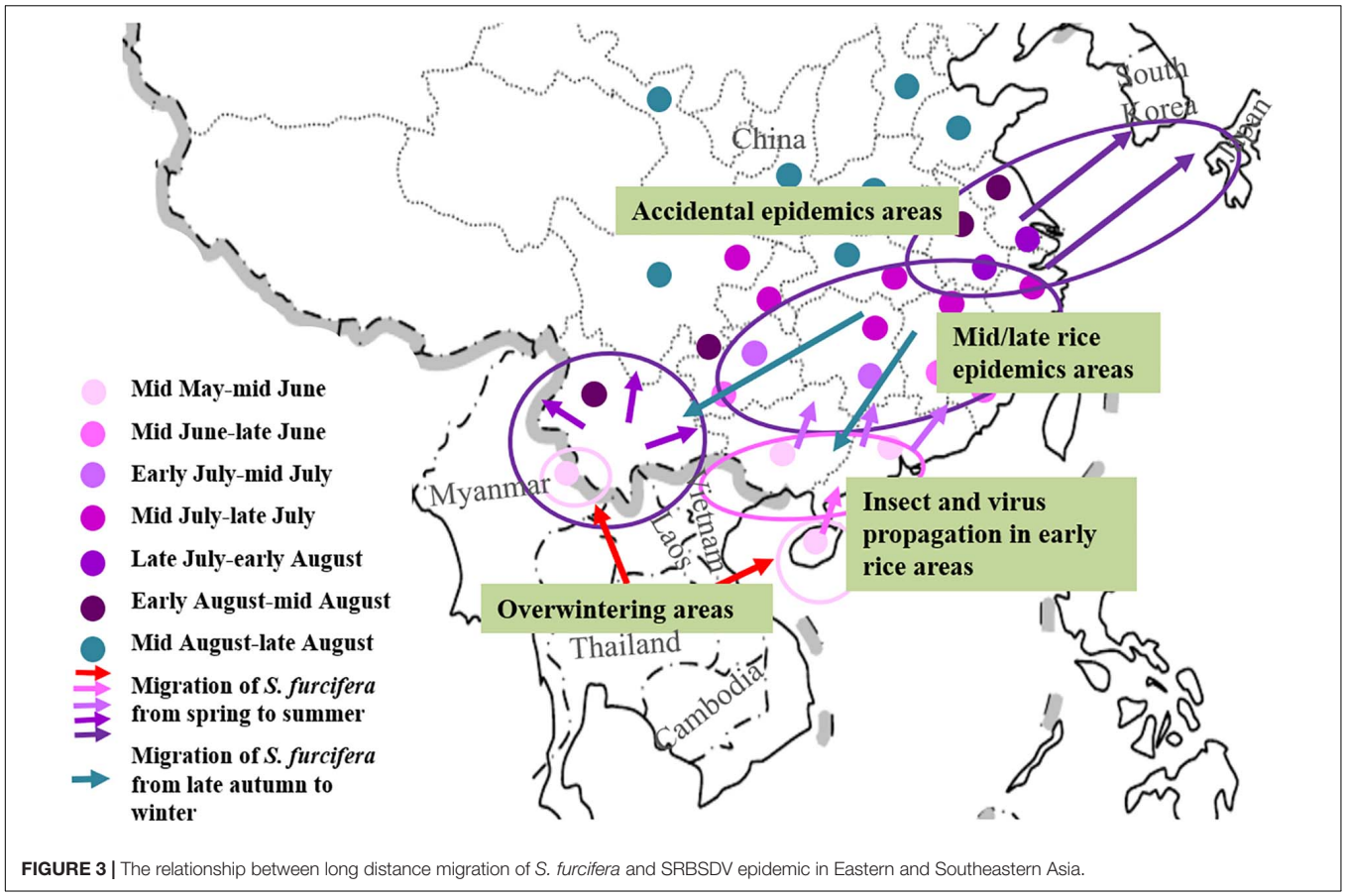

FIGURE 3 | The relationship between long distance migration of *S. furcifera* and SRBSDV epidemic in Eastern and Southeastern Asia.

immigration coinciding with the susceptible period of the rice. Seed dressing with pesticides is also recommended before sowing, and then the seedlings are applied pesticides three to 5 days before transplanting (Ren et al., 2016). For the management of Mal de Río Cuarto disease, the most important management practice is to advance the sowing so that the vector population peaks do not coincide with the emergency of the maize plants consulting a predictive model based on temperature variables and the disease intensity (March et al., 1995; Satapathy, 1998). Except managing insects, using virus-free vegetative materials and resistant varieties, removing infected stools or crops, and quarantining are existing effective methods to control FLG in Australia (Egan and Ryan, 1986; Dhileepan and Croft, 2003).

CONCLUDING REMARKS AND PROSPECTS

In general, field epidemics of plant fijiviruses have three typical stages: serious outbreak for 2–3 years, gradual mitigation over the next 2–3 years, and negligible disease for several years; thus, the disease tends to be intermittent over a longer period (Achon et al., 2013; Wu et al., 2020). Although existing virus management practices have played an important role during virus management, the underlying reasons for the epidemics are still poorly understood. Fijivirus epidemics are related to various biotic and non-biotic factors, so to better understand this complex pathosystem, and then provide accurate predictions and control measures, further study of transmission biology should be explored to reveal the reasons of the intermittent epidemics. Many aspects need to be addressed, including (a) the identification of determinants for vector specificity and viruses breaking through various transmission barriers in their vector insects. The roles of viral proteins, vector proteins, and insect symbionts in determining vector specialization also need to be further elucidated, which can provide targets for molecular design to inhibit transmission (Hajano et al., 2020). (b) Epigenetic RNA or DNA methylation of viral or host genes and changes in gene splicing upon virus infection can also affect interactions between the virus and vector insect and change vector specificity and transmission efficiency (Rivera-Serrano et al., 2017; Usama et al., 2019). (c) Global climate warming, organic farming methods to reduce the use of pesticides, and the commercialization of genetically modified crops that are resistant to lepidopterans or beetles may indirectly lead to the changes of planthopper population and the outbreaks of fijiviruses. Similar works have been done for other virus–vector insect systems (Wei and Li, 2016; Qin et al., 2018; Wang et al., 2019; Liu et al., 2020), but whether these results also apply to fijiviruses and their vector insects needs to be determined.

To further advance protection against these viruses, multidisciplinary approaches are needed. (a) Cooperative

research in plant pathology, insect ethology, ecology and other disciplines can help clarify mechanisms underpinning the four-way interactions in the plant–insect vector–virus–environment network. (b) Entomologists, plant virologists, crop breeders, and ecologists can coordinate and cooperate to advance the selection, cultivation and rational distribution of resistant varieties. (c) International exchange and cooperation should be strengthened to solve disease problems from a global perspective, focusing on the main places where the diseases occur, ascertain the migratory pathways of the vectors and the source of foreign insects, determine the source of the virus, and prevent outbreaks of the disease on an international scale. (d) A variety of experimental techniques for molecular biology, biochemistry, and environmental biology can be used to comprehensively study the pathogenic mechanism of viruses and their interactions with vectors and develop virus inhibitors or new technologies to block acquisition and transmission of viruses by the vectors.

AUTHOR CONTRIBUTIONS

XW conceived and designed the review. LZ, NW, YR, and XW wrote the manuscript. All authors contributed to the article and approved the submitted version.

FUNDING

This work was supported by the National Natural Science Foundation of China (31630058 and U1704234).

ACKNOWLEDGMENTS

We thank Dr. B. E. Hazen (Willows End scientific editing and writing, United States) for critically reading and revising the manuscript.

REFERENCES

Achon, M. A., Subira, J., and Sin, E. (2013). Seasonal occurrence of *Laodelphax striatellus* in Spain: effect on the incidence of maize rough dwarf virus. *Crop Prot.* 47, 1–5. doi: 10.1016/j.cropro.2013.01.002

Argüello Caro, E. B., Maroniche, G. A., Dumón, A. D., Sagadín, M. B., Mariana, D. V., and Truol, G. (2013). High viral load in the planthopper vector *Delphacodes Kuscheli* (Hemiptera: Delphacidae) is associated with successful transmission of Mal de Río Cuarto virus. *Ann. Entomol. Soc. Am.* 1, 93–99. doi: 10.1603/AN12076

Arneodo, J., Guzmán, F., Ojeda, S., Ramos, M. L., and Truol, G. (2005). Transmission of Mal de Río Cuarto virus by first and third-instar nymphs of *Delphacodes Kuscheli*. *Pesqui. Agropecu. Bras.* 40, 187–191. doi: 10.1590/s0100-204x2005000200014

Attoui, H., Mertens, P. P. C., Becnel, J., Belaganahalli, S., Bergoin, M., Brussaard, C., et al. (2012). "Family reoviridae," in *Virus Taxonomy: Ninth Report of the International Committee for the Taxonomy of Viruses*, eds A. M. Q. King, M. J. Adams, E. B. Carstens, and E. J. Lefkowits (New York: Elsevier), 541–637. doi: 10.1016/b978-0-12-384684-6.00051-3

Azuhata, F., Uyeda, I., Kimura, I., and Shikata, E. (1993). Close similarity between genome structures of rice black-streaked dwarf and maize rough dwarf viruses. *J. Gen. Virol.* 74, 1227–1232. doi: 10.1099/0022-1317-74-7-1227

Azuhata, F., Uyeda, I., and Shikata, E. (1992). Conserved terminal nucleotide sequences in the genome of rice black streaked dwarf virus. *J. Gen. Virol.* 73, 1593–1595. doi: 10.1099/0022-1317-73-6-1593

Blair, C. D. (2011). Mosquito RNAi is the major innate immune pathway controlling arbovirus infection and transmission. *Future Microbiol.* 6, 265–277. doi: 10.2217/fmb.11.11

Boito, G. T., and Ornaghi, J. A. (2008). Rol de los cereales de invierno y su sistema de manejo en la dinámica poblacional de Delphacodes kuscheli, insecto vector del MRCV. *Agriscientia* 25, 17–26.

Catherall, P. L. (1970). Oat sterile dwarf virus. *Plant Pathol.* 19, 75–78. doi: 10.1111/j.1365-3059.1970.tb00984.x

Chang, O. C. S. (1977). Transovarial transmission of the Fiji disease virus in Perkinsiella saccharicida Kirk. Sugarcane Pathologists'. *Newsletter* 18, 22–23.

Conti, M. (1974). Laodelphax striatellus as a vector of two cereal viruses in Italy. *Microbioligija* II, 49–54.

Conti, M. (1976). Epidemiology of maize of maize rough dwarf virus. II. Role of the different generations of vector in virus transmission. *Agric. Comp. Sci.* 39, 149–156.

Conti, M. (1984). "Epidemiology and vectors of plant reolike viruses," in *Current Topics in Vector Research*, Vol. 2, ed. K. E. Harris (New York, NY: Praeger), 111–139.

Conti, M. (1985). "Transmission of plant viruses by leafhoppers and planthoppers," in *The Leafhoppers and Planthoppers*, eds L. R. Nault and J. G. Rodriguez (New York, NY: John Wiley), 289–307.

Danthi, P., Guglielmi, K. M., Kirchner, E., Mainou, B., and Dermody, T. S. (2010). From touchdown to transcription: the reovirus cell entry pathway. *Curr. Top. Microbiol.* 343, 91–119. doi: 10.1007/82_2010_32

de Haro, L. A., Arellano, S. M., Novák, O., Feil, R., Dumón, A. D., Mattio, M. F., et al. (2019). Mal de río Cuarto virus infection causes hormone imbalance and sugar accumulation in wheat leaves. *BMC Plant Biol.* 19:112. doi: 10.1186/s12870-019-1709-y

de Haro, L. A., Dumón, A. D., Mattio, M. F., Argüello Caro, E. B., Llauger, G., Zavallo, D., et al. (2017). Mal de Río Cuarto Virus infection triggers the production of distinctive viral-derived siRNA profiles in wheat and its planthopper vector. *Front. Plant Sci.* 8:766. doi: 10.3389/fpls.2017.00766

Dhileepan, K., and Croft, B. J. (2003). Resistance to Fiji disease in sugarcane: role of cultivar preference by planthopper vector *Perkinsiella saccharicida* (Homoptera: Delphacidae). *J. Econ. Entomol.* 96, 148–155. doi: 10.1093/jee/96.1.148

Dhileepan, K., Greet, A., Ridley, A., Croft, B. J., and Smith, G. R. (2003). Fiji disease resistance in sugarcane: relationship to cultivar preference in field populations of the planthopper vector *Perkinsiella saccharicida*. *Ann. Appl. Biol.* 143, 375–379. doi: 10.1111/j.1744-7348.2003.tb00307.x

Di Feo, L. D. V., Laguna, I. G., and Biderbost, E. B. (2010). Physiological alterations associated to the Mal de Rio Cuarto virus (MRCV) infection and to vector (*Delphacodes kuscheli* Fennah) phytotoxicity in wheat. *Trop. Plant Pathol.* 35, 079–087. doi: 10.1590/S1982-56762010000200002

Ding, S. W. (2010). RNA-based antiviral immunity. *Nat. Rev. Immunol.* 10, 632–644. doi: 10.1038/nri2824

Dirven, J. G. P., and van Hoof, H. A. (1960). A destructive virus disease of pangola-grass. *Tijdschr Plantenziekten* 66, 344–349. doi: 10.1007/bf01987910

Distefano, A., Conci, L. R., Muñoz Hidalgo, M., Guzman, F. A., Hopp, H. E., and del Vas, M. (2002). Sequence analysis of genome segments S4 and S8 of Mal de Río Cuarto virus (MRVC): evidence that the virus should be a separate *Fijivirus* species. *Arch. Virol.* 147, 1699–1709. doi: 10.1007/s00705-002-0840-4

Donald, C. L., Kohl, A., and Schnettler, E. (2012). New insights into control of arbovirus replication and spread by insect RNA interference pathways. *Insects* 3, 511–531. doi: 10.3390/insects3020511

Dumón, A. D., Argüello Caro, E. B., Mattio, M. F., Alemandri, V., Del Vas, M., and Truol, G. (2017). Co-infection with a wheat rhabdovirus causes a reduction in Mal de Río Cuarto virus titer in its planthopper vector. *Bull. Entomol. Res.* 108, 232–240. doi: 10.1017/S0007485317000803

Dumón, A. D., Mattio, M. F., Argüello Caro, E. B., Alemandri, V. M., Puyané, N., del Vas, M., et al. (2015). Occurrence of a closely-related isolate to maize yellow striate virus in wheat plants. *Agriscientia* 32, 107–112.

Egan, B. T., and Ryan, C. C. (1986). "Predicting disease incidence and yield losses in sugarcane in a Fiji disease epidemic," in *Plant Virus Epidemics: Monitoring, Modelling and Predicting Outbreaks*, eds G. D. McLean, R. G. Garrett, and W. G. Ruesink (Sydney, NSW: Academic Press), 443–457.

Egan, B. T., Ryan, C. C., and Francki, R. I. B. (1989). "Fiji disease," in *Diseases of sugarcane; Major Diseases*, eds C. Ricaud, B. T. Egan, A. G. Gillespie, and C. G. Hughes (Amsterdam: Elsevier), 263–287. doi: 10.1016/b978-0-444-42797-7.50021-1

Firth, A. E., and Atkins, J. F. (2009). Analysis of the coding potential of the partially overlapping 3' ORF in segment 5 of the plant fijiviruses. *Virol. J.* 6, 32. doi: 10.1186/1743-422X-6-32

Fragkoudis, R., Attarzadeh-Yazdi, G., Nash, A. A., Fazakerley, J. K., and Kohl, A. (2009). Advances in dissecting mosquito innate immune responses to arbovirus infection. *J. Gen. Virol.* 90, 2061–2072. doi: 10.1099/vir.0.013201-0

Francki, R. I. B., and Boccardo, G. (1983). "The plant Reoviridae," in *The Reoviridae*, ed. W. K. Joklik (New York, NY: Plenum), 505–563. doi: 10.1007/978-1-4899-0580-2_10

Fu, Y., Cao, M., Wang, H., Du, Z., Liu, Y., and Wang, X. (2020). Discovery and characterization of a novel insect-specific reovirus isolated from *Psammotettix alienus*. *J. Gen. Virol.* 101, 884–892. doi: 10.1099/jgv.0.001442

Gammon, D. B., and Mello, C. C. (2015). RNA interference-mediated antiviral defense in insects. *Curr. Opin. Insect Sci.* 8, 111–120. doi: 10.1016/j.cois.2015.01.006

Greber, R. S., Gowanlock, D. H., Hicks, S., and Teakle, D. S. (1988). Transmission of pangola stunt virus by Sogatella kolophon. *Ann. Appl. Biol.* 113, 27–33. doi: 10.1111/j.1744-7348.1988.tb03278.x

Hajano, J. D., Raza, A., Zhang, L., Liu, W., and Wang, X. (2020). Ribavirin targets sugar transporter 6 to suppress acquisition and transmission of rice stripe tenuivirus by its vector *Laodelphax striatellus*. *Pest. Manag. Sci.* 76, 4086–4092. doi: 10.1002/ps.5963

Hajano, J. D., Wang, B., Ren, Y., Lu, C., and Wang, X. (2015). Quantification of southern rice black streaked dwarf virus and rice black streaked dwarf virus in the organs of their vector and nonvector insect over time. *Virus Res.* 208, 146–155. doi: 10.1016/j.virusres.2015.06.015

Harding, R. M., Burns, P., Geijskes, R. J., Mcqualter, R. M., Dale, J. L., and Smith, G. R. (2006). Molecular analysis of fiji disease virus segments 2, 4 and 7 completes the genome sequence. *Virus Genes* 32, 43–47. doi: 10.1007/s11262-006-5844-x

Harpaz, I. (1972). *Maize Rough Dwarf: A Planthopper Virus Disease Affecting Maize, Rice, Small Grains and Grasses*. Rome: Israel Universities Press.

Harpaz, I., and Klein, M. (1969). Vector-induced modifications in a plant virus. *Entomol. Exp. Appl.* 12, 99–106. doi: 10.1111/j.1570-7458.1969.tb02502.x

Hatta, T., and Francki, R. I. B. (1977). Morphology of Fiji disease virus. *Virology* 76, 797–807. doi: 10.1016/0042-6822(77)90260-4

Hogenhout, S. A., Ammar el, D., Whitfield, A. E., and Redinbaugh, M. G. (2008). Insect vector interactions with persistently transmitted viruses. *Ann. Rev. Phytopathol.* 46, 327–359. doi: 10.1146/annurev.phyto.022508.092135

Holder, M. W., and Wilson, S. W. (1992). Life history and descriptions of the immature stages of the planthopper *Prokelisia crocea* (Van Duzee) (Homoptera: Delphacidae). *J. New York Entomol. Soc.* 100, 491–497.

Huang, Y., and Li, Y. (2020). *Plant Reoviruses (reoviridae). Reference Module in Life Sciences*. Amsterdam: Elsevier, doi: 10.1016/B978-0-12-809633-8.21313-7

Hughes, C. G., and Robinson, P. E. (1961). "Fiji disease," in *Sugarcane Diseases of the World*, Vol. 1, eds J. P. Martin, E. V. Abbott, and C. G. Hughes (Amsterdam: Elsevier), 385–405.

Hughes, G. L., Allsopp, P. G., Brumbley, S. M., Johnson, K. N., and O'Neill, S. L. (2008). In vitro rearing of *Perkinsiella saccharicida* and the use of leaf segments to assay Fiji disease virus transmission. *Phytopathology* 98, 810–814. doi: 10.1094/phyto-98-7-0810

Hutchinson, P. B., and Francki, R. I. B. (1973). *Sugarcane Fiji Disease Virus. Description of Plant Viruses*, Vol. 119. Wallingford: Commonwealth Mycological Institute.

Isogai, M., Uyeda, I., and Lee, B. C. (1998). Detection and assignment of proteins encoded by rice black streaked dwarf fijivirus S7, S8, S9 and S10. *J. Gen. Virol.* 79, 1487–1494. doi: 10.1099/0022-1317-79-6-1487

Jia, D., Chen, H., Mao, Q., Liu, Q., and Wei, T. (2012). Restriction of viral dissemination from the midgut determines incompetence of small brown planthopper as a vector of southern rice black-streaked dwarf virus. *Virus Res.* 167, 404–408. doi: 10.1016/j.virusres.2012.05.023

Jia, D. S., Han, Y., Sun, X., Wang, Z. Z., Du, Z. G., Chen, Q., et al. (2016). The speed of tubule formation of two Fijiviruses corresponds with their dissemination efficiency in their insect vectors. *Virol. J.* 13, 174. doi: 10.1186/s12985-016-0632-1

Jia, D. S., Mao, Q., Chen, H. Y., Wang, A. M., Liu, Y. Y., Wang, H. T., et al. (2014). Virus-induced tubule: a vehicle for rapid spread of virions through basal lamina from midgut epithelium in the insect vector. *J. Virol.* 88, 10488–10500. doi: 10.1128/jvi.01261-14

Jupatanakul, N., Sim, S., and Dimopoulos, G. (2014). The insect microbiome modulates vector competence for arboviruses. *Viruses* 6, 4294–4313. doi: 10.3390/v6114294

Karan, M., Dale, J. L., Bateson, M. F., Harding, R. M., and Teakle, D. S. (1994). Detection and characterization of pangola stunt *Fijivirus* from Australia using cloned cDNA probes. *Arch. Virol.* 135, 397–404. doi: 10.1007/BF01310023

Klein, M., and Harpaz, I. (1969). Changes in resistance of graminaceous plants to delphacid planthoppers induced by maize rough dwarf virus (MRDV). *Zeitschrift für Angewandte Entomologie* 64, 39–43. doi: 10.1111/j.1439-0418.1969.tb03022.x

Kliot, A., Cilia, M., Czosnek, H., and Ghanim, M. (2014). Implication of the bacterial endosymbiont Rickettsia spp. in interactions of the whitefly Bemisia tabaci with tomato yellow leaf curl virus. *J. Virol.* 88, 5652–5660. doi: 10.1128/JVI.00071-14

Kliot, A., and Ghanim, M. (2013). The role of bacterial chaperones in the circulative transmission of plant viruses by insect vectors. *Viruses* 5, 1516–1535. doi: 10.3390/v5061516

Kuribayashi, K., and Shinkai, A. (1952). On the new disease of rice, black-streaked dwarf. *Ann. Phytopathol. Soc. Jap.* 16:41.

Laguna, I. G., Remes Lenicov, A. M., Virla, E., Avila, A., Gime' nez Pecci, M. P., Herrera, P., et al. (2002). Diffusion of Mal de Rio Cuarto virus (MRCV) of maize, its vector, associated planthoppers and alternative hosts in Argentina. *Rev. Soc. Entomol. Argent.* 61, 87–97.

Lan, H., Chen, H., Liu, Y., Jiang, C., Mao, Q., Jia, D., et al. (2016). Small interfering RNA pathway modulates initial viral infection in midgut epithelium of insect after ingestion of virus. *J. Virol.* 90, 917–929. doi: 10.1128/JVI.01835-15

Lefkowitz, E. J., Dempsey, D. M., Hendrickson, R. C., Orton R. J., Siddell, S. G., and Smith, D. B. (2018). Virus taxonomy: the database of the International Committee on Taxonomy of Viruses (ICTV). *Nucleic Acids Res.* 46, D708–D717. doi: 10.1093/nar/gkx932

Lei, W., Li, P., Han, Y., Gong, S., Yang, L., and Hou, M. (2016). EPG Recordings reveal differential feeding behaviors in Sogatella furcifera in response to plant virus infection and transmission success. *Sci. Rep.* 6:30240. doi: 10.1038/srep30240

Lenardón, S. L., March, G. J., Nome, S. F., and Ornaghi, J. A. (1998). Recent outbreak of "Mal de Río Cuarto" virus on corn in Argentina. *Plant Dis.* 82, 448–448. doi: 10.1094/PDIS.1998.82.4.448C

Li, J., Andika, I. B., Shen, J., Lv, Y., Ji, Y., and Sun, L. (2013). Characterization of rice black-streaked dwarf virus- and rice stripe virus-derived siRNAs in singly and doubly infected insect vector *Laodelphax striatellus*. *PLoS One* 8:e66007. doi: 10.1371/journal.pone.0066007

Li, S., Wang, H., and Zhou, G. H. (2014). Synergism between southern rice black-streaked dwarf virus and rice ragged stunt virus enhances their insect vector acquisition. *Phytopathology* 104, 794–799. doi: 10.1094/PHYTO-11-13-0319-R

Li, Y. Z., Cao, Y., Zhou, Q., Guo, H. M., and Ou, G. C. (2012). The efficiency of southern rice black-streaked dwarf virus transmission by the vector Sogatella furcifera to different host plant species. *J. Integr. Agr.* 11, 621–627. doi: 10.1016/S2095-3119(12)60049-5

Lindsten, K. (1974). Planthopper-transmitted virus diseases of cereals in Sweden. *Acta Biol. Iugoslavica B* 11, 55–66.

Liu, W., Hajano, J. U., and Wang, X. (2018). New insights on the transmission mechanism of tenuiviruses by their vector insects. *Curr. Opin. Virol.* 33, 13–17. doi: 10.1016/j.coviro.2018.07.004

Liu, W., Zhang, X., Wu, N., Ren, Y., and Wang, X. (2020). High diversity and functional complementation of alimentary canal microbiota ensure small brown planthopper to adapt different biogeographic environments. *Front. Microbiol.* 10:2953. doi: 10.3389/fmicb.2019.02953

Lot, H., Delecolle, B., Boccardo, G., Marzachi, C., and Milne, R. G. (1994). Partial characterization of reovirus-like particles associated with garlic dwarf disease. *Plant Pathol.* 43, 537–546. doi: 10.1111/j.1365-3059.1994.tb01588.x

Lovisolo, O. (1971). *Maize Rough Dwarf Virus. In Descriptions of Plant Viruses*. Surrey: Commonwealth Mycology Institute.

Lu, G. H., Zhang, T., He, Y. G., and Zhou, G. H. (2016). Virus altered rice attractiveness to planthoppers is mediated by volatiles and related to virus titre and expression of defence and volatile-biosynthesis genes. *Sci. Rep.* 6:38581. doi: 10.1038/srep38581

Magarey, R. C., Reynolds, M., Dominiak, B. C., Sergean, E., Agnew, J., Ward, A., et al. (2019). Review of sugarcane Fiji leaf gall disease in Australia and the declaration of pest freedom in Central Queensland. *Crop Prot.* 121, 113–120. doi: 10.1016/j.cropro.2019.03.022

Mainou, B. A., and Dermody, T. S. (2012). Transport to late endosomes is required for efficient reovirus infection. *J. Virol.* 86, 8346–8358. doi: 10.1128/JVI.00100-12

Mar, T. T., Liu, W., and Wang, X. (2014). Proteomic analysis of interaction between p7-1 of southern rice black-streaked dwarf virus and the insect vector reveals diverse insect proteins involved in successful transmission. *J. Proteomics* 102, 83–97. doi: 10.1016/j.jprot.2014.03.004

March, G. J., Balzarini, M., Ornaghi, J. A., Beviacqua, J. E., and Marinelli, A. (1995). Predictive Model for "Mal de Río Cuarto" Disease Intensity. *Plant Dis.* 79, 1051–1053. doi: 10.1094/PD-79-1051

March, G. J., Ornaghi, J. A., Beviacqua, J. E., Giuggia, J., Rago, A., and Lenardon, S. L. (2002). Systemic insecticides for control of *Delphacodes kuscheli* and the Mal de Río Cuarto virus on maize. *Int. J. Pest Manag.* 48, 127–132. doi: 10.1080/09670870110100695

March, G. J., Ornaghi, J. A., Beviacqua, J. E., Sanchez, G., and Guiggia, J. (1993). "Aportes para el desarrollo de una estrategia de manejo del Mal de río Cuarto," in *Actas Workshop "Mal de Río Cuarto del maize"*, (Cordoba), 47–48.

Maroniche, G. A., Mongelli, V. C., Peralta, A. V., Distéfano, A. J., Llauger, G., Taboga, O. A., et al. (2010). Functional and biochemical properties of Mal de Río Cuarto virus (*Fijivirus*, Reoviridae) P 9-1 viroplasm protein show further similarities to animal reovirus counterparts. *Virus Res.* 152, 96–103. doi: 10.1016/j.virusres.2010.06.010

Marzachi, C., Antoniazzi, S., Aquilio, M., and Boccardo, G. (1996). The double-stranded RNA genome of maize rough dwarf Fijivirus contains both mono and dicistronic segments. *Eur. J. Plant. Pathol.* 102, 601–605. doi: 10.1007/BF01877029

Matsukura, K. (2013). Dynamics of southern rice black-streaked dwarf virus in rice and implication for virus acquisition. *Phytopathology* 103, 509–512. doi: 10.1094/PHYTO-10-12-0261-R

Mattio, M. F., Cassol, A., de Remes Lenicov, A. M., and Truol, D. (2008). Tagosodes orizicolus: a new potential vector of Mal de Río Cuarto virus. *Trop. Plant Pathol.* 33, 237–240. doi: 10.1590/S1982-56762008000300010

Milne, R. G., Conti, M., and Lisa, V. (1973). Partial purification, structure and infectivity of complete maize rough dwarf virus particles. *Virology* 53, 130–141. doi: 10.1016/0042-6822(73)90472-8

Milne, R. G., and Lovisolo, O. (1977). Maize rough dwarf and related viruses. *Adv. Virus Res.* 21, 267–341. doi: 10.1016/S0065-3527(08)60764-2

Moreira, L. A., Iturbe-Ormaetxe, I., Jeffery, J. A., Lu, G., Pyke, A. T., Hedges, L. M., et al. (2009). A Wolbachia symbiont in Aedes aegypti limits infection with dengue. Chikungunya, and plasmodium. *Cell* 139, 1268–1278. doi: 10.1016/j.cell.2009.11.042

Mousson, L., Zouache, K., Arias-Goeta, C., Raquin, V., Mavingui, P., and Failloux, A. B. (2012). The native *Wolbachia symbionts* limit transmission of dengue virus in *Aedes albopictus*. *PLoS Negl. Trop. Dis.* 6:e1989. doi: 10.1371/journal.pntd.0001989

Mungomery, R. W., and Bell, A. F. (1933). Fiji disease of sugar-cane and its transmission. *Div. Pathol. Bur. Sugar Exp. Stations Bull.* 4, 28.

Nakasuji, F., and Kiritani, K. (1970). Effects of rice dwarf virus upon its vector, Nephotettix cincticeps Uhler (Hemiptera: Deltocephalidae), and its significance for changes in relative abundance of infected individuals among vector populations. *Appl. Entomol. Zool.* 5, 1–12. doi: 10.1303/aez.5.1

Nault, L. R. (1994). "Transmission biology, vector specificity and evolution of planthopper-transmitted plant viruses," in *Planthoppers*, eds R. F. Denno and T. J. Perfect (New York, NY: Chapman & Hall), 429–448. doi: 10.1007/978-1-4615-2395-6_13

Nome, S. F. (1981). Association of reovirus like particles with "Enfermedad de Río Cuarto" of maize in Argentina. *Phytopathology* 101, 7–15. doi: 10.1111/j.1439-0434.1981.tb03315.x

Ornaghi, J., Pecci, M. P. G., Herrera, P. S., Laguna, I. G., Pardina, P. R., and Borgogno, C. (2000). Rol de los cereales en la epidemiología del virus del Mal de Río Cuarto en Argentina. *Fitopatología* 35, 41–49. doi: 10.17104/0017-141720105455

Ornaghi, J. A., Boito, G., Sanchez, G., March, G., and Beviacqua, J. E. (1993). Studies on the populations of *Delphacodes kuscheli* Fennah in different years and agricultural areas. *J. Genet. Breed.* 47, 277–282.

Ornaghi, J. A., March, G. J., Boito, G. T., Marinelli, A., and Lenardon, S. L. (1999). Infectivity in natural populations of *Delphacodes kuscheli* vector of 'Mal de Río Cuarto virus. *Maydica* 44, 219–223.

Pardina, P. E. R., Pecci, M. P. G., Laguna, I. G., Dagoberto, E., and Truol, G. (1998). Wheat: a new natural host for the Mal de Río Cuarto virus in the endemic disease area, Río Cuarto, Córdoba province, Argentina. *Plant Dis.* 82, 149–152. doi: 10.1094/pdis.1998.82.2.149

Pu, L., Xie, G., Ji, C., Ling, B., Zhang, M., Xu, D., et al. (2012). Transmission characteristics of Southern rice black-streaked dwarf virus by rice planthoppers. *Crop Prot.* 41, 71–76. doi: 10.1016/j.cropro.2012.04.026

Qin, F., Liu, W., Wu, N., Zhang, L., Zhou, X., and Wang, X. (2018). Invasion of midgut epithelial cells by a persistently transmitted virus is mediated by sugar transporter in its insect vector. *PLoS Pathog.* 14:e1007201. doi: 10.1371/journal.ppat.1007201

Remes Lenicov, A. M. M., Virla, E., Tesón, A., Dagoberto, E., and Huguet, N. (1985). Hallazgo de uno de los vectores del "Mal de Río Cuarto" del maíz. *Gaceta Agron.* 5, 251–258.

Ren, Y., Lu, C., and Wang, X. (2016). Reason analysis about outbreak epidemics of rice black streaked dwarf disease: an example in Kaifeng, Henan Province. *Plant Prot.* 42, 8–16. doi: 10.3969/j.issn.0529-1542.2016.03.002

Rivera-Serrano, E. E., Fritch, E. J., Scholl, E. H., and Sherry, B. (2017). A cytoplasmic RNA virus alters the function of the cell splicing protein SRSF2. *J. Virol.* 91:e02488-16. doi: 10.1128/JVI.02488-16

Ryan, C. C. (1988). Epidemiology and control of Fiji disease virus of sugarcane. *Adv. Dis. Vector Res.* 5, 163–176.

Satapathy, M. K. (1998). Chemical control of insect and nematode vectors of plant viruses. *Plant Virus Dis. Control* 1, 188–195.

Shikata, E., and Kitagawa, Y. (1977). Rice black-streaked dwarf virus: its properties, morphology and intracellular localization. *Virology* 77, 826–842. doi: 10.1016/0042-6822(77)90502-5

Shimizu, T., Nakazono-Nagaoka, E., Akita, F., Uehara-Ichiki, T., Omura, T., and Sasaya, T. (2011). Immunity to rice black streaked dwarf virus, a plant reovirus, can be achieved in rice plants by rna silencing against the gene for the viroplasm component protein. *Virus Res.* 160, 400–403. doi: 10.1016/j.virusres.2011.05.011

Shinkai, A. (1962). Studies on insect transmission of rice virus diseases in Japan. *Bull. Natl. Inst. Agric. Sci. Jpn. C* 14, 1–112.

Teakle, D. S., Hicks, S., Harding, R. M., Greber, R. S., and Milne, R. G. (1988). Pangola stunt virus infecting pangola grass and summer grass in Australia. *Crop Pasture Sci.* 39, 1075–1083. doi: 10.1071/ar9881075

Teakle, D. S., and Steindl, D. R. L. (1969). Virus-like particles in galls of sugarcane plants affected by Fiji disease. *Virology* 37, 139–145. doi: 10.1016/0042-6822(69)90316-x

Than, W., Qin, F. L., Liu, W. W., and Wang, X. (2016). Analysis of Sogatella furcifera proteome that interact with P10 protein of southern rice black-streaked dwarf virus. *Sci. Rep.* 6:32445. doi: 10.1038/srep32445

Toohey, C. L., and Nielsen, P. J. (1972). Fiji disease at Bundaberg. *Proc. Old Soc. Sugar Cane Technol.* 39, 191–196.

Trumper, E. V., Gorla, D. E., and Grilli, M. P. (1996). The spatial pattern of "Malde Río Cuarto" (Río Cuarto Corn Disease) in corn fields. *Ecol. Aust.* 6, 131–136.

Usama, A., Clara, B., Vincent, L., Vincent, N., and Nadia, N. (2019). Advances in analyzing virus-induced alterations of host cell splicing. *Trends Microbiol.* 3, 268–281. doi: 10.1016/j.tim.2018.11.004

Vacke, J. (1966). Study of transovarial passage of the oat sterile-dwarf virus. *Biol. Plant.* 8, 127–130. doi: 10.1007/BF02930621

Velázquez, P. D., Arneodo, J. D., Guzmán, F. A., Conci, L. R., and Truol, G. A. (2003). Delphacodes haywardi Muir, a new natural vector of Mal de Río Cuarto virus in Argentina. *J. Phytopathol.* 151, 669–672. doi: 10.1046/j.1439-0434.2003.00786.x

Velázquez, P. D., Guzmán, F. A., Conci, L. R., de Remes Lenicov, A. M. M., and Truol, G. A. (2006). Pyrophagus tigrinus Remes Lenicov & Varela (Hemiptera: Delphacidae), nuevo vector del Mal de Río Cuarto virus (MRCV, *Fijivirus*) en condiciones experimentales. *Agriscientia* 23, 9–14.

Velázquez, P. D., Truol, G., and Lenicov, A. R. (2017). Caenodelphax teapae (Fowler) (Hemiptera: Delphacidae): a new natural vector of the Mal de Río Cuarto virus (MRCV, Fijivirus) in Argentina. *Agriscientia* 34, 39–45. doi: 10.31047/1668.298x.v34.n1.17357

Wang, H., Liu, Y., Zhang, L., Kundu, J. K., Liu, W., and Wang, X. (2019). ADP ribosylation factor 1 facilitates spread of wheat dwarf virus in its insect vector. *Cell Microbiol.* 21:e13047. doi: 10.1111/cmi.13047

Wang, H., Xu, D., Pu, L., and Zhou, G. (2013). Southern rice black-streaked dwarf virus alters insect vectors' host orientation preferences to enhance spread and increase rice ragged stunt virus co-infection. *Phytopathology* 104, 196–201. doi: 10.1094/PHYTO-08-13-0227-R

Wang, L., Tang, N., Gao, X., Guo, D., Chang, Z., Fu, Y., et al. (2016). Understanding the immune system architecture and transcriptome responses to southern rice black-streaked dwarf virus in *Sogatella furcifera*. *Sci. Rep.* 6:36254. doi: 10.1038/srep36254

Wei, T., and Li, Y. (2016). Rice reoviruses in insect vectors. *Ann. Rev. Phytopathol.* 54, 99–120. doi: 10.1146/annurev-phyto-080615-095900

Wu, N., Zhang, L., Ren, Y., and Wang, X. (2020). Rice black-streaked dwarf virus: from multiparty interactions among plant–virus–vector to intermittent epidemics. *Mol. Plant Pathol.* 21, 1007–1019. doi: 10.1111/mpp.12946

Wu, N., Zhang, P., Liu, W., Cao, M., and Wang, X. (2018). Sequence analysis and genomic organization of a new insect iflavirus, Sogatella furcifera honeydew virus 1. *Arch. Virol.* 163, 2001–2003. doi: 10.1007/s00705-018-3817-7

Wu, N., Zhang, P., Liu, W., Cao, M., and Wang, X. (2019). Complete genome sequence and characterization of a new iflavirus from the small brown planthopper (*Laodelphax striatellus*). *Virus Res.* 272:197651. doi: 10.1016/j.virusres.2019.197651

Xu, H. X., He, X. C., Zheng, X. S., Yang, Y. J., Tian, J. C., and Lu, Z. X. (2014). Southern rice black-streaked dwarf virus (SRBSDV) directly affects the feeding and reproduction behavior of its vector, *Sogatella furcifera* (Horváth) (Hemiptera: Delphacidae). *Virol. J.* 11:55. doi: 10.1186/1743-422X-11-55

Xu, H. X., He, X. C., Zheng, X. S., Yang, Y. J., Zhang, J. F., and Lu, Z. X. (2016). Effects of SRBSDV-infected rice plants on the fitness of vector and non-vector rice planthoppers. *J. Asia Pac. Entomol.* 19, 707–710. doi: 10.1016/j.aspen.2016.06.016

Zhang, C., Liu, Y., Liu, L., Lou, Z., Zhang, H., Miao, H., et al. (2008). Rice black streaked dwarf virus P9-1, an alpha-helical protein, self-interacts and forms viroplasms in vivo. *J. Gen. Virol.* 89, 1770–1776. doi: 10.1099/vir.0.2008/000109-0

Zhang, J., Zheng, X., Chen, Y. D., Hu, J., Dong, J. H., Su, X. X., et al. (2014). Southern rice black-streaked dwarf virus infection improves host suitability for its insect vector, *Sogatella furcifera* (Hemiptera: Delphacidae). *J. Econ. Entomol.* 107, 92–97. doi: 10.1603/ec13204

Zhang, T., Feng, W. D., Ye, J. J., Li, Z. B., and Zhou, G. H. (2018). Metabolomic changes in Sogatella furcifera under southern rice black-streaked dwarf virus infection and temperature stress. *Viruses* 10:344. doi: 10.3390/v10070344

Zhao, Y., Wu, C. X., Zhu, X. D., Jiang, X. H., Zhang, X. X., and Zhai, B. P. (2011). Tracking the source regions of southern rice black-streaked dwarf virus (SRBSDV) occurred in Wuyi county, Zhejiang province, China in 2009, transmitted by Sogatella furcifera (Horváth) (Homoptera: Delphacidae). *Acta Entomol. Sin.* 54, 949–959.

Zhao, Z. H., Pan, H., Du, J., Chen, J. B., Liu, Y., Zhang, S. B., et al. (2019). Identification of insect proteins interacting with P6 of SRBSDV in the midgut of white-backed planthopper (*Sogatella furcifera*). *J. Agri. Biotechnol.* 27, 712–719. doi: 10.3969/j.issn.1674-7968.2019.04.015

Zhou, G., Wen, J., Cai, D., Li, P., Xu, D., and Zhang, S. (2008). Southern rice black streaked dwarf virus: a new proposed *Fijivirus* species in the family Reoviridae. *Chinese Sci. Bull.* 53, 3677–3685. doi: 10.1007/s11434-008-0467-2

Zhou, G., Xu, D., Xu, D., and Zhang, M. (2013). Southern rice black-streaked dwarf virus: a white-backed planthopper-transmitted fijivirus threatening rice production in Asia. *Front. Microbiol.* 4:270. doi: 10.3389/fmicb.2013.00270

Zvereva, A. S., and Pooggin, M. M. (2012). Silencing and innate immunity in plant defense against viral and non-viral pathogens. *Viruses* 4, 2578–2597. doi: 10.3390/v4112578

Conflict of Interest: The authors declare that the research was conducted in the absence of any commercial or financial relationships that could be construed as a potential conflict of interest.

frontiers in Microbiology

MINI REVIEW
published: 12 March 2021
doi: 10.3389/fmicb.2021.656809

Plant Cell Wall as a Key Player During Resistant and Susceptible Plant-Virus Interactions

Edmund Kozieł[1], Katarzyna Otulak-Kozieł[1]* and Józef Julian Bujarski[2]*

[1]Institute of Biology, Department of Botany, Warsaw University of Life Sciences – SGGW, Warsaw, Poland, [2]Department of Biological Sciences, Northern Illinois University, DeKalb, IL, United States

The cell wall is a complex and integral part of the plant cell. As a structural element it sustains the shape of the cell and mediates contact among internal and external factors. We have been aware of its involvement in both abiotic (like drought or frost) and biotic stresses (like bacteria or fungi) for some time. In contrast to bacterial and fungal pathogens, viruses are not mechanical destructors of host cell walls, but relatively little is known about remodeling of the plant cell wall in response to viral biotic stress. New research results indicate that the cell wall represents a crucial active component during the plant's response to different viral infections. Apparently, cell wall genes and proteins play key roles during interaction, having a direct influence on the rebuilding of the cell wall architecture. The plant cell wall is involved in both susceptibility as well as resistance reactions. In this review we summarize important progress made in research on plant virus impact on cell wall remodeling. Analyses of essential defensive wall associated proteins in susceptible and resistant responses demonstrate that the components of cell wall metabolism can affect the spread of the virus as well as activate the apoplast- and symplast-based defense mechanisms, thus contributing to the complex network of the plant immune system. Although the cell wall reorganization during the plant-virus interaction remains a challenging task, the use of novel tools and methods to investigate its composition and structure will greatly contribute to our knowledge in the field.

Keywords: plant viruses, cell wall remodeling, defense response, hypersensitive reaction, ultrastructure

OPEN ACCESS

Edited by:
Rajarshi Kumar Gaur, Deen Dayal Upadhyay Gorakhpur University, India

Reviewed by:
Lei Huang, Purdue University, United States
Shabir Hussain Wani, Sher-e-Kashmir University of Agricultural Sciences and Technology, India

****Correspondence:***
Edmund Kozieł
edmund_koziel@sggw.pl;
edmund_koziel@sggw.edu.pl
Katarzyna Otulak-Kozieł
katarzyna_otulak@sggw.pl;
katarzyna_otulak@sggw.edu.pl

Specialty section:
This article was submitted to Microbe and Virus Interactions With Plants, a section of the journal Frontiers in Microbiology

Received: *21 January 2021*
Accepted: *19 February 2021*
Published: *12 March 2021*

Citation:
Kozieł E, Otulak-Kozieł K and Bujarski JJ (2021) Plant Cell Wall as a Key Player During Resistant and Susceptible Plant-Virus Interactions. Front. Microbiol. 12:656809. doi: 10.3389/fmicb.2021.656809

INTRODUCTION

Plant viruses are highly diversified and cause enormous alterations and deformations inside a plant host cell (Gergerich and Dolja, 2006). Their genome, which has the form of dsDNA, ssDNA, dsRNA, or ssRNA, is surrounded by a capsid consisting of coat protein molecules (Gergerich and Dolja, 2006; Hull, 2014). Generally, the viral genome encodes genetic information about proteins that play a crucial role in the induction and nondisturbed maintenance of viral infection *via* local/systemic transport (Hull, 2014). Thus, plant viruses are active only inside the host cell and induce multilevel changes in its internal system during infection.

Due to their constant exposure to a wide range of pathogenic microorganisms, plants have evolved both constitutive and inducible defense mechanisms (Underwood, 2012). Constitutive defenses of plants encompass physical barriers, such as waxy epidermal cuticles or cell walls on the surface, which prevent the penetration of pathogens. On the other hand, inducible defense

responses are activated in plants upon the recognition of potential pathogens by surveillance mechanisms (Jones and Dangl, 2006). Therefore, it can be considered that plants do not remain as "static components" during their interaction/contact with a viral pathogen. Rather, they induce complex systems of response to the invading virus (Mandadi and Scholthof, 2013). The speed, strength, and level of effectiveness of this response determines the susceptibility or resistance of a plant host. The cell wall is not only an inherent structural component in plant cells but also acts as an important "contact platform" during plant-pathogen interactions.

The structural polysaccharides present in the cell wall maintain the shape and size of the cell, while also providing mechanical strength required to endure extrinsic stresses and to preserve the inner turgor (Bacete et al., 2018; Voiniciuc et al., 2018). Numerous reviews have described that the polysaccharide (cellulose) and the non-saccharide fraction (lignin) of the plant cell wall play the main role in developmental, defense, and bioconversion processes (Chen et al., 2018a; Liu et al., 2018; Meents et al., 2018). According to the commonly known, classic model of cell wall structural networks, the surface of cellulose microfibrils is interconnected with hemicellulose fibers enclosed by a pectin matrix, which determines the flexibility or stiffness of the cell wall (Cosgrove, 2018). Broxterman and Schols (2018) postulated that the two components are linked by distinctive and strong covalent interactions in the primary cell wall architecture. Moreover, cell wall polysaccharides serve as a repository of molecules that are involved in intercellular signaling and that elicit the immune response to microbial invasion (Cosgrove, 2018).

A majority of previous studies have focused on the changes occurring in the plant cell wall and put forth different models of plant-pathogen interactions for organisms such as bacteria, nematodes, and fungi, but not viruses. Research on the engagement of the plant cell wall is highly focused on the changes occurring in plasmodesmata during the regulation/blockade of virus cell-to-cell transport. The results revealed the role of β-1,3 glucanase in controlling plant viruses during local and systemic transport (Beffa and Meins, 1996; Iglesias and Meins, 2000). However, recent studies indicate that the frequency of active remodeling and rebuilding of the cell wall, taking place in response to viral infection, is higher than assumed (Raggi, 2000; Ding et al., 2008; Park et al., 2017; Chen et al., 2018b,c; Otulak-Kozieł et al., 2018a). The process of wall rebuilding differs in susceptible and resistant plant hosts (Otulak-Kozieł et al., 2018b, 2020). This review presents the current knowledge about the role of plant cell wall in susceptible and resistance responses of plants to viruses and summarizes the potential fields of future research for a better understanding of this aspect of plant-pathogen interactions.

CELL WALL IN VIRAL INFECTION OF SUSCEPTIBLE HOST

During host-pathogen interactions, plant viruses build a complex system to evade or suppress the defense response of the plant (Garcia-Ruiz, 2018, 2019). If the virus manages to overcome the defense/response system, the plant host becomes susceptible to infection (Jin et al., 2018). The cell wall is a vital element of the host reaction system. Interestingly, novel comparative transcriptome profiling analysis as well as microarray gene expression analysis carried out in susceptible and resistant host plants after the viral infection has shown that the first target in the host cells is the cell wall (Shimizu et al., 2007, 2013; Zheng et al., 2013; Allie et al., 2014). The earlier reports demonstrating the involvement of the cell wall were based on tobacco mosaic virus (TMV) infection in susceptible tobacco plants (Beffa and Meins, 1996; Bucher et al., 2001). The authors of these studies demonstrated that cell wall-associated proteins and enzymes were involved in controlling the virus cell-to-cell transport. One of the main cell wall-associated polysaccharides—callose—was found to be extremely important in the specific control of TMV transport. The presence/distribution of this protein in the apoplast area was directly regulated by the ratio of two enzymes: callose synthase (which catalyzes the callose synthesis) and β-1,3 glucanase (which hydrolyzes callose; Kauss, 1996). In response to TMV (and other plant viruses), plants increase the synthesis and deposition of callose which can be observed near and inside the plasmodesmata. Callose deposited inside the plasmodesmata forms a physical barrier decreasing the size exclusion limit and blocking the cell-cell transport. However, this response could be frequently counteracted by some viruses, including cucumber mosaic virus (CMV), potato virus X (PVX), or TMV, through a mechanism that is rather universal among viruses. The class II β-1,3 glucanase includes the pathogenesis-related protein PR-2, which acts as an important host cellular factor governing the movement of the virus (Beffa and Meins, 1996). Iglesias and Meins (2000) clearly showed that infection by TMV enhances PR-2 activity in tobacco while also increasing the mobility and distribution of plasmodesmata, thus facilitating virus movement. Therefore, degradation of the callose physical barrier (due to increased deposition of β-1,3 glucanase) is essential for the maintenance of viral movement in a susceptible host (Bucher et al., 2001). The increased deposition of β-1,3 glucanase allows TMV and other viruses to overcome the natural blocking mechanism and promotes pathogen transportation. The changes of the cell wall are associated not only with plasmodesmata but also with apoplasts. The South African cassava mosaic virus is the first example reported to have this finding. Allie et al. (2014) postulated that susceptible cassava genotype T200 infected by SCMV induced mRNA transcripts of several components including proteins belonging to pectin lyase superfamily or plant invertase/pectin methylesterase inhibitor superfamily, which are responsible for the degradation of the plant cell wall. Similar transcriptome data were acquired by Zheng et al. (2013). The authors indicated that a susceptible rice cultivar (cv. Fengjin) responded to infection by rice stripe virus (RSV) by downregulating four genes that code for glycine-rich, cell wall structural protein, and a gene coding for cellulose synthase. Their results suggest that RSV and SCMV could structurally modify the cell wall by specific and complex regulation of cell wall structural proteins.

Changes occurring within the ultrastructure in a susceptible plant host were first reported for potato virus Y-NTN (PVY^{NTN})

infection by Otulak-Kozieł et al. (2018a). We ascertained that PVY^{NTN} could be folded into a loose structure. Moreover, they were associated with paramural bodies within the plasmodesmata in the affected portions of cell wall and with virus cytoplasmic inclusions. These changes correlated with alterations in the quantity and distribution of PR-2 and with the catalytic subunits of cellulose synthase (CesA4). Accumulation of PR-2 was noticeably elevated in the susceptible potato. Compared to mock-inoculated plants, the level of CesA4 was decreased in hosts that were susceptible to PVY^{NTN}. This infection also changed the distribution of both proteins inside the cells of compatible plant hosts. In the infected susceptible potato, PR-2 was more frequently accumulated in the cell wall and vacuoles compared to the healthy plants. Moreover, in susceptible plants, CesA4 was deposited in the cell wall, plasma membrane, and endoplasmic reticulum. This suggests that both the decrease in CesA4 and increase in PR-2 determined the susceptibility of potato (Otulak-Kozieł et al., 2018a), most likely by enabling cell-to-cell movement of the virus.

The results reported by Otulak-Kozieł et al. (2018b) shed some light on susceptible potato-PVY interactions (**Figure 1**). The authors studied the *in-situ* dissemination of various hemicellulosic cell wall matrix components during the interactions of susceptible and hypersensitive potato with PVY^{NTN}. Xyloglucan was identified as the major hemicellulose of the primary cell wall and was associated with the changes initiated by the pathogen (Pauly et al., 2013). Lotan and Fluhr (1990) and Bacete et al. (2018) postulated that xyloglucan metabolism is linked with cell wall expansion, and thus influences the infection by a pathogen. Organisms such as viruses disrupt the plant cell wall, as well as inducing β-1,4 xylanase, resulting in the production of endoxylanases. We ascertained that the cell wall loosening process occurs along with enhanced deposition of xylan in the event of susceptible interactions after infection of potato with the potyvirus. The cell wall of plants consists of several enzymes capable of modifying polysaccharides, of which xyloglucan endotransglucosylase/hydrolase (Xet, XTH) is of importance, as it is essential for wall architecture and elongation (Fry, 1995). It is commonly known that during the development of a plant, XTH/Xet is involved in cell wall loosening and expansion as well as improving its rigidity during infection by a pathogen (Rose et al., 2002). The PVY inoculation significantly redirected the deposition of xylan-1/xyloglucan and xyloglucan xyloglucosyl transferase (XTH-Xet5), compared to mock-inoculated tissues (Otulak-Kozieł et al., 2018b). Moreover, immunogold localization showed that Xet5 was dominant in cell wall and its nearby vesicles in the host susceptible to infection. The involvement of xyloglucan endotransglucosylases was also identified in the case of interactions of hosts with potato leafroll virus (DeBlasio et al., 2015) and with papaya meleira virus (Rodrigues et al., 2011).

The rebuilding of the cell wall during the growth and development of the plant cell or during the interaction of a plant with nonviral pathogens in the area associated with extensins and expansins, has been postulated by Marowa et al. (2016). However, Yang et al. (2007) stated that in *Arabidopsis* the patterns of expression of cell wall-related genes, including pectin methylesterase 3 (PME3), expansin 10 (EXP10), and xyloglucan transferase 6 (XTH6), varied based on the areas in which the samples were harvested. The authors also noticed a reduction in mRNA transcript accumulation after infection by turnip mosaic virus (TuMV). In addition, they found that the genes PME3, XTH6, and EXP10 were activated against TuMV after 10 days of inoculation. Moreover, Chen et al. (2018c) proposed that EXPA4 overexpression accelerated the replication of TMV and the development of symptoms in tobacco. Similar conclusions could be drawn based on studies analyzing the role played by extensins and expansins during infection of susceptible potato by PVY^{NTN} (Otulak-Kozieł et al., 2020). Otulak-Kozieł et al. (2020) indicated a remarkable induction of *StEXPA3* and slight induction of *StEXT4* during a susceptible response (**Figure 1**). In addition, the process of cell wall loosening occurred together with an increased deposition of StEXPA glycoproteins and hydroxyproline-rich glycoproteins (HRGPs) in PVY^{NTN}-susceptible potato. Interestingly, the StEXPA signal gradually increased in susceptible PVY^{NTN}-infected potato, unlike the resistance response which is often found within 1–7 days of inoculation in vascular tissues and 14–30 days of inoculation in most of the leaf tissues. In addition, StEXPAs were detected in the symplast of cells, mainly in the epidermal and stomata regions and in vascular bundles, especially in cell walls (Otulak-Kozieł et al., 2020). Furthermore, we showed the presence of StEXPAs in the plasmodesmata during the susceptible reaction as well as near the cytoplasmic inclusions of PVY—distinctive for the Potyvirus group. However, based on the results obtained from the microarray analysis of the expression of cell wall-related genes following RSV infection, Shimizu et al. (2007) reported marked suppression of other groups of extensins—proline-rich glycoproteins and glycine-rich glycoproteins. They concluded that different types of extensins could be up- or downregulated during interaction with different plant viruses.

PLANT CELL WALL AND THE PLANT-VIRUS RESISTANCE RESPONSE

Defense activation during the identification of exogenous or endogenous signals—known as pathogen-associated (PAMPs) and damage-associated molecular patterns (DAMPs), respectively—is the key function of innate immunity in plants (De Lorenzo et al., 2019). Damage detection is essential for plant cell survival. Mechanical damage and infections disturb the homeostatic cellular processes, which are recognized as a threat by plants (De Lorenzo et al., 2019). Perception of "damaged self" occurs independently of the infecting organism. Hence, the induced response may not be particular to a given pathogen (Heil and Land, 2014; De Lorenzo et al., 2019). DAMPs might result from the damage caused to cell structures by injuries and consequently developmental breaks; therefore, they not only protect against infection but also play a crucial role in processes that are not related to pathogens, including tissue injuries and repair (De Lorenzo et al., 2018). DAMPs can be exemplified by oligosaccharides discharged by the cell wall.

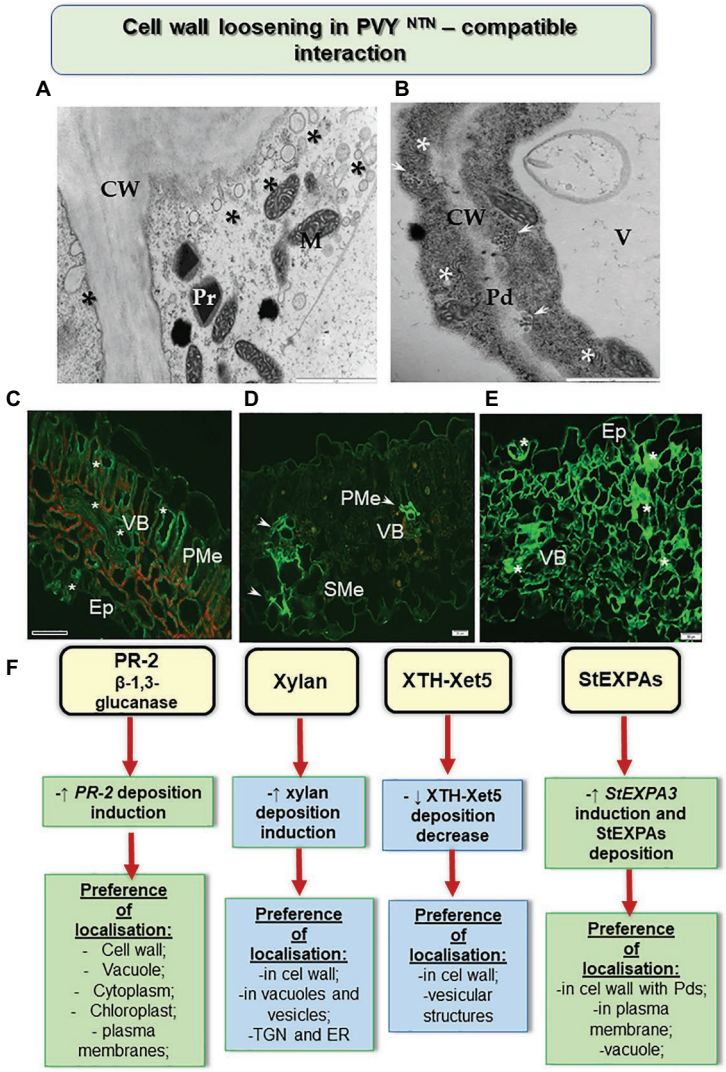

FIGURE 1 | Cell wall loosening in susceptible potato reaction to PVY^{NTN}. **(A)** Loosening of the cell wall structure with the distribution of vesicles (*) as shown by transmission electron microscopic analyses. Bar: 2 μm. **(B)** Paramular bodies (arrows) connected with plasmodesmata in association with viral cytoplasmic inclusion (*). Bar: 2 μm. **(C)** Green fluorescence of PR-2 protein (*) observed in the vascular bundle, palisade mesophyll, and epidermis with stomata in susceptible potato leaf. Bar: 200 μm. **(D)** Fluorescence of xyl-1/xyloglucan observed in vascular bundle (arrows; xylem and phloem) and spongy mesophyll cells after 14 days of inoculation with PVY^{NTN}. Bar: 20 μm. **(E)** StEXPA signal observed in the leaf tissues at 30 days of post inoculation—signals with the highest intensity (*) were observed in cell wall and symplast of necrotizing mesophyll cells, xylem tracheary elements, and stomata. Bar: 50 μm. **(F)** Schematic representation of the distribution changes of selected cell wall components in susceptible potato response to PVY^{NTN}. CW, cell wall; Ep, epidermis; M, mitochondria; Pd, plasmodesmata; PMe, palisade mesophyll; Pr, peroxisome; SMe, spongy mesophyll cells; V, vacuole; VB, vascular bundles. (Based on Otulak-Kozieł et al., 2018a,b, 2020, modified).

The structure of the plant cell wall is closely observed, upon cell wall remodeling. Moreover, it is significantly modified by mechanical injuries or by infection (Ferrari et al., 2013; Bellincampi et al., 2014; Hamann, 2015; De Lorenzo et al., 2019). According to the analyses of Benedetti et al. (2015) and Gramegna et al. (2016), the products resulting from the breakdown of homogalacturonan (HG), such as oligogalacturonides (OGs), are treated as DAMPs produced against microbial attack and as a local signal to repair mechanical damages. Moreover, Savatin et al. (2014) stated that during an infectious event, OGs are produced by the effect of enzymes that degrade microbial pectin. The defense responses are actively induced by OGs consisting of 10–15 residues, whereas shorter oligomers reveal lower activity, according to Davidsson et al. (2017). Cabrera et al. (2008) highlighted that the OGs function maximally when involved in calcium-mediated intermolecular ionic interactions that render these compounds with a conformational state referred to as "egg boxes." Moreover, the extent of HG methyl-esterification or acetylation, which differs in organs during the development of plants, may decide the characteristics of OGs released and their biological activity. As analyzed by Benedetti et al. (2015), average OG accumulation

triggers an appropriate and stable immune response, whereas excess OGs may induce hyper immunity, affecting growth and ultimately leading to cell death.

The PAMP and DAMP response pathways associated with the cell wall were not precisely recognized for plant viral infections. In fact, numerous results indicate that the cell wall is actively modified during a plant resistance response against viral pathogens. Years of plant-virus co-evolution did not only lead to susceptibility but also lead to resistance. Generally, resistance, or high resistance (associated with hypersensitive reaction), results from well-developed and effective defense mechanisms induced to prevent or limit the damage caused by infection by a viral pathogen (Soosaar et al., 2005). Plant resistance genes confer hosts with resistance against various pathogens, including viruses (Soosaar et al., 2005; Hull, 2014). The defense response initiated as a result of the recognition of a specific virus is stereotypical, and the associated cellular and physiological features have been well described by several authors (Soosaar et al., 2005; Hashimoto et al., 2016; Kumar, 2019).

The attribution of the cell wall to the resistance response against plant viruses is a newly emerging concept. Generally, several cell wall mutants or plants treated with cell wall biosynthesis inhibitors have been shown to exhibit a gamut of immune response, including the expression of defense genes and the accumulation of defense compounds, but it is rather limited in the case of plant-virus interactions (Hamann, 2015). The first investigations of plant-virus interactions concerned plasmodesmata. Inhibition of β-1,3 glucanase enzyme led to an elevated deposition of callose in some parts of the cell wall, thereby leading to a reduction in size exclusion limit. As a result, both short- and long-distance transport of CMV, TMV, PVX, and tobacco necrosis virus was reduced (Iglesias and Meins, 2000; Peña and Heinlein, 2012). Plants with suppressed β-1,3 glucanase restricted the access of plant viruses to a limited number of cells, in which it was possible to induce programmed cell death, thus repressing or even stopping virus infection (Iglesias and Meins, 2000). A similar limitation, characteristic of TMV, was observed in potato with a hypersensitive response (HR) against PVY^{NTN} (Otulak-Kozieł et al., 2018a). In this reaction, intense callose deposits were immuno-localized in plasmodesmata, accompanied by lower PR-2 deposition, as compared to the compatible interaction. In this case, PR-2 was mainly transported and deposited in vacuoles rather than in the cell wall. Apparently, potato actively redistributed this protein in the presence of the virus. In addition, resistant tobacco plants (VAM) that were infected with PVY responded with increased deposition of PR protein-related transcripts (Chen et al., 2016). On the other hand, the data presented by Lionetti et al. (2014) indicated the role of pectin methylotransferase inhibition in viral transport and plant resistance in *Arabidopsis thaliana* and *Nicotiana tabacum*. The authors showed that the overexpression of genes encoding pectin methylesterase inhibitors in *Nicotiana tabacum* and *Arabidopsis thaliana* from *Actinidia chinensis* generated some level of resistance and limited the transport of two different plant viruses namely TMV and turnip vein-clearing virus.

Moreover, the HR reaction of potato to PVY^{NTN} infection also led to changes in other components of cell walls (**Figure 2**; Otulak-Kozieł et al., 2018a,b, 2020). This included a decrease in the level of the catalytic subunit of cellulase synthase—CesA4. These changes were more intense than those observed in susceptible potato, and caused rebuilding of cell wall ultrastructure, resulting in a reinforced/thicker cell wall. In many cases of reinforced cell walls, phenolic compounds were also deposited. Otulak-Kozieł et al. (2019) postulated that respiratory burst oxidase homolog D (RbohD) and H_2O_2 were vital components of the resistance response in cell wall remodeling in potato-PVY pathosystem. Similarly, the reinforced cell wall and the role of H_2O_2 were suggested in the cases of immunity such as the reaction of quinoa to PDV (Kozieł et al., 2020). Along these lines, Zheng et al. (2013) showed that the HR response to RSV was associated with cell wall functions. The authors indicated that changes in peroxidase biosynthesis, glycine-rich cell wall structural protein, cellulose synthase, and XTH/Xet strengthened the physical barriers of rice against RSV. The role of xyloglucans in cell wall remodeling in HR was supported by the results of Otulak-Kozieł et al. (2018b). It was ascertained that during HR, the xylan content decreased but the levels of XTH-Xet5 increased (engaged in xyloglucan metabolism) in cell wall, cytoplasm, and the trans-Golgi network. Therefore, we postulated that the HR activated XTH-Xet5 in areas where xyloglucan endotransglucosylase is synthesized, and later the enzyme was transported to components such as cell wall, cytoplasm, and vacuoles. These findings were similar to those reported by Chen et al. (2016). Hypersensitive reaction is also associated with structural and modified cell wall proteins such as expansins and extensins. Park et al. (2017) showed in *Nicotiana benthamiana* that the absence of expansin A1 (*EXPA1*) gene leads to resistance against TuMV. Otulak-Kozieł et al. (2020) indicated that the *StEXT4* gene is often gradually activated and *StEXPA3* is repressed during HR against PVY^{NTN}. They demonstrated that the levels of StEXPAs in cell walls decreased, while the content of HRGPs dynamically increased in the reinforced cell walls; the HRGP extensins accumulated mainly in apoplast, but they were also observed to be deposited in the symplast in the case of resistant plants. Thus, we conclude that changes in the intracellular distribution of HRGPs and StEXPAs are differentially controlled based on the type of PVY^{NTN}-potato interactions. These observations confirm that apoplast as well as symplast is involved in defense response mechanisms.

FUTURE PROSPECTS

Plant cell wall performs a number of important functions in the cell. So far, the structural properties and composition of the cell wall as well as its involvement in the interaction of plants with bacterial and fungal pathogens have been well described. However, modifications occurring in the cell wall during viral infection remain poorly understood. This review presents recent interesting insights into the role the cell wall plays in compatible (susceptible) and incompatible (resistance)

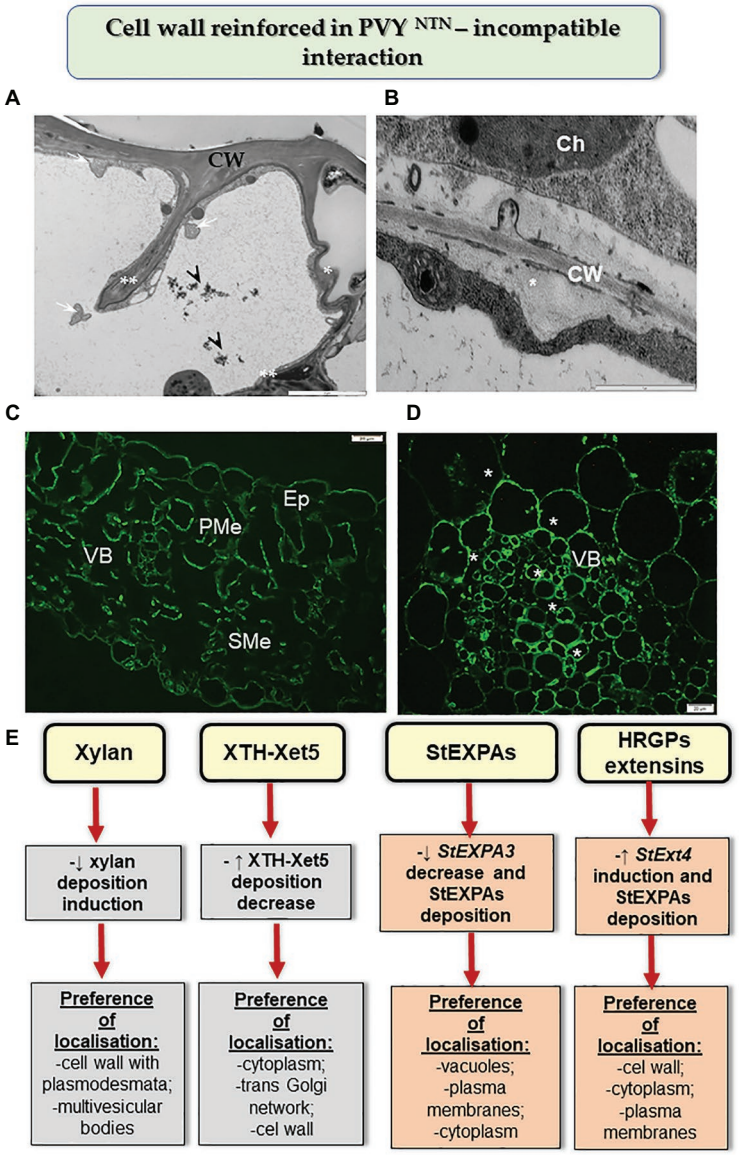

FIGURE 2 | Cell wall reinforced in resistance potato reaction to PVY^{NTN}. **(A)** Folded (*) and invaginated cell wall (**) observed in the epidermis during HR. Phenolic compounds (arrowhead) and multivesicular bodies (arrows) found in a vacuole. Bar: 2 μm. **(B)** Deposition of callose material (*) between plasma membrane and cell wall in mesophyll cells during HR. Bar: 1 μm. **(C)** Fluorescence detection of XTH-Xet5 in leaflet tissues after 10 days of PVY inoculation. Bar: 20 μm. **(D)** HRGP extensin signal (*) observed in the vascular bundle at 14 days post inoculation in hypersensitive potato response to PVY^{NTN}. Bar: 20 μm. **(E)** Schematic representation of the distribution changes of selected cell wall components in resistance potato response to PVY^{NTN}. Ch, chloroplast; CW, cell wall; Ep, epidermis; PMe, palisade mesophyll cells; SMe, spongy mesophyll cells; VB, vascular bundles. (Based on Otulak-Kozieł et al., 2018a,b, 2020, modified).

reactions. Significant progress has been made in identifying the important components of the cell wall. Results have shown that changes observed in the intracellular dissemination and accumulation of β-1,3 glucanase, components of hemicellulosic cell wall matrix, and cell wall structural and modifying proteins such as expansins, HRGPs, and extensins might be differentially controlled, based on the type of plant-virus interactions, leading to cell wall loosening or the appearance of a reinforced cell wall. This confirms that apoplast as well as symplast is activated as a mechanism of the defense response.

This research topic is promising and provides a better understanding of the multilevel complex network of plant responses to viruses. Further analysis of the functions of specific plant cell components is necessary to establish the regulatory pathways involved in communication between the plant and viral pathogen. This can be possible with the use of tools such as atomic force microscopy (AFM). AFM images can show, at the nanometer scale, the heterogeneity of the cell wall as well as the spatial distribution of both soft and rigid polymers of the cell wall matrix (Gierlinger, 2018). AFM can

be employed together with electron tomography to study the cell wall in mutants, for example, of cellulose synthase in the infected plants. Extensive computational simulations of mechanical properties may reveal the three-dimensional organization of the cell wall during interactions (Otegui and Pennington, 2019). Furthermore, spectroscopic techniques (such as confocal Raman spectroscopy) may non-disruptively indicate the cell wall structures and also be applied as a high-throughput method to describe the phenotypes of cell wall mutants. Transgenic/mutant plants are formed as a result of the generation of resistance to plant pathogens based on changes in cell wall-associated elements (Moscetti et al., 2013; Ferrari et al., 2014; Lionetti et al., 2014; Woo et al., 2014). Insertion of polygalacturonase-inhibiting proteins from bean and overexpression of natural wheat xylanase inhibitor TAXI-III induced resistance in wheat against *Fusarium graminearum* (Moscetti et al., 2013; Ferrari et al., 2014). Mutants or overexpression lines with lignin modification have been analyzed by many researchers, and they seem to play an important role in the pathogen resistance—as a passive or active regulatory component of immune response, such as in the case of cotton resistance to wilt (*Verticillium dahliae*) as presented by Xu et al. (2011) and Shi et al. (2012). Several examples of cell wall change-mediated immune reaction in genetically engineered plants have been reviewed in detail by Miedes et al. (2014), Smirnova and Kochotev (2016), and Bacete et al. (2018). The promising techniques for the generation of cell wall mutants include the T-DNA insertions, TILLING lines, and especially CRISPR/Cas9 lines, where crucial cell wall components and genes are blocked or overexpressed. In particular, the CRISPR/Cas9 system may provide an insight into the genetic control of the structure and functions of plant cell wall (Whitehead et al., 2018; Cao et al., 2020; McCarty et al., 2020). At present, these methods are generally used in studies focusing on cell wall synthesis pathways (including enzymes) and analyzing the exact functions of cell wall elements (Zhang and Showalter, 2020) for the improvement of crop products (Wang C. et al., 2019; Wang D. et al., 2019). However, Makarova et al. (2018) indicated the application of the CRISPR/Cas9 system for generating plant resistance (not precisely associated with cell wall) against various pathogens. Such studies can allow for a better understanding of the processes involved in the communication of the plant cell with viruses.

AUTHOR CONTRIBUTIONS

EK and KO-K conceived the project, analyzed data, and participated in writing the manuscript. JB analyzed data and helped with critical comments of the manuscript. All authors contributed to the article and approved the submitted version.

FUNDING

The work was conducted during the realization of a project financed by the National Science Center, Poland; NCN project decision number: 2019/03/X/NZ9/00499 given to EK and 2018/02/X/NZ9/00832 given to KO-K. Partial support for this investigation was also provided by the Statutory research fund of the Institute of Biology, Department of Botany (Warsaw University of Life Sciences-SGGW).

ACKNOWLEDGMENTS

We would like to express sincere thanks to Frederick Fenter and Frontiers Editorial Team for the discount opportunity.

REFERENCES

Allie, F., Pierce, E. J., Okoniewski, M. J., and Rey, C. (2014). Transcriptional analysis of South African cassava mosaic virus-infected susceptible and tolerant landraces of cassava highlights differences in resistance, basal defense and cell wall associated genes during infection. *BMC Genomics* 15:1006. doi: 10.1186/1471-2164-15-1006

Bacete, L., Mélida, H., Miedes, E., and Molina, A. (2018). Plant cell wall-mediated immunity: cell wall changes trigger disease resistance responses. *Plant J.* 93, 614–636. doi: 10.1111/tpj.13807

Beffa, R., and Meins, F. J. (1996). Pathogenesis-related functions of plant beta-1,3-glucanases investigated by antisense transformation—a review. *Gene* 179, 97–103. doi: 10.1016/S0378-1119(96)00421-0

Bellincampi, D., Cervone, F., and Lionetti, V. (2014). Plant cell wall dynamics and wall-related susceptibility in plant-pathogen interactions. *Front. Plant Sci.* 5:228. doi: 10.3389/fpls.2014.00228

Benedetti, M., Pontiggia, D., Raggi, S., Cheng, Z., Scaloni, F., Ferrari, S., et al. (2015). Plant immunity triggered by engineered in vivo release of oligogalacturonides, damage-associated molecular patterns. *Proc. Natl. Acad. Sci. U. S. A.* 112, 5533–5538. doi: 10.1073/pnas.1504154112

Broxterman, S. E., and Schols, H. A. (2018). Interactions between pectin and cellulose in primary plant cell walls. *Carbohydr. Polym.* 192, 263–272. doi: 10.1016/j.carbpol.2018.03.070

Bucher, G. L., Tarina, C., Heinlein, M., Di Serio, F., Meins, F. J., and Iglesias, V. A. (2001). Local expression of enzymatically active class I beta-1,3-glucanase enhances symptoms of TMV infection in tobacco. *Plant J.* 28, 361–369. doi: 10.1046/j.1365-313X.2001.01181.x

Cabrera, J. C., Boland, A., Messiaen, J., Cambier, P., and Van Cutsem, P. (2008). Egg box conformation of oligogalacturonides: the time-dependent stabilization of the elicitor-active conformation increases its biological activity. *Glycobiology* 18, 473–482. doi: 10.1093/glycob/cwn027

Cao, Y., Zhou, H., Zhaou, X., and Li, F. (2020). Control of plant viruses by CRISPR/Cas system-mediated adaptive immunity. *Front. Microbiol.* 11:593700. doi: 10.3389/fmicb.2020.593700

Chen, S., Li, F., Liu, D., Jiang, C., Cui, L., Shen, L., et al. (2016). Dynamic expression analysis of early response genes induced by potato virus Y in PVY-resistant *Nicotiana tabacum*. *Plant Cell Rep.* 36, 297–311. doi: 10.1007/s00299-016-2080-1

Chen, H. W., Persson, S., Grebe, M., and McFarlane, H. E. (2018a). Cellulose synthesis during cell plate assembly. *Physiol. Plant.* 164, 17–26. doi: 10.1111/ppl.12703

Chen, L. J., Zou, W. S., Fei, C. Y., Wu, G., Li, X. Y., Lin, H. H., et al. (2018b). α-Expansin EXPA4 positively regulates abiotic stress tolerance but negatively regulates pathogen resistance in *Nicotiana tabacum*. *Plant Cell Physiol.* 59, 2317–2330. doi: 10.1093/pcp/pcy155

Chen, L. J., Zou, W. S., Wu, G., Lin, H. H., and Xi, D. H. (2018c). Tobacco alpha-expansin EXPA4 plays a role in Nicotiana benthamiana defense against Tobacco mosaic virus. *Planta* 247, 355–368. doi: 10.1007/s00425-017-2785-6

Cosgrove, D. J. (2018). Diffuse growth of plant cell walls. *Plant Physiol.* 176, 16–27. doi: 10.1104/pp.17.01541

Davidsson, P., Broberg, M., Kariola, T., Sipari, N., Pirhonen, M., and Palva, E. T. (2017). Short oligogalacturonides induce pathogen resistance-associated gene expression in *Arabidopsis thaliana*. *BMC Plant Biol.* 17:19. doi: 10.1186/s12870-016-0959-1

DeBlasio, S. L., Johnson, R., Mahoney, J., Karasev, A., Gray, S. M., MacCoss, M. J., et al. (2015). Insights into the Polerovirus-plant interactome revealed by coimmunoprecipitation and mass spectrometry. *Mol. Plant-Microbe Interact.* 28, 467–481. doi: 10.1094/MPMI-11-14-0363-R

De Lorenzo, G., Ferrari, S., Cervone, F., and Okun, E. (2018). Extracellular DAMPs in plants and mammals: immunity, tissue damage and repair. *Trends Immunol.* 39, 937–950. doi: 10.1016/j.it.2018.09.006

De Lorenzo, G., Ferrari, S., Giovannoni, M., Mattei, B., and Cervone, F. (2019). Cell wall traits that influence plant development, immunity, and bioconversion. *Plant J.* 97, 134–147. doi: 10.1111/tpj.14196

Ding, X., Cao, Y., Huang, L., Zhao, J., Xu, C., Li, X., et al. (2008). Activation of the indole-3-acetic acid-amido synthetase GH3-8 suppresses expansin expression and promotes salicylate- and jasmonate-independent basal immunity in rice. *Plant Cell* 20, 228–240. doi: 10.1105/tpc.107.055657

Ferrari, S., Savatin, D. V., Sicilia, F., Gramegna, G., Cervone, F., and Lorenzo, G. D. (2013). Oligogalacturonides: plant damage-associated molecular patterns and regulators of growth and development. *Front. Plant Sci.* 4:49. doi: 10.3389/fpls.2013.00049

Ferrari, S., Sella, L., Janni, M., De Lorenzo, G. D., Favaron, F., and D'Ovidio, R. (2014). Transgenic expression of polygalacturonase-inhibiting proteins in *Arabidopsis* and wheat increases resistance to the flower pathogen *Fusarium graminearum*. *Plant Biol.* 14, 31–38. doi: 10.1111/j.1438-8677.2011.00449.x

Fry, S. C. (1995). Polysaccharide-modifying enzymes in the plant cell wall. *Annu. Review* 46, 497–520. doi: 10.1146/annurev.pp.46.060195.002433

Garcia-Ruiz, H. (2018). Susceptibility genes to plant viruses. *Viruses* 10:484. doi: 10.3390/v10090484

Garcia-Ruiz, H. (2019). Host factors against plant viruses. *Mol. Plant Pathol.* 20, 1588–1601. doi: 10.1111/mpp.12851

Gergerich, R. C., and Dolja, V. V. (2006). Introduction to plant Viruses, the invisible foe. *Plant Health Instr.* 414:1. doi: 10.1094/PHI-I-2006-0414-01

Gierlinger, N. (2018). New insights into plant cell walls by vibrational microspectroscopy. *Appl. Spectrosc. Rev.* 53, 517–551. doi: 10.1080/05704928.2017.1363052

Gramegna, G., Modesti, V., Savatin, D. V., Sicilia, F., Cervone, F., and De Lorenzo, G. (2016). GRP-3 and KAPP, encoding interactors of WAK1, negatively affect defense responses induced by oligogalacturonides and local response to wounding. *J. Exp. Bot.* 67, 1715–1729. doi: 10.1093/jxb/erv563

Hamann, T. (2015). The plant cell wall integrity maintenance mechanism–a case study of a cell wall plasma membrane signaling network. *Phytochemistry* 112, 100–109. doi: 10.1016/j.phytochem.2014.09.019

Hashimoto, M., Neriya, Y., Yamaji, Y., and Namba, S. (2016). Recessive resistance to plant viruses: potential resistance genes beyond translation initiation factors. *Front. Microbiol.* 7:1695. doi: 10.3389/fmicb.2016.01695

Heil, M., and Land, W. G. (2014). Danger signals - damaged-self recognition across the tree of life. *Front. Plant Sci.* 5:578. doi: 10.3389/fpls.2014.00578

Hull, R. (2014). *Plant. Virology*. London: Elsevier Academic Press.

Iglesias, V. A., and Meins, F. J. (2000). Movement of plant viruses is delayed in a beta-1,3-glucanase-deficient mutant showing a reduced plasmodesmatal size exclusion limit and enhanced callose deposition. *Plant J.* 21, 157–166. doi: 10.1046/j.1365-313x.2000.00658.x

Jin, X., Cao, X., Wang, X., Jiang, J., Wan, J., Laliberté, J. -F., et al. (2018). Three-dimensional architecture and biogenesis of membrane structures associated with plant virus replication. *Front. Plant Sci.* 9:57. doi: 10.3389/fpls.2018.00057

Jones, J. D., and Dangl, J. L. (2006). The plant immune system. *Nature* 444, 323–329. doi: 10.1038/nature05286

Kauss, H. (1996). "Callose synthesis" in *Membranes: Specialized Function in Plants*. eds. M. Smallwood, J. P. Knox and D. J. Bowles (Oxford: BIOS Scientific), 77–92.

Kozieł, E., Otulak-Kozieł, E., and Bujarski, J. J. (2020). Modifications in tissue and cell ultrastructure as elements of immunity-like reaction in *Chenopodium quinoa* against Prune dwarf virus (PDV). *Cell* 9:148. doi: 10.3390/cells9010148

Kumar, V. A. (2019). Plant antiviral immunity against Geminiviruses and viral counter-defense for survival. *Front. Microbiol.* 10:1460. doi: 10.3389/fmicb.2019.01460

Lionetti, V., Raiola, A., Cervone, F., and Bellincampi, D. (2014). Transgenic expression of pectin methylesterase inhibitors limits tobamovirus spread in tobacco and *Arabidopsis*. *Mol. Plant Pathol.* 15, 265–274. doi: 10.1111/mpp.12090

Liu, Q., Luo, L., and Zheng, L. (2018). Lignins: biosynthesis and biological functions in plants. *Int. J. Mol. Sci.* 19:335. doi: 10.3390/ijms19020335

Lotan, T., and Fluhr, R. (1990). Xylanase, a novel elicitor of pathogenesis-related proteins in tobacco, uses a non-ethylene pathway for induction. *Plant Physiol.* 93, 811–817. doi: 10.1104/pp.93.2.811

Makarova, S. S., Khromov, A. V., Spechenkova, N. A., Taliansky, M. E., and Kalinin, N. O. (2018). Application of the CRISPR/Cas system for generation of pathogen-resistant plants. *Biochem. Mosc.* 83, 1552–1562. doi: 10.1134/S0006297918120131

Mandadi, K. K., and Scholthof, K. B. G. (2013). Plant immune responses against viruses: how does a virus cause disease? *Plant Cell* 25, 1489–1505. doi: 10.1105/tpc.113.111658

Marowa, P., Ding, A., and Kong, Y. (2016). Expansins: roles in plant growth and potential applications in crop improvement. *Plant Cell Rep.* 35, 945–965. doi: 10.1007/s00299-016-1948-4

McCarty, N. S., Graham, A. E., Studená, L., and Ledesma-Amaro, R. (2020). Multiplexed CRISPR technologies for gene editing and transcriptional regulation. *Nat. Commun.* 11:1281. doi: 10.1038/s41467-020-15053-x

Meents, M. J., Watanabe, Y., and Samuels, A. L. (2018). The cell biology of secondary cell wall biosynthesis. *Ann. Bot.* 121, 1107–1125. doi: 10.1093/aob/mcy005

Miedes, E., Vanholme, R., Boerjan, W., and Molina, A. (2014). The role of the secondary cell wall in plant resistance to pathogens. *Front. Plant Sci.* 5:358. doi: 10.3389/fpls.2014.00358

Moscetti, I., Tundo, S., Janni, M., Sella, L., Gazzetti, K., Tauzin, A., et al. (2013). Constitutive expression of the xylanase inhibitor TAXI-III delays Fusarium head blight symptoms in durum wheat transgenic plants. *Mol. Plant-Microbe Interact.* 26, 1464–1472. doi: 10.1094/MPMI-04-13-0121-R

Otegui, M. S., and Pennington, J. G. (2019). Electron tomography in plant cell biology. *Microscopy* 68, 69–79. doi: 10.1093/jmicro/dfy133

Otulak-Kozieł, K., Kozieł, E., and Bujarski, J. J. (2018b). Spatiotemporal changes in xylan-1/xyloglucan and xyloglucan xyloglucosyl transferase (XTH-Xet5) as a step-in of ultrastructural cell wall remodeling in potato–Potato Virus Y (PVY^{NTN}) hypersensitive and susceptible reaction. *Int. J. Mol. Sci.* 19:2287. doi: 10.3390/ijms19082287

Otulak-Kozieł, K., Kozieł, E., and Lockhart, B. E. L. (2018a). Plant cell wall dynamics in compatible and incompatible potato response to infection caused by Potato Virus Y (PVY^{NTN}). *Int. J. Mol. Sci.* 19:862. doi: 10.3390/ijms19030862

Otulak-Kozieł, K., Kozieł, E., Lockhart, B. E. L., and Bujarski, J. J. (2020). The expression of potato expansin A3 (StEXPA3) and extensin4 (StEXT4) genes with distribution of StEXPAs and HRGPs-extensin changes as an effect of cell wall rebuilding in two types of PVY^{NTN}–*Solanum tuberosum* interactions. *Viruses* 12:66. doi: 10.3390/v12010066

Otulak-Kozieł, K., Kozieł, E., and Valverde, R. A. (2019). The respiratory burst oxidase homolog d (rbohd) cell and tissue distribution in potato–potato virus y (PVY^{NTN}) hypersensitive and susceptible reactions. *Int. J. Mol. Sci.* 20:2741. doi: 10.3390/ijms20112741

Park, S. H., Li, F., Renaud, J., Shen, W., Li, Y., Guo, L., et al. (2017). NbEXPA1, an α-expansin, is plasmodesmata-specific and a novel host factor for potyviral infection. *Plant J.* 92, 846–861. doi: 10.1111/tpj.13723

Pauly, M., Gille, S., Liu, L., Mansoori, N., de Souza, A., Schultink, A., et al. (2013). Hemicellulose biosynthesis. *Planta* 238, 627–642. doi: 10.1007/s00425-013-1921-1

Peña, E. J., and Heinlein, M. (2012). RNA transport during TMV cell-to-cell movement. *Front. Plant Sci.* 3:193. doi: 10.3389/fpls.2012.00193

Raggi, V. (2000). Hydroxyproline-rich glycoprotein accumulation in tobacco leaves protected against Erysiphe cichoracearum by potato virus Y infection. *Plant Pathol.* 49, 179–186. doi: 10.1046/j.1365-3059.2000.00442.x

Rodrigues, S. P., Ventura, J. A., Aguilar, C., Nakayasu, E. S., Almeida, I. C., Fernandes, P. M., et al. (2011). Proteomic analysis of papaya (*Carica papaya* L.) displaying typical sticky disease symptoms. *Proteomics* 11, 2592–2602. doi: 10.1002/pmic.201000757

Rose, J. K. C., Braam, J., Fry, S. C., and Nishitani, K. (2002). The XTH family of enzymes involved in xyloglucan endotransglucosylation and endohydrolysis: Current perspectives and a new unifying nomenclature. *Plant Cell Physiol.* 43, 1421–1435. doi: 10.1093/pcp/pcf171

Savatin, D. V., Gramegna, G., Modesti, V., and Cervone, F. (2014). Wounding in the plant tissue: the defense of a dangerous passage. *Front. Plant Sci.* 5:470. doi: 10.3389/fpls.2014.00470

Shi, H., Liu, Z., Zhu, L., Zhang, C., Chen, Y., Zhou, Y., et al. (2012). Over-expression of cotton (*Gossypium hirsutum*) dirigent 1 gene enhances lignification that blocks the spread of *Verticillium dahlia*. *Acta Biochim. Biophys. Sin.* 44, 555–564. doi: 10.1093/abbs/gms035

Shimizu, T., Ogamino, T., Hiraguri, A., Nakazono-Nagaoka, E., Uehara-Ichiki, T., Nakajima, M., et al. (2013). Strong resistance against Rice grassy stunt virus is induced in transgenic rice plants expressing double-stranded RNA of the viral genes for nucleocapsid or movement proteins as targets for RNA interference. *Phytopathology* 103, 513–519. doi: 10.1094/PHYTO-07-12-0165-R

Shimizu, T., Satoh, K., Kikuchi, S., and Omura, T. (2007). The repression of cell wall and plastid-related genes and the induction of defense-related genes in rice plants infected with Rice dwarf virus. *Mol. Plant-MiCcrobe Interact.* 20, 247–254. doi: 10.1094/MPMI-20-3-0247

Smirnova, O. G., and Kochetov, A. V. (2016). Plant cell wall and mechanisms of resistance to pathogens. *Russ. J. Genet. Appl. Res.* 6, 622–631. doi: 10.1134/S2079059716050130

Soosaar, J. L. M., Burch-Smitch, T. M., and Dinesh-Kumar, S. P. (2005). Mechanisms of plant resistance to viruses. *Nat. Rev. Microbiol.* 3, 789–798. doi: 10.1038/nrmicro1239

Underwood, W. (2012). The plant cell wall: a dynamic barrier against pathogen invasion. *Front. Plant Sci.* 3:85. doi: 10.3389/fpls.2012.00085

Voiniciuc, C., Pauly, M., and Usadel, B. (2018). Monitoring polysaccharide dynamics in the plant cell wall. *Plant Physiol.* 176, 2590–2600. doi: 10.1104/pp.17.01776

Wang, C., Liu, Q., Shen, Y., Hua, Y., Wang, J., Lin, J., et al. (2019). Clonal seeds from hybrid rice by simultaneous genome engineering of meiosis and fertilization genes. *Nat. Biotechnol.* 37, 283–286. doi: 10.1038/s41587-018-0003-0

Wang, D., Samsulrizal, N. H., Yan, C., Allcock, N. S., Craigon, J., Blanco-Ulate, B., et al. (2019). Characterization of CRISPR mutants targeting genes modulating pectin degradation in ripening tomato. *Plant Physiol.* 179, 544–557. doi: 10.1104/pp.18.01187

Whitehead, C., Ostos Garrido, F. J., Reymond, M., Simister, R., Distelfeld, A., Atienza, S. G., et al. (2018). A glycosyl transferase family 43 protein involved in xylan biosynthesis is associated with straw digestibility in *Brachypodium distachyon*. *New Phytol.* 218, 974–985. doi: 10.1111/nph.15089

Woo, M. O., Beard, H., MacDonald, M. H., Brewer, E. P., Youssef, R. M., Kim, H., et al. (2014). Manipulation of two α-endo-β-1,4-glucanase genes, AtCel6 and GmCel7, reduces susceptibility to *Heterodera glycines* in soybean roots. *Mol. Plant Pathol.* 15, 927–939. doi: 10.1111/mpp.12157

Xu, L., Zhu, L., Tu, L., Liu, L., Yuan, D., Jin, L., et al. (2011). Lignin metabolism has a central role in the resistance of cotton to the wilt fungus *Verticillium dahlia* as revealed by RNA-Seq-dependent transcriptional analysis and histochemistry. *J. Exp. Bot.* 62, 5607–5621. doi: 10.1093/jxb/err245

Yang, C., Guo, R., Jie, F., Nettleton, D., Peng, J., Carr, T., et al. (2007). Spatial Analysis of *Arabidopsis thaliana* Gene Expression in Response to Turnip mosaic virus Infection. *Mol. Plant-Microbe Interact.* 20, 358–370. doi: 10.1094/MPMI-20-4-0358

Zhang, Y., and Showalter, A. M. (2020). CRISPR/Cas9 genome editing technology: a valuable tool for understanding plant cell wall biosynthesis and function. *Front. Plant Sci.* 11:589517. doi: 10.3389/fpls.2020.589517

Zheng, W., Ma, L., Zhao, J., Li, Z., Sun, F., and Lu, X. (2013). Comparative transcriptome analysis of two rice varieties in response to Rice Stripe Virus and small brown Planthoppers during early interaction. *PLoS One* 8:e82126. doi: 10.1371/journal.pone.0082126

Conflict of Interest: The authors declare that the research was conducted in the absence of any commercial or financial relationships that could be construed as a potential conflict of interest.

frontiers in Microbiology

ORIGINAL RESEARCH
published: 22 March 2021
doi: 10.3389/fmicb.2021.645530

The P1 Protein of *Watermelon mosaic virus* Compromises the Activity as RNA Silencing Suppressor of the P25 Protein of *Cucurbit yellow stunting disorder virus*

*Maria Luisa Domingo-Calap[1,2], Ornela Chase[1], Mariona Estapé[1,3], Ana Beatriz Moreno[1] and Juan José López-Moya[1,4]**

[1]Centre for Research in Agricultural Genomics (CRAG), CSIC-IRTA-UAB-UB, Campus UAB Bellaterra, Barcelona, Spain, [2]Instituto Valencia de Investigaciones Agrarias, IVIA, Valencia, Spain, [3]Universitair Medisch Centrum, UMC, Utrecht, Netherlands, [4]Consejo Superior de Investigaciones Científicas (CSIC), Barcelona, Spain

Mixed viral infections in plants involving a potyvirus and other unrelated virus often result in synergistic effects, with significant increases in accumulation of the non-potyvirus partner, as in the case of melon plants infected by the potyvirus *Watermelon mosaic virus* (WMV) and the crinivirus *Cucurbit yellow stunting disorder virus* (CYSDV). To further explore the synergistic interaction between these two viruses, the activity of RNA silencing suppressors (RSSs) was addressed in transiently co-expressed combinations of heterologous viral products in *Nicotiana benthamiana* leaves. While the strong RSS activity of WMV Helper Component Proteinase (HCPro) was unaltered, including no evident additive effects observed when co-expressed with the weaker CYSDV P25, an unexpected negative effect of WMV P1 was found on the RSS activity of P25. Analysis of protein expression during the assays showed that the amount of P25 was not reduced when co-expressed with P1. The detrimental action of P1 on the activity of P25 was dose-dependent, and the subcellular localization of fluorescently labeled variants of P1 and P25 when transiently co-expressed showed coincidences both in nucleus and cytoplasm. Also, immunoprecipitation experiments showed interaction of tagged versions of the two proteins. This novel interaction, not previously described in other combinations of potyviruses and criniviruses, might play a role in modulating the complexities of the response to multiple viral infections in susceptible plants.

Keywords: RNA silencing suppression, watermelon mosaic potyvirus, cucurbit yellow stunting disease crinivirus, plant virus mixed infection, virus pathogenesis in plants

OPEN ACCESS

Edited by:
Rajarshi Kumar Gaur, Deen Dayal Upadhyay Gorakhpur University, India

Reviewed by:
Chrisa Orfanidou, Aristotle University of Thessaloniki, Greece
Narayan Rishi, Amity University, India

***Correspondence:**
Juan José López-Moya
juanjose.lopez@cragenomica.es

Specialty section:
This article was submitted to Virology, a section of the journal Frontiers in Microbiology

Received: *23 December 2020*
Accepted: *02 March 2021*
Published: *22 March 2021*

Citation:
Domingo-Calap ML, Chase O, Estapé M, Moreno AB and López-Moya JJ (2021) The P1 Protein of Watermelon mosaic virus Compromises the Activity as RNA Silencing Suppressor of the P25 Protein of Cucurbit yellow stunting disorder virus. Front. Microbiol. 12:645530. doi: 10.3389/fmicb.2021.645530

INTRODUCTION

The simultaneous presence of two unrelated viruses in mixed-infected plants can lead to different outcomes, including synergisms, antagonisms, and neutral interactions (Syller, 2012; Syller and Grupa, 2016; Moreno and López-Moya, 2020). Despite being a situation common in natural conditions, our knowledge of the interactions taking place in mixed infections is still rather limited, even for those combinations that cause plant diseases with more than one etiological viral agent. Particularly unknown is how the virus-virus interactions could influence pathogenicity and condition the ecology and evolution of viruses, even resulting in generation of new variants or shaping the genetic structure of viral populations (Tollenaere et al., 2016; Alcaide et al., 2020). Hence, a better knowledge of virus-virus interactions during mixed infections might be valuable for deploying efficient and durable virus control strategies (Syller, 2012; Wu et al., 2019).

Although the outcome of a mixed infection is difficult to predict in general, synergistic interactions are often expected when one of the partners is a potyvirus, assuming that the other unrelated virus would be "assisted" by the potyvirus. Initially characterized for the potyvirus *Potato virus Y* and the potexvirus *Potato virus X* (Damirdagh and Ross, 1967; Vance, 1991), the interactions of potyviruses and unrelated viruses produced outcomes remarkably coincidental in many cases (Taiwo et al., 2007; Zeng et al., 2007; Mascia et al., 2010). The identification of the potyviral Helper Component Proteinase (HCPro) as a candidate RNA silencing suppressor (RSS) (Anandalakshmi et al., 1998; Kasschau and Carrington, 1998) provided a sort of mechanistic model to explain the outcome, but the multifunctional nature of HCPro, including the complexities of its activity as RSS (Lakatos et al., 2006; Valli et al., 2018) makes specially challenging to reveal the underlying molecular aspects. Most of the interactions involving a potyvirus and an unrelated virus have been described only partially, mainly attending to the macroscopic and visible outcomes, likely leaving many unexplored molecular mechanisms. Indeed, the simplistic view in which a potent RSS would always work in a pro-viral direction for other viruses might not respond to the underlying complexities of these interactions. Interestingly, one remarkable exception to the potyvirus-assisted synergistic interactions was reported in sweet potato crops, where the potyvirus partners were benefited in co-infections with the crinivirus *Sweet potato chlorotic stunt virus* (SPCSV; Tairo et al., 2005; Untiveros et al., 2007; Clark et al., 2012). For this exception, a gene product different of HCPro, the P1N-PISPO, was associated to RSS activity in the potyvirus *Sweet potato feathery mottle virus* (SPFMV; Mingot et al., 2016; Untiveros et al., 2016).

In the present work, we have considered the mixed infection of the potyvirus *Watermelon mosaic virus* (WMV) and the crinivirus *Cucurbit yellow stunting disorder virus* (CYSDV). These two viruses belong to different taxonomic families, *Potyviridae* (Wylie et al., 2017) and *Closteroviridae* (Fuchs et al., 2020), they are transmitted by different vectors, but they are commonly found together in melon and other cucurbits, causing high production losses (Juarez et al., 2013). WMV is a widely spread aphid-transmitted potyvirus with the usual genomic and biological characteristics of the genus (Revers and García, 2015; Valli et al., 2015; Gibbs et al., 2020), and a remarkable natural variability (Moreno et al., 2004; Desbiez et al., 2011; Verma et al., 2020). CYSDV is a whitefly-transmitted crinivirus (Abrahamian and Abou-Jawdah, 2014; Wintermantel et al., 2017), and less widespread than WMV although lately it is becoming an emergent problem together with other whitefly-transmitted viruses (Navas-Castillo et al., 2011, 2014). We have already characterized the dynamic accumulation of these two partner viruses in melon and explored how that influences their vector-mediated dissemination (Domingo-Calap et al., 2020), although many molecular details of their interaction remained unaddressed, such as those dealing with RNA silencing processes.

To infect a host plant, viruses need to counteract its RNA silencing mechanism, considered an innate immune response (Voinnet, 2001; Baulcombe, 2004), by producing suppressor proteins that target different steps of the pathway to block this antiviral response (Csorba et al., 2015). In CYSDV, the role of RSS is associated to P25 (Kataya et al., 2009), and in WMV, we hypothesized that it might reside in HCPro, as this is the most common RSS in many other potyviruses (Valli et al., 2018). This assumption about WMV HCPro acting as RSS was confirmed experimentally for the first time in the present study.

To further explore virus-virus interactions in mixed infections of WMV and CYSDV, we decided to focus on their RNA silencing suppression machinery. In addition to the known RSSs, other viral gene products that might participate in the activity have been selected. For instance, the rather variable P1 of potyviruses (Valli et al., 2007; Shan et al., 2015) that has been considered a modulator of RSS in several viruses (Fernández et al., 2013; Pasin et al., 2014) and the P22 of CYSDV, the gene product downstream of the P25 region in the RNA1, located in a position where other criniviruses encode proteins involved in this function (Kreuze et al., 2005; Cañizares et al., 2008; Weinheimer et al., 2015; Kubota and Ng, 2016; Chen et al., 2019; Orfanidou et al., 2019).

In this study, thematically independent of our previous publication on the same mixed infection of WMV and CYSDV in melon (Domingo-Calap et al., 2020), we report an unexpected and dose-dependent negative effect of WMV P1 on the RNA silencing suppression activity of CYSDV P25 when co-expressed in a transient assay in *Nicotiana benthamiana*, and discuss its possible contribution to the complex virus-virus interactions during mixed infections.

MATERIALS AND METHODS

Plasmid Constructs

Gene fragments corresponding to CYSDV P25 (639 nts), CYSDV P22 (579 nts), WMV P1 (1,332 nts), and WMC HCPro (1,371 nts) were RT-PCR-amplified using viral genomes extracted respectively from CYSDV (for P25 and P22) and WMV (for P1 and HCPro) infected plants, using Phusion High Fidelity PCR System (Thermo Sciences) and the specific primers shown in **Table 1**. A cis construct spanning P1HCPro was also prepared

TABLE 1 | Sequence of primers used for cloning viral gene products.

Gene product	Sense[1]	Primer sequence[2]
WMV P1	Fw	5' **CACC**ATGGCAACAATCATGTTTGGAG 3'
	Rv	5' TCAATAATGTTGAATATCTTCTATCTCC 3'
WMV HCPro	Fw	5' **CACC**ATGTCTCACACTCCAGAAG 3'
	Rv	5' TCAACCAACCCTGTAAAACTTC 3'
CYSDV P22	Fw	5' **CACC**ATGCAGAGTGTTGGAGTAG 3'
	Rv	5' TCAAGGGATGGTGCCCATG 3'
CYSDV P25	Fw	5' **CACC**ATGGGAGAAGATTTACAAGAAC 3'
	Rv	5' CTACTCCAACACTCTGCATTC 3'

[1]*Sequence corresponding to the viral genome are considered Forward (Fw), while complementary are Reverse (Rv).*
[2]*Bold nucleotides correspond to 5' additions required for properly oriented cloning in pENTR-TOPO. In the case of potyviral gene products, a methionine codon inserted in the forward primer for Helper Component Proteinase (HCPro) and sequences complementary to stop codons added in the reverse dowstream primers of both P1 and HCPro are underlined.*

using primers forward and reverse upstream P1 and downstream HCPro, respectively. The amplified PCR products were purified and cloned into pENTRY D-TOPO *GATEWAY* expression system (Invitrogen), resulting in the constructs pENTRY_CYSDV-P22, pENTRY_CYSDV-P25, pENTRY_WMV-P1, pENTRY_WMV-HCPro, and pENTRY_WMV-P1HCPro. Subsequently, the different viral genes were mobilized through LR recombination into the different destination plasmid vectors (Tanaka et al., 2011), including pGWB-702 (containing the 35S promoter and the Ω enhancer) for silencing suppression analysis; pGWB-742 (containing 35S promoter and N-terminal phusion to EYFP) and pGWB-745 (same promoter and N-terminal phusion to ECFP) for subcellular localization; pGWB 715 (providing N-terminal tag 3xHa) and pGWB 718 (providing N-terminal tag 4xMyc) for protein detection and co-immunoprecipitation assays. For bimolecular fluorescence complementation (BiFC) assays (see below), the destination plasmid vectors pBiFC2 and pBiFC3 were used (Azimzadeh et al., 2008; Ochoa et al., 2019).

Agroinfiltration and Green Fluorescent Protein Imaging

Nicotiana benthamiana plants were grown at 23–25°C with a photoperiod of 16 h of light and 8 h of darkness. Cultures of *Agrobacterium tumefaciens* strain EHA105 carrying the different plasmids were grown overnight at 28°C, and cells were resuspended to an equal OD_{600} (=0.3) in induction buffer (10 mM MES/NaOH, pH 5.6, 10 mM $MgCl_2$, 150 μM acetosyringone) for 3 h before agroinfiltration of patches in leaves of *N. benthamiana* plants at the 4–6-leaf growth stage. For co-infiltration, the *A. tumefaciens* cultures were adjusted to the same optical density at OD_{600} (=0.3) and mixed in induction buffer to be agroinfiltrated at the same time.

The identification of RNA silencing suppression activity was done by visual inspection of green fluorescent protein (GFP) fluorescence in agroinfiltrated leaves, comparing the different independent viral proteins P22, P25, P1, HCPro, and the cis construct P1-HCPro when expressed transiently (see above) through co-agroinfiltrated with the construct pBIN-GFP, using always in every leaf for comparison purposes both a positive (corresponding to the CVYV P1b RSS) and negative (an empty vector named delta) controls kindly provided by Dr. A. Valli (CNB-CSIC, Madrid, Spain), and essentially following previously described procedures (Giner et al., 2010; Mingot et al., 2016). For the combinations of different constructs, the OD was adjusted to keep equal concentration of bacteria in the agroinfiltration solution. GFP fluorescence was observed under long-wavelength UV light (Black Ray model B 100AP, UV products), and pictures were taken using a Nikon digital camera.

Quantitative RT-PCR

Total RNA was extracted from two leaf disks of agroinfiltrated *N. benthamiana* plants using TRIzol reagent (Invitrogen) according to the provider's instructions, including an additional ethanol precipitation step to improve purity of RNA. Quality and concentration of RNA was estimated using a NanoDrop® spectrophotometer (ND-8000). After DNase treatment to eliminate genomic DNA, about 1 μg of total RNA extracted from plant samples was used to produce cDNA with the High-Capacity cDNA Reverse Transcription kit (Applied Biosystems™), following protocols provided by the manufacturer. SYBRGreen (Roche) was used to detect PCR products in a Light Cycler 480 (Roche) equipment using triplicates of 100 ng of the resulting single-stranded cDNA. Specific primers previously described for GFP (Leckie and Neal Stewart, 2011) and ubiquitin (Lacomme et al., 2003) sequences were used. Statistical analysis was performed applying *t*-test to ΔCt values using the program GraphPad Prism version 6.0.

Protein Extract Preparations and Western Blotting

Tagged versions of the different viral gene products were constructed using pGW 715 and pGW 718 backbones, and mobilized to *A. tumefaciens* for agroinfiltration in *N. benthamiana* (see above). Samples (four leaf disks) collected were processed from mock or agroinfiltrated *N. benthamiana* plants were collected and homogenized in 200 ul of extraction buffer (20 mM Tris-HCl pH 7.5, 30 mM NaCl, 1 mM EDTA, 0.5% NP-40, 2% b-mercaptoethanol). Cell debris were removed by centrifugation at 13,200 rpm at 4°C for 10 min, and an aliquot (30 μl) of the supernatant were boiled in Laemmli's sample buffer (250 mM Tris-HCl pH 7.5, 40% Glicerol, 8% SDS, 20% b-mercaptoethanol). Samples were separated on 12% SDS-PAGE, transferred to Amersham Protran nitrocellulose blotting membrane and subjected to Western blot analysis. For detection, Anti-Myc Tag Antibody, clone 4A6 (Millipore) and Anti-Ha (Sigma-Aldrich) were used followed by incubation with adequate secondary anti-mouse antibodies. The proteins were visualized by chemiluminescence (Super Signal West Femto, Thermo Scientifics) according to the manufacturer's instructions using a ChemiDoc imaging system (BioRad).

Subcellular Localization and Co-localization

The coding gene products for WMV P1 and CYSDV P25 proteins were inserted in the vectors pGWB742 (35S pro,

N-EYFP) and pGWB745 (35S pro, N-ECFP) respectively, generating constructs for expression of YFP-WMV-P1 and CFP-CYSDV-P25 fusion proteins. The transient expression of both products in *N. benthamiana* leaves was achieved co-agroinfiltrating the constructs with an additional plasmid for expression of the RSS P19 of TBSV, pBin-TBSV-P19 (kindly provided by Dr. Montse Martin, CRAG, Barcelona, Spain). A confocal laser scanning Leica TCS SP5 (Leica Microsystems, Germany) microscope was used to observe the *N. benthamiana* epidermal cells at the adequate wavelengths for each reporter.

BiFC Assays

Expression of fusion proteins with N- and C-fragments of the reporter YFP, denominated, respectively YFP^N and YFP^C was achieved in *A. tumefaciens* strain EHA105 carrying plasmid for YFP^C-WMV-P1, YFP^N-WMV-P1, YFP^C-CYSDV-P25, and YFP^N-CYSDV-P25. Each construct and pBIN-TBSV-P19 were cultured separately and the cells were resuspended to an equal OD_{600} (=0.3). Equal volumes of the combinations YFP^C- YFP^N- and pBIN-TBSV-P19 were mixed in induction buffer (10 mm MES/NaOH, pH 5.6, 10 mm $MgCl_2$, 150 µm acetosyringone). *Nicotiana benthamiana* plants at the 4–6-leaf stage were used for agroinfiltration. At 3, 5, and 7 days post agroinfiltration (dpa), epidermal cells of agroinfiltrated leaves were observed for fluorescence emission under a confocal laser scanning microscope (Leica TCS SP5) at a wavelength of 514 nm.

Co-immunoprecipitation of Tagged Proteins

For immunoprecipitation 50 ul of Anti-c-Myc agarose beads (Sigma) were washed before adding the samples with Phosphate-Buffered Saline (PBS) 1x. Samples (about 1 g) of mock-, HA-WMV-P1, MYC-CYSDV-P25, or HA-WMV-P1 + MYC-CYSDV-P25 agroinfiltrated *N. benthamiana* leaves were collected, ground in immunoprecipitation buffer (20 mM Tris-HCl pH 7.5, 30 mM NaCl, 1 mM EDTA, 0,5% NP-40, 2% b-mercaptoethanol) and cleared by centrifugation at 13,200 rpm for 10 min at 4°C. Supernatants of the different lysates were added to samples of washed beads and incubated for 1 h at 4°C. After immunoprecipitation, beads were washed three times with ice-cold PBS 1x for 1 min each. Input extracts and eluates of immunoprecipitations were used for Western blot analysis (see above).

RESULTS

Confirmation of RNA Silencing Suppression Activity for Transiently Expressed Viral Gene Products

Individual gene products from the viruses WMV and CYSDV were selected for testing their activities, including already known RSSs and others with potential modulator effects. For the potyvirus, P1 and HCPro proteins were tested, and in the crinivirus, we chose P25 and P22, both located in RNA1 (**Figure 1A**). The different constructs were tested individually using the standard transient expression assay in *N. benthamiana* leaves with GFP as reporter, and the corresponding CVYV P1b and delta constructs as positive and negative controls, following described procedures (Giner et al., 2010; Mingot et al., 2016). In the experiments with individual gene products, both WMV HCPro and CYSDV P25 exhibited activities as RSSs at 3 and 5 dpa, lasting up to at least 7 dpa in the case of HCPro, while P1 and P22 did not show detectable GFP at any of the tested time points, indicating that they do not suppress local RNA silencing in the assay (**Figure 1B**). These results served to confirm the RSS activity of the P25 protein in our CYSDV Spanish isolate, and to visually determine for the first time the RSS activity of the HCPro protein of WMV, as it was expected attending to the antecedents for many other viruses in the same genus (Valli et al., 2018). Since P1 and HCpro are naturally expressed in cis as part of a larger polyprotein, the construct P1-HCPro with the two gene products in cis was also tested, showing again a strong RSS activity, indistinguishable of the activity exhibited by the WMV HCPro alone (**Figure 1B**).

To verify the correct expression of all viral products constructs, MYC-tagged versions were agroinfiltrated and samples analyzed by SDS-PAGE and Western blot (**Figure 1C**).

Combination of Heterologous Gene Products: Negative Effect of WMV P1 on the RSS Activity of CYSDV P25

To determine possible interactions between gene products of the two viruses considered, a set of experiments were designed to compare the performance in assays of RSS activity of different combinations involving WMV P1 or HCPro, paired together with CYSDV P22 or P25 (**Figure 2A**). In the combinations including WMV HCPro as one of the partners, the high RSS activity remained apparently unaltered when comparing in the same leaf patches infiltrated with HCPro alone or co-expressed along with either P22 or P25, suggesting that the assay was not sensible enough to detect an additive effect of P25 on top of the very high activity exhibited by HCPro. However, in the reciprocal combinations involving WMV P1, while its expression in the control with P22 remained non-functional as expected, a negative effect of the non-suppressor WMV P1 was observed on the RSS activity of the CYSDV P25 protein. This unexpected result was consistently reproduced, always showing an obvious attenuation of the intensity of the GFP signal with respect to that observed when the suppressor was expressed alone (a representative example is shown in the upper left photograph of **Figure 2A**). The same effect could be observed along different time points during the experiment, as shown for 3 and 5 dpa, before the weak activity of P25 faded after 7 dpa (**Figure 2B**). To further confirm these observations, we performed relative qRT-PCR measuring the expression levels of the GFP mRNA (**Figure 2C**), showing that the negative effect was present as early as at 3 dpa, when visually only a weak RSS activity was observed in the patches co-agroinfiltrated with P1+P25 (**Figure 2B**, see below).

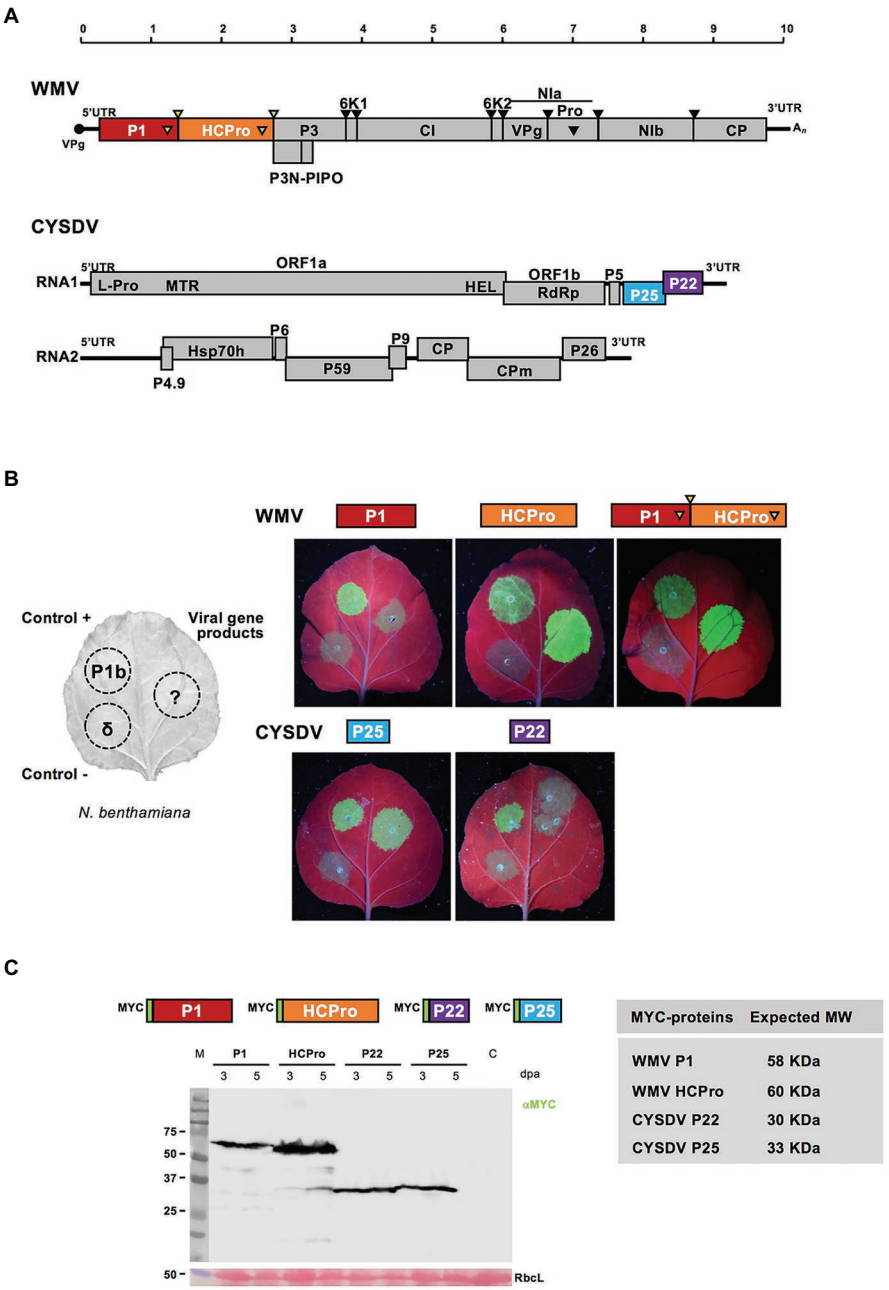

FIGURE 1 | Confirmation of RNA silencing suppression (RSS) activity in individually expressed viral gene products of *Watermelon mosaic virus* (WMV) and *Cucurbit yellow stunting disease virus* (CYSDV). **(A)** Genome maps of WMV and CYSDV. Below the size rule in kilobases, the viral ssRNAs are shown as solid horizontal lines (10,035 nucleotides for WMV, and 9,123 and 7,976 for the RNA1 and RNA2 of the bipartite CYSDV, respectively). In the WMV genome, VPg is depicted as a solid circle at the 5' end, and the poly-A tail as An at the 3' end. Viral ORFs are depicted as boxes with the names of the mature gene products. The PIPO region is shown below the polyprotein of the potyvirus leading to the partially out-of-frame product P3N-PIPO, and the protease-specific cleavages sites are indicated by arrows above and matching symbols in the gene products responsible of the proteolytic process. The different frames are shown for the crinivirus gene products. **(B)** The left part of the panel shows schematically the organization of patches in the *Nicotiana benthamiana* leaves used to test RSS activity in co-agroinfiltration of the selected gene products with the reporter green fluorescent protein (GFP). The positions for positive and negative controls, corresponding to the P1b of *Cucumber vein yellowing virus* (CVYV) and an empty vector (delta), respectively, are also shown. Constructs for expression of the individual gene products and the P1-HCPro cis construct are indicated above the pictures of leaves. Pictures were taken at 5 days post agroinfiltration (dpa) under UV light. **(C)** A representative Western blot analysis of the N-terminus MYC-tagged gene products shown in the diagrams with their expected molecular weights shown in the table. A representative blot revealed after incubation with the indicated anti-MYC specific antibody and the corresponding anti-mouse, is shown with agroinfiltrated samples, collected at 3 and 5 dpa time points, as indicated, and a non-agroinfiltrated *N. benthamiana* control lane labeled as C. M lane shows the migration of pre-stained molecular weight markers (sizes in KDa on the left side). RbcL corresponds to the Ponceau red-stained blot showing the large subunit of Rubisco protein as loading control.

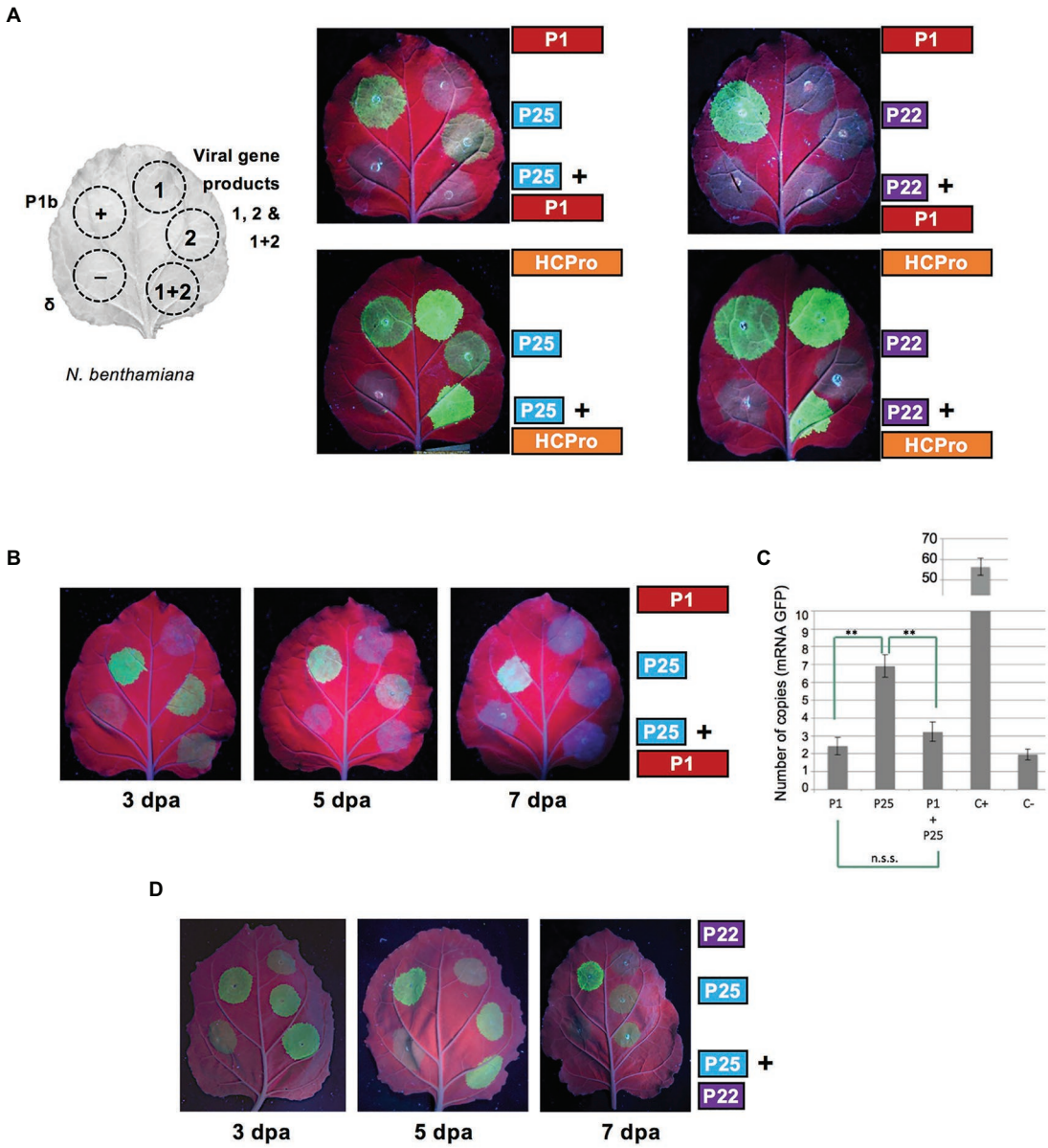

FIGURE 2 | Effect on RSS activity of the combination of heterologous selected gene products of WMV and CYSDV. **(A)** Schematic organization of patches in *N. benthamiana* leaves and comparison of effects on RSS activity of individual and combined gene products when co-agroinfiltrated with the reporter GFP. The positions for positive and negative controls, corresponding to the P1b of CVYV and an empty vector (delta), respectively, are also shown in the left half of every leaf. In the right side of the pictures and adjacent to the patches are depicted the constructs for expression of the individual gene products of WMV (P1 or HCPro) and of CYSDV (P25 or P22), with their corresponding combinations in the lower row. Pictures were taken at 5 dpa under UV light. **(B)** Time course evolution of RSS activity at 3, 5, and 7 dpa for the individual gene products WMV P1 (upper right patches), CYSDV P25 (central right patches), and their combination (lower right patches). Positive and negative controls as in A (patches in left side halves). **(C)** Quantification of GFP mRNA by qRT-PCR, relative to the reference gene ubiquitin, at 3 dpa, in patches agroinfiltrated with the constructs indicated below the bars. Mean values and SDs of three independent replicates are plotted, indicating statistically significant differences after *t*-test analysis (**indicate $p < 0.05$, values of $p = 0.0013$ for P25 vs. P1, and $p = 0.0022$ for P25 vs. P1+P25). **(D)** Absence of effect on RSS activity of CYSDV P25 when co-agroinfiltrated with CYSDV P22. Positive and negative controls as in **Figure 1B** (patches in left side half). Pictures were taken at 3, 5, and 7 dpa under UV light.

To rule out an unspecific effect on CYSDV P25 caused by co-expression of any other protein, we tested as an additional control if the co-expression of CYSDV P22 could also affect the RSS activity of P25. The experiment was performed as described above, finding that the capacity of P25 to exhibit RSS activity was unaltered by the co-expression of P22 at the same 3 and 5 dpa time points (**Figure 2D**).

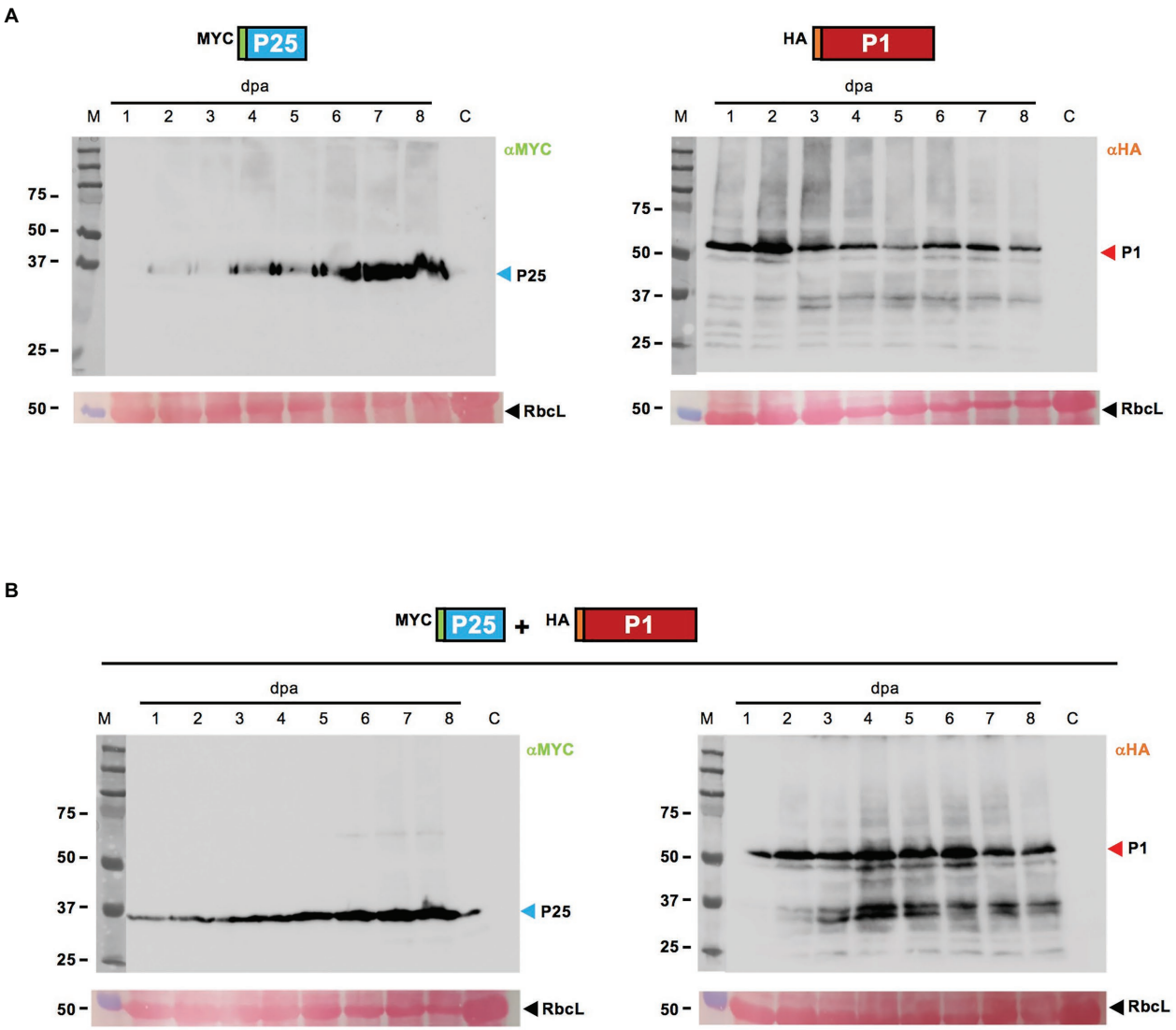

FIGURE 3 | Western blot analysis of selected N-terminus tagged proteins after transient expression, individually or combined. **(A)** Samples of *N. benthamiana* patches individually agroinfiltrated with MYC-P25 (left panel) and HA-P1 (right panel) constructs collected daily between 1 and 8 dpa are shown, besides a non-agroinfiltrated *N. benthamiana* control lane labeled as C. The blots are revealed after incubation with the corresponding anti-MYC or anti-HA specific antibodies. **(B)** Samples of patches co-agroinfiltrated with MYC-P25 and HA-P1 collected daily between 1 and 8 dpa are shown, besides a *N. benthamiana* control lane labeled as C, and revealed with anti-MYC (left panel) or anti-HA (right panel) specific antibodies. For both **(A,B)** lanes labeled with M show the migration of pre-stained molecular weight marker (sizes in KDa on the left side), and RbcL correspond to the Ponceau red-stained blots showing the large subunit of Rubisco protein as loading control.

Dynamics of Protein Expression in Patches Agroinfiltrated With CYSDV P25 and WMV P1, Both Individually and in Combination

Epitope tagged versions of the two gene products were tested for expression after agroinfiltration. Two different tags, MYC in the case of CYSDV P25 (MYC-P25) and HA in the case of WMV P1 (HA-P1), were chosen to allow independent detection of each gene product in the co-agroinfiltrated patches, and samples (pooled of three leaves from three independent plants) were taken daily up to 8 dpa. Representative Western blot analysis with the corresponding specific antibodies is shown in **Figure 3**. In the patches agroinfiltrated individually (**Figure 3A**), a steady increase of MYC-P25 expression was observed, probably reflecting its own RSS activity, reaching the highest amount of detectable protein at the end of the sampling period (8 dpa), while HA-P1 expression apparently peaked as early as 2 dpa, later showing a slight reduction followed by near constant levels until the last day sampled. In the case of the patches co-agroinfiltrated with MYC-P25 and HA-P1, the analysis also showed detection of both proteins along the

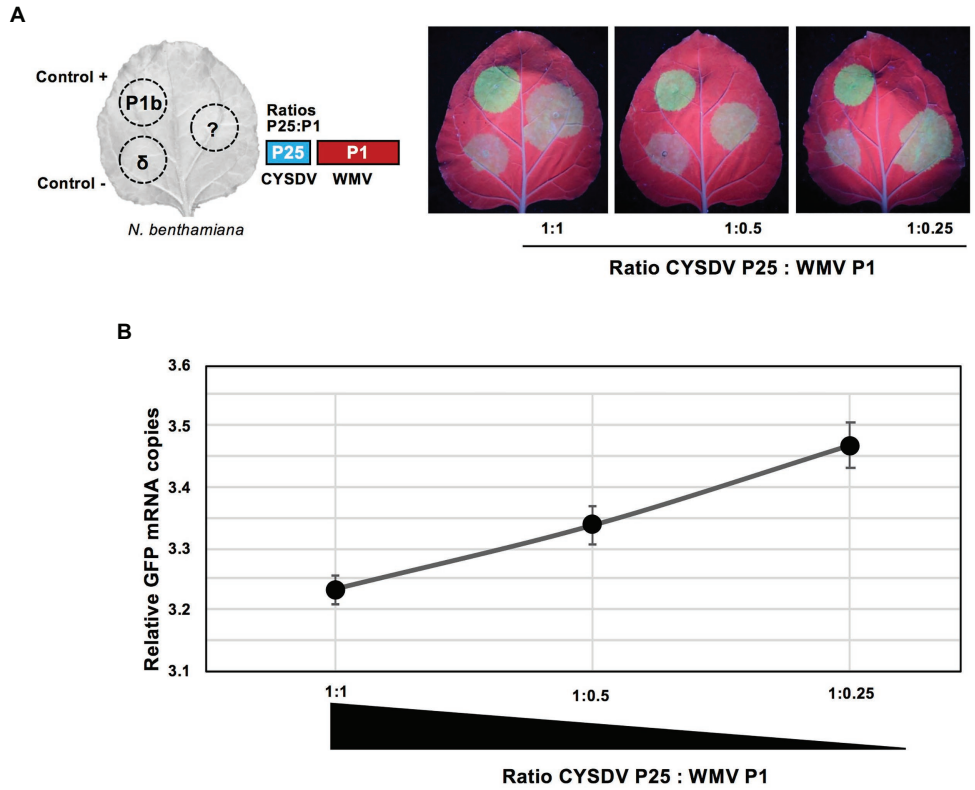

FIGURE 4 | Dose response of the presence of WMV P1 on the RSS activity of CYSDV P25. **(A)** Schematic organization of patches in *N. benthamiana* leaves co-agroinfiltrated with the reporter GFP. The same fixed concentration of P25 is used together with different amounts of P1 to reach the indicated ratios as shown in each picture, with positive and negative controls included in the left half of every leaf as in **Figure 1B**. Pictures were taken at 3 dpa under UV light. **(B)** Quantitative values showing inverse correlation of the ratio of CYSDV P25: WMV P1 and the relative copies of GFP mRNA measured by qRT-PCR with ubiquitin as reference gene. The graph shows the values for average and SD corresponding to three biological replicates per treatment.

complete period, with a delay in the peak of HA-P1 occurring around day 4, and a very similar dynamic of steady accumulation in the case of MYC-P25 (**Figure 3B**). These results proved that the reduced RSS activity of CYSDV P25 when co-expressed with WMV P1 was not caused by lack of expression.

Dose-Dependent Effect of the Presence of WMV on the RSS Activity of CYSDV P25

To evaluate if the observed negative effect was correlated to the relative expression levels of the two viral products, an experiment of dose-response was designed. Using the same concentration of *A. tumefaciens* culture transformed with the construct for expression of CYSDV P25, up to three dilutions of the culture harboring the partner product WMV P1 were tested for their effects on the RSS activity. Assuming that the quantities of CYSDV P25 were kept constant, the quantities of the partner WMV P1 were decreasing exponentially by a factor of 2, which correlated with a visible increase of GFP under UV light (**Figure 4A**), also detectable as a linear increase of mRNA levels corresponding to GFP (**Figure 4B**). These results indicated that the RSS activity of CYSDV P25 recovered when the relative amount of WMV P1 decreased.

Subcellular Localization of WMV P1 and CYSDV P25 in Nucleus and Cytoplasm

To investigate the subcellular localization of WMV P1 and CYSDV P25 proteins, we cloned them into constructs fused to fluorescent markers using the plasmids pGWB742 (containing YFP for fusion to the N-terminus of the cloned protein) and pGWB745 (for fusion to CFP, also in N-terminus). The constructs were transformed into *A. tumefaciens* strain EHA105 and agroinfiltrated into *N. benthamiana* leaves. Confocal microscopy examination showed that both fusion proteins, WMV P1 tagged with YFP and CYSDV P25 tagged with CFP, were located in the nucleus and the cytoplasm of the agroinfiltrated cells, and that they apparently co-localize in both compartments (**Figure 5**).

Interaction of WMV P1 and CYSDV P25

To test if there was a direct interaction between WMV P1 and CYSDV P25 when co-expressed transiently in *N. benthamiana*, we performed BiFC and co-immunoprecipitation assays. As shown by confocal microscopy observations, the split YFP fragments fused to WMV P1 and CYSDV P25 did reconstitute a visible fluorescence with the appropriate filter, indicating that the two proteins could interact in the cytoplasm of the agroinfiltrated cells (**Figure 6A**).

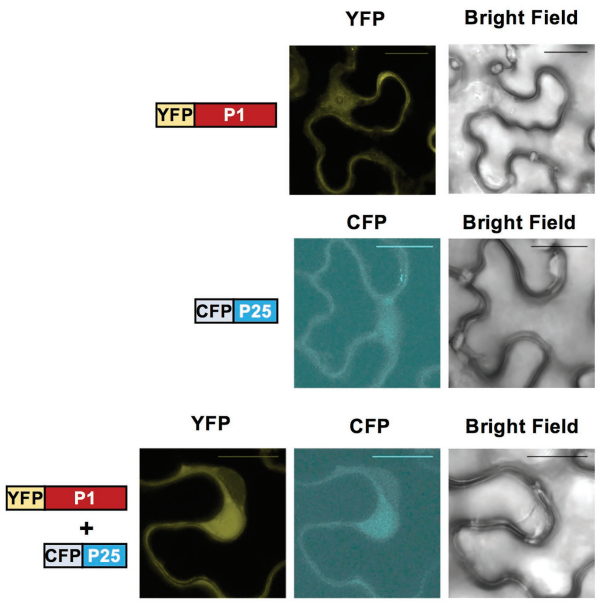

FIGURE 5 | Subcellular localization of fluorescently labeled WMV P1 and CYSDV P25 proteins. Confocal laser microscopy of *N. benthamiana* leaves agroinfiltrated with the constructs indicated schematically on the left: P1-YFP (upper lane), P25-CFP (central lane) and with both constructs at the same time (bottom lane). The images labeled with YFP correspond to the yellow color field, those labeled with CFP to the blue color field, and in the last column the bright field is shown, the column. In the samples agroinfiltrated with individual constructs observations were also performed with the conditions for the two YFP and CFP, without detecting any cross fluorescence (not shown). Bar size 20 μm.

Furthermore, when the same two tagged proteins with MYC and HA epitopes used in the previous time course analysis (see **Figure 3**) were co-agroinfiltrated and tested for co-inmunoprecipitation, a product corresponding to HA-P1 was precipitated along with the MYC-P25, indicating that indeed the two proteins can interact (**Figure 6B**).

DISCUSSION

Despite the common occurrence of multiple viral infections in plants, in many cases our understanding of the interactions occurring when two or more unrelated viruses share the same plant is still incomplete (Moreno and López-Moya, 2020). As an example, our recent analysis of melon plants co-infected by WMV and CYSDV revealed a complex scenario, with dynamic changes along the progress of the infections, that could even affect the transmissibility of the viruses by their insect vectors: briefly, the initial synergism and boost of CYSDV accumulation was later moderated and accompanied by a sort of recovery phenotype (Domingo-Calap et al., 2020). Intrigued by this peculiar behavior, we have addressed if virus-virus interactions between WMV and CYSDV might help to explain the outcome of the mixed infection. To start exploring at the molecular level the interactions between the two partner viruses, we decided to consider first the RSS function. Experiments were designed to transiently express the gene products known to participate in this function during individual infections, and then to combine them in order to find out possible interactions. In addition to known RSSs, we included other gene products that might modulate their activity in RNA silencing suppression. Following this strategy, an unexpected negative effect on the RSS activity of the P25 of CYSDV was observed when this viral product was expressed together with the P1 of WMV. To rule out a possible effect on the expression level of CYSDV P25 when co-expressed along with WMV P1, we have tested the amounts of tagged protein versions by Western blot analysis in agroinfiltrated patches. Compared with the individually expressed protein, we did not observed lack of expression in CYSDV P25 at different time points, therefore supporting a true affectation of the RSS activity. Interestingly, the dynamic of accumulation of tagged WMV P1 appeared to be altered in the co-agroinfiltrated samples, with a delayed peak compared with the individually expressed control. Unfortunately, the damage suffered after agroinfiltration precluded longer analysis, but it is tempting to speculate if these changes along this limited time might reflect somehow the peculiar dynamics mentioned to occur during mixed infections (Domingo-Calap et al., 2020).

To our knowledge, this is the first description of an interaction between viral gene products of two unrelated plant viruses that interfere on the RSS activity of one of them. Before speculating about the importance of this observation, a couple of previous considerations are cautionary needed: (i) the effect was observed in transient expression, not during viral infections; and (ii) it was occurring in a different plant of the natural common hosts where the two viruses might co-exist. Thus, we cannot assume directly that our observations after transient expression could reflect exactly what occurs during co-infection of the two viruses in a naturally infected cucurbit host. Indeed, the localization and behavior of the selected gene products expressed transiently in *N. benthamiana* might be quite different to what really happens during infections in cucurbits. In other words, could this negative interaction be occurring as well during WMV and CYSDV co-infection? Unfortunately, this question is difficult to address. First, adequate infectious clones of CYSDV that could be manipulated for tagging gene products in plants are not yet available, being only reported a version capable to replicate in protoplasts (Owen et al., 2016). We attempted to use this tool for whitefly transmission assays and to recreate mixed infections, unfortunately with no success (unpublished data). Another limitation to directly study mixed infections of the two viruses derives from difficulties to infect *N. benthamiana*, the model plant species, where the transient expression observations were performed: despite being a highly susceptible plant for many viruses, including isolates of WMV (Lecoq et al., 2011; Aragonés et al., 2019), CYSDV appears not to be able to infect and not even replicate in protoplasts of this species (Owen et al., 2016). The alternative approach to test the activity of P25 in susceptible cucurbits previously infected with WMV would require to knock-out the activity of WMV HCPro, a rather complex task, which could compromise the infectivity of WMV or modify its pathogeneicity, as suggested

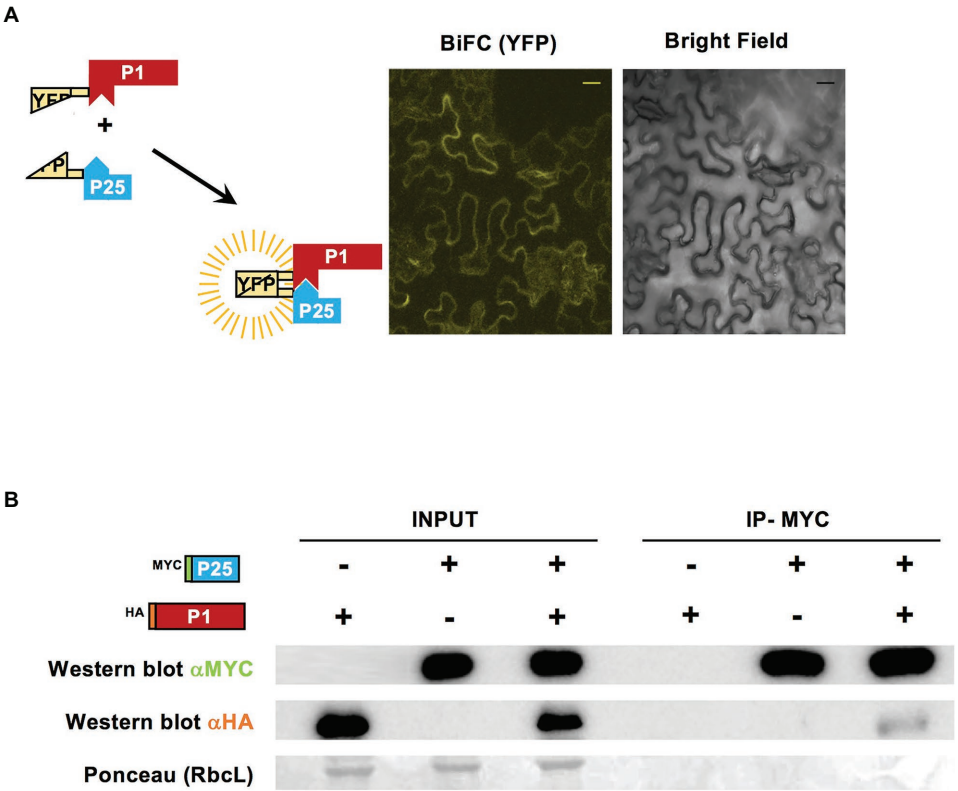

FIGURE 6 | Interaction of WMV P1 and CYSDV P25. **(A)** Schematic representation of bimolecular fluorescence complementation (BiFC) constructs with the split YFP fused to WMV P1 and CYSDV P25, and the observation using confocal laser microscopy of *N. benthamiana* leaves agroinfiltrated simultaneously with the two constructs. The picture YFP corresponds to the yellow color field and the same area is shown under bright field illumination. Control samples agroinfiltrated with individual constructs were analyzed without detecting any fluorescence (not shown). Bar size 20 μm. **(B)** Immunoprecipitation of viral protein variants tagged with MYC or HA, as indicated. Western blot analysis with anti-MYC and anti-HA antibodies, and Ponceau staining of the large subunit of Rubisco (RbcL) as control of loading, are shown for the input fractions and the corresponding immunoprecipitation samples, as indicated.

by previous mutagenesis and variability studies performed with other potyviruses (Torres-Barceló et al., 2008; Han et al., 2016).

Regarding localization in the plant, our knowledge on the distribution of WMV and CYSDV during mixed infections is also incomplete. Crinivirus are phloem-restricted viruses, and CYSDV distribution within the plant is particularly variable (Marco et al., 2003). A different crinivirus of cucurbits has been recently tagged with GFP (Wei et al., 2018), but unfortunately constructing a similar tool for CYSDV is not feasible nowadays, as already mentioned. On the other hand, there are no specific studies on the distribution of WMV within different tissues and cells in the plant, but comparing to other potyviruses it was expected to invade more cell types (Kogovsek et al., 2011). As a further complication, the distribution of viruses in mixed and individual infections could be different, as it was shown for instance in combinations of potyvirus and cucumovirus (Ryang et al., 2004; Mochizuki et al., 2016). Interestingly, in sweet potato plants co-infected by SPCSV and potyviruses, crinivirus components were detected outside the phloem, in contrast with its restricted phloem localization in single infections (Nome et al., 2007). Despite the lack of information about WMV, we can still make an educated guess, considering that the presence of potyviruses in phloem has been shown in certain cases (Rajamäki and Valkonen, 2003; Ion-Nagy et al., 2006). Also, another potyvirus of cucurbits, *Zucchini yellow mosaic virus* (ZYMV), showed a broad distribution in Zucchini when tagged with a visual marker (Majer et al., 2017). Although, at this point, we cannot provide evidence for the presence of the two viruses co-infecting the same cells, there are sufficient antecedents to make this possibility plausible. Further studies will be required to verify if indeed WMV and CYSDV might coincide in certain cells, and also if their distribution is altered or not during mixed infections.

With respect to intracellular localization, the P1 of potyviruses was found in the cytoplasm associated to other viral products (Lehto et al., 1998), and also trafficking to the nucleolus as recently reported (Martinez et al., 2014). Our results are compatible with these localizations. However, no information is available regarding intracellular localization of CYSDV P25, and only limited data are reported in other criniviruses and for other gene products, such as those involved in cell-to-cell movement (Qiao et al., 2018). Again, further investigations will be required to better understand if our observations of transiently expressed P25 reflect the intracellular localization of this viral protein during the virus infection.

The function(s) played by the P1 of potyviruses has remained elusive, and only recently some insights about its role(s) as modulator of essential activities during infection are being revealed. As a first important point to consider, the P1 is a remarkably variable product among potyviruses, what argues for its participation in host range determination, as it has been suggested by different authors (Valli et al., 2007; Revers and García, 2015; Cui and Wang, 2019; Nigam et al., 2019). Works with *Plum pox virus* (PPV) showed that P1 is involved in replication and pathogenicity (Maliogka et al., 2012; Pasin et al., 2014). Concerning RSS related functions, it has been proposed that P1 might stimulate the activity of HCPro (Anandalakshmi et al., 1998; Pruss et al., 2004; Rajamaki et al., 2005), but it is unclear if this stimulatory effect could be exerted on other RSSs, especially considering the importance of their expression in cis (Fernández et al., 2013). Interestingly, partial truncation of P1 in PPV revealed an antagonistic role for P1 in self-processing with a negative impact in local infection (Shan et al., 2018), but again it is uncertain if similar effects can be expected as well in other viruses. Our finding here might provide further clues to disentangle if the role(s) played by P1 are particularly relevant in the case of mixed infections. Indeed, although the interaction between CYSDV P25 and WMV P1 was revealed because it affected the RSS function of the crinivirus protein, the changes in the dynamic of accumulation of P1 observed in our western blot analysis might suggest an effect on the potyvirus infection.

It will be interesting to find out if this kind of interactions might occur as well in other combinations of potyviruses plus criniviruses. Many important crops are susceptible to criniviruses (Tzanetakis et al., 2013; Abrahamian and Abou-Jawdah, 2014; Fiallo-Olivé and Navas-Castillo, 2019; Ruiz Garcia and Janssen, 2020), and therefore co-infections with potyviruses are very likely to occur. Particularly intriguing could be the case of sweet potato, suffering strong synergism but in the opposite direction, with a boost of the potyviruses and other unrelated virus accumulation when co-infected by the crinivirus SPCSV (Untiveros et al., 2007; Cuellar et al., 2015). As mentioned, the RSS of sweet potato-infecting potyviruses appears to differ from the usual activity of HCPro, with the function shifted to a partially out-of-frame gene product P1N-PISPO produced after polymerase slippage (Mingot et al., 2016; Untiveros et al., 2016).

Finally, it should be noted that each one of the virus partners will be producing several proteins simultaneously during a mixed infection, at least 10 and 13 different mature products for the potyvirus and the crinivirus, respectively. Thus, our analysis testing only a few heterologous products in combination of two by two elements is just a first attempt to start exploring a presumably much richer landscape of interactions. As a novel observation, we hope our work will stimulate further research to better understand if these kind of interactions form part of the expected fine-tuning of RSS and other important functions during mixed infections, and how it can contribute to virus pathogenicity in the different situations.

DATA AVAILABILITY STATEMENT

The original contributions presented in the study are included in the article/supplementary material, further inquiries can be directed to the corresponding author.

AUTHOR CONTRIBUTIONS

MD-C, OC, AM, and JL-M designed the research, analyzed the data, composed figures, and wrote the manuscript. MD-C, OC, ME, AM, and JL-M performed the experiments. All authors contributed to the article and approved the submitted version.

FUNDING

Work in the author's laboratory was financed by grants AGL2016-75529-R and PID2019-105692RB-100 from Spanish Ministry of Science and Innovation. MD-C was supported by FPI contract BES-2014-068970 from Ministry of Science and Innovation and FEDER. OC was supported by 2018 FI_B 00329 from AGAUR, Generalitat de Catalunya, and Fons Social Europeu. AM was supported by European Union's Horizon 2020 research and innovation programme under the Marie Skłodowska-Curie grant agreement No 657527. We acknowledge financial support from the Spanish Ministry of Science and Innovation-State Research Agency (AEI), through the "Severo Ochoa Programme for Centres of Excellence in R&D" SEV-2015-0533 and CEX2019-000902-S, and from Generalitat de Catalunya CERCA Institution and support of the publication fee by the CSIC Open Access Publication Support Initiative through its Unit of Information Resources for Research (URICI).

ACKNOWLEDGMENTS

We want to thank our colleagues Montse Martin (CRAG) and Adrian Valli (CNB-CSIC, Madrid, Spain) for different constructs, and Ioannis Livieratos (Plant Virology Laboratory, CIHEAM-MAICh, Chania, Greece) for the gift of CYSDV cloned materials.

REFERENCES

Abrahamian, P. E., and Abou-Jawdah, Y. (2014). Whitefly-transmitted criniviruses of cucurbits: current status and future prospects. *Virusdisease* 25, 26–38. doi: 10.1007/s13337-013-0173-9

Alcaide, C., Rabadán, M. P., Moreno-Pérez, M. G., and Gómez, P. (2020). Implications of mixed viral infections on plant disease ecology and evolution. *Adv. Virus Res.* 106, 145–169. doi: 10.1016/bs.aivir.2020.02.001

Anandalakshmi, R., Pruss, G. J., Ge, X., Marathe, R., Mallory, A. C., Smith, T. H., et al. (1998). A viral suppressor of gene silencing in plants. *Proc. Natl. Acad. Sci. U. S. A.* 95, 13079–13084. doi: 10.1073/pnas.95.22.13079

Aragonés, V., Pérez-de-Castro, A., Cordero, T., Cebolla-Cornejo, J., López, C., Picó, B., et al. (2019). A watermelon mosaic virus clone tagged with the yellow visual maker phytoene synthase facilitates scoring infectivity in melon breeding programs. *Eur. J. Plant Pathol.* 153, 1317–1323. doi: 10.1007/s10658-018-01621-x

Azimzadeh, J., Nacry, P., Christodoulidou, A., Drevensek, S., Camilleri, C., Amiour, N., et al. (2008). *Arabidopsis* Tonneau1 proteins are essential for preprophase band formation and interact with centrin. *Plant Cell* 20, 2146–2159. doi: 10.1105/tpc.107.056812

Baulcombe, D. (2004). RNA silencing in plants. *Nature* 431, 356–363. doi: 10.1038/nature02874

Cañizares, M. C., Navas-Castillo, J., and Moriones, E. (2008). Multiple suppressors of RNA silencing encoded by both genomic RNAs of the crinivirus, tomato chlorosis virus. *Virology* 379, 168–174. doi: 10.1016/j.virol.2008.06.020

Chen, S., Sun, X., Shi, Y., Wei, Y., Han, X., Li, H., et al. (2019). Cucurbit chlorotic yellows virus p22 protein interacts with cucumber SKP1LB1 and its F-box-like motif is crucial for silencing suppressor activity. *Viruses* 11:818. doi: 10.3390/v11090818

Clark, C. A., Davis, J. A., Abad, J. A., Cuellar, W. J., Fuentes, S., Kreuze, J. F., et al. (2012). Sweetpotato viruses: 15 years of progress on understanding and managing complex diseases. *Plant Dis.* 96, 168–185. doi: 10.1094/PDIS-07-11-0550

Csorba, T., Kontra, L., and Burgyán, J. (2015). Viral silencing suppressors: tools forged to fine-tune host-pathogen coexistence. *Virology* 479–480, 85–103. doi: 10.1016/j.virol.2015.02.028

Cuellar, W. J., Galvez, M., Fuentes, S., Tugume, J., and Kreuze, J. (2015). Synergistic interactions of begomoviruses with sweet potato chlorotic stunt virus (genus Crinivirus) in sweet potato (*Ipomoea batatas* L.). *Mol. Plant Pathol.* 16, 459–471. doi: 10.1111/mpp.12200

Cui, H., and Wang, A. (2019). The biological impact of the hypervariable N-terminal region of potyviral genomes. *Annu. Rev. Virol.* 6, 255–274. doi: 10.1146/annurev-virology-092818-015843

Damirdagh, I. S., and Ross, A. F. (1967). A marked synergistic interaction of potato viruses X and Y in inoculated leaves of tobacco. *Virology* 31, 296–307. doi: 10.1016/0042-6822(67)90174-2

Desbiez, C., Joannon, B., Wipf-Scheibel, C., Chandeysson, C., and Lecoq, H. (2011). Recombination in natural populations of watermelon mosaic virus: new agronomic threat or damp squib? *J. Gen. Virol.* 92, 1939–1948. doi: 10.1099/vir.0.031401-0

Domingo-Calap, M. L., Moreno, A. B., Díaz Pendón, J. A., Moreno, A., Fereres, A., and López-Moya, J. J. (2020). Assessing the impact on virus transmission and insect vector behavior of a viral mixed infection in melon. *Phytopathology* 110, 174–186. doi: 10.1094/PHYTO-04-19-0126-FI

Fernández, F. T., González, I., Doblas, P., Rodríguez, C., Sahana, N., Kaur, H., et al. (2013). The influence of cis-acting P1 protein and translational elements on the expression of potato virus Y helper-component proteinase (HCPro) in heterologous systems and its suppression of silencing activity. *Mol. Plant Pathol.* 14, 530–541. doi: 10.1111/mpp.12025

Fiallo-Olivé, E., and Navas-Castillo, J. (2019). Tomato chlorosis virus, an emergent plant virus still expanding its geographical and host ranges. *Mol. Plant Pathol.* 20, 1307–1320. doi: 10.1111/mpp.12847

Fuchs, M., Bar-Joseph, M., Candresse, T., Maree, H. J., Martelli, G. P., Melzer, M. J., et al. (2020). ICTV virus taxonomy profile: Closteroviridae. *J. Gen. Virol.* 101, 364–365. doi: 10.1099/jgv.0.001397

Gibbs, A. J., Hajizadeh, M., Ohshima, K., and Jones, R. A. C. (2020). The potyviruses: an evolutionary synthesis is emerging. *Viruses* 12, 1–30. doi: 10.3390/v12020132

Giner, A., Lakatos, L., García-Chapa, M., López-Moya, J. J., and Burgyán, J. (2010). Viral protein inhibits RISC activity by argonaute binding through conserved WG/GW motifs. *PLoS Pathog.* 6:e1000996. doi: 10.1371/journal.ppat.1000996

Han, J.-Y., Chung, J., Kim, J., Seo, E.-U., Kilcrease, J. P., Bauchan, G. R., et al. (2016). Comparison of helper component-protease RNA silencing suppression activity, subcellular localization, and aggregation of three Korean isolates of turnip mosaic virus. *Virus Genes* 52, 592–596. doi: 10.1007/s11262-016-1330-1

Ion-Nagy, L., Lansac, M., Eyquard, J. P., Salvador, B., Garcia, J. A., Le Gall, O., et al. (2006). PPV long-distance movement is occasionally permitted in resistant apricot hosts. *Virus Res.* 120, 70–78. doi: 10.1016/j.virusres.2006.01.019

Juarez, M., Legua, P., Mengual, C. M., Kassem, M. A., Sempere, R. N., Gómez, P., et al. (2013). Relative incidence, spatial distribution and genetic diversity of cucurbit viruses in eastern Spain. *Ann. Appl. Biol.* 162, 362–370. doi: 10.1111/aab.12029

Kasschau, K. D., and Carrington, J. C. (1998). A counterdefensive strategy of plant viruses. *Cell* 95, 461–470. doi: 10.1016/S0092-8674(00)81614-1

Kataya, A. R. A., Suliman, M. N. S., Kalantidis, K., and Livieratos, I. C. (2009). Cucurbit yellow stunting disorder virus p25 is a suppressor of post-transcriptional gene silencing. *Virus Res.* 145, 48–53. doi: 10.1016/j.virusres.2009.06.010

Kogovsek, P., Kladnik, A., Mlakar, J., Znidaric, M. T., Dermastia, M., Ravnikar, M., et al. (2011). Distribution of potato virus Y in potato plant organs, tissues, and cells. *Phytopathology* 101, 1292–1300. doi: 10.1094/PHYTO-01-11-0020

Kreuze, J. F., Savenkov, E. I., Cuellar, W., Li, X., and Valkonen, J. P. T. (2005). Viral class 1 RNase III involved in suppression of RNA silencing viral class 1 RNase III involved in SUppression of RNA silencing. *J. Virol.* 79, 7227–7238. doi: 10.1128/JVI.79.11.7227-7238.2005

Kubota, K., and Ng, J. C. K. (2016). Lettuce chlorosis virus P23 suppresses RNA silencing and induces local necrosis with increased severity at raised temperatures. *Phytopathology* 106, 653–662. doi: 10.1094/PHYTO-09-15-0219-R

Lacomme, C., Hrubikova, K., and Hein, I. (2003). Enhancement of virus-induced gene silencing through viral-based production of inverted-repeats. *Plant J.* 34, 543–553. doi: 10.1046/j.1365-313X.2003.01733.x

Lakatos, L., Csorba, T., Pantaleo, V., Chapman, E. J., Carrington, J. C., Liu, Y. -P., et al. (2006). Small RNA binding is a common strategy to suppress RNA silencing by several viral suppressors. *EMBO J.* 25, 2768–2780. doi: 10.1038/sj.emboj.7601164

Leckie, B. M., and Neal Stewart, C. (2011). Agroinfiltration as a technique for rapid assays for evaluating candidate insect resistance transgenes in plants. *Plant Cell Rep.* 30, 325–334. doi: 10.1007/s00299-010-0961-2

Lecoq, H., Fabre, F., Joannon, B., Wipf-Scheibel, C., Chandeysson, C., Schoeny, A., et al. (2011). Search for factors involved in the rapid shift in watermelon mosaic virus (WMV) populations in South-Eastern France. *Virus Res.* 159, 115–123. doi: 10.1016/j.virusres.2011.05.004

Lehto, K., Pehu, E., Pehu, T., and Arbatova, J. (1998). Localization of the P1 protein of potato Y potyvirus in association with cytoplasmic inclusion bodies and in the cytoplasm of infected cells. *J. Gen. Virol.* 79, 2319–2323. doi: 10.1099/0022-1317-79-10-2319

Majer, E., Llorente, B., Rodríguez-Concepción, M., and Daròs, J. A. (2017). Rewiring carotenoid biosynthesis in plants using a viral vector. *Sci. Rep.* 7, 1–10. doi: 10.1038/srep41645

Maliogka, V. I., Salvador, B., Carbonell, A., Saenz, P., Leon, D. S., Oliveros, J. C., et al. (2012). Virus variants with differences in the P1 protein coexist in a plum pox virus population and display particular host-dependent pathogenicity features. *Mol. Plant Pathol.* 13, 877–886. doi: 10.1111/j.1364-3703.2012.00796.x

Marco, C. F., Aguilar, J. M., Abad, J., Gómez-Guillamón, M. L., and Aranda, M. A. (2003). Melon resistance to cucurbit yellow stunting disorder virus is characterized by reduced virus accumulation. *Phytopathology* 93, 844–852. doi: 10.1094/PHYTO.2003.93.7.844

Martinez, F., Daros, J. A., Martínez, F., Daròs, J.-A., Martinez, F., and Daros, J. A. (2014). Tobacco etch virus protein P1 traffics to the nucleolus and associates with the host 60S ribosomal subunits during infection. *J. Virol.* 88, 10725–10737. doi: 10.1128/JVI.00928-14

Mascia, T., Cillo, F., Fanelli, V., Finetti-Sialer, M. M., De Stradis, A., Palukaitis, P., et al. (2010). Characterization of the interactions between cucumber mosaic virus and potato virus Y in mixed infections in tomato. *Mol. Plant-Microbe Interact.* 23, 1514–1524. doi: 10.1094/MPMI-03-10-0064

Mingot, A., Valli, A., Rodamilans, B., San León, D., Baulcombe, D. C., García, J. A., et al. (2016). The P1N-PISPO trans-frame gene of sweet potato feathery mottle potyvirus is produced during virus infection and functions as an RNA silencing suppressor. *J. Virol.* 90, 3543–3557. doi: 10.1128/JVI.02360-15

Mochizuki, T., Nobuhara, S., Nishimura, M., Ryang, B. S., Naoe, M., Matsumoto, T., et al. (2016). The entry of cucumber mosaic virus into cucumber xylem is facilitated by co-infection with zucchini yellow mosaic virus. *Arch. Virol.* 161, 2683–2692. doi: 10.1007/s00705-016-2970-0

Moreno, A. B., and López-Moya, J. J. (2020). When viruses play team sports: mixed infections in plants. *Phytopathology* 110, 29–48. doi: 10.1094/PHYTO-07-19-0250-FI

Moreno, I. M., Malpica, J. M., Diaz-Pendon, J. A., Moriones, E., Fraile, A., and Garcia-Arenal, F. (2004). Variability and genetic structure of the population of watermelon mosaic virus infecting melon in Spain. *Virology* 318, 451–460. doi: 10.1016/j.virol.2003.10.002

Navas-Castillo, J., Fiallo-Olivé, E., and Sánchez-Campos, S. (2011). Emerging virus diseases transmitted by whiteflies. *Annu. Rev. Phytopathol.* 49, 219–248. doi: 10.1146/annurev-phyto-072910-095235

Navas-Castillo, J., López-Moya, J. J., and Aranda, M. A. (2014). Whitefly-transmitted RNA viruses that affect intensive vegetable production. *Ann. Appl. Biol.* 165, 155–171. doi: 10.1111/aab.12147

Nigam, D., LaTourrette, K., Souza, P. F. N., and Garcia-Ruiz, H. (2019). Genome-wide variation in potyviruses. *Front. Plant Sci.* 10:1439. doi: 10.3389/fpls.2019.01439

Nome, C. F., Nome, S. F., Guzmán, F., Conci, L., and Laguna, I. G. (2007). Localization of sweet potato chlorotic stunt virus (SPCSV) in synergic infection with potyviruses in sweet potato. *Biocell* 31, 23–31. doi: 10.32604/biocell.2007.31.023

Ochoa, J., Valli, A., Martín-Trillo, M., Simón-Mateo, C., García, J. A., and Rodamilans, B. (2019). Sterol isomerase HYDRA1 interacts with RNA silencing suppressor P1b and restricts potyviral infection. *Plant Cell Environ.* 42, 3015–3026. doi: 10.1111/pce.13610

Orfanidou, C. G., Mathioudakis, M. M., Katsarou, K., Livieratos, I., Katis, N., and Maliogka, V. I. (2019). Cucurbit chlorotic yellows virus p22 is a suppressor of local RNA silencing. *Arch. Virol.* 164, 2747–2759. doi: 10.1007/s00705-019-04391-x

Owen, C. A., Moukarzel, R., Huang, X., Kassem, M. A., Eliasco, E., Aranda, M. A., et al. (2016). In vitro synthesized RNA generated from cDNA clones of both genomic components of cucurbit yellow stunting disorder virus replicates in cucumber protoplasts. *Viruses* 8:170. doi: 10.3390/v8060170

Pasin, F., Simón-Mateo, C., and García, J. A. (2014). The hypervariable amino-terminus of P1 protease modulates potyviral replication and host defense responses. *PLoS Pathog.* 10:e1003985. doi: 10.1371/journal.ppat.1003985

Pruss, G. J., Lawrence, C. B., Bass, T., Li, Q. Q., Bowman, L. H., and Vance, V. (2004). The potyviral suppressor of RNA silencing confers enhanced resistance to multiple pathogens. *Virology* 320, 107–120. doi: 10.1016/j.virol.2003.11.027

Qiao, W., Medina, V., Kuo, Y. W., and Falk, B. W. (2018). A distinct, non-virion plant virus movement protein encoded by a crinivirus essential for systemic infection. *mBio* 9, e02230–e02218. doi: 10.1128/mBio.02230-18

Rajamaki, M. L., Kelloniemi, J., Alminaite, A., Kekarainen, T., Rabenstein, F., and Valkonen, J. P. (2005). A novel insertion site inside the potyvirus P1 cistron allows expression of heterologous proteins and suggests some P1 functions. *Virology* 342, 88–101. doi: 10.1016/j.virol.2005.07.019

Rajamäki, M.-L., and Valkonen, J. P. T. (2003). Localization of a potyvirus and the viral genome-linked protein in wild potato leaves at an early stage of systemic infection. *Mol. Plant-Microbe Interact.* 16, 25–34. doi: 10.1094/MPMI.2003.16.1.25

Revers, F., and García, J. A. (2015). Molecular biology of potyviruses. *Adv. Virus Res.* 92, 101–199. doi: 10.1016/bs.aivir.2014.11.006

Ruiz Garcia, L., and Janssen, D. (2020). Epidemiology and control of emerging criniviruses in bean. *Virus Res.* 280:197902. doi: 10.1016/j.virusres.2020.197902

Ryang, B. S., Kobori, T., Matsumoto, T., Kosaka, Y., and Ohki, S. T. (2004). Cucumber mosaic virus 2b protein compensates for restricted systemic spread of potato virus Y in doubly infected tobacco. *J. Gen. Virol.* 85, 3405–3414. doi: 10.1099/vir.0.80176-0

Shan, H., Pasin, F., Tzanetakis, I. E., Simón-Mateo, C., García, J. A., and Rodamilans, B. (2018). Truncation of a P1 leader proteinase facilitates potyvirus replication in a non-permissive host. *Mol. Plant Pathol.* 19, 1504–1510. doi: 10.1111/mpp.12640

Shan, H., Pasin, F., Valli, A., Castillo, C., Rajulu, C., Carbonell, A., et al. (2015). The Potyviridae P1a leader protease contributes to host range specificity. *Virology* 476, 264–270. doi: 10.1016/j.virol.2014.12.013

Syller, J. (2012). Facilitative and antagonistic interactions between plant viruses in mixed infections. *Mol. Plant Pathol.* 13, 204–216. doi: 10.1111/j.1364-3703.2011.00734.x

Syller, J., and Grupa, A. (2016). Antagonistic within-host interactions between plant viruses: molecular basis and impact on viral and host fitness. *Mol. Plant Pathol.* 17, 769–782. doi: 10.1111/mpp.12322

Tairo, F., Mukasa, S. B., Jones, R. A. C. C., Kullaya, A., Rubaihayo, P. R., and Valkonen, J. P. T. (2005). Unravelling the genetic diversity of the three main viruses involved in sweet potato virus disease (SPVD), and its practical implications. *Mol. Plant Pathol.* 6, 199–211. doi: 10.1111/j.1364-3703.2005.00267.x

Taiwo, M. A., Kareem, K. T., Nsa, I. Y., and Hughes, J. D. (2007). Cowpea viruses: effect of single and mixed infections on symptomatology and virus concentration. *Virol. J.* 4:95. doi: 10.1186/1743-422X-4-95

Tanaka, Y., Nakamura, S., Kawamukai, M., Koizumi, N., and Nakagawa, T. (2011). Development of a series of gateway binary vectors possessing a tunicamycin resistance gene as a marker for the transformation of *Arabidopsis thaliana*. *Biosci. Biotechnol. Biochem.* 75, 804–807. doi: 10.1271/bbb.110063

Tollenaere, C., Susi, H., and Laine, A. L. (2016). Evolutionary and epidemiological implications of multiple infection in plants. *Trends Plant Sci.* 21, 80–90. doi: 10.1016/j.tplants.2015.10.014

Torres-Barceló, C., Martín, S., Darós, J. A., and Elena, S. F. (2008). From hypo- to hypersuppression: effect of amino acid substitutions on the RNA-silencing suppressor activity of the tobacco etch potyvirus HC-pro. *Genetics* 180, 1039–1049. doi: 10.1534/genetics.108.091363

Tzanetakis, I. E., Martin, R. R., and Wintermantel, W. M. (2013). Epidemiology of criniviruses: an emerging problem in world agriculture. *Front. Microbiol.* 4:119. doi: 10.3389/fmicb.2013.00119

Untiveros, M., Fuentes, S., and Salazar, L. F. (2007). Synergistic interaction of sweet potato chlorotic stunt virus (Crinivirus) with carla-, cucumo-, ipomo-, and potyviruses infecting sweet potato. *Plant Dis.* 91, 669–676. doi: 10.1094/PDIS-91-6-0669

Untiveros, M., Olspert, A., Artola, K., Firth, A. E., Kreuze, J. F., and Valkonen, J. P. T. (2016). A novel sweet potato potyvirus open reading frame (ORF) is expressed via polymerase slippage and suppresses RNA silencing. *Mol. Plant Pathol.* 17, 1111–1123. doi: 10.1111/mpp.12366

Valli, A. A., Gallo, A., Rodamilans, B., López-Moya, J. J., and García, J. A. (2018). The HCPro from the Potyviridae family: an enviable multitasking helper component that every virus would like to have. *Mol. Plant Pathol.* 19, 744–763. doi: 10.1111/mpp.12553

Valli, A., García, J. A., and López-Moya, J. J. (2015). "Potyviridae" in *eLS Encyclopedia of life sciences*. Chichester, UK: John Wiley & Sons, Ltd, 1–10.

Valli, A., López-Moya, J. J., and García, J. A. (2007). Recombination and gene duplication in the evolutionary diversification of P1 proteins in the family Potyviridae. *J. Gen. Virol.* 88, 1016–1028. doi: 10.1099/vir.0.82402-0

Vance, V. B. (1991). Replication of potato virus X RNA is altered in coinfections with potato virus Y. *Virology* 182, 486–494. doi: 10.1016/0042-6822(91)90589-4

Verma, R. K., Mishra, M., Marwal, A., and Gaur, R. K. (2020). Identification, genetic diversity and recombination analysis of watermelon mosaic virus isolates. *3 Biotech* 10:257. doi: 10.1007/s13205-020-02248-8

Voinnet, O. (2001). RNA silencing as a plant immune system against viruses. *Trends Genet.* 17, 449–459. doi: 10.1016/S0168-9525(01)02367-8

Wei, Y., Han, X., Wang, Z., Gu, Q., Li, H., Chen, L., et al. (2018). Development of a GFP expression vector for cucurbit chlorotic yellows virus. *Virol. J.* 15:93. doi: 10.1186/s12985-018-1004-9

Weinheimer, I., Jiu, Y., Rajamäki, M.-L., Matilainen, O., Kallijärvi, J., Cuellar, W. J., et al. (2015). Suppression of RNAi by dsRNA-degrading RNaseIII enzymes of viruses in animals and plants. *PLoS Pathog.* 11:e1004711. doi: 10.1371/journal.ppat.1004711

Wintermantel, W. M., Gilbertson, R. L., Natwick, E. T., and McCreight, J. D. (2017). Emergence and epidemiology of cucurbit yellow stunting disorder virus in the American desert southwest, and development of host plant resistance in melon. *Virus Res.* 241, 213–219. doi: 10.1016/j.virusres.2017.06.004

Wu, X., Valli, A., García, J. A., Zhou, X., and Cheng, X. (2019). The tug-of-war between plants and viruses: great progress and many remaining questions. *Viruses* 11:203. doi: 10.3390/v11030203

Wylie, S. J., Adams, M., Chalam, C., Kreuze, J., López-Moya, J. J., Ohshima, K., et al. (2017). ICTV virus taxonomy profile: Potyviridae. *J. Gen. Virol.* 98, 352–354. doi: 10.1099/jgv.0.000740

Zeng, R., Liao, Q., Feng, J., Li, D., and Chen, J. (2007). Synergy between cucumber mosaic virus and zucchini yellow mosaic virus on cucurbitaceae hosts tested by real-time reverse transcription-polymerase chain reaction. *Acta Biochim. Biophys. Sin.* 39, 431–437. doi: 10.1111/j.1745-7270.2007.00292.x

Conflict of Interest: The authors declare that the research was conducted in the absence of any commercial or financial relationships that could be construed as a potential conflict of interest.

frontiers in Microbiology

REVIEW
published: 09 April 2021
doi: 10.3389/fmicb.2021.645419

Targets and Mechanisms of Geminivirus Silencing Suppressor Protein AC2

*Karuppannan Veluthambi[1] and Sukumaran Sunitha[2]**

[1]Department of Plant Biotechnology, School of Biotechnology, Madurai Kamaraj University, Madurai, India, [2]Department of Biological Sciences, Texas Tech University, Lubbock, TX, United States

Geminiviruses are plant DNA viruses that infect a wide range of plant species and cause significant losses to economically important food and fiber crops. The single-stranded geminiviral genome encodes a small number of proteins which act in an orchestrated manner to infect the host. The fewer proteins encoded by the virus are multifunctional, a mechanism uniquely evolved by the viruses to balance the genome-constraint. The host-mediated resistance against incoming virus includes post-transcriptional gene silencing, transcriptional gene silencing, and expression of defense responsive genes and other cellular regulatory genes. The pathogenicity property of a geminiviral protein is linked to its ability to suppress the host-mediated defense mechanism. This review discusses what is currently known about the targets and mechanism of the viral suppressor AC2/AL2/transcriptional activator protein (TrAP) and explore the biotechnological applications of AC2.

Keywords: geminivirus, AC2/C2, transcriptional activator, suppressor protein, silencing suppressor, biopharming, genome-editing

OPEN ACCESS

Edited by:
Rajarshi Kumar Gaur, Deen Dayal Upadhyay Gorakhpur University, India

Reviewed by:
Claudia Castillo-González, Texas A&M University, United States
Manoj Prasad, National Institute of Plant Genome Research (NIPGR), India

****Correspondence:***
Sukumaran Sunitha
sunitha.sukumaran@ttu.edu

Specialty section:
This article was submitted to Microbe and Virus Interactions With Plants, a section of the journal Frontiers in Microbiology

Received: *23 December 2020*
Accepted: *10 March 2021*
Published: *09 April 2021*

Citation:
Veluthambi K and Sunitha S (2021) Targets and Mechanisms of Geminivirus Silencing Suppressor Protein AC2. Front. Microbiol. 12:645419. doi: 10.3389/fmicb.2021.645419

INTRODUCTION

Geminiviruses are single-stranded (ss) DNA viruses that cause major losses to a number of economically important crops throughout the world (Scholthof et al., 2011; Rojas et al., 2018). *Geminiviridae* constitutes the largest family of plant viruses with nine genera and 485 species (Zerbini et al., 2017). Geminiviruses are characterized by their small, circular, ssDNA genomes encapsidated in twinned-icosahedral particles. They are vector-transmissible and infect both monocotyledonous and dicotyledonous plants (Zerbini et al., 2017). The viral genomes are either monopartite or bipartite with circular ssDNA molecules of 2.5 to 5.5 × 10^3 nucleotides. Bipartite geminiviruses, with DNA A and DNA B components, possess a highly conserved common region (CR) of ~200 nucleotides. An inverted repeat within the CR forms a hairpin loop, and within the loop is the conserved 9-nt sequence 5'-TAATATT$^{\downarrow}$AC-3'.

Geminiviruses are classified into nine genera namely *Becurtovirus*, *Begomovirus*, *Capulavirus*, *Curtovirus*, *Eragrovirus*, *Grablovirus*, *Mastrevirus*, *Topocuvirus*, and *Turncurtovirus*, based on the genome organization, host-range, and the type of insect vector which transmits the virus (Zerbini et al., 2017). Viruses in the genus *Begomovirus* have mono- or bipartite genomes while those of all other genera possess monopartite genome organization. Geminiviruses exhibit bidirectional transcription and encode 5–7 proteins that exploit and reprogram host machineries to establish infection (Hanley-Bowdoin et al., 2013; Aguilar et al., 2020). Two systems of gene nomenclature are currently in use. Both designate genes and gene products by numbers. One nomenclature

denotes genes as virion-sense (V) or complementary-sense (C), whereas the other indicates genes as oriented in the rightward (R; virion-sense; clockwise) or leftward (L; complementary-sense; counter clockwise) direction of the genome map. We have used in this review, the nomenclature based on the virion-sense (V) and complementary-sense (C) strands.

Begomovirus represents the largest and the best-studied geminivirus genus. The bipartite genomes of begomoviruses are designated as DNA A and DNA B (**Figure 1A**). DNA A encodes five or six open reading frames (ORFs) and DNA B encodes two ORFs. The virion-sense ORFs AV1 and AV2 of DNA A encode coat protein (CP) and pre-coat protein, respectively (Padidam et al., 1996). The complementary-sense strand ORFs of DNA A encode the replication-associated protein (AC1/Rep), the transcriptional activator protein (AC2/TrAP), the replication enhancer protein (AC3/REn), and AC4 (Hanley-Bowdoin et al., 2000). DNA B ORFs encode the nuclear-shuttle protein (BV1/NSP) and the movement protein (BC1/MP; Schaffer et al., 1995).

Monopartite begomoviruses lack the DNA B component (Kheyr-Pour et al., 1991; Navot et al., 1991). The single, circular ssDNA genome encodes six ORFs, two in the virion-sense (V1 and V2) and four in the complementary-sense (C1, C2, C3, and C4) strands (**Figure 1B**). Some monopartite begomoviruses do not cause typical disease symptoms in infected plants when acting alone. They require an ssDNA satellite molecule (betasatellite/alphasatellite/deltasatellites/defective satellites) to cause symptomatic disease and viral DNA accumulation (Saunders et al., 2000; Fiallo-Olivé et al., 2012, 2016).

Curtovirus genome organization is like that of monopartite begomoviruses (**Figure 1C**). The virion-sense strand of curtoviruses is more complex with three ORFS V1, V2, and V3. V1 encodes the coat protein and V3 encodes the movement protein. V2/Reg is a unique curtovirus protein that regulates relative ssDNA and dsDNA levels and hence the name "Reg" (Hormuzdi and Bisaro, 1993). The complementary-sense strand encodes four genes namely Rep/C1, C2, REn/C3, and C4

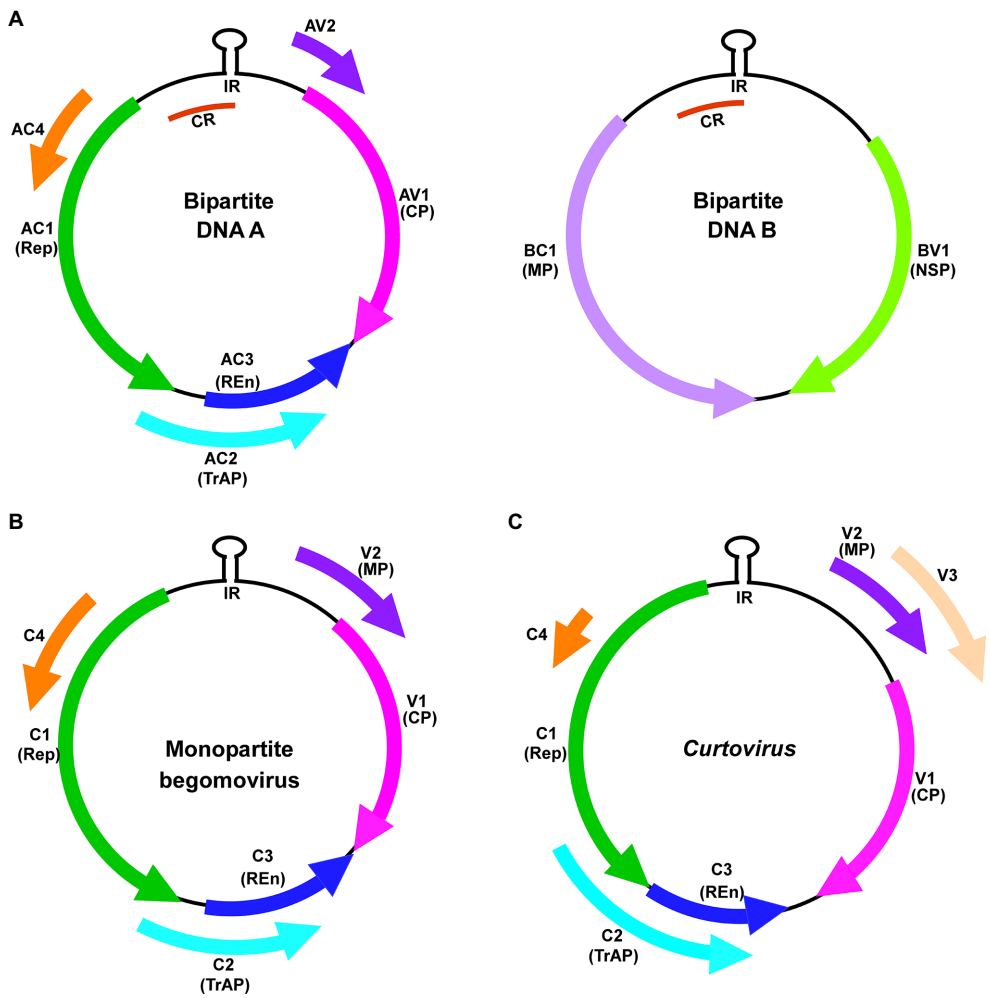

FIGURE 1 | Genomic organization of **(A)** bipartite begomovirus, **(B)** monopartite begomovirus, and **(C)** curtovirus. Virion-sense (V) or complementary-sense (C) strand open reading frames (ORFs) and corresponding protein products are coded by color. CR, common region; CP, coat protein; IR, intergenic region; MP, movement protein; NSP, nuclear shuttle protein; REn, replication enhancer protein; Rep, replication-associated protein; and TrAP, transcriptional activator protein.

(Stanley and Latham, 1992; Stanley et al., 1992). Rep/C1 (Luna and Lozano-Durán, 2020) and Ren/C3 are highly conserved between curtovirus and begomovirus. Curtovirus REn was shown to functionally complement the REn mutation in a bipartite begomovirus (Hormuzdi and Bisaro, 1995). However, curtovirus C2, and the positional homolog of begomovirus AC2, display only partial sequence and functional homology between them (Luna and Lozano-Durán, 2020).

Although the position of AC2/C2 ORFs is conserved in most geminivirus genera, the functions of AC2/C2 are known only in curtovirus and begomovirus. AC2, a 15 kDa multifunctional protein, is also known as C2, L2, AL2, or transcriptional activator protein (TrAP). AC2 is a delayed early gene product which transactivates late viral genes, *CP*, and *NSP* (Sunter and Bisaro, 1991, 1992; Haley et al., 1992; Shivaprasad et al., 2005), suppresses host defense mechanism (Bisaro, 2006; Raja et al., 2010), and acts as a symptom determinant (Hao et al., 2003; Rajeswaran et al., 2007; Siddiqui et al., 2008). *C2*, a positional homolog of *AC2* in monopartite begomoviruses, is highly similar to AC2 in sequence and function (**Figure 2A**; Noris et al., 1996; van Wezel et al., 2001, 2002, 2003; Dong et al., 2003; Gopal et al., 2007). The C2 protein which is encoded by the curtoviruses *Beet curly top virus* (BCTV), *Beet severe curly top virus* (BSCTV), and *Spinach curly top virus* (SCTV) exhibits very little sequence similarity when compared to begomovirus AC2/C2 except for the conserved Cys-His residues in the middle (**Figures 2A,D**; Luna and Lozano-Durán, 2020). AC2 has three highly conserved functional domains: (1) N-terminal basic domain with a bipartite nuclear localization signal (NLS), which consists of four consecutive arginine residues (**Figures 2A–C**; Dong et al., 2003; Trinks et al., 2005). (2) A conserved zinc finger-like domain comprising the conserved cysteine and histidine residues (CCHC) which is present in the middle. (3) The C-terminal which possesses an acidic transactivation domain (**Figures 2A,B**; Trinks et al., 2005). This review focuses on the host targets and versatile mechanisms deployed by the geminiviral silencing suppressor protein AC2/C2 to counter the plant defense.

PLANT DEFENSE AND VIRAL COUNTER-DEFENSE MECHANISMS

RNA silencing is a very effective antiviral defense mechanism. RNA silencing has evolved as the first line of defense against invading nucleic acids including viruses, transposons, transgenes, and repetitive sequences (Baulcombe, 2004; Voinnet, 2005; Shabalina and Koonin, 2008). In addition to structured ssRNA viral genomes, DNA viral transcripts which are structured and overlapping transcripts also act as precursors for viral siRNA pathway (Blevins et al., 2011; Aregger et al., 2012). The dsRNA is processed into 21 nt siRNAs by DICER-LIKE4/DCL4 protein (**Figure 3A**; Akbergenov et al., 2006; Blevins et al., 2006). DCL2 expression stimulates transitivity and secondary siRNA production and increases silencing efficiency in the absence of DCL4 (Parent et al., 2015). When DCL2 and DCL4 are present together, abundant RNAs from viruses and transgenes are processed hierarchically first by DCL4 which has high affinity and processivity to restrict off-target silencing caused by the secondary siRNAs generated by the transitivity-prone DCL2 (Parent et al., 2015). DCL1-mediated processing of geminiviral dsRNA into 21 nt siRNA is inefficient (Blevins et al., 2006); however, it acts as a positive regulator by making viral dsRNAs available to other DCLs to be processed into siRNAs (Blevins et al., 2006; Csorba et al., 2015). DCL1 also acts as a negative regulator of viral silencing by downregulating DCL4 and DCL3 (Qu et al., 2008). The 21 nt siRNA generated by DCL4 cleaves the target viral transcript in association with ARGONAUTE (AGO) proteins. AGO2 acts as a second layer of defense when AGO1 is suppressed in *Arabidopsis* (Harvey et al., 2011). AGO7 acts in coordination with AGO1 for viral clearance (Qu et al., 2008) but preferentially targets less structured viral RNA. The role of AGO7 in geminiviral defense is not clear.

The AGO-siRNA sliced target transcript serves as a template for RNA-DEPENDENT RNA POLYMERASE1/RDR1, RDR2, and RDR6 to convert it into dsRNA, which thereafter generates secondary siRNAs in RNA viruses (Garcia-Ruiz et al., 2010). Interestingly, geminiviral mRNAs appear to be poor templates for RDR-dependent secondary siRNA biogenesis. Aregger et al. (2012) showed that the viral siRNAs which accumulate in *Cabbage leaf curl virus* (CaLCuV)-infected *Arabidopsis* are RDR1/2/6-independent primary siRNAs. Interestingly, RDR6 was shown as a target of *Mungbean yellow mosaic India virus* (MYMIV) AC2 (Kumar et al., 2015). Although DCL4 has been implicated in the generation of 21 nt siRNAs, DCL2 and DCL3 appear to work in concert to generate the antiviral response (**Figures 3A,B**). Abundance of 21, 22, and 24 nt siRNAs is observed in cassava and *Nicotiana benthamiana* infected with *African cassava mosaic virus* (ACMV; Akbergenov et al., 2006). Prevalence of 21–22 nt siRNAs was observed in tomato infected with *Tomato yellow leaf curl Sardinia virus* (TYLCSV; Miozzi et al., 2013) and preferential accumulation of 22 nt siRNAs was observed in tomato and *N. benthamiana* infected with *Tomato yellow leaf curl China virus* (TYLCCNV; Yang et al., 2011). Interestingly, 24 nt siRNAs generated by DCL3 (**Figure 3B**) are the most abundant siRNAs in *Arabidopsis* infected with CaLCuV (Blevins et al., 2006).

RNA-directed DNA methylation (RdDM) of cytosine residues and histone H3 lysine 9 dimethylation (H3K9me2) of chromatin are hallmarks of epigenetic defense mechanism evolved by the plants against invading DNAs including geminiviruses and transposons. The equilibrium between repressed and active viral chromatin determines the outcome of infection and symptom remission. Host recovery is tightly associated with the equilibrium favoring repressed state (Ceniceros-Ojeda et al., 2016; Coursey et al., 2018). The canonical RdDM machinery includes RNA DEPENDENT RDR2, DCL3, AGO4, and two plant-specific RNA polymerases, Pol IV and Pol V (Zhang et al., 2018). Pol IV transcribes heterochromatic regions to produce a nascent transcript (Herr et al., 2005; Daxinger et al., 2009), which is recruited to the cajal bodies in the nucleolus, where they are converted into dsRNA by RDR2 (Li et al., 2006). The resultant dsRNA is processed by DCL3 into 24 nt siRNAs, which are methylated by HEN1 and used by AGO4 to base pair with the Pol V-generated scaffold transcript (Wierzbicki et al., 2008) to mediate RNA-directed DNA

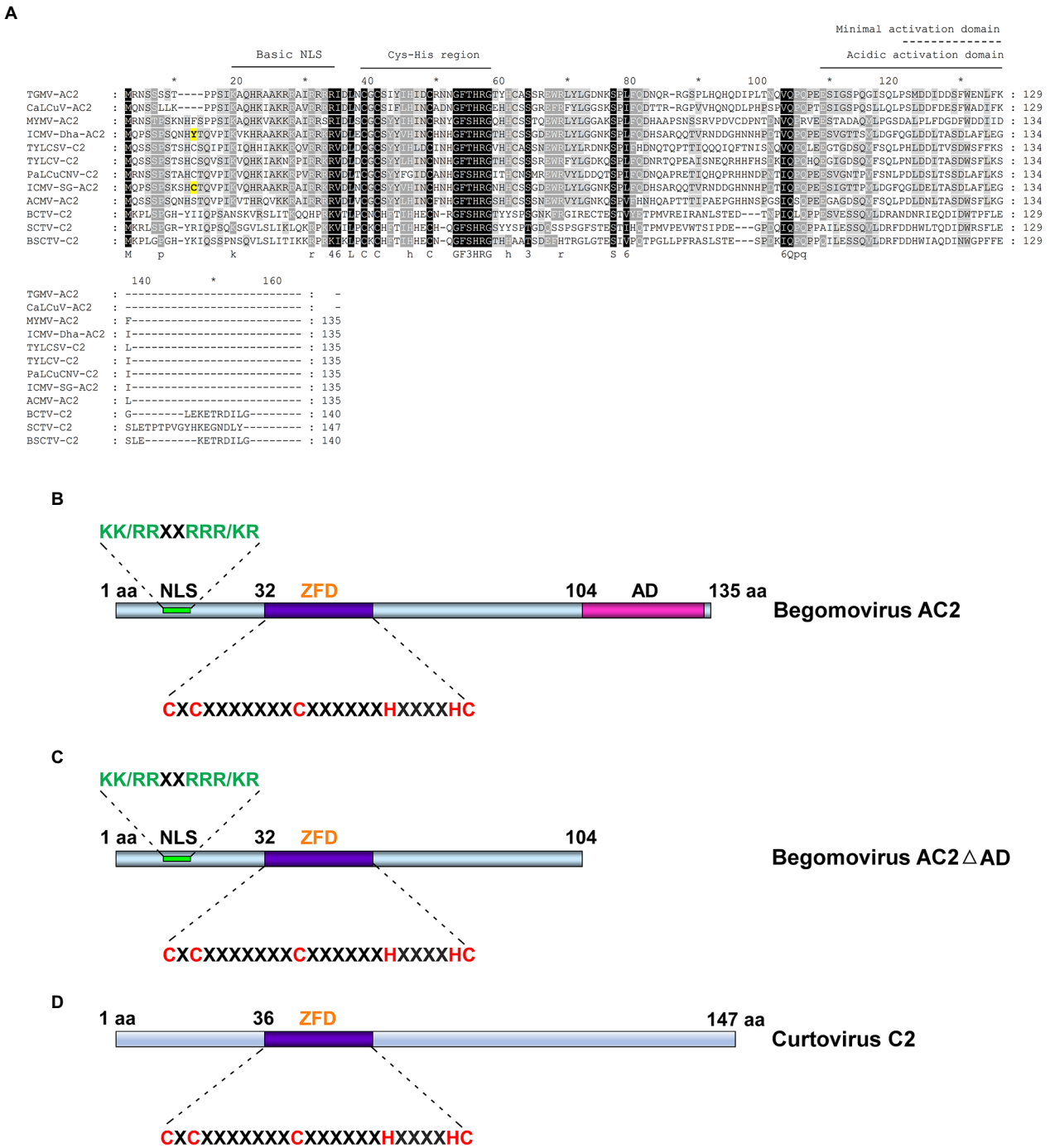

FIGURE 2 | Alignment of AC2 of bipartite, C2 proteins of monopartite begomovirus, and C2 of curtovirus. **(A)** Clustal alignment of AC2/C2 amino sequences of *Tomato golden mosaic virus* (TGMV; acc. no. NC_001507); *Mungbean yellow mosaic virus* (MYMV; acc. no. AJ132575); *African cassava mosaic virus* (ACMV; acc. no. NC_001467); *Indian cassava mosaic virus*-Singapore (ICMV-SG; acc. no. JX518289); *Indian cassava mosaic virus*-Dharwad (ICMV-Dha; acc. no. GQ924760); *Cabbage leaf curl virus* (CaLCuV; acc. no. NC_00386); *Tomato yellow leaf curl Sardinia virus* (TYLCSV; acc. no. L27708); *Tomato yellow leaf curl virus* (TYLCV; acc. no. AM282874); *Papaya leaf curl China virus* (PaLCuCNV; acc. no. FN256260); *Beet curly top virus* (BCTV; acc. no. AF379637); *Beet severe curly top virus* (BSCTV; acc. no. U02311); and *Spinach curly top virus* (SCTV; Acc. No. AY548948). The conserved N-terminal basic domain, the Cys-His residues in the middle and the C-terminal acidic activation domain are marked. The Tyr residue in ICMV-Dha strain and Cys residue in pathogenic ICMV-SG strain are highlighted in yellow. **(B)** Schematic representation of begomovirus AC2 involved in activation domain-dependent silencing suppression. **(C)** Schematic representation of begomovirus AC2 with deletion in activation domain (AC2ΔAD) involved in activation domain-independent silencing suppression. **(D)** Schematic representation of curtovirus C2 involved in activation domain-independent silencing suppression. NLS, nuclear localization signal; ZFD, zinc-finger like domain; and AD, activation domain.

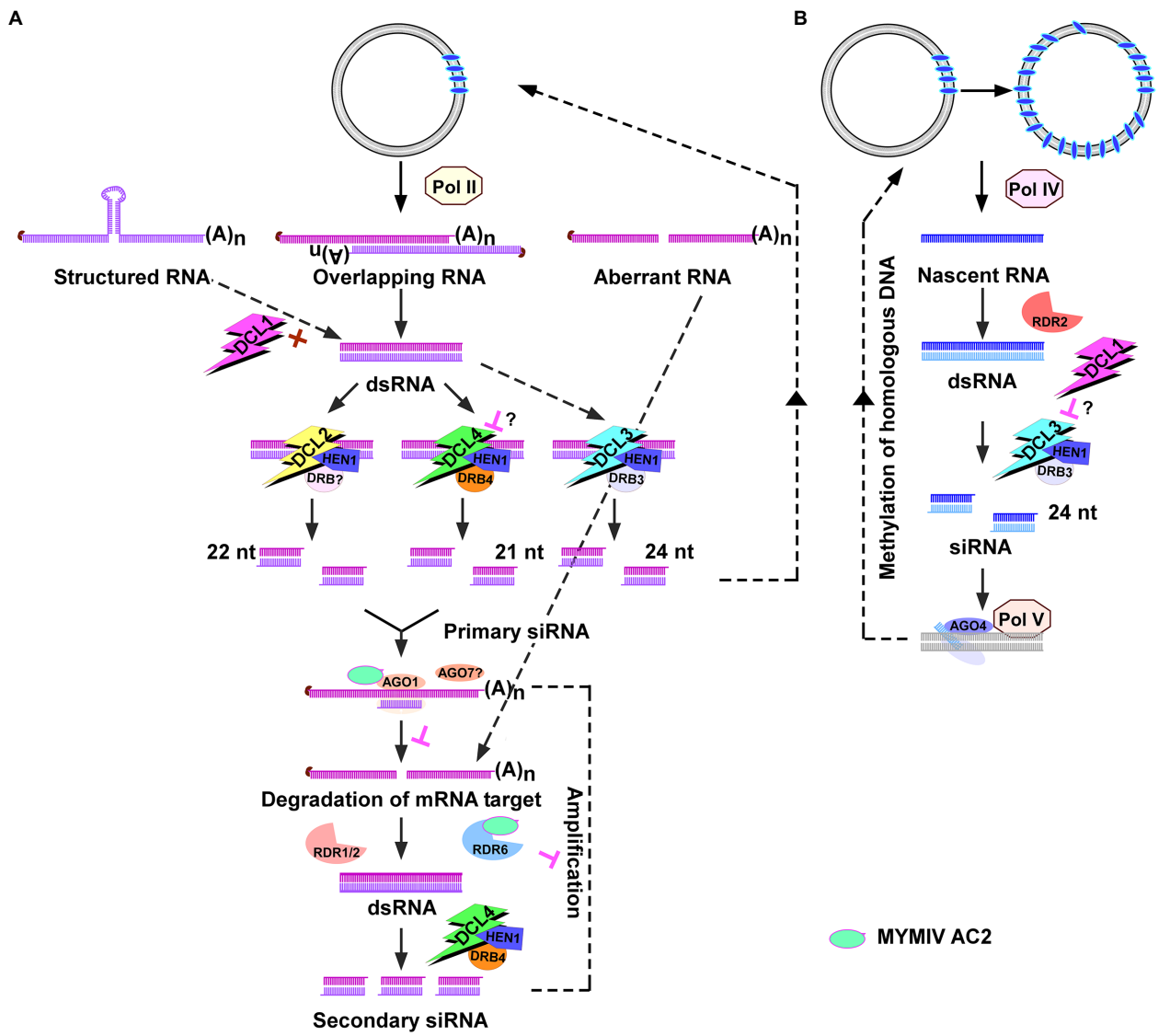

FIGURE 3 | Geminiviral siRNA pathways. **(A)** Post-transcriptional gene silencing (PTGS) pathway. The host RNA polymerase transcribes the replicative form of virus into structured/overlapping/aberrant transcripts which are processed into 21 nt siRNA by DICER-LIKE4/DCL4. DCL2 generates 22 nt siRNAs in the absence of DCL4. DCL1 acts as a positive regulator (+) by facilitating dsRNA access to other DCLs. The role of DCL1 as a negative regulator (⊣) of DCL4 and DCL3 in geminiviral siRNA pathway is not clear (?). The 21 nt siRNAs-Argonaute1 (AGO1) target viral transcripts for slicing by the endo-ribonuclease activity of AGO1. The role of AGO7 in geminiviral defense is not clear (?). The sliced mRNA transcript serves as a template for RNA-DEPENDENT RNA POLYMERASE1/2/6 (RDR1, -2, -6) to convert it into dsRNA, which thereafter generates secondary siRNAs to amplify the host defense response. Suppression of PTGS by binding AGO1 and RDR6 by *Mungbean yellow mosaic India virus* (MYMIV) AC2 is denoted. **(B)** Transcriptional gene silencing (TGS) pathway. The Pol II transcribed dsRNA is processed by DCL3 (when DCL2 and DCL4 are saturated) into 24 nt siRNAs which cause *de novo* methylation of viral genome. The methylated viral genome is transcribed by Pol IV to produce a nascent transcript, which is converted to dsRNA by RNA-DEPENDENT RNA POLYMERASE2/RDR2. dsRNA is processed by DCL3 into 24 nt siRNAs. The complex of 24 nt siRNA-AGO4 targets the Pol V-generated scaffold transcript to mediate RNA-directed DNA methylation. DRB, double-stranded RNA binding proteins and HEN1, HUA ENHANCER1 methyltransferase.

methylation (**Figure 3B**). Scaffold transcripts which originate from intergenic non-coding sequences are required for silencing adjacent siRNA-generating loci (Wierzbicki et al., 2009). AGO4 recruits chromatin modifying methyltransferase (MTase) and also slices the scaffold transcript which serves as a template for RDR2-mediated dsRNA production and amplification of 24 nt siRNA. Methylation of the invading geminiviral genome is mediated by 24 nt siRNAs (Raja et al., 2008; Buchmann et al., 2009). Interestingly, Pol IV and Pol V were shown to be not essential for *de novo* methylation of geminiviral genome (Jackel et al., 2016). *Arabidopsis* mutants *pol IV* and *pol V* reduced accumulation of all classes of virus-derived siRNAs suggesting that they are not so essential in viral siRNA biogenesis including 24 nt siRNA biogenesis. While Pol IV and Pol V

were not essential in establishing cytosine methylation in the viral genome, they were found to be critical for maintenance and amplification of methylation. Incidentally, the mechanism involving Pol II-RDR6-mediated methylation of retrotransposon (Marí-Ordóñez et al., 2013) was evoked to explain the *de novo* methylation of geminiviral genome (Jackel et al., 2016; **Figure 3B**). A study by Marí-Ordóñez et al. (2013) showed that EVADE (EVD), a retrotransposon, generates high levels of Pol II-RDR6 dependent dsRNA upon proliferation which could eventually quench the DCL2 and DCL4 dicers involved in 21 and 22 nt siRNA biogenesis. Thus, the Pol II-RDR6 dependent dsRNA are processed by DCL3 into 24 nt siRNAs from transcribed regions of the retrotransposon. The key role of Pol IV and Pol V in establishing chromatin methylation and in enabling recovery emphasized the importance of these enzymes in mounting antiviral defense through methylation.

The presence of a robust viral counter defense mechanism is underscored by the ubiquitous presence of one or more silencing suppressor proteins in the armor of a virus. The arms race between silencing and silencing suppression results in resistance or susceptibility to the pathogen. Geminiviruses encode several proteins namely AC2/C2, AC4/C4, AV2/V2, βC1, and Rep that suppress RNA silencing by targeting various components of the post-transcriptional gene silencing (PTGS) machinery, transcriptional gene silencing (TGS) machinery, and cellular regulatory genes (reviewed in Hanley-Bowdoin et al., 2013; Kumar, 2019; Rishishwar and Dasgupta, 2019; Yang et al., 2019; Guerrero et al., 2020). Of all the known geminiviral suppressor proteins, AC2 is the most well-studied and is known to target multiple plant genes and proteins. In this review, we have taken a comprehensive approach to document all known targets of the geminiviral suppressor protein AC2 and the interconnecting and/or unique mechanisms evolved by the viruses to counter the plant defense mechanism.

AC2-MEDIATED SUPPRESSION OF HOST DEFENSE MECHANISM

AC2 of begomoviruses and C2 of curtoviruses act as suppressors of silencing through two broadly classified mechanisms: (i) activation domain-dependent silencing suppression- begomovirus AC2 with a C-terminal acidic activation domain (**Figure 2B**) is involved in this mechanism and (ii) activation domain-independent silencing suppression, which is manifested by curtovirus C2 which lacks the activation domain (**Figure 2D**) and certain begomovirus AC2 proteins with deletions of the activation domain (**Figure 2C**). AC2/C2 also interacts with and inactivates many cellular regulatory proteins to circumvent the innate defense mechanism which is independent of siRNA-mediated silencing (Guerrero et al., 2020).

Activation Domain-Dependent Silencing Suppression

Suppression activity of AC2 was first demonstrated by Voinnet et al. (1999) in the *N. benthamiana* line 16c, in which the previously established silencing of *gfp* was reverted by the expression of the ACMV *AC2* in a potato virus X (PVX) vector. Similar studies with C2 of *Tomato yellow leaf curl virus*-China (TYLCV-C), a monopartite begomovirus, revealed that the suppression of silencing was associated with the presence of an intact zinc finger-like motif (van Wezel et al., 2002) and an NLS (Dong et al., 2003). *East African cassava mosaic Cameroon virus* (EACMCV) and *Indian cassava mosaic virus* (ICMV) are known to suppress silencing (Vanitharani et al., 2004). Although the mechanism of suppression is not clear, transient AC2 expression enabled ~8-fold increase in synergistic mixed infection with recovery type viruses ACMV and *Sri Lankan cassava mosaic virus* (SLCMV), which exhibit recovery from symptoms 2 to 3 weeks after infection (Vanitharani et al., 2004). The activation domain-dependent silencing suppression is also known as "transcription-dependent silencing suppression" (Bisaro, 2006). Trinks et al. (2005) demonstrated the requirement of the intact activation domain of *Mungbean yellow mosaic virus* (MYMV) AC2 in addition to the NLS and Zn-finger motifs to suppress silencing. The need for NLS, Zn-finger motif, and activation domain of AC2 for efficient silencing suppression suggested that MYMV and ACMV AC2 and TYLCV-C C2 regulate silencing suppression in the host cell nucleus and are dependent on DNA interaction and transcriptional activation.

Suppression of PTGS by Transactivation of Host Suppressor *WEL1*

Transient expression of MYMV and ACMV *AC2* in *Arabidopsis* protoplasts upregulated the expression of 30 plant genes. One such gene was Werner's exonuclease-like 1 (*WEL1*), a homolog of Werner Syndrome-like exonuclease (*WEX*). WEX, an RNase D exonuclease-like protein acts as a positive regulator of post-transcriptional gene silencing (PTGS; Glazov et al., 2003). WEL1 does not have the complete "DEDDY" signature conserved in WEX. Hence, AC2-mediated upregulation of *WEL1* is likely to exert a dominant negative effect on WEX function (**Figure 4A**; Trinks et al., 2005). Thereby, a novel mechanism of AC2-mediated induction of host silencing suppressors was proposed by Trinks et al. (2005). The authors showed induction of *WEL1* and five other genes by MYMV and ACMV AC2 in *Arabidopsis* and *Nicotiana plumbaginifolia* protoplasts. However, upregulation of *WEL1* upon ACMV or MYMV viral infection or an increase in viral load upon transgenic over-expression of *WEL1* has not been demonstrated to date; thus, the role of *WEL1* as a host silencing suppressor remains to be confirmed. Similarly, the authors did not evaluate whether silencing of *WEL1* abolished AC2-mediated suppression in *N. benthamiana* 16c line. Interestingly, Trinks et al. (2005) demonstrated that mutations of all three functional domains (NLS1-, ZF-, and AD-) abolished transactivation as well as silencing suppression property of AC2. MYMV AC2 being a small, multifunctional protein, the loss of silencing suppression of AC2 mutants by impaired folding or loss of interaction with host factors cannot be discounted.

Suppression of PTGS by Transactivation of Calmodulin-Like Protein

Tomato golden mosaic virus (TGMV) AC2 induces a calmodulin-like protein Nb-rgsCaM (Chung et al., 2014).

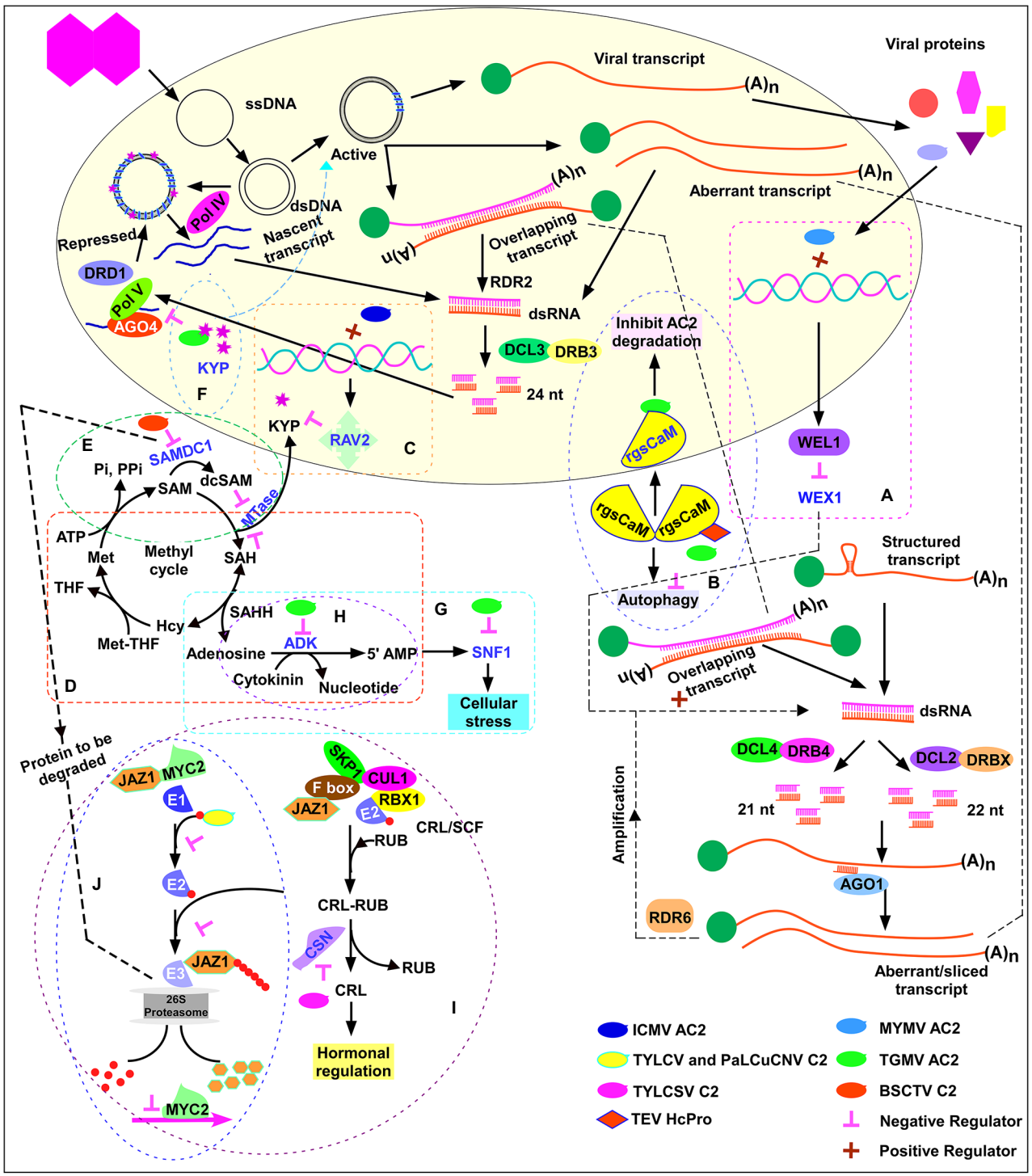

FIGURE 4 | AC2-mediated suppression of host defense mechanism. Activation domain-dependent mechanism: suppression of PTGS by activating the host silencing suppressors **(A)** Werner's exonuclease-like 1 (*WEL1*) by MYMV AC2, **(B)** calmodulin-like protein by TGMV AC2, and **(C)** RELATED TO ABI3 and VP1 (RAV2), transcription repression and downregulation of H3K9 histone methyltransferase KRYPTONITE (KYP) by *Indian cassava mosaic virus* (ICMV) AC2. Activation domain-independent mechanism: **(D)** The methyl cycle and suppression of PTGS/TGS by inactivating adenosine kinase by TGMV AC2 and BCTV C2. **(E)** Suppression of PTGS by stabilizing S-adenosyl methionine decarboxylase1 by BSCTV C2. **(F)** Suppression of TGS by inhibiting KYP enzymatic activity by TGMV and CaLCuV AC2 binding. **(G)** Suppression mediated by inactivation of SNF1 kinase by TGMV AC2 and BCTV C2. **(H)** Suppression mediated by elevation of cellular cytokinin levels by TGMV AC2 and C2 of SCTV. **(I)** Suppression mediated by inhibition of jasmonate signaling pathway by C2 of TYLCSV. **(J)** Suppression mediated by competitive binding of C2 of TYLCV and PaLCuCNV to ubiquitin.

rgsCaM over-expression leads to an increase in viral DNA load. rgsCaM was shown to be induced by HcPro, a silencing suppressor of *Tobacco etch virus* (TEV; Anandalakshmi et al., 1998) and over-expression of rgsCaM was shown to reverse PTGS (Anandalakshmi et al., 2000), suggesting the role of rgsCaM as an endogenous silencing suppressor. rgsCaM prevents TEV HcPro and Cucumber mosaic virus suppressor 2b from binding to dsRNAs/siRNAs and reduce the suppressor protein stability by autophagy, resulting in a more potent RNAi defense against viral infection. rgsCaM over-expressing lines were less susceptible to the virus (Nakahara et al., 2012). In contrast, rgsCaM over-expression resulted in increased susceptibility to TGMV and CaLCuV (Chung et al., 2014) likely because TGMV and CaLCuV are DNA viruses, whereas the viruses studied by Nakahara et al. (2012) were RNA viruses. TGMV AC2 does not bind dsRNAs/siRNAs unlike RNA viral suppressors HcPro, P19, and 2b. rgsCaM self-interaction was observed in cytoplasm while interaction with TGMV AC2 sequestered rgsCaM to the nucleus (**Figure 4B**). It was speculated that AC2-mediated localization of rgsCaM to the nucleus is the likely mechanism evolved by TGMV to evade degradation of AC2 by autophagy and thereby effectively suppress the plant defense mechanism. The cajal bodies in the nucleolus are the sites of 24 nt siRNA biogenesis (Pontes and Pikaard, 2008). Chung et al. (2014) speculated that nuclear localization of rgsCaM by TGMV AC2 might interfere with the overall host siRNA biogenesis and make the plants more susceptible to the virus. More studies are needed in future to confirm this hypothesis. TYLCCNV βC1 was shown to act as suppressor of PTGS by upregulating rgsCaM (Li et al., 2014). A recent study showed that TYLCCNV βC1-upregulated rgsCaM interacts with Suppressor of Gene Silencing 3 (SGS3), a cofactor of RDR6 and induces autophagic degradation of it and thereby suppresses PTGS (Li et al., 2017).

Suppression of TGS by Transactivation of Host Repressor

Indian cassava mosaic virus-Singapore (ICMV-SG) displayed higher pathogenicity in comparison to ICMV-Dharwad (ICMV-Dha). A single point mutation that changes Tyr to Cys in ICMV-Dha AC2 (ICMVDha^{Y11C}) significantly increased pathogenicity (**Figure 2A**; Sun et al., 2015). Increased ICMV-SG infection was associated with increased repression of H3K9 histone MTase KRYPTONITE (NbKYP), a key enzyme for maintenance of chromatin methylation. Downregulation of KYP was directly correlated with an increase in RELATED TO ABI3 and VP1 (RAV2), a transcription repressor. RAV2 is known to regulate RNA silencing and to get upregulated by suppressor proteins of potyvirus HcPro and cucomovirus P38 in *Arabidopsis* (Endres et al., 2010). Transient expression of ICMV-SG, ICMV-Dharwad (ICMV-Dha), and the ICMV-Dha^{Y11C}AC2 mutant in *N. benthamiana* 16c-TGS reversed the TGS of the 16c line as evidenced by reactivation of green fluorescence (Sun et al., 2015). Silencing of *NbRAV2* significantly reduced the viral titer, thus indicating a novel mechanism of silencing suppression. Activation of the putative transcription repressor *NbRAV2* by ICMV-AC2 interferes with TGS by suppressing the expression of KYP (**Figure 4C**). It is not known whether the RAV2 repressor protein directly binds to the *KYP* promoter sequence to downregulate its expression. A RAV2-dependent upregulation of *Arabidopsis* FIERY1 (FRY1) and CML38 (rgsCaM homolog) was observed in TuMV HC-Pro transgenic lines (Endres et al., 2010). It will be useful to study whether ICMV-SG induced RAV2 protein can induce rgsCaM in *N. benthamiana*.

Activation Domain-Independent Silencing Suppression

Reports on AC2-mediated silencing suppression in TGMV suggest that not all viruses require C-terminal activation domain in AC2 for mediating silencing suppression. The activation domain-independent silencing suppression observed in TGMV is also referred as "transcription-independent silencing suppression" (Bisaro, 2006). The unique mechanism evolved by the viruses encoding activation domain-independent silencing suppressors is by interfering with the methyl cycle. S-adenosyl methionine (SAM) is the methyl donor for most transmethylation reactions and is an essential MTase co-factor. An increase in the accumulation of SAM analogs would competitively inhibit MTase and prevent methylation and associated silencing. Activation domain-independent silencing suppressors interfere with the methyl cycle and increase the cellular levels of SAM analogs which compete with SAM. In addition to methyl cycle interference, TGMV and CaLCuV AC2 directly target and inhibit the H3K9me2 histone MTase Su(var)3-9 homolog 4/Kryptonite (SUVH4/KYP), an enzyme critical for histone methylation.

Suppression of PTGS by Inactivating Adenosine Kinase

TGMV AC2 with activation domain deletion (AC2-ΔAD; **Figure 2C**) and BCTV C2 (**Figure 2D**) interact with adenosine kinase (ADK) and inhibit the synthesis of 5'-AMP from adenosine and ATP (**Figure 4D**; Wang et al., 2003). C2 of BCTV and C2 of SCTV, both curtoviruses, lack the transcriptional activation domain which is present in AC2/C2 of begomoviruses (Sunter et al., 1994; Baliji et al., 2007). Although AC2 self-interacts and moves into the nucleus for transcriptional activation, AC2:ADK and C2:ADK complexes form in the cytoplasm (Yang et al., 2007). This emphasizes the dispensability of the activation domain for ADK interaction. AC2/C2 expression inhibited ADK activity in *Escherichia coli*, yeast, and transgenic plants (Wang et al., 2003). ADK plays a key role in the methyl cycle and in SAM-dependent MTase activity. MTase catalyzes methyl group transfer from SAM to a methyl acceptor converting SAM to S-adenosyl-homocysteine (SAH). S-adenosyl-homocysteine hydrolase (SAHH) hydrolyzes SAH to homocysteine (Hcy) and adenosine (**Figure 4D**). SAHH catalyzed reaction is reversible, and the removal of adenosine is essential to tilt the equilibrium of reaction toward hydrolysis of SAH, which otherwise lies strongly toward synthesis of SAH. SAH is also a competitive inhibitor of MTase. Phosphorylation of adenosine to 5'-AMP by ADK prevents resynthesis of SAH and promotes flux through the methyl

cycle to regenerate SAM. Removal of adenosine by phosphorylation facilitates methionine (Met) synthesis, wherein methionine synthase catalyzes the transfer of a methyl group from methylated folic acid [methyltetrahydrofolate (MTHF)] to homocysteine. Addition of adenosine to the sulfur group of methionine regenerates SAM. Thus, the removal of SAH is critical as it can strongly compete with SAM and inhibit MTase (**Figure 4D**). ADK-deficient plants displayed defects in silencing, thus implying an indirect role for ADK in regulating methyl cycle and silencing.

Wild-type *AC2* and *AC2*-ΔAD of TGMV and *C2* of BCTV suppressed PTGS which was directed against *gfp* in the *N. benthamiana* 16c line in an activation domain-independent manner (Wang et al., 2005). The local suppression caused by AC2 could be mimicked by using an invert repeat of ADK or by addition of an adenosine homolog (A-134974) that inhibited ADK activity (Wang et al., 2005). Methylation of the coding region of a gene is a hallmark of PTGS (Ingelbrecht et al., 1994; English et al., 1996). Thus, AC2-mediated inactivation of ADK is likely to have caused suppression of PTGS by its interference in the methylation of coding region (Raja et al., 2010).

Suppression of PTGS by Stabilizing S-Adenosyl Methionine Decarboxylase1

BSCTV C2 interaction with S-adenosyl methionine decarboxylase1 (SAMDC1) and resultant suppression of *de novo* DNA methylation were observed in *Arabidopsis* (Zhang et al., 2011). SAMDC1 is a key enzyme in the conversion of SAM to decarboxylate-S-adenosyl methionine (dcSAM). dcSAM acts as an aminopropyl donor for the biosynthesis of spermidine and spermine. dcSAM also competes with SAM and acts as a competitive inhibitor of MTase (**Figure 4E**). Hence, SAM/dcSAM balance is a key determinant of transmethylation. SAMDC1 possesses a conserved PEST (proline, glutamine, serine, and threonine) sequence that is associated with proteins with rapid turnover rates. BSCTV C2 interacts with SAMDC1 in the PEST region and stabilizes the enzyme by attenuating 26S proteasome-mediated degradation (**Figure 4E**). The resultant increase in dcSAM/SAM ratio affects the host *de novo* methylation. Infection of wild-type plants with BSCTV C2$^-$ mutant strain (engineered by introducing a stop codon in the C2 ORF) or infection of SAMDC1 mutant plant with wild-type BSCTV strain resulted in enhanced DNA methylation, reduced viral titer and reduced susceptibility confirming the key role of C2 and SAMDC1 in regulating host DNA methylation. Agroinfiltration of BSCTV *C2* and *SAMDC1* genes reverted *gfp* silencing in *N. benthamiana* 16c (Zhang et al., 2011).

Suppression of TGS by Inactivating Adenosine Kinase and Stabilizing SAMDC1

Adenosine kinase phosphorylation of adenosine is a prerequisite for sustaining cellular SAM levels. Thus, AC2-mediated interaction and inactivation of ADK invoked the possibility of methylation-mediated repression of viral genome as a possible host defense mechanism against the virus. The *Arabidopsis* mutants *adk*, *cmt3*, *drm1/2*, *drb3*, *clsy1*, *pol IV*, and *pol V* (mutants of RNA-directed DNA methylation components) were hypersensitive to viral infection. Cytosine methylation level of the viral genome was significantly reduced in the hypersusceptible mutant plants (Raja et al., 2008, 2014; Jackel et al., 2016). Infection of *Arabidopsis* with a BCTV mutant lacking *C2* (BCTV C2$^-$) resulted in a host recovery phenotype. The viral DNA in the recovered tissue was hypermethylated, suggesting methylation of the viral genome to be the cause of host recovery. Interestingly, *ago4*, *dcl3*, *drb3*, and *pol V* mutant *Arabidopsis* plants did not recover when infected with BCTV C2$^-$ (Raja et al., 2008, 2014; Jackel et al., 2016), whereas *pol IV* and *clsy1* mutants displayed a delayed recovery phenotype (Jackel et al., 2016). This finding underlined the requirement of AGO4, DCL3, DRB3, Pol IV, and Pol V for methylation of viral genome and resultant host recovery. These results confirmed that methylation of viral genome has been evolved as an epigenetic defense mechanism against geminiviruses (Raja et al., 2008, 2014; Jackel et al., 2016; Coursey et al., 2018).

The AC2/C2-mediated suppression of methylation was studied in the *N. benthamiana* (16-TGS) line, in which the 35S promoter-driven *gfp* transgene is transcriptionally silenced. The silencing of the 16-TGS plant was suppressed by wild-type *AC2* and *AC2*-ΔAD of TGMV and CaLCuV and also by BCTV *C2* when expressed from PVX vectors (Buchmann et al., 2009). Knocking down of SAHH and ADK expression using a *Tobacco rattle virus* VIGS vector reversed *gfp* silencing in 16-TGS. These observations further implied that reversal of silencing mediated by inhibition of methyl cycle is one of the prominent mechanisms evolved by viruses to suppress silencing (Buchmann et al., 2009). Infection of *N. benthamiana* 16-TGS with TGMV, CaLCuV, and BCTV restored GFP fluorescence in a manner consistent with the tissue tropism exhibited by the virus. TGMV and CaLCuV infection restored GFP expression in symptomatic vascular and mesophyll cells (Buchmann et al., 2009; Raja et al., 2010). Interestingly, BCTV-mediated suppression *of gfp* silencing was confined to the vascular tissue, which corroborated well with the vascular specificity of the virus. Transgenic expression of *AC2* and *AC2*-ΔAD of TGMV, BCTV *C2*, and ds*ADK* under a dexamethasone (dex)-inducible promoter reversed the methylation of transcriptionally silenced loci in *Arabidopsis*. The reversal of methylation by *AC2* and *AC2*-ΔAD of TGMV, and BCTV *C2* was found to be locus non-specific. Four independent regions, including one gene-coding region, two transposable elements, and one repetitive DNA region were used as markers to study the effect of *AC2* and *AC2*-ΔAD of TGMV, and BCTV *C2* on cytosine methylation. Reversal of cytosine methylation resulted in ectopic expression of TGS-silenced loci namely, a putative F-box gene, a retrotransposon *At*SN1 (SINE element), and *Athila* (LTR element) in all analyzed transgenic plants. The ability of *AC2* and *AC2*-ΔAD of TGMV and BCTV *C2* to suppress TGS indicates that the suppression is activation domain-independent. TGS in the CACTA-like transposon was reversed only upon wild-type *AC2* induction. This invoked the necessity of transcriptional

activation domain for mediating suppression of the CACTA TGS-loci. Thus, *AC2* transgenic plants reduced cytosine methylation of a wide spectrum of genomic regions and reversed methylation of the TGS loci in *Arabidopsis* by non-specifically inhibiting cellular transmethylation reactions (Buchmann et al., 2009). Although, methylation extension assays confirmed a decrease in 5-methylcytosine methylation of a wide range of genomic regions in *AC2* and *C2* transgenic lines (Buchmann et al., 2009), a whole-genome bisulfite sequencing would provide data on AC2 or C2-mediated reversal of genome-wide cytosine methylation at single-nucleotide resolution.

The attenuation of SAMDC1 degradation by BSCTV C2 may also result in suppression of TGS. SAMDC1 stabilization resulted in an increase in dcSAM/SAM ratio, which in turn reduced the host *de novo* methylation. BSCTV-C2 mutant infection resulted in enhanced DNA methylation of the viral genome (Zhang et al., 2011). In an interesting assay, an *FWA* genomic fragment containing tandem repeats in its promoter region was used to study the role of BSCTV C2 on *de novo* methylation. Methylation of the *FWA* promoter and consequent silencing of the *FWA* gene is essential for normal flowering. The absence of *de novo* methylation of *FWA* transgene in a MTase double mutant *Arabidopsis* plant (*drm1*/*drm2*) caused a delay in flowering (Cao and Jacobsen, 2002). Similar late flowering phenotype was observed when the *FWA* gene was transformed into C2-expressing transgenic lines (Zhang et al., 2011). This suggested a role for BSCTV-C2 in interfering with the *de novo* methylation of the *FWA* transgene.

Developmental Stage-Specific Silencing Suppression

CaLCuV AC2 with the transcription activation domain deletion, and BCTV C2 reversed PTGS and TGS in the vegetative phase of plants indicating a transcription-independent mechanism of silencing suppression. Interestingly, only CaLCuV AC2 but not BCTV C2 could reverse PTGS and TGS upon onset of flowering, indicating that a transcription-dependent activity is required during the reproductive transition. A third suppression mechanism was demonstrated in which CaLCuV $AC2_{1-114}$ lacking the transcription activation domain but not BCTV C2 effectively reversed TGS in reproductive plants (Jackel et al., 2015). Although TGS reversal was observed only in the vegetative phase of plants (plants with prolonged vegetative growth), reduced ADK activity was observed in both vegetative and reproductive plants upon BCTV infection or by silencing of ADK suggesting that TGS and ADK inhibition are uncoupled in reproductive *N. benthamiana* plants. In contrast, SAHH silencing resulted in reversal of TGS in both vegetative and reproductive plants. Thus, a new mechanism of TGS reversal that is independent of both transcription activation and ADK inactivation was observed in reproductive *N. benthamiana* plants expressing $AC2_{1-114}$.

Suppression of TGS by Inhibiting KYP

Interestingly, TGMV and CaLCuV AC2 were shown to inhibit the enzymatic activity of KYP by binding to the catalytic domain and thereby decreasing CHH methylation in gene-rich regions (Castillo-González et al., 2015). Over-expression of KYP enriched H3K9me2 mark of viral chromatin, leading to formation of viral heterochromatin. As a counter-defense strategy, inhibition of KYP activity by TGMV and CaLCuV AC2 protein restored the euchromatic status of the minichromosome which allowed active replication and transcription of viral genes and suppression of the host defense mechanism (**Figure 4F**). While *kyp* mutant was hypersusceptible to CaLCuV infection and accumulated significantly higher viral titers when compared to wild-type, over-expression of the *KYP* transgene in the *kyp* mutant reduced the disease severity significantly.

The necessity of functional AC2 for ssDNA accumulation (Hayes and Buck, 1989) and the requirement of AC2-mediated transactivation of the *CP* and *NSP* genes for systemic infection (Sunter and Bisaro, 1992) is well-known. CaLCuV $AC2^{-}$ strain was engineered by introducing a premature stop codon and was used to infect wild-type and *kyp* mutant plants. While CaLCuV lacking functional AC2 did not show any symptom or systemic accumulation of the mutant virus in wild-type plants, the *kyp* mutants showed low level of sustained systemic infection of the mutant CaLCuV. Although, the mutant viral titer was very low in *kyp* mutants, this exciting study confirmed the role of *KYP* in inhibiting viral replication. Whole genome bisulfite sequencing revealed that AC2 inhibited KYP-dependent CHH methylation. Interaction of AC2 with KYP blocks its methylation activity and relaxes the viral chromatin and facilitates viral replication (**Figure 4F**; Ré and Manavella, 2015).

Suppression of TGS by Ectopic Expression of VIM5

A recent work by Chen et al. (2020) revealed a unique mechanism in which BSCTV-encoded C2 recruits a host imprinted gene VIM5 to evade host silencing. While over-expressing BSCTV *Rep* transgene that also contained the *C2-C3* promoter sequence and C2 N-terminal sequence ($C2_N$), the authors serendipitously observed accumulation of the $C2_N$ transcript in addition to the *Rep* transcript in one of the transgenic *Arabidopsis* lines. Additional transcription from the *C2-C3* promoter was correlated with hypomethylation of the *C2-C3* promoter. Ectopic vegetative transcription of the endosperm-imprinted E3 ubiquitin ligase-encoding gene *VARIANT IN METHYLATION5* (*VIM5*) was observed only in the $C2_N$ transcript-expressing transgenic line, when compared to wild-type *Arabidopsis*. The role of VIM5 in hypomethylation was substantiated by over-expressing *VIM5* in another Rep transgenic line that did not originally accumulate the $C2_N$ transcript; Over-expression of *VIM5* triggered accumulation of the $C2_N$ transcript which correlated with decreased DNA methylation at the transgenic *C2-C3* promoter. Infection with BSCTV resulted in transient expression of the host endosperm-imprinted E3 ubiquitin ligase-encoding gene *VIM5* in rosette leaf tissues. BSCTV infection of *Arabidopsis vim5* mutants resulted in delayed accumulation of viral early gene transcripts *C2* and *C3*, thus confirming the role of VIM5 in contributing to the early expression of C2 and C3 from the viral genome. VIM5 was shown to interact with host CG MTase MET1 and the CHG MTase CMT3 and promote 26S proteasomal

degradation of MET1 and CMT3. MTase mutant plants *met1* and *cmt3* displayed reduced viral methylation at the *C2-C3* promoter. Similarly, infection of a modified BSCTV with substitutions at CG and CHG sites in the *C2-C3* promoter showed higher viral accumulation in *vim5* mutant when compared with the unmodified BSCTV. Thus, early expression of BSCTV silencing suppressor C2 and replication enhancer protein C3 immediately after the expression of Rep, by activating an imprinted E3 ubiquitin-ligase gene, is a strategy evolved by the virus to inhibit viral DNA methylation and establish disease (Chen et al., 2020).

Suppression of PTGS by Inhibiting RDR6 and AGO1

Silencing suppression activity of MYMIV AC2 was demonstrated *in gfp* silenced *Nicotiana xanthi* plants (Karjee et al., 2008; Rahman et al., 2012). The activation domain mutant of MYMIV-AC2 possessed the suppression activity. A two-pronged mechanism involving physical interaction of AC2 with RDR6 and AGO1 was shown as the basis of PTGS suppression of MYMIV AC2 (**Figure 3A**). AC2-mediated inhibition of RNA-dependent RNA polymerase activity and slicing activity of AGO1 protein resulted in reduced siRNA accumulation (**Figure 3A**; Kumar et al., 2015). An *in planta* assay using invert repeat of RDR6 to reverse *gfp* silencing only partially mimicked the suppression activity of AC2. The possibility of RDR6 paralogs partially compensating for the absence of RDR6 cannot be discounted. Future studies involving *rdr6* and *ago1* mutant plants and testing them for enhanced susceptibility would reveal any redundant function of paralogs.

Suppression of Defense Mechanism by Inactivating Cellular Regulatory Genes

Inactivation of SNF1 Kinase

AC2 of TGMV and C2 of BCTV have been shown to interact with SNF1-related kinase (SnRK1), a serine-threonine kinase, and inactivate it (Hao et al., 2003). SnRK1 has been implicated as a key regulator of cellular stress response including innate defense mechanism. AC2-SnRK1 interaction alters the cellular stress metabolism and causes a novel enhanced susceptibility (Hao et al., 2003). Although SNF1 inactivation does not involve suppression of silencing, interaction of AC2 with ADK reduces the cellular AMP levels (**Figure 4D**; Wang et al., 2003). AMP acts as an activator of SNF1 (**Figure 4G**), suggesting a dual strategy evolved by the virus to attenuate the cellular metabolism by inactivating SNF1 by direct interaction and indirectly by reducing cellular AMP levels (**Figure 4G**). *Arabidopsis* SnRK1 was shown to phosphorylate the serine residue at 109 (S^{109}) of CaLCuV AC2 protein. A phosphomimic mutation of the S^{109} reduced viral DNA accumulation and delayed symptom appearance in *Arabidopsis*, thus revealing phosphorylation of viral protein as a host defense mechanism against an invading virus (Shen et al., 2014). Guerrero et al. (2020) report that AC2 of all old world begomoviruses and cutoviruses C2 lack the S^{109} residue. While majority of the new world begomovirus AC2s possess the conserved SnRK1 phosphorylation site, some new world begomoviruses including TGMV AC2 lack the S^{109} residue and hence are not phosphorylated. Instead, TGMV AC2 is shown to inhibit the kinase activity of SnRK1 (Hao et al., 2003).

Elevation of Cellular Cytokinin Levels

Baliji et al. (2010) demonstrated a novel consequence of ADK inhibition by AC2 of TGMV and C2 of SCTV. ADK has a role in maintaining the cellular cytokinin level. ADK-mediated phosphorylation of cytokinin converts the bioactive form of cytokinin to a less bioactive form (**Figure 4H**). Silencing of ADK in *Arabidopsis* increased the cellular cytokinin levels, substantiated by increased activity of a cytokinin-responsive promoter. Over-expression of CaLCuV AC2 and SCTV C2 in *Arabidopsis* resulted in increased expression of endogenous cytokinin-responsive promoters. Thus, geminivirus AC2, by inactivating ADK, increased the cellular cytokinin levels. An enhanced cytokinin level is a prerequisite for cell cycle progression and to maintain an active state of replication. Increased cytokinin resulted in an enhanced susceptibility phenotype. Interestingly, cytokinin is known to negatively regulate the expression of SULTR1;2, a high affinity sulfate transporter in *Arabidopsis* roots (Maruyama-Nakashita et al., 2004). Cytokinin binding to the receptor cytokinin response 1/wooden leg/*Arabidopsis* histidine kinase 4 (CRE1/WOL/AHK) is the cue for negative regulation of sulfur assimilation, while *cre1* mutant is insensitive to cytokinin. In *sultr1;2* mutant, SULTR1;1 was downregulated by cytokinin. Downregulation of sulfate transporters by cytokinin correlated with the decrease in sulfate uptake. Another study by Ohkama et al. (2002) showed that exogenous application of cytokinins upregulated sulfur responsive genes APS reductase 1 (*APR1*) and *SULTR1;2* through a pathway independent of sulfur starvation; likely through increasing sucrose concentration which is known to upregulate *APR1* gene (Kopriva et al., 1999). Exogenous application of cysteine and glutathione (GSH) resulted in downregulation of ATP sulfurylase, APS reductase, and sulfate transporter (Vauclare et al., 2002).

TYLCSV-*C2* transgenic plants repressed the expression of three genes involved in sulfur assimilation namely ATP sulfurylase 3 (*APS3*), APS reductase 1 (*APR1*), and APS reductase 3 (*APR3*) and also accumulated reduced sulfur (Lozano-Durán et al., 2012). Adequate sulfate supply in tobacco plant resulted in a suppressed and delayed *Tobacco mosaic virus* (TMV) symptom development through a phenomenon named sulfur-induced resistance (SIR) or sulfur-enhanced defense (SED; Höller et al., 2010), thus revealing a role for sulfur in plant defense. Exogenous treatment of the TYLCSV-*C2* plants with methyl jasmonate (MeJA) reversed the repression of sulfur assimilation genes (Lozano-Durán et al., 2012). TYLCSV-*C2* transgenic plants over-accumulated cysteine and glutathione. The authors could not explain the reason behind the over-accumulation of cysteine and glutathione when the sulfur assimilation genes were repressed. Lozano-Durán et al. (2012) proposed that the C2 protein might suppress SIR/SED by suppressing jasmonate signaling pathway. However, it would be interesting to study in future if TYLCSV-*C2* plants had increased cellular cytokinin levels similar to

TGMV-*AC2*, CaLCuV-*AC2*, and SCTV-*C2* plants. Also, it is relevant to study if upregulation of sulfur assimilation genes by cytokinin is initially through sucrose-dependent pathway. It is also important to study if the reduction observed in the expression of sulfur assimilation genes is because of the accumulation of cysteine and glutathione in TYLCSV-*C2* transgenic plants. It would be informative to understand if the sulfate reduction in C2 transgenic plants might be because of the negative regulation of sulfate transport pathway by cytokinin binding to CRE1 receptor. Further studies are necessary to understand cross-talk between cytokinin, jasmonate, and sulfur assimilation pathways.

Inhibition of Jasmonate Signaling Pathway

COP9 signalosome (CSN), a highly conserved protein complex with eight subunits that resembles the 19S lid of the 26S proteasome (Dohmann et al., 2008), regulates the activity of E3 ligases. The CSN complex comprises eight subunits, named CSN1–CSN8, where CSN5 is the only catalytic subunit. TYLCSV C2 interacts with CSN5 and interferes with the cellular ubiquitination machinery (Lozano-Durán et al., 2011). Ubiquitination occurs through a cascade of enzymatic reactions namely ubiquitin activation by E1, conjugation by E2, and ligation by E3. E3 ligase comprises the multisubunit Cullin RING Ligases (CRLs). Among CRLs, cullin 1-based group or SCF (for Skp1/Cullin1/F-box), is comprised of four proteins, cullin 1 (CUL1), S-phase kinase-associated protein (SKP1/ASK), the RING subunit RBX1 (RING box 1) and an F-box substrate binding protein. The CRL activity is regulated by covalent attachment and removal of ubiquitin-like protein RUB (related to ubiquitin; **Figure 4I**). CSN5 is associated with the derubylation activity (Gusmaroli et al., 2007). CSN is a multisubunit isopeptidase which removes the RUB moiety from CRLs to function *in vivo*. C2 of TYLCSV interacts with CSN5 and inhibits the derubylation of CRL (**Figure 4I**). Rubylated CUL1 alters several SCF-dependent hormonal processes and also suppresses jasmonate responses in *C2* transgenic plants. Jasmonate signaling has been implicated in defense response and suppression of jasmonate response resulted in enhanced susceptibility phenotype, which was reverted upon exogenous treatment of methyl jasmonate (MeJA). TYLCV C2 and BCTV C2 were also shown to interact with CSN5 suggesting that CSN5-C2 interaction is a conserved function in geminiviruses (Lozano-Durán et al., 2011).

Jasmonate receptor SCF complex is also the receptor for the bacterial toxin coronatine, which is secreted by the plant pathogenic *Pseudomonas syringae* pv. tomato DC3000 (Pto DC3000). Coronatine application on plants facilitates stomatal opening and increases infection (Melotto et al., 2006; Geng et al., 2014). The hindrance of SCF complex by TYLCV C2 (Lozano-Durán et al., 2011) makes TYLCV/TYLCSV C2 transgenic plants less sensitive to coronatine, as evidenced by reduced Pto DC3000 bacterial growth (Rosas-Díaz et al., 2016). The mutant COR^- strain and wild-type strain had similar bacterial growth in C2 transgenic plants (Rosas-Díaz et al., 2016) confirming the role of C2 in altering SCF function (Lozano-Durán et al., 2011).

Jasmonic acid, which is involved in biotic and abiotic stress responses, is also known to induce the production of secondary metabolites including alkaloids, anthocyanins, and terpenoid compounds (Devoto et al., 2005). Whitefly-infested plants showed increased terpenoid production which was decreased in virus-infected plants (Luan et al., 2013). TYLCV-infected tobacco plants manifested increased survival and fecundity of whiteflies (Li et al., 2019). Terpene synthesis genes were downregulated in TYLCV and TYLCV-whitefly co-infected plants compared to whitefly-infested plants. TYLCV *C2* over-expression lines had decreased expression of terpene synthesis genes including MYC2, a transcription factor. MYC2 is under the regulatory control of JAZ1 protein and ubiquitination-mediated degradation of JAZ1 protein is the switch of MYC2 activation (Niu et al., 2011). TYLCV and *Papaya leaf curl China virus* (PaLCuCNV) C2 were shown to interact with RPS27A, a fusion protein consisting of ubiquitin at the N terminus and ribosomal protein S27a at the C terminus. C2 interaction was with the ubiquitin moiety of RPS27A. Li et al. (2019) demonstrated a novel suppression mechanism in which TYLCV C2 competitively bound to ubiquitin, which resulted in decreased JAZ1 protein ubiquitination (**Figure 4J**). Consequently, the MYC2 bound to JAZ1 is stabilized and interferes with the ability of MYC2 to induce the expression of downstream defense genes.

Suppression by Inhibiting Cell Cycle Regulator

Arabidopsis PEAPOD2 transcription factor (TIFY4B) was shown to interact with *AC2* and promoter sequences of TGMV and CaLCuV *CP* (Lacatus and Sunter, 2009) and TGMV *NSP* (Berger and Sunter, 2013). TIFY4B is known to limit cell proliferation in leaf epidermis and vascular tissues (White, 2006), which is substantiated by increased TIFY4B expression in callus tissue and during inflorescence emergence (Vanholme et al., 2007). TIFY4B has three conserved domains: PPD, TIFY, and CCT_2. While TIFY4B was shown to localize to nucleus (Lacatus and Sunter, 2009), mutant versions of TIFY4B including an 84–150-amino acid version were localized in the cytoplasm (Chung and Sunter, 2014). TGMV and CaLCuV AC2 interaction with the mutant TIFY4B altered the localization to nucleus. Increased TIFY4B expression was observed upon viral infection while the geminivirus infection is expected to downregulate a repressor of cell cycle progression. Over-expression of TIFY4B resulted in increased mean latent period and reduced CP expression suggesting a role of TIFYB in antiviral defense, wherein TIFYB inhibits cell proliferation, and therefore, viral replication. Chung and Sunter (2014) proposed a suppression mechanism in which AC2 sequesters TIFY4B and inhibits its role in cell cycle regulation, thereby creating a conducive environment for viral replication.

SUMMARY

This review highlights the different targets and mechanisms evolved by geminivirus AC2/C2 to counter PTGS and TGS.

Recent studies on cellular proteins that are targets of AC2/C2 have opened a third defense mechanism which does not involve PTGS and TGS (**Table 1**). Many studies show how a single suppressor protein like TGMV AC2 could deploy multiple targets. TGMV AC2 targets rgsCaM and ADK to suppress PTGS, targets ADK, and KYP to suppress TGS and inactivates SnRK1 and TIFY4B to inhibit the cellular defense response (**Table 1**). It is likely that silencing suppression is not limited to targeting of one viral protein and a host protein but rather involves a concerted effect on multiple host proteins as manifested in TGMV AC2. It would be interesting to see if other viral suppressor proteins also act on multiple targets. Most of our current knowledge regarding suppressor proteins and their targets is from curtoviruses and begomoviruses. Positional homologs of AC2/C2 are observed in other geminiviruses namely *Eragovirus*, *Topocuvirus*, and *Turncurtovirus*; however, they are not known to encode functional AC2/C2. Advancing our knowledge of suppressor proteins in other genera is essential. For example, *Grapevine red blotch virus* (GRBV), the type member of *Grablovirus*, is known to be a serious threat to the Californian wine industry. Understanding the GRBV suppressor proteins and their plant targets can present cogent strategies for mitigating this threat to a multibillion-dollar industry. Most of our current knowledge on silencing and silencing suppression is from dicot plants *Arabidopsis* and *N. benthamiana*. The genus *Mastrevirus* are monocot-infecting geminiviruses with 41 species. The only silencing suppressor protein identified till date in *Mastrevirus* is the Rep protein from *Wheat dwarf virus* which binds to ss- and ds-siRNA (Wang et al., 2014). It would be interesting to see if DCL5 and AGO18, the unique silencing machinery components of monocots, are targets of *Mastrevirus*.

FUTURE DIRECTIONS

Future research in AC2 suppressor protein should be focused on addressing the question of how the small AC2/AL2 protein (15 kDa) has evolved an ability to interact with so many different targets and make an impact on viral pathogenesis and plant metabolism. It would be interesting to know which of the studied target/targets is relevant in viral pathogenesis. Editing of the target genes in plants and study of viral pathogenesis and RNA silencing in the mutant plants infected with viruses will help in a more thorough evaluation of the AC2-interacting plant proteins. *Abutilon mosaic virus* (AbMV) AC2 was shown to act as a brake in geminivirus replication and was reported to enhance PTGS rather than suppress it

TABLE 1 | Geminivirus AC2/C2-plant protein interactions and associated functions.

Virus	Suppressor	Suppressing PTGS	Suppressing TGS	Cellular pathways
MYMV	AC2	Upregulates host suppressor protein WEL1 (Trinks et al., 2005)		
TGMV	AC2	Inactivates adenosine kinase (Wang et al., 2003, 2005)	Inactivates adenosine kinase (Buchmann et al., 2009)	Inactivates a serine-threonine kinase SnRK1 (Hao et al., 2003)
BCTV	C2			
BSCTV	C2	Stabilizes S-adenosyl methionine decarboxylase1 (SAMDC1; Zhang et al., 2011)	Activates VIM5, an endosperm-imprinted E3 ubiquitin-ligase gene (Chen et al., 2020)	
TGMV	AC2	Upregulates rgsCaM (Chung et al., 2014)	Inhibits histone methyltransferase KYP (Castillo-González et al., 2015)	Sequesters PEAPOD2 transcription factor (TIFY4B) and inhibits cell cycle regulation (Lacatus and Sunter, 2009; Chung and Sunter, 2014)
CaLCuV	AC2			
TGMV	AC2			Elevation of cellular cytokinin levels (Baliji et al., 2010)
SCTV	C2			
TYLCSV	C2			Interacts with CSN5 and inhibits jasmonate signaling (Lozano-Durán et al., 2011; Rosas-Díaz et al., 2016)
TYLCV	C2			
				Represses sulfur assimilation genes (Lozano-Durán et al., 2012)
ICMV-SG	AC2		Upregulation of RAV2, transcription repressor and repression of H3K9 histone methyltransferase KRYPTONITE (KYP; Sun et al., 2015)	
MYMIV	AC2	Interacts with RDR6 and AGO1(Kumar et al., 2015)		
TYLCV	C2			Downregulates terpene synthesis (Luan et al., 2013).
TYLCV	C2			Interaction with the ubiquitin moiety of RPS27A resulting in decreased JAZ1 degradation (Li et al., 2019)
PaLCuCNV	C2			

MYMV, Mungbean yellow mosaic virus; TGMV, Tomato golden mosaic virus; BCTV, Beet curly top virus; BSCTV, Beet severe curly top virus; CaLCuV, Cabbage leaf curl virus; SCTV, Spinach curly top virus; TYLCSV, Tomato yellow leaf curl Sardina virus; TYLCV, Tomato yellow leaf curl virus; MYMIV, Mungbean yellow mosaic India virus; ICMV-SG, Indian cassava mosaic virus-Singapore; and PaLCuCNV, Papaya leaf curl China virus.

(Krenz et al., 2015). It would be interesting to study if any other geminiviral AC2/C2 function as a facilitator of silencing. Besides the uniqueness of AbMV AC2 acting as a PTGS enhancer, a greater challenge is to understand how AbMV AC2 evolved as an enhancer. Does this confer any advantage to the virus or did the host evolve to inhibit viral replication or symptom development?

One major focus of future study should be in exploiting AC2 silencing suppressor function for biotechnological applications. The toxic effect of AC2, when expressed as a transgene, has been reported by several groups. This has limited the use of geminivirus AC2 in transgenic technology. Mutations of functional domains have been shown to alleviate the toxic effect (Rajeswaran et al., 2007). A study to precisely identify the amino acid residue/residues that contribute to the toxic effect of the 135 aa AC2 protein is highly desirable. DNA viral vectors containing only the replication origin and with Rep gene provided in *cis* or in *trans* have found application in biopharming (Rybicki and Martin, 2014). *Bean yellow dwarf virus* (BeYDV), a mild dicot infecting *Mastrevirus*, has been deconstructed and used widely as a replicon vector (Regnard et al., 2010). Huang et al. (2010) demonstrated high level expression of Ebola virus glycoprotein GP1 (6D8) recombinant monoclonal antibodies in *N. benthamiana* leaves by co-expressing the transgene in BeYDV replicon along with Rep and *Tomato bushy stunt virus* (TBSV) p19, a ds siRNA binding suppressor protein. Earlier work by Lacombe et al. (2018) has demonstrated that a combination of P19, P0, and P1 suppressors, that act at distinct steps of the RNA silencing pathway, allowed the highest ectopic protein expression. If the toxic effect of geminiviral AC2 can be negated without compromising on the silencing suppression function, *AC2*, which is known to target multiple steps of gene silencing, could find extensive use for over-expressing recombinant proteins in plants and plant cell cultures.

Both RNA and DNA viruses are widely used in Virus-Induced Gene Silencing (VIGS). The ease with which DNA viruses can be manipulated, the fact that geminiviral *CP* can be replaced with the gene of interest without affecting the systemic movement of virus (only in certain viruses), the recombinant vector derived from replacing *CP* is not vector transmissible and the broad host range of DNA viral vectors makes DNA viruses a good choice for VIGS over RNA viruses (Robertson, 2004). While several studies have shown the application of geminivirus as VIGS vector (Yang et al., 2017), the presence of suppressor proteins including AC2/C2 was shown to antagonize the silencing effect caused by the VIGS vector. The silencing efficiency is depleted as the suppressor protein accumulates in the plants. A null mutant in MYMIV-AC2, when used as VIGS vector, increased the silencing efficiency (Pandey et al., 2009). However, the mutation in the AC2 ORF reduced MYMIV replication efficiency by about 25%. A null mutation in CaLCuV AC2 abolished the viral replication (Castillo-González et al., 2015). Hence, future studies should investigate the possibility of mutating the AC2/C2 to mute the suppression function alone without compromising on the replication efficiency of the VIGS vector. Geminivirus VIGS vectors will help in performing functional genomics in a wide range of plants.

Baltes et al. (2014) demonstrated genome engineering using the BeYDV-based replicon system. Desired DNA changes were made when TALENs and CRISPR/Cas9 system were delivered using the BeYDV-based replicon system. A recent study by Mao et al. (2018) showed improved gene-editing efficiency by silencing AGO1 or by co-expressing TBSV p19 protein as part of CRISPR/Cas9 cassette. The challenge of gene editing technology is in identifying the edited events. Mao et al. (2018) established a suave means to phenotypically identify the edited events in the T_1 generation and T-DNA segregated events in T_2 generation. By co-expressing p19 as part of the CRISPR/Cas9 cassette, the authors could group the T_1 plants based on the severity of p19-induced leaf phenotype alteration. T_1 plants displaying severe phenotype associated with p19 over-expression were selected as edited lines. T_2 seedlings from the gene edited T_1 events were again grouped based on the leaf phenotype. Segregated plants with wild-type leaf phenotype were then identified as gene-edited plants from which the T-DNA was segregated out. The geminiviral suppressor protein AC2 can be co-expressed to increase the genome editing efficiency. Interestingly, AC2 is more attractive than TBSV p19 for the following reasons: (1) AC2 over-expression is known to cause pronounced phenotype in leaf (Siddiqui et al., 2008; Castillo-González et al., 2015). (2) TGMV AC2 over-expression resulted in early flowering (Castillo-González et al., 2015). (3) AC2 over-expression is likely to result in genome-wide hypomethylation (Castillo-González et al., 2015), and hence the tightly regulated genes involved in meiotic recombination are also likely to be upregulated. (4) MYMV AC2 and ACMV AC2, when transiently expressed in *Arabidopsis* protoplasts, upregulated the expression of the meiotic recombination protein AtDMC1 (Trinks et al., 2005; Da Ines et al., 2013). Thus, future studies would pave way to the evolution of AC2 from a core viral protein to a potent molecular tool with myriad applications.

AUTHOR CONTRIBUTIONS

SS: conceptualization and writing-original draft preparation. KV: conceptualization, reviewing, and editing. Both authors contributed to the article and approved the submitted version.

FUNDING

The costs of publication are supported by California Department of Food and Agriculture Pierce's Disease Board, agreement number 20-0248-000-SA to SS.

ACKNOWLEDGMENTS

We thank Christopher Rock, Texas Tech University for critical reading of the manuscript.

REFERENCES

Aguilar, E., Garnelo Gomez, B., and Lozano-Duran, R. (2020). Recent advances on the plant manipulation by geminiviruses. *Curr. Opin. Plant Biol.* 56, 56–64. doi: 10.1016/j.pbi.2020.03.009

Akbergenov, R., Si-Ammour, A., Blevins, T., Amin, I., Kutter, C., Vanderschuren, H., et al. (2006). Molecular characterization of geminivirus-derived small RNAs in different plant species. *Nucleic Acids Res.* 34, 462–471. doi: 10.1093/nar/gkj447

Anandalakshmi, R., Marathe, R., Ge, X., Herr, J. M., Mau, C., Mallory, A., et al. (2000). A calmodulin-related protein that suppresses posttranscriptional gene silencing in plants. *Science* 290, 142–144. doi: 10.1126/science.290.5489.142

Anandalakshmi, R., Pruss, G. J., Ge, X., Marathe, R., Mallory, A. C., Smith, T. H., et al. (1998). A viral suppressor of gene silencing in plants. *Proc. Natl. Acad. Sci. U. S. A.* 95, 13079–13084. doi: 10.1073/pnas.95.22.13079

Aregger, M., Borah, B. K., Seguin, J., Rajeswaran, R., Gubaeva, E. G., Zvereva, A. S., et al. (2012). Primary and secondary siRNAs in geminivirus-induced gene silencing. *PLoS Pathog.* 8:e1002941. doi: 10.1371/journal.ppat.1002941

Baliji, S., Lacatus, G., and Sunter, G. (2010). The interaction between geminivirus pathogenicity proteins and adenosine kinase leads to increased expression of primary cytokinin-responsive genes. *Virology* 402, 238–247. doi: 10.1016/j.virol.2010.03.023

Baliji, S., Sunter, J., and Sunter, G. (2007). Transcriptional analysis of complementary sense genes in spinach curly top virus and functional role of C2 in pathogenesis. *Mol. Plant-Microbe Interact.* 20, 194–206. doi: 10.1094/MPMI-20-2-0194

Baltes, N. J., Gil-Humanes, J., Cermak, T., Atkins, P. A., and Voytas, D. F. (2014). DNA replicons for plant genome engineering. *Plant Cell* 26, 151–163. doi: 10.1105/tpc.113.119792

Baulcombe, D. (2004). RNA silencing in plants. *Nature* 431, 356–363. doi: 10.1038/nature02874

Berger, M. R., and Sunter, G. (2013). Identification of sequences required for AL2-mediated activation of the tomato golden mosaic virus-yellow vein BR1 promoter. *J. Gen. Virol.* 94, 1398–1406. doi: 10.1099/vir.0.050161-0

Bisaro, D. M. (2006). Silencing suppression by geminivirus proteins. *Virology* 344, 158–168. doi: 10.1016/j.virol.2005.09.041

Blevins, T., Rajeswaran, R., Aregger, M., Borah, B. K., Schepetilnikov, M., Baerlocher, L., et al. (2011). Massive production of small RNAs from a non-coding region of cauliflower mosaic virus in plant defense and viral counter-defense. *Nucleic Acids Res.* 39, 5003–5014. doi: 10.1093/nar/gkr119

Blevins, T., Rajeswaran, R., Shivaprasad, P. V., Beknazariants, D., Si-Ammour, A., Park, H. S., et al. (2006). Four plant dicers mediate viral small RNA biogenesis and DNA virus induced silencing. *Nucleic Acids Res.* 34, 6233–6246. doi: 10.1093/nar/gkl886

Buchmann, R. C., Asad, S., Wolf, J. N., Mohannath, G., and Bisaro, D. M. (2009). Geminivirus AL2 and L2 proteins suppress transcriptional gene silencing and cause genome-wide reductions in cytosine methylation. *J. Virol.* 83, 5005–5013. doi: 10.1128/JVI.01771-08

Cao, X., and Jacobsen, S. E. (2002). Role of the *Arabidopsis* DRM methyltransferases in de novo DNA methylation and gene silencing. *Curr. Biol.* 12, 1138–1144. doi: 10.1016/S0960-9822(02)00925-9

Castillo-González, C., Liu, X., Huang, C., Zhao, C., Ma, Z., Hu, T., et al. (2015). Geminivirus-encoded TrAP suppressor inhibits the histone methyltransferase SUVH4/KYP to counter host defense. *elife* 4:e06671. doi: 10.7554/eLife.06671

Ceniceros-Ojeda, E. A., Rodríguez-Negrete, E. A., and Rivera-Bustamante, R. F. (2016). Two populations of viral minichromosomes are present in a geminivirus-infected plant showing symptom remission (recovery). *J. Virol.* 90, 3828–3838. doi: 10.1128/JVI.02385-15

Chen, Z. Q., Zhao, J. H., Chen, Q., Zhang, Z. H., Li, J., Guo, Z. X., et al. (2020). DNA geminivirus infection induces an imprinted E3 ligase gene to epigenetically activate viral gene transcription. *Plant Cell* 32, 3256–3272. doi: 10.1105/tpc.20.00249

Chung, H. Y., Lacatus, G., and Sunter, G. (2014). Geminivirus AL2 protein induces expression of, and interacts with, a calmodulin-like gene, an endogenous regulator of gene silencing. *Virology* 460–461, 108–118. doi: 10.1016/j.virol.2014.04.034

Chung, H. Y., and Sunter, G. (2014). Interaction between the transcription factor AtTIFY4B and begomovirus AL2 protein impacts pathogenicity. *Plant Mol. Biol.* 86, 185–200. doi: 10.1007/s11103-014-0222-9

Coursey, T., Regedanz, E., and Bisaro, D. M. (2018). *Arabidopsis* RNA polymerase V mediates enhanced compaction and silencing of geminivirus and transposon chromatin during host recovery from infection. *J. Virol.* 92, e1320–e1417. doi: 10.1128/JVI.01320-17

Csorba, T., Kontra, L., and Burgyán, J. (2015). Viral silencing suppressors: tools forged to fine-tune host-pathogen coexistence. *Virology* 479–480, 85–103. doi: 10.1016/j.virol.2015.02.028

Da Ines, O., Degroote, F., Goubely, C., Amiard, S., Gallego, M. E., and White, C. I. (2013). Meiotic recombination in *Arabidopsis* is catalysed by DMC1, with RAD51 playing a supporting role. *PLoS Genet.* 9:e1003787. doi: 10.1371/journal.pgen.1003787

Daxinger, L., Kanno, T., Bucher, E., van der Winden, J., Naumann, U., Matzke, A. J., et al. (2009). A stepwise pathway for biogenesis of 24-nt secondary siRNAs and spreading of DNA methylation. *EMBO J.* 28, 48–57. doi: 10.1038/emboj.2008.260

Devoto, A., Ellis, C., Magusin, A., Chang, H. S., Chilcott, C., Zhu, T., et al. (2005). Expression profiling reveals COI1 to be a key regulator of genes involved in wound- and methyl jasmonate-induced secondary metabolism, defence, and hormone interactions. *Plant Mol. Biol.* 58, 497–513. doi: 10.1007/s11103-005-7306-5

Dohmann, E. M., Levesque, M. P., De Veylder, L., Reichardt, I., Jürgens, G., Schmid, M., et al. (2008). The *Arabidopsis* COP9 signalosome is essential for G2 phase progression and genomic stability. *Development* 135, 2013–2022. doi: 10.1242/dev.020743

Dong, X., van Wezel, R., Stanley, J., and Hong, Y. (2003). Functional characterization of the nuclear localization signal for a suppressor of posttranscriptional gene silencing. *J. Virol.* 77, 7026–7033. doi:10.1128/JVI.77.12.7026-7033.2003

Endres, M. W., Gregory, B. D., Gao, Z., Foreman, A. W., Mlotshwa, S., Ge, X., et al. (2010). Two plant viral suppressors of silencing require the ethylene-inducible host transcription factor RAV2 to block RNA silencing. *PLoS Pathog.* 6:e1000729. doi: 10.1371/journal.ppat.1000729

English, J. J., Mueller, E., and Baulcombe, D. C. (1996). Suppression of virus accumulation in transgenic plants exhibiting silencing of nuclear genes. *Plant Cell* 8, 179–188. doi: 10.2307/3870263

Fiallo-Olivé, E., Martínez-Zubiaur, Y., Moriones, E., and Navas-Castillo, J. (2012). A novel class of DNA satellites associated with New World begomoviruses. *Virology* 426, 1–6. doi: 10.1016/j.virol.2012.01.024

Fiallo-Olivé, E., Tovar, R., and Navas-Castillo, J. (2016). Deciphering the biology of deltasatellites from the New World: maintenance by New World begomoviruses and whitefly transmission. *New Phytol.* 212, 680–692. doi: 10.1111/nph.14071

Garcia-Ruiz, H., Takeda, A., Chapman, E. J., Sullivan, C. M., Fahlgren, N., Brempelis, K. J., et al. (2010). *Arabidopsis* RNA-dependent RNA polymerases and dicer-like proteins in antiviral defense and small interfering RNA biogenesis during turnip mosaic virus infection. *Plant Cell* 22, 481–496. doi: 10.1105/tpc.109.073056

Geng, X., Jin, L., Shimada, M., Kim, M. G., and Mackey, D. (2014). The phytotoxin coronatine is a multifunctional component of the virulence armament of Pseudomonas syringae. *Planta* 240, 1149–1165. doi: 10.1007/s00425-014-2151-x

Glazov, E., Phillips, K., Budziszewski, G. J., Schöb, H., Meins, F., and Levin, J. Z. (2003). A gene encoding an RNase D exonuclease-like protein is required for post-transcriptional silencing in *Arabidopsis*. *Plant J.* 35, 342–349. doi: 10.1046/j.1365-313X.2003.01810.x

Gopal, P., Pravin Kumar, P., Sinilal, B., Jose, J., Kasin Yadunandam, A., and Usha, R. (2007). Differential roles of C4 and betaC1 in mediating suppression of post-transcriptional gene silencing: evidence for transactivation by the C2 of Bhendi yellow vein mosaic virus, a monopartite begomovirus. *Virus Res.* 123, 9–18. doi: 10.1016/j.virusres.2006.07.014

Guerrero, J., Regedanz, E., Lu, L., Ruan, J., Bisaro, D. M., and Sunter, G. (2020). Manipulation of the plant host by the geminivirus AC2/C2 protein, a central player in the infection cycle. *Front. Plant Sci.* 11:591. doi: 10.3389/fpls.2020.00591

Gusmaroli, G., Figueroa, P., Serino, G., and Deng, X. W. (2007). Role of the MPN subunits in COP9 signalosome assembly and activity, and their regulatory interaction with *Arabidopsis* cullin3-based E3 ligases. *Plant Cell* 19, 564–581. doi: 10.1105/tpc.106.047571

Haley, A., Zhan, X., Richardson, K., Head, K., and Morris, B. (1992). Regulation of the activities of African cassava mosaic virus promoters by the AC1,

AC2, and AC3 gene products. *Virology* 188, 905–909. doi: 10.1016/0042-6822(92)90551-Y

Hanley-Bowdoin, L., Bejarano, E. R., Robertson, D., and Mansoor, S. (2013). Geminiviruses: masters at redirecting and reprogramming plant processes. *Nat. Rev. Microbiol.* 11, 777–788. doi: 10.1038/nrmicro3117

Hanley-Bowdoin, L., Settlage, S. B., Orozco, B. M., Nagar, S., and Robertson, D. (2000). Geminiviruses: models for plant DNA replication, transcription, and cell cycle regulation. *Crit. Rev. Biochem. Mol. Biol.* 35, 105–140.

Hao, L., Wang, H., Sunter, G., and Bisaro, D. M. (2003). Geminivirus AL2 and L2 proteins interact with and inactivate SNF1 kinase. *Plant Cell* 15, 1034–1048. doi: 10.1105/tpc.009530

Harvey, J. J., Lewsey, M. G., Patel, K., Westwood, J., Heimstädt, S., Carr, J. P., et al. (2011). An antiviral defense role of AGO2 in plants. *PLoS One* 6:e14639. doi: 10.1371/journal.pone.0014639

Hayes, R. J., and Buck, K. W. (1989). Replication of tomato golden mosaic virus DNA B in transgenic plants expressing open reading frames (ORFs) of DNA A: requirement of ORF AL2 for production of single-stranded DNA. *Nucleic Acids Res.* 17, 10213–10222. doi: 10.1093/nar/17.24.10213

Herr, A. J., Jensen, M. B., Dalmay, T., and Baulcombe, D. C. (2005). RNA polymerase IV directs silencing of endogenous DNA. *Science* 308, 118–120. doi: 10.1126/science.1106910

Höller, K., Király, L., Künstler, A., Müller, M., Gullner, G., Fattinger, M., et al. (2010). Enhanced glutathione metabolism is correlated with sulfur-induced resistance in tobacco mosaic virus-infected genetically susceptible *Nicotiana tabacum* plants. *Mol. Plant-Microbe Interact.* 23, 1448–1459. doi: 10.1094/MPMI-05-10-0117

Hormuzdi, S. G., and Bisaro, D. M. (1993). Genetic analysis of beet curly top virus: evidence for three virion sense genes involved in movement and regulation of single- and double-stranded DNA levels. *Virology* 193, 900–909. doi: 10.1006/viro.1993.1199

Hormuzdi, S. G., and Bisaro, D. M. (1995). Genetic analysis of beet curly top virus: examination of the roles of L2 and L3 genes in viral pathogenesis. *Virology* 206, 1044–1054. doi: 10.1006/viro.1995.1027

Huang, Z., Phoolcharoen, W., Lai, H., Piensook, K., Cardineau, G., Zeitlin, L., et al. (2010). High-level rapid production of full-size monoclonal antibodies in plants by a single-vector DNA replicon system. *Biotechnol. Bioeng.* 106, 9–17. doi: 10.1002/bit.22652

Ingelbrecht, I., Van Houdt, H., Van Montagu, M., and Depicker, A. (1994). Posttranscriptional silencing of reporter transgenes in tobacco correlates with DNA methylation. *Proc. Natl. Acad. Sci. U. S. A.* 91, 10502–10506. doi: 10.1073/pnas.91.22.10502

Jackel, J. N., Buchmann, R. C., Singhal, U., and Bisaro, D. M. (2015). Analysis of geminivirus AL2 and L2 proteins reveals a novel AL2 silencing suppressor activity. *J. Virol.* 89, 3176–3187. doi: 10.1128/JVI.02625-14

Jackel, J. N., Storer, J. M., Coursey, T., and Bisaro, D. M. (2016). *Arabidopsis* RNA polymerases IV and V are required to establish H3K9 methylation, but not cytosine methylation, on geminivirus chromatin. *J. Virol.* 90, 7529–7540. doi: 10.1128/JVI.00656-16

Karjee, S., Islam, M. N., and Mukherjee, S. K. (2008). Screening and identification of virus-encoded RNA silencing suppressors. *Methods Mol. Biol.* 442, 187–203. doi: 10.1007/978-1-59745-191-8_14

Kheyr-Pour, A., Bendahmane, M., Matzeit, V., Accotto, G. P., Crespi, S., and Gronenborn, B. (1991). Tomato yellow leaf curl virus from Sardinia is a whitefly-transmitted monopartite geminivirus. *Nucleic Acids Res.* 19, 6763–6769. doi: 10.1093/nar/19.24.6763

Kopriva, S., Muheim, R., Koprivova, A., Trachsel, N., Catalano, C., Suter, M., et al. (1999). Light regulation of assimilatory sulphate reduction in *Arabidopsis thaliana*. *Plant J.* 20, 37–44. doi: 10.1046/j.1365-313X.1999.00573.x

Krenz, B., Deuschle, K., Deigner, T., Unseld, S., Kepp, G., Wege, C., et al. (2015). Early function of the Abutilon mosaic virus AC2 gene as a replication brake. *J. Virol.* 89, 3683–3699. doi: 10.1128/JVI.03491-14

Kumar, R. V. (2019). Plant antiviral immunity against geminiviruses and viral counter-defense for survival. *Front. Microbiol.* 10:1460. doi: 10.3389/fmicb.2019.01460

Kumar, V., Mishra, S. K., Rahman, J., Taneja, J., Sundaresan, G., Mishra, N. S., et al. (2015). Mungbean yellow mosaic Indian virus encoded AC2 protein suppresses RNA silencing by inhibiting *Arabidopsis* RDR6 and AGO1 activities. *Virology* 486, 158–172. doi: 10.1016/j.virol.2015.08.015

Lacatus, G., and Sunter, G. (2009). The *Arabidopsis* PEAPOD2 transcription factor interacts with geminivirus AL2 protein and the coat protein promoter. *Virology* 392, 196–202. doi: 10.1016/j.virol.2009.07.004

Lacombe, S., Bangratz, M., Brizard, J. P., Petitdidier, E., Pagniez, J., Sérémé, D., et al. (2018). Optimized transitory ectopic expression of promastigote surface antigen protein in *Nicotiana benthamiana*, a potential anti-leishmaniasis vaccine candidate. *J. Biosci. Bioeng.* 125, 116–123. doi: 10.1016/j.jbiosc.2017.07.008

Li, F., Huang, C., Li, Z., and Zhou, X. (2014). Suppression of RNA silencing by a plant DNA virus satellite requires a host calmodulin-like protein to repress RDR6 expression. *PLoS Pathog.* 10:e1003921. doi: 10.1371/journal.ppat.1003921

Li, P., Liu, C., Deng, W. H., Yao, D. M., Pan, L. L., Li, Y. Q., et al. (2019). Plant begomoviruses subvert ubiquitination to suppress plant defenses against insect vectors. *PLoS Pathog.* 15:e1007607. doi: 10.1371/journal.ppat.1007607

Li, C. F., Pontes, O., El-Shami, M., Henderson, I. R., Bernatavichute, Y. V., Chan, S. W., et al. (2006). An ARGONAUTE4-containing nuclear processing center colocalized with Cajal bodies in *Arabidopsis thaliana*. *Cell* 126, 93–106. doi: 10.1016/j.cell.2006.05.032

Li, F., Zhao, N., Li, Z., Xu, X., Wang, Y., Yang, X., et al. (2017). A calmodulin-like protein suppresses RNA silencing and promotes geminivirus infection by degrading SGS3 via the autophagy pathway in *Nicotiana benthamiana*. *PLoS Pathog.* 13:e1006213. doi: 10.1371/journal.ppat.1006213

Lozano-Durán, R., García, I., Huguet, S., Balzergue, S., Romero, L. C., and Bejarano, E. R. (2012). Geminivirus C2 protein represses genes involved in Sulphur assimilation and this effect can be counteracted by jasmonate treatment. *Eur. J. Plant Pathol.* 134, 49–59. doi: 10.1007/s10658-012-0021-6

Lozano-Durán, R., Rosas-Díaz, T., Gusmaroli, G., Luna, A. P., Taconnat, L., Deng, X. W., et al. (2011). Geminiviruses subvert ubiquitination by altering CSN-mediated derubylation of SCF E3 ligase complexes and inhibit jasmonate signaling in *Arabidopsis thaliana*. *Plant Cell* 23, 1014–1032. doi: 10.1105/tpc.110.080267

Luan, J. B., Yao, D. M., Zhang, T., Walling, L. L., Yang, M., Wang, Y. J., et al. (2013). Suppression of terpenoid synthesis in plants by a virus promotes its mutualism with vectors. *Ecol. Lett.* 16, 390–398. doi: 10.1111/ele.12055

Luna, A. P., and Lozano-Durán, R. (2020). Geminivirus-encoded proteins: not all positional homologs are made equal. *Front. Microbiol.* 11:878. doi: 10.3389/fmicb.2020.00878

Mao, Y., Yang, X., Zhou, Y., Zhang, Z., Botella, J. R., and Zhu, J. K. (2018). Manipulating plant RNA-silencing pathways to improve the gene editing efficiency of CRISPR/Cas9 systems. *Genome Biol.* 19:149. doi: 10.1186/s13059-018-1529-7

Marí-Ordóñez, A., Marchais, A., Etcheverry, M., Martin, A., Colot, V., and Voinnet, O. (2013). Reconstructing de novo silencing of an active plant retrotransposon. *Nat. Genet.* 45, 1029–1039. doi: 10.1038/ng.2703

Maruyama-Nakashita, A., Nakamura, Y., Yamaya, T., and Takahashi, H. (2004). A novel regulatory pathway of sulfate uptake in *Arabidopsis* roots: implication of CRE1/WOL/AHK4-mediated cytokinin-dependent regulation. *Plant J.* 38, 779–789. doi: 10.1111/j.1365-313X.2004.02079.x

Melotto, M., Underwood, W., Koczan, J., Nomura, K., and He, S. Y. (2006). Plant stomata function in innate immunity against bacterial invasion. *Cell* 126, 969–980. doi: 10.1016/j.cell.2006.06.054

Miozzi, L., Pantaleo, V., Burgyán, J., Accotto, G. P., and Noris, E. (2013). Analysis of small RNAs derived from tomato yellow leaf curl Sardinia virus reveals a cross reaction between the major viral hotspot and the plant host genome. *Virus Res.* 178, 287–296. doi: 10.1016/j.virusres.2013.09.029

Nakahara, K. S., Masuta, C., Yamada, S., Shimura, H., Kashihara, Y., Wada, T. S., et al. (2012). Tobacco calmodulin-like protein provides secondary defense by binding to and directing degradation of virus RNA silencing suppressors. *Proc. Natl. Acad. Sci. U. S. A.* 109, 10113–10118. doi: 10.1073/pnas.1201628109

Navot, N., Pichersky, E., Zeidan, M., Zamir, D., and Czosnek, H. (1991). Tomato yellow leaf curl virus: a whitefly-transmitted geminivirus with a single genomic component. *Virology* 185, 151–161. doi: 10.1016/0042-6822(91)90763-2

Niu, Y., Figueroa, P., and Browse, J. (2011). Characterization of JAZ-interacting bHLH transcription factors that regulate jasmonate responses in *Arabidopsis*. *J. Exp. Bot.* 62, 2143–2154. doi: 10.1093/jxb/erq408

Noris, E., Jupin, I., Accotto, G. P., and Gronenborn, B. (1996). DNA-binding activity of the C2 protein of tomato yellow leaf curl geminivirus. *Virology* 217, 607–612. doi: 10.1006/viro.1996.0157

Ohkama, N., Takei, K., Sakakibara, H., Hayashi, H., Yoneyama, T., and Fujiwara, T. (2002). Regulation of sulfur-responsive gene expression by exogenously applied cytokinins in *Arabidopsis thaliana*. *Plant Cell Physiol.* 43, 1493–1501. doi: 10.1093/pcp/pcf183

Padidam, M., Beachy, R. N., and Fauquet, C. M. (1996). The role of AV2 ("precoat") and coat protein in viral replication and movement in tomato leaf curl geminivirus. *Virology* 224, 390–404. doi: 10.1006/viro.1996.0546

Pandey, P., Choudhury, N. R., and Mukherjee, S. K. (2009). A geminiviral amplicon (VA) derived from tomato leaf curl virus (ToLCV) can replicate in a wide variety of plant species and also acts as a VIGS vector. *Virol. J.* 6:152. doi: 10.1186/1743-422X-6-152

Parent, J. S., Bouteiller, N., Elmayan, T., and Vaucheret, H. (2015). Respective contributions of *Arabidopsis* DCL2 and DCL4 to RNA silencing. *Plant J.* 81, 223–232. doi: 10.1111/tpj.12720

Pontes, O., and Pikaard, C. S. (2008). siRNA and miRNA processing: new functions for Cajal bodies. *Curr. Opin. Genet. Dev.* 18, 197–203. doi: 10.1016/j.gde.2008.01.008

Qu, F., Ye, X., and Morris, T. J. (2008). *Arabidopsis* DRB4, AGO1, AGO7, and RDR6 participate in a DCL4-initiated antiviral RNA silencing pathway negatively regulated by DCL1. *Proc. Natl. Acad. Sci. U. S. A.* 105, 14732–14737. doi: 10.1073/pnas.0805760105

Rahman, J., Karjee, S., and Mukherjee, S. K. (2012). MYMIV-AC2, a geminiviral RNAi suppressor protein, has potential to increase the transgene expression. *Appl. Biochem. Biotechnol.* 167, 758–775. doi: 10.1007/s12010-012-9702-z

Raja, P., Jackel, J. N., Li, S., Heard, I. M., and Bisaro, D. M. (2014). *Arabidopsis* double-stranded RNA binding protein DRB3 participates in methylation-mediated defense against geminiviruses. *J. Virol.* 88, 2611–2622. doi: 10.1128/JVI.02305-13

Raja, P., Sanville, B. C., Buchmann, R. C., and Bisaro, D. M. (2008). Viral genome methylation as an epigenetic defense against geminiviruses. *J. Virol.* 82, 8997–9007. doi: 10.1128/JVI.00719-08

Raja, P., Wolf, J. N., and Bisaro, D. M. (2010). RNA silencing directed against geminiviruses: post-transcriptional and epigenetic components. *Biochim. Biophys. Acta* 1799, 337–351. doi: 10.1016/j.bbagrm.2010.01.004

Rajeswaran, R., Sunitha, S., Shivaprasad, P. V., Pooggin, M. M., Hohn, T., and Veluthambi, K. (2007). The mungbean yellow mosaic begomovirus transcriptional activator protein transactivates the viral promoter-driven transgene and causes toxicity in transgenic tobacco plants. *Mol. Plant-Microbe Interact.* 20, 1545–1554. doi: 10.1094/MPMI-20-12-1545

Ré, D. A., and Manavella, P. A. (2015). Caught in a TrAP. *elife* 4:e11509. doi: 10.7554/eLife.11509

Regnard, G. L., Halley-Stott, R. P., Tanzer, F. L., Hitzeroth, I. I., and Rybicki, E. P. (2010). High level protein expression in plants through the use of a novel autonomously replicating geminivirus shuttle vector. *Plant Biotechnol. J.* 8, 38–46. doi: 10.1111/j.1467-7652.2009.00462.x

Rishishwar, R., and Dasgupta, I. (2019). Suppressors of RNA silencing encoded by geminiviruses and associated DNA satellites. *Virusdisease* 30, 58–65. doi: 10.1007/s13337-018-0418-8

Robertson, D. (2004). VIGS vectors for gene silencing: many targets, many tools. *Annu. Rev. Plant Biol.* 55, 495–519. doi: 10.1146/annurev.arplant.55.031903.141803

Rojas, M. R., Macedo, M. A., Maliano, M. R., Soto-Aguilar, M., Souza, J. O., Briddon, R. W., et al. (2018). World management of geminiviruses. *Annu. Rev. Phytopathol.* 56, 637–677. doi: 10.1146/annurev-phyto-080615-100327

Rosas-Díaz, T., Macho, A. P., Beuzón, C. R., Lozano-Durán, R., and Bejarano, E. R. (2016). The C2 protein from the geminivirus tomato yellow leaf curl Sardinia virus decreases sensitivity to jasmonates and suppresses jasmonate-mediated defences. *Plan. Theory* 5:8. doi: 10.3390/plants5010008

Rybicki, E. P., and Martin, D. P. (2014). Virus-derived ssDNA vectors for the expression of foreign proteins in plants. *Curr. Top. Microbiol. Immunol.* 375, 19–45. doi: 10.1007/82_2011_185

Saunders, K., Bedford, I. D., Briddon, R. W., Markham, P. G., Wong, S. M., and Stanley, J. (2000). A unique virus complex causes *Ageratum* yellow vein disease. *Proc. Natl. Acad. Sci. U. S. A.* 97, 6890–6895. doi: 10.1073/pnas.97.12.6890

Schaffer, R. L., Miller, C. G., and Petty, I. T. (1995). Virus and host-specific adaptations in the BL1 and BR1 genes of bipartite geminiviruses. *Virology* 214, 330–338. doi: 10.1006/viro.1995.0042

Scholthof, K. B., Adkins, S., Czosnek, H., Palukaitis, P., Jacquot, E., Hohn, T., et al. (2011). Top 10 plant viruses in molecular plant pathology. *Mol. Plant Pathol.* 12, 938–954. doi: 10.1111/j.1364-3703.2011.00752.x

Shabalina, S. A., and Koonin, E. V. (2008). Origins and evolution of eukaryotic RNA interference. *Trends Ecol. Evol.* 23, 578–587. doi: 10.1016/j.tree.2008.06.005

Shen, W., Dallas, M. B., Goshe, M. B., and Hanley-Bowdoin, L. (2014). SnRK1 phosphorylation of AL2 delays cabbage leaf curl virus infection in *Arabidopsis*. *J. Virol.* 88, 10598–10612. doi: 10.1128/JVI.00761-14

Shivaprasad, P. V., Akbergenov, R., Trinks, D., Rajeswaran, R., Veluthambi, K., Hohn, T., et al. (2005). Promoters, transcripts, and regulatory proteins of mungbean yellow mosaic geminivirus. *J. Virol.* 79, 8149–8163. doi: 10.1128/JVI.79.13.8149-8163.2005

Siddiqui, S. A., Sarmiento, C., Truve, E., Lehto, H., and Lehto, K. (2008). Phenotypes and functional effects caused by various viral RNA silencing suppressors in transgenic *Nicotiana benthamiana* and *N. tabacum*. *Mol. Plant-Microbe Interact.* 21, 178–187. doi: 10.1094/MPMI-21-2-0178

Stanley, J., and Latham, J. R. (1992). A symptom variant of beet curly top geminivirus produced by mutation of open reading frame C4. *Virology* 190, 506–509. doi: 10.1016/0042-6822(92)91243-N

Stanley, J., Latham, J. R., Pinner, M. S., Bedford, I., and Markham, P. G. (1992). Mutational analysis of the monopartite geminivirus beet curly top virus. *Virology* 191, 396–405. doi: 10.1016/0042-6822(92)90201-Y

Sun, Y. W., Tee, C. S., Ma, Y. H., Wang, G., Yao, X. M., and Ye, J. (2015). Attenuation of histone methyltransferase KRYPTONITE-mediated transcriptional gene silencing by geminivirus. *Sci. Rep.* 5:16476. doi: 10.1038/srep16476

Sunter, G., and Bisaro, D. M. (1991). Transactivation in a geminivirus: AL2 gene product is needed for coat protein expression. *Virology* 180, 416–419. doi: 10.1016/0042-6822(91)90049-H

Sunter, G., and Bisaro, D. M. (1992). Transactivation of geminivirus AR1 and BR1 gene expression by the viral AL2 gene product occurs at the level of transcription. *Plant Cell* 4, 1321–1331. doi: 10.1105/tpc.4.10.1321

Sunter, G., Stenger, D. C., and Bisaro, D. M. (1994). Heterologous complementation by geminivirus AL2 and AL3 genes. *Virology* 203, 203–210. doi: 10.1006/viro.1994.1477

Trinks, D., Rajeswaran, R., Shivaprasad, P. V., Akbergenov, R., Oakeley, E. J., Veluthambi, K., et al. (2005). Suppression of RNA silencing by a geminivirus nuclear protein, AC2, correlates with transactivation of host genes. *J. Virol.* 79, 2517–2527. doi: 10.1128/JVI.79.4.2517-2527.2005

Vanholme, B., Grunewald, W., Bateman, A., Kohchi, T., and Gheysen, G. (2007). The tify family previously known as ZIM. *Trends Plant Sci.* 12, 239–244. doi: 10.1016/j.tplants.2007.04.004

Vanitharani, R., Chellappan, P., Pita, J. S., and Fauquet, C. M. (2004). Differential roles of AC2 and AC4 of cassava geminiviruses in mediating synergism and suppression of posttranscriptional gene silencing. *J. Virol.* 78, 9487–9498. doi: 10.1128/JVI.78.17.9487-9498.2004

van Wezel, R., Dong, X., Liu, H., Tien, P., Stanley, J., and Hong, Y. (2002). Mutation of three cysteine residues in tomato yellow leaf curl virus-China C2 protein causes dysfunction in pathogenesis and posttranscriptional gene-silencing suppression. *Mol. Plant-Microbe Interact.* 15, 203–208. doi: 10.1094/MPMI.2002.15.3.203

van Wezel, R., Liu, H., Tien, P., Stanley, J., and Hong, Y. (2001). Gene C2 of the monopartite geminivirus tomato yellow leaf curl virus-China encodes a pathogenicity determinant that is localized in the nucleus. *Mol. Plant-Microbe Interact.* 14, 1125–1128. doi: 10.1094/MPMI.2001.14.9.1125

van Wezel, R., Liu, H., Wu, Z., Stanley, J., and Hong, Y. (2003). Contribution of the zinc finger to zinc and DNA binding by a suppressor of posttranscriptional gene silencing. *J. Virol.* 77, 696–700. doi: 10.1128/JVI.77.1.696-700.2003

Vauclare, P., Kopriva, S., Fell, D., Suter, M., Sticher, L., von Ballmoos, P., et al. (2002). Flux control of sulphate assimilation in *Arabidopsis thaliana*: adenosine 5'-phosphosulphate reductase is more susceptible than ATP sulphurylase to negative control by thiols. *Plant J.* 31, 729–740. doi: 10.1046/j.1365-313X.2002.01391.x

Voinnet, O. (2005). Induction and suppression of RNA silencing: insights from viral infections. *Nat. Rev. Genet.* 6, 206–220. doi: 10.1038/nrg1555

Voinnet, O., Pinto, Y. M., and Baulcombe, D. C. (1999). Suppression of gene silencing: a general strategy used by diverse DNA and RNA viruses of plants. *Proc. Natl. Acad. Sci. U. S. A.* 96, 14147–14152. doi: 10.1073/pnas.96.24.14147

Wang, H., Buckley, K. J., Yang, X., Buchmann, R. C., and Bisaro, D. M. (2005). Adenosine kinase inhibition and suppression of RNA silencing by geminivirus AL2 and L2 proteins. *J. Virol.* 79, 7410–7418. doi: 10.1128/JVI.79.12.7410-7418.2005

Wang, Y., Dang, M., Hou, H., Mei, Y., Qian, Y., and Zhou, X. (2014). Identification of an RNA silencing suppressor encoded by a mastrevirus. *J. Gen. Virol.* 95, 2082–2088. doi: 10.1099/vir.0.064246-0

Wang, H., Hao, L., Shung, C. Y., Sunter, G., and Bisaro, D. M. (2003). Adenosine kinase is inactivated by geminivirus AL2 and L2 proteins. *Plant Cell* 15, 3020–3032. doi: 10.1105/tpc.015180

White, D. W. (2006). PEAPOD regulates lamina size and curvature in *Arabidopsis*. *Proc. Natl. Acad. Sci. U. S. A.* 103, 13238–13243. doi: 10.1073/pnas.0604349103

Wierzbicki, A. T., Haag, J. R., and Pikaard, C. S. (2008). Noncoding transcription by RNA polymerase pol IVb/pol V mediates transcriptional silencing of overlapping and adjacent genes. *Cell* 135, 635–648. doi: 10.1016/j.cell.2008.09.035

Wierzbicki, A. T., Ream, T. S., Haag, J. R., and Pikaard, C. S. (2009). RNA polymerase V transcription guides ARGONAUTE4 to chromatin. *Nat. Genet.* 41, 630–634. doi: 10.1038/ng.365

Yang, X., Baliji, S., Buchmann, R. C., Wang, H., Lindbo, J. A., Sunter, G., et al. (2007). Functional modulation of the geminivirus AL2 transcription factor and silencing suppressor by self-interaction. *J. Virol.* 81, 11972–11981. doi: 10.1128/JVI.00617-07

Yang, Q.-Y., Ding, B., and Zhou, X.-P. (2017). Geminiviruses and their application in biotechnology. *J. Integr. Agric.* 16, 2761–2771. doi: 10.1016/S2095-3119(17)61702-7

Yang, X., Guo, W., Li, F., Sunter, G., and Zhou, X. (2019). Geminivirus-associated betasatellites: exploiting chinks in the antiviral arsenal of plants. *Trends Plant Sci.* 24, 519–529. doi: 10.1016/j.tplants.2019.03.010

Yang, X., Wang, Y., Guo, W., Xie, Y., Xie, Q., Fan, L., et al. (2011). Characterization of small interfering RNAs derived from the geminivirus/betasatellite complex using deep sequencing. *PLoS One* 6:e16928. doi: 10.1371/journal.pone.0016928

Zerbini, F. M., Briddon, R. W., Idris, A., Martin, D. P., Moriones, E., Navas-Castillo, J., et al. (2017). ICTV virus taxonomy profile: geminiviridae. *J. Gen. Virol.* 98, 131–133. doi: 10.1099/jgv.0.000738

Zhang, Z., Chen, H., Huang, X., Xia, R., Zhao, Q., Lai, J., et al. (2011). BSCTV C2 attenuates the degradation of SAMDC1 to suppress DNA methylation-mediated gene silencing in *Arabidopsis*. *Plant Cell* 23, 273–288. doi: 10.1105/tpc.110.081695

Zhang, H., Lang, Z., and Zhu, J. K. (2018). Dynamics and function of DNA methylation in plants. *Nat. Rev. Mol. Cell Biol.* 19, 489–506. doi: 10.1038/s41580-018-0016-z

Conflict of Interest: The authors declare that the research was conducted in the absence of any commercial or financial relationships that could be construed as a potential conflict of interest.

frontiers in Microbiology

ORIGINAL RESEARCH
published: 29 April 2021
doi: 10.3389/fmicb.2021.654697

Cucumber Ribosomal Protein CsRPS21 Interacts With P22 Protein of Cucurbit Chlorotic Yellows Virus

*Xue Yang†, Ying Wei†, Yajuan Shi†, Xiaoyu Han, Siyu Chen, Lingling Yang, Honglian Li, Bingjian Sun and Yan Shi**

College of Plant Protection, Henan Agricultural University, Zhengzhou, China

Cucurbit chlorotic yellows virus (CCYV) is a cucurbit-infecting crinivirus. RNA silencing can be initiated as a plant defense against viruses. Viruses encode various RNA silencing suppressors to counteract antiviral silencing. P22 protein encoded by RNA1 of CCYV is a silencing suppressor, but its mechanism of action remains unclear. In this study, the cucumber ribosomal-like protein CsRPS21 was found to interact with P22 protein *in vitro* and *in vivo*. A conserved CsRPS21 domain was indispensable for its nuclear localization and interaction with P22. Transient expression of CsRPS21 in *Nicotiana benthamiana* leaves interfered with P22 accumulation and inhibited P22 silencing suppressor activity. CsRPS21 expression in *N. benthamiana* protoplasts inhibited CCYV accumulation. Increasing numbers of ribosomal proteins are being found to be involved in viral infections of plants. We identified a P22-interacting ribosomal protein, CsRPS21, and uncovered its role in early viral replication and silencing suppressor activity. Our study increases knowledge of the function of ribosomal proteins during viral infection.

Keywords: cucurbit chlorotic yellows virus, P22, ribosomal protein, silencing suppressor, virus accumulation

OPEN ACCESS

Edited by:
Kristiina Mäkinen, University of Helsinki, Finland

Reviewed by:
Zongtao Sun, Ningbo University, China
Adrian Alejandro Valli, Centro Nacional de Biotecnología, Consejo Superior de Investigaciones Científicas (CSIC), Spain

***Correspondence:**
Yan Shi
shiyan00925@126.com

†These authors have contributed equally to this work

Specialty section:
This article was submitted to Microbe and Virus Interactions with Plants, a section of the journal Frontiers in Microbiology

Received: *17 January 2021*
Accepted: *07 April 2021*
Published: *29 April 2021*

Citation:
Yang X, Wei Y, Shi Y, Han X, Chen S, Yang L, Li H, Sun B and Shi Y (2021) Cucumber Ribosomal Protein CsRPS21 Interacts With P22 Protein of Cucurbit Chlorotic Yellows Virus. Front. Microbiol. 12:654697. doi: 10.3389/fmicb.2021.654697

INTRODUCTION

The members of the genus *Crinivirus* cause significant yield and quality losses in many cucurbit species (Kreuze et al., 2005; Navas-Castillo et al., 2011). Like most members of the genus *Crinivirus*, cucurbit chlorotic yellows virus (CCYV) has a bipartite genome. The genomes of criniviruses vary among species in the RNA1 3′ region downstream from RNA-dependent polymerase coding region, where the number of open reading frames (ORFs) varies from zero to three (Kataya et al., 2009). CCYV RNA1 contains four ORFs: ORF1a, ORF1b, ORF2, and ORF3. ORF1a encodes viral methyltransferase and RNA helicase 1; ORF1b encodes an RNA-dependent RNA polymerase motif; and ORF2 and ORF3 encode the predicted proteins P6 and P22, respectively. As RNA1 3′ ORFs are quite variable among criniviruses, both P6 and P22 show no significant similarity to corresponding proteins of other criniviruses (Okuda et al., 2010). In addition to CCYV P22, P22 proteins of tomato chlorosis virus (ToCV) and sweet potato chlorotic stunt virus (SPCSV), P23 of lettuce chlorosis virus (LCV), and P25 of cucurbit yellow stunting disorder virus (CYSDV) have also been identified as RNA silencing suppressors (Kreuze et al., 2005; Canizares et al., 2008; Kataya et al., 2009; Kubota and Ng, 2016; Orfanidou et al., 2019; Salavert et al., 2020).

Ribosomal proteins (RPs) are named according to their association with the small or large ribosomal subunit (Kaltschmidt and Wittmann, 1970). In *Arabidopsis*, 81 different RPs encoded

by 242 putatively functional RP genes have been identified (Hummel et al., 2015). Apart from RNA chaperone activity, some RPs regulate processes related to the cell cycle, apoptosis, development, oncogenesis, and rDNA transcription (Chen and Ioannou, 1999; Panic et al., 2007; Jeon et al., 2008; Lindstrom, 2009; Kim et al., 2014; Rajamaki et al., 2017). In plant viruses, P6 of cauliflower mosaic virus (CaMV) is found to interact with RPs L18, L24, and L13 (Bureau et al., 2004). These interactions may be involved in the translation reinitiation of polycistronic mRNAs (Bureau et al., 2004). RP L10 serves as the substrate for the kinase domain of nuclear shuttle protein interacting kinase, which is identified as a virulence target of the begomovirus nuclear shuttle protein and negatively affected tomato golden mosaic virus (TGMV) and tomato crinkle leaf yellows virus (TCrLYV) infection (Fontes et al., 2004; Rocha et al., 2008; Zorzatto et al., 2015). Many RP genes in *N. benthamiana* are upregulated at the mRNA level in response to infection by turnip mosaic virus (TuMV) and plum pox virus (PPV) (Dardick, 2007; Yang et al., 2009). In the case of tomato ringspot virus (ToRSV), the expression of plastid ribosomal genes is repressed (Dardick, 2007). RP S6 in *N. benthamiana* is involved in infections by various viruses and affects the accumulation of cucumber mosaic virus (CMV), TuMV, and potato virus A (PVA), but not turnip crinkle virus (TCV) or tobacco mosaic virus (TMV) (Rajamaki et al., 2017). Although increasing numbers of RPs are involved in viral infections of plants (Chen and Ioannou, 1999; Bureau et al., 2004; Panic et al., 2007; Jeon et al., 2008; Rocha et al., 2008; Rajamaki et al., 2017), the role of RPS21 during viral infection, if any, has not been characterized yet. In this study, we identified a cucumber ribosomal-like protein CsRPS21 that interacts with CCYV P22 protein *in vitro* and *in vivo*. A conserved domain of CsRPS21 was found to be indispensable for its nuclear localization and the interaction with P22; CsRPS21 interfered with the P22 accumulation to inhibit P22 silencing suppressor activity and viral accumulation.

MATERIALS AND METHODS

Plant Materials and Agrobacteria Inoculation

The *N. benthamiana* seeds were provided by Dr. Yanhong Qin from Henan Academy of Agricultural Sciences, and the plants were grown in pots in a growth room under a 16 h light/8 h dark photoperiod at 25°C with 60% humidity. For agroinfiltration, agrobacteria GV3101 carrying relevant clones were suspended in infiltration buffer (10 mM $MgCl_2$, 10 mM MES, and 200 μM acetosyringone, pH 5.6) at an OD_{600} of 1, kept at room temperature for 2–4 h, and infiltrated into *N. benthamiana* leaves using a 1 ml needleless syringe.

Yeast Two Hybrid Screen and Interaction Assay

The cucumber cDNA library screening was performed according to the protocol handbook provided by Matchmaker Gold Yeast Two-Hybrid System (Clontech, CA, United States). The cucumber library was used to screen P22 interacting proteins. The cDNA library screen and interaction assay were performed as described previously (Cheng et al., 2008).

Plasmid Construction

Supplementary Table 1 has the information regarding primers used in this study. All the constructs used were sequenced before use.

To construct vectors for yeast two-hybrid analysis, the full length of CCYV P22 (KU507601) was amplified and cloned into yeast vector pGBKT7 at the *Nde*I and *Bam*HI sites to generate the bait vector BDP22 using the primer pair BDP22F and BDP22R. The full-length coding sequence of CsRPS21 (XM_004145623) was amplified using the primer pair ADCsRPS21F/ADCsRPS21R, and subcloned into the vector pGADT7 at the *Eco*RI and *Xho*I sites to generate ADCsRPS21. We used the primer pairs ADCsRPS21$_{91}$F/ADCsRPS21R, ADCsRPS21F/ADCsRPS21$_{145}$R, ADCsRPS21$_{128}$F/ADCsRPS21R, ADCsRPS21F/ADCsRPS21$_{127}$R, ADCsRPS21$_{91}$F/ADCsRPS21$_{145}$R, ADCsRPS21F/ADCsRPS21$_{90}$R, and subcloned into the vector pGADT7 at the *Eco*RI and *Xho*I sites to generate ADRP1, ADRP2, ADRP3, ADRP4, ADRP5, and ADRP6.

For bimolecular fluorescence complementation (BiFC) analysis, the relevant vectors of P22, CsRPS21, and CsRPS21$_{1-145}$ were constructed using gateway strategy. P22, CsRPS21, and CsRPS21$_{1-145}$ were cloned into entry vector pDONR221 using primer pairs BPP22F/BPP22R, BPCsRPS21F/BPCsRPS21R, and BPCsRPS21F/BPCsRPS21$_{145}$R to generate BPCsRPS21, BPCsRPS21$_{1-145}$ and BPP22. The resultant clones were recombined into the binary expression vector pEarleyGate201-YN and pEarleyGate202-YC (Lu et al., 2010) by the LR reaction, constructing the gateway vector CsRPS21-cYFP, CsRPS21$_{1-145}$-cYFP and P22-nYFP.

For nuclear localization assay, sequences corresponding to 91-145 aa, 1-127 aa and 128-183 aa of CsRPS21 were amplified and cloned into entry vector pDONR221 using primer pairs BPCsRPS21$_{91}$F/BPCsRPS21$_{145}$R, BPCsRPS21F/BPCsRPS21$_{127}$R, and BPCsRPS21$_{128}$F/BPCsRPS21R to generate BPCsRPS21$_{91-145}$, BPCsRPS21$_{1-127}$, and BPCsRPS21$_{128-183}$. The resultant clones together with BPCsRPS21 were used to clone into the gateway vector pEarleyGate104 (Earley et al., 2006) to obtain the expression vector YFP-CsRPS21$_{91-145}$, YFP-CsRPS21$_{1-127}$, YFP-CsRPS21$_{128-183}$, and YFP-CsRPS21. BPP22 was cloned into pEG104 and pEG100-RFP to acquire YFP-P22 and P22-RFP.

For interaction with other CCYV proteins, BD vectors of P4.9, RNA1P6, RNA2P6, HSP70h, P9, P26, CP, CPm, and P59 (KU507602) were constructed and stored in our lab (Wang et al., 2015).

For P22 silencing suppressor activity, pGDFLag-P22 was constructed by introducing P22 into pGDFlag (Goodin et al., 2002) vector. P22 were amplified using primer pair FLAGP22F/FLAGP22R. PCR product was digested by *Sal*I and *Bam*HI, and cloned into pGDFlag vector to generate pGDFlag-P22. pGDMyc-CsRPS21 was constructed by introducing CsRPS21 into pGDMyc (Goodin et al., 2002) vector. CsRPS21 were amplified using primer pair MycRPS21F/MycRPS21R,

digested by *Pst*I and *Bam*HI, then cloned into pGDMyc vector to generate pGDMyc-CsRPS21.

Confocal Laser Scanning Microscopy

For BiFC and co-localization assay, agrobacteria carrying the corresponding constructs were infiltrated into *N. benthamiana* leaves as described previously (Walter et al., 2004). The leaves were detached at 48 h post infiltration (hpi) for fluorescence detection. Fluorescence signals were visualized under an inverted spectral confocal laser scanning microscope (Cal Zeiss LSM 710). Fluorescence of YFP and RFP was excited at 514 and 561 nm. Fluorescence of chlorophy II was excited at 637 nm.

Quantification of GFP Fluorescence Intensity

Images of GFP fluorescence from experimental and corresponding control plants were taken under the Nikon fluorescence microscope ECLIPSE Ti-S at 3 days post-infiltration (dpi). Thirty fluorescent spots were selected at random from two leaves, and the areas were measured using ImageJ2 software. Thirty independent images for each group were measured and values were analyzed via *t*-test. Three biological repeats were needed.

Western Blotting

Agro-infiltrated leaves were harvested at 3 dpi for western blotting assay. Total protein was extracted from 0.2 g leaf tissues using the extraction buffer containing 20% glycerol, 20 mM Tris-HCl pH 7.5, 1 mM EDTA, 150 mM NaCl, 1 mM PMSF, 1 × Protease inhibitor cocktail (Sigma, China). Total protein was separated in SDS-polyacrylamide gel electrophoresis, followed by transfer to nitrocellulose membranes. The membranes were probed using polyclonal anti-GFP (Sigma, China), anti-Flag (Sigma, China), and anti-Myc (Abmart, China) antibody followed by an HRP-conjugated secondary antibody. The detection signals were developed using an ECL reagent as instructed.

N. benthamiana Protoplasts Isolation and Transfection

Protoplasts were isolated from *N. benthamiana* seedlings and transfected using polyethylene glycol (PEG)-mediated method with modifications (Bak and Folimonova, 2015). Approximately 200 μl of protoplasts (2×10^5) were gently mixed with 5 μg of CCYV RNA1 and RNA2 which were obtained from *in vitro* transcription and incubated at room temperature for 15 min. The protoplasts were gently washed in W5 solution and incubated in the dark at 25°C. The transfected protoplasts were harvested at 24 h post transfection and used for quantitative reverse transcription PCR (RT-qPCR) analysis. Three independent experiments were conducted and protoplasts from two tubes were pooled for RNA isolation followed by RT-qPCR analysis.

Northern Blotting

Protoplasts, isolated from *N. benthamiana* seedlings and transfected with CCYV for 24 h, were sampled and pooled for total RNA extraction. RNA samples of 3 μg were used to detect CCYV RNA1 mRNA. Northern blotting analysis was conducted according to the manual of the Northern starter kit (Roche Diagnostics, Basel, Switzerland). RNA was labeled in an *in vitro* transcription reaction with CCYV RNA1 as a template using a labeling mixture. **Supplementary Table 1** shows the probe primers used to detect the CCYV RNA1. The intensities of bands for RNA1 were normalized against the intensities of loading bands with the relative value of YFP control as 1.00. The quantitative calculation of digital images of blots was done using ImageJ2 software.

Transient co-expression of GFP and CsRPS21 or GUS (as a control protein) in GFP-transgenic *N. benthamiana* plants (16c) at 5 dpi, were sampled and pooled for total RNA extraction. RNA samples of 3 μg were used to detect GFP mRNA with GFP probe. The quantitative calculation of digital images of blots was done using ImageJ2 software.

Quantitative Reverse Transcription PCR

Total RNA was extracted from harvested *N. benthamiana* protoplasts using Trizol reagent (Invitrogen, United States) and treated with RNase-free DNase I at 24 hpi. First strand cDNA was synthesized using 500 ng total RNA, an oligo d (T) primer, random primer, and M-MLV reverse transcriptase as instructed. Ten-fold diluted cDNA product was used for PCR on an Eppendorf Real-Time PCR system using an SYBR Green master mix (Takara, Japan). The *N. benthamiana* actin gene (AY179605) was used as the internal control. All the primers used for RT-qPCR are listed in **Supplementary Table 1**. The relative gene expression levels were calculated using the $2^{-\Delta\Delta CT}$ method (Livak and Schmittgen, 2001). Each treatment contains technical triplicates and three independent experiments to confirm the stable expression of genes of interest. *T*-test was performed on data using GraphPad Prism (Inc., San Diego, CA, United States). A two-sample unequal variance directional *t*-test was used to test the significance of the difference ($^*P < 0.05$; $^{**}P < 0.01$).

RESULTS

Identification of a P22-Interacting RPS21 Protein From Cucumber

To identify cucumber proteins that interact with CCYV P22 protein, we performed a yeast two-hybrid screen using a cucumber cDNA library (Chen et al., 2019). The coding sequence of P22 was placed in the pGBKT7 vector as bait. After screening, one clone that contained the entire ORF of a ribosomal-like protein was selected for further study (GenBank accession number XM_004145623). Using blastx, the ribosome-like protein identified here belonged to the ribosomal S21 superfamily, and showed 84.2% identity at the amino acid level with 30S RP S21 from *Cucurbita maxima*; hence, we designated it CsRPS21. Sequence analysis showed that RPS21 protein was conserved in cucurbits (**Supplementary Figure 1**). The CsRPS21 coding sequence was cloned into pGADT7 and the interaction with P22 was tested in the yeast strain Y2HGold using yeast co-transformation. The interaction was seen on

SD/–Leu/–Trp/–His/–Ade/Aba/X-α-gal plates (**Figure 1A**). To confirm the interaction between P22 and CsRPS21 *in planta*, we used BiFC analysis to test the interaction. The coding sequences of CCYV P22 and CsRPS21 were cloned into pEG201-YN and pEG202-YC, respectively, to generate P22-nYFP and CsRPS21-cYFP for infiltration into leaves. Yellow fluorescent protein (YFP) fluorescence was detected in *N. benthamiana* leaves agroinfiltrated with P22-nYFP and CsRPS21-cYFP at 2 dpi. Fluorescence was observed mainly in the nucleus, with weak fluorescence in the cytoplasm (**Figure 1B**). No such interaction was found between P22-nYFP and cYFP or nYFP and CsRPS21-cYFP (**Supplementary Figure 2**). To determine if the interaction influenced the localization of CsRPS21 and P22, YFP-CsRPS21 and YFP-P22 were transiently expressed in *N. benthamiana* leaves. YFP-CsRPS21 fluorescence was found mainly in the nucleus and some chloroplasts (**Figure 1C**). YFP-P22 was observed in both the cytoplasm and nucleus (**Figure 1D**) suggesting that the interaction changed the localization of CsRPS21. Besides co-localization of YFP-CsRPS21 and P22-RFP in *N. benthamiana* leaves showed the co-localization of P22 and CsRPS21 in the nucleus (**Supplementary Figure 3A**).

Interactions Between CsRPS21 and Other CCYV Proteins

The interaction between CsRPS21 and other CCYV proteins was tested using yeast co-transformation methods. AD-CsRPS21 was co-transformed with BD vectors of P4.9, RNA1P6, RNA2P6, HSP70h, P9, P26, CP, CPm, and P59, and plated on SD/–Leu/–Trp/–His/–Ade/Aba/X-α-gal plates for selection. In addition to P22, interactions with CsRPS21 occurred with P4.9, RNA2P6, and P59 (**Figure 2**).

The Conserved NLS Domain of CsRPS21 Is Indispensable for Nuclear Localization and P22-CsRPS21 Interaction

Since the interaction was observed mainly in the nucleus, we identified the nuclear localization domain of CsRPS21 and tested

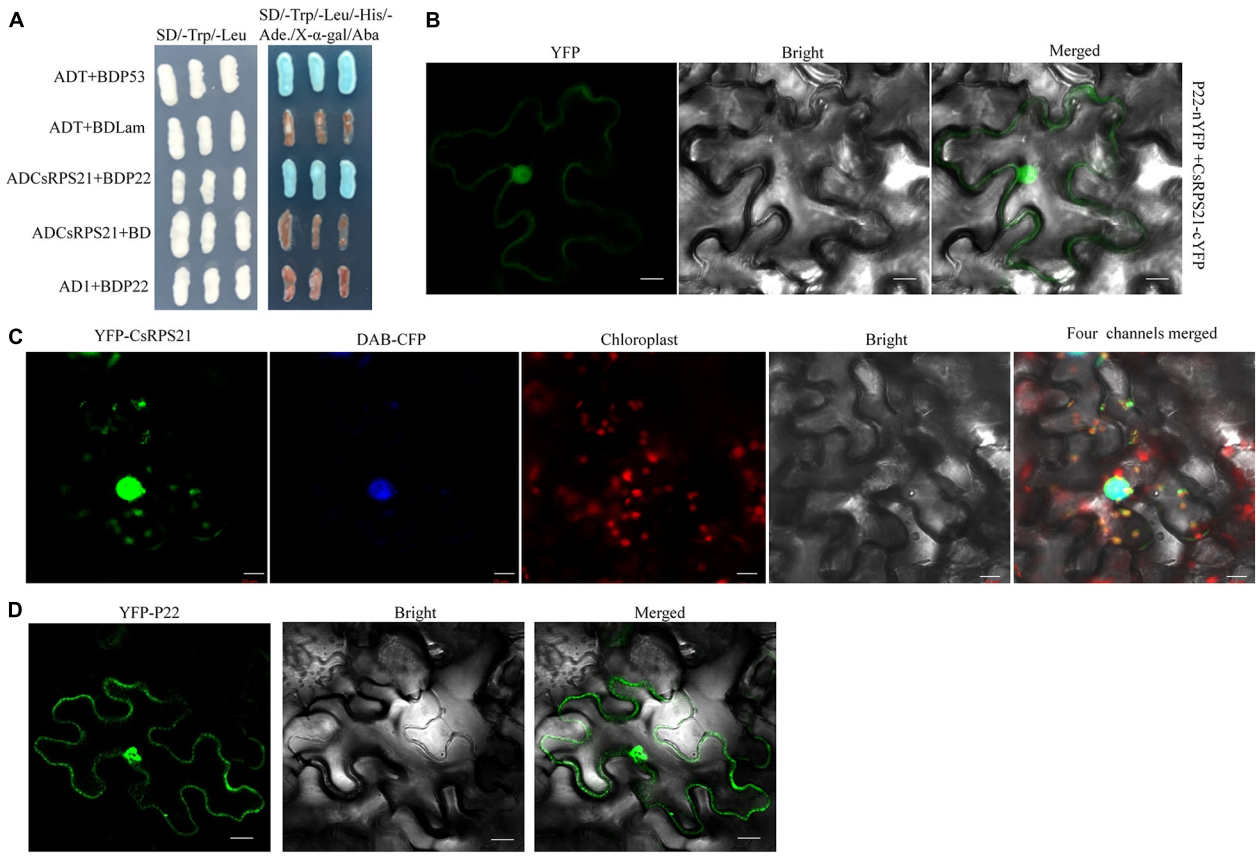

FIGURE 1 | Identification of the interaction between P22 and CsRPS21. **(A)** Growth of Y2HGold yeast cells co-transformed with ADCsRPS21 and BDP22 on low-(SD/–Trp/–Leu) and high-(SD/–Trp/–Leu/–His/–Ade/Aba/X-α-gal) stringency selection media. ADT + BDP53 and ADT + BDLam served as positive and negative controls, respectively. **(B)** Visualization of the interaction between P22 and CsRPS21 in *N. benthamiana* epidermal cells using BiFC. P22 fused with the N-terminal portion of YFP (P22-nYFP) was transiently co-expressed with CsRPS21 fused with the C-terminal portion of YFP (CsRPS21-cYFP). Bar represents 10 μm. Photos were taken at 2 dpi using a Zeiss LSM710 laser scanning microscope. **(C)** Localization of CsRPS21 in *N. benthamiana* epidermal cells. YFP-tagged CsRPS21 (YFP-CsRPS21) was expressed *in planta*. Confocal images were taken at 2 dpi. Nuclear localization protein DAB-CFP was used as a nucleus indicator. Bar represents 10 μm. **(D)** Localization of P22 in *N. benthamiana* epidermal cells. YFP-tagged P22 (YFP-P22) was expressed *in planta*. Confocal images were taken at 2 dpi. Bar represents 10 μm.

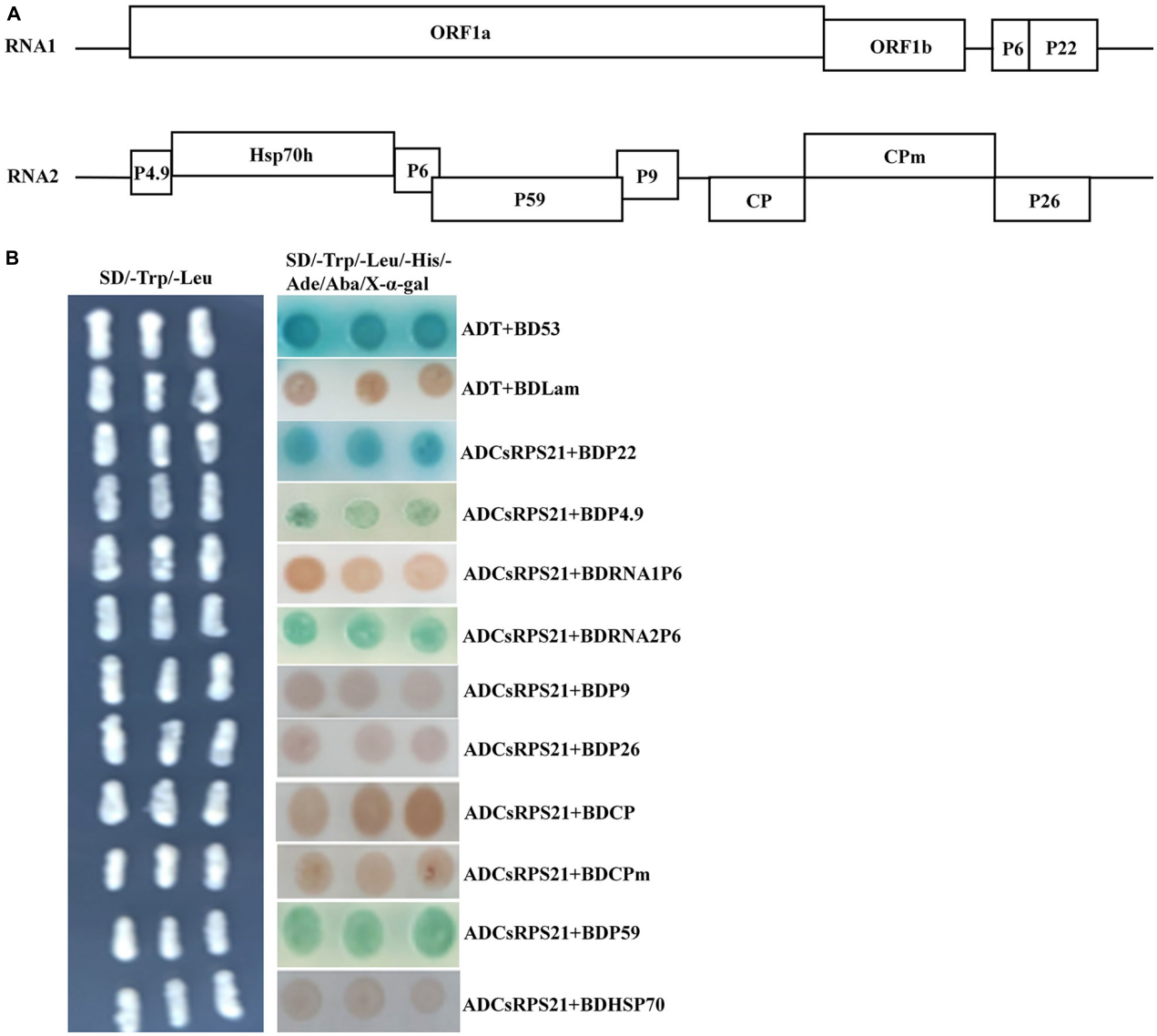

FIGURE 2 | Identification of the interaction between CsRPS21 and CCYV proteins **(A,B)** ADCsRPS21 was co-transformed with CCYV proteins, as P4.9, P1-6, P2-6, P9, P26, CP, CPm, P59, and HSP70, into Y2HGold yeast cells and plated on a low-(SD/–Trp/–Leu) and high-(SD/–Trp/–Leu/–His/–Ade/Aba/X-α-gal) stringency selection media. ADT + BDP53 and ADT + BDLam served as positive and negative controls, respectively.

its role in the interaction. Using the cNLS mapper program[1], the nuclear localization signal was predicted to be located between amino acids 113 and 139 (**Figure 3A**). Using the SMART protein prediction tool, the conserved domain of RP S21 was identified at amino acids 91–145. Next, we constructed the CsRPS21 deletion mutants YFP-CsRPS21$_{91-145}$ (RP5), YFP-CsRPS21$_{1-127}$ (RP4), and YFP-CsRPS21$_{128-183}$ (RP3) and observed fluorescence after agroinfiltration into leaves. The nuclear localization signal was found to be located between amino acids 91 and 145 (**Figure 3B**). We tested the necessity for the localization signal in the interaction of P22 and CsRPS21 using a series of CsRPS21 deletion constructs (**Figure 3C**, left). Yeast cotransformation results showed that AD-CsRPS21$_{1-145}$ (RP2) interacted with BDP22, indicating that the N-terminal 145 amino acids containing the nuclear localization signal are necessary for the interaction (**Figure 3C**, right). Using BiFC analysis, YFP fluorescence was detected in leaves agroinfiltrated with P22-nYFP and CsRPS21$_{1-145}$-cYFP (RP2) at 2 dpi (**Figure 3D** and **Supplementary Figure 4**).

CsRPS21 Negatively Regulates P22 Silencing Suppressor Activity

Previously, P22 was identified as a weak silencing suppressor (Chen et al., 2019; Orfanidou et al., 2019). To determine whether CsRPS21 expression affects the P22 silencing suppressor activity,

[1]http://nls-mapper.iab.keio.ac.jp/

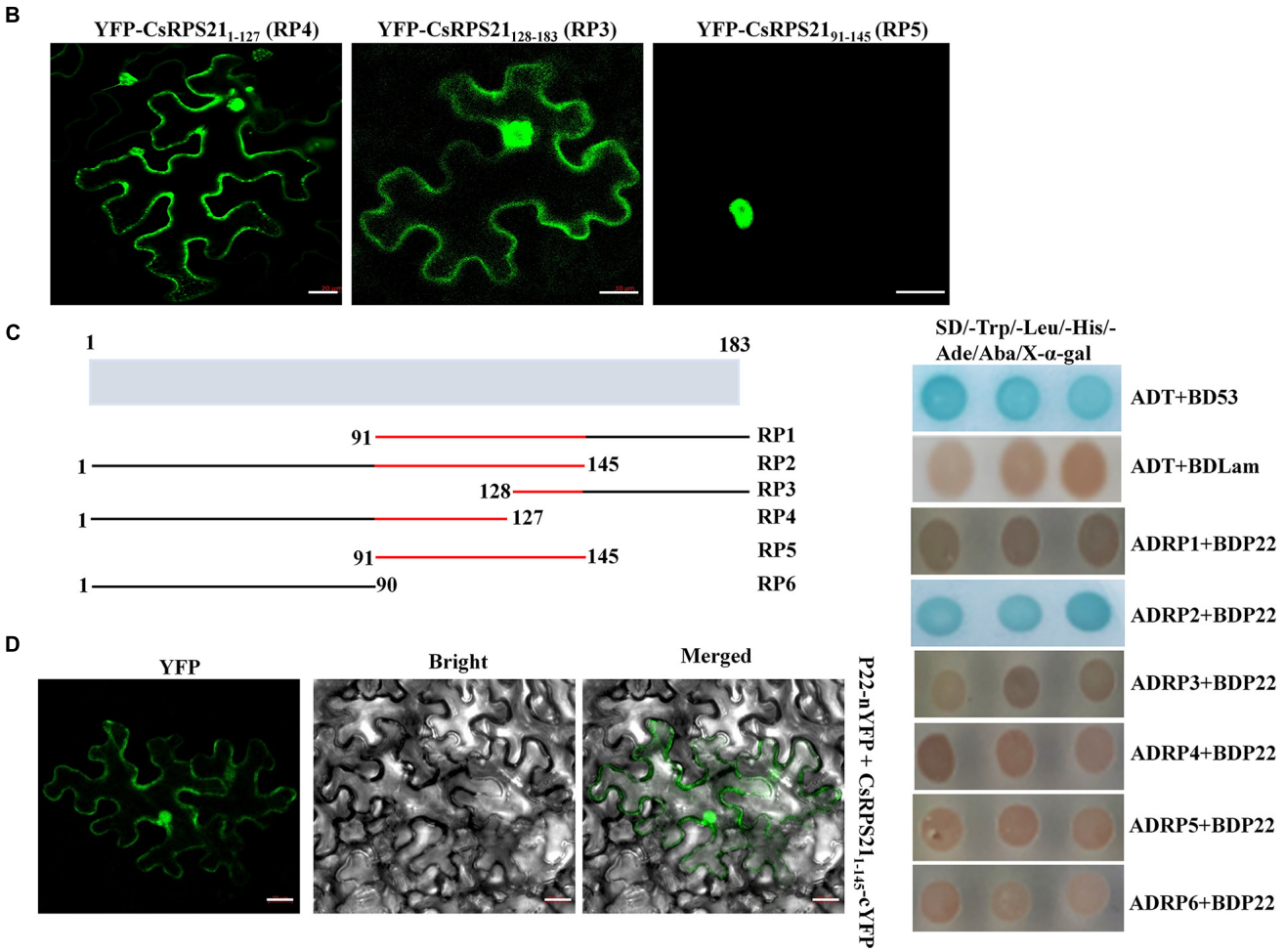

FIGURE 3 | Nuclear localization signal determination and its involvement in the interaction. **(A)** The full amino acid sequence of CsRPS21. Amino acids constituting the nuclear localization signal predicted using cNLS mapper are shown in red. The conserved ribosomal protein S21 domain predicted using the SMART protein prediction tool is underlined. **(B)** Three YFP-tagged deletion mutants of CsRPS21 (YFP-CsRPS21$_{1-127}$, YFP-CsRPS21$_{128-183}$, and YFP-CsRPS21$_{91-145}$) were transiently expressed in *N. benthamiana* leaves. Bar represents 20 μm. Photos were taken at 2 dpi using a Zeiss LSM710 laser scanning microscope. **(C)** Left panel: schematic representation of the CsRPS21 deletion mutants. Six CsPRS21 deletion mutants were used: RP1 (residues 91–183), RP2 (residues 1–145), RP3 (residues 128–183), RP4 (residues 1–127), RP5 (residues 91–145), and RP6 (residues 1–90). Right panel: Interaction between BDP22 and the CsRPS21 deletion mutants. Growth of Y2HGold yeast cells co-transformed with BDP22 and ADRP1, ADRP2, ADRP3, ADRP4, ADRP5, or ADRP6 on high-stringency selection medium (SD/–Leu/–Trp/–His/–Ade/Aba/X-α-gal). **(D)** Interaction between P22 and CsRPS21$_{1-145}$ (RP2) in *N. benthamiana* epidermal cells using BiFC. P22 fused with the N-terminal portion of YFP (P22-nYFP) was transiently co-expressed with CsRPS21$_{1-145}$ fused with the C-terminal portion of YFP (CsRPS21$_{1-145}$-cYFP). Bar represents 20 μm. Photos were taken at 3 dpi using a Zeiss LSM710 laser scanning microscope.

we tested the ability of P22 to suppress RNA silencing by ectopic expression of GFP together with CsRPS21 or GUS in *N. benthamiana* and GFP-transgenic *N. benthamiana* plants (16c) leaves. In these experiments, silencing of the GFP transgene was initiated by infiltration with an *Agrobacterium* culture carrying a second copy of the GFP gene. As shown in **Figure 4A**, at 5 dpi, the amount of GFP fluorescence was observable in leaf patches co-infiltrated with plasmids expressing GFP + P22 + pGDMyc-GUS and GFP + P19 + pGDMyc-GUS (as the positive control). These results demonstrated that P22 was able to suppress silencing of the GFP gene in these infiltrated patches. In contrast, GFP fluorescence was much lower in a patch co-infiltrated with GFP and P22 plus pGDMyc-CsRPS21, indicating that the pGDMyc-CsRPS21 could prevent P22 from suppressing silencing of the GFP gene. Western blotting and northern blotting were done to confirm that the levels of apparent GFP fluorescence correctly reflected the level of GFP protein and mRNA accumulation in the various patches (**Figures 4B,C**).

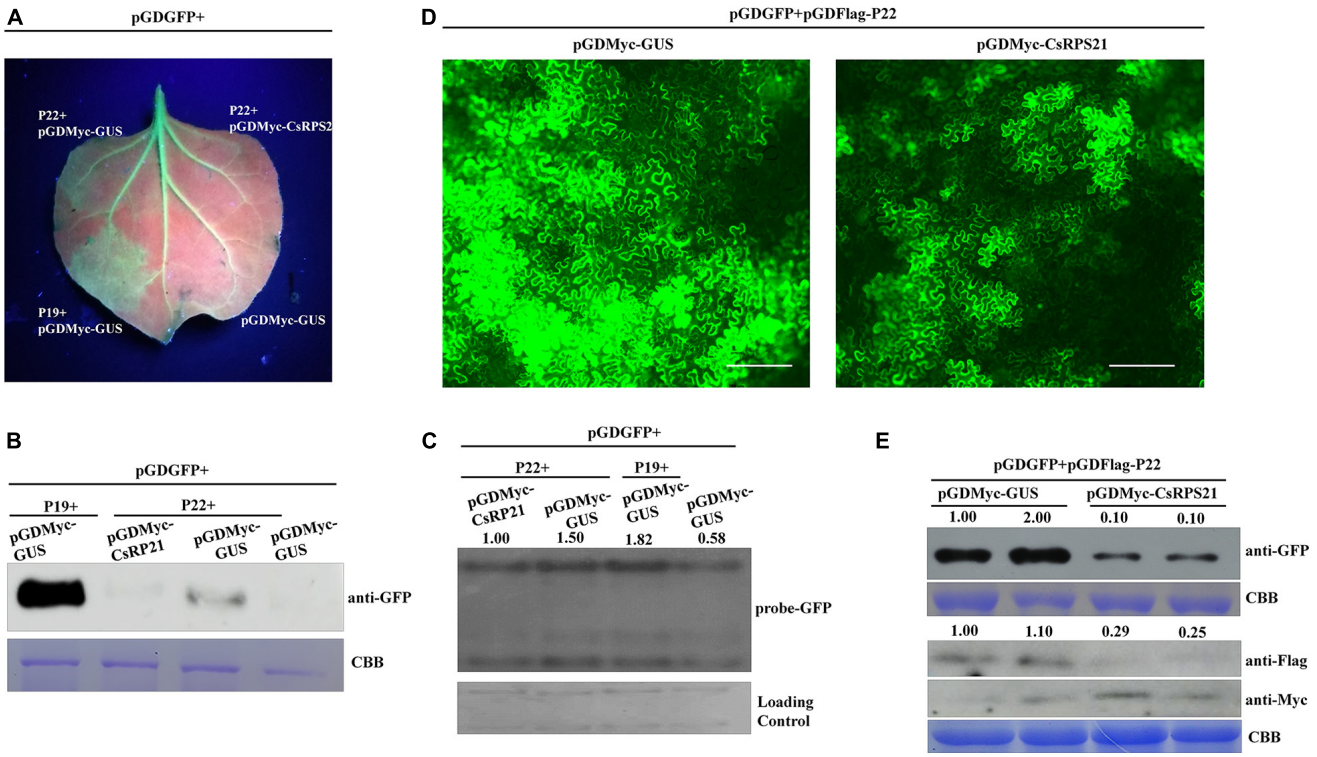

FIGURE 4 | CsRPS21 negatively regulates P22 silencing suppressor activity **(A–C)** Silencing suppression ability of P22 was tested in 16c *N. benthamiana* plants, with transient co-expression of GFP and CsRPS21 or GUS (as a control protein). GFP fluorescence was revealed by UV illumination at 5 dpi with *Agrobacterium* constructs. Western blotting **(B)** and northern blotting **(C)** were used to detect the accumulation of GFP. **(D)** *N. benthamiana* leaves were infiltrated with a mixture of three *Agrobacterium* cultures carrying pGDGFP, pGDFlag-P22, pGDMyc-GUS, or pGDMyc-CsRPS21 and photographed at 3 dpi. Images of GFP fluorescence from agroinfiltrated leaves were taken under a Nikon ECLIPSE Ti-S fluorescence microscope. Bar represents 200 μm. **(E)** Western blotting analysis of protein extracted from the *N. benthamiana* leaves indicated above. GFP, CsRPS21 and P22 expression were confirmed using anti-GFP, anti-Myc and anti-Flag antibody. Coomassie Brilliant Blue (CBB) staining of the large subunit of Rubisco served as a loading control (**Supplementary Figure 5**).

Using fluorescence microscopy, strong GFP fluorescence was observed in *N. benthamiana* leaves agroinfiltrated with pGDGFP and pGDFLag-P22 together with pGDMyc-GUS (as control treatment). When co-expression of pGDGFP + pGDFLag-P22 and pGDMyc-CsRPS21, the fluorescence was weaker than control indicating that CsRPS21 expression inhibits P22 silencing suppressor activity (**Figure 4D**). The fluorescence intensity per visual field of the GUS control was significantly higher than that with the pGDMyc-CsRPS21 treatment (**Supplementary Figure 5**). Western blotting showed that the expression of GFP was consistent with previous findings. We also detected the expression of pGDMyc-CsRPS21 and pGDFlag-P22. CsPRS21 inhibited the P22 expression (**Figure 4E**). Based on these results we speculate that CsRPS21 interfere with P22 expression to attenuate the RNA silencing suppression function of P22.

CsRPS21 Inhibits CCYV Accumulation in *N. benthamiana* Protoplasts

To investigate the role of CsRPS21 in CCYV replication, protoplasts were isolated from *N. benthamiana* leaves agroinfiltrated with YFP-CsRPS21 and transfected *in vitro* with CCYV RNA1 and RNA2 transcripts. At 1 dpi, the total RNA of the transfected protoplasts was extracted and analyzed by northern blotting and RT-qPCR. The results showed that, with the increased CsRPS21 expression, CCYV RNA1 accumulation was significantly decreased in YFP-CsRPS21-treated protoplasts compared with the YFP control (**Figure 5**), indicating the negative regulation of CCYV accumulation by CsRPS21.

DISCUSSION

RPs are involved in processes related to the cell cycle, apoptosis, development, oncogenesis, and control of rDNA transcription, in addition to their RNA chaperone activity (Jeon et al., 2008; Lindstrom, 2009; Kim et al., 2014). In *Arabidopsis thaliana*, knockout of plastid RP S21 impaired the photosynthesis activity and sugar response, possibly via reduced protein synthesis (Morita-Yamamuro et al., 2004). Besides, plastid RPS21 plays role in the response to C/N balance (Dong et al., 2020). In microorganisms, S21 is involved in stress resistance, growth, and motility (Akanuma et al., 2012; Metselaar et al., 2015; Koomen et al., 2018). Different RPs like RPL10, RPL13, RPL18, RPL24, and

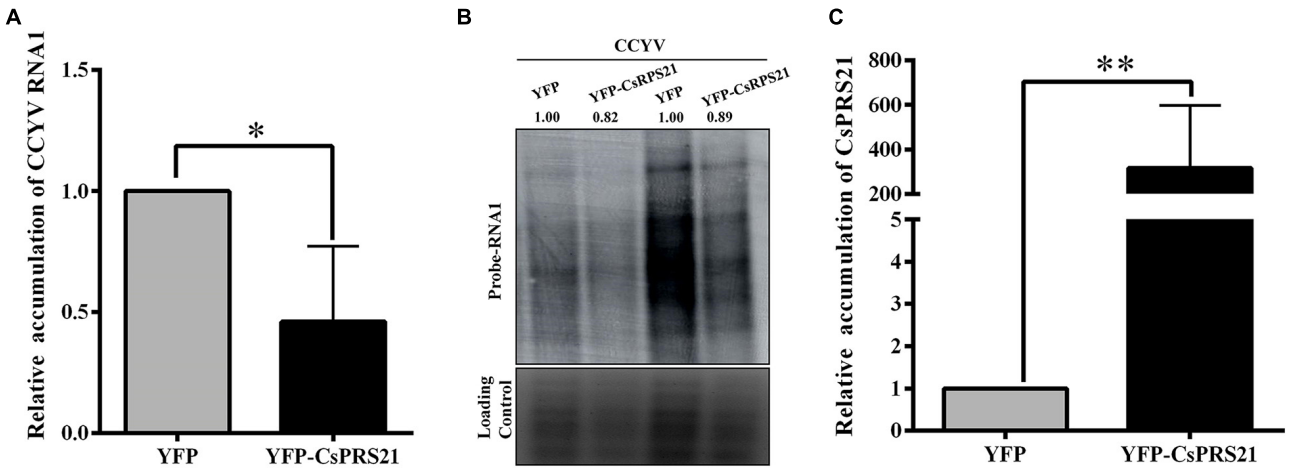

FIGURE 5 | Transient expression of CsRPS21 in *N. benthamiana* protoplasts inhibited CCYV accumulation. **(A,B)** Accumulation of CCYV RNA1 of transfected protoplasts was measured using RT-qPCR and northern blotting with the probe of CCYV RNA1 at 24 hpi. **(C)** Protoplasts isolated from YFP-CsRPS21 and YFP agroinfiltrated *N. benthamiana* leaves were transfected with CCYV RNA1 and RNA2. Accumulation of CsRPS21 was measured using RT-qPCR at 24 hpi. Data were pooled across experiments and statistically analyzed using *t*-tests. Bars represents the mean ± standard deviation (SD). Single and double asterisks indicate significant differences at $^{*}p < 0.05$ and $^{**}p < 0.01$, respectively.

RPS6 are involved in viral infections of plants (Bureau et al., 2004; Rocha et al., 2008; Hafren et al., 2013; Zorzatto et al., 2015; Chen et al., 2016; Ivanov et al., 2016; Rajamaki et al., 2017; Li et al., 2018). The function of RP S21 during viral infections of plants is unknown. In our study we found that CsRPS21 interacted with CCYV P22 and negatively regulated CCYV P22 accumulaiton and silencing suppressor activity, and early viral accumulaiton. CCYV P22, a weak silencing suppressor, is able to suppress local RNA silencing induced by dsRNA (Orfanidou et al., 2019). Using *in vitro* RNA binding analysis P22 is able to bind to ss and ds long RNAs, in addition to ss and ds small interfering (si) RNA molecules *in vitro* (Salavert et al., 2020). A previous study reported that CCYV P22 interacts with SKP1 and F-box like domain of CCYV P22 is essential for the RNA silencing activity (Chen et al., 2019). In this study we found that the interaction down-regulated the CCYV P22 accumulation, and interfered with the silencing suppressor activity of CCYV P22 suggesting that various pathways are possibly involved in the process of CCYV P22 silencing suppression and host defense response.

ToCV P22 was found to be dispensable for viral replication (Landeo-Rios et al., 2016), so the effect on replication is likely due to interaction with viral proteins other than P22. Here, we used protoplasts to uncover the possible role of CsRPS21 in the early infection of CCYV (**Figure 5**). In a viral RNA transfection experiment, the earliest steps in virus life cycles, such as genomic RNA replication and translation, can be monitored because the virus propagation is restricted within single protoplasts (Zhu et al., 2014). Using northern blotting to detect CCYV RNA accumulaiton we found that overexpression of RPS21 in *N. benthamiana* protoplasts caused slight down-regulation of rRNAs indicating that RPS21 was negatively involved in regulating rDNA transcription. As previously reported RPS6 was involved in down-regulation of rRNA in *Arabidospsis* protoplast (Kim et al., 2014).

CsRPS21 shares a high identity with chloroplast RPS21 from cucurbits, although we found that cucumber RPS21 localized in both the nuclei and chloroplasts of *N. benthamiana* epidermal cells. The localization of other cucurbit RPS21s in *N. benthamiana* is unknown. In *Arabidopsis thaliana*, cytosolic RPS21 is localized in the cytosol and nuclear, and plastid RPS21 is localized in the chloroplast (Wang et al., 2018; Dong et al., 2020).

Analysis combining the Nuclear Localization and SMART Protein prediction tools indicated that the domains for interaction and nuclear localization overlapped (**Figure 3**), suggesting the importance of nuclear localization during the interaction. The full length of the domain is important for nuclear localization since both deletion mutants with half coverage of the domain were localized in both the cytoplasm and nuclei.

According to our result CsRPS21 interacts with three other CCYV encoded proteins besides P22 (**Figure 2**). It is possible that CsPRS21 plays multifunctional roles during viral infection through regulating different viral proteins at various infection stages. Currently, the function of P4.9, P2-6, and P59 was limitedly studied, the interaction will give a hint on the further study of P4.9, P2-6, and P59.

We identified a cucumber ribosomal-like protein, termed CsRPS21, that interacts with CCYV P22. A conserved CsRPS21 domain was identified and found to be indispensable for its nuclear localization and interaction with P22. Transient expression of CsRPS21 in *N. benthamiana* leaves interfered with the P22 accumulation to inhibit P22 silencing suppressor activity. In addition, CsRPS21 expression in *N. benthamiana* protoplasts inhibited CCYV accumulaiton. These results suggest that CsRPS21 negatively regulates CCYV infection, possibly by inhibition of P22 accumulation and silencing suppressor activity, and increase our knowledge of the function of RPs during viral infection. RPS21 probably represents one of the translation machinery that is usurped by CCYV P22 protein.

It would be interesting to see if other RPs are involved in the recognition of P22.

DATA AVAILABILITY STATEMENT

The datasets presented in this study can be found in online repositories. The names of the repository/repositories and accession number(s) can be found in the article/ **Supplementary Material**.

AUTHOR CONTRIBUTIONS

YS designed the experiment. YW, YJS, XH, SC, and LY performed the experiments. HL critically reviewed the manuscript. BS contributed to the data discussion. YS, XY, and YW wrote the manuscript. All authors read and approved the manuscript.

FUNDING

This work was funded by the Henan Science Fund for Excellent Young Scholars (Grant No. 202300410194) and Henan Agriculture Research System (S2014-11-G06).

SUPPLEMENTARY MATERIAL

The Supplementary Material for this article can be found online at: https://www.frontiersin.org/articles/10.3389/fmicb.2021.654697/full#supplementary-material

Supplementary Figure 1 | Alignment of amino acid sequences of CsRPS21 from different cucurbit plants.

Supplementary Figure 2 | YFP fluorescence was not detected in the combination of P22-nYFP + cYFP and nYFP + CsRPS21-cYFP. Bar scale represents 20 μm.

Supplementary Figure 3 | (A) Colocalization of YFP-CsRPS21 and P22-RFP in *N. benthamiana*. Confocal images were taken at 2 dpi. Bar represents 20 μm. **(B)** Free YFP was expressed as a control. Bar scale represents 20 μm.

Supplementary Figure 4 | YFP fluorescence was not detected in the combination of P22-nYFP + $CsRPS21_{1-90}$-cYFP, P22-nYFP + cYFP, nYFP + $CsRPS21_{1-90}$-cYFP, nYFP + $CsRPS21_{1-145}$-cYFP. Bar scale represents 20 μm.

Supplementary Figure 5 | GFP fluorescence intensity of **Figure 4D** was measured using ImageJ2 software. Thirty independent images for each group were measured and values were statistically analyzed with *t*-tests. Three biological repeats were performed.

Supplementary Table 1 | Primers used in the paper.

REFERENCES

Akanuma, G., Nanamiya, H., Natori, Y., Yano, K., Suzuki, S., Omata, S., et al. (2012). Inactivation of ribosomal protein genes in *Bacillus subtilis* reveals importance of each ribosomal protein for cell proliferation and cell differentiation. *J. Bacteriol.* 194, 6282–6291. doi: 10.1128/Jb.01544-12

Bak, A., and Folimonova, S. Y. (2015). The conundrum of a unique protein encoded by citrus tristeza virus that is dispensable for infection of most hosts yet shows characteristics of a viral movement protein. *Virology* 485, 86–95. doi: 10.1016/j.virol.2015.07.005

Bureau, M., Leh, V., Haas, M., Geldreich, A., Ryabova, L., Yot, P., et al. (2004). P6 protein of Cauliflower mosaic virus, a translation reinitiator, interacts with ribosomal protein L13 from *Arabidopsis thaliana*. *J. Gen. Virol.* 85, 3765–3775. doi: 10.1099/vir.0.80242-0

Canizares, M. C., Navas-Castillo, J., and Moriones, E. (2008). Multiple suppressors of RNA silencing encoded by both genomic RNAs of the crinivirus, tomato chlorosis virus. *Virology* 379, 168–174. doi: 10.1016/j.virol.2008.06.020

Chen, F. W., and Ioannou, Y. A. (1999). Ribosomal proteins in cell proliferation and apoptosis. *Int. Rev. Immunol.* 18, 429–448. doi: 10.3109/08830189909088492

Chen, S., Sun, X., Shi, Y., Wei, Y., Han, X., Li, H., et al. (2019). Cucurbit chlorotic yellows virus p22 protein interacts with cucumber SKP1LB1 and its F-Box-like motif is crucial for silencing suppressor activity. *Viruses* 11:818. doi: 10.3390/v11090818

Chen, Y. M., Lu, Z., Zhang, L. Z., Gao, L., Wang, N., Gao, X., et al. (2016). Ribosomal protein L4 interacts with viral protein VP3 and regulates the replication of infectious bursal disease virus. *Virus Res.* 211, 73–78. doi: 10.1016/j.virusres.2015.09.017

Cheng, Y. Q., Liu, Z. M., Xu, J., Zhou, T., Wang, M., Chen, Y. T., et al. (2008). HC-Pro protein of sugar cane mosaic virus interacts specifically with maize ferredoxin-5 in vitro and in planta. *J. Gen. Virol.* 89, 2046–2054. doi: 10.1099/vir.0.2008/001271-0

Dardick, C. (2007). Comparative expression profiling of *Nicotiana benthamiana* leaves systemically infected with three fruit tree viruses. *Mol. Plant Microbe Interact.* 20, 1004–1017. doi: 10.1094/Mpmi-20-8-1004

Dong, X., Duan, S., Wang, H.-B., and Jin, H.-L. (2020). Plastid ribosomal protein LPE2 is involved in photosynthesis and the response to C/N balance in *Arabidopsis thaliana*. *J. Integr. Plant Biol.* 62, 1418–1432. doi: 10.1111/jipb.12907

Earley, K. W., Haag, J. R., Pontes, O., Opper, K., Juehne, T., Song, K., et al. (2006). Gateway-compatible vectors for plant functional genomics and proteomics. *Plant J.* 45, 616–629. doi: 10.1111/j.1365-313X.2005.02617.x

Fontes, E. P., Santos, A. A., Luz, D. F., Waclawovsky, A. J., and Chory, J. (2004). The geminivirus nuclear shuttle protein is a virulence factor that suppresses transmembrane receptor kinase activity. *Genes Dev.* 18, 2545–2556. doi: 10.1101/gad.1245904

Goodin, M. M., Dietzgen, R. G., Schichnes, D., Ruzin, S., and Jackson, A. O. (2002). pGD vectors: versatile tools for the expression of green and red fluorescent protein fusions in agroinfiltrated plant leaves. *Plant J.* 31, 375–383. doi: 10.1046/j.1365-313x.2002.01360.x

Hafren, A., Eskelin, K., and Makinen, K. (2013). Ribosomal protein P0 promotes potato virus A infection and functions in viral translation together with VPg and eIF(iso)4E. *J. Virol.* 87, 4302–4312. doi: 10.1128/Jvi.03198-12

Hummel, M., Dobrenel, T., Cordewener, J., Davanture, M., Meyer, C., Smeekens, S., et al. (2015). Proteomic LC-MS analysis of *Arabidopsis* cytosolic ribosomes: identification of ribosomal protein paralogs and re-annotation of the ribosomal protein genes. *J. Proteom.* 128, 436–449. doi: 10.1016/j.jprot.2015.07.004

Ivanov, K. I., Eskelin, K., Basic, M., De, S., Lohmus, A., Varjosalo, M., et al. (2016). Molecular insights into the function of the viral RNA silencing suppressor HCPro. *Plant J.* 85, 30–45. doi: 10.1111/tpj.13088

Jeon, Y. J., Kim, I. K., Hong, S. H., Nan, H., Kim, H. J., Lee, H. J., et al. (2008). Ribosomal protein S6 is a selective mediator of TRAIL-apoptotic signaling. *Oncogene* 27, 4344–4352. doi: 10.1038/onc.2008.73

Kaltschmidt, E., and Wittmann, H. G. (1970). Ribosomal proteins. VII: Two-dimensional polyacrylamide gel electrophoresis for fingerprinting of ribosomal proteins. *Anal. Biochem.* 36, 401–412.

Kataya, A. R., Suliman, M. N., Kalantidis, K., and Livieratos, I. C. (2009). Cucurbit yellow stunting disorder virus p25 is a suppressor of post-transcriptional gene silencing. *Virus Res.* 145, 48–53. doi: 10.1016/j.virusres.2009.06.010

Kim, Y. K., Kim, S., Shin, Y. J., Hur, Y. S., Kim, W. Y., Lee, M. S., et al. (2014). Ribosomal protein S6, a target of rapamycin, is involved in the regulation of

rRNA genes by possible epigenetic changes in *Arabidopsis*. *J. Biol. Chem.* 289, 3901–3912. doi: 10.1074/jbc.M113.515015

Koomen, J., den Besten, H. M. W., Metselaar, K. I., Tempelaars, M. H., Wijnands, L. M., Zwietering, M. H., et al. (2018). Gene profiling-based phenotyping for identification of cellular parameters that contribute to fitness, stress-tolerance and virulence of Listeria monocytogenes variants. *Int. J. Food Microbiol.* 283, 14–21. doi: 10.1016/j.ijfoodmicro.2018.06.003

Kreuze, J. F., Savenkov, E. I., Cuellar, W., Li, X., and Valkonen, J. P. T. (2005). Viral class 1 RNase III involved in suppression of RNA silencing. *J. Virol.* 79, 7227–7238. doi: 10.1128/jvi.79.11.7227-7238.2005

Kubota, K., and Ng, J. C. (2016). Lettuce chlorosis virus P23 suppresses RNA silencing and induces local necrosis with increased severity at raised temperatures. *Phytopathology* 106, 653–662. doi: 10.1094/PHYTO-09-15-0219-R

Landeo-Rios, Y., Navas-Castillo, J., Moriones, E., and Canizares, M. C. (2016). The p22 RNA Silencing suppressor of the crinivirus tomato chlorosis virus is dispensable for local viral replication but important for counteracting an antiviral RDR6-mediated response during systemic infection. *Viruses* 8, 129–136.

Li, S., Li, X., and Zhou, Y. J. (2018). Ribosomal protein L18 is an essential factor that promote rice stripe virus accumulation in small brown planthopper. *Virus Res.* 247, 15–20. doi: 10.1016/j.virusres.2018.01.011

Lindstrom, M. S. (2009). Emerging functions of ribosomal proteins in gene-specific transcription and translation. *Biochem. Biophys. Res. Commun.* 379, 167–170. doi: 10.1016/j.bbrc.2008.12.083

Livak, K. J., and Schmittgen, T. D. (2001). Analysis of relative gene expression data using real-time quantitative PCR and the $2^{-\Delta\Delta CT}$ method. *Methods* 25, 402–408. doi: 10.1006/meth.2001.1262

Lu, Q., Tang, X., Tian, G., Wang, F., Liu, K., Nguyen, V., et al. (2010). *Arabidopsis* homolog of the yeast TREX-2 mRNA export complex: components and anchoring nucleoporin. *Plant J.* 61, 259–270. doi: 10.1111/j.1365-313X.2009.04048.x

Metselaar, K. I., den Besten, H. M. W., Boekhorst, J., van Hijum, S. A. F. T., Zwietering, M. H., and Abee, T. (2015). Diversity of acid stress resistant variants of *Listeria monocytogenes* and the potential role of ribosomal protein S21 encoded by rpsU. *Front. Microbiol.* 6:422. doi: 10.3389/fmicb.2015.00422

Morita-Yamamuro, C., Tsutsui, T., Tanaka, A., and Yamaguchi, J. (2004). Knock-out of the plastid ribosomal protein S21 causes impaired photosynthesis and sugar-response during germination and seedling development in *Arabidopsis thaliana*. *Plant Cell Physiol.* 45, 781–788. doi: 10.1093/pcp/pch093

Navas-Castillo, J., Fiallo-Olive, E., and Sanchez-Campos, S. (2011). Emerging virus diseases transmitted by Whiteflies. *Annu. Rev. Phytopathol.* 49, 219–248. doi: 10.1146/annurev-phyto-072910-095235

Okuda, M., Okazaki, S., Yamasaki, S., Okuda, S., and Sugiyama, M. (2010). Host range and complete genome sequence of cucurbit chlorotic yellows virus, a new member of the genus crinivirus. *Phytopathology* 100, 560–566. doi: 10.1094/Phyto-100-6-0560

Orfanidou, C. G., Mathioudakis, M. M., Katsarou, K., Livieratos, I., Katis, N., and Maliogka, V. I. (2019). Cucurbit chlorotic yellows virus p22 is a suppressor of local RNA silencing. *Arch. Virol.* 164, 2747–2759. doi: 10.1007/s00705-019-04391-x

Panic, L., Montagne, J., Cokaric, M., and Volarevic, S. (2007). S6-haploinsufficiency activates the p53 tumor suppressor. *Cell Cycle* 6, 20–24. doi: 10.4161/cc.6.1.3666

Rajamaki, M. L., Xi, D. H., Sikorskaite-Gudziuniene, S., Valkonen, J. P. T., and Whitham, S. A. (2017). Differential requirement of the ribosomal protein S6 and ribosomal protein S6 kinase for plant-virus accumulation and interaction of S6 kinase with potyviral VPg. *Mol. Plant Microbe Interact.* 30, 374–384. doi: 10.1094/Mpmi-06-16-0122-R

Rocha, C. S., Santos, A. A., Machado, J. P. B., and Fontes, E. P. B. (2008). The ribosomal protein L10/QM-like protein is a component of the NIK-mediated antiviral signaling. *Virology* 380, 165–169. doi: 10.1016/j.virol.2008.08.005

Salavert, F., Navarro, J. A., Owen, C. A., Khechmar, S., Pallás, V., and Livieratos, I. C. (2020). Cucurbit chlorotic yellows virus p22 suppressor of RNA silencing binds single-, double-stranded long and short interfering RNA molecules in vitro. *Virus Res.* 279:197887. doi: 10.1016/j.virusres.2020.197887

Walter, M., Chaban, C., Schutze, K., Batistic, O., Weckermann, K., Nake, C., et al. (2004). Visualization of protein interactions in living plant cells using bimolecular fluorescence complementation. *Plant J.* 40, 428–438. doi: 10.1111/j.1365-313X.2004.02219.x

Wang, R. J., Zhao, J., Jia, M., Xu, N., Liang, S., Shao, J. X., et al. (2018). Balance between cytosolic and chloroplast translation affects leaf variegation. *Plant Physiol.* 176, 804–818. doi: 10.1104/pp.17.00673

Wang, Z. Y., Wang, Y. Z., Sun, H., Gu, Q. S., Li, H. L., Sun, B. J., et al. (2015). Two proteins of cucurbit chlorotic yellows virus, P59 and P9, are self-interacting. *Virus Genes* 51, 152–155. doi: 10.1007/s11262-015-1203-z

Yang, C. L., Zhang, C. Q., Dittman, J. D., and Whitham, S. A. (2009). Differential requirement of ribosomal protein S6 by plant RNA viruses with different translation initiation strategies. *Virology* 390, 163–173. doi: 10.1016/j.virol.2009.05.018

Zhu, M., Chen, Y. T., Ding, X. S., Webb, S. L., Zhou, T., Nelson, R. S., et al. (2014). Maize Elongin C interacts with the viral genome-linked protein, VPg, of sugarcane mosaic virus and facilitates virus infection. *New Phytol.* 203, 1291–1304. doi: 10.1111/nph.12890

Zorzatto, C., Machado, J. P. B., Lopes, K. V. G., Nascimento, K. J. T., Pereira, W. A., Brustolini, O. J. B., et al. (2015). NIK1-mediated translation suppression functions as a plant antiviral immunity mechanism. *Nature* 520, 679–682. doi: 10.1038/nature14171

Conflict of Interest: The authors declare that the research was conducted in the absence of any commercial or financial relationships that could be construed as a potential conflict of interest.

frontiers in Microbiology

ORIGINAL RESEARCH
published: 12 May 2021
doi: 10.3389/fmicb.2021.663948

Retention and Transmission of Grapevine Leafroll-Associated Virus 3 by *Pseudococcus calceolariae*

Brogan McGreal[1,2], Manoharie Sandanayaka[1], Rebecca Gough[1], Roshni Rohra[2], Vicky Davis[1], Christina W. Marshall[3], Kate Richards[1], Vaughn A. Bell[3], Kar Mun Chooi[1] and Robin M. MacDiarmid[1,2]*

[1] The New Zealand Institute for Plant and Food Research Limited (PFR), Auckland, New Zealand, [2] School of Biological Sciences, The University of Auckland, Auckland, New Zealand, [3] The New Zealand Institute for Plant and Food Research Limited (PFR), Hastings, New Zealand

Grapevine leafroll-associated virus 3 (GLRaV-3), an economically significant pathogen of grapevines, is transmitted by *Pseudococcus calceolariae*, a mealybug commonly found in New Zealand vineyards. To help inform alternative GLRaV-3 control strategies, this study evaluated the three-way interaction between the mealybug, its plant host and the virus. The retention and transmission of GLRaV-3 by *P. calceolariae* after access to non-*Vitis* host plants (and a non-GLRaV-3 host) White clover (*Trifolium repens* L. cv. "Grasslands Huia white clover"), Crimson clover (*T. incarnatum*), and *Nicotiana benthamiana* (an alternative GLRaV-3 host) was investigated. For all experiments, *P. calceolariae* first instars with a 4 or 6 days acquisition access period on GLRaV-3-positive grapevine leaves were used. GLRaV-3 was detected in mealybugs up to 16 days on non-*Vitis* plant hosts but not after 20 days. GLRaV-3 was retained by second instars (n = 8/45) and exuviae (molted skin, n = 6/6) following a 4 days acquisition period on infected grapevines leaves and an 11 days feeding on non-*Vitis* plant hosts. Furthermore, GLRaV-3 was transmitted to grapevine (40–60%) by *P. calceolariae* second instars after access to white clover for up to 11 days; 90% transmission to grapevine was achieved when no alternative host feeding was provided. The 16 days retention period is the longest observed in mealybug vectoring of GLRaV-3. The results suggest that an alternative strategy of using ground-cover plants as a disrupter of virus transmission may be effective if mealybugs settle and continue to feed on them for 20 or more days.

Keywords: ***Pseudococcus calceolariae*, grapevine leafroll-associated virus 3, alternative host, retention, transmission, clover, *Trifolium repens***

OPEN ACCESS

Edited by:
Xifeng Wang,
Institute of Plant Protection (CAAS), China

Reviewed by:
Marc Fuchs,
Cornell University, United States
Kent Marshall Daane,
University of California, Berkeley, United States

****Correspondence:***
Brogan McGreal
Brogan.McGreal@plantandfood.co.nz

Specialty section:
This article was submitted to Virology, a section of the journal Frontiers in Microbiology

Received: *04 February 2021*
Accepted: *16 April 2021*
Published: *12 May 2021*

Citation:
McGreal B, Sandanayaka M, Gough R, Rohra R, Davis V, Marshall CW, Richards K, Bell VA, Chooi KM and MacDiarmid RM (2021) Retention and Transmission of Grapevine Leafroll-Associated Virus 3 by Pseudococcus calceolariae. Front. Microbiol. 12:663948. doi: 10.3389/fmicb.2021.663948

INTRODUCTION

Grapevine leafroll-associated virus 3 (GLRaV-3) is the main and most widespread etiological agent of grapevine leafroll disease (GLD) worldwide (Maree et al., 2013). GLD negatively affects berry yield and qualitative characteristics like soluble solids, titratable acidity, and anthocyanins (Over de Linden and Chamberlain, 1970; Cabaleiro et al., 1999; Charles et al., 2006; Lee and Martin, 2009; Lee et al., 2009; Vega et al., 2011; Martelli, 2014; Montero et al., 2016). GLRaV-3 is transmitted by propagation and grafting of infected grapevine material and by insect vectors, namely mealybugs,

soft scale and scale insects (Maree et al., 2013). It has never been demonstrated that GLRaV-3 is transmitted mechanically.

Mealybugs (Hemiptera: Pseudococcidae) are commonly found in New Zealand vineyards. Two cosmopolitan species are especially problematic because they transmit GLRaV-3: *Pseudococcus calceolariae* and *P. longispinus* (Charles, 1993).

Pseudococcus calceolariae and *P. longispinus* are both polyphagous, feeding on numerous plant species throughout New Zealand, including horticultural crops such as apple and pear, and ground-cover species such as white clover, red clover, and doves foot (Charles, 1993; Charles et al., 2006). New Zealand's cool climate status means *P. calceolariae* and *P. longispinus* have two to three generations per year, but can reach a fourth generation under favorable warmer conditions (Charles et al., 2006). *Pseudococcus calceolariae* colonizes all parts of the grapevine, including the roots. Petersen and Charles (1997) demonstrated that *P. calceolariae* first instars transmit GLRaV-3 efficiently but little is known about the length of time required for virus to be acquired and retained by this vector species.

In New Zealand, mealybugs are the key contributor of GLRaV-3 spread from infected grapevines to adjacent healthy vines in vineyards (Bell et al., 2018). Consequently, active control of mealybug populations is recognized as an integral component of a successful GLRaV-3 management program (Bell et al., 2018). Knowledge of virus acquisition, retention, and transmission is fundamental to understanding the interaction between plant viruses and the insect vectors in the context of a range of mealybug plant hosts. Specifically, understanding transmission biology and the impact of non-*Vitis* food sources for mealybug could be important for the further development and enhancement of GLRaV-3 management responses (Almeida et al., 2013; Krüger et al., 2015).

Mealybug numbers are generally maintained at low population densities in New Zealand vineyards through spring applications of insecticides compatible with integrated pest management (IPM; e.g., buprofezin). This response helps facilitate biological control later in the growing season (Charles et al., 2010). Thus, IPM-compatible chemistry and biological control are believed to greatly minimize the risk of vector-mediated transmission of GLRaV-3 (Bell et al., 2018). In addition, grapevines identified as GLRaV-3 infected are rogued (removed) to reduce inoculum in target areas, with the missing vines replaced with those sourced from a nursery certified by the wine sector to supply healthy vines (Bell et al., 2018). However, within New Zealand's Hawke's Bay viticulture region, two organically managed (minimal application of pesticides) vineyards presented high initial GLD incidence but low GLRaV-3 transmission despite apparent high mealybug numbers observed on the ground cover plants (Bell et al., 2018). Notably, mealybug populations on grapevines in both vineyards were low (<3 mealybugs per 100 vine leaves inspected) for at least 6 years (Bell et al., 2018). In other words, there was no evidence of large-scale *P. calceolariae* migration from groundcover to grapevine in either vineyard, an observation supported by a substantially reduced influence of GLRaV-3 over time. In 2009, GLRaV-3 incidence was quantified at 10% in one organically managed vineyard planted in mature Merlot vines, and at 16% in the second planted in mature Cabernet Sauvignon. Once the initial infected vines in each vineyard were removed, annual incidence was consistently less than 1% from years 2 to 6, when monitoring concluded (Bell et al., 2018). Therefore, high mealybug numbers within vineyards may not always result in GLRaV-3 transmission to grapevine. This may be associated with mealybug feeding on ground-cover plants rather than grapevines.

Preliminary retention and transmission experiments were carried out in 2015, with retention experiments repeated in 2019–2020 (2020 Retention experiments). The aims of this study were to determine (i) the GLRaV-3 retention period in viruliferous first instar *P. calceolariae* after feeding on non-*Vitis* plant hosts, (ii) whether GLRaV-3 is retained in second instar *P. calceolariae* and exuviae molted by the first instar *P. calceolariae* after feeding on non-*Vitis* plant hosts, and (iii) whether GLRaV-3 is transmissible by viruliferous first and second instar *P. calceolariae* after feeding on non-*Vitis* plant hosts. White clover (*Trifolium repens* L. cv. Grasslands Huia white clover), Crimson clover (*Trifolium incarnatum*) and *Nicotiana benthamiana* were used as non-*Vitis* plant hosts, of which only *N. benthamiana* has been demonstrated as an alternative host for GLRaV-3.

MATERIALS AND METHODS

Plant Material

For the retention and transmission experiments in 2015, GLRaV-3-positive leaf material was obtained from *V. vinifera* cv. Pinot noir and *V. vinifera* cv. Sauvignon blanc grapevines infected with GLRaV-3 group I maintained in controlled growth rooms (23°C with a 16 h light and 8 h dark cycle). For GLRaV-3-negative plant material, Cabernet franc were sourced from a New Zealand grapevine collection (Lincoln, New Zealand; New Zealand Winegrowers) and Merlot from Riversun Nursery (Gisborne, New Zealand). The virus status of all plants was confirmed by enzyme-linked immunosorbent assay (ELISA) or immunocapture RT-qPCR (Blouin et al., 2017). White clover (*Trifolium repens* L. cv. Grasslands Huia White clover) plants were grown from seed and were used as the non-*Vitis* host plant.

For 2020 retention experiments, GLRaV-3 was obtained from Pinot noir grapevines infected with at least two GLRaV-3 genetic variants representative of phylogenetic groups I and VI. White clover (*Trifolium repens* L. cv. Grasslands Huia white clover), Crimson clover (*Trifolium incarnatum*) and *Nicotiana benthamiana* plants were grown from seed and used as supplied to *P. calceolariae*. These the non-*Vitis* host plants were maintained within a glasshouse (at average 24°C with 16 h light and 8 h dark cycle) within separate, species-specific units with adequate space between plants. To ensure each donor leaf was infected with GLRaV-3 and sufficient GLRaV-3 was acquired by mealybugs, the petiole from each grapevine donor leaf was collected and tested by RT-qPCR (McGreal et al., 2019).

Pseudococcus calceolariae Colonies

Pseudococcus calceolariae mealybugs were reared and maintained at The New Zealand Institute for Plant and Food Research (PFR), Auckland campus, within vented, plastic containers

held under controlled laboratory conditions (22°C with 16 h light and 8 h dark cycle). The colonies were sustained on seed potatoes over multiple generations without exposure to grapevines or GLRaV-3.

GLRaV-3 Retention by *Pseudococcus calceolariae*

Retention experiments were performed in both 2015 and 2020 as detailed below and summarized in **Table 1**.

2015 Retention Experiment (Days 1–4 on Grapevine or a Non-*Vitis* Host)

Pseudococcus calceolariae eggs were collected from the colony and placed on a moist, black filter paper for emergence of first instars. Less than 24 h old nymphs were transferred to excised GLRaV-3-positive Cabernet franc grapevine leaves for an acquisition access period (AAP) or to GLRaV-3-free grapevine leaves for a mock AAP. Excised leaves were kept in good condition within vertically-orientated Petri dishes with the petiole extending through a fitted foam plug placed through the base of both lid and dish into a tube of water. After a 4 days AAP, *P. calceolariae* nymphs were transferred with a paint brush to White clover (Virus/White clover), GLRaV-3-free grapevine leaves (Virus/Grapevine), or maintained on the virus-infected leaves as a positive control (Virus). After a 4 days mock AAP, nymphs were transferred to White clover (No virus/White clover) or maintained on the uninfected grapevine leaves as a negative control (No virus). For all five treatments (Virus/White clover, No virus/White clover, Virus/Grapevine, Virus, and No virus), first instar *P. calceolariae* were collected after 1, 2, 3, and 4 days feeding on grapevine or the non-*Vitis* host. To minimize disruption to mealybug feeding they were collected from separate grapevine or White clover leaves each day. Second instar and exuviae were collected from four treatments (Virus/White clover, No virus/White clover, Virus, and No virus). For the Virus treatment, late first instar mealybugs close to molt (AAP 10–12 days) were transferred onto moist filter paper in a Petri dish to ensure that no nascent second instar mealybugs had an opportunity to feed on GLRaV-3-positive leaves. A maximum of 10 first instar mealybugs were transferred into each Petri dish, thereafter the plates were checked daily for exuviae and second instar mealybugs. The second instar mealybugs with recently removed exuviae were identified based on their shiny brown skin and the absence of the wooly appearance characteristic of first instars. For treatments Virus/White clover, No virus/White clover or No virus, second instar and exuviae were sampled directly from White clover or virus-free grapevine leaves, respectively. GLRaV-3 status in mealybugs and exuviae was detected by one-step RT-qPCR as described previously (McGreal et al., 2019). The GLRaV-3 retention assay was repeated in the same year.

2020 Retention Experiment (Days1–40 on a Non-*Vitis* Host)

Pseudococcus calceolariae egg masses with emerging nymphs were added to an excised GLRaV-3 donor grapevine leaf (∼400 eggs per grapevine leaf). Each grapevine leaf was maintained in a Petri dish as described above. After 24 h the unhatched eggs were removed, leaving the newly emerged nymphs on the leaf surface (∼300 mealybug nymphs/leaf). After a 6 days AAP on virus donor grapevine leaves (two additional days to the 2015 experiment in an attempt to increase the percentage of viruliferous individuals) viruliferous mealybugs were transferred most delicately onto recipient plants by cutting donor grapevine leaf pieces harboring ∼40 mealybugs (per non-*Vitis* host plant) and placing the mealybug-loaded leaf piece(s) onto each non-*Vitis* host plant. The grapevine leaf pieces were removed once they were mealybug free. Mealybugs remained on each non-*Vitis* host for up to 40 days, with harvesting of subsets at 5, 10, 16, 20, and 40 days. Once the mealybug collection was completed, the remaining mealybugs were killed by spraying

TABLE 1 | Summary of retention experiments performed in 2015 and 2020.

Treatment name	Year (number of experimental replicates)	Acquisition access period (AAP) or mock (mealybug age)	Days post initial acquisition on grapevine or non-*Vitis* host (mealybug age)
Virus	2015 (×2)	GLRaV-3 positive grapevine (1–4 days old)	Days 1–4 on original GLRaV-3 positive grapevine (5–8 days old[a,b′])
Virus/White clover	2015 (×2)	GLRaV-3 positive grapevine (1–4 days old)	Days 1–4 on White clover (5–8 days old[a,b])
Virus/Grapevine	2015 (×2)	GLRaV-3 positive grapevine (1–4 days old)	Days 1–4 on GLRaV-3 negative grapevine (5–8 days old[a])
No Virus	2015 (×2)	GLRaV-3 negative grapevine (1–4 days old)	Days 1–4 on GLRaV-3 negative grapevine (5–8 days old[a,b])
No Virus/White clover	2015 (×2)	GLRaV-3 negative grapevine (1–4 days old)	White clover (5–8 days old[a,b])
Virus/White clover	2020 (×1)	GLRaV-3 positive grapevine (1–6 days old)	Days 1–40 on White clover (7–46 days old[c])
Virus/Crimson clover	2020 (×1)	GLRaV-3 positive grapevine (1–6 days old)	Days 1–40 on Crimson clover (7–46 days old[c′])
Virus/*Nicotiana benthamiana*	2020 (×1)	GLRaV-3 positive grapevine (1–6 days old)	Days 1–16 on *Nicotiana benthamiana* (7–22 days old[c′′])

[a] *First instar mealybugs collected after 1, 2, 3, and 4 days after feeding on this plant host then tested for GLRaV-3.*
[b] *Second instar and excuviae collected directly from this treatment then tested for GLRaV-3.*
[b′] *Second instar and excuviae collected from this treatment following transfer of first instars at AAP 10–12 days to Petri dish, then tested for GLRaV-3.*
[c] *First instar mealybugs collected after 5, 10, 15, 20, and 40 days after feeding on this plant host then tested for GLRaV-3.*
[c′] *First instar mealybugs collected after 5, 10, 15, and 20 days after feeding on this plant host then tested for GLRaV-3, as the plants were sprayed at day 35 to treat a pest infestation.*
[c′′] *First instar mealybugs collected after 5 and 10 days after feeding on this plant host then tested for GLRaV-3, as no mealybugs were present on the plant thereafter.*

the plants with insecticide (a mixture of Movento®, Avid®, and Confidor® with Partner®).

To test GLRaV-3 retention in mealybugs after feeding on clover or *N. benthamiana*, five mealybugs from each non-*Vitis* host plant per time point were collected, with individual mealybugs placed into Eppendorf tubes. Mealybug males in cocoons were also included in the sample collection. No mealybugs were present on *N. benthamiana* plants after 16 days. At 35 days post-inoculation, Crimson clover plants were treated with Confidor® for an infestation of aphids, mites and whiteflies that killed 14 plants. After the final mealybug sample collection on day 40, all the plants were treated with a mixture of Movento®, Avid®, and Confidor® with Partner®. At Day 0 (after 6 days AAP), three mealybugs from each donor leaf were collected into individual Eppendorf tubes. The individual donor petioles and the individual mealybug samples were tested for GLRaV-3 as described previously (McGreal et al., 2019). A negative mealybug control (not fed on GLRaV-3 infected host plant) and a buffer only control was included in each batch (10–22 mealybugs) of RNA extractions and RT-qPCR to ensure that no false positives were recorded within the 1,288 mealybug dataset. The GLRaV-3 status in mealybugs on the non-*Vitis* plant for 5, 10, 16, 20, and 40 days was assessed by RT-qPCR (McGreal et al., 2019).

GLRaV-3 Transmission by *Pseudococcus calceolariae*

After a 4 days AAP on excised GLRaV-3-positive grapevine leaves, *P. calceolariae* nymphs were transferred to White clover leaves (as performed for the 2015 retention experiments). Following either a 5 or 11 days non-*Vitis* plant feeding on White clover, *P. calceolariae* nymphs were inoculated on GLRaV-3-free Merlot grapevine plants, as first (Treatment 1) or second instars (Treatment 2), respectively. As a positive control, *P. calceolariae* nymphs were maintained on GLRaV-3-positive leaves for a total of 10 or 16 days AAP, and thereafter transferred to GLRaV-3-free Merlot grapevine plants as either first (Treatment 3) or second instars (Treatment 4), respectively. For the inoculation of GLRaV-3-free grapevine plants, large healthy leaves, two or three nodes above the grapevine graft union, were selected. White clover or GLRaV-3 positive leaves with 25–50 mealybugs were secured to the underside of the grapevine leaf with Blu-Tack (Bostik). Mealybugs were maintained for a 7–10 days inoculation access period (IAP) on GLRaV-3-free grapevines, thereafter plants were sprayed with Movento®. Plants were physically separated during the IAP. Grapevines were pruned and maintained in the glasshouse for 5 months and were sprayed with insecticides once a month. Previous research by Cohen et al. (2004) showed that initial GLRaV-3 spread after transmission was basipetal from the graft point. Therefore, pruning of growth more than three nodes above the marked leaf (on which the mealybugs were inoculated), should have had a minimal effect on distribution of the transmitted GLRaV-3. The GLRaV-3 transmission experiment was performed twice in 2015. Four (Block 2) to five months (Block 1) after GLRaV-3 transmission onto previously GLRaV-3-negative grapevine plants, each inoculated leaf to which mealybugs had been transferred and basipetal cane sections were sampled and tested for GLRaV-3 as described previously (McGreal et al., 2019). As a negative control, GLRaV-3-free Merlot grapevine plants were maintained in the glasshouse until all plants were tested for GLRaV-3 (Prator et al., 2017).

Statistical Analysis

To provide accuracy when expected values are small, Fisher's Exact Test was used to analyze the proportion of GLRaV-3 positive mealybugs to the total number of mealybugs tested for the different feeding treatments and to compare the proportion of GLRaV-3 positive grapevine to the total number of grapevines. To enable comparison between treatments where mealybugs were fed on GLRaV-3 positive grapevine leaves (which was skewed when compared with negative controls where mealybugs were fed on GLRaV-3-free grapevine leaves), the 2015 retention dataset was blocked based on expected positive samples (Virus, Virus/White clover and Virus/Grapevine) and expected negative samples (No virus and No virus/White clover). The following variables were compared: GLRaV-3 status, days feeding on alternate host (grapevine or non-*Vitis*), treatment, source plant and alternate host. The false discovery rate correction (fdr) was applied when performing multiple *post-hoc* pairwise comparisons (Benjamini and Hochberg, 1995). Analyses were implemented in R version 3.6.1 (Team, 2015).

RESULTS

GLRaV-3 Retention in *Pseudococcus calceolariae*

2015 Retention Experiments: Days 1–4 on Grapevine or a Non-*Vitis* Host

Samples positive for GLRaV-3 generated Ct values that ranged between 24 and 38. The percentage of single, viruliferous mealybugs was 7, 15, 81, and 84% after 1, 2, 3, and 4 days post initial AAP, respectively (**Figure 1A**). Based on pairwise comparison using the Fisher exact test and fdr correction, there was evidence of a statistically significant difference between Day 1 (7%), and Day 3 (81%) and Day 4 (84%) ($p < 0.001$) and between Day 2 (15%) and both Days 3 and 4 ($p < 0.001$). When feeding on a non-*Vitis* host plant (Virus/White clover) or on GLRaV-3-free grapevine leaves (Virus/Grapevine), *P. calceolariae* nymphs retained GLRaV-3 for at least 4 days (**Figure 1A**). For the Virus/White clover treatment, the percentage of viruliferous mealybugs ranged over time from 18 to 31%. Over time for the Virus/Grapevine treatment, the percentage of viruliferous mealybugs ranged from 5 to 30%. For both Virus/White clover and Virus/Grapevine treatments, there was no evidence of statistically significant difference in the percentage of viruliferous mealybugs ($p > 0.05$). The percentages of viruliferous mealybugs varied for each of the GLRaV-3 retention treatments (Virus/White clover, Virus/Grapevine and Virus) on Days 3 and 4 post initial AAP (**Figure 1A**). At Day 3, there was evidence of a difference between the Virus (81%) and both Virus/White clover (31%) and Virus/Grapevine (10%) treatments

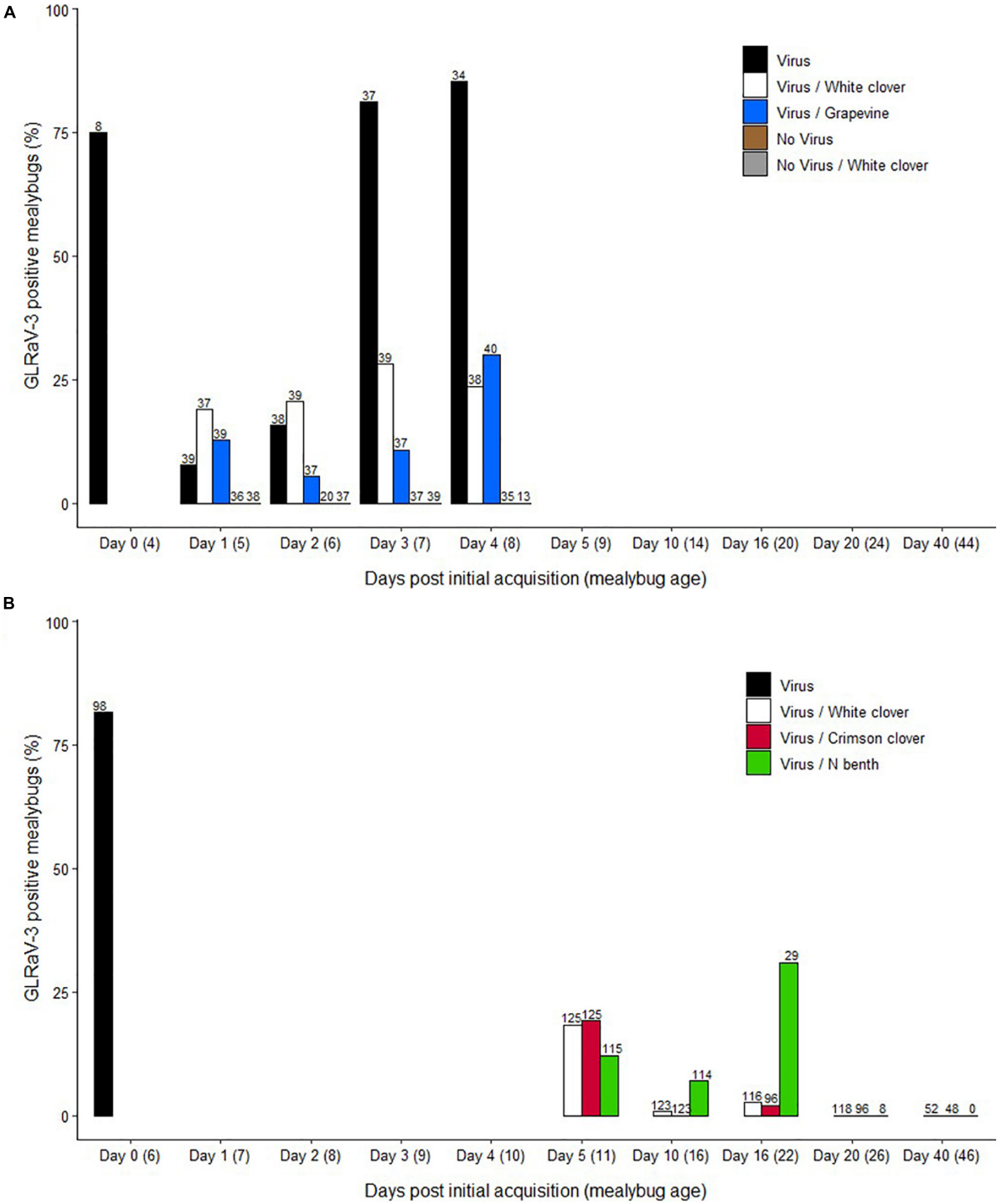

FIGURE 1 | Retention of grapevine leafroll-associated virus 3 (GLRaV-3) in *Pseudococcus calceolariae* after feeding on non-*Vitis* plant host based on results from experiments conducted in **(A)** 2015 and **(B)** 2020. **(A)** Day 0 (Virus acquisition): First instar nymphs had a 4 days acquisition access period (AAP) on GLRaV-3 positive grapevine leaves, and a sub-sample were tested for GLRaV-3. Days 1–4: Nymphs were transferred to and allowed a 1–4 days access period on White clover (*Trifolium repens* L.) (Virus/White Clover) or GLRaV-3 negative grapevines (Virus/Grapevine). As a positive control, mealybugs were left on GLRaV-3 positive grapevine leaves for the duration of the experiment (Virus). Two negative controls were: mealybugs with a 4 days AAP on GLRaV-3 negative grapevine leaves, and then transferred on to White clover (No virus/White Clover) and mealybugs left on GLRaV-3 negative grapevine leaves for the duration of the experiment (No virus). Mealybugs were sampled each day and tested for GLRaV-3. **(B)** Day 0: First instar nymphs had a 6 days AAP on GLRaV-3 positive grapevine leaves and a sub-sample was tested for GLRaV-3 (Virus). Days 5–40: Nymphs were transferred to allow a 5–40 days access period on Crimson clover (*T. incarnatum*), White clover or *Nicotiana benthamiana*. Mealybugs were sampled from White clover (Virus/White clover), Crimson clover (Virus/Crimson clover), and *N. benthamiana* (Virus/N benth) in ∼5 days increments and tested for GLRaV-3. Sample numbers (n) are included above each bar.

(p = 0.028 and <0.001, respectively). Similarly, at Day 4, there was evidence of a difference between the Virus (85%) and both Virus/White clover (23%) and Virus/Grapevine (30%) treatments ($p < 0.001$). All first instar mealybugs sampled from negative control treatments for all blocks (No virus and No virus/White clover treatments) tested negative for GLRaV-3. GLRaV-3 was successfully detected in 17% of second instar *P. calceolariae* from the Virus treatment. One second instar *P. calceolariae*, which fed on GLRaV-3-free grapevine leaves, tested positive for GLRaV-3 (No virus, n = 22), suggesting contamination during the virus retention assay or total RNA extraction procedure. GLRaV-3 was not detected in second instar *P. calceolariae* from the No virus/White clover and Virus/White clover treatments. Composite exuviae samples (10 exuviae per tube) were tested for GLRaV-3. GLRaV-3 was successfully detected in 100% of exuviae samples from the Virus treatment. GLRaV-3 was not detected in exuviae from the No virus, No virus/White clover, and Virus/White clover treatments.

2020 Retention Experiments: Days 1–40 on a Non-*Vitis* Host

A total of 1,288 mealybugs was tested by RT-qPCR as single mealybug samples comprising five time points; 5, 10, 16, 20, and 40 days on a non-*Vitis* host plant. Samples positive for GLRaV-3 generated Ct values that ranged between 31.5 and 35. Notably, there was a gradual reduction of mealybugs collected per time point as the experiment progressed. This result was likely because of poor mealybug settlement on the non-*Vitis* plant host (particularly for *N. benthamiana*) and the natural attrition of Crimson and White clover plants and the mealybugs they supported. The percentage of mealybugs that tested positive for GLRaV-3 by RT-qPCR reduced gradually, with no GLRaV-3 detected from 20 days on any of the non-*Vitis* host plants (**Figure 1B**). The percent viruliferous mealybugs on Crimson and White clover species was 19 and 18% at 5 days, 0 and 1% at 10 days, and 2 and 3% at 16 days, respectively. By contrast, at 10 and 16 days on *N. benthamiana* a greater percentage of mealybugs tested GLRaV-3 positive (7 and 31%, respectively). There was evidence of a statistically significant difference at Day 10 between Crimson clover and *N. benthamiana* ($p < 0.01$). At Day 16, there was evidence of a statistically significant difference between both clover species and *N. benthamiana* ($p < 0.001$). There was no evidence of any statistically significant difference for the *N. benthamiana* treatment between the different time points ($p > 0.05$).

GLRaV-3 Transmission by First Instar *Pseudococcus calceolariae*

GLRaV-3 was successfully transmitted by *P. calceolariae* nymphs when they were transferred directly (Treatment 3) or indirectly (via the non-*Vitis* host White clover, Treatment 1) to recipient grapevines (**Table 2**). Greater transmission success was observed for direct transfer of mealybugs to the recipient grapevines compared with those that had an intermediary 5 days feeding period on the alternative host. For the first instar positive control (Treatment 3), GLRaV-3 was detected in 9 out of 10 grapevine plants based on both cane and leaf samples. By contrast, GLRaV-3 was detected in only 6 out of 10 grapevine plants based on leaf and cane samples for first instars fed intermediary on an alternate host (Treatment 1). There was no evidence of a statistically significant difference in transmission success between Treatments 1 and 3 (Fisher's exact test; p = 0.23).

GLRaV-3 Transmission by Second Instar *Pseudococcus calceolariae*

Overall for Block 1 and Block 2, GLRaV-3 was successfully transmitted by second instar mealybugs when transferred directly (Treatment 4) or indirectly (via the non-*Vitis* host White clover, Treatment 2) to recipient grapevines (**Table 2**). Greater transmission success was observed for the second instars directly transferred (Treatment 4) compared to second instars fed on the alternate host (Treatment 2). For the second instar positive control (Treatment 4), GLRaV-3 was detected in six out of seven grapevine plants based on leaf and cane samples. In contrast when second instars were fed on White clover (Treatment 2), GLRaV-3 was detected in four out of nine recipient grapevine plants based on leaf samples, and five out of nine plants based on cane samples. There were differences in transmission success for second instars fed on White clover (Treatment 2) between Block 1 and Block 2. For Block 1, GLRaV-3 was detected in one out of four recipient grapevine plants compared to four out of five grapevine plants for Block 2. Though there was a statistically significant difference in transmission success between Block 1 and 2 for Treatment 2 (Fisher's exact test; p = 0.015) there was no evidence of a difference in transmission success between Block 1 and Block 2 for Treatment 4 ($p > 0.05$). GLRaV-3 was not detected in any of the negative controls grown in parallel to the inoculated grapevines (seven plants).

Pseudococcus calceolariae Internal Control

A subset of RNA extracted from mealybugs was tested for *P. calceolariae* elongation factor 1a gene and all samples were positive (data not shown).

DISCUSSION

GLRaV-3 Persistence in *P. calceolariae* Nymphs: GLRaV-3 Is Retained 16 Days After Feeding on Non-*Vitis* Plant Hosts but Lost by 20 Days

This study demonstrated that more than 4 days is needed to ensure optimal virus acquisition by individual *P. calceolariae* within the mealybug populations in this study. In the 2015 retention experiment, *P. calceolariae* nymphs were given a 4 days AAP on GLRaV-3-positive grapevine leaves and showed an increased percentage of viruliferous mealybugs over time for the positive control (Virus). In the 2020 retention experiment, a 6 days AAP was used and resulted in 81% acquisition of GLRaV-3. Neither the 2015 nor the 2020 experiments resulted in a drop in GLRaV-3 Ct values over time of mealybug feeding on the non-*Vitis* host, thereby supporting a non-propagative interaction

TABLE 2 | Transmission of grapevine leafroll-associated virus 3 (GLRaV-3) by first and second instar *Pseudococcus calceolariae* initially fed on GLRaV-3-infected grapevine leaves and later transferred to White clover (*Trifolium repens* L., a non-*Vitis* host plant) prior to access to healthy grapevines for transmission of GLRaV-3 (Blocks 1 and 2).

Treatment	AAP[a]	NVF[b]	IAP[c]	Mealybugs per plant	Positive plants/Inoculated plants		Mealybugs per plant	Positive plants/Inoculated plants			
					Block 1[e]			Block 2[e]		Combined results[e]	
					Leaf	Cane		Leaf	Cane	Leaf	Cane
1—First instar White clover	5 days	5 days	1 week	30–37	3/5	1/5	47–52	3/5	5/5	6/10	6/10
2—Second instar White clover	5 days	11 days	1 week	31–38	0/4	1/4	50–52	4/5	4/5	4/9	5/9
3—First instar No alternate host	5 days		1 week	32–38	4/5	4/5	50	5/5	5/5	9/10	9/10
4—Second instar No alternate host	16 days		1 week	26–31	4/4	3/4	30–40	2/2[d]	3/3	6/6	6/7
Negative controls										0/7	0/7

[a] *Acquisition access period.*
[b] *Non-Vitis feeding.*
[c] *Inoculation access period.*
[d] *Leaf samples were collected from two out of three grapevine plants, as the inoculated leaf on one of the plants senesced.*
[e] *Leaf and cane material collected from same plant.*

between vector and virus. Variability in virus acquisition of GLRaV-3 by mealybugs has been reported previously. Charles et al. (2006) suggested that GLRaV-3 acquisition by mealybugs is shorter than the typical AAP of other plant viruses, usually occurring within 0.25–12 h. Krüger et al. (2006) reported that *P. longispinus* first instar nymphs transmitted GLRaV-3 after an AAP of 1.5 h. Mahfoudhi et al. (2009) detected GLRaV-3 in 58.3% of first and second instar groups and 41.7% of composited adult female *P. ficus* fed on GLRaV-3 positive grapevine leaves for a 7 days AAP. Sandanayaka et al. (2013) found *P. longispinus* adults did not acquire GLRaV-3 in less than 24 h. Krüger et al. (2015) found that *P. ficus* was able to transmit GLRaV-3 after a 15-min AAP and a 15 min IAP, and for *P. longispinus*, GLRaV-3 was transmitted after an AAP of 10 min and an IAP of 1 h.

The 2015 experiment used a single set of excised GLRaV-3-positive Cabernet franc grapevine leaves on which all mealybugs fed prior to distribution to White clover or GLRaV-3-free grapevine leaves for collection at Days 1–4 (**Table 1** and **Figure 1**). The Virus treatment comprised those mealybugs that remained on the original source leaves (**Table 1**). At Days 1 and 2 post initial AAP the mealybugs for the Virus treatment had only a brief time to recover from the disturbance caused by the distribution of mealybugs from those leaves. This disturbance may have resulted in less feeding and lower GLRaV-3 incidence at Days 1 and 2 compared with Days 3 and 4. Due to this presumed feeding disturbance we altered the method in the 2020 experiment to a gentler, mealybug-motivated movement from source grapevine leaves to alternative host plant leaves.

This study demonstrated that the GLRaV-3 retention period in *P. calceolariae* was at least 16 days, i.e., between when the first instar acquired the virus and subsequently fed on either White clover, Crimson clover or *N. benthamiana*. In the 2015 experiments, GLRaV-3 was detected from 23.7% of the mealybugs collected after 4 days of feeding on White clover. Furthermore, GLRaV-3 was detected from 17% of second instar citrophilus mealybugs left on GLRaV-3 positive grapevine leaves for up to 9 days then removed to Petri dishes before the mealybugs molted to become second instar mealybugs. Moreover, GLRaV-3 was transmitted to grapevines even after the inoculating mealybugs were sustained on White clover plants for 11 days. The 2020 experiments extended past 4 days access to a non-*Vitis* host and GLRaV-3 was detected in *P. calceolariae* after 16 days feeding on White clover or *N. benthamiana*, but at 20 days and beyond, no GLRaV-3 was detected in the test mealybugs.

Notably, the number of mealybugs available to be collected from *N. benthamiana* plants dramatically declined during the 2020 experiment. This result was most likely because of the poorer mealybug settlement on *N. benthamiana* compared with the clover plants. The poor mealybug settlement and consequent lack of feeding may have led to the slightly higher number of GLRaV-3 positive mealybugs from *N. benthamiana* plants compared with the clover as the virus would have had less opportunity to be transmitted from the mealybug into the solanaceous plant. GLRaV-3 detection in *N. benthamiana* plants only occurs months after inoculation (Prator et al., 2017) therefore this non-*Vitis* plant is unlikely to have provided GLRaV-3 inoculum to mealybugs within the timeframe of this retention experiment.

Reported GLRaV-3 retention time varies throughout the literature and appears to differ with mealybug species, their maturity, and the AAP. For example, it has been reported that *Planococcus citri* nymphs lose GLRaV-3 after 1 h of being removed from GLRaV-3 positive grapevines on which they had been feeding for 3 days (Cabaleiro and Segura, 1997). In another study, first and second instar nymphs of *P. longispinus* were found to retain GLRaV-3 for more than 3 days, with the percentage of viruliferous mealybugs declining over time from 81 to 17% (Krüger et al., 2006). In addition, individual *P. longispinus* first and second instar nymphs were reported to transmit GLRaV-3, after an AAP of 5 days followed by 5 days of feeding on virus-free plants (Douglas and Krüger, 2008). Krüger et al. (2015) observed

GLRaV-3 retention in *P. ficus* for 8 days when feeding on a non-virus host (*Ficus benjamini*) or GLRaV-3-free grapevine, and for 2 days when starving. By contrast, *P. longispinus* retained GLRaV-3 for at least 3 days when fed on GLRaV-3-free grapevine or starving (Krüger et al., 2015). Several studies have also noted that mealybug adults (which do not feed) have lower transmission efficiency than first instar mealybugs (Petersen and Charles, 1997; Sandanayaka et al., 2013). First instar *P. longispinus* were found to start feeding earlier in their life stage and feed for longer than adults, suggesting they are more efficient vectors (Sandanayaka et al., 2013).

Collectively, based on the acquisition and retention times from previous studies, GLRaV-3 transmission by mealybugs has been described as non-circulative, non-propagative, and semi-persistent, i.e., GLRaV-3 does not breach the gut barrier of the mealybug and is retained in the stylet or foregut prior to transmission (Cabaleiro and Segura, 1997; Krüger et al., 2006, 2015; Cassone et al., 2014). Thus, GLRaV-3 is shed from the maturing mealybug with the exuviae through the molt. From the current study, the detection of GLRaV-3 in the exuviae (n = 6/6) and the decrease in percentage viruliferous mealybugs over time on clover or *N. benthamiana* and the eventual lack of detection of GLRaV-3 in individual mealybugs by 20 days, supports the non-circulative and non-propagative descriptors for the transmission of GLRaV-3.

If GLRaV-3 was semi-persistent, the virus would likely be bound to the stylet alimentary channel or the foregut epicuticle. Cid et al. (2007) presented results that supported circulative transmission in *Pl. citri*. When dissected after feeding on GLRaV-3 infected grapevine leaves, in all cases GLRaV-3 was detected in the salivary glands, mid-gut, hindgut, Malpighian tubes, bacteriome, and exuviae, and in some instances, in the reproductive apparatus, suboesophageal ganglion, and mouth apparatus. The virus was not detected in bundles or replication sites in *Pl. citri*, suggesting GLRaV-3 does not replicate inside the insect (Cid et al., 2007). By contrast, the dissection of *P. maritimus* after feeding on an *in vitro* solution with GLRaV-3 revealed virus accumulation in the cibarium, a pumping organ of the foregut located proximal to the esophagus (Herrbach et al., 2017), but not in other body parts (Prator and Almeida, 2020). Similarly, lettuce infectious yellows virus (LIYV; genus *Crinivirus*, family *Closteroviridae)* is transmitted by *Bemisia tabaci* (whitefly) in a non-circulative, semi-persistent transmission and LIYV was shown to localize in the anterior of the foregut or cibarium (Chen et al., 2011). The results from the current study suggests GLRaV-3 or parts of the virus are potentially moving further down the foregut of *P. calceolariae* and/or are located in parts of the insect that are not removed effectively during molt. GLRaV-3 was detected from mealybugs after an extended amount of time on a non-*Vitis* host plant (16 days) and in second instar mealybugs (n = 8/45), even when first instars that had been feeding on GLRaV-3-positive grapevine leaves were transferred to Petri dishes prior to molt so that mealybugs could not feed as second instars prior to virus testing. This raises the question of whether the detected GLRaV-3 is present as a whole virion and is therefore still infectious. Similar feeding/dissection studies of *P. calceolariae* will validate the GLRaV-3 binding locations for this particular mealybug species and virus, and may verify or refute the previously reported circulative manner of the GLRaV-3-vector interaction. These experiments could also be used to reveal any differences between the transmission of GLRaV-3 genetic variants (Diaz-Lara et al., 2018).

No difference in the retention of GLRaV-3 in mealybugs was observed between the two clover species that are known to be preferred hosts of *P. calceolariae* (Sandanayaka et al., 2018). Some non-*Vitis* mealybug hosts, e.g., those with high lectin content, may be capable of causing a faster decrease in mealybug GLRaV-3 retention by blocking or competing for GLRaV-3 binding to the cuticular surface of its insect vectors (Prator and Almeida, 2020). The effect of plant host, beyond grapevine, clover and *N. benthamiana*, on GLRaV-3 retention by *P. calceolariae* is yet to be determined. Given GLRaV-3 can be transmitted to at least one non-*Vitis* host i.e., *N. benthamiana*, consideration must also be given to the possibility of other plant species found within vineyards being GLRaV-3 reservoirs (Prator et al., 2017).

GLRaV-3 Is Transmitted by Both First and Second Instar *P. calceolariae* After Feeding on Non-*Vitis* Plant Hosts of Mealybugs

The ability of second instar *P. calceolariae* to transmit GLRaV-3 was demonstrated by the 90% transmission rate by second instar nymphs following continuous feeding on GLRaV-3-infected grapevine leaves and the 40–60% transmission rate after access to white clover for up to 11 days. These data underscored the importance of mealybug control in vineyards and demonstrated that managing only the nascent mealybug instars is insufficient; long-term management is required to reduce vector-mediated GLRaV-3 transmission. A period of 16 days was assumed to be sufficiently long for the mealybugs to molt and transition into second instars. Thus, it is possible a small number of mealybugs had not molted at the time of transfer from the non-*Vitis* and *Vitis* (experimental positive control) plants. Future transmission studies will benefit from transferring mealybugs from plants to Petri dishes prior to molt, similar to the 2015 retention experiment. Furthermore, as noted above, the GLRaV-3-*P. calceolariae* relationship would benefit from investigation by feeding/dissection studies including second instar and later life stages. In particular, the use of electron microscopy to view immunologically tagged GLRaV-3 virions within mealybugs at different time points in the life-cycle and on a non-*Vitis* plant, in combination with transmission studies, would help elucidate where the infectious virion is located within the vector. The underlying question still remains, at what point in time does the GLRaV-3 virion lose its infection capacity following mealybug acquisition?

Previous studies have hypothesized that the GLRaV-3 genetic variant has an effect on the efficiency of virus transmission by mealybugs (Jooste et al., 2011; Chooi et al., 2013; Blaisdell et al., 2015). It is also possible that the genetic differences between the GLRaV-3 variants could affect the interaction between the virus and its vector, with impacts on minimal required AAP and IAP.

Such differences may be direct (e.g., affecting virus retention within the insect) or indirect (e.g., affecting virus titre in the grapevine and subsequently its transmission efficiency).

Implications for GLRaV-3 and Mealybug Management

Mealybug instars influence the spread of GLRaV-3 within and between vineyards by crawling between vines, movement via vineyard management activities and aerial dispersal (Charles et al., 2009). Dispersal of viruliferous mealybug nymphs result in vine-to-vine spread of GLRaV-3, which is typically most pronounced within vine rows (Bell et al., 2018). Several epidemiology studies supported this form of dispersal, with infection shown to spread more rapidly along rows than between rows and often appeared clustered (Cabaleiro and Segura, 1997). Vine management activities such as machinery use, leaf trimmers, and machine harvesters may also transport mealybugs within the vineyard and between adjoining vineyards (Charles et al., 2009). Aerial dispersal of mealybugs, particularly nymphs can result in movement of GLRaV-3 between blocks and vineyards (Charles et al., 2006). There is a strong correlation between mealybug numbers and GLRaV-3 infection levels in the subsequent seasons; accordingly the rapid spread of GLRaV-3 is purported to be a consequence of high-density mealybug populations (Charles et al., 2009; Franco et al., 2009; Daane et al., 2012).

Here, we have shown that GLRaV-3 can be retained and transmitted by first or second instar *P. calceolariae* after either feeding on a non-*Vitis* mealybug host or GLRaV-3-free grapevine leaves for up to 16 days. These results demonstrated the insidious nature of GLRaV-3 in vineyards and they go some way to explaining issues around virus persistence, spread, and barriers to effective management. Measures to control GLRaV-3 spread that do not rely on insecticides only could include the use of ground-cover plants that host the mealybug vector but not the virus, thereby interrupting the GLRaV-3 transmission pathway from grapevine to grapevine. However, alternative hosts like clover must be a sink for mealybugs for a period of time sufficient to transition viruliferous individuals to non-viruliferous. In New Zealand, this novel addition to the integrated response to GLRaV-3 management is being evaluated (V. Bell unpublished data), and comes at a time when the wine sector is actively reducing its reliance on insecticides.

DATA AVAILABILITY STATEMENT

The raw data supporting the conclusions of this article will be made available by the authors, without undue reservation.

AUTHOR CONTRIBUTIONS

MS, KC, and RM: conceptualization and supervision. BM, RG, RR, KC, VD, and CM: data generation and curation. BM, KC, RG, and KR: formal analysis. KC, RM, and VB: Funding acquisition. BM, MS, RG, RR, VD, CM, KR, VB, KC, and RM: methodology, writing—review, and editing. BM, MS, KC, RM, and RG: writing—original draft. All authors contributed to the article and approved the submitted version.

FUNDING

The 2015 retention experiment and the transmission experiments were supported by the Bio-Protection Research Centre, New Zealand, the Agricultural and Marketing Research and Development Trust (AGMARDT), New Zealand, and The New Zealand Institute for Plant and Food Research Limited (PFR) Virus-Vector project. The 2020 retention experiment was supported by the New Zealand Winegrowers Research Centre Limited, New Zealand. Preparation of the manuscript was supported by the PFR Rejuvenating Crop Ecosystems Programme.

ACKNOWLEDGMENTS

We thank Dr. Grant Smith for his helpful suggestions prior to submission of the manuscript.

REFERENCES

Almeida, R. P. P., Daane, K. M., Bell, V. A., Blaisdell, G. K., Cooper, M. L., Herrbach, E., et al. (2013). Ecology and management of grapevine leafroll disease. *Front. Microbiol.* 4:94. doi: 10.3389/fmicb.2013.00094

Bell, V. A., Hedderley, D. I., Pietersen, G., and Lester, P. J. (2018). Vineyard-wide control of grapevine leafroll-associated virus 3 requires an integrated response. *J. Plant Pathology* 100, 399–408. doi: 10.1007/s42161-018-0085-z

Benjamini, Y., and Hochberg, Y. (1995). Controlling the false discovery rate: a practical and powerful approach to multiple testing. *J. R. Stat. Soc.* 1, 289–300. doi: 10.1111/j.2517-6161.1995.tb02031.x

Blaisdell, G., Zhang, S., Bratburd, J., Daane, K., Cooper, M., and Almeida, R. (2015). Interactions within susceptible hosts drive establishment of genetically distinct variants of an insect-borne pathogen. *J. Econo. Entomol.* 108, 1531–1539. doi: 10.1093/jee/tov153

Blouin, A., Chooi, K., Cohen, D., and Macdiarmid, R. (2017). "Serological methods for the detection of major grapevine viruses," in *Grapevine Viruses: Molecular Biology, Diagnostics and Management*, eds B. Meng, G. P. Martelli, D. A. Golino, and M. Fuchs, (Cham: Springer), 409–429. doi: 10.1007/978-3-319-57706-7_21

Cabaleiro, C., and Segura, A. (1997). Field transmission of grapevine leafroll associated virus 3 (GLRaV-3) by the mealybug *Planococcus* citri. *Plant Disease* 81, 283–287. doi: 10.1094/pdis.1997.81.3.283

Cabaleiro, C., Segura, A., and Garcia-Berrios, J. J. (1999). Effects of Grapevine Leafroll-Associated Virus 3 on the Physiology and Must of Vitis vinifera L. cv. Albarifio following contamination in the field. *Am. J. Enol. Viticult.* 50, 40–44.

Cassone, B. J., Wijeratne, S., Michel, A. P., Stewart, L. R., Chen, Y., Yan, P., et al. (2014). Virus-independent and common transcriptome responses of leafhopper vectors feeding on maize infected with semi-persistently and persistent propagatively transmitted viruses. *BMC Genomics* 15:133. doi: 10.1186/1471-2164-15-133

Charles, J. G. (1993). A survey of mealybugs and their natural enemies in horticultural crops in North Island, New Zealand, with implications for biological control. *Biocontrol Sci. Technol.* 3, 405–418. doi: 10.1080/09583159309355295

Charles, J. G., Bell, V. A., Lo, P. L., Cole, L. M., and Chhagan, A. (2010). Mealybugs (*Hemiptera: Pseudococcidae*) and their natural enemies in New Zealand vineyards from 1993-2009. *New Zealand Entomol.* 33, 84–91. doi: 10.1080/00779962.2010.9722195

Charles, J. G., Cohen, D., Walker, J. T. S., Forgie, S. A., Bell, V. A., and Breen, K. C. (2006). A review of Grapevine Leafroll associated Virus type 3 (GLRaV-3) for the New Zealand wine industry. *HortRes. Client Rep.* 59, 330–337. doi: 10.30843/nzpp.2006.59.4590

Charles, J. G., Froud, K. J., Van Den Brink, R., and Allan, D. J. (2009). Mealybugs and the spread of grapevine leafroll-associated virus 3 (GLRaV-3) in a New Zealand vineyard. *Aust. Plant Pathol.* 38, 576–583. doi: 10.1071/ap09042

Chen, A. Y., Walker, G. P., Carter, D., and Ng, J. C. (2011). A virus capsid component mediates virion retention and transmission by its insect vector. *Proc. Natl. Acad. Sci.* 108, 16777–16782. doi: 10.1073/pnas.1109384108

Chooi, K. M., Cohen, D., and Pearson, M. N. (2013). Molecular characterisation of two divergent variants of Grapevine leafroll-associated virus 3 in New Zealand. *Arch. Virol.* 158, 1597–1602. doi: 10.1007/s00705-013-1631-9

Cid, M., Pereira, S., Cabaleiro, C., Faoro, F., and Segura, A. (2007). Presence of Grapevine leafroll-associated virus 3 in primary salivary glands of the mealybug vector Planococcus citri suggests a circulative transmission mechanism. *Eur. J. Plant Pathol.* 118, 23–30. doi: 10.1007/s10658-006-9090-8

Cohen, D., Van Den Brink, R., and Habill, N. (2004). *Detection of Leafroll Virus in Newly-Infected Grapevines*. The Australian & New Zealand Grapegrower & Winemaker, 56–59.

Daane, K. M., Almeida, R. P. P., Bell, V. A., Walker, J. T. S., Botton, M., Fallahzadeh, M., et al. (2012). "Biology and management of mealybugs in vineyards," in *Arthropod Management in Vineyards*, eds N. J. Bostanian, C. Vincent, and R. Isaacs, (Netherlands: Springer).

Diaz-Lara, A., Klaassen, V., Stevens, K., Sudarshana, M. R., Rowhani, A., Maree, H. J., et al. (2018). Characterization of grapevine leafroll-associated virus 3 genetic variants and application towards RT-qPCR assay design. *PLoS One* 13:e0208862. doi: 10.1371/journal.pone.0208862

Douglas, N., and Krüger, K. (2008). Transmission efficiency of Grapevine leafroll-associated virus 3 (GLRaV-3) by the mealybugs Planococcus ficus and Pseudococcus longispinus (*Hemiptera: Pseudococcidae*). *Eur. J. Plant Pathol.* 122, 207–212. doi: 10.1007/s10658-008-9269-2

Franco, J. C., Zada, A., and Mendel, Z. (2009). "Novel approaches for the management of mealybug pests," in *Biorational Control of Arthropod Pests*, eds I. Ishaaya, and A. Horowitz, (Dordrecht: Springer), 233–278. doi: 10.1007/978-90-481-2316-2_10

Herrbach, E., Alliaume, A., Prator, C. A., Daane, K., Cooper, M., and Almeida, R. P. (2017). "Vector transmission of grapevine leafroll-associated viruses," in *Grapevine viruses: Molecular Biology, Diagnostics and Management*, eds B. Meng, G. P. Martelli, D. A. Golino, and M. Fuchs, (Cham: Springer), 483–503. doi: 10.1007/978-3-319-57706-7_24

Jooste, A. E., Pietersen, G., and Burger, J. T. (2011). Distribution of grapevine leafroll associated virus-3 variants in South African vineyards. *Eur. J. Plant Pathol.* 122131, 371–381. doi: 10.1007/s10658-011-9814-2

Krüger, K., Saccaggi, D., and Douglas, N. (2006). "Grapevine leafroll associated virus 3–vector interactions: Transmission by the mealybugs Planococcus ficus and Pseudococcus longispinus (*Hemiptera: Pseudococcidae*)," in *15th Meeting of the International Council for the Study of Virus and Virus-like Diseases of the Grapevine (ICVG)*, Stellenbosch, 3–7.

Krüger, K., Saccaggi, D. L., Van Der Merwe, M., and Kasdorf, G. G. F. (2015). Transmission of grapevine leafroll-associated virus 3 (GLRaV-3): Acquisition, inoculation and retention by the mealybugs Planococcus ficus and Pseudococcus longispinus (*Hemiptera: Pseudococcidae*). *South African J. Enol. Viticult.* 36, 223–230.

Lee, J., Keller, K. E., Rennaker, C., and Martin, R. R. (2009). Influence of grapevine leafroll associated viruses (GLRaV-2 and-3) on the fruit composition of Oregon Vitis vinifera L. cv. *Pinot Free Amino Acids, Sugars Organic Acids. Food Chem.* 117, 99–105. doi: 10.1016/j.foodchem.2009.03.082

Lee, J., and Martin, R. R. (2009). Influence of grapevine leafroll associated viruses (GLRaV-2 and-3) on the fruit composition of Oregon Vitis vinifera L. cv. *Pinot noir: Phenolics. Food Chemistry* 112, 889–896. doi: 10.1016/j.foodchem.2008.06.065

Mahfoudhi, N., Digiaro, M., and Dhouibi, M. H. (2009). Transmission of Grapevine Leafroll Viruses by Planococcus ficus (*Hemiptera: Pseudococcidae*) and Ceroplastes rusci (Hemiptera: Coccidae). *Plant Disease* 93, 999–1002. doi: 10.1094/pdis-93-10-0999

Maree, H. J., Almeida, R. P. P., Bester, R., Chooi, K. M., Cohen, D., Dolja, V. V., et al. (2013). Grapevine leafroll-associated virus 3. *Front. Microbiol.* 4:82. doi: 10.3389/fmicb.2013.00082

Martelli, G. P. (2014). Directory of virus and virus-like diseases of the grapevine and their agents. *J. Plant Pathol.* 96, S1–S136.

McGreal, B., Sandanayaka, M., Chooi, K. M., and MacDiarmid, R. (2019). Development of sensitive molecular assays for the detection of grapevine leafroll-associated virus 3 in an insect vector. *Arch. Virol.* doi: 10.1007/s00705-019-04310-0

Montero, R., Mundy, D., Albright, A., Grose, C., Trought, M., Cohen, D., et al. (2016). Effects of Grapevine Leafroll associated Virus 3 (GLRaV-3) and duration of infection on fruit composition and wine chemical profile of Vitis vinifera L. cv. *Sauvignon Blanc. Food Chem.* 197, 1177–1183. doi: 10.1016/j.foodchem.2015.11.086

Over de Linden, A. J., and Chamberlain, E. E. (1970). Effect of grapevine leafroll virus on vine growth and fruit yield and quality. *New Zealand J. Agric. Res.* 13, 689–698. doi: 10.1080/00288233.1970.10421616

Petersen, C. L., and Charles, J. G. (1997). Transmission of grapevine leafroll-associated closteroviruses by Pseudococcus longispinus and P. calceolariae. *Plant Pathol.* 46, 509–515. doi: 10.1046/j.1365-3059.1997.d01-44.x

Prator, C. A., and Almeida, R. P. (2020). A Lectin Disrupts Vector Transmission of a Grapevine Ampelovirus. *Viruses* 12, 843. doi: 10.3390/v12080843

Prator, C. A., Kashiwagi, C. M., Vončina, D., and Almeida, R. P. (2017). Infection and Colonization of Nicotiana benthamiana by Grapevine leafroll-associated virus 3. *Virology* 510, 60–66. doi: 10.1016/j.virol.2017.07.003

Sandanayaka, W. M., Davis, V. A., and Jesson, L. K. (2018). Mealybug preference among clover cultivars: testing potential groundcover plants to dissociate mealybugs from grapevines. *New Zealand Plant Protection* 71, 248–254. doi: 10.30843/nzpp.2018.71.138

Sandanayaka, W. R. M., Blouin, A. G., Prado, E., and Cohen, D. (2013). Stylet penetration behaviour of Pseudococcus longispinus in relation to acquisition of grapevine leafroll virus 3. *Arthropod-Plant Interactions* 7, 137–146. doi: 10.1007/s11829-012-9238-8

Team, R. C. (2015). *R: A Language and Environment for Statistical Computing*. Vienna: Foundation for Statistical Computing.

Vega, A., Gutierrez, R. A., Pena-Neira, A., Cramer, G. R., and Arce-Johnson, P. (2011). Compatible GLRaV-3 viral infections affect berry ripening decreasing sugar accumulation and anthocyanin biosynthesis in Vitis vinifera. *Plant Mol. Biol.* 77, 261–274. doi: 10.1007/s11103-011-9807-8

Conflict of Interest: The authors declare that the research was conducted in the absence of any commercial or financial relationships that could be construed as a potential conflict of interest.

frontiers in Plant Science

ORIGINAL RESEARCH
published: 21 July 2021
doi: 10.3389/fpls.2021.682879

High-Throughput Sequencing of Small RNAs for the Sanitary Certification of Viruses in Grapevine

Leonardo Velasco[1] and Carlos V. Padilla[2]*

[1] *Instituto Andaluz de Investigación y Formación Agraria, Málaga, Spain,* [2] *Instituto Murciano de Investigación y Desarrollo Agrario y Alimentario, Murcia, Spain*

Biological indexing is the method generally recognized for the certification of propagative grapevines in many countries, and it is mandatory in the European Union. It consists of the evaluation of the plant material after grafting on indicators that are inspected for symptom development. This is a lengthy process that requires well-trained workers, testing field, etc. Alternative diagnostic methods such as serology and RT-qPCR have been discarded for certification because of their intrinsic drawbacks. In turn, high-throughput sequencing (HTS) of plant RNA has been proposed as a plausible alternative to bioassay, but before it is accepted, different aspects of this process must be evaluated. We have compared the HTS of small RNAs with bioassays and other diagnostic methods from a set of 40 grapevine plants submitted for certification. The results allowed the authors the identification of numerous grapevine viruses in the samples, as well as different variants. Besides, relationships between symptom expression and viromes were investigated, in particular leafroll-associated viruses. We compared HTS results using analytical and bioinformatics approaches in order to define minimum acceptable quality standards for certification schemes, resulting in a pipeline proposal. Finally, the comparison between HTS and bioassay resulted favorable for the former in terms of reliability, cost, and timing.

Keywords: grapevine, high-throughput sequencing, bioassay, diagnostics, virus, viroid, certification, cost analysis

OPEN ACCESS

Edited by:
Kristiina Mäkinen,
University of Helsinki, Finland

Reviewed by:
Victor Golyaev,
Centre de Coopération Internationale en Recherche Agronomique pour le Développement (CIRAD), France
Rajarshi Kumar Gaur,
Deen Dayal Upadhyaya Gorakhpur University, India

****Correspondence:***
Leonardo Velasco
leonardo.velasco@juntadeandalucia.es

Specialty section:
This article was submitted to Plant Pathogen Interactions, a section of the journal Frontiers in Plant Science

Received: *19 March 2021*
Accepted: *24 June 2021*
Published: *21 July 2021*

Citation:
Velasco L and Padilla CV (2021) High-Throughput Sequencing of Small RNAs for the Sanitary Certification of Viruses in Grapevine. Front. Plant Sci. 12:682879. doi: 10.3389/fpls.2021.682879

INTRODUCTION

Plant viruses are responsible for billions of losses in the economies of many countries, damages that are increased by unrestricted movements of infected plant materials, particularly in vegetatively propagated crops (Mumford et al., 2016). In the case of grapevine, two main groups of viruses are responsible for most of the losses, either in yield or quality of berries for wine-making. One is the nepoviruses, such as grapevine fanleaf virus (GFLV) and Arabis mosaic virus (ArMV), responsible for the so-called infectious degeneration that eventually can cause death of a plant. Others are those responsible for grapevine leafroll disease (GLRD), caused by members of the family *Closteroviridae* such as the closterovirus grapevine leafroll-associated virus 2 (GLRaV-2) and by a complex of different species of the genus *Ampelovirus* (Almeida et al., 2013). Other diseases of viral origin in vines, such as the rugose wood, are considered to be minority diseases, and their etiology is not always well defined but sometimes, especially if there are multiple infections -which is very frequent

in vines-, they can be harmful for a crop, e.g., in grafting incompatibility (reviewed in Martelli, 2017). The economic losses caused by all the grapevine viruses have not been established, although for certain viruses and growing areas some estimates have been made. For the most widespread GLRD causal agent, grapevine leafroll-associated virus 3 (GLRaV-3), losses of around 20–40% of crop yield have been reported, representing over €1,000 Ha/year (Maree et al., 2013). In the region of Galicia in northern Spain, the accumulated losses from a 100% GLRaV-3-infected vineyard over 30 years have been estimated at more than €74,000 Ha (Cabaleiro et al., 2013).

Control of plant virus-borne diseases is mainly based on two strategies: immunization and prophylaxis to limit virus dispersion (Rubio et al., 2020). Immunization approaches, which include introgression of genetic resistance by classical breeding and genetic transformation, are not suitable for the control of grapevine viruses. Natural sources of resistance to GLRD viruses have not been found so far, although in some cases lack of symptoms, in some infected varieties, has been reported (Oliver and Fuchs, 2011), but in the case that it is, genetic breeding is very difficult to carry out in this crop, given the varietal identity requirements that are mandatory for grapevine cultivation, especially for wine grapes, as well as the lengthy processes of breeding in woody species. Therefore, all the control measures for this crop must rely on preventive strategies such as quarantine measures, certification, roguing of infected plants, control of natural vectors, limiting the propagation of infected material, cleaning of stocks by virus elimination by heat therapy, and meristem tip culture, and importantly, the training of staff at nurseries, agronomists, growers, etc. Many, if not all, of the measures described for the control of grapevine viruses rely on their effective identification and diagnostics. Given the clonal multiplication of grapevine, the presence of viruses in a propagation material is subjected to strict regulations in many countries aiming at minimizing the impact of the diseases produced by these viruses (Golino et al., 2017). Currently, certification schemes for grapevine in the EU and specifically in Spain rely on biological indexing (bioassay) assisted by other diagnostic tools such as serology and RT-qPCR. This practice is generally effective and provides reliable diagnostics for the five viruses required in Spanish official certification scheme: GLRaV-1, GLRaV-3, ArMV, GFLV, and grapevine fleck virus (GFkV) (this lasts only in rootstocks). Serological analysis and RT-qPCR for detection of grapevine viruses are limited by several factors. In the case of serology, it depends on the availability of specific antisera that are commercially purchased to providers that use their own virus isolates for their obtention. Given the intrinsic variability of grapevine viruses, specific detection is not always produced. Another inconvenience of serology-based methods is the lower sensitivity compared with other diagnostic tools and that sometimes is limited by virus concentration in plant tissues. This low sensitivity is overcome by molecular diagnostics based on PCR, but in turn, it presents the inconvenience of reliability, given that viruses, and, in particular, grapevine viruses, present sequence variability that restricts the universality of designed primers for effective amplification. Moreover, even if general degenerate primers are designed that can detect all known isolates of a given virus species, this does not ensure that they will be able to detect new variants that may eventually appear. Degenerate primers also increase the chance of false positive results. In the experience of the authors and others, diagnosis of grapevine viruses by serology or RT-qPCR sometimes offers dubious results that require double-checking, increasing the cost and difficulty of the analysis, even for experienced staff. In other examples, some plants show virus symptoms, but there is no virus detection. This is the case of GLRD that can be produced by different virus species that, in addition, have intrinsically high genetic variability.

Since the availability of high-throughput sequencing (HTS) for plant transcriptomics, the detection and identification of plant viruses by this technology has become widely used (reviewed in Maliogka et al., 2018; Maree et al., 2018). Among the sources of nucleic acids for determination of plant virus and viroids, small RNA (sRNA) fraction has been revealed as a valuable tool compared with total RNA (Pecman et al., 2017). Among the sRNAs, and as product of the plant RNA silencing mechanism appear the small interfering RNAs (siRNAs). They are produced through the Dicer/RISC complex that targets viral dsRNAs, product of virus replication, that results cleaved into the siRNAs, that are more specifically called virus small interfering RNAs (vsiRNAs). vsiRNAs are then used for HTS and subsequent virus identification with bioinformatics pipelines. HTS raw sequences that are usually massive.fastq files need to be processed in order to extract the information required, which is the identification of the viruses present in the samples. This involves trimming the adapters and discarding the low-quality sequences. Given that these sequences that are in the order of million reads and of short length cannot be generally used directly for virus detection in databases, thus *de novo* assembly of contigs must be obtained prior to analysis (Seguin et al., 2014). This is performed with different algorithms such as BinPacker, SPAdes, Oases, Trinity, or Velvet (Geniza and Jaiswal, 2017). Unlike Oases, SPAdes, Trinity and Velvet, which use de Bruijn graphs to construct transcripts, BinPacker is based on a splicing graph construction. Once the *de novo* contigs are obtained, then they are submitted to BLASTN and BLASTX analysis of NCBI for virus identification based on similarity to viruses present in the databases. Several platforms have been offered to the community for virus detection using HTS reads or contigs. ViroBLAST is an online server that accepts .fasta files of up to 5M, and it allows adjustment of several parameters and comparison with several viral databases (Deng et al., 2007). Another pipeline is VirFind, which performs *de novo* assembly from HTS reads and compares with NCBI virus databases (Ho and Tzanetakis, 2014). More recently, a Yabi web-based analytical environment has been developed for virus identification from sRNA sequences (Barrero et al., 2017). A different approach was used through a Galaxyweb-based platform that uses reference viral genomes for mapping HTS reads (Miozzi and Pantaleo, 2015), producing SAM files of alignments that can be visualized with, e.g., the MISIS program (Seguin et al., 2016). Finally, VirusDetect is a powerful tool specifically designed for the detection of viruses from small RNA sequences (Zheng et al., 2017). The development of such platforms and pipelines must offer not only reliability,

specificity, and efficiency but also ease of use and traceability. In addition, in order to include HTS in certification schemes, there are some control points that must be addressed in order to reach proficiency and reproducibility (Massart et al., 2019; Maree et al., 2018).

High-throughput sequencing has been valuable in the detection and characterization of grapevine viruses and viroids in Spain (Velasco et al., 2014, 2015; Cretazzo and Velasco, 2017). In the country, only Instituto Murciano de Investigación y Desarrollo Agrario (IMIDA) is qualified to perform sanitary certification of grapevine, and it follows the methodology described in the Spanish regulations, i.e., bioassay accompanied by serological tests. Thus, we aimed to evaluate HTS as a plausible approach for sanitary certification in comparison with the bioassays. For this purpose, we selected a set of samples among the candidate clones sent for certification to IMIDA. In addition to investigating the feasibility of HTS derived from grapevine sRNA in diagnostics, plants were specifically selected to further research the etiology of GLRD. These samples were processed for HTS in three batches, consisting of 6, 10, and 24 plants each, and for which different Illumina sequencing depths were requested. HTS through a bioinformatics pipeline allowed the determination of a number of grapevine viruses in the plants. This process allowed the identification of key internal control points to assess the quality of the diagnostics. The plants were also evaluated in addition to the bioassays by DAS-ELISA and RT-qPCR, and the results compared with HTS.Viruseq, a platform for BLASTN and BLASTX analysis from *de novo* contigs for virus determination was specifically developed (Velasco et al., 2016). Finally, a pipeline for HTS certification of grapevine candidate clones is proposed based on these results.

MATERIALS AND METHODS

Plant Material and Bioassays on Indicators

A set of 40 samples received at IMIDA for sanitary certification from 2015 to 2017 was analyzed for virus presence by four methodologies: serology, RT-qPCR, bioassay, and HTS. The samples consisted of dormant canes that are received annually as submitted by nurseries and research institutions from all over Spain. Bioassays consisted of bud grafting of the testing scions on five plants each of *Vitis vinifera* Cabernet Sauvignon and *V. rupestris* du Lot as indicators. Indexing was performed from March to April, and plants were evaluated by visual inspection of the symptoms using a 0–5 rating scale during a 3-year period. Cuttings from the canes were rooted and kept in pots for RNA extractions and DAS-ELISA diagnostics.

Serological Diagnostics

DAS-ELISA was performed using the following antisera from Bioreba (Berna, Spain): ArMV, GFLV, GFkV, GLRaV-1, GLRaV-2, GLRaV-3, GLRAV-4 strains 4–9, and GLRaV-4 strain 6, following the indications of the manufacturer.

RNA Extractions for RT-qPCR Detection

RNAs were extracted from approximately 100 mg of phloem scrapings of the canes at the stage of vine ripening with the Spectrum Plant RNA kit (Sigma-Aldrich, St. Louis, MO, United States). The RNAs were quantified using NanoDrop ND-1000 (Thermo Fisher Scientific, Waltham, MA, United States). For the RT-qPCR, we used 10 ng of total RNA extract from each plant that was added to the AgPath-ID One-step RT-PCR master mix (Applied Biosystems, Waltham, MA, United States) supplemented with 200 nM of the forward and reverse primers and 200 nM of the TaqMan probe to a final volume of 25 ml. For the qPCR, we used specific primers for GFLV, GFkV, GLRaV-1, GLRaV-2, GLRaV-3, GLRaV-3, GLRaV-4, GLRaV-4 strains 5, and GLRaV-4 strain 9 (Osman et al., 2008). Reverse transcription and qPCR cycling amplification conditions were as follows: 45°C for 35 min, 95°C for 10 min, followed by 45 cycles of 95°C for 15 s and 60°C for 1 min. The RT-qPCR was run in the StepOne Plus thermocycler (Applied Biosystems, Waltham, MA, United States). In each run, the StepOne Plus 2.0 software (Ambion) plotted the fluorescence intensity against the number of cycles and provided the quantification cycle (Cq) value.

RNA Extractions for HTS

sRNA-enriched samples were also obtained from 100 mg of phloem tissue using the miRCURY RNA isolation kit (Exiqon, Vedbaek, Denmark) following the recommendations of the manufacturer. The samples were quantified using NanoDrop, and the quality was assessed with Bioanalyzer 2100 using RNA 6000 Nano Kit (Agilent Technologies, Santa Clara, CA, United States). The sRNA fraction (1 ng, ∼21 nt length) from the RNA extractions was eluted from polyacrylamide gels, and the corresponding cDNA libraries were prepared. The libraries were constructed for each extract using the TruSeq Small RNA kit (Illumina, San Diego, CA, United States), and paired-end 2 × 50 pb RNAseq was performed on the Hiseq 2500 Illumina deep sequencing platform of CRG (Barcelona, Spain). The 40 samples were processed in three batches, one consisting of six samples separating them using sequence barcodes (Batch #1: 29085-30123), for which the sequencing depth in a single run was >200 M reads, another consisting of 10 samples (Batch #2: 31004-31099) for which a sequence depth in a run was >250 M reads, and a third batch of 24 samples (Batch #3: 3200-33121) that were processed in a run of >450 M reads.

Bioinformatics Analysis

The sequencing Illumina RNA adapter was removed from the HTS raw sequences, and the low-quality reads were discarded using Geneious prime v. 2019.2.3 (Biomatters, Auckland, New Zealand). For the subsequent analysis, reads ranging from 18 to 24 nt were selected. These reads were assembled into contigs by the *de novo* assembly function of Velvet v. 1.2.08 (Zerbino and Birney, 2008) implemented in the SCBI Picasso server. For that, we used the k-mer values 13, 14, 15, 16, and 17. Contigs obtained from each accession were subjected to BLASTX and BLASTN analysis against the non-redundant database of NCBI as available in the ViruSeq v0.1a1 platform from the Picasso supercomputing

SCBI server that can be freely accessed at: http://www.scbi.uma.es/ingebiol/session/new/viruseq. BLASTN *E*-value was set as default (1e-5); and for BLASTX, the parameter was adjusted for optimization. In addition to the BLASTX and BLASTN analysis, both the set of contigs and the 18–24 nt reads from each sample were aligned to sequences of reference virus genomes using the Map to Reference tool with default parameters as available in Geneious to search for matches indicative of specific virus sequences.

RESULTS

HTS Reads and Contigs Obtained From the sRNAs

RNA extractions performed with the Exiqon kit from grapevine phloem scrapings rendered specifically low-weight RNAs and sRNAs (**Supplementary Figure 1**). Most of the samples produced a high yield in the range of 18–24 nt length sRNAs (that include the vsiRNAs), but in some cases, RNAs of higher weight (50–150 nt) were majoritarian (e.g., samples 32000, 32014, and 32019). Gel-purified sRNAs were used for cDNA library preparation and sequencing. Illumina sequencing produced 4.95–29.15 M reads after discarding the low-quality reads and adapter trimming. From this, after selecting the sequencing reads ranging 18–24 nt, we obtained 2.7–19.4 M reads. This makes a ratio between the total sRNA reads and the 18–21 ntsRNA reads of 32–81% (**Supplementary Table 1**). Within the 18–24 ntsRNAs those of 21 nt were predominant, averaging 44.6% (**Supplementary Figure 2** and **Supplementary Table 1**). Using different k-mer values, Velvet assembled the 18–24 nt reads and produced contigs of different range of sizes and number (**Supplementary Table 2**). For the first batch of samples, we obtained 6331–8277, 2006–2936, and 815–1232 contigs for k-mers 13, 15, and 17, respectively. In the second batch, the k-mer values allowed the obtention of 4071–8500, 1446–3708, and 534–1490 contigs for k-mers 13, 15, and 17, respectively. In the third batch, we obtained contigs of 431-6550, 164-1787, and 75-789 for k-mer 13, 15, and 17 (**Supplementary Table 2**). Thus, contigs generated with k-mer 13 produced more contigs than when using k-mer 15 followed by k-mer 17 (**Figure 1**). However, as can be seen in **Supplementary Figure 3**, the profiles generated of contig sizes using k-mer 13 differed from those obtained with k-mer 15 or k-mer 17. For k-mer 17, it produced contigs with a minimal length of 33 nt, which reduced to 29 for k-mer 15 and to 25 when using k-mer 13 (**Supplementary Table 2**). The length of the contigs generated with k-mer 13 is size-limited (average 130 nt) while longer contigs were obtained with k-mer 15 (average 500 nt) or k-mer 17 (average 660 nt) (**Figure 1**).

For the taxonomic identification of viruses in the samples, the contigs were submitted to BLASTX and BLASTN analysis against the NCBI viral databases as implemented in the platform Viruseq. For that, we used the contigs generated by Velvet for k-mers 13, 15, and 17. Next, we adjusted the BLASTX E-value for maximum reliability and tested the contigs generated with the different k-mer values. Results showed that the highest number of matches to grapevine viruses was obtained when k-mer was 15 and the *E*-value of BLASTX was 1e-3 (**Supplementary File 1**). Although k-mer13 produced a higher number of contigs than k-mer 15, BLASTX produced the highest number of matches to grapevine viruses when k-mer was 15, pointing many contigs as artifacts (chimeras) when k-mer 13 was set in Velvet. The results of virus identification using Viruseq that we describe hereafter refer to the contigs generated for Velvet (k-mer = 15) and BLASTX *E*-value = 1e-3. Ontology analysis of the contigs allowed the determination of the cellular origin of the sRNAs by BLASTX at the NCBI GenBank. Among the pool of contigs from batch#1 of the set of samples used as representative of all the samples, virus-derived contigs were in a high percentage, being 1–12% of the total (**Figure 2**). Viroid contigs were also well represented, although in a lower ratio (0.21–4.6%).

Identification of Grapevine Viruses From the Contigs and HTS Reads

Among the virus species identified in the pool of samples according to Viruseq BLAST analysis of each set of contigs in addition to genetic analysis of the individual contigs, results showed GLRaV-1, GLRaV-2, GLRaV-3, grapevine leafroll-associated virus 4-like viruses (GLRaV-4LVs), GFLV, GFkV, grapevine rupestris stem pitting-associated virus (GRSPaV), grapevine rupestris vein feathering virus (GRVFV), grapevine Red Globe virus (GRGV), grapevine Pinot Gris virus (GPGV), grapevine virus A (GVA), grapevine virus B (GVB), and grapevine virus L (GVL) (**Tables 1**, **2** and **Supplementary File 1**). Among the viroids, grapevine yellow speckle viroid 1 (GYSVd-1) and hop stunt viroid (HSVd) were present in all the samples. In addition to Viruseq, we performed alignments of the sRNA reads to the reference genomes (**Supplementary Table 3**) to seek for virus sequences in the samples for which contigs were not obtained. After examination of the reads matching with the reference sequences, we set up a lower limit of less than 2% of genome coverage for discarding a given virus in the sample, considering those reads as not specific. According to this guideline, the result showed that the most frequent virus found was GRSPaV, found in all the samples. Two different variants of this virus seem to be present. The most frequent variants were similar to isolate SK704-A (KX274274) found in all but one sample (31099) where the variant present was similar to GRSPaV isolate GG (JQ922417). The closterovirus GLRaV-2 was present in 26 samples (**Table 1**). Among the ampeloviruses, GLRaV-1 was present only in samples 29170 and 31099. GLRaV-4LVs were frequent, present in nine samples, while GLRaV-3 was present in four samples. GFkV was found in 14 samples (**Table 2**). GRVFV (12 samples) is another virus frequently found in the pool of samples (**Table 3**). The vitivirus GVA was present in five samples, whereas GVB was found in another seven. Other viruses present were GPGV (32097) and GRGV (30039, 30123, 31004, and 32097). GFLV was identified by HTS in one sample (33111) but only from a few reads aligning to the reference genome. All samples but one (32023) showed multiple virus infection, harboring at least two different viruses.

Six groups of GLRaV-2 variants have been identified by the workers so far, arranged in six distinct lineages represented by

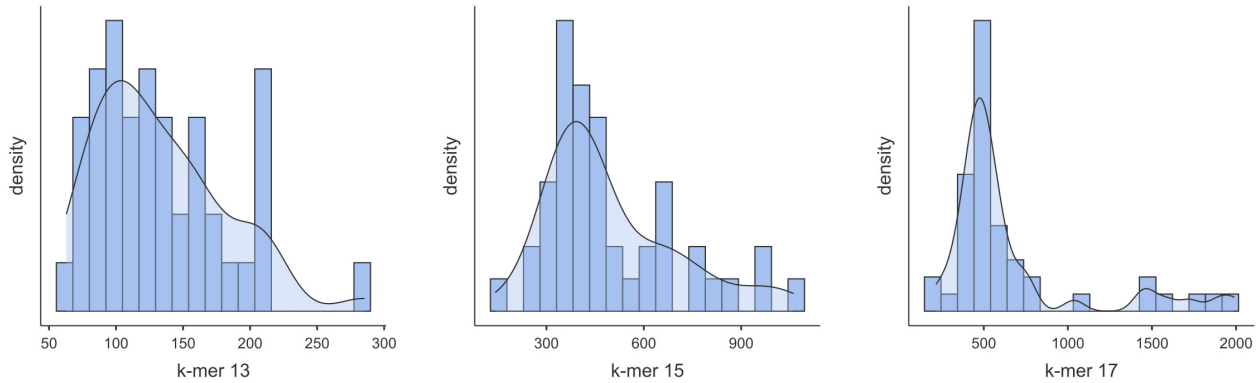

FIGURE 1 | Distribution of the contigs according to sizes as obtained from the 18–24 nt reads using Velvet (k-mer = 13, 15 or 17).

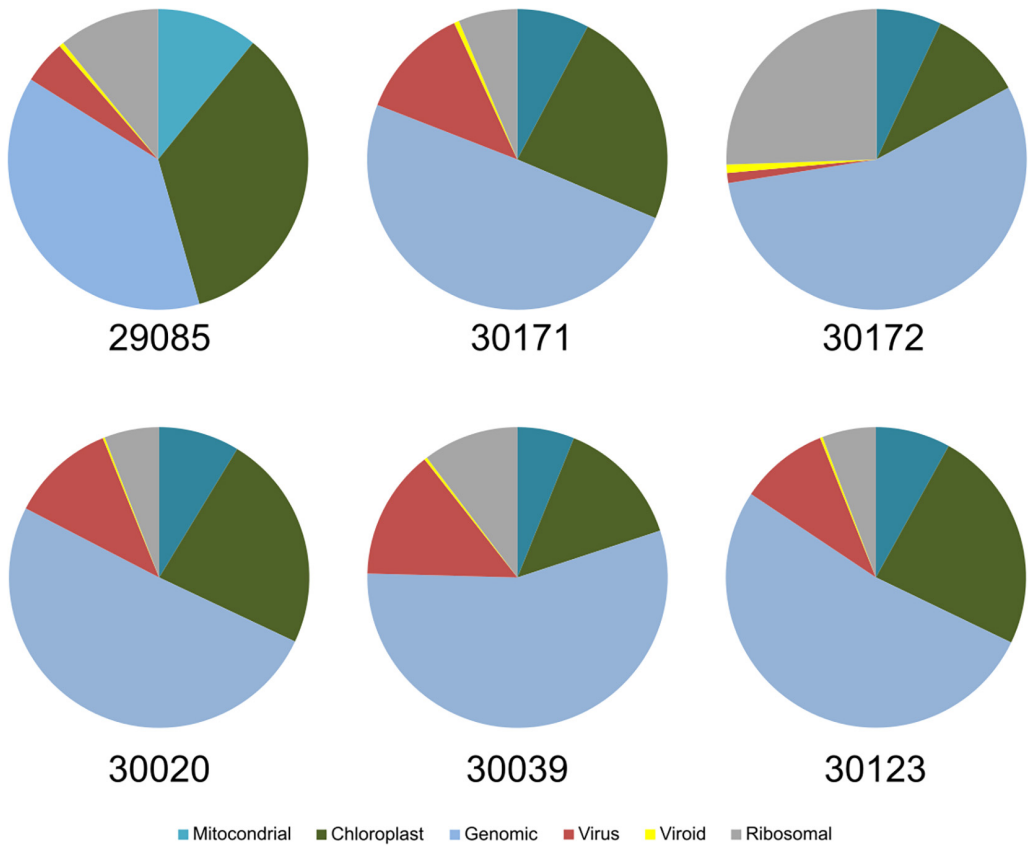

FIGURE 2 | Ontology of the contigs obtained from the samples of batch #1 after BLAST analysis. Virus and viroid contigs represent between 2 and 15% of the total contigs derived from the HTS of sRNAs.

the type isolates 93/955, PN, PV20, RG, H4, and BD (Angelini et al., 2017). These variants show a high degree of variations in their genomic sequences and have been related to differences in symptoms induced on their host or graft incompatibility. We constructed the GLRaV-2 genomes from the scaffolds of contigs and reads aligning to the reference genomic sequences. As a result, 10 of the GLRaV-2 isolates present in the plants investigated in this study were found phylogenetically clustered with variant 93/955 (AY881628; Meng et al., 2005; **Table 2** and **Figure 3**). These isolates were present in plants inducing generally strong to very strong symptoms (rating 4–5) in the bioassays, although in other three cases the symptoms were mild to moderate (rating 2–3), whereas in one case there was no symptom exhibition (29172) (**Table 3**). In other plants, genetic and phylogenetic analysis clustered GLRaV-2 isolates with the type variant PV20 (Acc. No. EF012721; Beuve et al., 2007) and

TABLE 1 | Quantitation of contigs, and reads and percentage of genome coverage aligning to GLRD viruses.

Sample	Virus	Contigs (k-mer = 15)	Reads (18-24 nt)	Coverage	Total reads 18-24 nt	% Total reads
29085	GLRaV-2 93/955	282	2,510,386	99.7	12673748	19.81
29170	GLRaV-1	111	4,574	36.0	13134664	0.03
	GLRaV-2 93/955	83	219,860	35.2	13134664	1.67
	GLRaV-4 str. 6	82	5,960	19.3	13134664	0.05
29172	GLRaV-2 93/955	93	4,313	51.8	9026152	0.05
32000	GLRaV-2 93/955	1	254	17.7		0.00
30020	GLRaV-2 93/955	122	37,835	56.5	10,599,368	0.36
30039	GLRaV-2 93/955	351	2,328,022	75.5	18369925	12.67
30123	GLRaV-2 PN	1	1,043	53.0	9,583,027	0.01
31004	GLRaV-2 PN	154	1,702,792	96.9	11513269	14.79
31006	GLRaV-2 PN	163	34,550	93.4	9726535	0.36
31008	GLRaV-2 PV20	2	1,520	56.5	9344564	0.02
31032	GLRaV-2 93/955	40	176,963	17.0	10875760	1.63
31035	GLRaV-2 PV20	14	3,377	71.3	8023183	0.04
31036	GLRaV-2 PV20	5	2,325	66.1	8141625	0.03
31044	GLRaV-2 PV20	1	1,175	51.7	6121372	0.02
31052	GLRaV-2 PV20	232	13,504,528	99.8	19393837	69.63
31065	GLRaV-2 PV20	270	9,279,850	99.9	12550158	73.94
	GLRaV-4 strn. 6	59	7,549	21.1	12550158	0.06
31099	GLRaV-2 PN	38	748,497	99.4	7313344	10.23
	GLRaV-4 strn. 6	65	2,183	15.5	7313344	0.03
	GLRaV-1	157	167,862	60.0	7313344	2.30
32000	GLRaV-2 PN	0	316	22.8	19393837	0.00
32001	GLRaV-2 PV20	16	8,920	80.0	5,328,968	0.17
32002	GLRaV-4 strn. 6	34	3,083	33.9	6,067,849	0.05
32007	GLRaV-2 93/955	530	1,037,609	99.6	6,828,892	15.19
32010	GLRaV-2 93/955	490	487,844	99.3	3,078,924	15.84
32014	GLRaV-2 93/955	307	920,915	98.9	4,230,205	21.77
	GLRaV-4 strn. 5	11	3,083	35.1	4,230,205	0.07
32017	GLRaV-4 strn. 5	117	23,812	63.2	5,152,525	0.46
32019	GLRaV-2 93/955	696	7,219,608	100.0	16,936,974	42.63
32022	GLRaV-4 strn. 5	86	14,828	85.4	7,043,346	0.21
32075	GLRaV-2 PN	130	2,744,265	100.0	9,135,104	30.04
32097	GLRaV-2 PN	98	991,045	100.0	6,838,454	14.49
33109	GLRaV-3 group VI	54	1,346	6.8	6,792,474	0.02
33111	GLRaV-3 group II	43	32,164	83.6	4,017,775	0.80
	GLRaV-4 strn. 5	0	2,110	25.7	4,017,775	0.05
	GLRaV-2 PN	0	272	8.5		0.00
33115	GLRaV-3 group I?	0	9	1.0	4,998,909	0.00
	GLRaV-2 PV20	0	157	10.1	4,998,909	0.00
33116	GLRaV-3 group II	136	85,633	94.8	5,692,071	1.50
	GLRaV-4 strn. 6	31	7,131	29.5	5,692,071	0.13
33121	GLRaV-3 group VI	15	394	5.7	7,113,170	0.01

with 12G402B (MH814492; Rott et al., 2017), which is genetically close to PV20. Remarkably, when isolates similar to variant PV20 were present in the samples, symptoms on the indicator plant were mild (rating 2–3) or even absent (32001). However, strong symptoms (rating 4) were induced by a plant harboring both a GLRaV-2 PV20-like isolate and GLRaV-4 (31065). The GLRaV-2 isolates present in other group of plants were phylogenetically close to GLRaV-2 variant PN (AF039204; Zhu et al., 1998; **Table 1** and **Figure 3**). Plants harboring this variant induced mild to very strong GLRD symptoms (rating 2–5) but resulted asymptomatic in the bioassay in other two cases (31006 and 32003). This is, to the knowledge of the authors, the first report distinguishing GLRaV-2 variants in Spain. With respect to GLRaV-3, the variants found in the samples belonged to group II and group VI (two samples each), and one plant possibly was host of a GLRaV-3 group I isolate, after the identification of reads aligning to this genomic sequence (**Table 1**). In all the cases when GLRaV-3 was present, symptoms in the bioassay were strong or very strong (rating 4–5) (**Table 3**). Regarding the GLRaV-4LVs, genetic analysis using reference genomes revealed that GLRaV-4

TABLE 2 | Quantitation of reads and percentage of genome coverage aligning to non-GLRD viruses identified by HTS.

	GRSPaV		GFkV		GFLV		GVA		GVB		GVL		GPGV		GRGV		GRVFV	
Sample	**Coverage**	**Reads**	**Coverage**	**Reads**	**Coverage**	**Reads**	**Coverage**	**Reads**	**Coverage**	**Reads**	**Coverage**	**Reads**	**Coverage**	**Reads**	**Coverage**	**Reads**	**Coverage**	**Reads**
29085	89.7	9,233																
29170	88.7	9,575					7.2	212							26.3	1,046		
29172	92	12,941																
30020	91	11,694																
30039	76.4	8,759							17.2	33,849					47	8,304		
30123	87.4	7,910													37.5	8,306	36	24,843
31004	93.3	15,804							17.9	3,530					20.8	265	17.8	3,530
31006	93.6	15,456							12.9	1,045							22.7	564
31008	93.7	21,990																
31032	90	9,144																
31035	93.5	27,181															11.7	142
31036	92.3	21,986															15.8	325
31044	92.4	21,432															14.6	286
31052	90.1	9,544																
31065	91.6	11,401															117	11
31099	90.1	11,725					24.6	5,659										
32000	27.1	455																
32001	72.6	3,069	34.1	898														
32002	71.5	2,620																
32003	84.4	5,749																
32004	83.6	6,024																
32007	53.7	759	60.3	5,336					14.3	5,364								
32010	61.4	1,151	32.5	883					12.7	1,849								
32013	82.1	4,772	51.9	3,583														
32014	39.3	1,066							12.3	1,453								
32017	85.9	8,841																
32019	77.1	3,344	48.9	4,226														
32022	87.5	5,580															14.3	282
32023	86.7	8,382															9.1	6,616
32024	77.8	5,050																
32042	86	7,051	35.8	1,295														
32049	85	7,200	50.6	3,177					3.2	89								
32059	82.9	5,127																
32063	85.2	8,294																
32064	87.8	10,939																
32075	86.4	6,393	11.1	362													16.2	731
32097	79	4,812	70.8	13,386									68.9	4,229	68	19,239		
32113	75.9	4,713	11.2	411														
33109	77.4	6,520					3.8	306			42	9,033						
33111	54.5	3,906			2.1	104	12.3	884										
33113	41.3	979																
33115	49.1	1,147																
33116	66.8	5,253																
33121	79.9	5,756					9.1	628										

TABLE 3 | Comparison among the four diagnostics methods used in this study for the diagnostics of viruses in the grapevine samples.

Sample	Cultivar	Origin	DAS-ELISA	RT-qPCR	RL Bioassay*	CS Bioassay*	HTS
29085	Malfar	Extremadura	Negative	GLRaV-2		5	GLRaV-2 93/955, GRSPaV
29170	Verdejo Colorado	Castilla y León	GLRaV-1	Negative		2	GLRaV-4 str. 6, GRSPaV, GLRaV-1, GLRaV-2 93/955, GVA
29172	Verdejo Serrano	Castilla y León	Negative	Negative	3		GLRaV-2 93/955, GRSPaV, GFkV
30020	Cayetana	Extremadura	Negative	GLRaV-2		2	GLRaV-2 93/955, GRSPaV
30039	Godello	Navarra	GLRaV-2	GLRaV-2		4	GRGV, GLRaV-2 93/955, GRSPaV, GVB
30123	Carrasquín	Asturias	Negative	GLRaV-2		2	GRVFV, GRGV, GRSPaV, GLRaV-2 PN
31004	Tempranillo	Navarra	Negative	n/t	2	2	GRSPaV, GLRaV-2 PN, GRVFV, GRGV, GVB
31006	Tempranillo	Navarra	Negative	n/t	2		GRSPaV, GLRaV-2 PN, GRVFV, GVB
31008	Tempranillo	Navarra	Negative	n/t		2	GRSPaV GLRaV-2 PV20
31032	Tempranillo	Madrid	Negative	n/t		4	GRSPaV, GLRaV-2 93/955
31035	Tempranillo	Madrid	Negative	n/t		2	GRSPaV, GRVFV, GLRaV-2 PV20
31036	Tempranillo	Madrid	Negative	n/t		2	GRSPaV, GRVFV, GLRaV-2 PV20
31044	Garnacha	Madrid	Negative	n/t		2	GRSPaV, GRVFV, GLRaV-2 PV20
31052	Malvar	Madrid	GLRaV-2	n/t		3	GRSPaV, GLRaV-2 PV20
31065	Mandón	Castilla y León	GLRaV-4 strns.	n/t		4	GLRaV-4 strain 6, GRSPaV, GLRaV-2 PV20, GRVFV
31099	Garnacha	Madrid	GLRaV-1, GLRaV-2, GLRaV-4 strns.	GLRaV-1, GLRaV-2, GLRaV-5		5	GLRaV-4 strain5, GLRaV-1, GRSPaV, GLRaV-2 PN, GVA
32000	Beba	Extremadura	GLRaV-1, GLRaV-4 strns., GFkV	GLRaV-1, GLRaV-9, GLRaV-5, GFkV	3	2	GFkV, GLRaV-2 PN
32001	Beba	Extremadura	GLRaV-4 strns., GLRaV-4 strn. 6, GFkV	GLRaV-5, GFLV, GFkV	3		GLRaV-2 PV20; GFkV
32002	Beba	Extremadura	GLRaV-4 strns., GFkV	GFLV, GLRaV-9, GFkV		4	GFkV, GLRaV-4 strn. 6
32003	Beba	Extremadura	Negative	GLRaV-5			GRSPaV, GLRaV-2 PN
32007	Beba	Extremadura	Negative	GLRaV-5, GLRaV-2, GFkV	2	5	GLRaV-2 93/955, GVB, GFkV
32010	Beba	Extremadura	GLRaV-2, GFkV	GLRaV-2, GFkV	2	5	GLRaV-2 93/955, GVB, GFkV
32013	Beba	Extremadura	GFkV	GLRaV-5, GLRaV-2, GFkV	2		GFkV, GRSPaV
32014	Beba	Extremadura	GLRaV-4 strns., GLRaV-4 strn. 6	GLRaV-5, GLRaV-2		3	GLRaV-2 93/955, GVB, GLRaV-4 strn. 5
32017	Beba	Extremadura	GLRaV-4 strns.	GLRaV-5, GLRaV-2		5	GLRaV-4 strn. 5, GRSPaV
32019	Beba	Extremadura	GFkV, GLRaV-2	GLRaV-5, GLRaV-2, GFkV	4	5	GLRaV-2 93/955, GFkV
32022	ZocaZarra	Navarra	GLRaV-4 strns.	GLRaV-5, GLRaV-2		2	GRSPaV, GLRaV-4 strn. 5, GRVFV, Betaflexivirus?
32023	Castellana Blanca	Navarra	Negative				GRSPaV, GRVFV
32042	Blasco	Andalucía	GFkV		4		GFkV, GRSPaV
32049	Manto Negro	Baleares	GFkV	GFkV	5		GFkV, GRSPaV, GRVFV, GVB
32059	Cabernet Sauvignon	Valencia	GFkV	GLRaV-4, GFkV			GFkV
32063	Riesling	Valencia	Negative	GFkV			GRSPaV
32075	Albillo Dorado	Castilla-La Mancha	Negative	GLRaV-2, GFkV	4	5	GLRaV-2 PN, GRSPaV GRVFV, GFkV

(Continued)

TABLE 3 | Continued

Sample	Cultivar	Origin	DAS-ELISA	RT-qPCR	RL Bioassay*	CS Bioassay*	HTS
32097	Tempranillo Blanco	La Rioja	GLRaV-2, GLRaV-4 strns., GFkV, GLRaV-3	GLRaV-2, GFkV	3	5	GLRaV-2 PN, GRGV, GFkV, GPGV
32113	Albarín negro	Galicia	Negative	GLRaV-2, GFkV	5		GRSPaV, GFkV
33109	Albillo criollo	Canary	GLRaV-3	GLRaV-3	2	4	GLRaV-3, GVL, GVA, GRSPaV
33111	Verijadiego	Canary	GFLV, GLRaV-3, GLRaV-4 strns., GLRaV-4 strn. 6	GLRaV-5, GLRaV-3, GFLV	*5 (FL)*	5	GLRaV-3, GVA, GLRaV-4 strn. 5, GRSPaV, GFLV?
33115	Castellana	Canary	GLRaV3, GLRaV-4 strns.	GLRaV-3		5	GLRaV-2 PV20, GLRaV-3?
33116	Bastardo blanco	Canary	GLRaV-2, GLRaV-3, GLRaV-4 strns.	GLRaV-3, GLRaV-5		5	GLRaV-3, GLRaV-4 strn. 6, GRSPaV
33121	Burrablanca	Canary	GLRaV-3	GLRaV-2		5	GLRaV-3, GVA

The bioassay was performed by grafting the test plants on Rupestris du Lot (RL) and Cabernet Sauvignon (CS) for detection of fan leaf, fleck, and leafroll symptoms. The rating scale was from very mild symptoms (1) to very strong (5).
**Rating scale of symptoms on indicator plants: 1 (very mild), 2 (mild), 3 (moderate), 4 (strong), 5 (very strong).*
n/t, not tested.

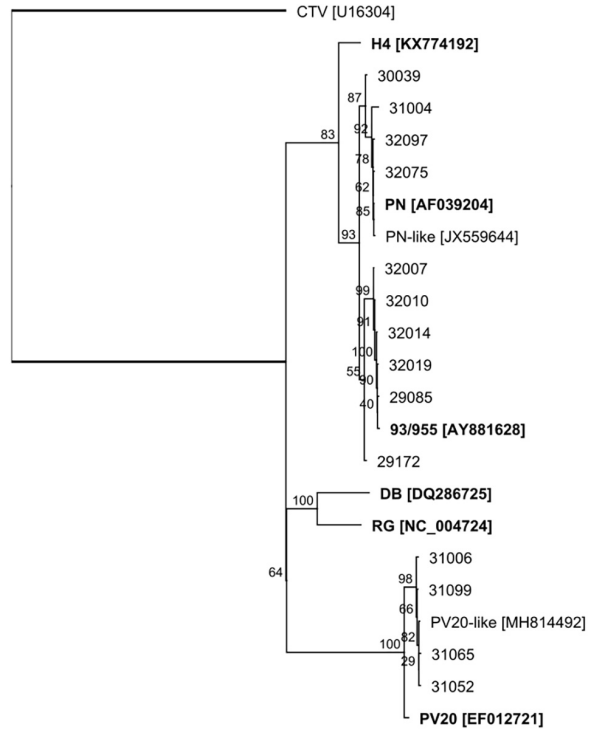

FIGURE 3 | ML phylogenetic tree of the 3′ end (2.7 Kb) of the genomes of GLRaV-2 isolates. Reference genomic sequences for the type variants of the virus are included and highlighted in bold. The closterovirus Citrus tristeza virus (CTV) was included as outgroup. The sequences were aligned using MAFFT, and the phylogenetic tree was generated with the PHYML plugin (HKY85 substitution model, 100 bootstraps) available in Geneious. Branches represent bootstrap support (%).

strain 5 (31099, 32014, 32017, 32022, and 33111) and GLRaV-4 strain 6 (29170, 31065, 32002, and 33116) were the only GLRaV-4 variants present in this set of samples (**Table 1**). Plants harboring GLRaV-4LVs were host for another GLRD virus in six out of the nine plants where this virus was present. In all these cases, symptoms appeared in the bioassay. In other three plants, the only GLRD virus present was GLRaV-4 strain 5 (32017, 32022) or GLRaV-4 strain 6 (32002). In these three cases, the GLRaV-4LVs induced symptoms that varied from mild (32022) to strong (32017) (**Table 3**).

Quantitation of GLRD Viruses From sRNA Reads

Availability of sRNA reads and contigs allowed the quantitation of alignments to reference sequences for the viruses found in the samples (**Tables 1**, **2**). Comparison of the aligned reads (vsiRNAs) provided an estimation of the virus titers in the phloem tissue of the plants. In general, vsiRNAs aligning to GLRaV-2 were, in most of the cases, majoritarian when compared with the other virus species. In some of the cases, when this virus is present, a high ratio of the total sRNAs corresponded to GLRaV-2 vsiRNAs. For this virus, and in the three variants identified in the samples, most of the 21 nt class vsiRNAs aligning to the genomes were

of positive polarity (58.2–80.5%, depending on the isolate and sample) (**Supplementary Figure 4**). Remarkably, in most cases when isolates genetically clustered with the 93/955 variant were present, their vsiRNAs were very abundant (**Table 1**). In sample 32019, GLRaV-2 93/955 vsiRNAs were 43% of the total (>7.2 M reads). The GLRaV-2 variant PV20 included 69.6 and 74% of the total vsiRNA in samples 31052 and 31065, respectively. In sample 32072, the GLRaV-2 PNvsiRNAs were 30% of the reads (2.7 M reads). However, in most cases the number of vsiRNAs was much lower for PN and PV20 variants. Strikingly, there were some samples that did not show contigs that matched GLRaV-2 but did show few vsiRNAs that aligned with the PV20 or PN variant. In particular, GLRaV-2 PV20-like isolates showed the lowest number of vsiRNAs. Among the ampeloviruses, GLRaV-3 showed the highest number of vsiRNAs, mostly of positive polarity (51%) (**Table 1** and **Supplementary Figure 4**). VsiRNAs aligning to GLRaV4 strain 6 were mostly of positive polarity (59%). On the contrary, most of the vsiRNAs aligning to GLRaV-1 in samples 29170 and 31099 resulted from the negative strand (55%). Remarkably, in this sample that is host both for GLRaV-1 and GLRaV-4, the number of aligning-vsiRNAs was in the same magnitude order. However, in samples 33111 and 33116, specific GLRaV-3-vsiRNAs accumulated about 10 times the number of reads that aligned to GLRaV-4 strn. 5 or GLRaV-4 strn. 6 (**Table 1**).

Novel Grapevine Viruses in Spain Derived From the HTS Analysis of the Samples

BLAST analysis of the contigs allowed the identification of viruses not previously reported in Spain, besides the different variants of GLRaV-2 described here. Sample 33109 (Albillo criollo, Canary Islands) showed contigs matching to vitiviruses (**Supplementary File 1**). When the contigs were analyzed, they showed the highest similarity to Grapevine virus L (GVL), a vitivirus recently described (MH681991; Debat et al., 2019). Specific consensus primers were designed based on the sequences of the contigs matching to the coat protein (CP) gene of the virus (GVLF1: GCAGTCCCTTAGTAGTAATAT and GVLR1: CCACCTGAGACTGAGCATCGA) and used for RT-PCR, resulting one amplicon (488 bp) from the RNA extraction of the sample. The amplicon was used for direct Sanger sequencing, and the resulting sequence was compared with isolate resulting 98.2% identical in the nucleotide sequence to the corresponding cp gene in GVL. This is, to the knowledge of the authors, the first report of GVL in Spain. Other samples (32010, 32014) showed hits in BLASTX matching to GVE (**Supplementary File 1**), but close examination of the contigs revealed that they corresponded instead to GVB. Finally, sample 32022 (Zocazarra) showed contigs matching to genomic regions of different betaflexiviruses (**Supplementary File 2**), indicating the plausible presence of an unknown virus of the family.

Validation of HTS for Virus Detection Using Internal Controls

To investigate the quality of the HTS process and its reliability for virus detection in grapevine, we explored some other parameters in addition to quality of the sRNA extraction and the total number of HTS reads obtained. The consistent presence of two viroids and GRSPaV in the samples provided internal references. Hence, we investigated the number of vsiRNAs matching to their genomes. Statistical analysis showed significant correlation between the specific vsiRNA amounts of the three species in the samples (**Figure 4**). There are clear differences in the samples regarding the relative abundance of GRSPaV, GYSVd, and HSVd vsiRNAs (**Table 2** and **Supplementary Table 4**). Samples from batches #1 and #2 showed higher viroid/GRSPaV vsiRNA titers when compared with samples from batch #3. Significantly, sample 32000 had the lowest number of viroid and GRSPaV vsiRNAs. Moreover, inspection of the profiles of GSYVd vsiRNAs and the ratio of the 21 nt vsiRNAs showed differences among the samples (**Supplementary Figure 2**). Analysis of vsiRNAs aligning to GYSVd-1 showed that among the 18–24 nt siRNAs, the 21 nt followed by the 22 and 24 nt class of vsiRNAs were predominant, averaging a of ratio 5:0.94:0.98 (∼5:1:1), indicating the major involvement of Dicer-like protein 4 (DCL4) in the silencing mechanism. This ratio is generally observed in the three batches; however, for sample 32000, this ratio was not followed but was instead 5:1.11:0.39. In sample 32007, the ratio was 5:0.45:0.45. Plausibly, in these samples, a significant part of the population of sRNAs was product of degradation of plant RNAs in the extractions and not product of RNA silencing. In general, results significantly deviating from the 5[21nt]:1[22 nt]:1[24 nt] ratio should be considered as not acceptable.

Comparison of the Reliability of Different Diagnostics Methods

Bioassays showed that 15 plants of the collection were capable of inducing fleck-like symptoms on *V. rupestris* du Lot (**Table 3**), one plant induced strong fanleaf symptoms in that indicator (33111) and 29 plants induced GLRD symptoms in Cabernet. From these, nine plants induced symptoms in both indicators. Only four plants did not induce symptoms after grafting on the indicators. Among them, according to HTS in one plant (32063), the only virus present was GRSPaV; while in plant 32023 (Riesling), only GRSPaV and GRVFV were found. In another plant (32003, Beba) only GRSPaV and GLRaV-2PN were found. There was another plant (32059, Cabernet Sauvignon) that did not induce symptoms in which HTS detected GFkV and GRSPaV. All the plants that induced leafroll symptoms in the indicator had at least a GLRD virus, according to HTS. However, not all the plants harboring leafroll viruses were capable of inducing symptoms; and in these cases, the virus present was always some variant of GLRaV-2 (29172, 32003, 31006, and 32001). Two other plants that harbored GFkV failed to induce symptoms in the indicators (32002 and 32059). Thus, the bioassay and the HTS were not fully coincident, being HTS capable of detecting viruses even if not inducing symptoms. Regarding GFLV, the virus was not detected by the BLAST analysis of the contigs in 33111, but it was identified after aligning to a reference genome. Although the vitiviruses GVA, GVB, and GVL were detected by HTS, unfortunately, in the bioassays, we dismissed

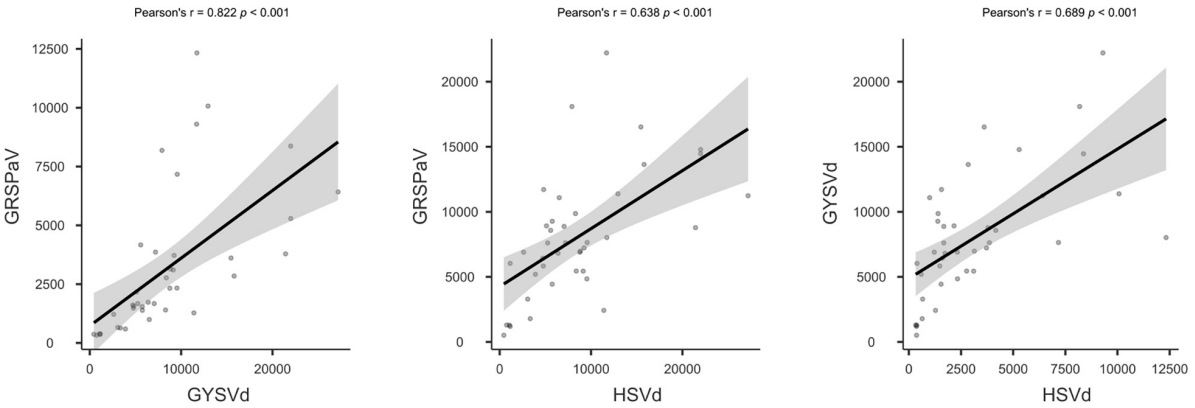

FIGURE 4 | Correlation plot of vsiRNA reads amounts specific for GRSPaV, GYSVd, and HSVd. The statistical analysis was performed with Jamovi v.1.6.

the registration of rugose wood symptoms. Other viruses not detected in the bioassays included GRVFV, GPGV, and GRGV.

Serology and RT-qPCR were, in general, more erratic, failing in detecting viruses in some cases (**Table 3**). For example, GLRaV-2 was detected by serology only in six plants out of the 26 testing positive to HTS. RT-qPCR detected GLRaV-2 in 10 of the samples positive in HTS but provided positive results in another five samples that tested negative in HTS. Compared with the bioassay, serology detected GFkV only in eight of the 15 plants that induced symptoms on Rupestris.GLRaV-1 diagnostic results coincided in serology and RT-qPCR where the virus was detected in three samples, while HTS revealed it in only two samples. However, HTS failed to detect the virus in sample 32000 that, according to reference values (Bioanalyzer and GRSPaV/GYSVd reads), was of lower quality (**Table 2**, **Supplementary Figure 1**, and **Supplementary Table 4**). Detection of GLRaV-3 by serology was concurrent in the five plants that tested positive by HTS. However, in plant 33115, HTS detected only few reads corresponding to GLRaV-3. According to the Bioanalyzer results and the scarce GRSPaV/GYSVd/HSVd reads used as a reference, HTS from this sample should not be considered acceptable. Serology detected GLRaV-4 variants in 13 samples, confirmed by HTS only in nine samples. In contrast, one plant (29170) positive in HTS to GLRaV-4 strain 6 resulted negative in serology and RT-qPCR. It is worth mentioning that a plant that tested negative both in the bioassay and HTS tested positive to GLRaV-4 variants in DAS-ELISA (32001). RT-qPCR detected GLRaV-3 in four plants that were coincident with four of the five positives of the serological test and HTS. Regarding GFLV, this virus was detected only in one sample (33111) according to the bioassay, serology, RT-qPCR, and few HTS reads aligning to the genome.

A Pipeline for Virus Certification Using HTS of sRNAs in Grapevine

We devised a flux diagram for virus certification using HTS of sRNAs in grapevine (**Figure 5**). In this process, we consider the critical steps assessing the quality of the results. Hence, sRNA quality is inspected through the Bioanalyzer prior to submitting the RNA to HTS. A sequence depth of at least 10 M reads per sample will be requested. Once the raw reads are received from the sequencing service, FastQC[1] or another equivalent tool will help to inspect the quality of the readings, and a threshold will be set to decide to continue with the analysis process (e.g., Phred score $>$ 34). Besides, a minimum number of 18–24 nt reads will be necessary ($>$5 M reads). In addition, we recommend that the ratio of 21 nt vs. 18–24 nt siRNAs in the sample should be $>$30%. If there are viroids or GRSPaV in the sample, as frequently happens in grapevine, an additional quality parameter could be the titers and profile of vsiRNAs aligning to the viroid/GRSPaV genomes (e.g., a ratio 5:1:1 in GSVd-1 for the 21, 22, and 24 nt vsiRNAs). In the pipeline, contigs will be generated from the 18–24 nt reads using Velvet (combined k-mers 13, 15, and 17) and submitted to BLASTN (*E*-value = 1e-5) and BLASTX (*E*-value = 1e-3) against the virus databases of NCBI as available in Viruseq. If there are hits with some of the viruses included in the certification standards, the material may be reported as non-compliant. If not, the 18–24 nt reads are aligned with reference genomic sequences. Next, if significant reads appear (e.g., $>$50 reads aligning across the reference genome covering $>$ 5% of the genome), then the presence of regulated virus species will be reported, and the material will be classified as unsuitable for certification. Negative results from the alignments would mean healthy plant material. Each diagnostic procedure could be validated by including in the analysis a control plant that has been previously analyzed. Finally, this certification scheme, provided all the steps are carried out properly, would take about 6 months after receipt of the plant material.

DISCUSSION

Virus Identification by HTS in the Grapevine Samples

In the last years, performing RNA-sequencing analysis for determination and discovery of plant viruses in crop plants has become widespread (Rott et al., 2017; Zheng et al., 2017;

[1]http://www.bioinformatics.babraham.ac.uk/projects/fastqc/

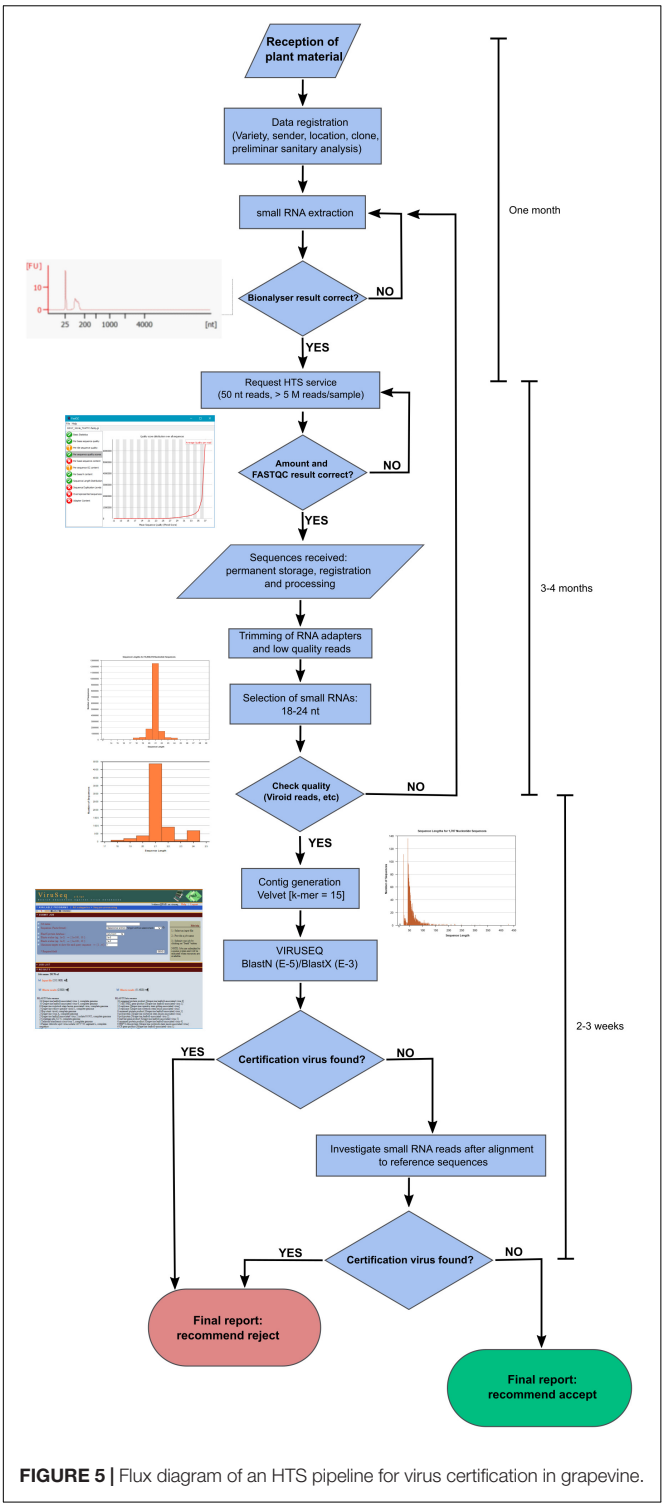

FIGURE 5 | Flux diagram of an HTS pipeline for virus certification in grapevine.

Maliogka et al., 2018; Massart et al., 2019; Rajamäki et al., 2019; Mehetre et al., 2021). More specifically, Al Rwahnih et al. (2009) pioneered the use of HTS for virus determination in grapevine; and since then, it has proved a valuable tool (Coetzee et al., 2010; Pantaleo et al., 2010; Al Rwahnih et al., 2015; Maree et al., 2015; Jo et al., 2015; Czotter et al., 2018; Hily et al., 2018; Vigne et al., 2018). In Spain, we have used Ion Torrent or Illumina for sequencing sRNAs for the diagnostics and characterization of these viruses (Velasco et al., 2014, 2015; Cretazzo and Velasco, 2017). VsiRNAs are present in a high rate in the pool of sRNAs collected for HTS, making this class of RNAs suitable for virus diagnostics. Their inconvenience is that the short reads obtained can be prone to incorrect assembly leading to false positives that can be overcome with longer reads obtained from total RNA (Maliogka et al., 2018). However, the advantage of using the sRNA fraction for HTS is the elevated rate of virus and viroid vsiRNAs (Pecman et al., 2017; Santala and Valkonen, 2018). In the samples, the sRNAs corresponding to viruses was 0.1–72%, averaging 9%. Viroid siRNAs were 0.15% of the total sRNAs.

There are two types of questions regarding diagnostics that usually need to be addressed by researchers. One is what virus or virus combination is causing the disease symptoms in a given plant, including novel viruses. The other is to determine whether the plant is virus-free or has some already known viruses, i.e., in phytosanitary certification and quarantine controls. To give answer to both type of questions, HTS reads must be processed and compared with sequences already present in databases. The first step after curating the raw reads is to perform *de novo* assembly to generate contigs using SPAdes, Trinity, Velvet, or some other tool appropriate for sRNAs. The algorithm of choice should be carefully evaluated for each particular situation to select the best option. Multiple k-mer mode tools such as the one used in Oases, a derivative of Velvet, and SPAdes are considered good for contig assembly of sRNAs (Pirovano et al., 2015; Hölzer and Marz, 2019). Next, the contigs can be analyzed by comparing with known reference viral genomes or submitting to BLASTN and BLASTX that will render hits to viral sequences present in databases. The advantage of this second method is that novel viruses with similarity to other viruses, mainly in the RNA-dependent RNA polymerase, can be identified. This second method is computationally more demanding, and in practice submitting a bulk of sequences directly to the BLAST platform of NCBI is unfeasible. For this reason, several web-based tools/services have been developed that, in some cases, include the viral sequences or built-in databases of NCBI in their own server that allows online analysis (Wang et al., 2013; Ho and Tzanetakis, 2014; Zheng et al., 2017; reviewed in Jones et al., 2017). ViruSeq was designed aiming at developing an easy-to-use and quick platform for the identification of viruses in HTS sequences. We observed that the number of reads and contigs aligning to reference sequences or matching to grapevine viruses decreased when reducing the sequencing depth, as previously reported (Massart et al., 2019). In the analysis, obtention and generation of contigs from the sRNA reads was performed with Velvet, and it was shown that k-mer 15 was optimal for obtaining a higher number of contigs with meaningful results. When using k-mer 13, more contigs were obtained in each sample but resulted in less significant results in BLASTX and BLASTN, pointing out to the generation of chimeric contigs derived from non-contiguous reads. Thus, the combined use of the contigs generated with the three k-mer values 13, 15, and 17 for BLAST analysis allowed reaching the optimal number of hits to grapevine viruses. Similar results were reported in HTS analysis of sRNAs

from grapevines collected in Hungary when using Velvet (Czotter et al., 2018). In a wide cross-laboratory sRNA-derived HTS study for identification of plant viruses, the authors reported the combination of k-mer 13-15-17 as the most reliable in BLAST analysis (Massart et al., 2019). In any case, the alignment of sRNA reads to reference genomes allowed the identification of viruses that were not detected by BLAST analysis of the contigs.

Among the ampeloviruses, in this study, we identified GLRaV-1, GLRaV-3, and GLRaV-4LVs. In Spain, field surveys for GLRaV-1 and GLRaV-3 are limited, but the latter appears to be well distributed (Bertolini et al., 2010; López-Fabuel et al., 2013; Pesqueira et al., 2016), corresponding with the general observation of higher occurrence of GLRaV-3 worldwide (Maree et al., 2013; Burger et al., 2017). Although GLRaV-4LVs have been detected previously in Spain, scarce field data on the occurrence of these viruses are available (Padilla et al., 2010a,b; Velasco et al., 2014, 2015). Serological analysis showed recurrent GLRaV-4LVs infections in candidate clones submitted for certification (Padilla et al., 2012). Significantly, GLRaV-4 strain 5 and GLRaV-4 strain 6 alone were able to induce leafroll symptoms in the absence of other GLRD viruses. GLRaV-2 occurrence was very high in the samples and was capable of inducing GLRD in many cases, particularly if 93/955-like isolates were present. Not surprisingly, as a result, many plants got infected by viruses not included in regulations, such as GRSPaV and GFkV. The latter is sanctioned in the EU regulations only for the rootstocks (Golino et al., 2017). Thus, although it could eventually be detected by serology during the selection programs of the varieties, the result is not considered relevant. Other viruses frequently found in the samples were the vitiviruses (GVA, GVB, and GVL) and other non-regulated viruses, such as GRVFV, GRGV, and GPGV, and some possible unknown-to-date virus. All the plants in this study were hosts for at least one virus species and two viroids (HSVd and GYSVd-1).

The relationship between virus titers and disease incidence has been reported for plant viruses (Gray et al., 1991; Linak et al., 2020). In the samples, the amount of GLRaV-3 vsiRNAs is 10 times higher than that of GLRaV-4LVs when co-infecting a plant. In a previous study, we showed by RT-qPCR that GLRaV-3 titers are one order of magnitude higher than those of GLRaV-4LVs (Velasco et al., 2014). Differential ratios in titers of ampeloviruses have been previously reported for the viral dsRNAs (Hu et al., 1991), and it is corroborated by other authors (Aboughanem-Sabanadzovic et al., 2017). Higher viral titers may be related to the incidence of GLRaV-3, as it increases the likelihood of a vector carrying the virus and its infectivity. Moreover, this could contribute to the high occurrence of the closterovirus GLRaV-2 for which, at present, the natural vector is unknown. Another factor that has been correlated with viral titer is disease severity, as reported in other pathosystems (Galipienso et al., 2013). Evidence is accumulating relating GLRaV-4LVs with mild to moderate GLRD symptoms when compared with GLRaV-3 (Aboughanem-Sabanadzovic et al., 2017). In this study, a vine harboring only GLRaV-4 strain 6 induced strong symptoms on the indicator plant when compared with the very strong symptoms induced by cultivars bearing only GLRaV-3. Another grapevine plant harboring GLRaV-4 strain 6 and GLRaV-2 variant PV20 induced strong leafroll symptoms on the indicator. Other plants that showed mild or moderate symptoms were host for GLRaV-4 strains in addition to GLRaV-2. Therefore, besides the lower incidence, reduced virus titers may also explain the lower GLRD symptomatology caused by GLRaV-4LVs as compared with GLRaV-3.

HTS for Virus Certification in Grapevine

Prior to this study, a comparative study between bioassay and HTS in grapevine virus certification has been performed (Al Rwahnih et al., 2015). These authors reported that HTS of dsRNAs was superior to the bioassay in terms of reliable virus detection, independence of environmental conditions, economical cost, and time required for the analysis. In fact, in some cases, HTS was capable of detecting viruses not shown by bioassays such as GRVFV and others, similar to what happened in the samples with GRVFV, GPGV, GRGV, and, in some cases, GLRaV-2, and GFkV. Another advantage of HTS is the permanent availability of the sequences, that can be analyzed at any time, including their re-evaluation for the detection of newly identified viruses that is not possible for bioassays once the assay has been completed and plants removed. In our case, we dismissed rugose wood in the bioassays that could not be inspected again in field after the removal of the plants. All these advantages have led to the proposal of a plausible standard internationally recognized "metagenome passport" for propagative material resulting of HTS-generated metadata that would include information on plant viromes (Saldarelli et al., 2017). The use of HTS in grapevine certification is an opportunity to be considered in the future EU and international regulations, but before arriving at this "metagenome passport," several points need to be considered, such as which viruses should be included in the certification schemes. For example, EU regulations on the phytosanitary status of propagative grapevine plants follow the Directive 68/193/EEC and Council Directive 2002/11/EC that states: "The following test methods may be applied: for all virus diseases the indexing methods in the case of vine plants; for fanleaf, in addition to the preceding methods, the indexing method in the case of herbaceous plants, and also the serology method," but harmonization among EU countries is far from reaching a consensus regarding the phytosanitary status and the diagnostics methods for certified propagation material (Golino et al., 2017). Another issue to be addressed is the set of viruses included in the regulations, which vary from country to country, as some countries include rough wood diseases and/or GLRaV-2, while in all cases GFkV is excluded, except for rootstocks.

Validation of a diagnostic test in plant virology depends on its intrinsic characteristics that differ with respect to its sensitivity, specificity, and selectivity (Roenhorst et al., 2018). Therefore, agents such as nurseries, breeders, scientists, growers, and regulators must reach a consensus to develop and establish standard protocols for the application of HTS technologies in grapevine certification. In addition, viruses excluded from certification and in which conditions (e.g., in traditional minority varieties, the presence of viruses could be accepted as long as no healthy material is available) need to be determined. A standard methodology for HTS certification should clarify the origin of

the tissue for the analysis (phloem scrapings, leaves, petioles, etc.), vegetative stage of the plant material (dormant, flowering, ripening, harvesting), type of nucleic acid (dsRNA, sRNA, or total RNA), and protocol for extractions and cDNA library generation. For example, in addition to sRNAs, the dsRNAs, which are a fraction of nucleic acids enriched in plant RNA viruses, can be a highly valuable source for HTS (Gaafar and Ziebell, 2020). They have been successfully used for virus characterization and identification (Velasco et al., 2018, 2019), and specifically have shown in grapevine to be suitable when compared with bioassays (Al Rwahnih et al., 2015).

In any HTS certification pipeline, library quality, number of reads per sample, and standard bioinformatics analysis must be optimized and a consensus must be attained. For example, HTS detection of GLRaV-1 in a cross-laboratory study required > 2.5 M sRNA reads for a sensitive detection at a percentage > 70–80% (Massart et al., 2019). Therefore, minimum quality standards for RNA extraction, libraries, and sequencing must be guaranteed. Importantly, given the high sensitivity of HTS, special care must be taken to avoid contamination among samples. The high frequency of appearance of viroids in grapevine make them plausible as internal controls of HTS efficiency and quality. For example, Massart et al. (2019) reported the simultaneous presence of HSVd and GYSVd-1 in four samples considered and showed comparable results in terms of the number of reads and proportions to those described in this study. A similar number of HSVd and GYSVd-1 vsiRNAs have been reported in GLRaV-3-infected and uninfected grapevines and in comparable ratios to those found in the samples (Alabi et al., 2012). Finally, we have previously reported the simultaneous presence of HSVd, GYSVd-1, and GRSPaV in grapevine plants collected all over Spain (Velasco et al., 2014; and unpublished results).

In this study, we have compared HTS versus bioassays in terms of reliability, but the economic cost and time required for both diagnostic methods, in addition to other factors, must also be taken into account. In the case of HTS, expenses include RNA extractions, library preparation, sequencing, and bioinformatics analysis. For bioassays, we must include indicator plants, soil preparation and sanitation, grafting, plant maintenance, and symptom inspection visits over 3 years. Both methods require qualified personnel although with different expertise. Although both methodologies currently have a comparable cost (excluding personnel expenses), in the case of HTS it will probably decrease in the coming years, while bioassay costs are likely to remain the same, or may increase considering inflation. Another advantage of HTS is the ability to detect additional viruses and viroids in samples, such as those that are not included in the regulations but that may have effects on yield and quality. Finally, HTS offers the possibility of achieving a widely accepted standard and replacing bioassays.

CONCLUSION

We have analyzed 40 grapevine plants in three sets at different HTS depths and quality of RNA extractions for virus detection. Numerous grapevine viruses could be identified in the samples, such as non-regulated viruses. Leafroll viruses, even non-regulated ones, resulted capable of inducing symptoms in indicator hosts in most of the cases. The results have shown the suitability of HTS in comparison with bioassays and other diagnostic tools. As a result, we propose a pipeline using HTS for virus certification in grapevine with the aim of addressing several problems identified by workers and breeders: timely results, identification of key parameters in sRNA extractions and bioinformatics processing, a user-friendly platform for BLAST analysis, and, finally, the procedure is susceptible of validation using different controls. The HTS pipeline is intended to be operated by non-scientific experts, so that interpretation of results can be performed by a technician with minimal training.

DATA AVAILABILITY STATEMENT

The datasets presented in this study can be found in online repositories. The names of the repository/repositories and accession number(s) can be found below: https://www.ncbi.nlm.nih.gov/genbank/, PRJNA715068; MW715828; MW715829; MW715830; MW715831; MW715832; MW715833; MW715834; MW715835; MW715836.

AUTHOR CONTRIBUTIONS

LV and CP: conceptualization, methodology, investigation, writing—review and editing, and funding acquisition. LV: bioinformatic analysis and writing—original draft preparation. Both authors read and agreed to the published version of the manuscript.

FUNDING

This research was funded by the Oficina Española de Variedades Vegetales (OEVV, MAPAMA) and IFAPA, Grant No: TRA2019.007 (TRANSVITI), co-financed by FEDER. This study is part of the collaboration agreement 045/2017 signed by IFAPA and IMIDA in 2017.

ACKNOWLEDGMENTS

The authors wish to thank I. Hita and E. Salmerón for the technical assistance in the inspection of virus symptoms and diagnostics. They also thank D. Guerrero-Fernández and M. G. Claros (SCBI, Universidad de Málaga) for the development and maintenance of Viruseq.

SUPPLEMENTARY MATERIAL

The Supplementary Material for this article can be found online at: https://www.frontiersin.org/articles/10.3389/fpls.2021.682879/full#supplementary-material

Supplementary Figure 1 | Electropherograms of RNA extractions according to the Bioanalyzer (Agilent) from phloem scrapings of grapevine canes. Except for the Tempranillo sample that is included as a reference for which the total RNA was extracted using the Sigma Plant RNA extraction kit, the RNAs of the samples for HTS were extracted with the Exiqon RNA kit. RIN is the Agilent RNA integrity number. The RNAs of about 18–24 nt are the small RNAs that include the vsiRNAs.

Supplementary Figure 2 | Profiles of small RNA population (18–24 nt) and specific vsiRNAs aligning to GYSVd-1 genomes for the samples studied in this study.

Supplementary Figure 3 | Profiles of contig sizes generated at different k-mers for representative samples belonging to batch #1 **(A)** 30020 and batch #3 **(B)** 32022.

Supplementary Figure 4 | (Left) Distribution of vsiRNA reads of different lengths that align to reference virus sequences. Negative numbers refer to vsiRNAs aligned to the negative strand of the viral genome. **(Right)** Alignment of the 21 nt class vsiRNAs (reads) to the viral genomes of GLRaV-1, GLRaV-2 variant 95/933, GLRaV-2 variant PN, and GLRaV-3 group II. Reads belong to samples 29170 (GLRaV-1; GLRaV-2 95/933), 32024 (GLRaV-2 PN), and 33116 (GLRaV-3). Reads below the *x*-axes represent the vsiRNAs aligning to the negative strand of the viral genomes. For the analysis, vsiRNA populations were aligned to the indexed genomes and the BAM alignment file produced was processed using MISIS (Seguin et al., 2016). The genomes are not to the same scale.

Supplementary Table 1 | Data of trimmed Illumina reads from the grapevine small RNAs.

Supplementary Table 2 | Contigs generated from the Illumina reads of small RNAs (18–24 nt) using Velvet 12.08 and different k-mer.

Supplementary Table 3 | Grapevine viruses and their GenBank numbers used as references in this study.

Supplementary Table 4 | Number of vsiRNAs and genome coverage aligning to Grapevine yellow speckle viroid 1 and Hop stunt viroid 1 in the samples.

Supplementary Table 5 | GenBank accession numbers of the sequences obtained in this study.

Supplementary File 1 | Summary of the hits to viral sequences of the samples studied in this study after submission to Viruseq BLASTN and BLASTX using different k-mer values.

Supplementary File 2 | Result of Viruseq BLASTX analysis for sample 33109. Contigs matching with betaflexiviruses are highlighted.

REFERENCES

Aboughanem-Sabanadzovic, N., Maliogka, V., and Sabanadzovic, S. (2017). "Grapevine leafroll-associated virus 4," in *Grapevine Viruses: Molecular Biology, Diagnostics and Management*, eds B. Meng, G. P. Martelli, D. A. Golino, and M. Fuchs (Cham: Springer), 197–216. doi: 10.1007/978-3-319-57706-7_9

Al Rwahnih, M., Daubert, S., Golino, D., and Rowhani, A. (2009). Deep sequencing analysis of RNAs from a grapevine showing Syrah decline symptoms reveals a multiple virus infection that includes a novel virus. *Virology* 387, 395–401. doi: 10.1016/j.virol.2009.02.028

Al Rwahnih, M., Daubert, S., Golino, D., Islas, C., and Rowhani, A. (2015). Comparison of next-generation sequencing versus biological indexing for the optimal detection of viral pathogens in grapevine. *Phytopathology* 105, 758–763. doi: 10.1094/phyto-06-14-0165-r

Alabi, O. J., Zheng, Y., Jagadeeswaran, G., Sunkar, R., Naidu, R. A., and Rayapati, A. N. (2012). High-throughput sequence analysis of small RNAs in grapevine (*Vitis vinifera* L .) affected by grapevine leafroll disease. *Mol. Plant Pathol.* 13, 1060–1076. doi: 10.1111/j.1364-3703.2012.00815.x

Almeida, R. P. P., Daane, K. M., Bell, V. A., Blaisdell, G. K., Cooper, M. L., Herrbach, E., et al. (2013). Ecology and management of grapevine leafroll disease. *Front. Microbiol.* 4:94.

Angelini, E., Aboughanem-Sabanadzovic, N., Dolja, V. V., and Meng, B. (2017). "Grapevine leafroll-associated virus 2," in *Grapevine Viruses: Molecular Biology, Diagnostics and Management*, eds B. Meng, G. P. Martelli, D. A. Golino, and M. Fuchs (Cham: Springer).

Barrero, R. A., Napier, K. R., Cunnington, J., Liefting, L., Keenan, S., Frampton, R. A., et al. (2017). An internet-based bioinformatics toolkit for plant biosecurity diagnosis and surveillance of viruses and viroids. *BMC Bioinformatics* 18:26.

Bertolini, E., García, J., Yuste, A., and Olmos, A. (2010). High prevalence of viruses in Table grape from Spain detected by real-time RT-PCR. *Eur. J. Plant Pathol.* 128, 283–287. doi: 10.1007/s10658-010-9663-4

Beuve, M., Sempé, L., and Lemaire, O. (2007). A sensitive one-step real-time RT-PCR method for detecting Grapevine leafroll-associated virus 2 variants in grapevine. *J. Virol. Methods* 141, 117–124. doi: 10.1016/j.jviromet.2006.11.042

Burger, J. T., Maree, H. J., Gouveia, P., and Naidu, R. A. (2017). "Grapevine leafroll-associated virus 3," in *Grapevine Viruses: Molecular Biology, Diagnostics and Management*, eds B. Meng, G. P. Martelli, D. A. Golino, and M. Fuchs (Cham: Springer), 172–195.

Cabaleiro, C., Pesqueira, A. M., Barrasa, M., and Garcia-Berrios, J. J. (2013). Analysis of the losses due to grapevine leafroll disease in albariño vineyards in RíasBaixas (Spain). *Cienc. e Tec. Vitivinic* 28, 43–50.

Cretazzo, E., and Velasco, L. (2017). High throughput sequencing allowed the completion of the genome of grapevine red globe virus and revealed recurring co-infection with other tymoviruses in grapevine. *Plant Pathol.* 66, 1202–1213. doi: 10.1111/ppa.12669

Coetzee, B., Freeborough, M.-J., Maree, H. J., Celton, J.-M., Rees, D. J. G., and Burger, J. T. (2010). Deep sequencing analysis of viruses infecting grapevines: virome of a vineyard. *Virology* 400, 157–163. doi: 10.1016/j.virol.2010.01.023

Czotter, N., Molnar, J., Szabó, E., Demian, E., Kontra, L., Baksa, I., et al. (2018). NGS of virus-derived small RNAs as a diagnostic method used to determine viromes of hungarian vineyards. *Front. Microbiol.* 9:122.

Debat, H., Zavallo, D., Brisbane, R. S., Vončina, D., Almeida, R. P. P., Blouin, A. G., et al. (2019). Grapevine virus L: a novel vitivirus in grapevine. *Eur. J. Plant Pathol.* 155, 319–328. doi: 10.1007/s10658-019-01727-w

Deng, W., Nickle, D. C., Learn, G. H., Maust, B., and Mullins, J. I. (2007). ViroBLAST: a stand-alone BLAST web server for flexible queries of multiple databases and user's datasets. *Bioinformatics* 23, 2334–2336. doi: 10.1093/bioinformatics/btm331

Gaafar, Y. Z. A., and Ziebell, H. (2020). Comparative study on three viral enrichment approaches based on RNA extraction for plant virus/viroid detection using high-throughput sequencing. *PLoS One* 15:e0237951. doi: 10.1371/journal.pone.0237951

Galipienso, L., Janssen, D., Rubio, L., Aramburu, J., and Velasco, L. (2013). Cucumber vein yellowing virus isolate-specific expression of symptoms and viral RNA accumulation in susceptible and resistant cucumber cultivars. *Crop Prot.* 43, 141–145. doi: 10.1016/j.cropro.2012.08.004

Geniza, M., and Jaiswal, P. (2017). Tools for building de novo transcriptome assembly. *Curr. Plant Biol.* 11–12, 41–45. doi: 10.1016/j.cpb.2017.12.004

Golino, D. A., Fuchs, M., Al Rwahnih, M., Farrar, K., Schmidt, A., and Martelli, G. P. (2017). "Regulatory aspects of grape viruses and virus diseases: certification, quarantine, and harmonization," in *Grapevine Viruses: Molecular Biology, Diagnostics and Management*, eds B. Meng, G. P. Martelli, D. A. Golino, and M. Fuchs (Cham: Springer), 581–598. doi: 10.1007/978-3-319-57706-7_28

Gray, S., Power, A., Smith, D., Seaman, A., and Altman, N. (1991). Aphid transmission of barley yellow dwarf virus: acquisition access periods and virus concentration requirements. *Phytopathology* 81, 539–545. doi: 10.1094/phyto-81-539

Hily, J. M., Candresse, T., Garcia, S., Vigne, E., Tannière, M., Komar, V., et al. (2018). High-throughput sequencing and the viromic study of grapevine leaves: from the detection of grapevine-infecting viruses to the description of a new environmental Tymovirales member. *Front. Microbiol.* 9:1782.

Ho, T., and Tzanetakis, I. E. (2014). Development of a virus detection and discovery pipeline using next generationsequencing. *Virology* 471–473, 54–60. doi: 10.1016/j.virol.2014.09.019

Hölzer, M., and Marz, M. (2019). De novo transcriptome assembly: a comprehensive cross-species comparison of short-read RNA-Seq assemblers. *Gigascience* 8, 1–16.

Hu, J. S., Gonsalves, D., Boscia, D., Maixner, M., and Golino, D. (1991). Comparison of rapid detection assays for grapevine leafroll disease associated closteroviruses. *Vitis* 30, 87–95.

Jones, S., Baizan-Edge, A., MacFarlane, S., and Torrance, L. (2017). Viral diagnostics in plants using next generation sequencing: computational analysis in practice. *Front. Plant Sci.* 8:1770.

Jo, Y., Choi, H., Kyong Cho, J., Yoon, J. Y., Choi, S. K., and Kyong Cho, W. (2015). In silico approach to reveal viral populations in grapevine cultivar Tannat using transcriptome data. *Sci. Rep.* 5, 1–11. doi: 10.1038/srep15841

Linak, J. A., Jacobson, A. L., Sit, T. L., and Kennedy, G. G. (2020). Relationships of virus titers and transmission rates among sympatric and allopatric virus isolates and thrips vectors support local adaptation. *Sci. Rep.* 10:7649.

López-Fabuel, I., Wetzel, T., Bertolini, E., Bassler, A., Vidal, E., Torres, L. B., et al. (2013). Real-time multiplex RT-PCR for the simultaneous detection of the five main grapevine viruses. *J. Virol. Methods* 188, 21–24. doi: 10.1016/j.jviromet.2012.11.034

Maliogka, V. I., Minafra, A., Saldarelli, P., Ruiz-García, A. B., Glasa, M., Katis, N., et al. (2018). Recent advances on detection and characterization of fruit tree viruses using high-throughput sequencing technologies. *Viruses* 10:486.

Maree, H. J., Almeida, R. P. P., Bester, R., Chooi, K. M., Cohen, D., Dolja, V. V., et al. (2013). Grapevine leafroll-associated virus 3. *Front. Microbiol.* 4:82.

Maree, H. J., Fox, A., Al Rwahnih, M., Boonham, N., and Candresse, T. (2018). Application of HTS for routine plant virus diagnostics: state of the art and challenges. *Front. Plant Sci.* 9:1082.

Maree, H. J., Pirie, M. D., Oosthuizen, K., Bester, R., Jasper, D., Rees, G., et al. (2015). Phylogenomic analysis reveals deep divergence and recombination in an economically important grapevine virus. *PLoS One* 10:e0126819. doi: 10.1371/journal.pone.0126819

Martelli, G. P. (2017). "An overview on grapevine viruses, viroids, and the diseases they cause," in *Grapevine Viruses: Molecular Biology, Diagnostics and Management*, eds B. Meng, G. P. Martelli, D. A. Golino, and M. Fuchs (Cham: Springer).

Massart, S., Chiumenti, M., De Jonghe, K., Glover, R., Haegeman, A., Koloniuk, I., et al. (2019). Virus detection by high-throughput sequencing of small RNAs: large-scale performance testing of sequence analysis strategies. *Phytopathology* 109, 488–497. doi: 10.1094/phyto-02-18-0067-r

Mehetre, G. T., Leo, V. V., Singh, G., Sorokan, A., Maksimov, I., Yadav, M. K., et al. (2021). Current developments and challenges in plant viral diagnostics: a systematic review. *Viruses* 13:412. doi: 10.3390/v13030412

Meng, B., Li, C., Goszczynski, D. E., and Gonsalves, D. (2005). Genome sequences and structures of two biologically distinct strains of Grapevine leafroll-associated virus 2 and sequence analysis. *Virus Genes* 31, 31–41. doi: 10.1007/s11262-004-2197-0

Miozzi, L., and Pantaleo, V. (2015). "Drawing siRNAs of viral origin out from plant siRNAs libraries," in *Plant Virology Protocols: Newapproaches to Detect Viruses and Host Responses*, eds I. Uyeda and C. Masuta (New York, NY: Springer), 111–123. doi: 10.1007/978-1-4939-1743-3_10

Mumford, R. A., Macarthur, R., and Boonham, N. (2016). The role and challenges of new diagnostic technology in plant biosecurity. *Food Secur.* 8, 103–109. doi: 10.1007/s12571-015-0533-y

Oliver, J. E., and Fuchs, M. (2011). Tolerance and resistance to viruses and their vectors in vitis sp.: a virologist's perspective of the literature. *Am. J. Enol. Vitic.* 62, 438–451. doi: 10.5344/ajev.2011.11036

Osman, F., Leutenegger, C., Golino, D., and Rowhani, A. (2008). Comparison of low-density arrays, RT-PCR and real-time TaqMan® RT-PCR in detection of grapevine viruses. *J. Virol. Methods* 149, 292–299. doi: 10.1016/j.jviromet.2008.01.012

Padilla, C. V., Cretazzo, E., López, N., García, De Rosa, B., Padilla, V., et al. (2010a). First report of Grapevine leafroll-associated virus 4 (GLRaV-4) in Spain. *New Dis.Rep.* 21:21. doi: 10.5197/j.2044-0588.2010.021.021

Padilla, C. V., Cretazzo, E., López, N., Padilla, V., and Velasco, L. (2010b). First report of Grapevine leafroll-associated virus 5 in Spain. *Plant Dis.* 94, 1507. doi: 10.1094/pdis-07-10-0508

Padilla, C. V., Garcia, de Rosa, B., López, N., Velasco, L., Salmerón, E., et al. (2012). "Grapevine leafroll virus in candidate clones for plant certification in Spain," in *Proceedings of the 17th Congress of the International Council for the Study of Virus and Virus-like Diseases of the Grapevine (ICVG)*, ed. B. Ferguson (California: University of California), 268–269.

Pantaleo, V., Saldarelli, P., Miozzi, L., Giampetruzzi, A., Gisel, A., Moxon, S., et al. (2010). Deep sequencing analysis of viral short RNAs from an infected Pinot Noir grapevine. *Virology* 408, 49–56. doi: 10.1016/j.virol.2010.09.001

Pecman, A., Kutnjak, D., Gutiérrez-Aguirre, I., Adams, I., Fox, A., Boonham, N., et al. (2017). Next generation sequencing for detection and discovery of plant viruses and viroids: comparison of two approaches. *Front. Microbiol.* 8:1998.

Pesqueira, A. M., Cabaleiro, C., and Velasco, L. (2016). Genetic analysis of Grapevine leafroll-associated virus 3 population from Galicia. Spain. *Plant Pathol.* 65, 310–321. doi: 10.1111/ppa.12413

Pirovano, W., Miozzi, L., Boetzer, M., and Pantaleo, V. (2015). Bioinformatics approaches for viral metagenomics in plants using short RNAs: model case of study and application to a *Cicer arietinum* population. *Front. Microbiol.* 5:790.

Rajamäki, M. L., Lemmetty, A., Laamanen, J., Roininen, E., Vishwakarma, A., Streng, J., et al. (2019). Small-RNA analysis of pre-basic mother plants and conserved accessions of plant genetic resources for the presence of viruses. *PLoS One* 14:e0220621. doi: 10.1371/journal.pone.0220621

Roenhorst, J. W., de Krom, C., Fox, A., Mehle, N., Ravnikar, M., and Werkman, A. W. (2018). Ensuring validation in diagnostic testing is fit for purpose: a view from the plant virology laboratory. *EPPO Bull.* 48, 105–115. doi: 10.1111/epp.12445

Rott, M., Xiang, Y., Boyes, I., Belton, M., Saeed, H., Kesanakurti, P., et al. (2017). Application of next generation sequencing for diagnostic testing of tree fruit viruses and viroids. *Plant Dis.* 101, 1489–1499. doi: 10.1094/pdis-03-17-0306-re

Rubio, L., Galipienso, L., and Ferriol, I. (2020). Detection of plant viruses and disease management: relevance of genetic diversity and evolution. *Front. Plant Sci.* 11:1092.

Saldarelli, P., Giampetruzzi, A., Maree, H. J., and Al Rwahnih, M. (2017). "High-throughput sequencing: advantages beyond virus identification," in *Grapevine Viruses: Molecular Biology, Diagnostics and Management*, eds B. Meng, G. P. Martelli, D. A. Golino, and M. Fuchs (Cham: Springer), 625–642. doi: 10.1007/978-3-319-57706-7_30

Santala, J., and Valkonen, J. P. T. (2018). Sensitivity of small RNA-based detection of plant viruses. *Front. Microbiol.* 9:939.

Seguin, J., Otten, P., Baerlocher, L., Farinelli, L., and Pooggin, M. M. (2016). MISIS-2: a bioinformatics tool for in-depth analysis of small RNAs and representation of consensus master genome in viral quasispecies. *J. Virol. Methods* 233, 37–40. doi: 10.1016/j.jviromet.2016.03.005

Seguin, J., Rajeswaran, R., Malpica-López, N., Martin, R. R., Kasschau, K., Dolja, V. V., et al. (2014). De novo reconstruction of consensus master genomes of plant RNA and DNA viruses from siRNAs. *PLoS One* 9:e0088513.

Velasco, L., Arjona-Girona, I., Ariza-Fernández, M. T., Cretazzo, E., and López-Herrera, C. (2018). A novel hypovirus species from Xylariaceae fungi infecting avocado. *Front. Microbiol.* 9:778.

Velasco, L., Arjona-Girona, I., Cretazzo, E., López-Herrera, C., Velasco, L., et al. (2019). Viromes in Xylariaceae fungi infecting avocado in Spain. *Virology* 532, 11–21. doi: 10.1016/j.virol.2019.03.021

Velasco, L., Bota, J., Montero, R., and Cretazzo, E. (2014). Differences of three ampeloviruses ' multiplication in plant may explain their incidences in vineyards. *Plant Dis.* 98, 395–400. doi: 10.1094/pdis-04-13-0433-re

Velasco, L., Cretazzo, E., Padilla, C. V., and Janssen, D. (2015). Grapevine leafroll associated virus 4 strain 9: complete genome and quantitative analysis of virus-derived small interfering RNA populations. *J. Plant Pathol.* 97, 149–152.

Velasco, L., Guerrero, D., Claros, M. G., and Cretazzo, E. (2016). "ViruSeq, un servicio de identificación de virus a partir de secuencias múltiples (POST-173)," *XVIII Congreso de la Sociedad Española de Fitopatología, 20-23 Septiembre 2016, Palencia* (Spain).

Vigne, E., Garcia, S., Komar, V., Lemaire, O., and Hily, J. M. (2018). Comparison of serological and molecular methods with high-throughput sequencing for the detection and quantification of grapevine fanleaf virus in vineyard samples. *Front. Microbiol.* 9:2726.

Wang, Q., Jia, P., and Zhao, Z. (2013). VirusFinder: software for efficient and accurate detection of viruses and their integration sites in host genomes through next generation sequencing data. *PLoS One* 8:e64465. doi: 10.1371/journal.pone.0064465

Zerbino, D. R., and Birney, E. (2008). Velvet: algorithms for de novo short read assembly using de Bruijn graphs. *Genome Res.* 18, 821–829. doi: 10.1101/gr.074492.107

Zheng, Y., Gao, S., Padmanabhan, C., Li, R., Galvez, M., and Gutierrez, D. (2017). VirusDetect: an automated pipeline for efficient virus discovery using deep sequencing of small RNAs. *Virology* 500, 130–138. doi: 10.1016/j.virol.2016.10.017

Zhu, H., Ling, K., Goszczynski, D., McFerson, J., and Gonsalves, D. (1998). Nucleotide sequence and genome organization of grapevine leafroll-associated virus-2 are similar to beet yellows virus, the closterovirus type member. *J. Gen. Virol.* 79, 1289–1298. doi: 10.1099/0022-1317-79-5-1289

Conflict of Interest: The authors declare that the research was conducted in the absence of any commercial or financial relationships that could be construed as a potential conflict of interest.

frontiers in Plant Science

ORIGINAL RESEARCH
published: 29 July 2021
doi: 10.3389/fpls.2021.685382

Enhanced Age-Related Resistance to Tomato Yellow Leaf Curl Virus in Tomato Is Associated With Higher Basal Resistance

*Jing-Ru Zhang, Shu-Sheng Liu and Li-Long Pan**

Ministry of Agriculture Key Laboratory of Molecular Biology of Crop Pathogens and Insects, Institute of Insect Sciences, Zhejiang University, Hangzhou, China

Tomato yellow leaf curl virus (TYLCV) is one of the most notorious plant pathogens affecting the production of tomato worldwide. While the occurrence of age-related resistance (ARR) against TYLCV has been reported, the factors impacting its development remain unknown. We conducted a series of experiments with three tomato cultivars that vary in basal resistance to TYLCV to explore factors involved in the development of ARR. Our data indicate that ARR is more pronounced in tomato cultivars with higher basal resistance. Additionally, increased plant biomass in older plants does not contribute to ARR. Virus source plants with a younger age at initial inoculation facilitates virus acquisition by whiteflies. Finally, an analysis on plant hormones suggests that salicylic acid (SA) may play a major role in the development of ARR in tomato against TYLCV. These findings provide new insights into the developmental resistance in tomato against TYLCV as well as clues for the deployment of ARR in the management of diseases caused by TYLCV.

Keywords: TYLCV, age-related resistance, salicylic acid, virus quantity, infection rate, plant biomass

OPEN ACCESS

Edited by:
Rajarshi Kumar Gaur, Deen Dayal Upadhyay Gorakhpur University, India

Reviewed by:
Pranav Pankaj Sahu, Global Change Research Centre (ASCR), Czechia
Xiufang Xin, Institute of Plant Physiology and Ecology, Chinese Academy of Sciences, China

***Correspondence:**
Li-Long Pan
panlilong@zju.edu.cn

Specialty section:
This article was submitted to Plant Pathogen Interactions, a section of the journal Frontiers in Plant Science

Received: *25 March 2021*
Accepted: *07 July 2021*
Published: *29 July 2021*

Citation:
Zhang J-R, Liu S-S and Pan L-L (2021) Enhanced Age-Related Resistance to Tomato Yellow Leaf Curl Virus in Tomato Is Associated With Higher Basal Resistance. Front. Plant Sci. 12:685382. doi: 10.3389/fpls.2021.685382

INTRODUCTION

Plant viral diseases pose serious threats to the production of many crops worldwide (Jones, 2020). In recent decades, diseases caused by tomato yellow leaf curl virus (TYLCV) (family *Geminiviridae*, genus *Begomovirus*) have imposed substantial losses to tomato production (Navas-Castillo et al., 2011; Dhaliwal et al., 2019). TYLCV infection in tomato plants results in yellowing and reduced size of the apical leaves, curling of leaf margins and stunted plant growth (Cohen and Harpaz, 1964; Prasad et al., 2020). First discovered in Jordan Valley in the 1930s, TYLCV was biologically characterized and named in 1960s (Cohen and Harpaz, 1964). Whilst TYLCV was confined to a few countries in Middle East in the first few decades post its characterization, its global spread started in 1980s when the Israel and Mild strains emerged and its whitefly vectors invaded many regions worldwide (Lefeuvre et al., 2010). Subsequently, TYLCV has become one of the most important plant pathogens in tomato production in dozens of countries around the globe as well as a focus for research in plant virology (Lefeuvre et al., 2010; Mabvakure et al., 2016; Prasad et al., 2020). Under natural conditions, TYLCV is transmitted by whiteflies of the *Bemisia tabaci* complex in a persistent circulative manner (Fiallo-Olivé et al., 2020; Wang and Blanc, 2021).

To date, various measures have been adopted to control TYLCV, including chemical, cultural and physical strategies, and breeding resistant plants (Rojas et al., 2018). Chemical control of its whitefly vectors, whilst commonly used, has resulted in the development of pesticide resistance and deleterious effects on the environment and human health (Gilbertson et al., 2015; Basit, 2019). Successful implementation of some cultural and physical tactics such as the application of a whitefly host-free period, colored shading nets and polyester covers, have also been reported (Polston and Anderson, 1997; Ben-Yakir et al., 2012; Al-Shihi et al., 2016). Nevertheless, increasing resistance in tomato plants via breeding represents the most effective measure to combat TYLCV (Islam and Wu, 2017; Dhaliwal et al., 2019). In resistance breeding, the most widely used resistance genes are *Ty-1*, *Ty-2*, and *Ty-3* that originate from *Solanum chilense* and *S. habrochaites* (Dhaliwal et al., 2019). However, to date genetic resources against TYLCV have been found in only a few wild relatives of cultivated tomato and introgression of resistance into tomato cultivars may take years and end up unsuccessful (Dhaliwal et al., 2019). More importantly, resistance break-down has been found in southeast Spain where severe epidemics of TYLCV in tomato cultivars carrying the *Ty-1* gene were reported (Torre et al., 2018). Therefore, alternative measures to improve the resistance in tomato plants are needed.

Post entry of viruses into plants, the outcome of virus-plant interaction may vary from immune to severe disease progression depending on many intrinsic and environmental factors (Osterbaan and Fuchs, 2019). Environmental factors, such as temperature and water availability, may significantly impact the interactions between plants and plant pathogens such as viruses, leading to altered disease development (Velásquez et al., 2018). Intrinsically, plant resistance and infectivity of viruses represent the most important factors affecting virus-plant interactions. On the plant side, many factors such as plant cultivar and age, among others, have been shown to modulate resistance to viruses (Osterbaan and Fuchs, 2019). The increase of resistance with plant age, often referred to as age-related resistance (ARR), has been shown to substantially affect virus-plant interactions (Panter and Jones, 2002; Hu and Yang, 2019). For example, the susceptibility of pepper to tomato spotted wilt tospovirus and soybean to bean pod mottle virus decreased with the increase of plant age (Moriones et al., 1998; Beaudoin et al., 2009; Byamukama et al., 2015). Likewise, the expression of genetic resistance to TYLCV was shown to increase with plant age (Levy and Lapidot, 2008). However, our knowledge of ARR in tomato against TYLCV is limited. Many key questions remain, for example, does plant age impact virus quantity in plants and in turn virus transmission by whiteflies that acquire TYLCV from these plants? Moreover, the ecological and molecular mechanisms underlying ARR against TYLCV in tomato remain unknown.

In the present study, we explored the factors involved in ARR against TYLCV in tomato plants. First, we compared TYLCV resistance among three tomato cultivars. Second, we characterized the impact of plant age on TYLCV resistance in plants of these cultivars. Third, we examined the effects of plant biomass at inoculation on ARR. Fourth, we analyzed the effects of virus source plants with varying ages at initial inoculation on acquisition and transmission of TYLCV by whiteflies. Finally, we examined the roles of plant hormones in ARR. Our findings provide insights into how ARR develops in tomato against TYLCV and how it might be utilized to combat the diseases caused by TYLCV.

MATERIALS AND METHODS

Plants and Insects

Three cultivars of tomato (*S. lycopersicum* Mill), namely Pufen7, Pufen5, and Hezuo903, and one cultivar of cotton (*Gossypium hirsutum* cv. Zhe-Mian 1793), were used. Tomato seeds were purchased from Shanghai Funong Seed Co., Ltd., and cotton seeds were provided by the Institute of Crop Sciences, Zhejiang University. All plants were grown in insect-proof greenhouses under natural lighting at 25 ± 3°C. Unless specified otherwise, all plants were watered with solutions containing 0.17 g/L macromineral water-soluble fertilizer (DeMei LvYuan, China). For insects, a culture of MEAM1 whiteflies of the *B. tabaci* complex (mt*COI* GenBank accession code: KM821540) was used. Whiteflies were reared on cotton plants in insect-proof cages in climate chambers at 26 ± 2°C, 60–80% relative humidity and 14/10 h light/dark cycles. In all experiments, newly emerged female whiteflies (0–3 days post emergence) were used. The purity of the whitefly culture was assessed every 3 months using PCR-restriction fragment length polymorphism and mt*COI* sequencing (Qin et al., 2013).

PCR and Quantitative PCR Detection of TYLCV in Tomato Plants and Whitefly

For the detection of TYLCV in tomato plants, the first apical fully-expanded leaves were harvested and subjected to DNA extraction. For TYLCV detection in whiteflies, adults were collected as groups of 15 and then subjected to DNA extraction. DNA extraction was done using procedures described previously (Pan et al., 2017). PCR detection of TYLCV was performed with primers TYLCV-F (5′-ATCGAAGCCCTGATATCCCCCGTGG-3′) and TYLCV-R (5′-CAGAGCAGTTGATCATG-3′). Quantitative PCR (qPCR) analysis of TYLCV was performed using SYBR Premix Ex Taq II (Takara, Japan) and CFX96 Real-Time PCR Detection System (Bio-Rad, Unted States) with the primers TYLCV-RTF (5′-GAAGCGACCAGGCGATATAA-3′) and TYLCV-RTR (5′-GGAACATCAGGGCTTCGATA-3′) for TYLCV, and primers WF-Actin-F (5′-TCTTCCAGCCATCCT TCTTG-3′) and WF-Actin-R (5′-CGGTGATTTCCTT CTGCATT-3′) for whitefly *actin*, and Tom-Actin-F (5′-TGGAGGATCCATCCTTGCATCAC-3′) and Tom-Actin-R (5′-TCGCCCTTTGAAATCCACATCTGC-3′) for tomato *actin*.

Standard Procedure of Agrobacteria-Mediated Virus Inoculation

An infectious clone of TYLCV isolate SH2 (GenBank accession code: AM282874.1), provided by Professor Xueping Zhou (Institute of Biotechnology, Zhejiang University), was used

(Wu et al., 2006). To perform agro-inoculation, agrobacteria containing infectious clones of TYLCV were first cultured until OD600 reached 1.5–2.0, and then resuspension buffer (10 mM $MgCl_2$, 10 mM MES, 200 μM Acetosyringone) was used to re-suspend the agrobacteria. Re-suspended agrobacteria were then incubated at room temperature for 1 h and 1 mL syringes were used to introduce the agrobacteria into leaves of tomato plants. In virus inoculation experiments using agrobacteria, 0.6 mL of agrobacteria solution was introduced into each seedling and the test plants were then cultivated for 28 days before being sampled for PCR and qPCR detection of TYLCV.

Standard Procedure of Whitefly-Mediated Virus Inoculation

In virus inoculation experiments using viruliferous whiteflies, TYLCV-infected Hezuo903 plants that were agro-inoculated at two true-leaf stage and had grown to 7–8 true-leaf stage were used as the source of inoculum. Whiteflies were collected from the lab culture and released onto TYLCV-infected plants to feed for 48 h for virus acquisition. Viruliferous whiteflies were then collected and placed on leaves (enclosed with leaf-clip cages) of test plants for 48 h for virus transmission. The number of whiteflies per test plants was five. Leaf-clip cages were made as reported before (Ruan et al., 2007). Whitefly survival was recorded during virus transmission and the live whiteflies were collected at the end of transmission and subjected to TYLCV quantification. Immediately after whitefly removal, imidacloprid (20 mg/L) was sprayed to kill whitefly eggs and the plants were cultivated for a further 28 days before being sampled for PCR and qPCR detection of TYLCV.

Comparison of TYLCV Resistance Among Three Tomato Cultivars

Tomato seedlings of the three cultivars were grown to two true-leaf stage. Virus inoculation was conducted using the standard procedure of agrobacteria-mediated virus inoculation (Variable I, **Table 1**). Measurement of plant height (stem length in centimeters from soil level to stem tip) was conducted 4 weeks post virus inoculation as described before (Murphy and Bowen, 2006). In addition, two experiments of virus inoculation by whiteflies were conducted: in experiment 1, the standard procedure of whitefly-mediated virus inoculation was used; in experiment 2, the durations of both virus acquisition and virus inoculation were increased to 96 h and the number of viruliferous whiteflies was increased to 10 per plant (Variable I, **Table 1**).

Comparison of TYLCV Resistance Among Plants of Different Ages

Tomato seeds were sown on a weekly basis, and seedlings were transplanted when they had reached two true-leaf stage. For each of the three cultivars, four batches of seedlings with the age of 0, 7, 14, and 21 days post transplanting (DPT), respectively, were prepared. Typical images of seedlings at different ages are presented in **Supplementary Figure 1**. Comparison of TYLCV resistance among plants of the four age-batches were conducted using the standard procedures of agrobacteria-mediated and whitefly-mediated virus inoculation (Variable II, **Table 1**).

Comparison of TYLCV Resistance Among Plants of the Same Chronological Age With Different Biomass

Pufen7 and Hezuo903 seedlings at 0 DPT were prepared. For each of the two cultivars, seedlings were divided into three groups. The three groups of seedlings were watered with water, a solution containing 0.17 g/L macromineral water-soluble fertilizer and a solution containing 0.34 g/L macromineral water-soluble fertilizer, respectively. At 21 DPT, virus inoculation was conducted for the three groups of plants using the standard procedure of agrobacteria-mediated inoculation (Variable III, **Table 1**).

Comparison of Virus Acquisition and Transmission by Whiteflies When Plants Inoculated at Different Ages Were Used as the Source of Inoculum

Two age groups of Hezou903 plants at 0 and 21 DPT were prepared and then agro-inoculated. Four weeks later, whiteflies were collected from the lab culture and released onto these plants to feed for 48 h for virus acquisition. Some viruliferous whiteflies were then collected and subjected to analysis of virus quantity. Further, virus transmission capacity of the viruliferous whiteflies from plants of each of the two age groups were tested with Hezuo903 seedlings of 0 DPT using the standard procedure of whitefly-mediated virus inoculation (Variable IV, **Table 1**).

Analysis of Salicylic Acid and Jasmonates Contents

Pufen7 and Hezuo903 plants at 0 and 21 DPT were prepared. For the analysis of salicylic acid (SA) and jasmonates (JA) contents, leaves from three seedlings were mixed and used as one sample. For each treatment (cultivar × plant age), four and nine-ten replicates were conducted for SA and JA, respectively. Samples were first powdered in liquid nitrogen and then 0.15 g of leaf powder was transferred into centrifuge tubes. Plant hormones were extracted using 1 mL of ethyl acetate containing 10 ng of D4-SA and D6-JA. All samples were vortexed and centrifuged and supernatants collected and concentrated using a vacuum concentrator. The dry residues were re-suspended in 110 μL of MeOH: H_2O (50: 50, v/v). After mixing and centrifugation, 100 μL of the supernatants were collected. SA and JA were analyzed using an Agilent 6460 triple quadrupole mass spectrometer (Agilent Technologies, United States) equipped with an electrospray ionization (ESI) source that operated in the negative ion multiple-reaction monitoring (MRM) mode. Agilent Mass Hunter Workstation was used for data acquisition and processing.

TABLE 1 | Variables tested in experiments for comparing resistance to Tomato yellow leaf curl virus (TYLCV) among tomato plants of different cultivars, of the same cultivar with different ages and of the same age with different biomass as well as for examining the effects of age of inoculum virus-infected plants on virus acquisition and transmission by whiteflies.

Variables	Method of virus inoculation	Duration of virus acquisition (h)	Virus inoculation via whitefly feeding		No. of treatments /No. of replicates	No. of plants per replicates
			Duration (h)	No. of whiteflies per plant		
Variable I: TYLCV	Agrobacteria	n/a-	n/a	n/a	3/3	7–8
resistance among three	Whitefly: experiment 1	48	48	5	3/3	7–8
tomato cultivars	Whitefly: experiment 2	96	96	10	3/3	7–8
Variable II: TYLCV	Agrobacteria	n/a-	n/a	n/a	4/3	6–10
resistance among plants of four different ages	Whitefly	48	48	5	4/3	6–10
Variable III: TYLCV resistance among plants of the same age with three different biomass	Agrobacteria	n/a-	n/a	n/a	3/8–15	1
Variable IV: Effects of age of inoculum virus-infected plants on virus acquisition and transmission by whitefly	Whitefly	48	48	5	2/3	8–9

n/a stands for not applicable.

Quantitative Reverse Transcription PCR Analysis of SA Biosynthesis Genes

Seedlings of Pufen7 and Hezuo903 of different ages were prepared. For each treatment (cultivar × plant age), six replicates were conducted. Total RNAs were extracted with TRIzol and cDNA was synthesized using the PrimeScript RT reagent Kit with gDNA Eraser (Takara, Japan). qRT-PCR was performed using SYBR Premix Ex Taq II (Takara, Japan) and CFX96 Real-Time PCR Detection System (Bio-Rad, United States) with the primers ICS1-RTF (5′-GGCTTTAGCTGGAACACGG-3′) and ICS1-RTR (5′-CAATCTTCTTCTTATGCACTCCC-3′) for *ICS1*, and primers PAL-F (5′-CGTTATGCTCTCCGAACATC-3′) and PAL-R (5′-GAAGTTGCCACCATGTAAGG-3′) for *PAL*, and Tom-Actin-F (5′-TGGTCGGAATGGGACAGAAG-3′) and Tom-Actin-R (5′-CTCAGTCAGGAGAACAGGGT-3′) for tomato *actin*, and Tom-EF1α-F (5′-ATTGGAAATGGATATGCTCCA-3′) and Tom- EF1α-R (5′-TCCTTACCTGAACGCCTGTCA-3′) for tomato *EF1*α. Each gene was analyzed in two technical replicates.

Statistical Analysis

For the analysis of virus quantity, real time data were calculated using $2^{-\Delta Ct}$ as normalized to *actin*. For the analysis of gene expression level, real time data were calculated using $2^{-\Delta Ct}$ as normalized to the geometric mean of two reference genes *actin* and elongation factor 1α (*EF1*α; Vandesompele et al., 2002). All percentage data were arcsine square root transformed for statistical analysis and back-transformed for presentation. For the comparison of virus transmission efficiency, virus quantity, plant hormone contents and gene expression level, one-way analysis of variance (ANOVA) along with Fisher's least significant difference (LSD) was used when three or more treatments were conducted, and Student's independent *t*-test was used when only two treatments were conducted. All data in this study were presented as the mean ± standard errors of mean (mean ± SEM). The differences between treatments were considered significant when $p < 0.05$. All statistical analysis was performed using SPSS 20.0 Statistics and EXCEL.

RESULTS

Resistance to TYLCV in Three Tomato Cultivars

Tomato yellow leaf curl virus infection did not induce noticeable symptom in Pufen7 plants (**Figure 1A**). In Pufen5 plants yellowing of several apical leaves was observed; in Hezou903 plants both yellowing and severe leaf curl were observed (**Figures 1B,C**). TYLCV infection significantly reduced the height of Pufen5 (by 32.1%) and Hezou903 (by 53.4%) plants, but did not affect the height of Pufen7 plants (**Figures 1D–F**). Some yellowing was observed in cotyledons and old leaves that were agro-inoculated in both un-infected and TYLCV-infected plants for each cultivar. Post agro-inoculation, 95.2% of Pufen7 plants and all the plants of Pufen5 and Hezou903 were infected by TYLCV (**Figure 2A**). The highest quantity of TYLCV was found in Hezou903, followed by Pufen5 and then Pufen7 (**Figure 2B**). Similarly, two whitefly transmission assays revealed that the highest TYLCV infection rate was always found in Hezou903, followed by Pufen5 and then Pufen7 (**Figures 2C,D**). Notably, no successful transmission was found for Pufen7 plants. During virus transmission, there was no significant difference in whitefly survival rate and TYLCV quantity in recovered whiteflies among plants of different cultivars (**Figures 2E–G**).

Effects of Plant Age on TYLCV Resistance in Pufen7 Plants

As whiteflies were unable to transmit TYLCV to Pufen7 plants, TYLCV resistance in Pufen7 plants of different ages was assayed only by agro-inoculation and virus infection status was assessed 4 weeks post inoculation. TYLCV infection rate decreased

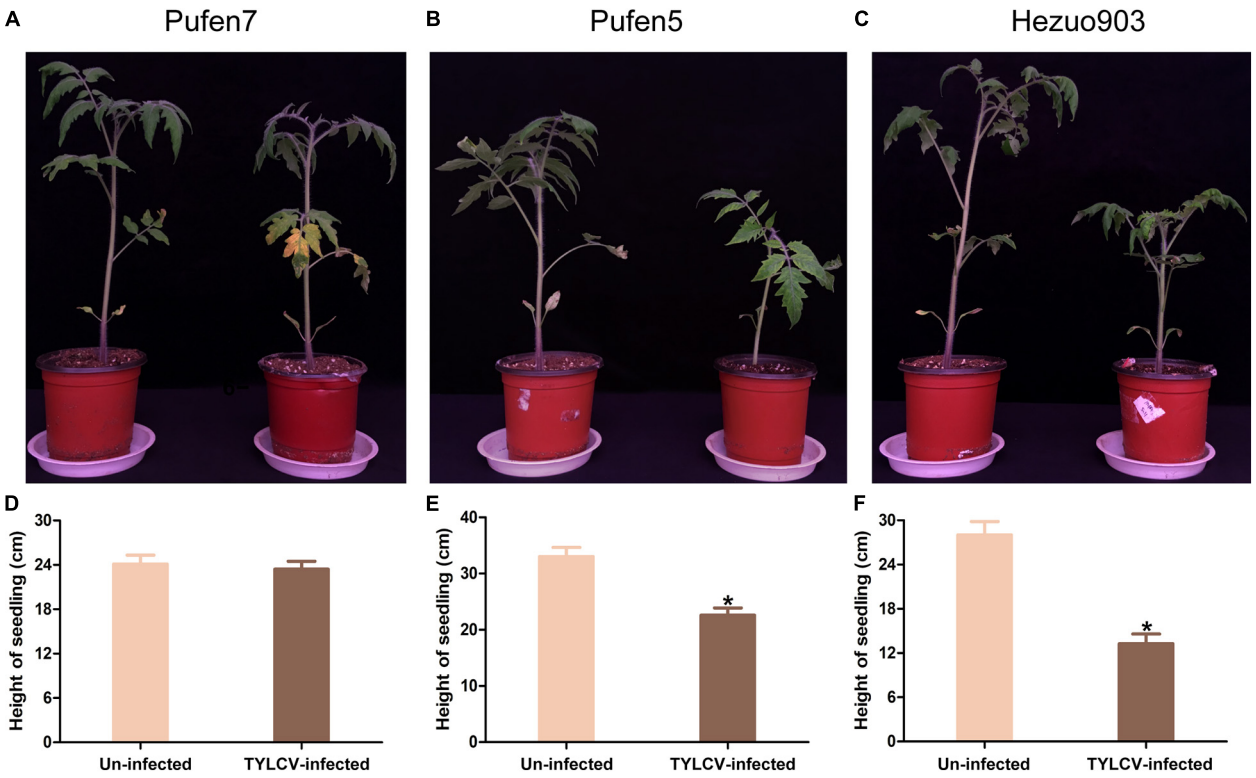

FIGURE 1 | Typical images and height of un-infected and tomato yellow leaf curl virus (TYLCV)-infected tomato plants of different cultivars. **(A–C)** Image of Pufen7, Pufen5, and Hezuo903. **(D–F)** Height of un-infected and TYLCV-infected tomato plants. Photographing and measurement of plant height were conducted 4 weeks post virus inoculation. Values are means ± SEM in panels **(D–F)** (n = 8–15). *Above columns indicate significant differences (independent t-test, $p < 0.05$).

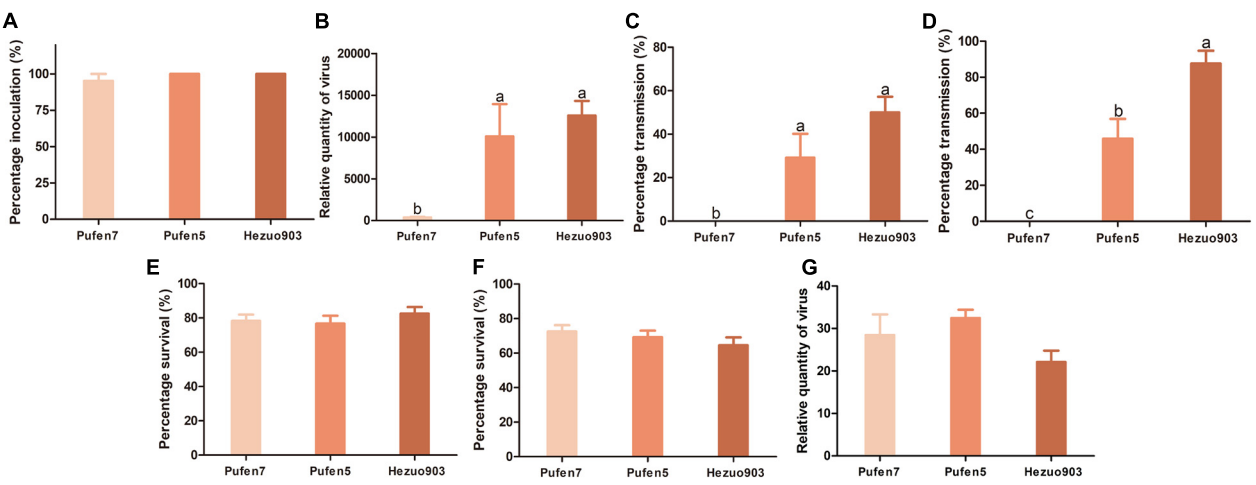

FIGURE 2 | Resistance to tomato yellow leaf curl virus (TYLCV) in plants of tomato cultivars Pufan7, Pufen5, and Hezuo903. **(A)** Percentage of TYLCV-infected plants in agro-inoculated plants; **(B)** Relative quantity of virus in agro-inoculated plants; **(C)** Percentage of TYLCV-infected plants in whitefly-inoculated plants when the durations of both virus acquisition and transmission were 48 h and five whiteflies were used per test plant; **(D)** Percentage of TYLCV-infected plants in whitefly-inoculated plants when the durations of both virus acquisition and transmission were 96 h and ten whiteflies were used per test plant; **(E)** Whitefly survival on plants when five whiteflies were used per test plant; **(F)** Whitefly survival on plants when ten whiteflies were used per test plant; **(G)** Relative quantity of virus in whiteflies recovered from plants post virus transmission when 10 whiteflies were used per test plant. Values are means ± SEM (n = 3 for panels **(A,C,D)** and in each replicate 7–8 plants were used; n = 14 for panel **(B)**; n = 24 for panels **(E,F)**; n = 4 for panel **(G)**]. Different letters above the columns indicate significant differences (one-way ANOVA, $p < 0.05$).

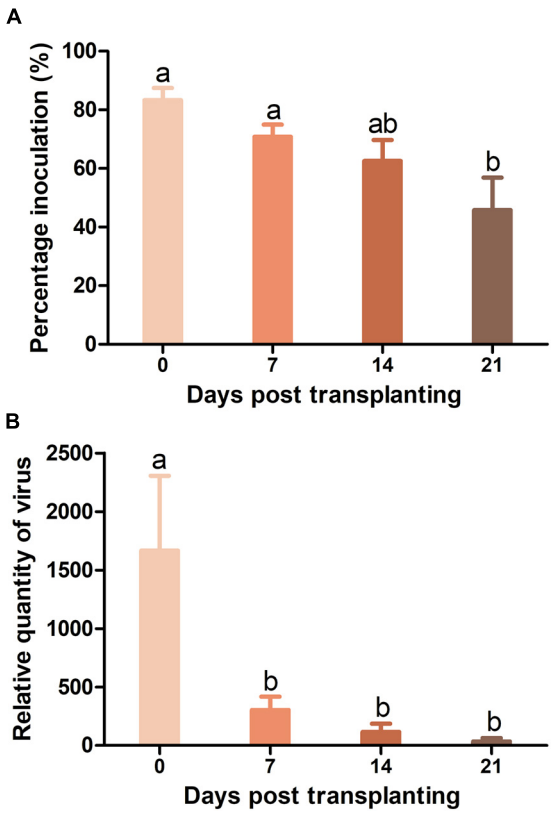

FIGURE 3 | Resistance to tomato yellow leaf curl virus (TYLCV) in Pufen7 seedlings of 0, 7, 14, and 21 DPT. **(A)** Percentage of TYLCV-infected plants in agro-inoculated plants; **(B)** Relative quantity of virus. Values are means ± SEM (n = 3 and in each replicate 7–8 plants were used for panel **(A)**; n = 8 for panel **(B)**]. Different letters above the columns indicate significant differences (one-way ANOVA, $p < 0.05$).

sequentially from 83.3 to 45.8% with the increase of plants age (**Figure 3A**). An obvious reduction in TYLCV quantity was observed with the increase of plant age (**Figure 3B**).

Effects of Plant Age on TYLCV Resistance in Pufen5 Plants

When TYLCV was agro-inoculated into plants, TYLCV infection rate in Pufen5 plants did not differ significantly between plants of 0 and 7 DPT. However, for plants of 7–21 DPT, a slight decrease of TYLCV infection rate from 100 to 80.7% was observed with the increase of plant age (**Figure 4A**). No significant difference was found for TYLCV quantity in plants of different ages post agro-inoculation (**Figure 4B**). When whitefly transmission was used, TYLCV infection rate decreased from 87.5% at 7 DPT to 50% at 21 DPT (**Figure 4C**). Sequential decreases of TYLCV quantity with the increase of plant age was observed (**Figure 4D**). For whiteflies, during virus transmission their survival rate on plants at 14 DPT (92.2%) was significantly higher than that on plants at 0 DPT (77.1%) and 21 DPT (81.7%) (**Figure 4E**). No significant difference in TYLCV quantity in whiteflies recovered from plants of different ages was found (**Figure 4F**).

Effects of Plant Age on TYLCV Resistance in Hezuo903 Plant

There was no significant difference in TYLCV infection rate in Hezuo903 plants of different ages when TYLCV was agro-inoculated into plants (**Figure 5A**). However, TYLCV quantity in plants decreased significantly from 0 to 7 DPT and did not differ significantly among plants of 7, 14, and 21 DPT (**Figure 5B**). When whitefly transmission was used, there was no significant difference in TYLCV infection rate among plants of different ages (**Figure 5C**), but again TYLCV quantity decreased significantly with the increase of plant age (**Figure 5D**). For whiteflies, during virus transmission their survival rate on plants was similar except that survival rate on plants of 7 DPT was slightly lower than that on plants of 21 DPT (**Figure 5E**). There was no significant difference in TYLCV quantity in whiteflies recovered from plants of different ages (**Figure 5F**).

Effects of Plant Biomass at Inoculation on Virus Quantity

Plants differed in biomass (size) among the three fertilizer treatments for both Pufen7 (**Figure 6A**) and Hezuo903 (**Figure 6B**). In the data of relative quantity of virus of the three fertilizer treatments in Pufen7, we noted one outlier with exceptionally high virus quantity in each of the three treatments: 41.2, 18.9, and 23.1 for water, 0.17 g/L, and 0.34 g/L, respectively. After elimination of the outliers, Kolmogorov–Smirnov analysis showed that the remaining data followed a normal distribution and thus were analyzed using ANOVA. Following virus inoculation, virus quantity was significantly higher in plants watered with a solution containing 0.34 g/L macromineral water-soluble fertilizer than that in the other two treatments for Pufen7 (**Figure 6C**). Virus quantity did not differ significantly among plants of the three fertilizer treatments for Hezuo903 (**Figure 6D**).

Effects of Virus Inoculum Plants Inoculated at Different Ages on Virus Acquisition and Transmission by Whiteflies

Tomato yellow leaf curl virus-infected Hezuo903 plants that were agro-inoculated at 0 and 21 DPT were presented to whiteflies for virus acquisition. TYLCV quantity in whiteflies was significantly higher when the source of inoculum was agro-inoculated at 0 DPT than that at 21 DPT (**Figure 7A**). Virus transmission rate by whiteflies did not differ significantly between the two treatments (**Figure 7B**).

Effects of Plant Age on the Contents of SA and JA

For both cultivars, the level of endogenous SA was significantly higher in seedlings of 21 DPT than that in seedlings of 0 DPT (**Figures 8A,B**). Similarly, endogenous JA level was significantly

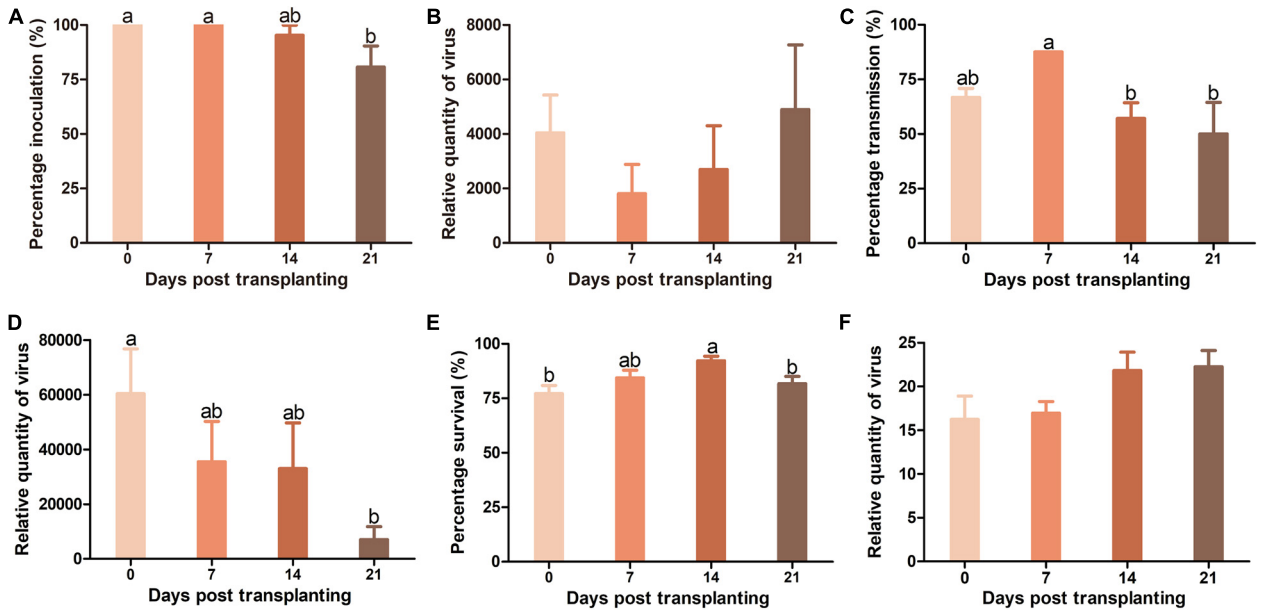

FIGURE 4 | Resistance to tomato yellow leaf curl virus (TYLCV) in Pufen5 seedlings of 0, 7, 14, and 21 DPT. **(A)** Percentage of TYLCV-infected plants in agro-inoculated plants; **(B)** Relative quantity of virus in agro-inoculated plants; **(C)** Percentage of TYLCV-infected plants in whitefly-inoculated plants; **(D)** Relative quantity of virus in whitefly-inoculated plants; **(E)** Whitefly survival on tomato seedlings of different ages; **(F)** Relative quantity of virus in whiteflies recovered post virus transmission. Values are means ± SEM [n = 3 and in each replicate 7–8 plants were used for panels **(A,C)**; n = 7–8 for panels **(B,D)**; n = 21–24 for panel **(E)**; n = 4 for panel **(F)**]. Different letters above the columns indicate significant differences (one-way ANOVA, $p < 0.05$).

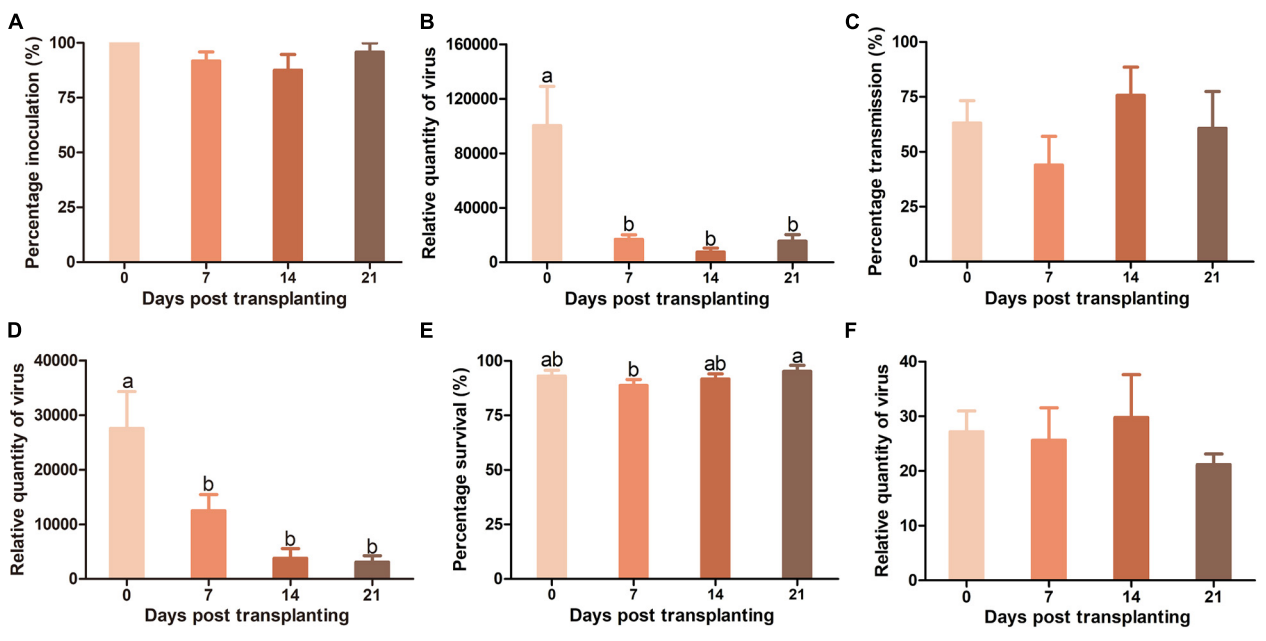

FIGURE 5 | Resistance against tomato yellow leaf curl virus (TYLCV) in Hezuo903 seedlings of 0, 7, 14, and 21 DPT. **(A)** Percentage of TYLCV-infected plants in agro-inoculated plants; **(B)** Relative quantity of virus in agro-inoculated plants; **(C)** Percentage of TYLCV-infected plants in whitefly-inoculated plants; **(D)** Relative quantity of virus in whitefly-inoculated plants; **(E)** Whitefly survival on tomato seedlings; **(F)** Relative quantity of virus in whiteflies recovered post virus transmission. Values are means ± SEM [n = 3 and in each replicate 6–10 plants were used for panels **(A,C)**; n = 7–8 for panels **(B,D)**; n = 21–24 for E; n = 3 for panel **(F)**]. Different letters above the columns indicate significant differences (one-way ANOVA, $p < 0.05$).

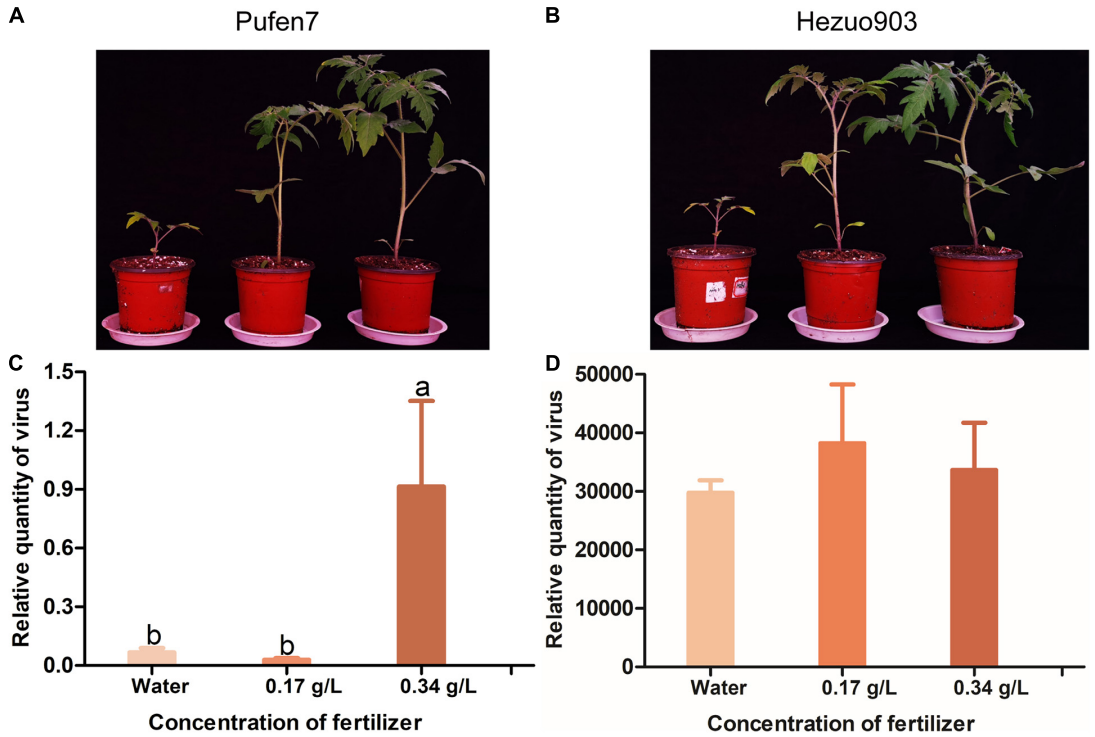

FIGURE 6 | Picture of tomato seedlings that were treated with water or solutions containing different concentration of fertilizer for 21 days and relative quantity of virus in these plants post agro-inoculation. **(A)** Pufen7 seedlings; **(B)** Hezuo903 seedlings; **(C)** Relative quantity of virus in Pufen7 plants; **(D)** Relative quantity of virus in Hezuo903 plants. Values are means ± SEM in panels **(C,D)** [n = 15 for panel **(C)** and 8 for panel **(D)**]. Different letters above the columns in panels **(C,D)** indicate significant differences (one-way ANOVA, $p < 0.05$).

higher in seedlings of 21 DPT than that in seedlings of 0 DPT (**Figures 8C,D**). Expression of gene *ICS1* in Pufen7 increased significantly at the early stages and then decreased to levels lower than that at 0 DPT (**Figure 8E**). *ICS1* expression in Hezuo903 decreased significantly from 0 to 14 DPT but then increased to a level similar to that at 0 DPT (**Figure 8F**). For *PAL*, its expression in Pufen7 increased significantly from 0 to 7 DPT but decreased thereafter (**Figure 8G**). *PAL* expression in Hezuo903 decreased significantly from 0 to 14 DPT and then increased to levels similar to that at 0 DPT (**Figure 8H**).

DISCUSSION

In this study, we explored the influence of basal resistance to TYLCV in tomato on ARR using three cultivars that differ in TYLCV resistance. Our data indicate: (1) virus quantity in plants mostly decreased with the increase of plant age at the initial inoculation (**Figures 3–5**), (2) ARR appeared more evident in cultivars with higher basal resistance (**Figures 3–5**), (3) tomato plants with higher biomass at inoculation contained similar or higher quantity of TYLCV later in the plants (**Figure 6**), and (4) virus source plants with a younger age at initial inoculation facilitated virus acquisition by whiteflies (**Figure 7**). In addition, our analysis on plant hormones suggest that endogenous SA and JA level increased with plant age (**Figure 8**).

In the management of TYLCV, resistance breeding by introgression of genes from wild relatives of tomato into cultivated tomato has been considered as one of the most effective strategies in combating TYLCV (Islam and Wu, 2017; Dhaliwal et al., 2019). As the genetic resources of resistance from wild relatives of tomato are limited (Dhaliwal et al., 2019), employment of ARR may facilitate better utilization of them. Here we found that ARR is more pronounced in tomato cultivars with higher basal resistance. Hence, ARR can be used in combination with resistance from other sources such as *Ty-1*, *Ty-2*, and *Ty-3* to obtain higher overall resistance. Moreover, even in the susceptible cultivar Hezuo903, reduced TYLCV quantity was observed with increased plant age at initial inoculation. The reduced TYLCV quantity may in turn reduce the subsequent spread of the virus by whitefly vectors. Therefore, maintaining tomato seedlings free of TYLCV to an older age in well-protected nurseries before transplanting into open fields can be a cost-effective measure in disease management (Riley and Srinivasan, 2019).

Since plants of different ages differ significantly in biomass and resistance to TYLCV, we sought to explore the contribution of biomass in ARR. Intriguingly, tomato plants of the same chronological age with higher biomass at inoculation contained similar or higher quantity of TYLCV later in the plants, indicating that increased biomass in older plants did not contribute to ARR. As regards one outlier with exceptionally high virus quantity in

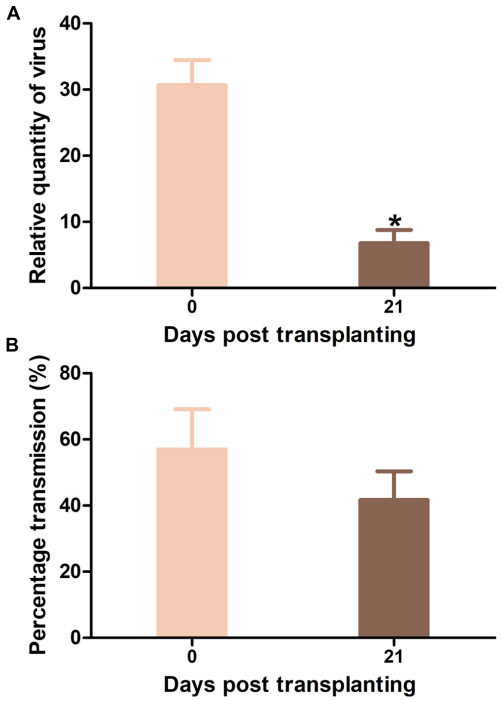

FIGURE 7 | Tomato yellow leaf curl virus (TYLCV) quantity in whiteflies and virus transmission efficiency by whiteflies when Hezou903 plants inoculated at 0 and 21 DPT were used as the source of inoculum. **(A)** TYLCV quantity in whiteflies; **(B)** TYLCV transmission efficiency by whiteflies. Values are means ± SEM (n = 4 for panel **(A)**; n = 3 and each replicate contains 8–9 test plants for panel **(B)**. *Above columns indicate significant differences (independent t-test, $p < 0.05$).

each of the three fertilizer treatments for Pufen7 (**Figure 6C**), we suspect that the Pufen7 seeds used in the experiment, which we obtained from a commercial source, may contain a small proportion of seeds that were partially susceptible to TYLCV.

As plants grow, substantial changes of many important traits, such as physical barriers, chemical defense and innate immunity may occur and contribute to ARR (Hu and Yang, 2019). For example, physical barriers contributed to ARR in potato against potato virus Y by modulating the systemic movement of virions in the foliage (Chikh-Ali et al., 2020). In cucumber fruit ARR against *Phytophthora capsici* can be attributable to the increases in transcriptional level of R-genes and activity of resistance related transcription factors (Mansfeld et al., 2020). Additionally, SA or other components in the SA-signaling pathway may contribute to ARR in *Arabidopsis thaliana* against several pathogens (Carviel et al., 2010; Wilson et al., 2017). Here, we analyzed the contents of SA and JA, two major defense-related plant hormones (Pieterse et al., 2012; Pan et al., 2021; Ye et al., 2021); we found that both endogenous SA and JA increased with plant age. Since SA is well-known for conferring resistance against biotrophic pathogens such as viruses (Pieterse et al., 2012; Pan et al., 2021; Ye et al., 2021), we propose that SA may play a major role in ARR against TYLCV in tomato plants. However, whether JA contribute to ARR against TYLCV warrants further investigations. Further, gene expression analysis was conducted to determine whether increase in plant hormone level resulted from increase in expression level of plant hormone biosynthesis genes. So far, two SA biosynthesis pathways have been identified in plants, namely phenylalanine ammonia lyase (PAL)-mediated phenylalanine pathway and isochorismate synthase (ICS)-mediated isochorismate pathway (An and Mou, 2011; Chen et al., 2020). In the present study, we found that the relative expression level of *ICS1* and *PAL* did not increase appreciably when tomato plants became older, suggesting that the increased SA contents in older plants may be due to the accumulation of this hormone in plants during development.

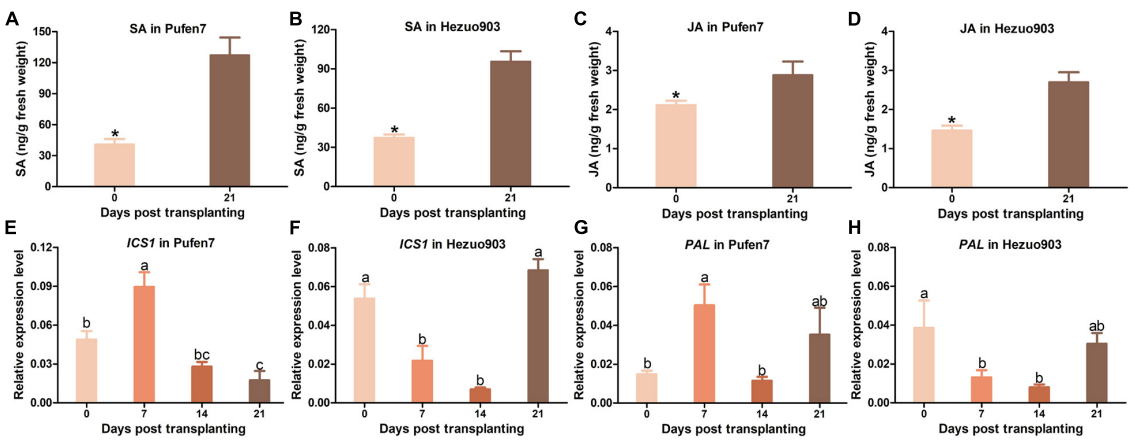

FIGURE 8 | Contents of salicylic acid (SA) and jasmonates (JA) and relative expression of SA biosynthesis genes in Pufen7 and Hezuo903 seedlings. **(A)** Contents of SA in Pufen7 seedlings of 0 and 21 DPT; **(B)** Contents of SA in Hezuo903 seedlings; **(C)** Contents of JA in Pufen7 seedlings; **(D)** Contents of JA in Hezuo903 seedlings; **(E)** Relative expression level of *ICS1* in Pufen7 seedlings of 0, 7, 14, and 21 DPT; **(F)** Relative expression level of *ICS1* in Hezuo903 seedlings; **(G)** Relative expression level of *PAL* in Pufen7 seedlings; **(H)** Relative expression level of *PAL* in Hezuo903 seedlings. Values are means ± SEM [n = 4 for panels **(A,B)**; n = 9–10 for panels **(C,D)**; n = 6 for panels **(E–H)**]. * above columns in panels **(A–D)** and different letters in panels **(E–H)** indicate significant differences among plants of different ages [independent t-test, $p < 0.05$ for panels **(A–D)**; one-way ANOVA, $p < 0.05$ for panels **(E–H)**].

SA is produced in a wide range of prokaryotic and eukaryotic organisms (An and Mou, 2011). In plants, SA plays important roles in regulating many biological processes including growth and immune response (Koo et al., 2020). In the SA-signaling pathway, SA binds to two classes of receptors NPR1 and NPR3/NPR4, thereby regulating the expression of downstream genes (Liu et al., 2020). So far, three main stages of plant-virus interactions, namely intercellular trafficking, long-distance movement and replication of viruses, have been found to be regulated by SA (Zhao and Li, 2021). In addition, SA may modulate plant-virus interactions indirectly by affecting other antiviral pathways such as RNA silencing, pathogen-associated molecular pattern-triggered and effector-triggered immunity (Campos et al., 2014; Yang et al., 2015; Palukaitis and Yoon, 2020). Here we found that SA may directly contribute to ARR in tomato against TYLCV. However, how SA modulates resistance in an age-dependent manner warrants further investigations.

Taken together, we have found that ARR against TYLCV in tomato plants is more evident in plants with higher basal resistance. We revealed that plant biomass does not contribute to ARR in tomato against TYLCV, but virus source plants with a younger age at initial inoculation facilitates virus acquisition by whiteflies. We also showed that SA may directly contribute to ARR. Our findings provide new knowledge of ARR in tomato against TYLCV as well as clues for the deployment of ARR in the management of diseases caused by TYLCV.

DATA AVAILABILITY STATEMENT

The original contributions presented in the study are included in the article/**Supplementary Material**, further inquiries can be directed to the corresponding author.

AUTHOR CONTRIBUTIONS

J-RZ, S-SL, and L-LP contributed to conception and design of the study. J-RZ and L-LP performed the experiments. J-RZ performed the statistical analysis. J-RZ wrote the first draft of the manuscript. S-SL and L-LP revised the manuscript. All authors contributed to manuscript revision, read, and approved the submitted version.

FUNDING

Financial support for this study was provided by the earmarked fund for China Agricultural Research System (Grant Number: CARS-23-D07) and Fundamental Research Funds for the Central Universities (Grant Number: K20210058).

ACKNOWLEDGMENTS

We thank Myron Zalucki, the University of Queensland, Australia for his help in revising the manuscript. We also thank Xiao-Dan Wu of the Analysis Center of Agrobiology and Environmental Sciences of Zhejiang University for assistance in analyzing SA and JA contents.

SUPPLEMENTARY MATERIAL

The Supplementary Material for this article can be found online at: https://www.frontiersin.org/articles/10.3389/fpls.2021.685382/full#supplementary-material

REFERENCES

Al-Shihi, A. A., Al-Sadi, A. M., Al-Said, F. A., Ammara, U. E., and Deadman, M. L. (2016). Optimising the duration of floating row cover period to minimise the incidence of tomato yellow leaf curl disease and maximise yield of tomato. *Ann. Appl. Biol.* 168, 328–336. doi: 10.1111/aab.12266

An, C., and Mou, Z. (2011). Salicylic acid and its function in plant immunity. *J. Integr. Plant Biol.* 53, 412–428. doi: 10.1111/j.1744-7909.2011.01043.x

Basit, M. (2019). Status of insecticide resistance in *Bemisia tabaci*: resistance, cross-resistance, stability of resistance, genetics and fitness costs. *Phytoparasitica* 47, 207–225. doi: 10.1007/s12600-019-00722-5

Beaudoin, A. L. P., Kahn, N. D., and Kennedy, G. G. (2009). Bell and banana pepper exhibit mature-plant resistance to tomato spotted wilt tospovirus transmitted by *Frankliniella fusca* (Thysanoptera: Thripidae). *J. Econ. Entomol.* 102, 30–35. doi: 10.1603/029.102.0105

Ben-Yakir, D., Antignus, Y., Offir, Y., and Shahak, Y. (2012). Colored shading nets impede insect invasion and decrease the incidences of insect-transmitted viral diseases in vegetable crops. *Entomol. Exp. Appl.* 144, 249–257. doi: 10.1111/j.1570-7458.2012.01293.x

Byamukama, E., Robertson, A. E., and Nutter, F. W. (2015). Bean pod mottle virus time of infection influences soybean yield, yield components, and quality. *Plant Dis.* 99, 1026–1032. doi: 10.1094/PDIS-11-14-1107-RE

Campos, L., Granell, P., Tarraga, S., Lopez-Gresa, P., Conejero, V., Bellés, J. M., et al. (2014). Salicylic acid and gentisic acid induce RNA silencing-related genes and plant resistance to RNA pathogens. *Plant Physiol. Bioch.* 77, 35–43. doi: 10.1016/j.plaphy.2014.01.016

Carviel, J. L., Al-Daoud, F., Neumann, M., Mohammad, A., Provart, N. J., and Moeder, W. (2010). Forward and reverse genetics to identify genes involved in the age-related resistance response in *Arabidopsis thaliana*. *Mol. Plant Pathol.* 10, 621–634. doi: 10.1111/J.1364-3703.2009.00557.X

Chen, J., Clinton, M., Qi, G., Wang, D. W., Liu, F. Q., and Fu, Z. Q. (2020). Reprogramming and remodeling: transcriptional and epigenetic regulation of salicylic acid-mediated plant defense. *J. Exp. Bot.* 71, 5256–5268. doi: 10.1093/jxb/eraa072

Chikh-Ali, M., Tran, L. T., Price, W. J., and Karasev, A. V. (2020). Effects of the age-related resistance to potato virus Y in potato on the systemic spread of the virus, incidence of the potato tuber necrotic ringspot disease, tuber yield, and translocation rates into progeny tubers. *Plant Dis.* 104, 269–275. doi: 10.1094/PDIS-06-19-1201-RE

Cohen, S., and Harpaz, I. (1964). Periodic, rather than continual acquisition of a new tomato virus by its vector, the tobacco whitefly (*Bemisia tabaci* Gennadius). *Entomol. Exp. Appl.* 7, 155–166. doi: 10.1007/BF00305053

Dhaliwal, M. S., Jindala, S. K., Sharmaa, A., and Prasannab, H. C. (2019). Tomato yellow leaf curl virus disease of tomato and its management through resistance breeding: a review. *J. Hortic. Sci. Biotech.* 95, 425–444. doi: 10.1080/14620316.2019.1691060

Fiallo-Olivé, E., Pan, L. L., Liu, S. S., and Navas-Castillo, J. (2020). Transmission of begomoviruses and other whitefly-borne viruses: dependence on the vector species. *Phytopathology* 110, 10–17. doi: 10.1094/PHYTO-07-19-0273-FI

Gilbertson, R. L., Batuman, O., Webster, C. G., and Adkins, S. (2015). Role of the insect supervectors *Bemisia tabaci* and *Frankliniella occidentalis* in the

emergence and global spread of plant viruses. *Annu. Rev. Virol.* 2, 67–93. doi: 10.1146/annurev-virology-031413-085410

Hu, L., and Yang, L. (2019). Time to fight: molecular mechanisms of age-related resistance. *Phytopathology* 109, 1500–1508. doi: 10.5423/PPJ.RW.12.2019.0295

Islam, W., and Wu, Z. J. (2017). Genetic defense approaches against begomoviruses. *J. Appl. Virol.* 6, 26–49. doi: 10.21092/jav.v6i3.81

Jones, R. A. C. (2020). Disease pandemics and major epidemics arising from new encounters between indigenous viruses and introduced crops. *Viruses* 12:1388. doi: 10.3390/v12121388

Koo, Y. M., Heo, A. Y., and Choi, H. W. (2020). Salicylic acid as a safe plant protector and growth regulator. *Plant Pathol. J.* 36, 1–10. doi: 10.5423/PPJ.RW.12.2019.0295

Lefeuvre, P., Martin, D. P., Harkins, G., Lemey, P., Gray, A. J. A., Meredith, S., et al. (2010). The spread of tomato yellow leaf curl virus from the Middle East to the world. *PLoS Pathog.* 6:e1001164. doi: 10.1371/journal.ppat.1001164

Levy, D., and Lapidot, M. (2008). Effect of plant age at inoculation on expression of genetic resistance to tomato yellow leaf curl virus. *Arch. Virol.* 153, 171–179. doi: 10.1007/s00705-007-1086-y

Liu, Y., Sun, T., Sun, Y., Zhang, Y., Radojicic, A., Ding, Y., et al. (2020). Diverse roles of the salicylic acid receptors NPR1 and NPR3/NPR4 in plant immunity. *Plant Cell* 32, 4002–4016. doi: 10.1105/tpc.20.00499

Mabvakure, B., Martin, D. P., Kraberger, S., Cloete, L., Brunschot, S. V., Geering, A. D. W., et al. (2016). Ongoing geographical spread of tomato yellow leaf curl virus. *Virology* 498, 257–264. doi: 10.1016/j.virol.2016.08.033

Mansfeld, B. N., Colle, M., Zhang, C., Lin, Y. C., and Grumet, R. (2020). Developmentally regulated activation of defense allows for rapid inhibition of infection in age-related resistance to *Phytophthora capsici* in cucumber fruit. *BMC Genom.* 21:628. doi: 10.1186/s12864-020-07040-9

Moriones, E., Aramburu, J., Riudavets, J., Arnó, J., and Laviña, A. (1998). Effect of plant age at time of infection by tomato spotted wilt tospovirus on the yield of field-grown tomato. *Eur. J. Plant Pathol.* 104, 295–300. doi: 10.1023/A:1008698731052

Murphy, J. F., and Bowen, K. L. (2006). Synergistic disease in pepper caused by the mixed infection of cucumber mosaic virus and pepper mottle virus. *Phytopathology* 96, 240–247. doi: 10.1094/PHYTO-96-0240

Navas-Castillo, J., Fiallo-Olivé, E., and Sánchez-Campos, S. (2011). Emerging virus diseases transmitted by whiteflies. *Annu. Rev. Phytopathol.* 49, 219–248. doi: 10.1146/annurev-phyto-072910-095235

Osterbaan, L. J., and Fuchs, M. (2019). Dynamic interactions between plant viruses and their hosts for symptom development. *J. Plant Pathol.* 101, 885–895. doi: 10.1007/s42161-019-00323-5

Palukaitis, P., and Yoon, J. Y. (2020). R gene mediated defense against viruses. *Curr. Opin. Virol.* 45, 1–7. doi: 10.1016/j.coviro.2020.04.001

Pan, L. L., Chen, Q. F., Zhao, J. J., Guo, T., Wang, X. W., Hariton-Shalev, A., et al. (2017). Clathrin-mediated endocytosis is involved in tomato yellow leaf curl virus transport across the midgut barrier of its whitefly vector. *Virology* 502, 152–159. doi: 10.1016/j.virol.2016.12.029

Pan, L. L., Miao, H. Y., Wang, Q. M., Walling, L. L., and Liu, S. S. (2021). Virus-induced phytohormone dynamics and their effects on plant-insect interactions. *New Phytol.* 230, 1305–1320. doi: 10.1111/nph.17261

Panter, S. N., and Jones, D. A. (2002). Age-related resistance to plant pathogens. *Adv. Bot. Res.* 38, 251–280. doi: 10.1016/S0065-2296(02)38032-7

Pieterse, C. M., Van der Does, D., Zamioudis, C., Leon-Reyes, A., and Van Wees, S. C. (2012). Hormonal modulation of plant immunity. *Annu. Rev. Cell Dev. Biol.* 28, 489–521. doi: 10.1146/annurev-cellbio-092910-154055

Polston, J. E., and Anderson, P. K. (1997). The emergence of whitefly-transmitted geminiviruses in tomato in the western hemisphere. *Plant Dis.* 81, 1358–1369. doi: 10.1094/PDIS.1997.81.12.1358

Prasad, A., Sharma, N., Hari-Gowthem, G., Muthamilarasan, M., and Prasad, M. (2020). Tomato yellow leaf curl virus: impact, challenges, and management. *Trends Plant Sci.* 25, 897–911. doi: 10.1016/j.tplants.2020.03.015

Qin, L., Wang, J., Bing, X. L., and Liu, S. S. (2013). Identification of nine cryptic species of *Bemisia tabaci* (Hemiptera: Aleyrodidae) (in Chinese with English abstract) from China by using the mtCOI PCR-RFLP technique. *Acta Entomol. Sin.* 56, 186–194. Available at: http://www.insect.org.cn/CN/Y2013/V56/I2/186

Riley, D. G., and Srinivasan, R. (2019). Integrated management of tomato yellow leaf curl virus and its whitefly vector in tomato. *J. Econ. Entomol.* 112, 1526–1540. doi: 10.1093/jee/toz051

Rojas, M. R., Macedo, M. A., Maliano, M. R., Soto-Aguilar, M., Souza, J. O., Briddon, R. W., et al. (2018). World management of geminiviruses. *Annu. Rev. Phytopathol.* 56, 637–677. doi: 10.1146/annurev-phyto-080615-100327

Ruan, Y. M., Luan, J. B., Zang, L. S., and Liu, S. S. (2007). Observing and recording copulation events of whiteflies on plants using a video camera. *Entomol. Exp. Appl.* 124, 229–233. doi: 10.1111/j.1570-7458.2007.00575.x

Torre, C., Donaire, L., Gómez-Aix, C., Juárez, M., Peterschmitt, M., Urbino, C., et al. (2018). Characterization of begomoviruses sampled during severe epidemics in tomato cultivars carrying the Ty-1 gene. *Int. J. Mol. Sci.* 19:2614. doi: 10.3390/ijms19092614

Vandesompele, J., Preter, K. D., Pattyn, F., Poppe, B., Roy, N. V., Paepe, A. D., et al. (2002). Accurate normalization of real-time quantitative RT-PCR data by geometric averaging of multiple internal control genes. *Genom. Biol.* 3:research0034.1. doi: 10.1186/gb-2002-3-7-research0034

Velásquez, A. C., Castroverde, C. D. M., and He, S. Y. (2018). Plant-pathogen warfare under changing climate conditions. *Curr. Biol.* 28, 619–634. doi: 10.1016/j.cub.2018.03.054

Wang, X. W., and Blanc, S. (2021). Insect transmission of plant single-stranded DNA viruses. *Annu. Rev. Entomol.* 66, 389–405. doi: 10.1146/annurev-ento-060920-094531

Wilson, D. C., Kempthorne, C. J., Carella, P., Liscombe, D. K., and Cameron, R. K. (2017). Age-related resistance in Arabidopsis thaliana involves the MADS-domain transcription factor SHORT VEGETATIVE PHASE and direct action of salicylic acid on *Pseudomonas* syringae. *Mol. Plant Microbe Interact.* 30, 919–929. doi: 10.1094/MPMI-07-17-0172-R

Wu, J. B., Dai, F. M., and Zhou, X. P. (2006). First report of tomato yellow leaf curl virus in China. *Plant Dis.* 90:1359. doi: 10.1094/PD-90-1359C

Yang, Y. X., Ahammed, G., Wu, C., Fan, S. Y., and Zhou, Y. H. (2015). Crosstalk among jasmonate, salicylate and ethylene signaling pathways in plant disease and immune responses. *Curr. Protein Pept. Sci.* 16, 450–461. doi: 10.1016/j.tplants.2020.10.009

Ye, J., Zhang, L., Zhang, X., Wu, X., and Fang, R. (2021). Plant defense networks against insect-borne pathogens. *Trends Plant Sci.* 26, 272–287. doi: 10.1016/j.tplants.2020.10.009

Zhao, S. S., and Li, Y. (2021). Current understanding of the interplays between host hormones and plant viral infections. *PLoS Pathog.* 17:e1009242. doi: 10.1371/journal.ppat.1009242

Conflict of Interest: The authors declare that the research was conducted in the absence of any commercial or financial relationships that could be construed as a potential conflict of interest.

Publisher's Note: All claims expressed in this article are solely those of the authors and do not necessarily represent those of their affiliated organizations, or those of the publisher, the editors and the reviewers. Any product that may be evaluated in this article, or claim that may be made by its manufacturer, is not guaranteed or endorsed by the publisher.

frontiers in Microbiology

REVIEW
published: 04 August 2021
doi: 10.3389/fmicb.2021.686025

Occurrence, Distribution, Evolutionary Relationships, Epidemiology, and Management of Orthotospoviruses in China

Zhongkai Zhang, Kuanyu Zheng, Lihua Zhao, Xiaoxia Su, Xue Zheng and Tiantian Wang*

Key Lab of Agricultural Biotechnology of Yunnan Province, Biotechnology and Germplasm Resources Research Institute, Yunnan Academy of Agricultural Sciences, Kunming, China

Orthotospoviruses are responsible for serious crop losses worldwide. Orthotospoviral diseases have spread rapidly in China over the past 10 years and are now found in 19 provinces. Currently, 17 *Orthotospovirus* species have been reported in China, including eight newly identified species from this genus. The number of new highly pathogenic *Orthotospovirus* strains or species has increased, likely because of the virus species diversity, the wide range of available hosts, adaptation of the viruses to different climates, and multiple transmission routes. This review describes the distribution of *Orthotospovirus* species, host plants, typical symptoms of infection under natural conditions, the systemic infection of host plants, spatial clustering characteristics of virus particles in host cells, and the orthotospoviral infection cycle in the field. The evolutionary relationships of orthotospoviruses isolated from China and epidemiology are also discussed. In order to effectively manage orthotospoviral disease, future research needs to focus on deciphering the underlying mechanisms of systemic infection, studying complex/mixed infections involving the same or different *Orthotospovirus* species or other viruses, elucidating orthotospovirus adaptative mechanisms to multiple climate types, breeding virus-resistant plants, identifying new strains and species, developing early monitoring and early warning systems for plant infection, and studying infection transmission routes.

Keywords: *Orthotospovirus*, species diversity, systemic infection, multiple transmission routes, monitoring and early warning

OPEN ACCESS

Edited by:
Xiaofei Cheng,
Northeast Agricultural University, China

Reviewed by:
Xiaorong Tao,
Nanjing Agricultural University, China
Nagendran Krishnan,
Indian Institute of Vegetable Research (ICAR), India

****Correspondence:***
Zhongkai Zhang
zhongkai99@sina.com

Specialty section:
This article was submitted to Virology, a section of the journal Frontiers in Microbiology

Received: *26 March 2021*
Accepted: *25 June 2021*
Published: *04 August 2021*

Citation:
Zhang Z, Zheng K, Zhao L, Su X, Zheng X and Wang T (2021) Occurrence, Distribution, Evolutionary Relationships, Epidemiology, and Management of Orthotospoviruses in China. Front. Microbiol. 12:686025. doi: 10.3389/fmicb.2021.686025

INTRODUCTION

Orthotospoviruses have a worldwide distribution and cause serious economic losses in a variety of crops (Komoda et al., 2017). Before 2017, orthotospoviruses were considered to be part of the genus *Tospovirus* in the family Bunyaviridae and were divided into seven or nine serogroups based on serology (Chen et al., 2012b, 2016). However, in 2020, the International Committee on Taxonomy of Viruses (ICTV) announced that the genus *Orthotospovirus* belongs to the family Tospoviridae, order Bunyavirales, class Ellioviricetes, realm Riboviria, subphylum Polyploviricotina, phylum Negarnaviricota, and kingdom Orthornavirae (Hong et al., 2020).

As with other members of the order Bunyavirales, orthotospovirus particles are spherical, and multi-virions form aggregations in host-derived vesicles. Mature virions range in diameter from 80 to 120 nm. The surface of the virions is composed mainly of two glycoproteins (Gn and Gc), which are responsible for the virus acquisition and transmission by the thrips vectors. The core

of the virion contains three viral RNA fragments, named L RNA, M RNA, and S RNAs according to their lengths, encapsulated by the nucleocapsid protein (N). The orthotospovirus are single-negative-stranded, ambisense RNA viruses. The L RNA (∼8.9 kb) encodes the RNA-dependent RNA polymerase (RdRp) in the complementary (vcRNA) strand; M RNA (∼4.8 kb) encodes the movement protein (NSm) in the viral (vRNA) strand and the Gn and Gc proteins in the vcRNA strand; and RNA S (∼2.9 kb) encodes the N protein in the vcRNA and silencing suppressor (NSs) in the vRNA strand (Oliver and Whitfield, 2016).

To date, many articles have illustrated details of the global occurrence, epidemiology, and molecular interactions between orthotospoviruses and their thrips vectors (Pappu et al., 2009; Oliver and Whitfield, 2016). In this article, we will summarize the latest research progress on species diversity, occurrence, distribution, epidemiology, and management of orthotospoviruses in China.

SYMPTOMATOLOGY

Symptoms of orthotospoviral disease in host plants are very similar, with only minor differences between species of virus. The major symptoms are ringspots (including chlorotic, yellow, necrotic, and zonate spots), bud necrosis, silver mottle, and vein banding. Zonate spots are characteristic of orthotospovirus infection. Although symptoms vary between disease stages, chlorotic, yellow, and necrotic ringspots can occur at all stages (early, middle, and late). Herbaceous plants with severe disease die in the late stage. The symptoms occur in the leaves and fruit, with a few cases of stem necrosis (**Figure 1**).

HOST RANGE

The host range of orthotospovirus has expanded from crops to other plants, including weeds such as *Bidens bipinnata* (Zhang et al., 2020) and even to woody plants such as kiwifruit, mulberry, and macadamia nut (Fang et al., 2013; Meng et al., 2015; Wang et al., 2016). Orthotospoviral diseases in China mainly involve diseases of vegetables, fruits, tobacco, groundnuts, and ornamental plants, including crops of the families Solanaceae, Cucurbitaceae, Asteraceae, Brassicaceae, Fabaceae, Orchidaceae, and Amaryllidaceae (Alliaceae), weeds (such as *B. bipinnata* L.), and woody plants (such as kiwifruit, macadamia nut, and mulberry) (**Table 1**).

DIVERSITY AND EVOLUTIONARY RELATIONSHIPS

There are currently 30 *Orthotospovirus* species known worldwide, comprising 11 definitive species (written in italics) and 19 tentative species (written in upright letters) (**Figure 2A**; International Committee on Taxonomy of Viruses Executive Committee [ICTVEC], 2020; Zheng et al., 2020). Orthotospoviruses can be divided into five phylogenetic clades based on the amino acid sequence of nucleocapsid (N) protein (**Figure 2A**), namely the *tomato spotted wilt orthotospovirus* (TSWV) clade, *watermelon silver mottle orthotospovirus* (WSMoV) clade, soybean vein necrosis-associated orthotospovirus (SVNV) clade, *iris yellow spot orthotospovirus* (IYSV) clade, and *groundnut yellow spot orthotospovirus* (GYSV) clade (Peng et al., 2011; Oliver and Whitfield, 2016). Based on the geography of the recent epidemics, viruses from the WSMoV and IYSV clades are mainly found in Asia and Europe (**Figure 3A**). Viruses from the WSMoV clade are most commonly found in East Asia and mainly infect crops in the families Solanaceae, Cucurbitaceae, and Asteraceae, with several new species from this clade reported in recent years (Dong et al., 2008; Yin et al., 2014b; Zheng et al., 2017, 2020). Viruses from the IYSV clade are mainly found in Central Asia and Europe. Some of the species in this clade, including IYSV and tomato yellow ring orthotospovirus (TYRV), were originally isolated from plants in the Middle East but have become endemic in Europe in recent years (Bag et al., 2015; Zarzynska-Nowak et al., 2016). Viruses in the GYSV clade, which is also Asian, have been reported from Taiwan province, China, and India (Satyanarayana et al., 1996; Chao et al., 2001). The SVNV and TSWV clades belong to the group found in the Americas. Soybean vein necrosis-associated orthotospovirus (SVNV) and bean necrotic mosaic orthotospovirus (BeNMV), two species in the SVNV clade, have been reported to infect bean plants in the United States and Brazil (Zhou et al., 2011; de Oliveira et al., 2012). Several members of the TSWV clade were originally found in the Americas (Torres et al., 2012; Webster et al., 2015). However, TSWV, which belongs to the TSWV clade, is now widely distributed throughout the world, and indeed is considered to be the most harmful of the *Orthotospovirus* species, causing great damage and large crop losses globally (Pappu, 2008; Pappu et al., 2009).

The country from which the largest number of *Orthotospovirus* species has been reported is China. A total of 17 *Orthotospovirus* species are known in China to date (**Table 1**), comprising 8 definitive and 10 tentative species. These species belong to four phylogenetic clades (TSWV, WSMoV, IYSV, and GYSV) (**Figure 2B**). Of the *Orthotospovirus* clades found in China, the WSMoV clade is the most diverse. Several new virus species in this clade have been reported for the first time in China (Dong et al., 2008; Yin et al., 2014b; Zheng et al., 2017, 2020), and it has been speculated that the WSMoV clade originated in China. TSWV, which belongs to the Americas group (Pappu et al., 2009), has become the virus posing the largest threat to agricultural production in China. Compared with native WSMoV clade viruses, TSWV has wider geographical adaptability (**Figure 3B**), and evidence of adaptive evolution of TSWV in China can be found in the phylogenetic analysis of TSWV *N* gene diversity (Mao et al., 2019; Liu et al., 2021).

OCCURRENCE AND GEOGRAPHICAL DISTRIBUTION

Before 2000, only two *Orthotospovirus* species had been reported from China. The earliest record of TSWV symptoms in peanuts was published in 1986 by Xu in Guangdong and Guangxi

FIGURE 1 | Typical symptoms of host plants infected with orthotospoviruses under natural field conditions. **(A)** Zonate spot in leaf of chili pepper (*Capsicum annuum* L.) infected with tomato zonate spot orthotospovirus (TZSV). **(B)** Necrotic spot in leaf of macadamia nut (*Macadamia ternifolia* F. Muell.) infected with *watermelon silver mottle virus* (WSMoV) serogroup member. **(C)** Yellow spot and ringspot in tomato (*Solanum lycopersicum* L.) infected with *tomato spotted wilt orthotospovirus* (TSWV). **(D)** Necrotic zonate spot in tomato infected with tomato necrotic spot-associated orthotospovirus (TNSaV). **(E)** Chlorotic spot in sweet pepper (*C. annuum* L.) infected with TZSV. **(F)** Necrotic ringspot in potato (*Solanum tuberosum* L.) infected with TZSV.

provinces (Xu et al., 1986). Subsequently, TSWV-like virus particles were observed using transmission electron microscopy in tomato and tobacco from Sichuan and Yunnan provinces (Su et al., 1987; Yao, 1992; Zhang et al., 1998). WSMoV was first reported in Taiwan and identified as a new *Orthotospovirus* species through sequencing analysis (Chu and Yeh, 1998).

After 2000, the new *Orthotospovirus* species tomato zonate spot orthotospovirus (TZSV) was reported in tomatoes from Yunnan province, based on whole-genome sequencing and viral particle clustering characteristics in host cells (Dong et al., 2008). TZSV has a wide host range, causing harm in tomato, pepper, tobacco, and other crops, and it is now the dominant *Orthotospovirus* species found in these crops in Yunnan province (Huang et al., 2015; Zheng et al., 2015c).

Different *Orthotospovirus* species have been reported from different provinces, but TSWV is currently spreading rapidly from the south to the north of China. A total of 17 *Orthotospovirus* species have been reported from 19 Chinese provinces (**Table 1** and **Figure 3B**). Yunnan has extremely high *Orthotospovirus* diversity, with 13 species identified, while most other Chinese provinces harbor only one or two *Orthotospovirus* species. Of all the *Orthotospoviruses*, TSWV has the most extensive distribution, occurring in 18 provinces to date (**Table 1** and **Figure 3B**).

Yunnan has a high incidence of orthotospoviral disease, with diverse species of viruses and host plants, and a wide distribution. We identified 13 *Orthotospovirus* species from areas with very different climates (including tropical, subtropical, temperate, and cold temperate) (**Figure 3C**) and more than 20 species of natural host plants in Yunnan. The natural host range included most of the plants in China known to become infected with orthotospoviruses (**Table 1**). The orthotospoviruses isolated from Yunnan belonged to four phylogenetic clades, with the majority (seven species) belonging to the WSMoV clade. Three new *Orthotospovirus* species were first reported in Yunnan: TZSV (Dong et al., 2008), hippeastrum chlorotic

TABLE 1 | Orthotospoviruses reported by China.

Phylogenetic clade[a]	Species[b]	Abbreviation	Region	Host	Citations
WSMoV	Calla lily chlorotic spot orthotospovirus	CCSV	Taiwan, Zhejiang, Yunnan	Calla lilies (*Zantedeschia* sp.), Celtuce (*Lactuca sativa* var. *augustana*), Tobacco (*Nicotiana tabacum* L.)	Chen et al., 2005; Liu et al., 2012; Wu et al., 2018
WSMoV	Capsicum chlorosis orthotospovirus	CaCV	Taiwan, Sandong, Yunnan, Hubei, Guangdong	Phalaenopsis (*Phalaenopsis aphrodite Rchb.* F.), Calla lilies, Peanut (*Arachis hypogaea Linn.*), Tomato (*Lycopersicon esculentum* Mill.), Zucchini (*Cucurbita pepo* L.)	Chen et al., 2006, 2007, Chen et al., 2012a; Zheng et al., 2008; Huang et al., 2010; Yin et al., 2015; Sun et al., 2018
WSMoV	Mulberry vein banding orthotospovirus	MVBaV	Guangxi	Mulberry (*Morus alba* L.)	Meng et al., 2015.
WSMoV	Melon yellow spot orthotospovirus	MYSV	Taiwan, Guangdong, Hainan	Watermelon (*Citrullus lanatus* (Thunb.) Matsum. et Nakai), Cucumber (*Cucumis sativus* L.), Melon (*Cucumis melo* L.)	Chao et al., 2010; Chen et al., 2010; Liu et al., 2010; Peng et al., 2011
WSMoV	Pepper chlorotic spot orthotospovirus	PCSV	Taiwan, Yunnan	Sweet pepper (*Capsicum frutescens* L.), Chili pepper (*Capsicum annuum* L.)	Cheng et al., 2013; Zheng et al., 2017
WSMoV	Tomato necrotic spot-associated orthotospovirus	TNSaV	Guizhou	Tomato, Kiwifruit (*Actinidia* sp.)	Yin et al., 2014b; Wang et al., 2016; Zheng et al., 2016
WSMoV	Tomato zonate spot orthotospovirus	TZSV	Yunnan, Guangxi	Tomato, tabacco, Potato(*Solanum tuberosum* L.), Chili pepper, Iris tectorum (*Iris tectorum* Maxim.)	Dong et al., 2008; Cai et al., 2011; Li et al., 2014; Huang et al., 2015; Zheng et al., 2015a,c
WSMoV	Watermelon bud necrosis orthotospovirus	WBNV	Taiwan	Watermelon	Li et al., 2011
WSMoV	*Watermelon silver mottle orthotospovirus*	WSMoV	Taiwan, Yunnan, Guangdong,	Watermelon	Chu and Yeh, 1998; Chu et al., 2001; Rao et al., 2013; Yin et al., 2014a
WSMoV	Chili yellow ringspot orthotospovirus	CYRSV	Yunnan	Tomato, Chili Pepper	Zheng et al., 2020
TSWV	*Groundnut ringspot orthotospovirus*	GRSV	Yunnan	Potato	Ding et al., 2004
TSWV	*Impatiens necrotic spot orthotospovirus*	INSV	Taiwan, Yunnan	*Hippeastrum*.sp., Phalaenopsis, Dendrobium (*Dendrobium nobile*)	Adam et al., 1993; Zhang Q. et al., 2010
TSWV	*Tomato spotted wilt orthotospovirus*	TSWV	Yunnan, Taiwan, Beijing, Liaoning, Guangdong, Heilongjiang, Shaanxi, Ningxia, Sichuan, Qinghai, Shandong, Gansu, Guizhou, Tianjin, Chongqin, Hubei	Tomato, Watermelon, Peanut, *Chrysanthemum morifolium*, Chili pepper, Celtuce, *Allium sativum* L.Chinese, Parsley (*Petroselinum crispum*), Tobacco,Potato, *Pelargonium hortorum*, *Bidens bipinnata* L.	Adam et al., 1993; Zhang et al., 1998, 2017, 2020; Liu et al., 2010; Ren et al., 2014; Zheng et al., 2015b; Gao et al., 2016, 2020; Jie et al., 2017; Sun et al., 2017; Zhu et al., 2017; Song et al., 2019; Wang et al., 2019; Liu et al., 2019; Du et al., 2020; Jin et al., 2020; Wu et al., 2020; Zhang and Feng, 2020
IYSV	Hippeastrum chlorotic ringspot orthotospovirus	HCRV	Yunnan	*Hippeastrum* sp., *Zephyranthes candida*	Dong et al., 2013; Xu et al., 2013; Wu and Liu, 2017
IYSV	*Iris yellow spot orthotospovirus*	IYSV	Yunnan	Tobacoo	Wu and Liu, 2017
GYSV	Groundnut chlorotic fan-spot orthotospovirus	GCFSV	Taiwan,	Peanut	Chao et al., 2001
GYSV	*Groundnut yellow spot orthotospovirus*	GYSV	Yunnan	Chili pepper	Zhang Z. K. et al., 2010

[a] *List updated from clades defined by Peng et al. (2011) and Oliver and Whitfield (2016).*
[b] *Definitive species write in italics and tentative species write in upright letters.*

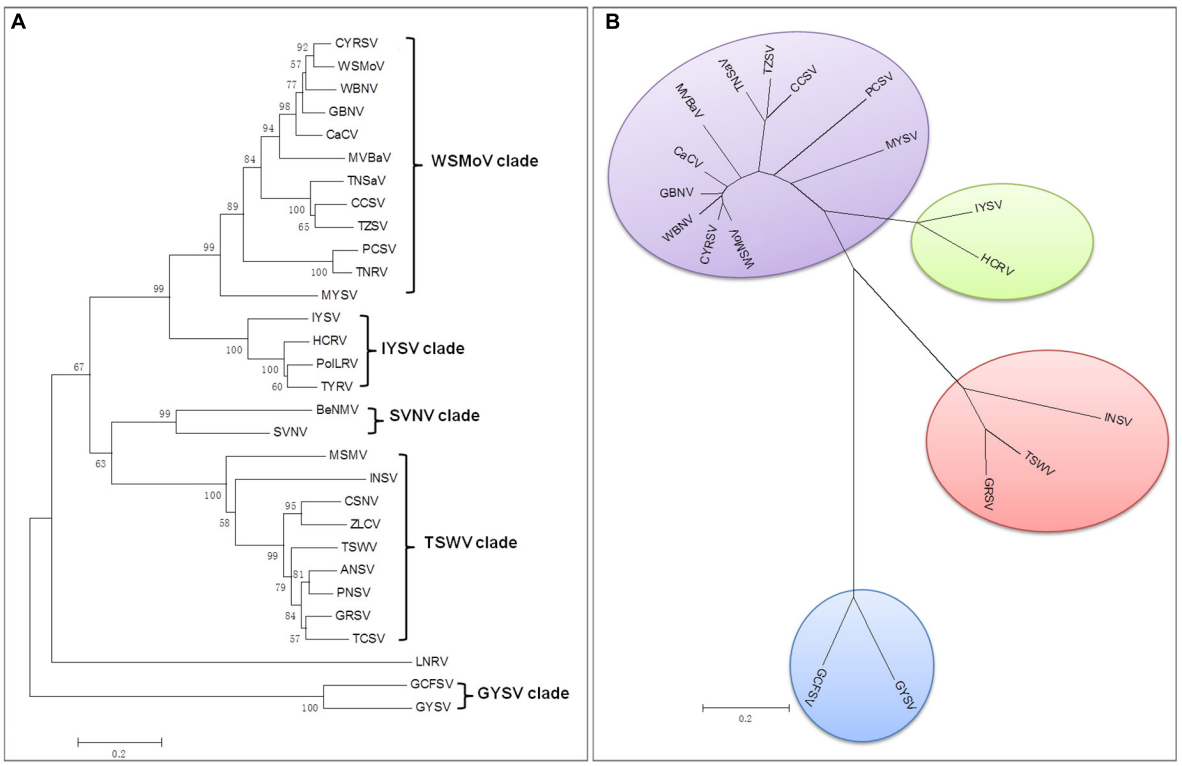

FIGURE 2 | Phylogenetic tree of orthotospoviruses based on the amino acid sequence of nucleocapsid (N) protein. **(A)** Phylogenetic tree of 30 orthotospoviruses reported worldwide. **(B)** Phylogenetic tree of the 17 orthotospoviruses reported from China. Bootstrap values on the branches represent support for the branches based on 1,000 bootstrap replicates. Definitive species are written in italics and tentative species are written in upright letters. Abbreviations (and NCBI no.): ANSV, Alstroemeria necrotic spot orthotospovirus (GQ478668); BeNMV, Bean necrotic mosaic orthotospovirus (NC_018071); CaCV, Capsicum chlorosis orthotospovirus (NC_008301); CCSV, Calla lily chlorotic spot orthotospovirus (AY867502); CSNV, Chrysanthemum stem necrosis orthotospovirus (NC_027719); CYRSV, Chili yellow ringspot orthotospovirus (MH779495); GBNV, *Groundnut bud necrosis orthotospovirus* (NC_003619); GRSV, *Groundnut ringspot orthotospovirus*; GYSV, *Groundnut yellow spot orthotospovirus* (AF013994); HCRV, Hippeastrum chlorotic ringspot orthotospovirus (KC290943); INSV, *Impatiens necrotic spot orthotospovirus* (NC_003624); IYSV, *Iris yellow spot orthotospovirus* (AF001387); LNRV, Lisianthus necrotic ringspot orthotospovirus (AB852525); MSMV, Melon severe mosaic orthotospovirus (EU275149); MVBaV, Mulberry vein banding associated orthotospovirus (KM819701); MYSV, Melon yellow spot orthotospovirus (AB038343); GCFSV, Groundnut chlorotic fan-spot orthotospovirus (AF080526); PCSV, Pepper chlorotic spot orthotospovirus (KF383956); PolRSV, *Polygonum ringspot orthotospovirus* (KF383956); PNSV, Pepper necrotic spot orthotospovirus (HE584762); SVNV, Soybean vein necrosis-associated orthotospovirus (HQ728387); TCSV, *Tomato chlorotic spot orthotospovirus* (S54325); TSWV, *Tomato spotted wilt orthotospovirus* (NC_002051); TNRV, Tomato necrotic ringspot orthotospovirus (FJ489600); TNSaV, Tomato necrotic spot-associated orthotospovirus (KM355773); TYRV, Tomato yellow ring orthotospovirus (AY686718); TZSV, Tomato zonate spot orthotospovirus (NC_010489); WBNV, *Watermelon bud necrosis orthotospovirus* (EU249351); WSMoV, *Watermelon silver mottle orthotospovirus* (NC_003843); and ZLCV, *Zucchini lethal chlorosis orthotospovirus* (AF067069).

ringspot orthotospovirus (HCRV; Dong et al., 2013), and chili yellow ringspot virus (CYRSV; Zheng et al., 2020). TSWV and TZSV were the dominant species, based on disease epidemics and severity (Zhang et al., 2016). The orthotospoviruses in Yunnan province have caused serious harm to crops including tomato, chili pepper, potato, and tobacco (Solanaceae); zucchini, watermelon, and squash (Cucurbitaceae); Phalaenopsis and Dendrobium (Orchidaceae); lettuce and chrysanthemum (Asteraceae); soybean and groundnut (Fabaceae), and more than 10 weed species.

TRANSMISSION

Orthotospoviruses are becoming more and more harmful due to their multiple transmission routes and wide host ranges. The main transmission routes under natural conditions are via the vector thrips, which are insects in the order *Thysanoptera.* More than 14 species of thrips are known to act as vectors for orthotospoviruses.

The thrips that are known to transmit orthotospovirus include *Ceratothrip oidesclaratris*, *Dictyothrips betae*, *Frankliniella occidentalis*, *Frankliniella schultzei*, *Frankliniella gemina*, *Frankliniella intonosa*, *Frankliniella cephalica*, *Frankliniella bispinosa*, *Frankliniella fusca*, *Frankliniella zucchini*, *Scirtothrips dorsalis*, *Neohydatothrips variabilis, Thrips palmi*, and *Thrips tabaci* (Pappu et al., 2009; Whitfield et al., 2015). A single *Orthotospovirus* species can be transmitted by one or many species of thrips (e.g., TSWV is transmitted by nine species of thrips). A single species of thrips can transmit one or many *Orthotospovirus* species (e.g., *F. occidentalis* can transmit five *Orthotospovirus* species) (Whitfield et al., 2015).

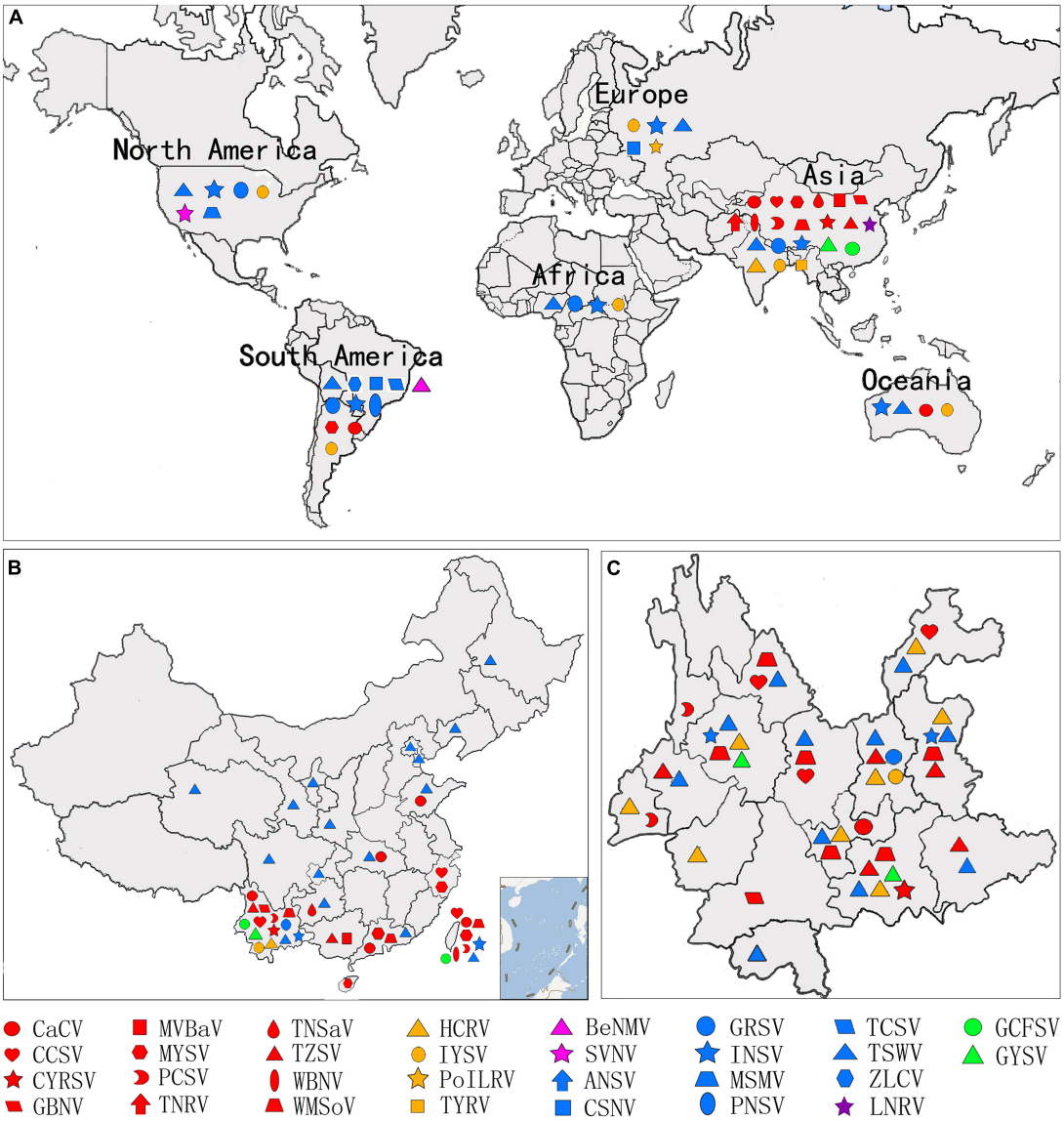

FIGURE 3 | Geographic distribution of orthotospoviruses. **(A)** Worldwide geographic distribution of orthotospoviruses. **(B)** Geographic distribution of orthotospoviruses in China. **(C)** Geographic distribution of orthotospoviruses in Yunnan province, China.

Besides transmission by thrips, other routes of transmission facilitate spread of orthotospoviruses. Orthotospoviruses such as SVNV spread through seeds (Groves et al., 2016). In addition, spreading seedings infected with orthotospoviruses is also an important source for the virus to spread in different places (Zhang et al., 2020). Weeds, as an important primary infection source, provide potential conditions for the secondary infection and outbreak of orthotospoviruses in the field.

EPIDEMIOLOGY

Orthotospoviruses have spread rapidly through China in recent years. Before 2015, orthotospoviral diseases mainly occurred in Southwest and Southeast China. However, over the last 5 years, orthotospoviral diseases have also occurred in Central, Northwest, and Northeast China. Although TSWV is the main epidemical *Orthotospovirus* species, we have recently found WSMoV, TZSV, and HCRV in Tibet, Hainan, and other Chinese provinces. Orthotospoviruses tend to quickly replace other viral pathogens (such as tobacco mosaic virus and cucumber mosaic virus) or form complex/mixed infections with other viruses (such as potato virus Y and whitefly transmitted geminivirus) in solanaceous crops, based on our research results over the past 20 years in Yunnan province.

The main reasons for the rapid expansion of *Orthotospovirus* species, especially TSWV, in China are as follows: (1) Over the last 20 years, the rapid popularization and development

of greenhouses in China has provided perfect conditions for the propagation of the vector insects, thrips. Particularly in the north of China, greenhouses provide suitable temperatures for the overwintering of the virus-transmitting thrips, and indeed the orthotospoviral diseases in most northern provinces occur mainly in greenhouses (Jie et al., 2017; Liu et al., 2021). In southern China, as well as the greenhouse-thrips-vegetables infection pathway, a secondary infection cycle can be formed by weeds and other intermediate hosts, and weeds also provide thrips with overwintering habitats (Zhang et al., 2020). (2) Changes in planting structure have also led to the rapid expansion of TSWV. With the popularization of greenhouses, monocultures of a single crop variety with susceptibility to orthotospoviruses, such as pepper, tomato, and other Solanaceous crops, have been planted in large quantities (Miao, 2018). This is particularly obvious in Yunnan province, where the planting structure, which usually includes flowers, tomatoes, peppers, tobacco, and potatoes, provides very favorable conditions for the reproduction of the thrips population and susceptibility to orthotospoviruses (Zhao et al., 2021).

HISTOPATHOLOGICAL ASPECTS

Orthotospoviruses in host cells have distinct histopathological characteristics that mainly relate to the virus species rather than to the host plant species, and these characteristics have important diagnostic value. The histopathological characteristics differ between the different stages of infection. In general, at 3 days post inoculation (dpi), there are a large number of vesicles in the host cells. At 7 dpi, virus particles form in the vesicles. At this stage (in the early stages of infection), double-enveloped virions (DEV) are also observed in host cells. At 9 dpi, virus particle aggregates appear in the host cells. By 12 dpi (in the late stages of infection), the cells are filled with virus particles (Zhang, 2015).

The virus particle clustering characteristics differ among *Orthotospovirus* species. TSWV virus particles always cluster in the endoplasmic reticulum (ER) or in special vesicles (based on transmission electron microscopy of ultrathin sections or negative staining). TZSV virus particles usually cluster in a moniliform structure in the ER membrane (vertical section) or as double-enveloped virions (cross-section) (Zhang et al., 2016). WSMoV virus particles always cluster in vesicles connected to other empty vesicles or in host cell vacuoles (unpublished data). *Impatiens necrotic spot orthotospovirus* (INSV) virus particles usually cluster in the lumen of the ER (Zhang Z. K. et al., 2010; **Figure 4**). Although these virus particle clustering characteristics are not necessarily unique to these viruses in the host cells, histopathological ultrastructure characteristics can help to identify *Orthotospovirus* species.

Systemic Infection

To establish a systemic infection in a host plant, the TSWV ribonucleoprotein (RNP) complex migrates along the ER membrane. The N protein wraps with TSWV RNAs to form the RNP complex, and these RNPs are subsequently driven along the ER membrane and actin by the action of myosin, after which the viral RNPs enter into the Golgi body, where they form mature virus particles (Feng et al., 2013; Ribeiro et al., 2013). To infect a new cell, the RNP complexes move to the plasmodesmata, traversing the plasmodesmata through the action of the viral movement protein NSm to reach a neighboring cell. This process involves the interaction of the N-terminal of the NSm protein with nucleocapsid protein N and assists the movement of the RNPs toward the plasmodesmata using the actin microfilament/ER transport system (Leastro et al., 2015; Tripathi et al., 2015; Feng et al., 2016). The viral movement protein NSm plays a decisive role in the intercellular and long-distance movement of viral RNPs. However, research also shows that nucleocapsid protein N plays a key role in long-distance movement, and it has been confirmed that both TSWV N and NSm are necessary for the long-distance movement of movement-deficient TMV (Lewandowski and Adkins, 2005; Zhang et al., 2011). Deletion mutations have demonstrated that NSm mediates virus intercellular movement and long-distance movement using different domains, suggesting that the mechanisms by which NSm mediates virus intercellular movement and long-distance movement are different (Li et al., 2009). Interestingly, TSWV and TZSV virus particles with vesicles have been also found in plant vascular tissue, suggesting that viral particles can also load/unload from vascular tissues and establish systematic infection through long-distance movement (Zhang, 2015; Wen et al., 2020).

MANAGEMENT

Biological Control

Biological control is an effective method to control thrips-borne orthotospovirus disease, which includes diversified prevention and control measures. These include a reasonable rotation or continuous replanting mode (Bokil et al., 2019); release of predatory mites, mirids, and other natural enemies to the greenhouse environment (Bouagga et al., 2020); and adding beneficial microorganisms to the soil environment to help plants enhance disease resistance (Beris et al., 2018; Bonanomi et al., 2020). In disease management, integrated pest management (IPM) has been proved to be more effective than chemical control (Rodríguez et al., 2019).

Screening of Virus-Resistant Plant Varieties

Growing highly virus-resistant plant varieties can be an effective way to prevent and control viral diseases. TSWV-resistant tomato and pepper varieties have been bred by Bayer, Syngenta, and other companies. These varieties possess the *Sw-5* and *Tsw* resistance genes, respectively. After selection trials, virus-resistant plants were grown in areas of high TSWV occurrence in China. However, the resistance of these plants was poor, due to single-gene resistance combined with the existence of complex/mixed infections. To date, there are no varieties with high levels of comprehensive resistance.

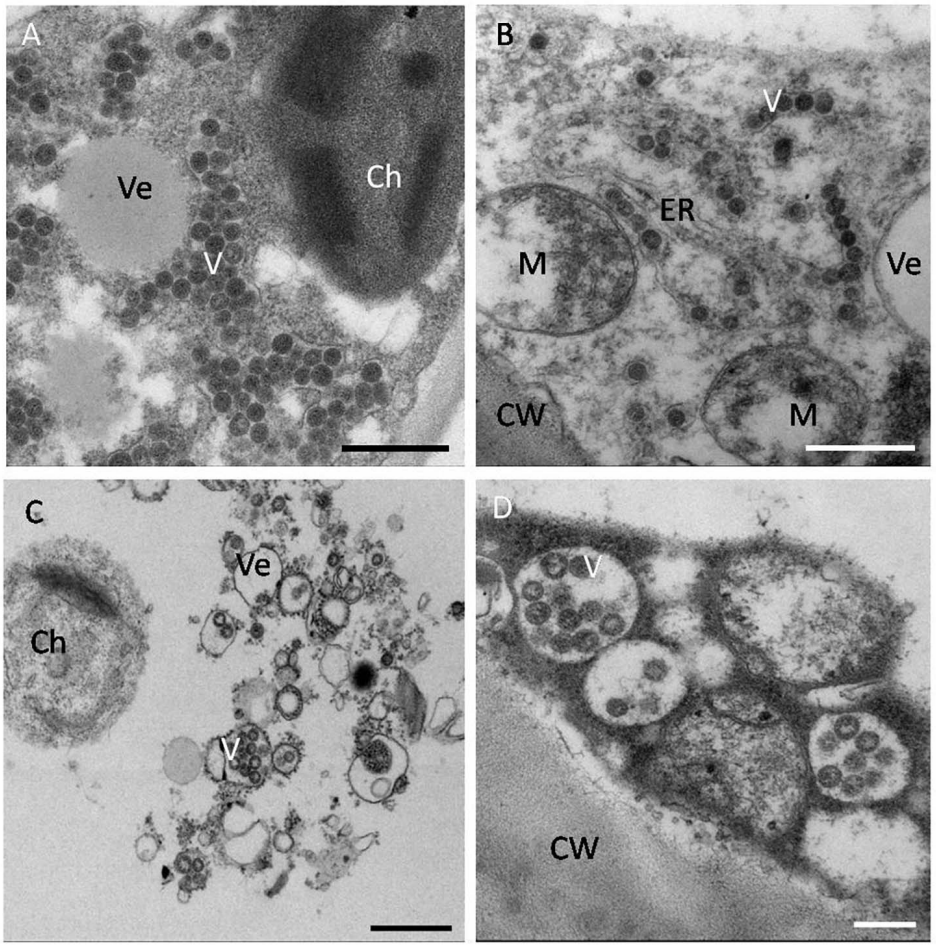

FIGURE 4 | Histopathological characteristics of orthotospoviruses in host cells. **(A)** TSWV virus particles clustered in the cytoplasm of a tomato leaf cell. Bar = 500 nm. **(B)** TZSV virus particles clustered in the endoplasmic reticulum (ER) membrane of a tomato fruit cell. Bar = 500 nm. **(C)** WSMoV virus particles clustered in vesicles in a tomato fruit cell. Bar = 500 nm. **(D)** INSV virus particles clustered in the lumen of the ER in a tomato fruit cell. Bar = 20 nm. Ve, vesicle; V, virus particle; Ch, chloroplast; M, mitochondrion; ER, endoplasmic reticulum; CW, cell wall.

Transgenic Resistance Breeding

Transgene technology is a rapid method for plants to acquire resistance to orthotospoviruses. So far, transgenic tobacco with broad-spectrum resistance against four other serologically unrelated *Orthotospovirus* TSWV, GYSV, INSV, and GCFCV has been developed by transforming the conserved motifs of the *RdRp* gene of WSMoV through hagrobacterium-mediated transformation (Kung et al., 2012; Peng et al., 2014).

Screening of Natural Anti-orthotospoviral Chemicals

Natural chemicals have attracted increasing attention and have become the most promising strategy in the defense against pathogenic infections. These naturally occurring chemicals are popular because they are environmentally friendly and leave little residue, they are highly identifiable, and they have low toxicity for the plant hosts. Because of the serious damage to agricultural crops caused by TSWV infection, natural products able to limit TSWV have attracted a great deal of interest. One potential natural derivative is atin-3-acetonyl-3-hydroxyoxindole (AHO), isolated from *Strobilanthescusia*, which is able to up-regulate PR-10 genes in the salicylic acid (SA) pathway, as well as up-regulate the levels of miRNAs (miR156, miR172f, miR172g, miR408a) that contribute to inhibiting TSWV infection (Chen et al., 2014, 2017). Actigard, imidacloprid, and *Bacillus amyloliquefaciens* strain MBI600 have also been found to induce the SA signaling pathway and to prevent TSWV infection (Csinos et al., 2001; McPherson et al., 2005; Beris et al., 2018). The terpenoid compound 3α-angeloyloxy-9β-hydroxy-ent-kaur-16-en-19-oic acid (AHK) has been isolated from *Wedeliatrilobata* and found to defend against TSWV activity and infection, with an inhibition rate of 62.4% in curative effects assays and 76.5% in protective effects assays, mainly through activation of the jasmonic acid (JA) signaling pathway and inhibition of *NSs*, *NSm,* and *RdRp* gene expression (Zhao et al., 2019). Tagitinin A is a sesquiterpene isolated from *Tithonia diversifolia* and was found to have even higher curative and protective effects against

TSWV, with an inhibition rate of over 75%. Furthermore, the expression of the genes *NSs* and *NSm* was inhibited in inoculated and systemic leaves in the protective assay, with an inhibition rate of more than 85% in systemic leaves (Zhao et al., 2017, 2020). It is therefore possible that these natural products can be used as chemical elicitors to trigger systemic acquired resistance (SAR), stimulating natural plant immunity. There is a wide variety of potential applications for such chemicals in agriculture.

The Use of Virus-Free Seeding

Viral infection at the seedling stage (a highly susceptible stage) is the main reason for disease outbreaks in the middle and late plant growth periods. To obtain virus-free seeds and effectively reduce the occurrence and loss caused by orthotospovirus diseases, seedlings should be grown in greenhouses with insect-proof netting or maximal barrier precautions, yellow or blue sticky plates should be used to attract and trap the vector insects (thrips), and the virus carriage rate of the seedlings should be regularly monitored. Comprehensive measures to reduce the vector insects (thrips) should also be applied.

CONCLUDING REMARKS AND FUTURE PROSPECTS

Orthotospoviruses are expected to further expand worldwide because of their wide host range, multiple transmission routes, and ability to adapt to diverse climates. Additionally, increases in agricultural trade have accelerated global transmission. In China, new species or strains with high pathogenicity (because of mutation, reassortment, and recombination within and/or among *Orthotospovirus* species) have increased the frequency of disease. Orthotospoviruses are therefore a threat to crop production because of their high pathogenicity and the complex/mixed infections involving different *Orthotospovirus* species or other viruses.

It is necessary to enhance the monitoring of orthotospovirus infections and set up early warning systems in high-incidence areas; to allow the rapid diagnosis of symptoms caused by *Orthotospovirus* species in host plants; to assess virus carriage rates in seeds, seedlings, thrips, and weeds; and to allow dynamic monitoring of thrips levels. A deeper understanding of the mechanisms of systemic infection, of the pathogenesis of complex/mixed infections involving the same or different *Orthotospovirus* species or other viruses, and of *Orthotospovirus* adaptation mechanisms to multiple climate types is required, as is the screening and breeding of virus-resistant plant varieties. Furthermore, to ensure environmentally friendly prevention and control of orthotospoviral diseases, highly effective biological antiviral agents should be developed, and several techniques should be popularized, including the use of virus-free seeds and standardized seedling propagation technology (such as building greenhouses with insect-proof nets, sterilizing tools before raising seedlings, controlling the number of insects by using yellow or blue sticky plates, and releasing predatory mites, mirids, or the other natural enemies of thrips, and monitoring of virus incidence on seedlings before transplantation).

AUTHOR CONTRIBUTIONS

ZZ conceived and designed the review and wrote most of the manuscript. KZ wrote the text on orthotospoviruses evolutionary relationships, conducted the statistical analyses shown in **Figure 2** and **Table 1**, and revised the manuscript. LZ wrote the text on the screening of natural anti-orthotospoviral products. XS conducted the statistical analyses shown in **Figure 3**. XZ wrote the text on orthotospoviruses transmission by thrips. TW conducted the transmission electron microscopy procedures. All authors contributed to the article and approved the submitted version.

FUNDING

This study was supported by the National Natural Science Foundation of China (U1802235), the Yunling Scholar Programme of the Yunnan Provincial Government (2016-2020), and Science and Technology Program of Yunnan Province (2018FB028).

ACKNOWLEDGMENTS

We thank the reviewer XT (Nanjing Agricultural University, China) and Sijun Zheng (Yunnan Academy of Agricultural Science, China/Alliance of Bioversity International and CIAT) for critically reading and revising the manuscript.

REFERENCES

Adam, G., Yeh, S. D., Reddy, D. V., and Green, S. K. (1993). Serological comparison of tospovirus isolates from Taiwan and India with impatiens necrotic spot virus and different Tomato spotted wilt virus isolates. *Arch. Virol.* 130, 237–250. doi: 10.1007/BF01309657

Bag, S., Schwartz, H. F., Cramer, C. S., Havey, M. J., and Pappu, H. R. (2015). Iris yellow spot virus (Tospovirus: bunyaviridae): from obscurity to research priority. *Mol. Plant Pathol.* 16, 224–237. doi: 10.1111/mpp.12177

Beris, D., Theologidis, L., Skandalis, N., and Vassilakos, N. (2018). *Bacillus amyloliquefaciens* strain MBI600 induces salicylic acid dependent resistance in tomato plants against Tomato spotted wilt virus and Potato virus Y. *Sci. Rep.* 8:10320. doi: 10.1038/s41598-018-28677-3

Bokil, V. A., Allen, L. J. S., Jeger, M. J., and Lenhart, S. (2019). Optimal control of a vectored plant disease model for a crop with continuous replanting. *J. Biol. Dyn.* 13, 325–353. doi: 10.1080/17513758.2019.1622808

Bonanomi, G., Alioto, D., Minutolo, M., Marra, R., Cesarano, G., and Vinale, F. (2020). Organic amendments modulate soil microbiota and reduce virus disease incidence in the TSWV-tomato pathosystem. *Pathogens* 9:379. doi: 10.3390/pathogens9050379

Bouagga, S., Urbaneja, A., Depalo, L., Rubio, L., and Pérez-Hedo, M. (2020). Zoophytophagous predator-induced defences restrict accumulation of the tomato spotted wilt virus. *Pest Manag. Sci.* 76, 561–567. doi: 10.1002/ps.5547

Cai, J. H., Qin, B. X., Wei, X. P., Huang, J., Zhou, W. L., Lin, B. S., et al. (2011). Molecular Identification and Characterization of Tomato zonate spot virus in Tobacco in Guangxi, China. *Plant Dis.* 95:1483. doi: 10.1094/PDIS-06-11-0486

Chao, C. H., Chen, T. C., Kang, Y. C., Li, J. T., Huang, L. H., and Yeh, S. D. (2010). Characterization of Melon yellow spot virus infecting cucumber (*Cucumissativus* L.) in Taiwan. *Plant Pathol. Bull.*19, 41–52.

Chao, J. C. J., Chu, K. F., Peng, Y. Y., Lin, S. C., Yeh, E. S., and Chen, C. (2001). Serological and Molecular Characterization of Peanut chlorotic fan-spot virus, a New Species of the Genus *Tospovirus*. *Phytopathology* 91, 856–863. doi: 10.1094/PHYTO.2001.91.9.856

Chen, C. C., Chen, T. C., Lin, Y. H., Yeh, S. D., and Hsu, H. T. (2005). A chlorotic spot disease on calla lilies (*Zantedeschia* spp.) is caused by a Tospovirus serologically but distantly related to Watermelon silver mottle virus. *Plant Dis*. 89, 440–445. doi: 10.1094/PD-89-0440

Chen, K., Xu, Z., Yan, L., and Wang, G. (2007). Characterization of a new strain of capsicumchlorosis virus from peanut (Arachishypogaea l.) in China. *J. Phytopathol*. 155, 178–181. doi: 10.1111/j.1439-0434.2007.01217.x

Chen, K. R., Xu, Z. Y., Yan, L. Y., and Wang, G. P. (2006). Complete genome sequence of mulberry vein banding associated virus, a new Tospovirus infecting mulberry. *PLoS One* 10:e0136196. doi: 10.1371/journal.pone.0136196

Chen, T. C., Chang, C. A., Kang, Y. C., Yeh, S. D., Huang, C. H., and Chen, C. C. (2012a). Identification of capsicum chlorosis virus causing chlorotic spots and stripes on calla lily. *Agric. Res. Taiwan* 61, 64–74. doi: 10.6156/JTAR/2012.06101.06

Chen, T. C., Li, J. T., Lin, Y. P., Yeh, Y. C., Kang, Y. C., Huang, L. H., et al. (2012b). Genomic characterization of calla lily chlorotic spot virus and design of broad: pectrum primers for detection of tospoviruses. *Plant Pathol.* 61, 183–194.

Chen, T. C., Lu, Y. Y., Cheng, Y. H., Li, J. T., Yeh, Y. C., Kang, Y. C., et al. (2010). Serological relationship between Melon yellow spot virus and Watermelon silver mottle virus and differential detection of the two viruses in cucurbits. *Arch. Virol*. 155, 1085–1095. doi: 10.1007/s00705-010-0688-y

Chen, Y. D, Dong, J. H, Bennetzen, J. L., Zhong, M., Yang, J., Zhang, J., et al. (2017). Integrating transcriptome and microRNA analysis identifies genes and microRNAs for AHO-induced systemic acquired resistance in *N. tabacum*. *Sci. Rep*. 7:12504. doi: 10.1038/s41598-017-12249-y

Chen, Y. D, Zhang, J., Wu, K., Liu, C. M., Xiao, J. H., Li, X. Y., et al. (2014). Field control effect of plant-derived natural product AHO on tospovirus disease. *J. Southern Agric*. 45, 2167–2171. doi: 10.3969/j:issn.2095-1191.2014.12.2167

Chen, Y. H., Dong, J., Chien, W. C., Zheng, K. Y., Wu, K., Yeh, S. D., et al. (2016). Monoclonal antibodies for differentiating infections of three serological-related tospoviruses prevalent in Southwestern China. *Virol. J*. 13:72. doi: 10.1186/s12985-016-0525-3

Cheng, Y. H., Zheng, Y. X., Tai, C. H., Yen, J. H., Chen, Y. K., and Jan, F. J. (2013). Identification, characterisation and detection of a new tospovirus on sweet pepper. *Ann. Appl. Biol*. 164, 107–115. doi: 10.1111/aab.12084

Chu, F. H., Chao, C. H., Peng, Y. C., Lin, S. S., Chen, C. C., and Yeh, S. D. (2001). Serological and molecular characterization of Peanut chlorotic fan-spot virus, a new species of the genus *Tospovirus*. *Phytopathology* 91, 856–863.

Chu, F. H., and Yeh, S. D. (1998). Comparison of ambisense M RNA of watermelon silver mottle virus with other tospoviruses. *Phytopathology* 88, 351–358.

Csinos, A. S., Pappu, H. R., McPherson, R. M., and Stephenson, M. G. (2001). Management of Tomato spotted wilt virusin flue-cured tobacco with acibenzolar-S-methyl and imidacloprid. *Plant Dis*. 85, 292–296. doi: 10.1094/PDIS.2001.85.3.292

de Oliveira, A. S., Melo, F. L., Inoue-Nagata, A. K., Nagata, T., Kitajima, E. W., and Resende, R. O. (2012). Characterization of Bean necrotic mosaic virus: a member of a novel evolutionary lineage within the genus *Tospovirus*. *PLoS One* 7:e38634. doi: 10.1371/journal.pone.0038634

Ding, M., Zhang, L. Z., Fang, Q., Li, T., Su, T., X, X., et al. (2004). Identification, purification and antiserum preparation of tospovirus isolate affecting potato. *Southwest Chin. J. Agric. Sci*. S1, 160–162. doi: 10.16213/j.cnki.scjas.2004.s1.038

Dong, J. H., Cheng, X. F., Yin, Y. Y., Fang, Q., Ding, M., Li, T. T., et al. (2008). Characterization of Tomato zonate spot virus, a new tospovirus in China. *Arch. Virol*. 153, 855–864. doi: 10.1007/s00705-008-0054-5

Dong, J. H., Yin, Y. Y., Fang, Q., McBeath, J. H., and Zhang, Z. K. (2013). A new tospovirus causing chlorotic ringspot on *Hippeastrum* sp. in China. *Virus Genes* 46, 567–570. doi: 10.1007/s11262-012-0873-z

Du, X., Wu, K., Liu, X., Zhang, L. Z., Su, X. X., Zhang, H. R., et al. (2020). The occurrence trends of dominant species of potato viruses and thrips in Yunnan Province. *Sci. Agric. Sin*. 53, 551–562. doi: 10.3864/j.issn.0578-1752.2020.03.008

Fang, Q., Ding, M., Dong, J. H., Yin, Y. Y., Zhang, L., Su, X. X., et al. (2013). Preliminary report of tospovirus infecting macadamia seedlings in Yunnan, China. *Acta Hortic. Sin*. 40, 350–354. doi: 10.16420/j.issn.0513-353x.2013.02.004

Feng, Z., Chen, X., Bao, Y., Dong, J., Zhang, Z., and Tao, X. R. (2013). Nucleocapsid of Tomato spotted wilt tospovirus forms mobile particles that traffic on an actin/endoplasmic reticulum network driven by myosin XI-K. *New Phytol*. 200, 1212–1224. doi: 10.1111/nph.12447

Feng, Z., Xue, F., Xu, M., Chen, X. J., Zhao, W. Y., Garcia-Murria, M. J., et al. (2016). The ER-membrane transport system is critical for intercellular trafficking of the NSm movement protein and Tomato spotted wilt tospovirus. *PLoS Pathog*. 12:e1005443. doi: 10.1371/journal.ppat.1005443

Gao, W., Wang, Y., Zhang, C. X., Zhang, A. S., and Zhu, X. P. (2016). Investigation and Pathogen Preliminary Identification of Pepper Virus Disease in Tianjin. *Shandong Agric. Sci* 48, 91–94.

Gao, X., Wang, S., Li, Z., Yang, B., and Liu, Y. T. (2020). Investigation and identification of orthotospovirus on tobacco in Yunnan province, china. *Acta Tabacaria Sin*. 26, 84–90. doi: 10.16472/j.chinatobacco.2019.164

Groves, C., German, T., Dasgupta, R., Mueller, D., and Smith, D. L. (2016). Seed transmission of soybean vein necrosis virus: the first tospovirus implicated in seed transmission. *PLoS One*. 11:e0147342. doi: 10.1371/journal.pone.0147342

Han, S., Zhang, Q. H., Wu, J., Li, H. H., and Xi, Y. D. (2020). Identification and detection of Tomato spotted wilt virus and pepper mild mottle virus infecting pepper in Sichuan using RNA sequencing. *Acta Phytopathol. Sin*. 50, 147–154. doi: 10.13926/j.cnki.apps.000417

Hong, J., Xie, L., Zhang, Z. K., and Zhou, X. P. (2020). Plant viruses in the new 15-rank taxonomic system of ICTV. *Acta Phytopathol. Sin.* 51, 143–162. doi: 10.13926/j.cnki.apps.000554

Huang, C., Yong, L., Yu, H., and Li, B. (2015). Occurrence of Tomato zonate spot virus on potato in China. *Plant Dis*. 99:733. doi: 10.1094/PDIS-08-14-0851-PDN

Huang, C. H., Zheng, Y. X., Cheng, Y. H., Lee, W. S., and Jan, F. J. (2010). First report of capsicum chlorosis virus infecting tomato in Taiwan. *Plant Dis*. 94:1263. doi: 10.1094/PDIS-04-10-0275

International Committee on Taxonomy of Viruses Executive Committee [ICTVEC]. (2020). The new scope of virus taxonomy: partitioning the virosphere into 15 hierarchical ranks. *Nat. Microbiol.* 5, 668–674. doi: 10.1038/s41564-020-0709-x

Jie, L., Chi, S., Yang, Q., Ding, T., and Dong, C. (2017). Identification of Tomato spotted wilt virus disease in Shandong, China. *Plant Prot.* 43, 228–232. doi: 10.3969/j.issn.0529-1542.2017.01.043

Jin, F. M., Song, J., Xue, J., Chen, D. L., Wang, S., Zhang, Y., et al. (2020). Molecular detection and partial genome sequence analysis of Tomato spotted wilt virus infected chrysanthemum in Beijing. *Acta Agric. Boreali Sin.* 35, 175–184.

Komoda, K., Narita, M., Yamashita, K., Tanaka, I., and Yao, M. (2017). Asymmetric trimeric ring structure of the nucleocapsid protein of tospovirus. *J. Viro*. 91, e01002–17. doi: 10.1128/JVI.01002-17

Kung, Y. J., Lin, S. S., and Huang, Y. L. (2012). Multiple artificial micrornas targeting conserved motifs of the replicase gene confer robust transgenic resistance to negative-sense single-stranded rna plant virus. *Mol. Plant Pathol.* 13, 303–317. doi: 10.1111/j.1364-3703.2011.00747.x

Leastro, M. O., Pallás, V., Resende, R. O., and Sánchez-Navarro, J. A. (2015). The movement proteins (NSm) of distinct tospoviruses peripherally associate with cellular membranes and interact with homologous and heterologous NSm and nucleocapsid proteins. *Virology* 478, 39–49. doi: 10.1016/j.virol.2015.01.031

Lewandowski, D. J., and Adkins, S. (2005). The tubule-forming Nsm protein from Tomato spotted wilt virus complements cell-to-cell and long-distance movement of tobacco mosaic virus hybrids. *Virology* 342, 26–37. doi: 10.1016/j.virol.2005.06.050

Li, J. T., Yeh, Y. C., Yeh, S. D., Raja, J. A., Rajagopalan, P. A., Liu, L. Y., et al. (2011). Complete genomic sequence of watermelon bud necrosis virus. *Arch. Virol*. 156, 359–362. doi: 10.1007/s00705-010-0881-z

Li, Q. F., Zhi, L., Li, M., Xu, Y., Huang, Y. N., and Liu, Y. T. (2014). Tomato zonate spot virus as a Pathogen Found in Iris tectorum. *J. Yunnan Agric. Univ*. 29, 167–172. doi: 10.3969/j.issn.1004-390X(n).2014.02.004

Li, W., Lewandowski, D. J., Hilf, M. E., and Adkins, S. (2009). Identification of domains of the Tomato spotted wilt virus Nsm protein involved in tubule

formation, movement and symptomatology. *Virology* 390, 110–121. doi: 10.1016/j.virol.2009.04.027

Liu, J., Chen, D., Liang, Y., Liu, D., and Huang, C. (2021). Identification of tomato spotted wilt virus on Beijing pepper and tomato. *Plant Quar.* 35, 44–48. doi: 10.19662/j.cnki.issn1005-2755.2021.00.009

Liu, Z., Li, Y., Wu, Y., Rao, X. (2010). Identification of tospovirus on pepper in Guangzhou. *Acta Phytophylacica Sin.* 37, 383–384. doi: 10.13802/j.cnki.zwbhxb.2010.04.016

Liu, Y., Li, F., Li, Y. Y., Zhang, B. S., Gao, X. W., Xie, Y., et al. (2019). Identification, distribution and occurrence of viruses in the main vegetables of China. *Entia Agric. Sin.* 52, 239–261. doi: 10.3864/j.issn.0578-1752.2019.02.005

Liu, Y. T., Zhi, X. P., and Zheng, Y. X. (2012). Calla lily chlorotic spot virus from spider lily (*Hymenocallislitteralis*) and tobacco (*Nicotianatabacum*) in the south-west of China. *J. Phytopathol.* 160, 201–205. doi: 10.1111/j.1439-0434.2011.01873.x

Mao, L., Zhao, K., Deng, M., Yang, Z., Tang, D., and Zhu, H. (2019). Variation analysis of nucleocapsid protein and movement protein of Tomato spotted wilt virus around Kunming area. *Acta Botanica Boreali Occidentalia Sin.* 39, 1929–1934. doi: 10.7606/j.issn.1000-4025.2019.11.1929

McPherson, R. M., Stephenson, M. G., Lahue, S. S., and Mullis, S. W. (2005). Impact of early-season thrips management on reducing the risks of spotted wilt virus and suppressing aphid population in flue-cured tobacco. *J. Econ. Entomol.* 98, 129–134. doi: 10.1603/0022-0493-98.1.129

Meng, J., Liu, P., Zhu, L., Zou, C., Li, J., and Chen, B. (2015). Complete genome sequence of mulberry vein banding associated virus, a new tospovirus infecting mulberry. *PLoS One* 10:e0136196.

Miao, J. (2018). Problems and Development Countermeasures of Facility Vegetable Industry in China From Macroscopic and Microscopic Perspectives. *Northern Hortic.* 2018, 185–190. doi: 10.11937/bfyy.20172601

Oliver, J. E., and Whitfield, A. E. (2016). The genus *Tospovirus*: emerging Bunyaviruses that threaten food security. *Annu. Rev. Virol.* 3, 101–124. doi: 10.1146/annurev-virology-100114-055036

Pappu, H. R. (2008). "Tomato spotted wilt virus (Bunyaviridae)," in *Encyclopedia of Virology*, eds B. W. J. Mahy and M. H. V. Van Regenmortel (Oxford, UK: Elsevier Ltd), 133–138.

Pappu, H. R., Jones, R. A., and Jain, R. K. (2009). Global status of tospovirus epidemics in diverse cropping systems: successes achieved and challenges ahead. *Virus Res.* 141, 219–236. doi: 10.1016/j.virusres.2009.01.009

Peng, J. C., Chen, T. C., Raja, J., Yang, C. F., Wan-Chu, C., and Lin, C. H. (2014). Broad-spectrum transgenic resistance against distinct tospovirus species at the genus level. *PLoS One* 9:e96073. doi: 10.1371/journal.pone.0096073

Peng, J. C., Yeh, S. D., Huang, L. H., Li, J. T., and Chen, T. C. (2011). Emerging threat of thrips-borne melon yellow spot virus on melon and watermelon in Taiwan. *Eur. J. Plant Pathol.* 130, 205–214. doi: 10.1007/s10658-011-9746-x

Rao, X., Wu, Z., and Li, Y. (2013). Complete genome sequence of a Watermelon silver mottle virus isolate from China. *Virus Genes* 46, 576–580. doi: 10.1007/s11262-013-0885-3

Ren, X., Liu, Y., Tan, Y., Sun, C., Huang, Y., and Liu, Z. (2014). Distribution characteristics of main tobacco virus diseases in Guizhou. *Guizhou Agric. Sci.* 42, 117–120. doi: 10.6041/j.issn.1000-1298.2014.07.017

Ribeiro, D., Jung, M., Moling, S., Borst, J. W., Goldbach, R., and Kormelink, R. (2013). The cytosolic nucleoprotein of the plant-infecting Bunyavirus tomato spotted wilt recruits endoplasmic reticulum-resident proteins to endoplasmic reticulum export sites. *Plant Cell* 25, 3602–3614. doi: 10.2307/23598370

Rodríguez, E., Téllez, M. M., and Janssen, D. (2019). Whitefly Control Strategies against Tomato Leaf Curl New Delhi Virus in Greenhouse Zucchini. *Int. J. Environ. Res. Public Health* 16:2673. doi: 10.3390/ijerph16152673

Satyanarayana, T., Reddy, K. L., Ratna, A. S., Deom, C. M., and Reddy, D. V. R. (1996). Peanut yellow spot virus: a distinct tospovirus species based on serology and nucleic acid hybridisation. *Ann. App. Biol.* 129, 237–245. doi: 10.1111/j.1744-7348.1996.tb05748.x

Song, X., Liu, Y., Chen, J., Shi, X., Zhang, D., and Branch, L. (2019). Systemic infection of Chinese garlic by Tomato spotted wilt tospovirus. *Plant Prot.* 45, 149–151. doi: 10.16688/j.zwbh.2018266

Su, D. K., Yuan, X. Z., Xie, Y. H., Wang, S. R., and Ding, H. (1987). Tomato spotted wilt virus in tomato in Chengdu and Dukou. *Acta Phytopathol. Sin.* 14, 255–256. doi: 10.13926/j.cnki.apps.1987.04.023

Sun, M., Jing, C., Chu, C., Wu, G., and Qing, L. (2017). Serological detection and molecular identification of tomato spotted wilt virus in pepper in Chongqing. *Acta Hortic. Sin.* 44, 487–494. doi: 10.16420/j.issn.0513-353x.2016-0733

Sun, S. E., Wang, J. Q., Chen, S., Zhang, S. B., Zhang, D. Y., and Liu, Y. (2018). First report of Capsicumchloros is orthotospovirus Infecting Zucchini (*Cucurbitapepo*) in China. *Plant Dis.* [Epub Online ahead of print]. doi: 10.1094/PDIS-12-17-1876-PDN

Torres, R., Larenas, J., Fribourg, C., and Romero, J. (2012). Pepper necrotic spot virus, a new tospovirus infecting solanaceous crops in Peru. *Arch. Virol.* 157, 609–615. doi: 10.1007/s00705-011-1217-3

Tripathi, D., Raikhy, G., and Pappu, H. R. (2015). Movement and nucleocapsid proteinscoded by two tospovirus species interact through multiple binding regions in mixed infections. *Virology*. 478, 137–147. doi: 10.1016/j.virol.2015.01.009

Wang, K., Zhan, B., and Zhou, X. (2019). Detection and partial biological characterization of Tomato spotted wilt tospovirus in Heilongjiang Province. *Plant Prot.* 45, 37–43. doi: 10.16688/j.zwbh.2018117

Wang, Y., Yang, Z., Wang, G., Wang, L., and Ni, H. (2016). First report of the tospovirus Tomato necrotic spot associated virus infecting kiwifruit (*Actinidia* sp.) in China. *Plant Dis* 100, 2539–2539. doi: 10.1094/PDIS-05-16-0629-PDN

Webster, C. G., Frantz, G., Reitz, S. R., Funderburk, J. E., and Mellinger, H. C. (2015). Emergence of Groundnut ringspot virus and Tomato chlorotic spot virus in vegetables in Florida and the southeastern United States. *Phytopathology* 105, 388–398. doi: 10.1094/PHYTO-06-14-0172-R

Wen, Z. D., Ding, Y., Shang, W. N., Wang, T. T., Wu, S. Z., Zhang, J., et al. (2020). Distribution characteristics of TSWV virions in vascular tissues of the systemic host tobacco K326. *J. Southwest For. Univ.* 40, 124–131. doi: 10.11929/j.swfu.202001020

Whitfield, A. E., Falk, B. W., and Rotenberg, D. (2015). Insect vector-mediated transmission of plant viruses. *Virology* 479, 278–289. doi: 10.1016/j.virol.2015.03.026

Wu, B., and Liu, Y. (2017). First report of *Hippeastrum* chlorotic ringspot virus infecting *Zephyranthescandida* in China. *Plant Dis.* 101:1960. doi: 10.1094/PDIS-12-16-1837-PDN

Wu, S. H., Xu, L. Q., Xian, W. R., Ren, J. H., Gao, D. N., Ji, Y., et al. (2020). Detection and Identification of Tomato spotted wilt tospovirus on pepper from Qinghai Province. *Acta Hortic. Sin.* 47, 1391–1400. doi: 10.16420/j.issn.0513-353x.2019-0920

Wu, X., Wu, X., Li, W., and Cheng, X. (2018). Molecular characterization of a divergent strain of calla lily Chlorotic spot virus infecting lettuce (*Lactuca sativa* var. augustana) in China. *Arch. Virol.* 163, 1375–1378. doi: 10.1007/s00705-018-3743-8

Xu, Y., Lou, S. G., Li, X. L., Zheng, Y. X., and Wang, W. C. (2013). The complete S RNA and M RNA nucleotide sequences of a Hippeastrum chlorotic ringspot virus (HCRV) isolate from *Hymenocallislittoralis* (Jacq.) Salisb. in China. *Arch. Virol.* 158, 2597–2601. doi: 10.1007/s00705-013-1756-x

Xu, Z. Y., Reddy, D. V. R., Rajeshwari, R., Zhang, Z. Y., and Huang, L. X. (1986). A new peanut virus disease caused by tomato spotted wilt virus in southern China. *Chin. J. Virol.* 03, 271–274.

Yao, G. (1992). Tomato spotted wilt virus (TSWV) found in Sichuan tobacco. *Chin. J. Tob.* 6, 39–40. doi: 10.13496/j.issn.1007-5119.1992.04.001

Yin, Y., Li, T., Xun, L., Qi, F., and Zhang, Z. K. (2015). First report of capsicum chlorosis virus infecting tomato in Yunnan, Southwest of China. *Plant Dis.* 100:230. doi: 10.1094/PDIS-01-15-0088-PDN

Yin, Y. Y., Fang, Q., Lu, X., Li, T. T., and Zhang, Z. K. (2014a). Detection of Watermelon silver mottle virus infecting watermelon in Yunnan, southwest of China. *J. Plant. Pathol.* 96:S4.123. doi: 10.1002/chin.199620258

Yin, Y. Y., Zheng, K. Y., Dong, J. H., Fang, Q., Wu, S., Wang, L. S., et al. (2014b). Identification of a new tospovirus causing necrotic ringspot on tomato in China. *Virol. J.* 11:213. doi: 10.1186/s12985-014-0213-0

Zarzynska-Nowak, A., Rymelska, N., Borodynko, N., and Hasiow-Jaroszewska, B. (2016). The occurrence of Tomato yellow ring virus on tomato in Poland. *Plant Dis.* 100:234. doi: 10.1094/PDIS-05-15-0521-PDN

Zhang, Q., Ding, Y. M., and Li, M. (2010). First report of *Impatiens* necrotic spot virus infecting *Phalaenopsis* and *Dendrobium* orchids in Yunnan Province. *Chin. Plant Dis.* 94:915. doi: 10.1094/PDIS-94-7-0915A

Zhang, W. H., and Feng, K. (2020). The infection of TSWV was first found in Shandong tobacco growing areas. *Chin Tob. Sci*. 41, 87–91. doi: 10.13496/j.issn.1007-5119.2020.05.011

Zhang, Y., Hou, M., and Li, C. (2017). Detection of main viral species of vegetable virus diseases in Hubei Province. *J. Huazhong Agric. Univ*. 36, 1–38. doi: 10.13300/j.cnki.hnlkxb.2017.06.005

Zhang, Y., Zhang, C., and Li, W. (2011). The nucleocapsid protein of an enveloped plant virus, tomato spotted wilt virus, facilitates long-distance movement of Tobacco mosaic virus hybrids. *Virus Res*. 163, 246–253. doi: 10.1016/j.virusres.2011.10.006

Zhang, Z. K. (2015). *The Mechanism of Assembly and Movement of Tospoviruses Virion in Host Plant*. Beijing: Graduate School of Chinese Academy of Agricultural Sciences.

Zhang, Z. K., Fang, Q., Wu, Z. Q., He, Y. K., Li, Y. H., and Huang, X. Q. (1998). The occurrence and distribution of main Solanacae crop viruses in Yunnan. *J. Yunnan Univ*. 20, 128–131.

Zhang, Z. K., He, Y. F., Fang, Q., Cheng, X. F., Dong, J. H., Yin, Y. Y., et al. (2010). Cytopathological characterization of three distinct tospovirus species in infected host plants. *Southwest Chin. J. Agric. Sci.* 23, 1522–1524. doi: 10.3724/SP.J.1142.2010.40491

Zhang, Z. K., Ma, X. Y., Wu, K., Zheng, K. Y., Pei, W. H., Chen, Y. D., et al. (2020). Infection cycle and epidemic characteristics of spotted wilt diseases on genera *Lactuca* vegetables in Luliang county, Yunnan province, southwest China. *J. Agric. Sci*. 33, 2827–2832.

Zhang, Z. K., Zheng, K. Y., Dong, J. H., Hong, J., and Wang, X. F. (2016). Clustering and cellular distribution characteristics of virus particles of Tomato spotted wilt virus and Tomato zonate spot virus in different plant hosts. *Virol. J*. 13:11.

Zhao, J., Liu, Y., Li, Y., Dong, L., Xie, J., Wang, L., et al. (2021). Sales status and development countermeasures of vegetable products in yunnan province in 2019. *Yangtze River Vegetables* 4, 72–76. doi: 10.3865/j.issn.1001-3547.2021.04.023

Zhao, L. H., Dong, J. H., Su, X. X., Li, S. L., Zhang, J., Xu, T., et al. (2017). Inhibition effects of sesquiterpenoids from *Tithoniadiversifolia* on Tomato spotted wilt virus. *Tob. Sci. Technol*. 50, 21–25. doi: 10.16135/j.issn1002-0861.2016.0553

Zhao, L. H., Hu, Z. H., Li, S. L., Zhang, L. Z., Yu, P., Zhang, J., et al. (2020). Tagitinin A from *Tithoniadiversifolia* provides resistance to Tomato spotted wilt orthotospovirus by inducing systemic resistance. *Pestic. Biochem. Phys*. 169:104654. doi: 10.1016/j.pestbp.2020.104654

Zhao, L. H., Hu, Z. H., Li, S. L., Zhou, X. P., Li, J. P., Su, X. X., et al. (2019). Diterpenoid compounds from *Wedeliatrilobata* induce resistance to Tomato spotted wilt virus via the JA signal pathway in tobacco plants. *Sci. Rep*. 9:2763. doi: 10.1038/s41598-019-39247-6

Zheng, K., Chen, T. C., Yeh, S. D., Rahman, M. S., Su, X., Wu, K., et al. (2017). Characterization of a new isolate of pepper chlorotic spot virus from Yunnan province, China. *Arch. Virol*. 162, 2809–2814. doi: 10.1007/s00705-017-3402-5

Zheng, K. Y., Chen, T. C., Wu, K., Kang, Y. C., Yeh, S. D., Zhang, Z. K., et al. (2020). Characterization of a new orthotospovirus from chilli pepper in Yunnan Province. *Chin. Plant Dis*. 104, 1175–1182. doi: 10.1094/PDIS-09-19-1925-RE

Zheng, K. Y., Dong, J. H., Fang, Q., Li, T. T., Yin, Y. Y., and Zhang, Z. K. (2015a). Detection of Tomato zonate spot virus by immunogold labeling electron microscopy. *J. Chin. Electron. Microsc. Soc*. 34, 67–70.

Zheng, K. Y., Liu, H. Y., Yin, Y. Y., Chen, T. C., Yeh, S. D., Zhang, Z. K., et al. (2016). Full-length M and L RNA sequences of tospovirus isolate 2009-GZT, which causes necrotic ringspot on tomato in China. *Arch. Virol*. 161, 1411–1414. doi: 10.1007/s00705-016-2788-9

Zheng, K. Y., Wu, K., Dong, J. H., Fang, Q., and Zhang, Z. K. (2015b). Infection and damage of Tomato spotted wilt virus on lettuce vegetables in Yunnan. *Plant Prot*. 41, 174–178. doi: 10.3969/j.issn.0529-1542.2015.05.033

Zheng, X., Zhang, J., Chen, Y. D., Wu, K., Dong, J. H., and Zhang, Z. K. (2015c). Occurrence dynamics and control status of *Tospoviruses* in vegetables of Yunnan in 2014. *Shandong Agric. Sci*. 47, 83–87. doi: 10.14083/j.issn.1001-4942.2015.10.021

Zheng, Y. X., Chen, C. C., Yang, C. J., Yeh, S. D., and Jan, F. J. (2008). Identification and characterization of a tospovirus causing chloroticringspots on *Phalaenopsis* orchids. *Eur. J. Plant Pathol*. 120, 199–209. doi: 10.1007/s10658-007-9208-7

Zhou, J., Kantartzi, S. K., Wen, R. H., Newman, M., Hajimorad, M. R., Rupe, J. C., et al. (2011). Molecular characterization of a new tospovirus infecting soybean. *Virus Genes* 43, 289–295. doi: 10.1007/s11262-011-0621-9

Zhu, M., Wang, B., Huang, Y., Jia, L. I., and Tao, X. (2017). Tomato spotted wilt virus was found as a pathogen of geranium (*Pelargonium hortorum*) in Yunnan Province. *J. Nanjing Agric. Univ*. 40, 450–456. doi: 10.7685/jnau.201612021

Conflict of Interest: The authors declare that the research was conducted in the absence of any commercial or financial relationships that could be construed as a potential conflict of interest.

Publisher's Note: All claims expressed in this article are solely those of the authors and do not necessarily represent those of their affiliated organizations, or those of the publisher, the editors and the reviewers. Any product that may be evaluated in this article, or claim that may be made by its manufacturer, is not guaranteed or endorsed by the publisher.

Advantages of publishing in Frontiers

OPEN ACCESS
Articles are free to read for greatest visibility and readership

FAST PUBLICATION
Around 90 days from submission to decision

HIGH QUALITY PEER-REVIEW
Rigorous, collaborative, and constructive peer-review

TRANSPARENT PEER-REVIEW
Editors and reviewers acknowledged by name on published articles

Frontiers
Avenue du Tribunal-Fédéral 34
1005 Lausanne | Switzerland

Visit us: www.frontiersin.org
Contact us: frontiersin.org/about/contact

REPRODUCIBILITY OF RESEARCH
Support open data and methods to enhance research reproducibility

DIGITAL PUBLISHING
Articles designed for optimal readership across devices

FOLLOW US
@frontiersin

IMPACT METRICS
Advanced article metrics track visibility across digital media

EXTENSIVE PROMOTION
Marketing and promotion of impactful research

LOOP RESEARCH NETWORK
Our network increases your article's readership